MINUTES
OF THE FIFTEENTH
EXPLOSIVES SAFETY SEMINAR

VOLUME II

D D C

MAR 21 1974

C

HYATT REGENCY HOTEL

SAN FRANCISCO, CALIF.

18-20 SEPTEMBER 1973

Sponsored by

DEPARTMENT OF DEFENSE EXPLOSIVES SAFETY BOARD

Washington, D.C. 20314
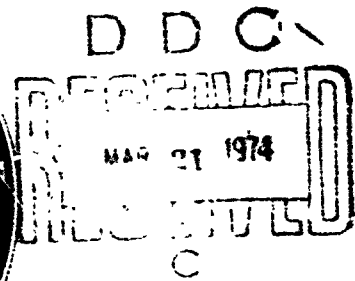
MINUTES

OF THE FIFTEENTH

EXPLOSIVES SAFETY SEMINAR

VOLUME II

HYATT REGENCY HOTEL

SAN FRANCISCO, CALIFORNIA

18-19-20 September 1973

Sponsored by

Department of Defense Explosives Safety Board

Washington, D. C. 20314

i

TABLE OF CONTENTS

VOLUME II

iii

GROUND SHOCK ENERGY COUPLING - TOOELE CONTAINERIZATION STUDY

J. D. Day

U. S. Army Engineer
Waterways Experiment Station
Vicksburg, Mississippi

INTRODUCTION

In 1972-73, twelve munitions detonations tests were conducted at the Hill Air Force Base Test Range, Lakeside, Utah. The explosives used, consisted of various configurations of munition containers, i.e., Milvans, stuffed with typical ammunition loads (Figure 1).

These tests were designed to simulate certain aspects of an accidental explosion aboard a munition laden cargo ship. Specifically, standard, 8' x 8' x 20', Milvans were used to house the explosives. The Milvans were loaded with various types of munitions as would be typically found aboard a ship and were placed together in an excavated pit in order to approximate the loaded configuration of a ship's cargo hold (Figure 2).

The tests were conducted under the direction of the Department of Defense Explosive Safety Board (DoDESB) with the support of the Ammunition Equipment Office (AEO), TEAD. The Tooele project engineer requested the Weapons Effects Laboratory (WEL) of the U. S. Army Engineer Waterways Experiment Station (WES) to provide support in the instrumentation and measurment of the ground shock associated with such tests. The U. S. Army Munitions Command in conjunction with the U. S. Coast Guard will use the overall tests results to aid in specifying appropriate cargo mixtures of varying classes of explosives.

OBJECTIVES

The test objective was to determine the possible percentage of the total explosive weight of a loaded cargo ship which would

FIGURE 1   TYPICAL MUNITIONS USED

TYPE	EXPLOSIVE WT./ MILVAN (LBS)	EXPLOSIVE
MINE, M15	8,736	COMPOSITION B
BOMB, 500 LBS	13,824	TRITONAL
PROPELLING CHARGES, 155 mm, M13	17,064	SINGLE BASE PROPELLANT
CARTRIDGES, 30 mm	5,676	23% COMPOSITION B 77% PROPELLANT
CARTRIDGES, 50 CAL.	3,384	PROPELLANT
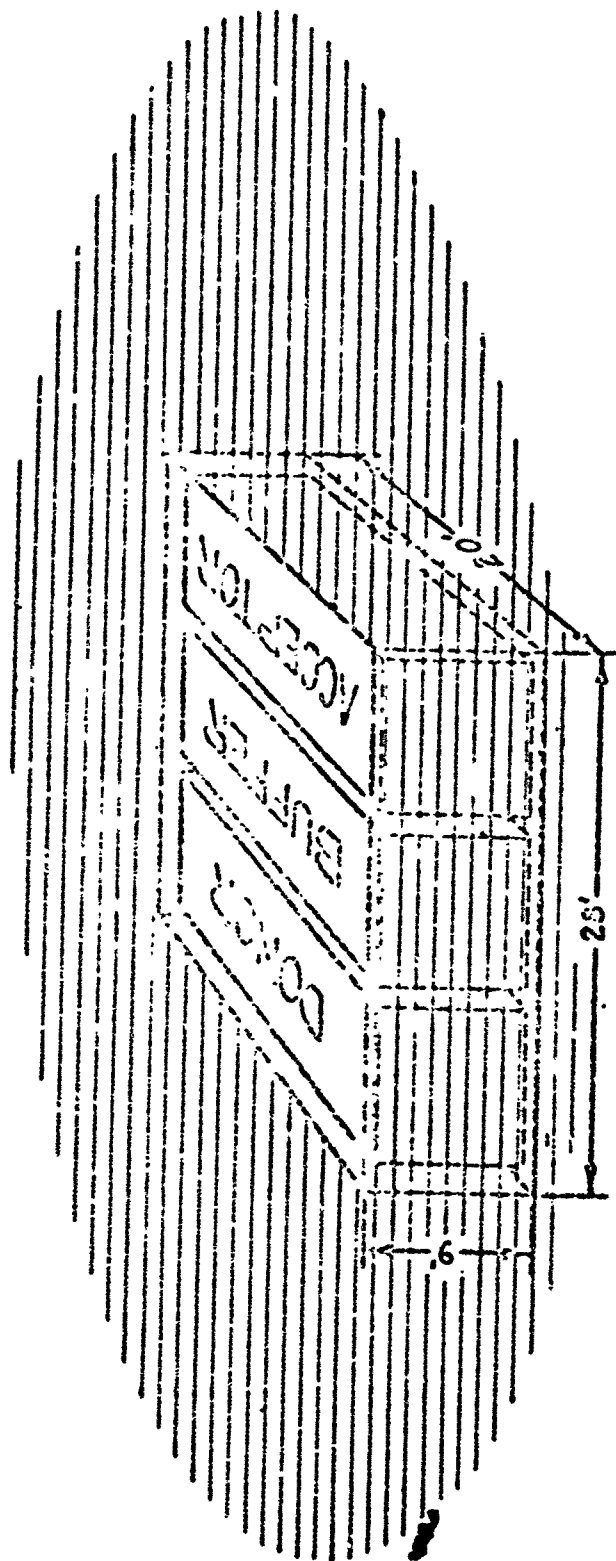
FIGURE 2   VAN PLACEMENT

contribute to blast overpressure and shock if one or more vans accidentally exploded. The likelihood of sympathetic detonations of surrounding containers, depending on explosive type, was to be studied also.

The objectives of the instrumentation projects were to document the blast or explosion characteristics in order to ascertain the sequence and the completeness of the detonations. High speed photography was used to determine the explosion sequence, and airblast measurements were used to determine the shock magnitudes. Since the Milvans were placed in open earthen pits, ground shock was measured to complement the photographic and airblast measurements.

PROCEDURES

On each detonation, one van was selected as the detonator or donor van. This van was detonated using a blasting cap with several pounds of Composition B as a booster, attached in the fuze well of an explosive item, either a mine or a bomb. One or more vans (buffer vans) were used to mitigate or buffer the remaining vans. The final vans in the array were the acceptor vans used to verify if a sympathetic detonation had been propagated. Figure 3 shows the combinations of vans and munitions used for each test.

Ground shock gages were positioned along a line, essentially emanating radially, from the ground zero (GZ) points. Since the van arrangement was not always symmetrical, the GZ was defined as the geometrical center of the excavated pit. All shots, except 11, had a single gage radial. Shot 11, with a 33 van stack, used two gage radials, i.e., an additional line perpendicular to the main line. This shot had a total of 40 gages, all others had 24 gages.

Since the airblast parameter was a primary measurement, the ground shock stations were laid out adjacent to the airblast stations. Overpressure of interest was the 1-50 psi level which spanned a ground

FIGURE 3 MILVAN CONFIGURATIONS

TEST NO.	DONOR VAN(S) NO.	MUNITION	BUFFER VAN(S) NO.	MUNITION	ACCEPTOR VAN(S) NO.	MUNITION	EXPLOSIVE WEIGHT LBS
1	1	MINES	1	CARTRIDGE, 90 mm	1	MINES	23,148
2	1	MINES	2	CARTRIDGE, 90 mm	1	MINES	28,824
3	1	MINES	2	PROPELLANT, ARTY.	1	MINES	51,600
4	1	MINES	1	CARTRIDGE, 50 CAL.	1	MINES	20,856
5	1	BOMBS	2	CARTRIDGE, 90 mm	1	MINES	33,912
6	1	BOMBS	2	CARTRIDGE, 90 mm	1	BOMBS	39,000
7	2	BOMBS	2	CARTRIDGE, 90 mm	1	BOMBS	52,824
8	1	BOMBS	1	CARTRIDGE, 90 mm	1	BOMBS	33,324
9	1	BOMBS	0	--	0	--	13,824
10	1	BOMBS	2	CARTRIDGE, 90 mm	1	BOMBS	36,930
11	2	BOMBS	15	CARTRIDGE, 90 mm	16	BOMBS	316,947
12	1	BOMBS	0	--	0	--	13,824

range from 100 feet to approximately 1500 feet from GZ, depending on the various explosive weights. Two depths were instrumented, 1.5 ft and 5 ft. The majority of the gages were at the 1.5-ft depth in order to measure the airblast-induced ground shock. Three, 5-ft stations were used to check shock propagation downward and to sense any refracted shock wave propagation, should such occur. The 1.5-ft stations consisted of a soil stress gage and a vertically and a horizontally oriented accelerometer; 5-ft stations had accelerometers culy.

The accelerometers were contained in blast resistant canisters, each canister containing a vertically and horizontally oriented pair of gages. These canisters were then firmly grouted in boreholes using a soil-cement backfill material. The stress gages were individually backpacked into separate shallow gage holes.

The gage cables were placed in trenches and run back to a common junction box where all were connected through a single multipair telephone trunch cable to the recording equipment, some 3000 ft away. Here the recording van was located under a barricaded shelter, which provided protection from possible flying shrapnel.

DISCUSSION OF RESULTS

The data from this ground shock study will be used to augment that from the photographic and airblast projects. For the purpose of this discussion, however, it is assumed that this other data is not available. If such were the case, what then can be gleaned solely from the ground shock data?

Since the instrumentation was near the ground surface and in close proximity to the airblast gages, the ground shock should reflect, to a degree, the nature of the airshock. Examination of the typical data in Figure 4 yields this type information. This station was 1250 ft from GZ on Shot 1. The directly coupled ground shock arrives approximately 150 milliseconds (msec) after zero time (ZT) and the
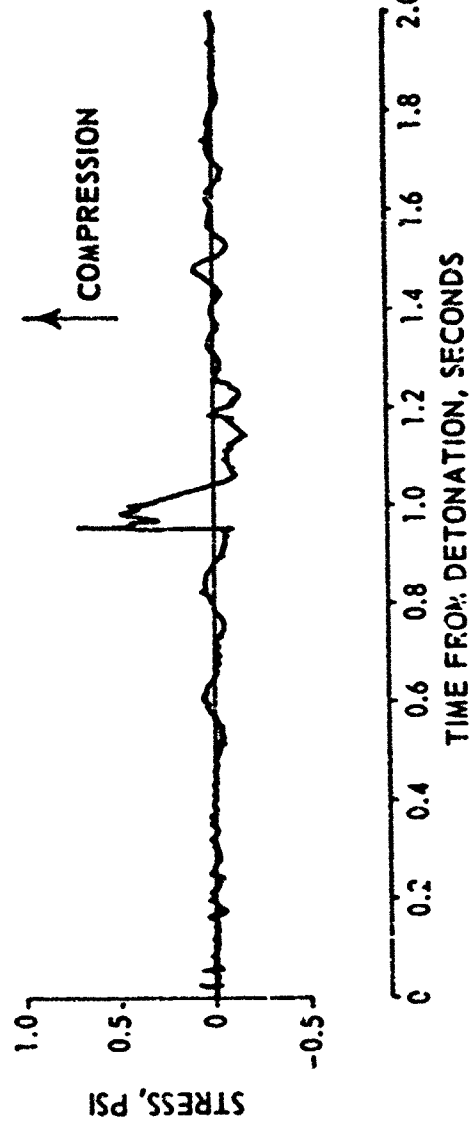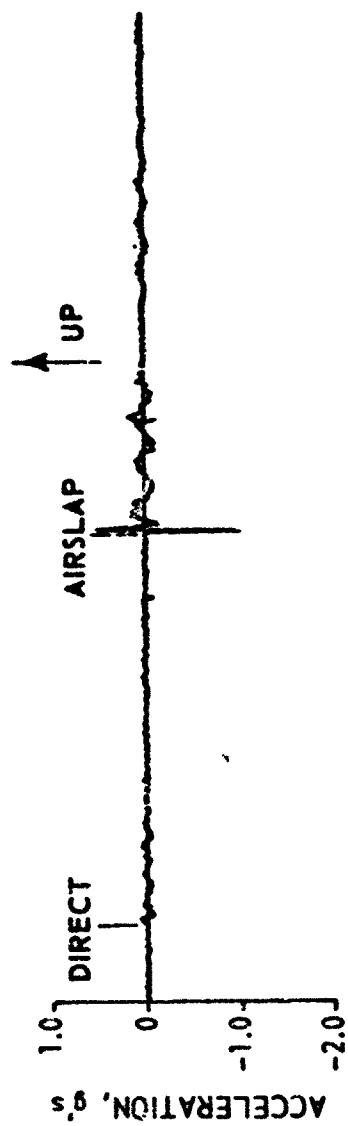
FIGURE 4   TYPICAL GROUND SHOCK DATA

airblast induced shock arrives at 940 msec after ZT. The airslap motions clearly dominate the direct motions here and also at the other stations of interest (<50 psi). Since these peak motions are the maxima in every case, the airblast peak values will be used hereafter in the discussion.

If a single explosive source were assumed to be the charge and the degree of charge coupling to the soil were known, one could simply scale (Sachs scaling law) the charge weights, determine overpressure versus distance and compare this to the measured airblast induced motions. The difference between these values would indicate degree of completeness of the detonation. If this were the case, the blast data should be relatable to the explosive ranking given in Figure 5.

Figure 6 shows a plot of peak acceleration versus ground range where mines were used as both donor and acceptor. Shots 1, 2 and 4 are directly comparable, since all used cartridge vans as buffers. (Shot 3 used bagged propellant as a buffer). If ranked by weight, Shot 2 was largest, 1 next, then 4. We see the effects of buffering. Shot 1 with one van of 9C mm's produced stronger shocks than 2 with two buffers. Shot 4 with one van of 50 caliber cartridges as a buffer showed less shock. Shot 3 used two vans of artillery propellant, obviously not a good buffer, and 9 was a single van control shot.

Figure 7 shows soil stress versus ground range for the same series of shots. We see the same trends here, with Shots 4 and 2 nearly equal however.

Figure 8 shows acceleration data obtained from the shots using 500 lb bombs as donors and acceptors. Shot 11 stands out by itself as it should; it used 33 vans of explosives. It certainly should be ranked No. 1. Shots 7 and 5 show strong shocks, then Shots 8, 6 and 10.

FIGURE 5   TOTAL EXPLOSIVE WEIGHT, RANKED

SHOT NO.	WEIGHT (LBS)	CUBE ROOT
11	319,947	67.9
7	52,824	37.4
3	51,600	37.2
6	39,000	33.8
10	36,930	33.2
5	33,912	32.3
8	33,324	32.1
2	28,824	30.6
1	23,148	28.4
4	20,856	27.4
9	13,824	23.9
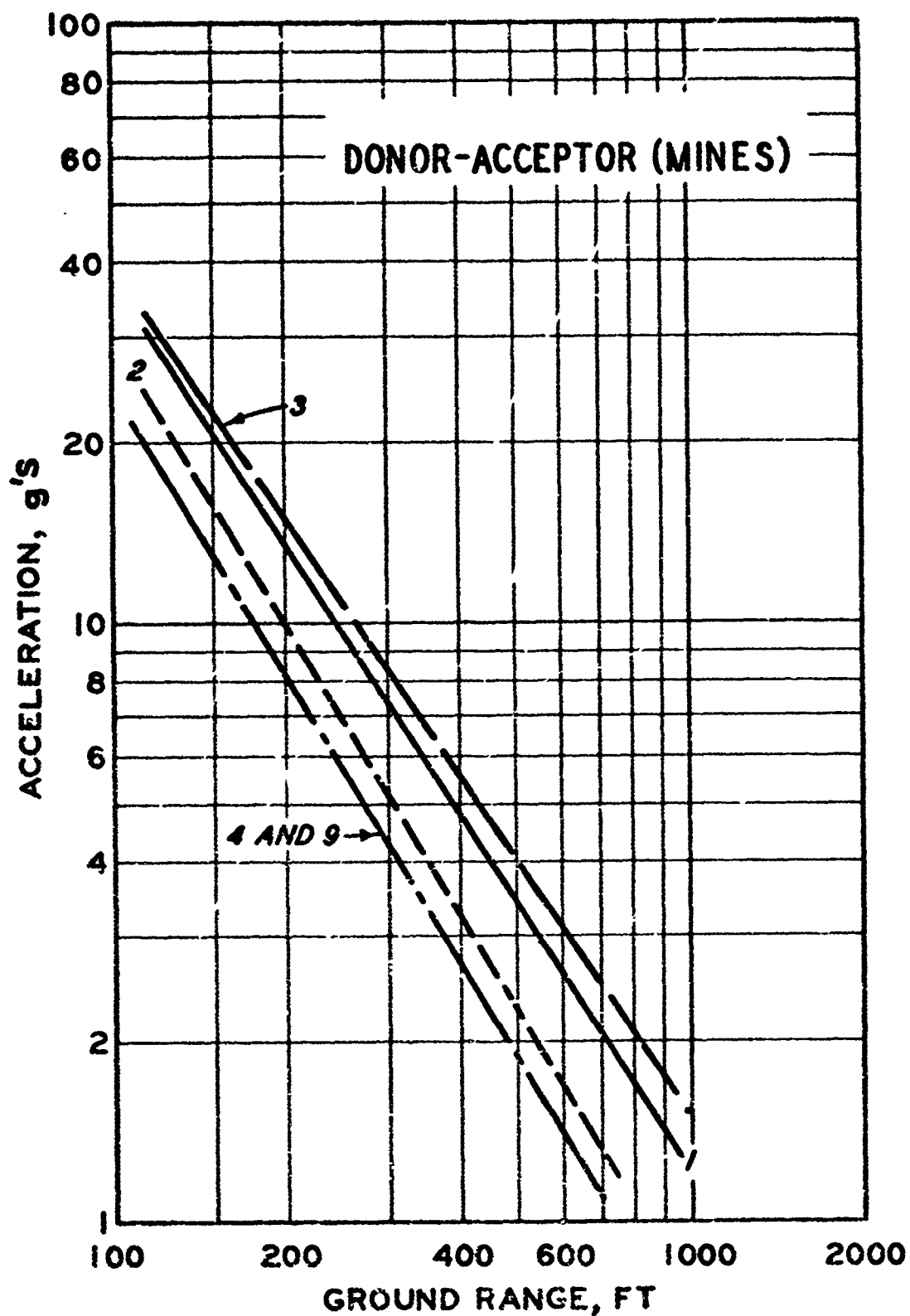
ACCELERATION VS DISTANCE

FIGURE 6
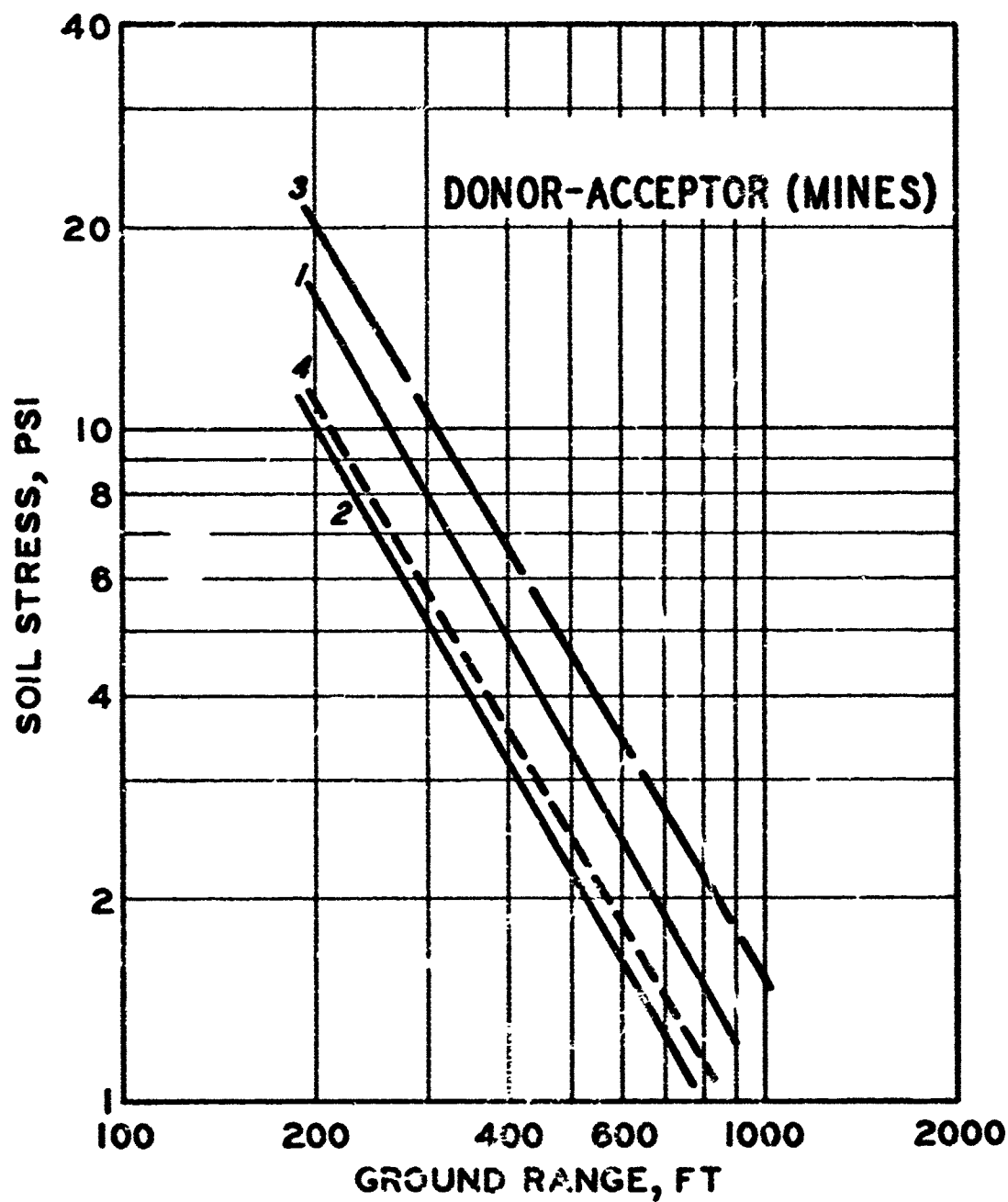
SOIL STRESS VS DISTANCE
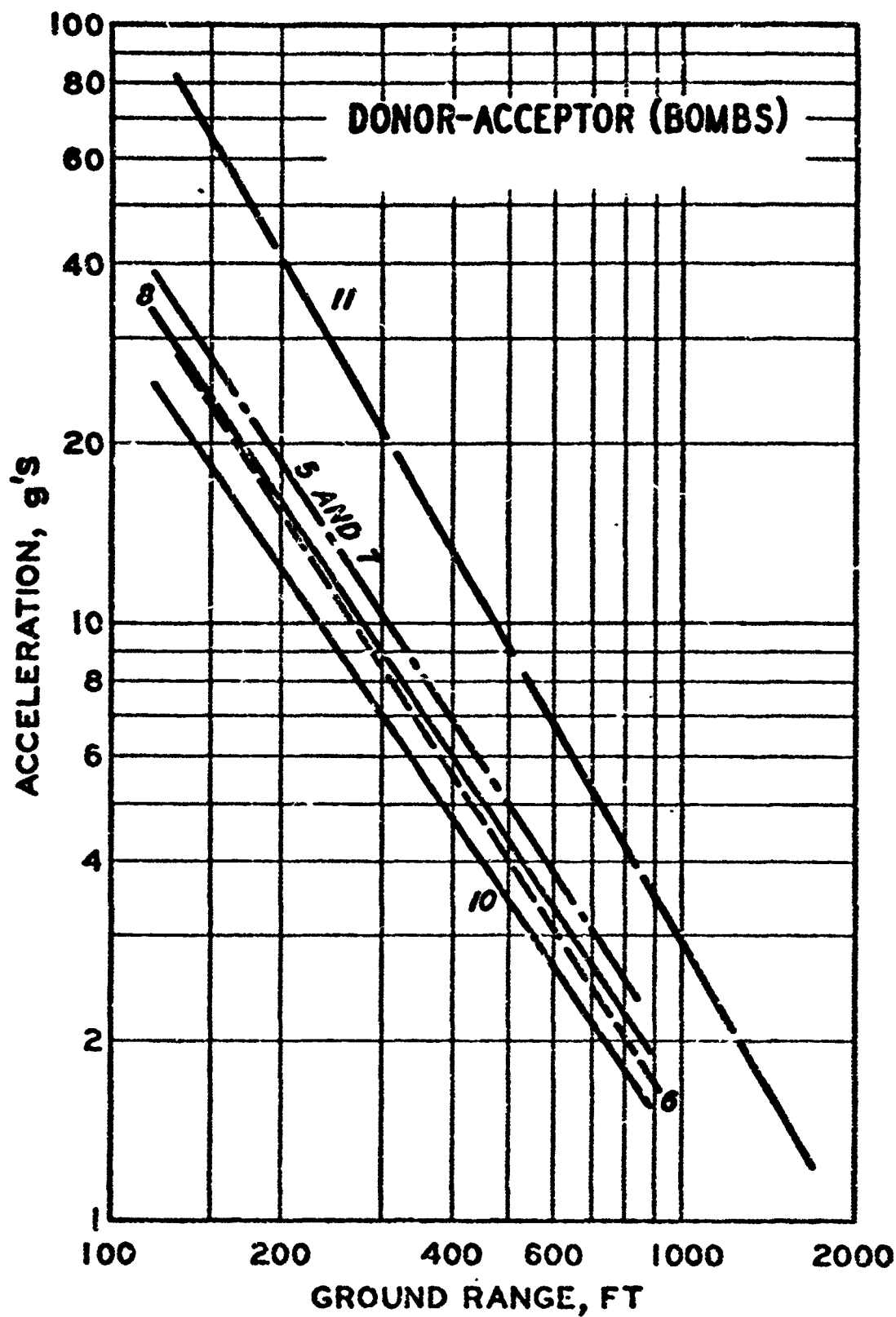
FIGURE 1

ACCELERATION VS DISTANCE

FIGURE 8

The stress data from the bomb shots are shown in Figure 9. The relative order is changed; but also there is a trend for the data to decrease with each succeeding shot. Compared to the stress data from the mines (Figure 7), it is becoming lower and lower, which is not true with the acceleration data. The indication here is not decreasing explosive sources but probably one of the gages becoming more disassociated from the media as shot after shot is fired over the same area. The top layer becomes powdered which attenuates the stress. The accelerometers, tightly grouted into the surrounding in situ material, does not degrade with suceeding shots. For this reason, the stress data is not felt reliable after the first several shots. The discussion then will center on the acceleration data.

If the data from Figures 6 and 8 are used together, the shock strengths may be ranked in terms of the acceleration data. Although graphic distinctions are lacking for several shots, this ranking appears to group thusly: Shots 11, 7, 5, 8, 3, 1, 6, 10, 2, 9 and 4.

Figure 10 refers back to the original ranking by total weight. Another column is added here showing the significance of discounting the non-mass detonating propellants from the buffers. Comparing the ground shock rankings at this point, does not yield a very good agreement. From the earlier data review, there was evidence of buffering which probably meant some Class 7 items were not detonated and therefore their charge weights should not be used as part of the total weight.

At this point, one piece of corroborative evidence should be used, i.e., the results from the explosive ordnance disposal (EOD) teams. After each shot the EOD teams gathered the unexploded items for disposal, and a tabulation was made of these unexploded weights. If these values are subtracted from the original values, we obtain the data shown in
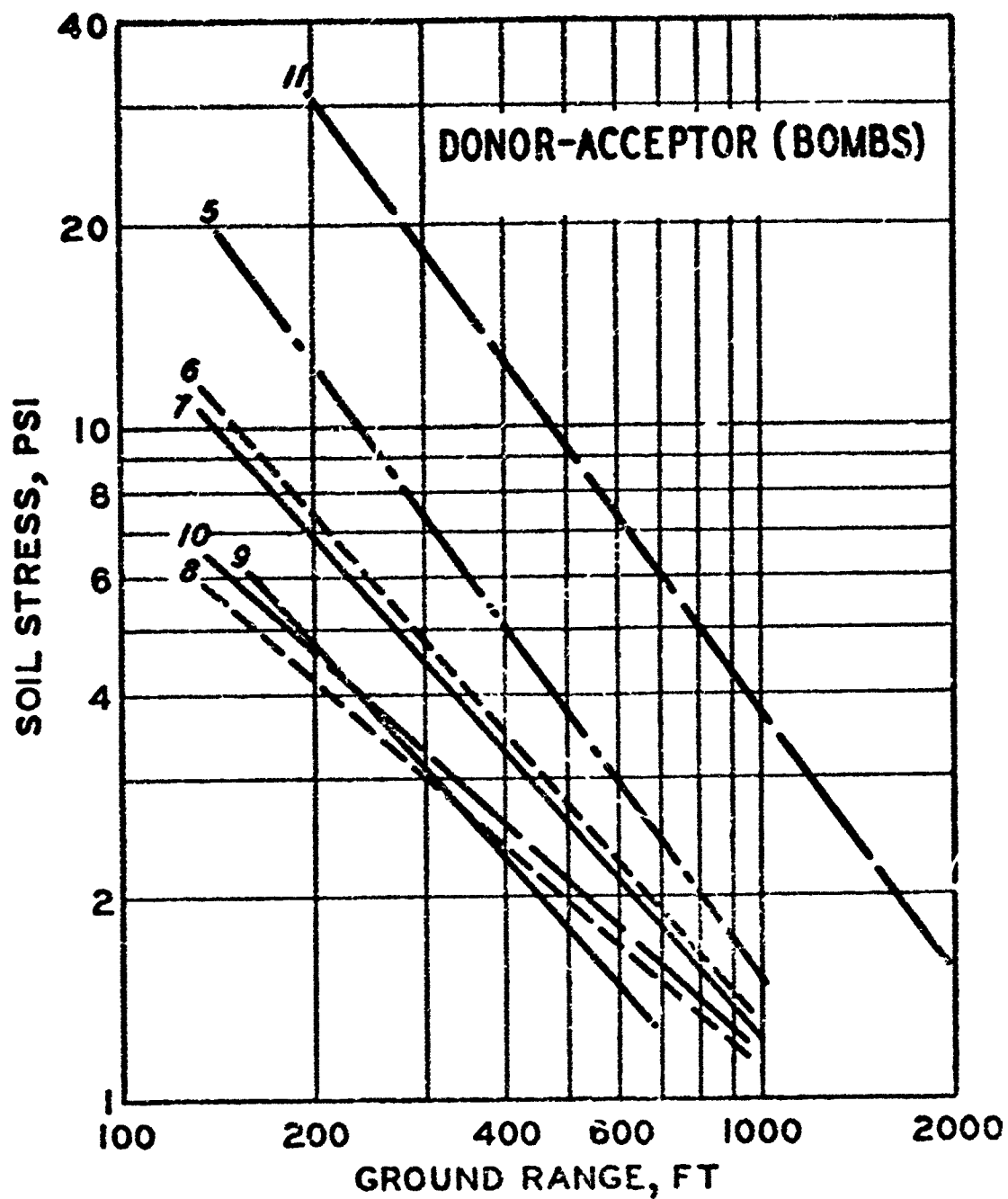
SOIL STRESS VS DISTANCE

FIGURE 9

770

FIGURE 10   TOTAL WEIGHTS OR ADJUSTED WEIGHTS

ORIGINAL RANK	GROUND SHOCK RANKING	ADJUSTED RANK (LBS/LBS)
11	11	11 - 319,947/264,312
7	7	7 - 52,824/44,052
3	5	6 - 39,000/30,280
6	8	10 - 36,930/29,912
10	(3)	8 - 33,324/28,938
5	1	5 - 33,912/25,140
8	6	2 - 28,824/20,052
2	10	1 - 23,148/18,762
1	2	4 - 20,856/17,471
4	9	3 - 51,600/1,722
9	4	9 - 13,824/13,824

Figure 11. In some cases the change is significant. For the final comparison, the ground shock rankings are shown. The agreement speaks for itself.

The data from the near-surface accelerometers can be used to infer the completeness of the explosion and hence the buffering accomplished in these tests.

One final piece of data should be added. Once the effective charge weights were ranked by the ground shock, the cube root of these weights can be used on the unscaled airblast data. Figure 12 presents the airblast arrival time data. The raw data is scaled by the final weights and this scaled data collapses nicely. Figure 13 gives the overpressures and hence again, the scaled data supports the ranking by the ground shock/EOD results.

FIGURE 11   FINAL RANKINGS

TOTAL (CUBE ROOT)		GROUND SHOCK RANKING	ADJUSTED (CUBE ROOT)	
11	67.9	11	11	64.2
7	37.4	7	7	30.1
3	37.2	5	5	29.3
6	33.8	8	8	29.1
10	33.2	(3)	1	26.5
5	32.3	1	6	26.2
8	32.1	6	3	25.9
2	30.6	10	10	25.4
1	28.4	2	2	24.0
4	27.4	9	9	23.7
9	23.9	4	4	22.8
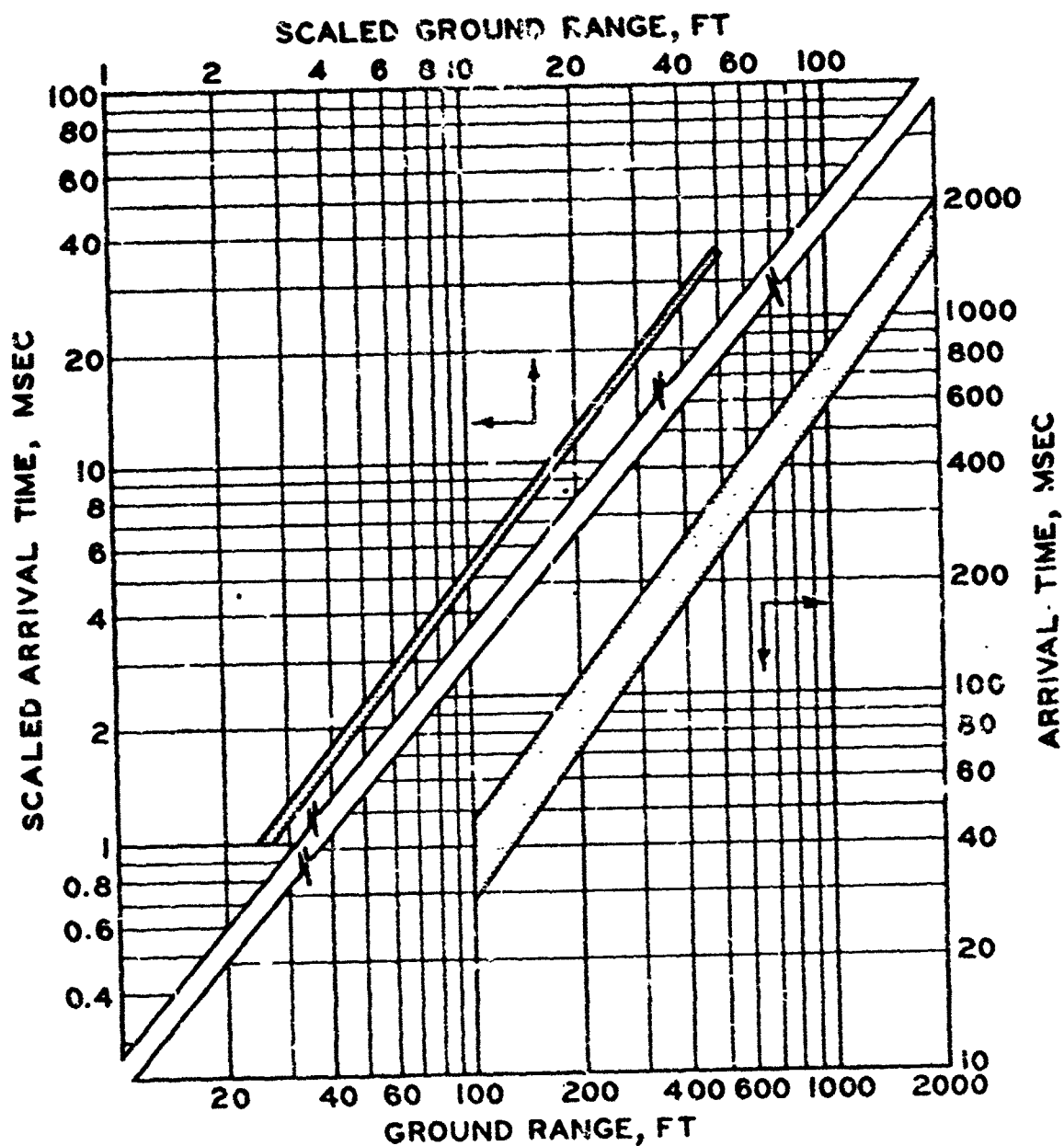
ARRIVAL TIMES-UNSCALED VS SCALED (EOD WTS)

FIGURE 12
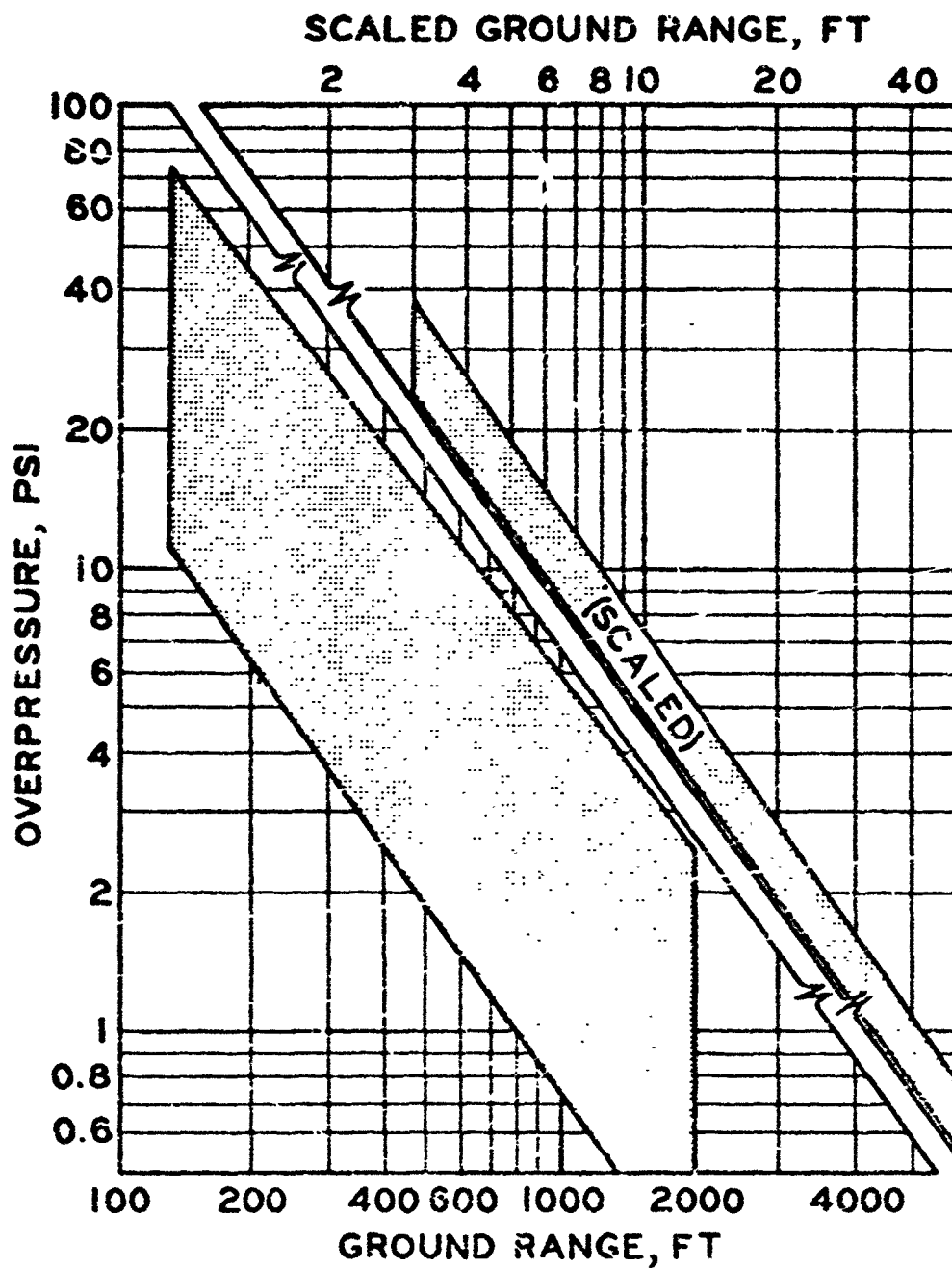
OVERPRESSURES – UNSCALED VS
SCALED (EOD WTS)

FIGURE 13

THE MIXING AND PUMPING OF GELLED NITROMETHANE

CAPT H. H. Reed, USA
Explosive Excavation Research Lab., Livermore, Calif.

1. __Introduction.__ The Explosive Excavation Research Laboratory (EERL) of the Corps of Engineers' Waterways Experiment Station is colocated with the Atomic Energy Commission's Lawrence Livermore Laboratory (LLL) in Livermore, California. EERL is currently involved in a comprehensive program of nuclear explosion simulation tests using chemical explosives. Design of specific experiments of this program required selection of an acceptable chemical explosive and placement system. The selection process was complicated by a need to meet two specific constraints generated by the program objectives.

2. __Constraints.__ Complex computer codes, available at LLL, are able to calculate the chemical explosive yields required to simulate a buried nuclear detonation. These codes require that an equation-of-state be developed for the chemical explosive being used for the numerical calculation. Testing is required to develop a well defined equation-of-state for an explosive. A truly valid equation-of-state can be generated only if an explosive's detonation is reliable and its detonation characteristics are reproducible.

The second technical constraint impacting on explosive and placement system selection was the fallout tracer program. Fallout simulation using the tracer technique calls for uniformly suspending tagged sand particles in the explosive. Iridium, a neutron activable chemical element, is surface absorbed on these quartz particles which are of known size and density. Trays are placed at measured intervals in the shot area to collect material ejected on detonation. The collected material is weighed, sized, activated, and analyzed. Numerical calculations on this data produce fallout patterns and the fraction vented for each event.[2] This simulation technique requires

an explosive with the capability of uniformly suspending sand particles and holding them in suspension for at least a week.

3.   Explosive Selection.   Based on its use during experimentation conducted during the late 60's at Fort Peck, Montana, nitromethane was selected as the prime candidate for use in the nuclear simulation program.   Reproducibility of nitromethane's detonation characteristics is excellent and its equation-of-state had already been determined (see Table 1).   Testing of nitromethane by the Chemistry Department of LLL revealed that reproducible detonations could be obtained after the addition of up to 40% by weight of inert materials. Naturally, a corresponding reduction in energy and detonation velocity occurred, however, these reductions were constant for a given percentage of dilution.[3]   Thus, nitromethane was well suited for use in the computer code.   Unfortunately, the suspension of sand in a nitromethane solution proved to be a much more complex problem.   During the Fort Peck tests, efforts to gell nitromethane were unsuccessful with gelling agents available at the time. At this point, it was decided that aluminized ammonium nitrate slurry would be investigated as an alternative.   Although slurry is well suited for sand suspension, tests performed in an effort to define its equation-of-state revealed that this task would be extremely difficult and could probably not be accomplished in the time available.   Thus, efforts were turned to the task of developing an acceptable gelling technique for nitromethane.

4.   Gelling Agent.   Discussions were held with Commercial Solvents Corporation, the sole producers of nitromethane in the United States, on systems and methods of gelling or thickening nitromethane.   Nitro cellulose has been used, but it is a high explosive in itself, and when mixed with nitromethane readily forms lumps which are difficult to disperse.[1]   This system was not considered practical or safe in terms of the quantities or conditions required

Table 1. Physical and detonation properties of nitromethane.[1]

Boiling Point (at 1 atm)	101.2°C
Vapor Pressure (at 20°C)	27.3 torr
Freezing Point	-28.55°C
Density (at 20°C)	1.138 g/ml
Viscosity (at 20°C)	0.647 cp
Heat of vaporization (at b.p.)	8.225 kcal/mole
Heat of Combustion	169.4 kcal/mole
Flash Point (tag open cup)	112°F
Flash Point (tag closed cup)	96°F
Solubility in water (at 20°C)	10.5% wt
Solubility of water in NM (at 20°C)	1.75% wt
Heat of Explosion	1227 cal/g
Volume of Gases	936 1/kg
Rate of Detonation	6300 m/sec

for the simulation program. Polyoxyethylene can be used to thicken nitromethane but a rigid gell is formed which will begin to liquefy after about a week of storage at room temperature.[1] This gell can be further stabilized, but the rigid gell produced is not considered compatible with the need to mix, then pump, or pour the gelled nitromethane into a subsurface cavity. Most starches, natural gums, and synthetic polymers used in water gelling systems are ineffective with nitromethane. General Mills, Inc., had been doing development work with a modified guargum, a cyanoethylether derivative of a galacto-mannan gum, specifically directed at thickening or gelling nitromethane.[2] This gelling agent is identified as XG 512 by General Mills, Inc. It is a free-flowing, white powder which must be quickly dispersed throughout the nitromethane to prevent the formation of lumps which are difficult to break up.

5. Explosive Testing. The Chemistry Department of LLL obtained samples of XG 512 and laboratory testing was conducted. Various percentages of the agent were mixed with tracer sand and nitromethane. These samples were observed over a period of a few weeks. No liquefaction was observed although perceptible sand settlement was noted at the end of the second week. A formulation containing 87/10/3 weight percentages of nitromethane/sand/gelling agent was chosen for further study. The complete settling of sand did not occur until several months had elapsed.[4]

Industrial grade nitromethane is relatively insensitive to shock as compared with conventional commercial or military explosives. It cannot be detonated by a number 8 blasting cap. It may be detonated if a booster of sufficient size is used. There are many ways in which pure nitromethane may be sensitized to make it cap-sensitive.[1] The ease with which it can be sensitized was an important consideration in the use of gelled nitromethane.

To insure that the gelling process and the sand did not sensitize the nitromethane, various safety tests were performed, including: differential thermal analysis, impact sensitivity, a number 8 blasting cap test, gap tests, a gell stability test, and a burn test.

The differential thermal analysis tests showed a large endotherm due to evaporating nitromethane. No exotherms were observed. Impa.t sensitivity was determined using the LLL drop hammer test. Tests of gelled nitromethane and the composition with sand failed to show reaction using a 2.5 kg weight at the limiting height of 177 cm.[2] A number 8 blasting cap failed to detonate the explosive.

Gap tests were conducted on industrial nitromethane, a sensitized nitromethane, and the gelled nitromethane. The gelled samples appeared to be only slightly more shock-sensitive than industrial nitromethane as seen in Table 2.

The gell stability test consisted of keeping a sample in an oven set at 100°F for several weeks. No appreciable gell breakdown was noted.

The burn test consisted of placing several pounds of explosive within a ring of combustible material and igniting the combustible material. The gelled nitromethane did burn, but at a very slow rate with very little hea: output and a very low, almost imperceptible, flame.[4,5] Field tests conducted at Fort Peck again demonstrated the slow burning rate and low heat output of burning gelled nitromethane.

The detonation parameters were determined using the LLL cylinder test.[6] A summary of the cylinder performance tc.t results of the gelled nitromethane compared with pure nitromethane is given in Table 3. The cylinder test data was also used to determine an equation-of-state for the detonation products.

Table 2[4]

Explosive	NM (industrial)	Sensitized NM (95% NM/5% Ethylene Diamine)	Gelled NM (87/10/3)
Density (g/cc)	1.13	1.12	1.21
G_{50} (mils)	15	144	30-50
95% Confidence Interval	±5	±5	-
Number of Usable Shots	11	11	14

Samples were 1/3-inch in diameter and 1 inch long and confined in mild steel. The donor system was PBX 9404, 1/3-inch diameter by 0.3 inches long with a type K detonator. The inert barrier was brass.

Table 3[4]. Cylinder performance of gelled nitromethane (87/10/3) and nitromethane.

Performance	Gelled NM (87/10/3)	NM
Wall Velocity - mm/μsec at 6mm expansion	1.00	1.06
Time - μsec to 6mm expansion	7.92	7.51
Wall Velocity - mm/μsec at 19mm expansion	1.17	1.22
Time - μsec to 19mm expansion	19.68	18.71
Detonation Velocity - mm/μsec	6.11	6.37

6. **Mixing and Pumping Equipment Selection.** The first planned operation using gelled nitromethane was a one-ton cratering shot planned for the fall of 1972 at Fort Peck, Montana. The mixing and pumping equipment selected for field use had to meet several criteria. Most importantly, it had to be safe for use in field operations. As nitromethane is sensitive to detonation from the heat of the compression of gases, it is shipped in 55-gallon drums which are designed to vent if the internal pressure exceeds about 100 psi. Conditions which might lead to accidental detonation from this phenomenon had to be avoided both in the pump and the discharge lines. The mixer had to be able to disperse the sand uniformly throughout the nitromethane and create enough mixing action so the gelling agent could be added quickly to avoid clumps forming in the mix. The mixing container had to be compatible with both the pump and the mixer, and the entire system must mix batches large enough to insure efficient loading would be accomplished.

Within the limited time available for selecting and testing the mixing and pumping system, the simplest, safe system was chosen. Air-driven equipment was chosen because of its inherent safety in processing explosives. The mixer was a Lightning Model NAG 100 manufactured by the Mixing Equipment Company, Rochester, New York. It used a 3-foot shaft and a 7.8-inch diameter, 3-blade propeller (Figure 1). The unit was clamped to the rim of a 55-gallon drum which was used as the mixing barrel for 400-pound batches. Testing showed that this unit produced the deep vortex required for rapid and thorough mixing. After mixing, the mixer was removed from the drum and the drum was placed under a barrel pump. The pump and ram unit was manufactured by Grayco, Inc., Minneapolis, Minnesota, and was particularly designed for pumping viscous materials from 55-gallon drums. The pump consisted of three separate units as shown in Figure 2. The ram piston fit

Figure 1. Nitromethane mixing unit.
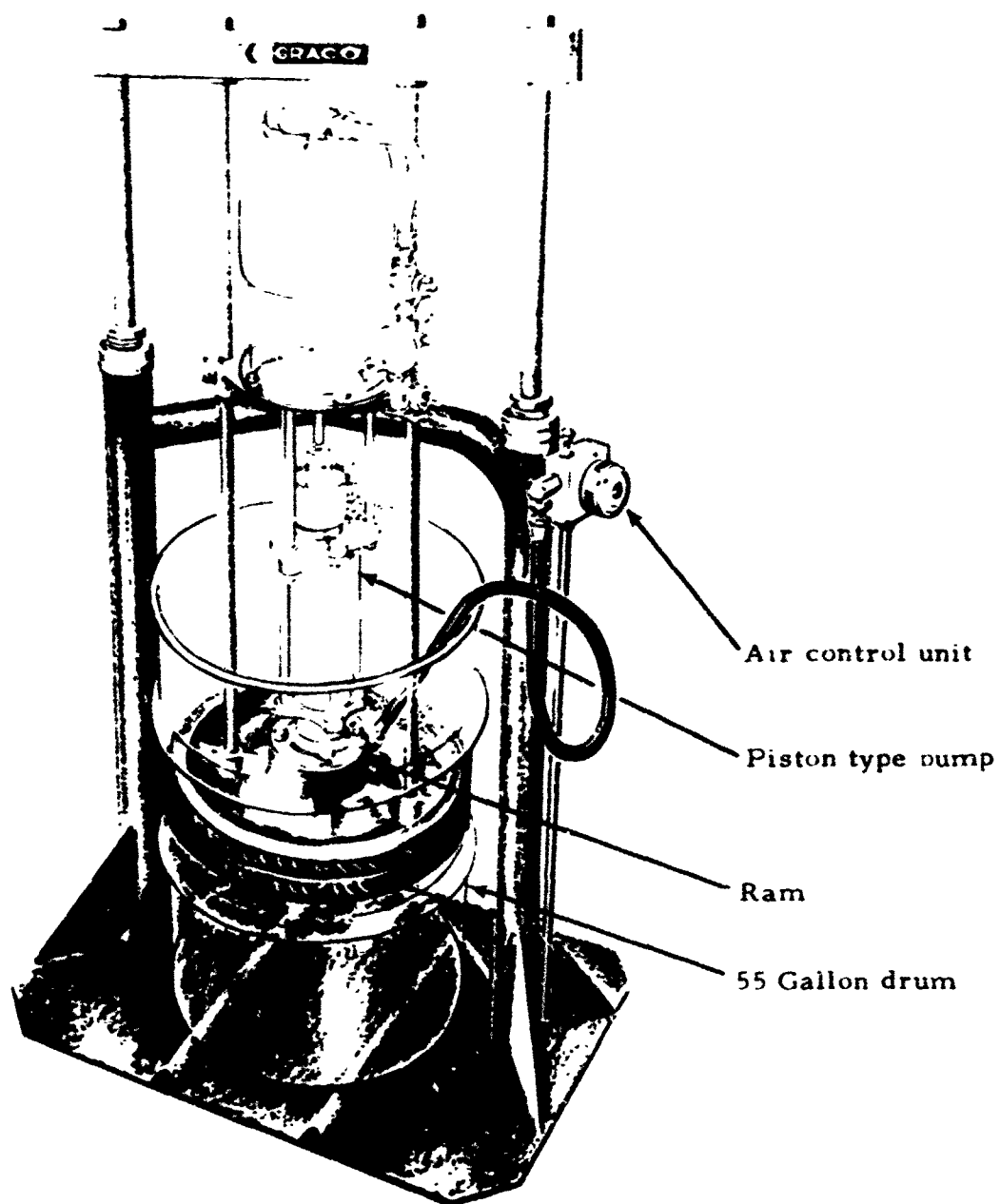
Figure 2. GRAYCO pump unit used for pumping nitromethane in DIAMOND ORE tests.

snugly inside the 55-gallon drum and maintained about 1 psi pressure on the gelled nitromethane. The double action piston pump was mounted on the ram assembly. The air control unit was used to regulate the pressure in both the ram and the pump. The pump produced a 5 to 1 pressure ratio (output to input). An approximately 125 psi pump discharge pressure was required to force 8 gallons per minute of gel through 35 feet of 1-1/2-inch I.D., natural rubber-lined fire hose. Certain modifications were made to the pump to avoid any possible traps in the double-action piston pump.

Under the less than ideal field conditions where the mixing and pumping equipment was mounted on a truck body, a total mix and pump time of only two hours was required to fill the shot. Gelling time was less than one minute for each 400-pound batch. Detonation velocity measurements taken using a piezoelectric pin rate stick gave an average detonation velocity over a 30-cm path of 6.14mm/ sec, which compares favorably with 6.11mm/ sec obtained from the laboratory cylinder test.[7]

Careful evaluation of the system during the 1-ton test resulted in the conclusion that for future shots a safer method should be developed in which the explosive was separated from any mechanical functions of the pumping system. A further consideration was the projected requirement for pumping larger shots. This required a bigger and faster system.

A survey of industrial pumps led to a detailed examination of concrete pumps. These pumps have the capability of pumping fairly large amounts of viscous materials at a fairly high rate. A Challenge Squeeze-Crete 120 made by Challenge-Cook Brothers, Inc., Industry, California, was obtained for testing (Figure 3). This pump accomplishes a "squeeze-action" by two rollers alternately compressing a tough steel-banded rubber pumping tube, forcing the concrete through the pump and lines. The concrete contacts only the tube. A partial vacuum is created at the inlet to insure material flows into the tube.

1. Frame
2. Hopper
3. Hydrostatic Transmission
4. Speed Reducer
5. Sheaves
6. Vacuum Pump Sheave
7. Reducer Drive Belts
8. Vacuum Pump Drive Belt
9. Vacuum Drive Sheave
10. Coupling
11. Vacuum Pump
12. Belt Guard
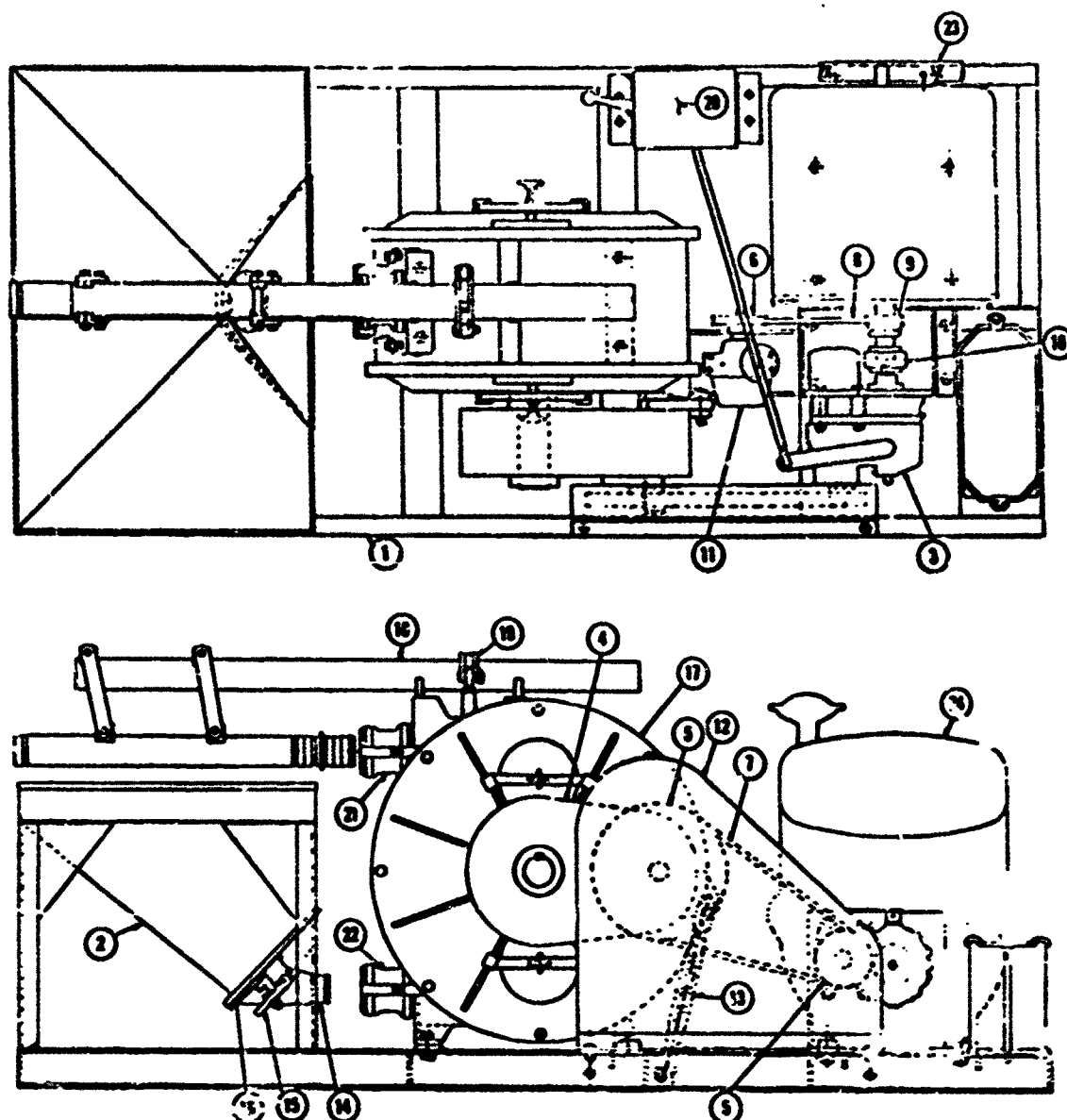
13. Reducer Turnbuckle Belt Adjustment
14. Hopper Outlet
15. Toggle Clamps
16. Gasket
17. Pump Housing
18. Tube Support Arm
19. Support Arm Clamp
20. Controls and Hydraulic Tank
21. Upper Boot
22. Lower Boot
23. Hyd. Heat Exchanger
24. Engine

Figure 3.   Schematic Diagram of Challenge Model Squeeze-Crete 120
            Concrete Pump Selected for Pumping Gelled Nitromethane

This pump was tested at the LLL explosives testing site and performed extremely well. At full speed, outlet pressures did not exceed 100 psi, and at half speed, a pumping rate of 195 pounds per minute was maintained. As a result of the testing, this pumping system was chosen for tests conducted during the summer of 1973 at Fort Polk, Louisiana. These tests, consisting of a series of four shots, required a total of over 45 tons of explosives.

Extensive modifications were made in the commercial system based on the considerations addressed in picking the first mixing and pumping system. All motors were replaced with air-driven motors for safety. As large amounts of explosive were to be mixed and pumped, a working platform was built. The pumping equipment was mounted under the platform and the top was used for transfer of the nitromethane from 55-gallon drums to the mixing barrel. This barrel was designed to handle two 55-gallon drums of nitromethane at one time. Mixing was performed with the Lightning air mixer used during the Fort Peck test.

7. <u>Summary</u>. Nuclear simulation tests using chemical explosives required an explosive with reliable and reproducible detonation properties so that an equation-of-state could be determined for it. The explosive also had to be able to hold sand particles in a uniform suspension. Gelled nitromethane was chosen as the explosive and extensive safety and detonation performance tests were performed. Finally, two mixing and pumping systems were developed: one for a 1-ton shot at Fort Peck, Montana, in the fall of 1972; and the second for a series of large-scale detonations at Fort Polk, Louisiana, during the summer of 1973. In both cases, the nitromethane and mixing and pumping units performed quite well.

References

1. Egly, Richard S., "Recent Developments in Nitromethane-Based Liquid Explosives," Proceedings of the Symposium on Military Applications of Commercial Explosives, The Technical Cooperation Program Working Panel 0-2 (Explosives), 28-29 August 1972.

2. O'Connor, John M., Explosive Selection and Fallout Simulation Experiments: Nuclear Cratering Device Simulation (Project DIAMOND ORE), U.S. Army Engineer Explosive Excavation Research Laboratory, Livermore, California, TR-E-73-102 (to be published).

3. Finger, Milton, et al., Explosive Investigations in Support of Project DIAMOND ORE, Lawrence Livermore Laboratory, Livermore, California, UCID ____ (to be published).

4. Helm, Frank, Lawrence Livermore Laboratory, personal communication (1972-73).

5. Guarienti, Richard, Lawrence Livermore Laboratory, personal communication (1973).

6. Finger, Milton, et al., Metal Acceleration by Composite Explosives, Lawrence Livermore Laboratory, Livermore, California, Proceedings of the 5th Symposium on Detonation, 1969.

7. Boat, Ronald, Lawrence Livermore Laboratory, personal communication (1972).

BIOLOGICAL DEGRADATION OF TRINITROTOLUENE

William D. Won and Robert J. Heckly

Naval Biomedical Research Laboratory

School of Public Health

University of California, Berkeley, California

As with many established practices in waste disposal, the disposal of dilute aqueous trinitrotoluene (TNT) solutions has come under close scrutiny during the past few years. Although TNT is not particularly toxic, our current objective is to remove all traces of TNT, and intermediate degradation products, from waste waters before they are released into the environment. This removal can be done chemically, or by adsorption on charcoal, but these methods are relatively uneconomical. In contrast, since bacteria can grow in dilute nutrient solutions, a biological system is potentially feasible. A number of investigators have been working on this problem of developing a biological process using various approaches. The approach we have employed was to select a number of isolates by a culture enrichment technique from soil that had been contaminated with TNT. To this end, 15 soil and water samples were taken at the Naval Ammunition Depot, McAlester, Oklahoma, at various points along the ditch or stream carrying the TNT waste water. The bacteria in the samples collected near the source of this waste water would have been exposed to practically a saturated solution of TNT, whereas, at the most distant point, the TNT concentration would be virtually "0". Three yellow-pigment-producing organisms were isolated from mud and water samples using the culture enrichment technique, where about 35×10^{-5} M of TNT was included in a basal salt solution consisting of 86×10^{-3} M NaCl, 4×10^{-3} M $MgSO_4$ and 0.02 M sodium-potassium phosphate (pH 7.0). The relative rate of TNT degradation by the various isolates was first determined by measuring the relative rate of oxygen uptake, using a Warburg respirometer according to the standard procedures (1). Results typical of active cultures are shown in Fig. 1. On the basis of the Warburg tests, four strains were selected for more detailed study. Three of these were _Pseudomonas_ and a fourth appears to be a _Klebsiella_. It may be significant that the latter was isolated from a pond into which a sulfide-containing waste solution was discharged.

The relative rate of TNT degradation under various conditions was measured by incubating 100 ml volumes, in 250 ml flasks, at 32 C on a rotary shaker operated at 200 strokes per minute. This provides a highly aerobic environment. All media contained 100 µg TNT/ml in the basal salt medium described above, to which various additives were added. Residual TNT was extracted into benzene which was then assayed using a Hewlett-Packard gas chromatograph fitted with a flame ionization detector. The internal standard was m-dinitrobenzene. The number of viable cells was

estimated by plating 0.1 ml of appropriate dilutions on nutrient agar containing 0.5% glucose. The results of a typical experiment are shown in Figure 2. Of the substances tested, glucose best supported growth of the Pseudomonas strains. In similar experiments, as shown in Figure 3, the optimum pH appears to be near 6.4, and that none of the organisms survived well at pH values above 8 or below 5. As is shown in Figure 4, TNT disappeared from the media in the presence of glucose but there was a significant increase in at least 2 intermediates, 6-dinitro-4-aminotoluene and 2-amino-4,6-dinitrotoluene. The decrease in the number of viable cells in this experiment can be attributed to acid production in the metabolism of glucose in unbuffered media. By using large inoculae, in the order of 10^8 viable cells/ml, the TNT was degraded much more rapidly and less than 6 hours was required to reduce the TNT concentration to 0.1 μg/ml. Figure 5 shows one of the small devices used for continuous culture studies. In this assembly the pH electrodes are located in the effluent stream so that they can be cleaned without disturbing the culture. Airation was at a high rate through a medium porosity scintered glass filter. TNT was added with one peristaltic pump and other nutrients, such as sugar, cornsteep water, or yeast extract, were added via separate lines. The results of one of the earlier experiments is shown in Figure 6. In this experiment, both TNT and 0.5% yeast extract was added at 1/10 volume per hour. The pH was not controlled and therefore, the concentration of viable cells and the residual TNT fluctuated considerably. Addition of sugar to the system produced acid, whereas protein, such as the yeast extract, caused the solution to become alkaline. Salts of organic acids such as sodium acetate produced an alkaline reaction. Because cornsteep water contains 47% protein, and 26% lactic acid, this material may provide a nearly ideal balance for maintaining proper pH.

Work is currently underway to determine the optimum conditions for reducing the concentration of certain intermediates as well as TNT in the effluent solution of these continuous culture systems. The most refractory of these intermediates appear to be the 2-amino-4,6-dinitrotoluene and 2,6-dinitro-4-aminotoluene. However, results of recent experiments indicate that it will be possible to eliminate even these intermediates from the effluent but the precise conditions have not yet been established.
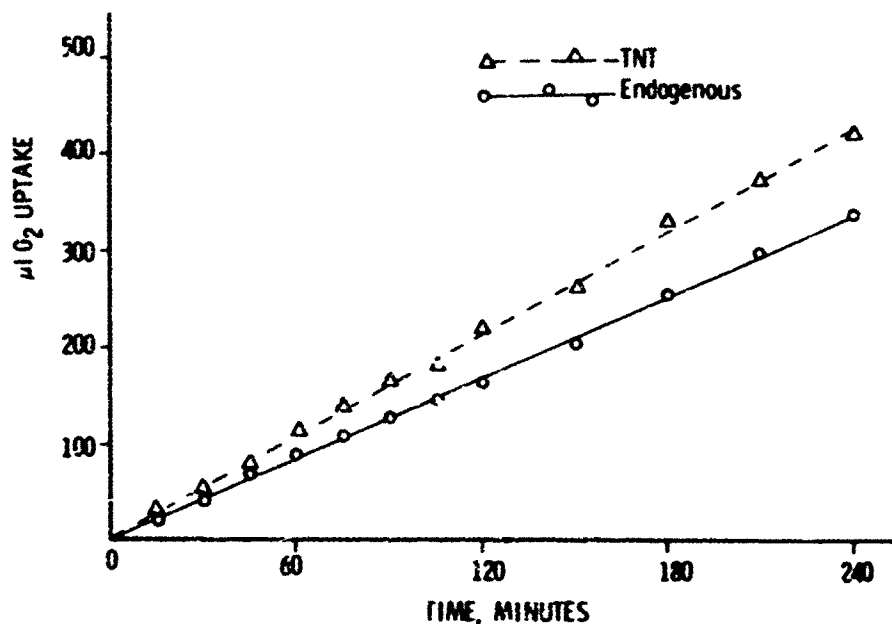
Fig. 1.   The oxidation of TNT by isolate Y at 35 C, pH 6.0
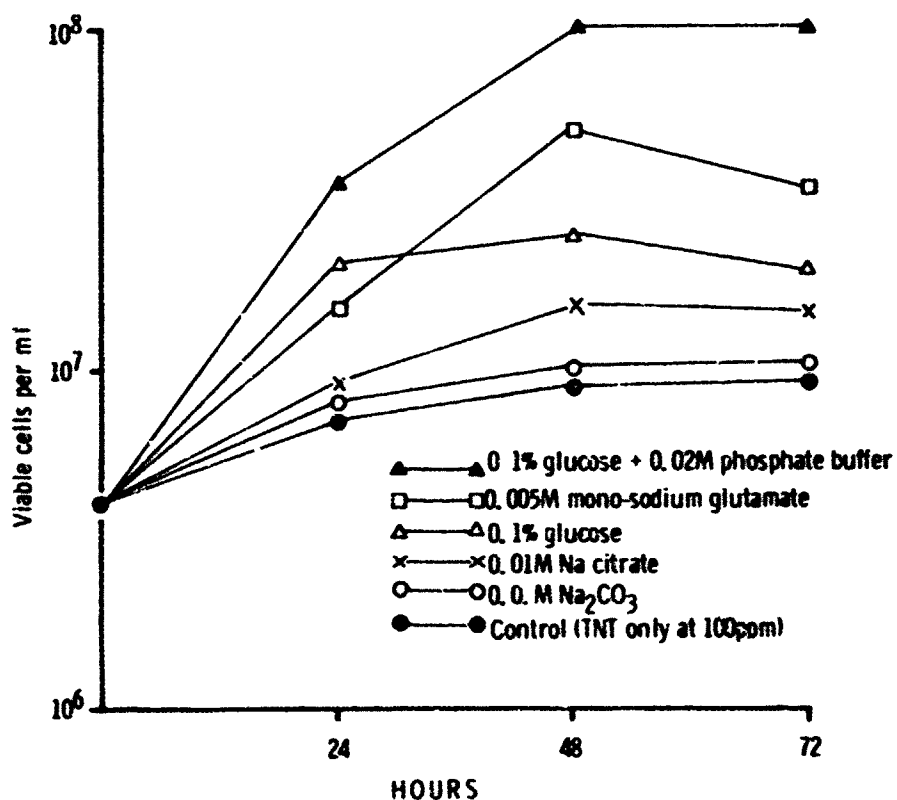
Fig. 2.   Growth of isolate "I" in fortified TNT media.
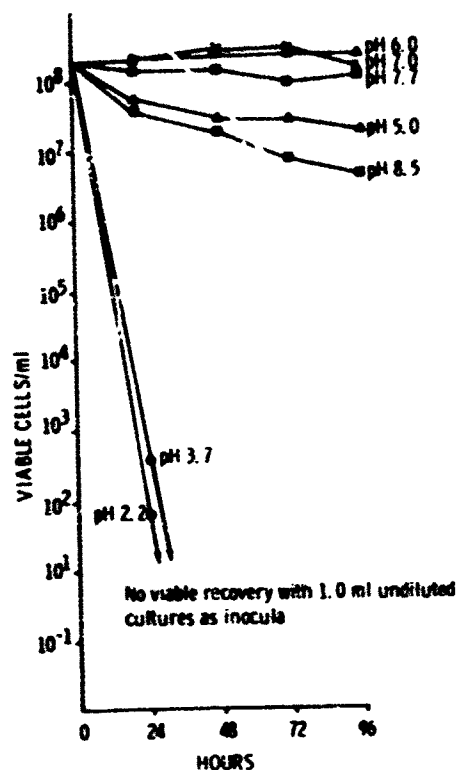
Fig. 3. Effect of pH on survival of isolate "Y" at 32 C in 100 ppm TNT solutions.
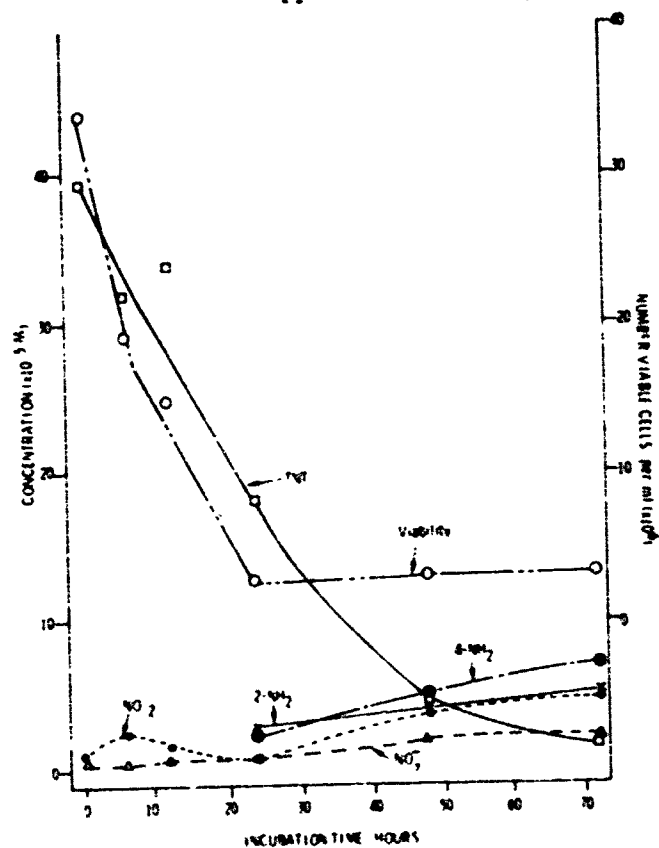
Fig. 4. Effect of isolate "Y" on TNT solution containing 0.005 M glucose. 4-NH$_2$ = 2,6-dinitro-4-aminotoluene. 2-NH$_2$ = 2-amino-4,6-dinitrotoluene.
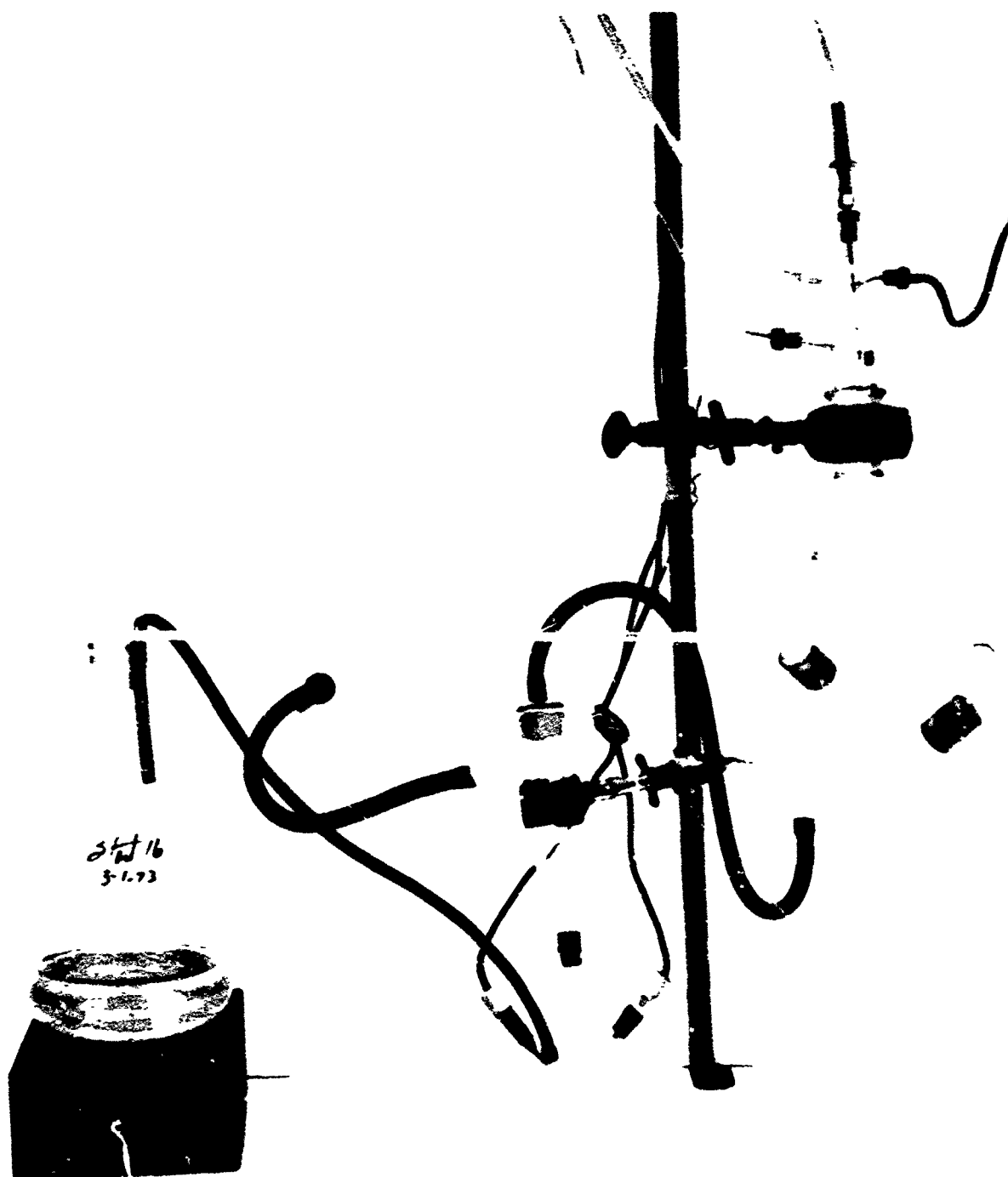
Fig. 5.   Photograph of a small apparatus used to study TNT degradation
in continuous culture.
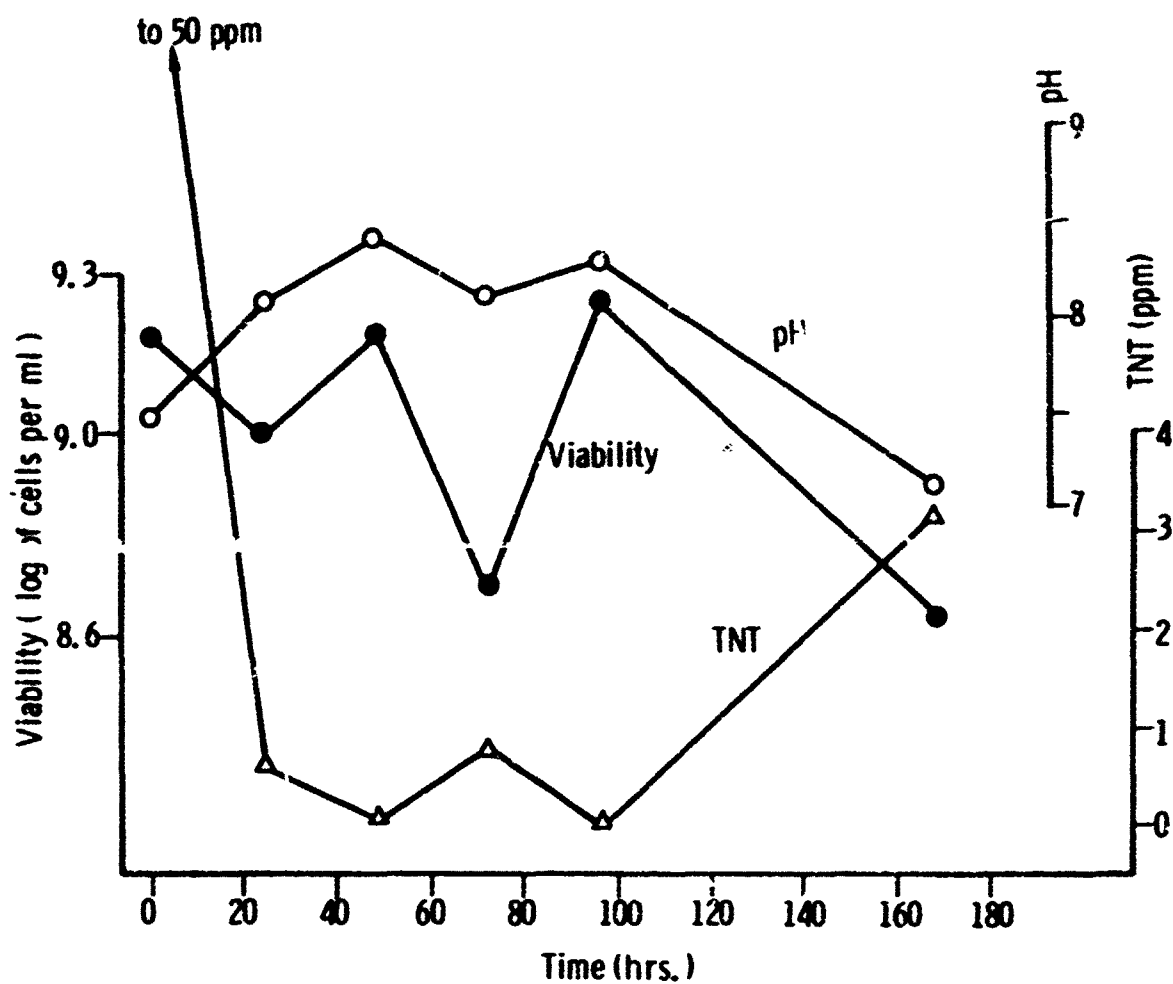
Fig. 6.   Results of a continuous culture of isolate "I". Solutions 0.5% yeast extract and 100 ppm TNT were each added at 0.1 volume per hr.

BIODEGRADABILITY OF EXPLOSIVES

F. D. Lonadier, W. H. Hedley and L. D. Haws

Monsanto Research Corporation
Mound Laboratory*
Miamisburg, Ohio

The feasibility of using biodegradation for disposal of explosives such as PETN is being explored. In an initial feasibility study, an ecologically acceptable method for disposal of explosives by biological means will be sought. This program is expected to provide a basis for either initiating process development studies to evaluate a promising method in greater detail, or for discarding this approach because it is not feasible.

This program consists of three tasks:

1. Literature Survey and Analysis
2. Development of a Biological Method for Degradation of PETN
3. Small-Scale Batch Treatability Studies and Economic Analysis.

LITERATURE SURVEY AND ANALYSIS

Three approaches to the disposal of PETN were considered as part of the literature search:

1. Biological Degradation of PETN
2. Enzymatic Degradation of PETN
3. Combinations of Biological and Chemical Degradation of PETN.

Compounds used in early investigations into bacterial methods for destroying nitro compounds were nitrobenzene, picric acid, trinitro-resorcinol, nitrophenols, dinitrophenols, chloramphenicol, and dinitro-o-cresol, all of which are aromatic nitro compounds.

Bacterial degradation has also been used in treatment of waste-waters with a high content of aromatic nitro compounds obtained from organic synthesis plants.

These processes use activated sludges with acclimatized cultures. It was found that the nitro derivatives were very difficult to destroy biologically, even though they were first reduced chemically to amines. It has been suggested that the bacteria required other sources of energy in the medium.

Other bacteria or organisms that have been used in the decomposition of aromatic nitro compounds include Actinomyces, Pseudomones, Coryne bacterium, McAlester bacteria, and sediment bacteria as well as yeasts and cellular preparations.

The nitro groups can be reduced chemically and biologically, but the pentaerythrityl derivatives resulting are resistant to further degradation in the systems that can be used. The neocarbon skeleton of PETN or pentaerythritol is extremely stable. It is resistant to biological degradation and to attack by all but the most active chemicals.

$$\begin{bmatrix} & C & \\ & | & \\ C\text{-}C\text{-}C \\ & | & \\ & C & \end{bmatrix}$$

The pentaerythrityl skeleton can be destroyed by oxidation with chromic acid to form CO_2 and formic acid, alkaline permanganate to form CO_2 and oxalic aicd, oxygen with barium hydroxide and palladium catalyst to form CO_2 and formic acid, and hydrogen perioxide with ferrous sulfate and sulfuric acid to form CO_2 and formic acid. It can also be destroyed by hydrogenation over a copper-chromium-barium oxide catalyst (99% conversion to methanol and isobutanol). One of these methods may have to be used in conjunction with the biological or chemical denitration methods to achieve complete destruction of the pentaerythrityl nucleus.

Partial biological degradation of PETN has been accomplished by mammalian enzymes, i.e., the nitro reductases. The enzymes used were primarily those from rat (mouse) livers which partially

denitrate PETN in the presence of reduced glutathione. It has
been found that blood plasma and erythrocytes have a strong
affinity for PETN and apparently represent the first step in
PETN detoxification by the intact animal body.

Enzymic reduction of nitro compounds has also been observed with
extracts of the cells of Bacillus Pumilus and of hemolytic strep-
tococci, both of which are bacteria. PETN was denitrated to
pentaerythritol and lower pentaerythrityl nitrates by the mammalian
and bacterial enzymes.

Some promising leads were uncovered during the literature analysis
phase of Task 1. The most promising was from a paper which describes
the complete biodegradation of pentaerythritol (PE) using organisms
(pond benthic bacteria) of the flavobacterium, F.oxydans, which
appears to be a new species of flavobacterium.

Large colonies from the culture medium grew well in a medium con-
taining pentaerythritol as the sole carbon source. They did not
accumulate nonvolatile metabolites, which indicates total bio-
degradation of pentaerythritol. However, it was observed that
small peripheral colonies began to form on continuous plating of
the large colonies in fresh pentaerythritol medium. These small
colonies were found to be mutants which had lost their ability to
grow significantly or survive in the pentaerythritol medium. These
mutants grew well on other carbon sources, and when pentaerythritol
was incorporated with the other assimilable carbon sources
(co-oxidation technique), high yields of a metabolite, tris(hydroxy-
methyl) acetic acid, accumulated. A process for producing
tris(hydroxymethyl) acetic acid utilizing these mutants (F.oxydans
ATCC 21245) has been patented.

Up until this time, pentaerythritol was considered as being
resistant to biodegradation. As late as 1968, Traxler found that
alkanes (octanes) with branches of the 2 position only were oxidized
by Pseudomonas strains using an assimilable carbon source (co-oxi-
dation). However, other branched isomers, among which was the
pentaerythritol neocarbon skeleton, were not dissimilated.
Although they can be biologically oxidized, the kinetic oxidation
rates of branched alkanes are very low as compared to the equivalent
normal alkane. This can be attributed primarily to steric effects.

The co-oxidation technique (inclusion of other assimilable carbon sources) provides another promising lead. It was reported that nitro derivatives alone obtained from organic synthesis plants were very difficult to destroy biologically even though they were first reduced to amines. However, the authors obtained a removal efficiency of 90% biochemical oxygen demand (BOD) and 80% chemical oxygen demand (COD) removal by inclusion of other assimilable organic carbon sources in activated sludge applications. The average oxidizability was 20% prior to use of the co-oxidation technique. The key supporting statement for the co-oxidation technique in the article is that "activated sludge developed on effluents with complex composition is more stable (in the purification efficiency ---) than other developed --- with a simple composition."

The third lead consists of the use of acclimatized cultures produced from activated sludge. There are reports wherein the aqueous effluent is first aerated after an inoculation with bacteria and then inoculated with activated sludge, or the effluent is aerated and the sludge so formed is incubated with micro-organisms which were cultivated in aerators. The acclimatized bacteria were then able to dissimilate the undesirable effluent contents. Azotobacter Agilis species of Pseudomonas and 15 species of Bacillus were acclumatized in this manner. After acclimatization, the organisms could be isolated and cultured, and were able to dissimilate the undesirable products without prolonged adaptation.

DEVELOPMENT OF A BIOLOGICAL METHOD FOR DEGRADATION OF PETN

Amole Cultûre Initial experimentation began using cultures (nutritionally-like and morphologically similar to Pseudomonas, but not Pseudomonas) in test tube experiments." A culture (nutritionally-like and morphologically similar to Pseudomonas, but not Pseudomonas) was obtained from Mr. Henry Hess of Amole, Inc., Dayton, Ohio. The following quantities of chemicals were added for a liter of media:

Sodium Chloride	3.0 g
Dextrose	10.0 g
PETN	0.1 g
Sodium Nitrate	4.0 g
Dipotassium hydrogen phosphate	2.0 g
Potassium dihydrogen phosphate	1.4 g

Two liters of solution were prepared with tap water. Casein (0.1 g) was added as a protein supplement to one of the nutrient solutions. Ten milliliters of culture media, both types, was added to a series of screw top test tubes. To each was added 1 ml of culture.

Anaerobic Digesters I Two anaerobic digesters were constructed using a 3-liter flask with a CNP of 87:7:1. The flasks were blanketed with nitrogen and sealed. Attempts were made to acclimatize a benthic culture from the Mound Laboratory sump drain and stabilization pond in reactors at 35°C. After two weeks, samples were taken and analyses were made to ascertain the viability of the sludge. Microscopic investigation revealed no sign of biological activity.

Anaerobic Digestion II Another anaerobic reactor was designed and seeded with a sludge seed of the following composition:

> 1000 ml sump and pond sediments
> 1000 ml activated sludge from Miamisburg Plant
> 2000 ml total

The anaerobic digester was being fed with acetone-PETN solution and maintained at 40°C.

Since the anaerobic reactor did not indicate any sign of biological activity over a period of nearly two months, its operation was discontinued.

Activated Sludge Unit I The benthic culture from Mound Laboratory sump drain and stabilization pond was acclimatized by using a straight PETN feed in an activated sludge unit. Acclimation was by fill and draw techniques in a 3500-ml aeration basin. The initial filling was with an aqueous benthic sample obtained from Mound Laboratory which was diluted to 3250 ml with tap water. Then 250 ml of solution containing 58 ppm of total organic carbon (TOC) was added to bring the volume to 3500 ml. Results indicated that pH decreased from 8.0 to 5.4 over 14 days.

Activated Sludge Unit II The continuous activated sludge unit described above was modified by being mixed with additional domestic waste sludge from the Miamisburg Plant, sump sediments

and pond mud from Mound Laboratory, and the Amole culture in the following ratio:

```
    5C ml Amole culture
    50 ml PETN sludge
    50 ml sump sediments from Mound
    50 ml pond mud from Mound
   700 ml activated sludge from Miamisburg Plant
  1000 ml total
```

This ratio of cultures was used to seed five activated sludge units. These units consists of 5 one-liter graduated cylinders that are stirred and aerated. The units are being fed daily with acetone, lactose, phosphorus, and nitrogen feed in the ratio C:N:P = 100:5:1.

During the first five days of operation the acetone feed was maintained at 1 ml/liter in the first reactor, and was increased to 2 ml/liter, 3 ml/liter, 4 ml/liter, and 5 ml/liter in the second, third, fourth, and fifth reactor, respectively. In addition to acetone, lactose feed is maintained in each reactor at the constant rate 200 ppm and PETN in the range of 100-300 ppm. The objective of this experiment is to acclimate the bacteria culture in the reactors to higher concentrations of acetone that will eventually lead to higher solubility of PETN. To increase the solubility of PETN in the reactors is considered very important for proper and sufficient PETN feed for the bacteria.

The reactors are regularly analyzed for PETN concentration and TOC in the filtrate. The PETN analysis of the five reactors produced the results shown in Table 1. Samples for PETN analysis were obtained by drawing approximately 200 ml of each of the reactor contents into a beaker, and while the contents of the beaker were continuously stirred to insure homogeneity, a 10-ml sample was pipetted out, evaporated, dissolved in a known volume of ethyl acetate solvent, and analyzed for PETN. The first set of samples was collected on June 21 immediately after the reactors were fed with PETN. Two days later, a second set was obtained and analyzed. The same sample collection procedure was used in both cases.

As can be seen from the data presented in Table 1, the first results of PETN analysis are quite inconsistent. Because of these erratic

PETN ANALYSIS IN BATCH ACTIVATED SLUDGE REACTORS

Date	PETN (ppm)				
	Reactor 1	Reactor 2	Reactor 3	Reactor 4	Reactor 5
6/21/73	190	16	80	150	96
6/23/73	140	44	26	150	100

results, we collected a large number of samples from different points of a reactor before and after feeding. The results obtained revealed that stratification of PETN in the reactors exists even though the reactors are continuously stirred and aerated. Also, even vigorous stirring of the sampling beaker contents did not prevent the PETN from settling.

To study the effect of the presence of bacterial sludge on the PETN analysis, we have also designed a reactor which was fed with PETN and contained no sludge. The results of these experiments are summarized in Table 2.

Samples for PETN analysis were removed immediately after feeding the reactors with PETN-acetone solution, and each day in the following five days. The reactors were continuously stirred and aerated at the rate of approximately $2\frac{1}{2}$ ft^3/hr of premoistened air per liter of reactor content. Samples for PETN analysis were removed by a pipette technique while the reactors were in full operation. Additionally, some samples were removed through the sampling spout by means of a 10-ml graduated cylinder (see Table 3). The pH of each reactor was measured daily and adjusted to about 7.5, if necessary. The results of this experiment are summarized in Table 3.

To support the indication that PETN is biodegraded and not absorbed on the walls of the reactors, we performed the following experiment. We emptied the contents of reactors 1, 3, and 5 and rinsed each reactor with distilled water. Then, we rinsed the walls of each of those three reactors with acetone. Two-hundred ml of acetone were used for rinsing. An aliquot of the 200-ml rinses was taken

Table 2

SUMMARY OF STRATIFICATION EXPERIMENTS

Sample	Description	Concentration (ppm)
	I Before feeding	
75-3A	900-ml level	160
75-3B	500-ml level	160
75-3C	200-ml level	190
75-3D	Sampling spout @300-ml level after two flushings	28
	II-A Fed with 1 ml acetone saturated with PETN. Samples taken without mixing, aerated.	
75-3E	900-ml level	230
75-3F	500-ml level	240
75-3G	200-ml level	310
	II-B Samples taken with mixing, aerated	
75-3H	900-ml level	260
75-3I	500-ml level	330
75-3J	200-ml level	290
75-3K	Sampling spout @300-ml level after two flushings	320
	III Reactor with no bacterial sludge, samples taken with mixing and aerated.	
75-BA	900-ml level	120
75-BB	500-ml level	110
75-BC	200-ml level	120
75-BD	Sampling spout @300-ml level after two flushings	94

Table 3

PETN ANALYSIS SUMMARY FROM THE ACTIVATED SLUDGE EXPERIMENT

Date	PETN Concentration (average) (ppm)				
	Reactor 1	Reactor 2	Reactor 3	Reactor 4	Reactor 5
7/11/73	115	105	190	88	87
7/12/73	100	120	170	120	66
7/13/73	32	79	98	46	26
7/16/73	50	11	108	37	12
7/17/73	20	34	120	22	-

and anclyzed for PETN. The same procedure was followed on a so-called blank reactor which was set up to study the effect of the presence of bacterial sludge on the PETN analysis. The reactor originally contained 110 to 120 ppm of PETN. The results and the blank reactor are summarizeo in Table 4.

Table 4

ACETONE RINSING PETN RECOVERIES

Reactor	PETN Recovered (mg)		Average
1	8	8	8
3	6.4	3.2	4.8
5	1.6	2.4	2.0
Blank	80	80	80

The fact that almost the whole amount of PETN introduced into the blank reactor was recovered indicates that PETN can absorb on the reactor walls, but it can be removed quantitatively by dissolving in acetone. The rinses of the reactors 1, 3, and 5 showed no significant amount of PETN.

Flavobacterium I The seventh activated sludge batch reactor was set up and seeded with the sludge obtained from the continuous activated sludge reactor and Flavobacterium F.Oxidans species. The reactor is presently acclimating to PETN-acetone feed. No additional nitrogen food is supplied to this reactor.

BIBLIOGRAPHY

1. D. Erikson, J. Bacteriol. 41, 271 (1941).

2. F. W. Moore, J. Gen. Microbiol. 3, 143 (1949).

3. T. I. Rogovskaya, Mikrobiologiya (Moscow) 20, 265 (1951).

4. J. R. Simpson and W. C. Evans, Brochem. J. 55, XXIV (1953).

5. H. J. Petersen in H. J. Jensen and K. Gundersen, Nature 175, 341 (1955).

6. V. Popescu and M. Mihail, Stud. Prot. Epurarea Apeior 1969, 12, 203-23; Chem. Abstr. 74 130115e (1971).

7. R. Radovic, Kem. Ind. (Zagreb) 16, 192-6 (1967); Chem. Abstr. 67, 76141a (1967).

8. B. W. Dickerson, Ontario Indus. Waste Conf., 11th Proc., June 1964, pp. 1-22.

9. J. Wichmann, F. I. Honea, E. E. Leake, and T. K. Mehrhoff, "Disposal of Waste or Excess High Explosives," Progress Report October-December 1972, MHSMP 73-1.

10. C. Neubert and E. Reinfurth, Biochem. Z. 138, 561-8 (1923).

11. W. Lipschitz and J. Osterroth, Arch. ges. Physiol. 205, 364-5 (1924).

12. P. Needleman and F. E. Hunter, Jr., Mol. Pharmacol. 1, 77-86 (1965).

13. F. J. DiCarlo, C. B. Coutinho, N. J. Sklow, L. J. Haynes, and M. C. Crew, Proc. Soc. Exptl. Biol. Med. 120, 705-9 (1965).

14. I. Yamashina, Bull. Chem. Soc. Japan 27, 85-9 (1954).

15. Encyclopedia of Chemical Technology, Vol. 6, R. E. Kirk and D. F. Othmer, Ed., Interscience Encyclopedia Inc., New York, 1951, p. 32.

16. E. Berlow, R. H. Barth, and J. E. Snow, "The Pentaerythritols," American Chemical Society Monograph No. 136, Reinhold Publishing Corp., New York, 1958, pp. 47-48.

POLLUTION ABATEMENT/CONTROL OF PARTICULATE
AND GASEOUS EMISSIONS FROM THE EXHAUST OF A
DEMILITARIZATION FURNACE FOR AMMUNITION

Prepared by

J. R. Roach
Naval Ordnance Systems Command
Naval Ammunition Production Engineering Center
Crane, Indiana

THIS PRESENTATION WILL DESCRIBE A PROJECT RECENTLY COMPLETED BY
THE NAVAL ORDNANCE SYSTEMS COMMAND/NAVAL AMMUNITION PRODUCTION
ENGINEERING CENTER AT NAD CRANE, INDIANA. THE PROJECT FORMED
THE BASIS FOR A PROJECT COST ESTIMATE FOR A MILITARY CONSTRUCTION
PROJECT FOR THAT ACTIVITY. THIS PROJECT WAS SO SCOPED THAT DATA
RESULTING FROM IT COULD PROVIDE A BASIS FOR STANDARDIZATION OF
POLLUTION ABATEMENT/CONTROL EQUIPMENT FOR DEMILITARIZATION OR
DEACTIVATION FURNACES.

THE HIGHLIGHT OF THE PROJECT WAS THE STACK SAMPLING OF BOTH GASEOUS
AND PARTICULATE EMISSIONS FROM THE FURNACE UNDER ACTUAL OPERATING
CONDITIONS.

THIS TEST WAS CONDUCTED AND COMPLETED IN DECEMBER OF 1972 AND
FORMALLY APPROVED FOR IMPLEMENTATION ON 3 APRIL 1973.

IN THE ARENA OF DEMILITARIZATION/DISPOSAL OF AMMUNITION THERE ARE
4 BASIC METHODS AVAILABLE. AS CAN BE SEEN FROM THE FIRST SLIDE
THE 4 METHODS ARE:

Preceding page blank

1. Detonation
2. Open Burning
3. Washout

(3)   4. Furnace

(4)   This presentation will concern the furnace method for demil/
      disposal of ammunition. Specifically, the 4 barrel rotary contin-
(5)   uous type vice the batch type of incinerator, as shown in the next
(6)   six slides, was the subject of this project.

      There are approximately 22 of these furnaces located at various
(7)   Army and Navy activities at the present time. There are 5 at Navy
      activities and 17 at Army activities.

      At the present time none of these furnaces have any pollution
      control/abatement equipment installed and operating on a production
      basis. The rotary demil furnaces have the capability to demil the
      following types of ammunition as shown in the following slides:

(8) (9)   2 SLIDES   1. Small Arms Ammunition
(10) (11)   2 SLIDES   2. 20mm Ammunition
(12) (13) (14) 2 SLIDES   3. Projectile Fuzes
(15) (16)   2 SLIDES   4. Cartridge Actuated Device
(17) (18)   2 SLIDES   5. Pyro Illuminating Signal

(19)   The next slide(s) shows the various materials which make up small
(20)   arms ammunition, 20mm HEI Mk 106, Mod 0 in particular as can be
(21)

SEEN. IT CAN BE ASSUMED THAT WHEN MATERIAL SUCH AS THIS UNDER GOES COMBUSTION OR THERMAL DEGRADATION, MANY TOXIC MATERIALS OR PRODUCTS OF COMBUSTION WILL RESULT. IT CAN FURTHER BE ASSUMED THAT SECOND-ARY REACTIONS COULD OCCUR THROUGH CATALYTIC ACTION WHICH COULD ADD TO THE COMPLEXITY OF THE FURNACE EXHAUST GAS.

(22) THE FOLLOWING SLIDE SHOWS THE MAJOR TYPES OF ENERGETIC MATERIALS CONTAINED IN MOST TYPES OF AMMUNITION BURNED WHICH IS OF THE GREATEST CONCERN AT THE PRESENT TIME.

THIS LEADS UP TO THE CRUX OF THIS TOTAL EFFORT. THE MAIN OBJECTIVE WAS TO CONCLUSIVELY DETERMINE WHAT WAS COMING OUT OF THE EXHAUST GAS STACK OF THE 4 BARREL ROTARY DEMIL FURNACE DURING ACTUAL OPERATION IN THE DEACTIVATION OF VARIOUS TYPES OF AMMUNITION.

(23) THE FOLLOWING SLIDES SHOW WHAT PRODUCTS OF COMBUSTION WERE EXPECTED TO BE PRESENT IN THE EXHAUST GASES. THESE PRODUCTS OF COMBUSTION, DEPENDING ON THEIR PRESENCE AND/OR CONCENTRATION, COULD BE POTENTIAL POLLUTANTS. THESE POTENTIAL POLLUTANTS WERE CLASSIFIED AS:

1. PARTICULATE
2. GASEOUS

IT SHOULD BE NOTED THAT NOISE WAS ALSO CONSIDERED AND THE DETONA-TION NOISE LEVEL WAS ALSO SAMPLED FOR EACH OF THE FIVE AMMUNITION

TYPES UNDERGOING THERMAL DEACTIVATION IN THIS TEST.

IT SHOULD ALSO BE NOTED THAT ANY FURTHER BREAKDOWN OR IDENTIFICA-
TION OF EMISSIONS INTO VAPORS, FUMES, DUSTS, AEROSOLS, FOGS,
MISTS, AND SMOKES WAS NOT MADE IN THIS SPECIFIC PROJECT.

KNOWING THE COMPOSITION OF THE FURNACE EXHAUST WITH REGARD TO BOTH
A QUALITATIVE AND A QUANTATIVE ANALYSIS IS ONLY ONE HALF THE
PROBLEM. THE OTHER ONE HALF OF THE PROBLEM BEING THE COMPARISON
OF THE COLLECTED DATA WITH THE ESTABLISHED AND REGULATORY
STANDARDS FOR LIMITING AIR POLLUTION, IN ORDER TO DETERMINE COMPLI-
ANCE OR NON-COMPLIANCE. AT THE PRESENT TIME THERE ARE THREE
SOURCES FOR STANDARDS:

1. FEDERAL
2. STATE
3. LOCAL

IT WAS ASSUMED THAT THE DEMIL FURNACE SHOULD BE CLASSIFIED AS A
STATIONARY SOURCE.

(24) AT THE TIME OF THIS TEST THE EPA SOURCE STANDARDS SHOWN IN THE NEXT
SLIDE WERE IN EFFECT. THE STATE OF INDIANA HAD THE EMISSION
(25) STANDARDS AS SHOWN ON THE NEXT SLIDE.
(26)

812

As a result in NAVORD's (Naval Ordnance Systems Command) partici-
pation in the Joint Service effort in the problem of demil/disposal
ashore of ammunition, NAVORD has decided to use the so called APSA
(Ammunition Procurement and Supply Agency)/Army developed emission
levels or guidelines as design criteria for pollution abatement
and control. Considerable effort and expense has been expended by
the Army in this effort and the Navy considers it to be the best
effort to date concerning our unique "industry." Utilization of
these APSA guidelines as shown in this slide also lends to
standardization within DOD. These APSA guidelines were established
with state and local regulations in mind due to having Army plants
in many states and regions of the United States as does the Navy.
These standards are considered to be good for the future as well
as for today; In other words, the best thing available for use at
the time.

Naturally, since we are dealing with EPA we decided to use only
the EPA approved methods for stack sampling. As this was the
first test of its kind within the Navy for the five ammunition
types under production conditions, it was determined that the
scope of the test should cover a broad area relating to the
ultimate objective of determining pollution abatement/control
equipment. For this test the EPA methods 1-9 were utilized as
can be seen on the next slide.

(27)

(28) THE CONTRACTOR UTILIZED TWO EPA DESIGN/TYPE SAMPLING TRAINS AS DEPICTED IN THE NEXT SLIDE FOR ALL WEIGHT AND CHEMICAL ANALYSIS OF EMISSIONS.

THE EPA SAMPLING TRAIN CONSISTS OF THE FOLLOWING COMPONENTS:
A SAMPLING NOZZLE AND HEATED PROBE (1) THAT CONNECTS DIRECTLY TO A FILTER HOLDER WITH A PERFORATED STAINLESS STEEL FILTER SUPPORT (2). THE FILTER IS POSITIONED IN A HEATED SAMPLING BOX, WHICH IS MAINTAINED BETWEEN 240° AND 280°F. THE FILTER IS GLASS FIBER OF 0.3 MICRON POROSITY (99.975% EFF. ON 0.3 MICRON PARTICLES). NEXT IN LINE ARE FOUR GREENBERG-SMITH IMPINGERS (3) IN AN ICE BATH. ONLY THE SECOND IMPINGER HAS THE ORIGINAL TIP, THE OTHERS HAVE HAD THE TIPS REMOVED TO DECREASE THE PRESSURE DROP THROUGH THEM. THE FIRST AND SECOND IMPINGERS, DURING PARTICULATE SAMPLING, ARE FILLED WITH 100 MILLILITERS OF DISTILLED AND DEIONIZED WATER. THE THIRD IMPINGER ACTS AS A MOISTURE TRAP FOR THE FIRST TWO IMPINGERS. THE LAST IMPINGER CONTAINS 200 GRAMS OF PRECISELY WEIGHED SILICA GEL TO REMOVE ANY REMAINING MOISTURE.

THE UMBILICAL CORD (6) CONNECTS THE LAST GREENBERG-SMITH IMPINGER, THE S-TYPE PITOT TUBE (17) AND THE HEATING ELEMENTS (PROBE AND SAMPLING BOX) TO THE METER BOX WHICH CAN BE LOCATED IN A CONVENIENT PLACE WITHIN 100 FEET OF THE SAMPLING PORT.

THE UMBILICAL CORD CONSISTS OF THE FOLLOWING THREE PARTS:

1. A 1/2 inch vacuum hose connecting the sample box to the meter box, a thermometer (4) and check valve (5) are built into the quick disconnect connector at the sampling box.

2. Two 1/4 inch lines of tubing with quick disconnects on both ends of the tubing (connects S-pitot tube (17) to meter box manometer (15))

3. Six insulated conductors with Jones plug connectors on both ends (connects probe and sample box heater to meter box power supply).

The umbilical cord connects to the meter box, which contains a vacuum pump (11), regulating valves (8 and 9) instantaneous (14) and integrating (13) flow meters, pitot tube and instantaneous flowmanometers (15), vacuum gauge (7), and electrical controls.

A bypass valve (9) is in parallel with the vacuum pump (11) to give fine flow control and to permit recirculation of gases at low sample rate so that the pump motor is not overloaded. Downstream of the pump (11) and bypass valve (9) are a thermometer (4), dry gas meter (13), another thermometer (4), and a calibrated orifice (14) with an inclined/vertical manometer (15) in parallel. The calibrated orifice (14) and inclined/vertical manometer (15) read in inches of water are used to indicate the instantaneous volume sampling rate. The dry gas meter (13) gives an integrated gas

SAMPLE VOLUME. THE AVERAGE OF THE INLET AND OUTLET TEMPERATURES OF THE DRY GAS METER (13) GIVES THE TEMPERATURE AT WHICH THE VOLUME IS SAMPLED. THE METER PRESSURE IS THE ATMOSPHERIC PRESSURE PLUS THE ORIFICE PRESSURE DROP.

(29) THE SAMPLE RECOVERY TECHNIQUE IS SHOWN ON THE NEXT SLIDE. GAS ANALYSIS WAS MADE BY USING SAMPLES FROM TEFLON GAS BAGS AS INDICA-
(30) TED IN THE FOLLOWING SLIDE.

(31) THE PARTICLE SIZE SAMPLING TRAIN WAS THE SAME AS THE ABOVE SAMPLING TRAIN WITH THE EXCEPTION OF THE ADDITION OF AN ANDERSON SIZING HEAD AS SHOWN IN THE NEXT SLIDE.

THE ANDERSON SIZING HEAD (2) IS ADDED TO THE TRAIN BETWEEN THE SAMPLING NOZZLE (1) AND THIMBLE HOLDER (3).

THE ANDERSON SIZING HEAD CONTAINS NINE JET PLATES EACH HAVING A PATTERN OF PRECISION-DRILLED ORIFICES. THE NINE PLATES, SEPARATED BY 2.5 MILLIMETER STAINLESS STEEL SPACERS, DIVIDE THE SAMPLE INTO EIGHT FRACTIONS OR PARTICLE SIZE RANGES. THE JETS ON EACH PLATE ARE ARRANGED IN CONCENTRIC CIRCLES WHICH ARE OFFSET ON EACH SUCCEEDING PLATE. THE SIZE OF THE ORIFICES IS THE SAME ON A GIVEN PLATE, BUT IS SMALLER FOR EACH SUCCEEDING DOWNSTREAM PLATE. THEREFORE, AS THE SAMPLE IS DRAWN THROUGH THE SAMPLER AT A CONSTANT FLOW RATE, THE JETS OF AIR FLOWING THROUGH ANY PARTICULAR PLATE DIRECT THE PARTICULATES TOWARD THE COLLECTION AREA ON THE DOWN-STREAM PLATE DIRECTLY BELOW THE CIRCLES OF JETS ON THE PLATE

ABOVE. SINCE THE JET DIAMETERS DECREASE FROM PLATE TO PLATE, THE VELOCITIES INCREASE SUCH THAT WHENEVER THE VELOCITY IMPARTED TO A PARTICLE IS SUFFICIENTLY GREAT, ITS INERTIA WILL OVERCOME THE AERO- DYNAMIC DRAG OF THE TURNING AIRSTREAM AND THE PARTICLE WILL BE IMPACTED ON THE COLLECTION SURFACE. OTHERWISE, THE PARTICLE REMAINS IN THE AIRSTREAM AND PROCEEDS TO THE NEXT PLATE. SINCE THE PARTICLE DEPOSIT AREAS ARE DIRECTLY BELOW THE JETS, SEVEN OF THE PLATES ACT AS BOTH A JET STAGE AND A COLLECTION PLATE. THUS, NO. 0 PLATE IS ONLY A JET STAGE AND NO. 8 PLATE IS ONLY A COLLECTION PLATE.

THE CALIBRATIONS WERE REFERENCED TO UNIT DENSITY (1G/CC), SPHERICAL PARTICLES SO THAT THE AERODYNAMICALLY EQUIVALENT SIZED PARTICLES COLLECTED ON EACH STAGE ARE ALWAYS IDENTICAL FOR ANY GIVEN FLOW RATE. FOR THIS REASON, A STACK SAMPLE CONTAINING A MIXTURE OF SHAPES AND DENSITIES IS FRACTIONATED AND COLLECTED ACCORDING TO ITS AERODYNAMIC CHARACTERISTICS AND IS AERODYNAMICALLY EQUIVALENT IN SIZE TO THE UNIT DENSITY SPHERES COLLECTED ON EACH SPECIFIC STAGE DURING CALIBRATION. THE AERODYNAMIC SIZE OF A PARTICLE GIVES INFORMATION RELATING TO THE PHYSICAL SIZE, SHAPE, AND DENSITY OF THE PARTICLE AND INDICATES HOW THE PARTICLE WILL BEHAVE IN ANY ENVIRONMENT. IF THE AERODYNAMIC SIZE DISTRIBUTION OF THE PARTICU- LATES IN A STACK SAMPLE IS KNOWN, THEN THE FOLLOWING PERTINENT INFORMATION CAN BE DETERMINED:

1. PARTICLE BEHAVIOR AFTER LEAVING THE STACK.
2. APPROXIMATE AREA OF ENVIRONMENTAL DEPOSITION.
3. PROBABLE POINT OF RESPIRATORY DEPOSITION.
4. TYPE OF CONTROL EQUIPMENT NEEDED TO COLLECT THE PARTICLES.

THIS TYPE OF INFORMATION IS IMPOSSIBLE TO OBTAIN WITH ONLY PHYSICAL SIZING DATA WHICH IS NORMALLY OBTAINED BY MEANS OF MICROSCOPIC SIZING OR WET AND/OR DRY SCREENING.

AS CAN BE SEEN STACK SAMPLING IS VERY COMPLEX AND IS VERY EXPENSIVE. SITE PREPARATION IS VERY IMPORTANT.

PROCEDURE - IN GENERAL, THE SAMPLING TRAIN IS USED ONLY FOR COLLECTION OF PARTICULAR MATTER IN THE EXHAUST GASES BEING TESTED. GASES SUCH AS CO_2, SO_2, H_2S, AND NITROGEN OXIDES CONSIST OF MOLECULAR SIZE PARTICLES AND DO NOT CONDENSE IN THE EQUIPMENT. THUS, THEY PASS ON THROUGH AND ARE MERELY MEASURED AS A GAS FLOW.

THE SAMPLING TRAIN IS DESIGNED TO INTERCEPT AND COLLECT PARTICLES DOWN TO AT LEAST 0.3 MICRON IN SIZE PLUS MOLECULAR CONSTITUENTS THAT WILL CONDENSE AT NORMAL ATMOSPHERIC TEMPERATURES, 70 F. THUS, THE SAMPLING TRAIN CONSISTS OF SEVERAL COMPONENTS IN SERIES, EACH WITH A FUNCTION TO PERFORM IN THE OVERALL OPERATION. THESE FUNCTIONS ARE: (1) INTERCEPT THE STACK GASES IN THE FLUE; (2)

COLLECT THE PARTICULATE MATTER BY FILTERS, CYCLONES, ETC.; (3) CONDENSE AND COLLECT THE CONDENSIBLES; AND (4) MEASURE THE FLOW OF THE RESIDUAL DRY GAS.

IN COLLECTING PARTICULATE MATERIAL, THE ULTIMATE OBJECTIVE IS TO GET A MEASUREMENT OF THE STACK EMISSIONS TO THE ATMOSPHERE (POLLUTANT MASS RATE) IN UNITS PRESCRIBED BY THE APPLICABLE CODES (LB/HR, FOR EXAMPLE). THIS IS DONE ESSENTIALLY BY WEIGHING THE COLLECTED MATTER, MEASURING THE TOTAL SAMPLE GAS FLOW DURING THE TEST, AND DIVIDING TO GET GRAINS PER CUBIC FOOT. THIS FIGURE IS THEN CONVERTED TO POUNDS PER HOUR BY MULTIPLYING BY THE MEASURED STACK GAS VELOCITY.

PARTICULATE SAMPLING IS DONE ON SOURCES WHERE SOLID AND LIQUID PARTICLES ARE BEING EMITTED. PARTICULATE SAMPLING INVOLVES THE ADDED COMPLICATION OF CONTINUOUS STACK GAS VELOCITY DETERMINATION BECAUSE OF INERTIAL EFFECTS OF MANY PARTICLES. IT IS NECESSARY TO DRAW THE SAMPLE GAS INTO THE SAMPLE PROBE AT THE SAME VELOCITY AS THE AVERAGE VELOCITY OF THE FLUE GAS STREAM AT THAT POINT IN ORDER TO OBTAIN A REPRESENTATIVE SAMPLE. THIS CONDITION IS KNOWN AS ISOKINETIC SAMPLING, AND MUST BE MAINTAINED THROUGHOUT PARTICULATE SAMPLING. AT EACH POINT IN THE TRAVERSE, THE SAMPLE FLOW RATE MUST BE ADJUSTED TO ATTAIN ISOKINETIC CONDITIONS AT THE SAMPLE NOZZLE. NOMOGRAPHS OR OTHER CALCULATION AIDS ARE AVAILABLE TO ENABLE RAPID DETERMINATION OF THE REQUIRED SAMPLE FLOW.

GASEOUS SAMPLING IN FLUE GASES IS SIMPLER THAN PARTICULATE SAMPLING, PRINCIPALLY BECAUSE THE GAS MOLECULES ARE SMALL ENOUGH TO BE GOVERNED BY THE RANDOM NATURE OF BROWNIAN MOTION; INERTIAL EFFECTS BECOME INSIGNIFICANT. IN CONTINUOUS SAMPLING IT IS NECESSARY ONLY TO WITHDRAW A SAMPLE FROM THE FLUE AT A KNOWN RATE. THE TASK OF OBTAINING A REPRESENTATIVE SAMPLE, THEREFORE, IS CONSIDERABLY EASIER BECAUSE THE SAMPLING RATE CAN BE INDEPENDENT OF THE VELOCITY IN THE DUCT. THIS IS TRUE, OF COURSE, ONLY FOR THOSE POLLUTANTS THAT EXIST EXCLUSIVELY AS GASES. FOR POLLUTANTS SUCH AS MERCURY AND FLUORIDES WHICH EXIST AS BOTH PARTICULATES AND GASES, AN ISOKINETIC SAMPLING PROCEDURE MUST BE FOLLOWED.

SEVERAL METHODS ARE AVAILABLE FOR COLLECTION OF GASEOUS CONSTITU- ENTS FROM FLUE GAS STREAMS. THESE INCLUDE ABSORPTION INTO A LIQUID PHASE, COLLECTION IN AN EVACUATED CONTAINER, COLLECTION IN A FLEXIBLE FABRIC BAG, ABSORPTION ON A SOLID MATERIAL, AND FREEZE- OUT TECHNIQUES. EACH METHOD IS USEFUL FOR PARTICULAR APPLICATION, DEPENDING ON THE TEMPERATURE AND MOISTURE CONTENT OF THE FLUE GAS, THE MATERIAL BEING ANALYZED, AND THE METHOD OF ANALYSIS USED.

THE FOLLOWING SLIDES SHOW:

(32)	STACK SCAFFOLDING
(33)	STACK SCAFFOLDING
(34)	STACK PORTS
(35)	TRAVERSE MECHANISM FRAME
(36)	STACK SAMPLE PORT PLATE

(37)   Traverse Frame

(38)   Demil Furnace (Burner End)

(39)   Demil Furnace (Burner End)

(40)   Impinger/Collectors

(41)   Probe Assembly

(42)   Probe Assembly on Traverse Mechanism

(43)   Probe Assembly on Traverse Mechanism

(44)   Probe Assembly on Traverse Assembly

(45)   Stack Scaffolding

(46)   Control Instrumentation

(47)   Anderson Sizing Head Assembly

(48)   Anderson Sizing Head Assembly

(49)   Noise Recording Instrumentation

(50)   Noise Recording Instrumentation

(51)   Noise Pollution Definition

(52)   Stack Elevation

The initial test was a furnace background or base test for the purpose of establishing any and all polluting emissions which were attributable to the test furnace system. This test was conducted prior to any stack sampling involving the demil of ammunition items in the furnace. This test included both gaseous and particulate sampling at a steady state operating condition with regard to furnace RPM and a retort barrel skin temperature of 750 to 800 F.

(53)   Subsequent test runs were made for each of the five types of ammunition shown in this slide at the feed rate indicated. A sufficient

PERIOD OF TIME OF BACKGROUND FURNACE OPERATION (WITHOUT ANY AMMU-
NITION BEING RUN) WAS ALLOWED TO LAPSE TO "CLEAN" THE FURNACE
BETWEEN SPECIFIC AMMUNITION ITEM TESTS SO AS TO ELIMINATE ANY
ADVERSE EFFECT OF ONE ITEM PREVIOUSLY RUN ON ANOTHER ITEM.

THE FURNACE RPM WAS VARIED ACCORDINGLY TO ALLOW THE CONTROL OF THE
AMMUNITION DEACTIVATION (DETONATION/DEFLAGRATION) WITHIN THE NEXT
TO THE LAST RETORT BARREL SECTION.

(53)
Thru
(71)
THE NEXT SLIDES REPRESENT THE DATA COLLECTED DURING THE STACK
SAMPLING PROJECT INCLUDING THE NOISE LEVELS MEASURED AT 3
SELECTED POSITIONS.

THE NEXT SLIDE(S) SHOWS THE GASEOUS EMISSION DATA IN A TABULATED
FORM.

(72)
(73)
THE NEXT TWO SLIDES LIST THE PERTINENT DATA RESULTING FROM THE STACK
SAMPLING TESTS.

WITH THIS INFORMATION AT HAND THE PROBLEM THEN SHIFTED TO SELECTION
OF POLLUTION ABATEMENT/CONTROL EQUIPMENT FOR BOTH PARTICULATE AND
GASEOUS POLLUTANTS OR POTENTIAL POLLUTANTS BASED ON HOW ONE
INTERPRETS THE VARIOUS REGULATIONS.

(74) A COMPREHENSIVE ANALYSIS OF THE VARIOUS POLLUTION ABATEMENT/CONTROL EQUIPMENT AVAILABLE FOR PARTICULATE EMISSIONS WAS MADE. THE FOLLOWING SLIDES DESCRIBE THE TYPES OF EQUIPMENT CONSIDERED:

SLIDE (75) SCHEMATIC OF A MECHANICAL COLLECTOR (DRY CENTRIFUGAL)

THIS TYPE OF COLLECTOR WAS NOT GIVEN SERIOUS CONSIDERATION BECAUSE OF LOW EFFICIENCIES AND INABILITY TO COLLECT SMALL PARTICLES (BELOW 20 - 40 MICRONS).

SLIDE (76) SCHEMATIC OF A FILTER TYPE COLLECTOR

THE FABRIC COLLECTORS ARE RECOMMENDED AS THE BEST TYPE OF PARTICULATE COLLECTOR AS THEIR COLLECTION EFFICIENCY EXCEEDS 99% AND WILL COLLECT PARTICULATES HAVING A SIZE OF 0.5 MICRON WITH EASE. THE DIRTIER THE FILTER MEDIA (BAG), THE HIGHER PERCENT OF RECOVERY/FILTRATION AND THE FINER THE PARTICLES RECOVERED. FABRIC FILTERS ARE MEDIUM COST UNITS. FILTERS OF THE INTERMITTENT SHAKER TYPE WHICH COLLECT DUST IN HOPPERS THROUGH ROTARY AIR LOCK VALVES ARE DESIRABLE. BAGS HAVING AN AIR TO CLOTH RATIO OF 2.5 TO 1 AND OF "IONEX" MATERIAL WOULD BE APPLICABLE. THIS TYPE OF FILTER IS NOT EFFECTIVE IN THE ABATEMENT OF GASEOUS EMISSIONS.

SLIDE (77) SCHEMATIC OF AN ELECTROSTATIC PRECIPITATOR

THIS TYPE OF PARTICULATE COLLECTOR WOULD PROVIDE EFFICIENCIES COMPARABLE TO THE FABRIC COLLECTORS FOR PARTICULATE EMISSIONS BUT WOULD HAVE NO ADVANTAGE OVER THEM FOR THIS PROJECT. ELECTROSTATIC PRECIPITATORS WOULD ADD SOME LIABILITIES REGARDING HIGH INITIAL

FIRST COST, CRITICAL CONTROL, AND MAINTENANCE PROBLEMS. THEY ARE
NOT USUALLY USED ON SUCH SMALL VOLUMES OF GASES SUCH AS IN THIS
UNIT. POWER FAILURE WOULD ALLOW PARTICULATE EMISSIONS TO ESCAPE
AND WITH REGARD TO GASEOUS EMISSIONS THE ELECTROSTATIC PRECIPITATOR
IS NOT EFFECTIVE.

SLIDE (78) SCHEMATIC OF A WET COLLECTOR

WET COLLECTORS ARE EFFECTIVE FOR REMOVAL OF BOTH PARTICULATE AND
GASEOUS EMISSIONS. PACKED TOWER TYPE SCRUBBERS WITH A "MARBLE BED"
CAN EFFECTIVELY CAPTURE PARTICLES MEASURING 1-2 MICRONS AT MEDIUM
PRESSURE DROPS. HIGHER PRESSURE DROPS OR (HIGH ENERGY) VENTURI
TYPES OF WET COLLECTORS CAN EFFECTIVELY REMOVE SUBMICRON PARTICLES
BUT AT A HIGH COST PER CFM. WET COLLECTORS ARE IN THE MODERATE
COST AREA AND THE EFFLUENT (SLUDGE) RESULTING FROM THEIR OPERATION
INHERENTLY CREATES ANOTHER WASTE DISPOSAL PROBLEM. FREEZE PROTECT-
ION IS REQUIRED FOR WET COLLECTORS INSTALLED OUTSIDE.

(79) A COMPREHENSIVE ANALYSIS OF THE VARIOUS POLLUTION ABATEMENT/CONTROL
EQUIPMENT AVAILABLE FOR GASEOUS EMISSIONS WAS MADE. THE FOLLOWING
SLIDES DESCRIBE THE TYPES OF EQUIPMENT CONSIDERED:

SLIDE (80) SCHEMATIC OF A TYPICAL ADSORPTION SYSTEM
THIS SYSTEM UTILIZES A FIXED BED OF VARIOUS DRY MEDIA DEPENDING ON
VAN DER WAALS FORCES AND CAPILLARY ACTION TO ADSORB GAS MOLECULES
ON AND/OR IN THE ADSORBENT.

ALTHOUGH A GREAT VARIETY OF CLAYS, CHARS, GELS, OXIDES, SILICATES
AND ACTIVATED CARBON HAVE BEEN USED AS SORBENTS, MOST EFFORT AND

APPLICATION IN THE AIR POLLUTION FIELD HAS BEEN CONFINED TO ACTIVATED CARBONS. MORE RECENTLY SOME OF THE SYNTHETIC HYDROUS SILICATES (MODIFIED ZEOLITES/MOLECULAR SIEVES) HAVE BEEN ALSO CONSIDERED. THESE MATERIALS SHOW PROMISE FOR EFFICIENT REMOVAL OF NO_X AND SO_X. STATE OF THE ART IS NOT DEVELOPED TO THE POINT WHERE THEY CAN BE APPLIED ON THIS PROJECT. REGENERATION OF ADSORBENT IS REQUIRED AND IT IS NOT 100% REVERSIBLE AT THIS TIME (ONLY 50% - 75%).

SLIDE (81) SCHEMATIC OF A PACKED TOWER (WET SCRUBBER)

THE COUNTERCURRENT FLOW PACKED TOWER UTILIZING A CERAMIC MARBLE BED IS CONCLUDED TO GENERALLY THE BEST TYPE OF WET COLLECTOR FOR THE REMOVAL OF GASES. OTHER TYPES OF PACKINGS SUCH AS "TELLERETTES," "RASCHIG" RINGS, "PALL" RINGS, "BERL" SADDLES, "INTALOX" SADDLES AND "GLITCH" RINGS ARE CONSIDERED TO BE LESS DESIRABLE FOR THIS APPLICATION AS THEY WOULD BE MORE SUBJECT TO CLOGGING. CHEMICAL TREATMENT OF THE SCRUBBING WATER IS OPTIONAL. WATER RECIRCULATION IS POSSIBLE BUT A SLUDGE EFFLUENT IS GENERATED WHICH CREATES ANOTHER DISPOSAL PROBLEM. HOWEVER, IN THIS APPLICATION THE SLUDGE WOULD BE SUITABLE FOR SANITARY LAND FILL.

SLIDE (82) SCHEMATIC OF A SPRAY CHAMBER SCRUBBER

THIS TYPE IS A VERY SIMPLE TYPE IN WHICH WATER SPRAY NOZZLES ARE MOUNTED IN THE UPPER SECTION OF A CYLINDRICAL CHAMBER AND THE WATER DROPLETS ARE MADE TO FALL DOWNWARD USUALLY COUNTER CURRENT TO THE GAS FLOW. THE WATER ABSORBS SOME OF THE SOLUBLE GASES. THIS IS CONSIDERED TO BE A LOW EFFICIENCY METHOD.

SLIDE (83) SCHEMATIC OF A VENTURI SCRUBBER

THE VENTURI SCRUBBER IS ESSENTIALLY A HIGH ENERGY SPRAY TOWER IN WHICH AN EFFORT IS MADE TO MAXIMIZE THE MIXING OF THE GAS STREAM PASSING THROUGH THE MAIN SECTION OF THE VENTURI WITH THE LIQUID (WATER) INTRODUCED AT THE THROAT OF THE VENTURI. A DEGREE OF GAS ADSORPTION TAKES PLACE IN THE WATER DROPLETS THEN THEY MOVE TO AN ENTRAINMENT SEPARATOR (DEMISTER) TO REMOVE THE LIQUID FROM THE WASHED GASES. THIS SYSTEM REQUIRES A PRESSURE DROP OF FROM 10 - 100 INCHES OF WATER AND GAS VELOCITIES REACHING 5000 FEET PER MINUTE.

SLIDE ⑧⑧ SCHEMATIC OF A GAS/VAPOR INCINERATOR (AFTERBURNER)

AFTERBURNERS ARE USED MAINLY ON ORGANIC EMISSIONS SUCH AS SMOKE HOUSES, PAINT BAKING OVENS, ETC., WHERE COMBUSTIBLE MATTER EXISTS IN THE GAS STREAM. AFTERBURNERS REQUIRE AUXILIARY FUEL BURNERS WHICH CONTRIBUTE TO HYDRO CARBON, SO_x, CO_x AND NO_x EMISSIONS.

SCHEMATIC OF A CATALYTIC COMBUSTOR (AFTERBURNER)

THIS SLIDE SHOWS AN ADDITION OF A CATALYTIC ELEMENT IN AN AFTER-BURNER. THE MAIN IDEA IS TO IMPROVE THE COMBUSTION AT LOWER TEMPERATURES. CATALYTIC AFTERBURNERS ARE USED MAINLY IN NITRIC ACID PLANTS AND OIL REFINERIES AND HAVE NOT BEEN COMMERCIALLY APPLIED ON COMBUSTION PROCESSES.

THE OBJECTIVE WAS TO SELECT THE BEST TYPE OF ABATEMENT METHOD(S) THAT WILL MEET THE CRITERIA OF:

1. EFFICIENT REMOVAL OF CONTAMINANTS (POLLUTANTS) BOTH PARTICULATE AND GASEOUS

2. COMPLIANCE WITH ALL PREVAILING AIR POLLUTION REGULATIONS

3. ECONOMY OF FIRST COST, OPERATION AND MAINTENANCE

THE PRINCIPAL REQUIREMENT IN THIS PROJECT, AS DETERMINED BY THE STACK EMISSION TESTS AND ANALYSIS WAS TO REDUCE THE PARTICULATE CONCENTRATIONS OF THE STACK EMISSIONS AND THEREBY MEET THE REQUIREMENTS OF THE INDIANA AIR POLLUTION CONTROL REGULATION APC 7 (INCINERATORS) WHICH IS THE SAME AS THE EPA REG ATIONS. THE MEASURED MAXIMUM PARTICULATE EMISSION RATE (1.29 POUNDS PER 1000 LBS OF DRY GAS FOR THE .50 CALIBER AMMUNITION) EXCEEDS THE 0.7 POUNDS PER 1000 POUNDS OF DRY GAS LIMIT OF APC 7 AND THE EPA REGULATION. IT WAS ALSO DESIRABLE TO REDUCE THE LEVEL OF GASEOUS POLLUTANTS TO THE LOWEST POSSIBLE LEVEL WITHIN REASONABLE MEANS.

SOUND MEASUREMENTS WERE TAKEN AT VARIOUS LOCATIONS NORMALLY OCCUPIED BY WORKERS DURING DEMIL OPERATIONS. SOUND LEVELS OF 85 DBA WERE NOT EXCEEDED INSIDE THE BUILDING PROPER. THE READINGS WERE TAKEN BY WALK THROUGH SOUND MEASUREMENT EQUIPMENT. SOUND MEASUREMENTS WERE RECORDED AT SEVERAL POSITIONS WITHIN THE CONTROL ROOM. SOUND LEVELS OF 90 DBA WERE EXCEEDED DURING DETONATION OF FUZES, .50 CALIBER AND 20MM AMMUNITION WITH MAXIMUM READINGS OF APPROXIMATELY 105 DBA OCCURRING AT TIMES. IT WAS RECOMMENDED THAT

NO NOISE ABATEMENT (INSULATION, ENCLOSURES, ETC.) BE REQUIRED FOR
THIS PROJECT BASED ON THIS SURVEY. SOUND LEVELS EXCEED 90 DBA
IN THE FURNACE CONTROL ROOM ONLY WHEN CERTAIN TYPES OF AMMUNITION
ARE DETONATED. THESE LEVELS ARE INTERMITTENT NOT CONTINUOUS.
EAR PROTECTION IS PRESENTLY WORN BY PERSONNEL WHEN WORKING IN THE
CONTROL ROOM AND THIS IS CONSIDERED TO BE ADEQUATE AND IN COMPLI-
ANCE WITH THE OSHA (OCCUPATIONAL SAFETY AND HEALTH ACT).

(85) THE NEXT SLIDE SHOWS THE POLLUTION ABATEMENT/CONTROL EQUIPMENT
ULTIMATELY SELECTED FOR THIS APPLICATION FOR BOTH PARTICULATE AND
GASEOUS EMISSIONS. AS THIS INSTALLATION ON A ROTARY DEMIL FURNACE
WILL BE A FIRST-OF-ITS-KIND WE ARE GOING TO BE INTERESTED IN THE
PERFORMANCE OF THE EQUIPMENT IN ACTUAL PRODUCTION. THE EQUIPMENT
IS PLANNED FOR INSTALLATION ON A MOBILE/RELOCATABLE ROTARY FURNACE
SYSTEM IN THE FALL OF 1974. A FOLLOW-UP PERFORMANCE TEST AND
EVALUATION WILL SUBSEQUENTLY BE MADE AND THE INFORMATION WILL BE
MADE AVAILABLE TO ALL CONCERNED VIA THE DDC (DEFENSE DOCUMENTATION
CENTER).

PERIODIC MONITORING OF SELECTED VARIABLES WILL BE PERFORMED FOR
OPERATION CONTROL AS COMPLEX STACK SAMPLING IS NOT CONSIDERED
NECESSARY FOR THIS TYPE OF SYSTEM ONCE IN OPERATION.

LIST OF VISUAL AIDS

SLIDE NO.   DESCRIPTION

1.   NAVORD EMBLEM

2.   4 BASIC DEMIL METHODS

3.   PROCESS FLOW SCHEMATIC DIAGRAM

4.   GENERAL OVERALL RENDERING OF A 4 BARREL ROTARY DEMIL
            FURNACE SYSTEM

5.   CROSS SECTION OF THE RETORT SECTION SHOWING THE BURNER,
            INTERNAL HELICAL SPIRALS AND FEED/EXHAUST

6.   ACTUAL PHOTOGRAPH OF THE 4 BARREL ROTARY DEMIL FURNACE
            SYSTEM

7.   ACTUAL PHOTOGRAPH OF THE 4 BARREL RETORT ASSEMBLY

8.   DESCRIPTIVE DRAWING OF SMALL ARMS AMMUNITION DEMIL IN
            THE FURNACE (.22, .38, .45, .30 CAL, 5.56MM, 7.62 MM
            AND .50 CAL)

9.   ACTUAL PHOTOGRAPH OF .50 CAL SMALL ARMS AMMUNITION

10.   DESCRIPTIVE DRAWING OF 20MM AMMUNITION

11.   ACTUAL PHOTOGRAPH OF 20MM HEI AMMUNITION

12.   DESCRIPTIVE DRAWING OF A TYPICAL GUN AMMUNITION
            PROJECTILE FUZE

13.   ACTUAL PHOTOGRAPH OF A 5" PROJECTILE NOSE FUZE

14.   ACTUAL PHOTOGRAPH OF A 5" PROJECTILE BASE FUZE

15.   DESCRIPTIVE DRAWING OF A TYPICAL CAD (CARTRIDGE
            ACTUATED DEVICE)

16.   ACTUAL PHOTOGRAPH OF A CARTRIDGE ACTUATED DEVICE (CAD)

17.   DESCRIPTIVE DRAWING OF A TYPICAL PYROTECHNIC ILLUMINATING
            SIGNAL

18.   ACTUAL PHOTOGRAPH OF AN ILLUMINATIVE SIGNAL

19.   MATERIAL AND SUB-COMPONENT BREAKDOWN OF AN AMMUNITION ITEM
            (20MM) TO SHOW COMPLEX COMPOSITION BY WEIGHT PERCENTAGE

SLIDE NO.	DESCRIPTION
20.	MATERIAL AND SUB-COMPONENT BREAKDOWN OF AN AMMUNITION ITEM (20MM) TO SHOW COMPLEX COMPOSITION BY WEIGHT PERCENTAGE
21.	MATERIAL AND SUB-COMPONENT BREAKDOWN OF AN AMMUNITION ITEM (20MM) TO SHOW COMPLEX COMPOSITION BY WEIGHT PERCENTAGE
22.	CHART OF TYPICAL ENERGETIC MATERIALS (PROPELLANTS, EXPLOSIVES, PYROTECHNICS - PEP) WHICH BURN, DEFLAGRATE OR DETONATE DURING THERMAL DEGRADATION IN THE DEMIL FURNACE
23.	CHART LISTING EXPECTED/POTENTIAL PRODUCTS OF COMBUSTION AND REACTION PRODUCTS RESULTING FROM THERMAL DEACTIVATION/ DEGRADATION IN THE ROTARY DEMIL FURNACE
24.	POLLUTANT EMISSION LEVELS FOR STATE OF INDIANA, LOCAL
25.	POLLUTANT EMISSION LEVELS FOR FEDERAL LAW (EPA)
26.	POLLUTANT EMISSION LEVELS AS AGREED BY JPAD/JCAP (APSA GUIDELINES)
27.	EPA PROMULGATED TEST PLAN FOR STACK SAMPLING OF STATIONARY SOURCES (LIST OF METHODS)
28.	TEST EQUIPMENT SELECTED FOR USE IN STACK SAMPLING (LIST) (EPA APPROVED SAMPLING TRAINS)
29.	GASEOUS SAMPLE RECOVERY TECHNIQUE
30.	PARTICULATE SAMPLE RECOVERY TECHNIQUE
31.	PARTICULATE SAMPLING TRAIN (ANDERSON SIZING HEAD)
32.	STACK SCAFFOLDING (SAMPLE PORT PREPARATION)
33.	STACK SCAFFOLDING (SAMPLE PORT PREPARATION)
34.	STACK SAMPLE PORTS
35.	TRAVERSE MECHANISM FRAME
36.	STACK SAMPLE PORT PLATE
37.	TRAVERSE MECHANISM FRAME
38.	DEMIL FURNACE (BURNER END)
39.	DEMIL FURNACE (BURNER END)
40.	PROBE IMPINGER BOX

SLIDE NO.		DESCRIPTION
41.		PROBE ASSEMBLY
42.		PROBE ASSEMBLY ON TRAVERSE MECHANISM
43.		PROBE ASSEMBLY ON TRAVERSE MECHANISM
44.		PROBE ASSEMBLY ON TRAVERSE ASSEMBLY
45.		STACK SCAFFOLDING
46.		CONTROL INSTRUMENTATION
47.		ANDERSON SIZING HEAD ASSEMBLY
48.		ANDERSON SIZING HEAD ASSEMBLY
49.		NOISE RECORDING INSTRUMENTATION
50.		NOISE RECORDING INSTRUMENTATION
51.		DEFINITION OF NOISE POLLUTION
52.		SIDE ELEVATION OF DEMIL FURNACE STACK
53.		SPECIFIC SAMPLING PLAN FOR AMMUNITION DEMILED
54. THRU 71.		SAMPLES OF VARIOUS DATA COLLECTED DURING THE STACK SAMPLING TEST
72.		PERTINENT DATA RESULTING FROM THE STACK SAMPLING TESTS
73.		PERTINENT DATA RESULTING FROM THE STACK SAMPLING TESTS
74.		POLLUTION ABATEMENT/CONTROL EQUIPMENT ALTERNATIVES FOR PARTICULATES
75.		SCHEMATIC OF A MECHANICAL COLLECTOR
76.		SCHEMATIC OF A FILTER TYPE COLLECTOR
77.		SCHEMATIC OF A WET COLLECTOR
78.		SCHEMATIC OF AN ELECTRO STATIC PRECIPITATOR
79.		POLLUTION ABATEMENT/CONTROL EQUIPMENT ALTERNATIVES FOR ABSORPTION OF GASEOUS POLLUTANTS
80.		SCHEMATIC OF A TYPICAL ABSORPTION SYSTEM

SLIDE NO.	DESCRIPTION
81.	SCHEMATIC OF A PACKED TOWER (WET) SCRUBBER
82.	SCHEMATIC OF A SPRAY CHAMBER SCRUBBER
83.	SCHEMATIC OF A VENTURI CHAMBER SCRUBBER
84.	SCHEMATIC OF A GAS/VAPOR INCINERATOR (AFTERBURNER)
	SCHEMATIC OF A CATALYTIC COMBUSTOR INCINERATION OF GASEOUS POLLUTANTS
85.	EQUIPMENT TYPE (DRY FABRIC FILTER/BAGHOUSE) SELECTED FOR PARTICULATE ABATEMENT FOR THIS APPLICATION
	EQUIPMENT TYPE (MARBLE BED, WET SCRUBBER) SELECTED FOR BOTH PARTICULATE AND GASEOUS POLLUTANT ABATEMENT FOR THIS APPLICATION
	SCHEMATIC OF THE SELECTED POLLUTION ABATEMENT/CONTROL EQUIPMENT ON THE 4 BARREL ROTARY DEMIL FURNACE

SLIDE NO. 1
NAVORD EMBLEM

PROJECTILE DEMIL/DISPOSAL ALTERNATIVES FOR METHODS/PROCESSES

DETONATION

BURN OUT

WASH OUT
• water
• steam

MECH. PREP.

DEMIL FURNACE

PROCESS

SLIDE NO. 2

834
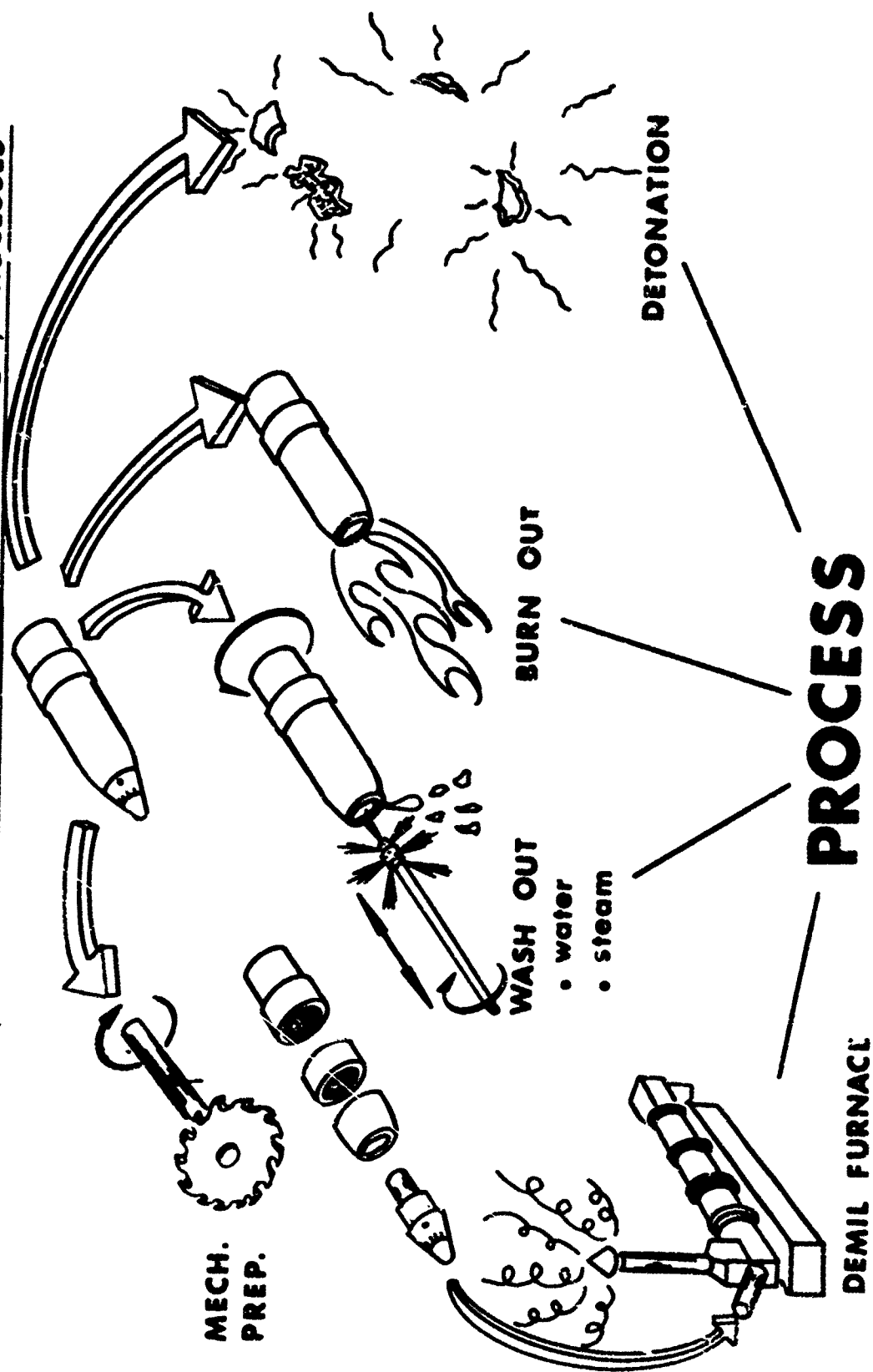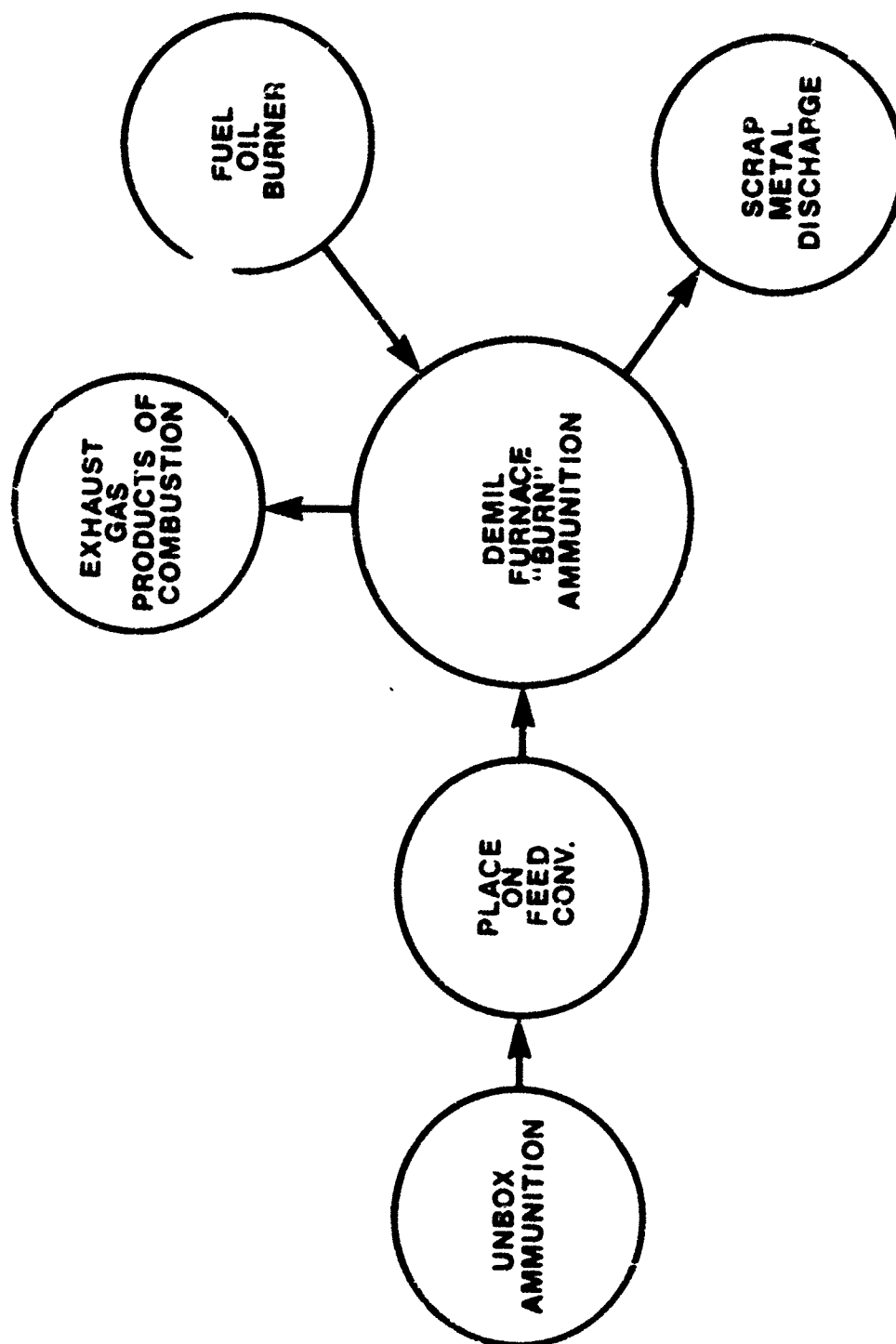
DEMIL FURNACE PROCESS FLOW

SLIDE NO. 3

835

SIMPLIFIED RENDERING OF 4 BARREL ROTARY DEMIL FURNACE SYSTEM

BURNER

DISCHARGE

BLOWER

INTERNAL SPIRAL
(CUTAWAY VIEW)

RETORT SECTION

EXISTING
EXHAUST
STACK

FEED
TUBE

DRIVE ROLLERS

SLIDE NO. 4

-35-
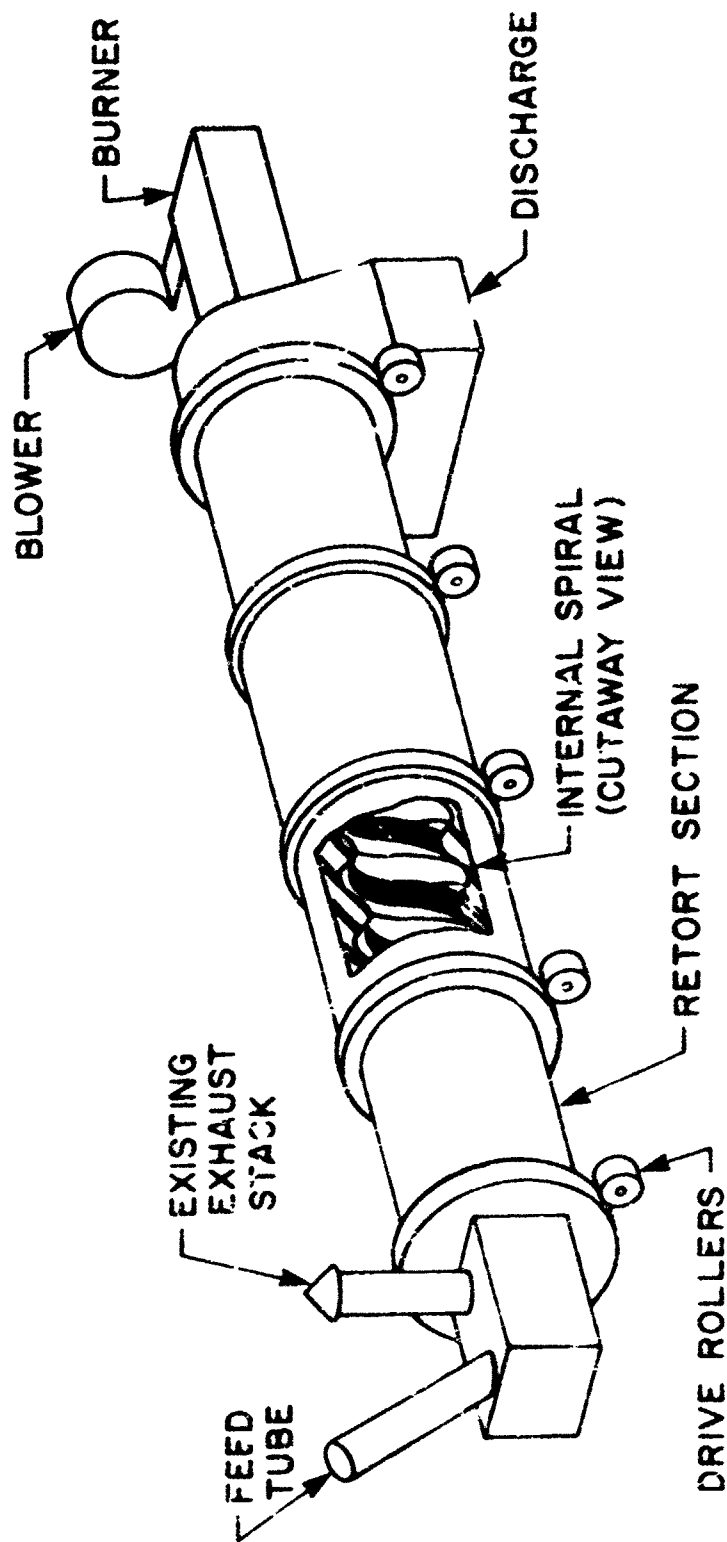
CROSS SECTION OF RETORT SECTIONS
SHOWING BURNER, SPIRALS, FEED AND EXHAUST

FUEL OIL
BURNER NOZZLE

AMMUNITION ITEM
BETWEEN INTERNAL
SPIRAL LEADS

ONE OF 4
RETORT
BARREL
SECTIONS

EXHAUST
STACK

FEED TUBE

SLIDE NO. 5

SMALL ARMS AMMUNITION

BULLET

TRACER MATERIAL

SMOKELESS POWDER

CARTRIDGE CASE

PERCUSSION PRIMER

.50 CAL

7.62 mm

5.56 mm

.30 CAL

.45 CAL

.38 CAL

.22 CAL

SLIDE NO. 8

840
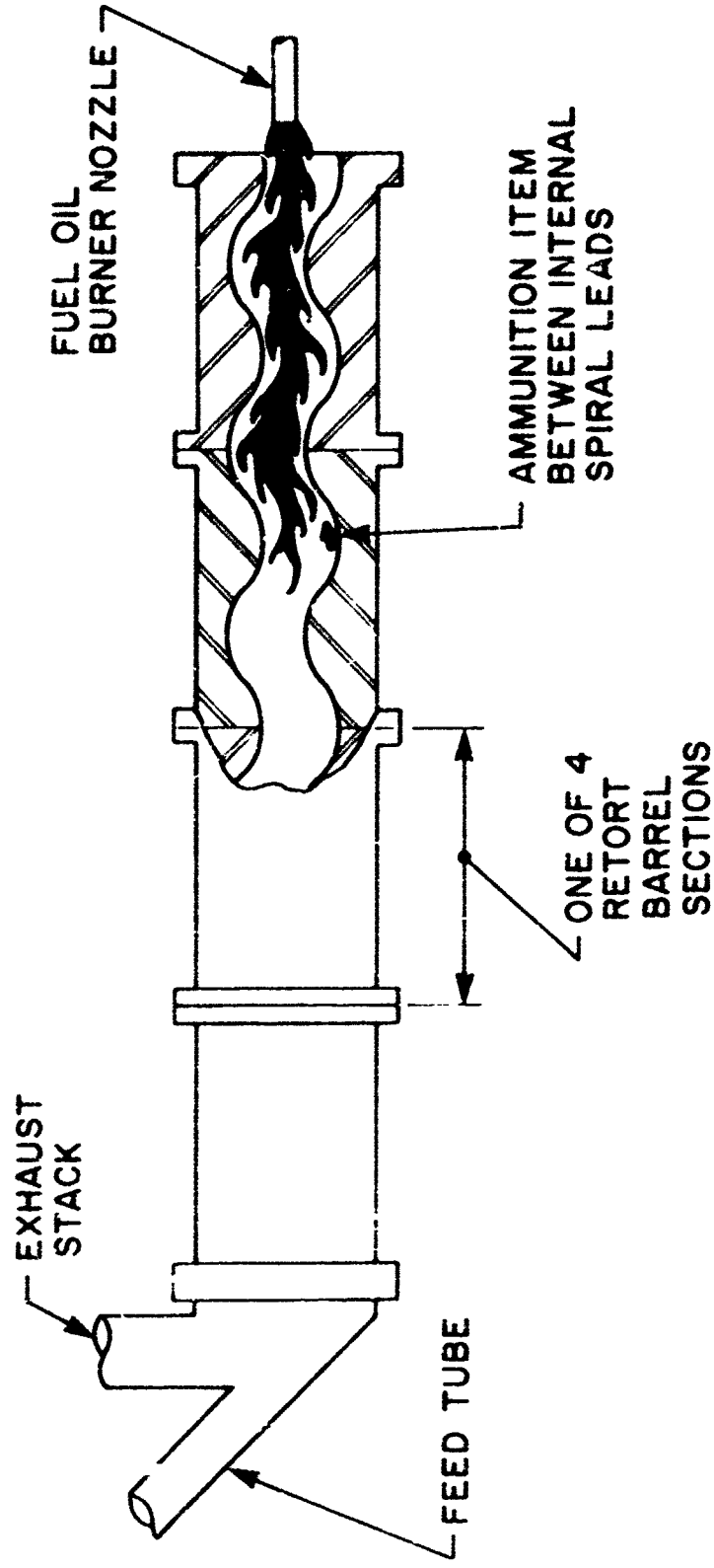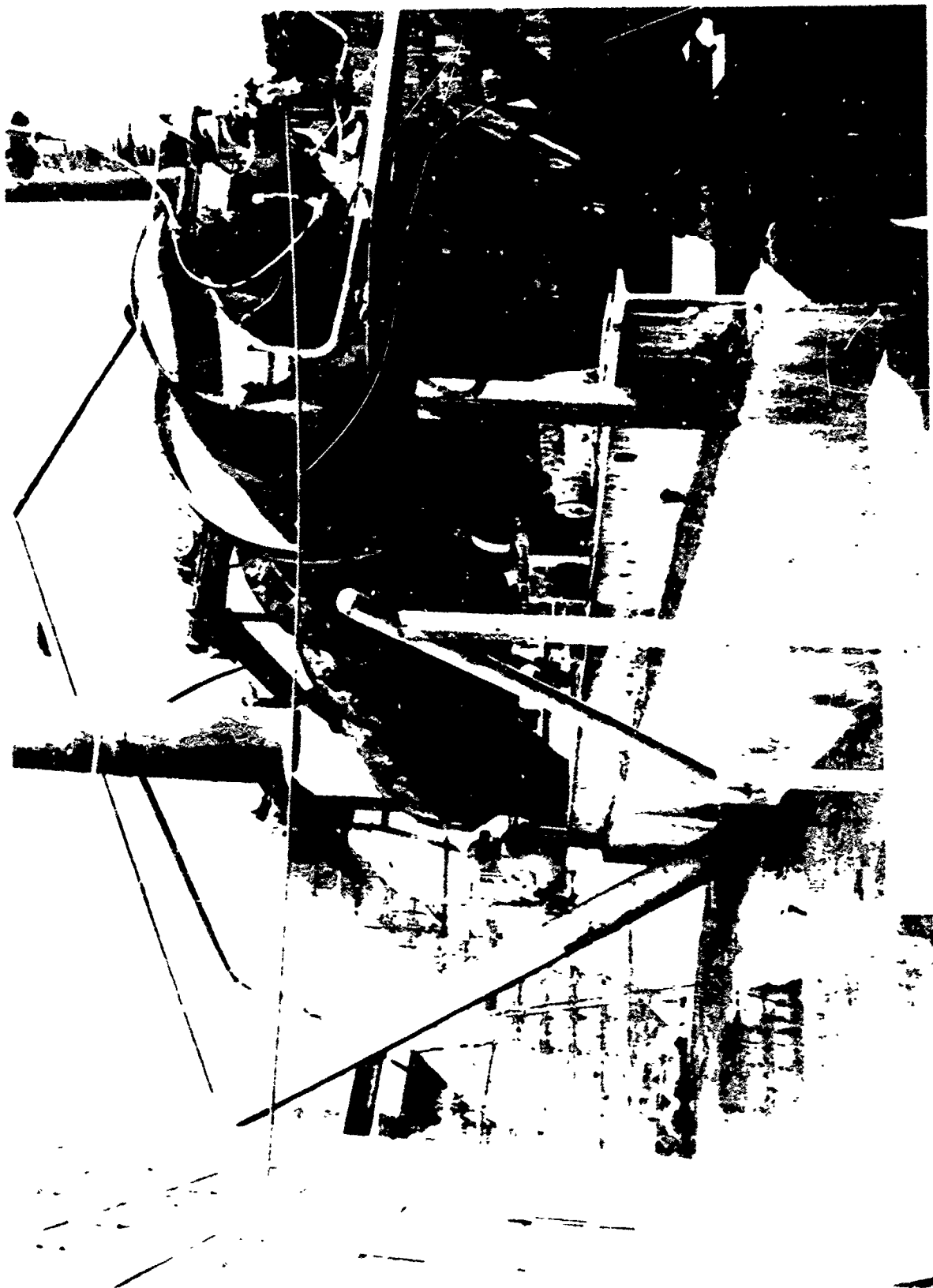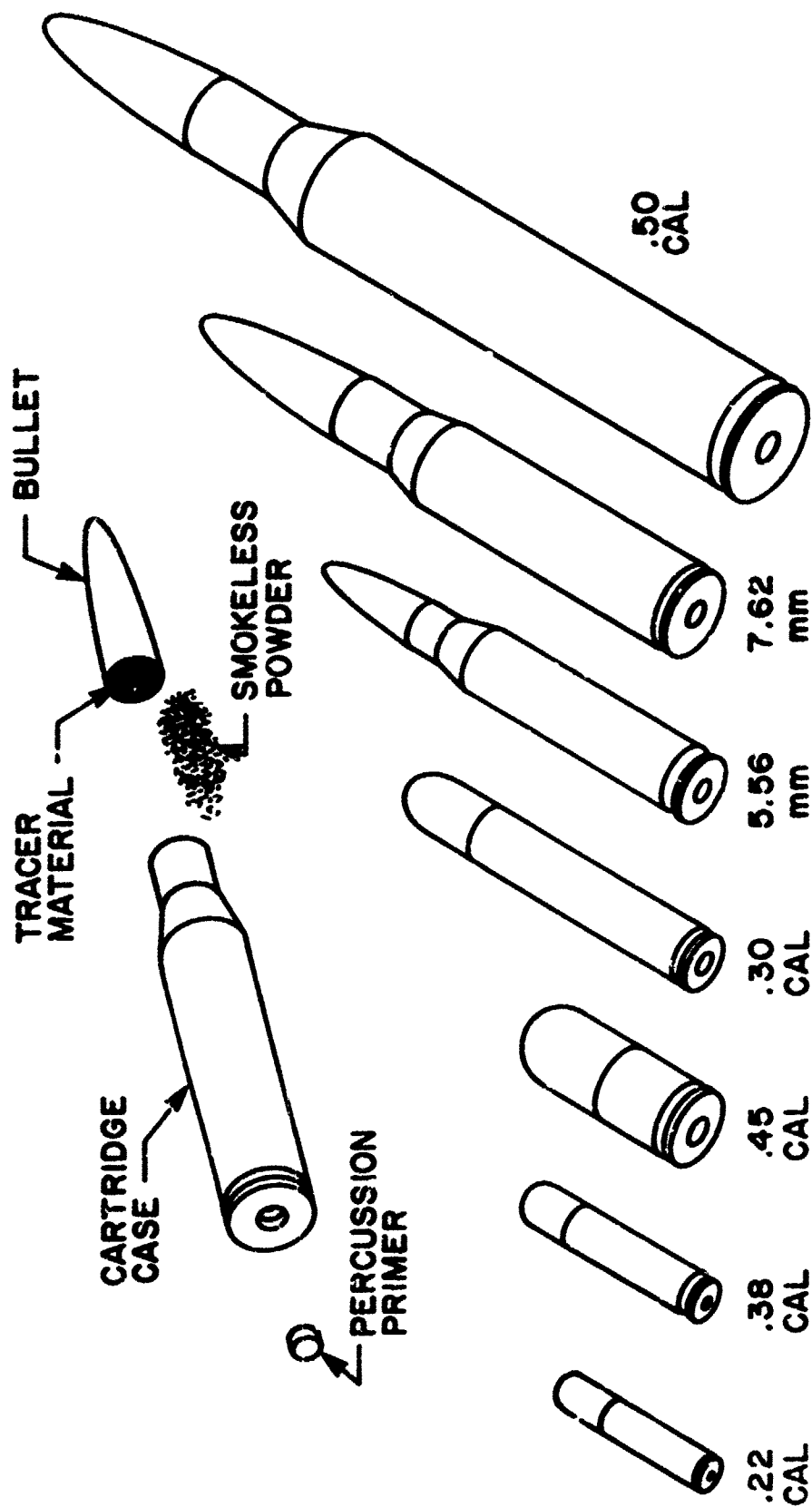
SLIDE NO. 9
.50 CAL SMALL ARMS AMMUNITION

841

20mm AMMUNITION

FUZE

HE EXPLOSIVE LOAD

INCENDIARY LOAD

ARMOR PIERCING BALL

PROJECTILE BODY

TRACER MATERIAL

ROTATING BAND (COPPER)

CASE (STEEL & BRASS)

PRIMER

SLIDE NO. 10

842

SLIDE NO. 11
20MM HEI AMMUNITION

843
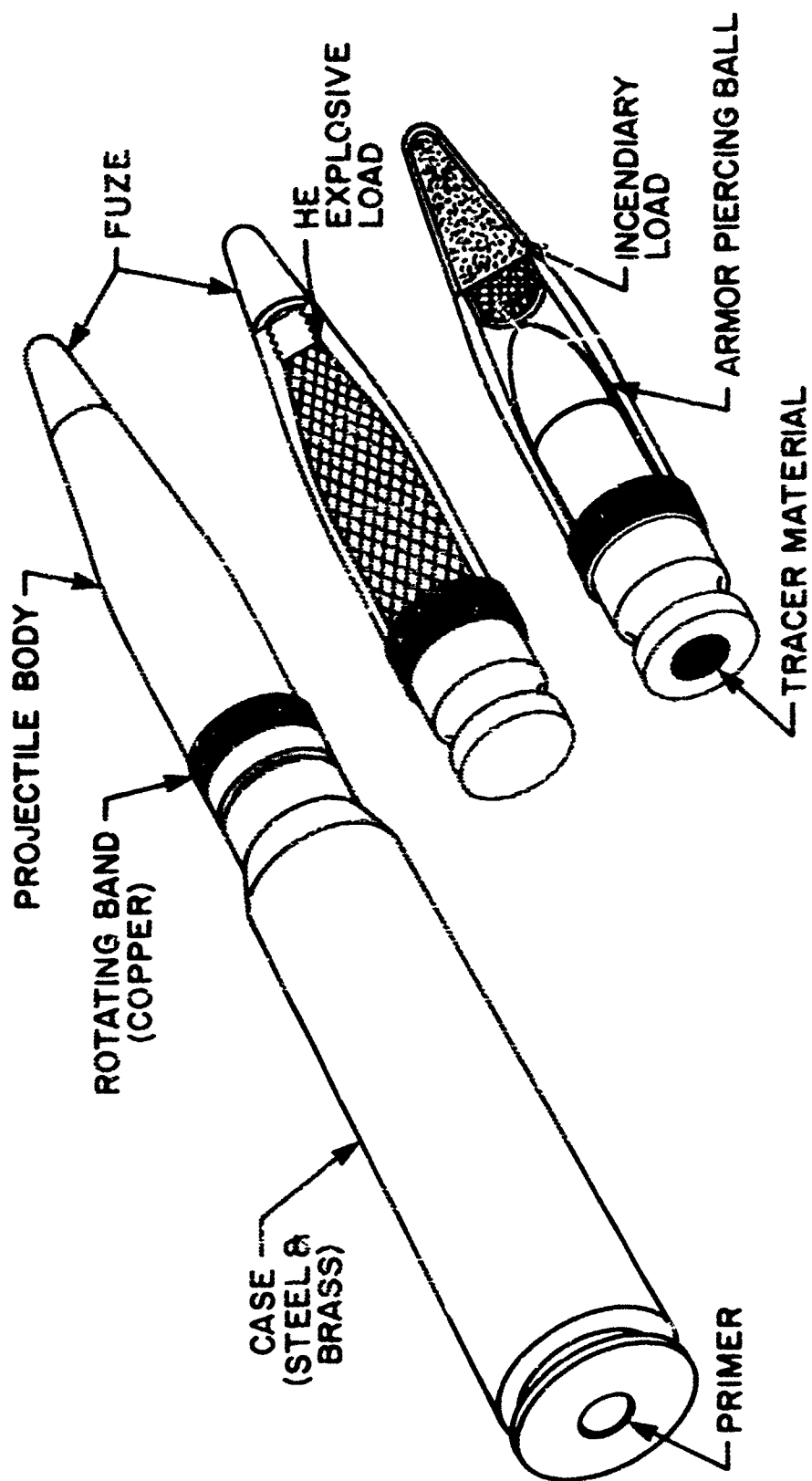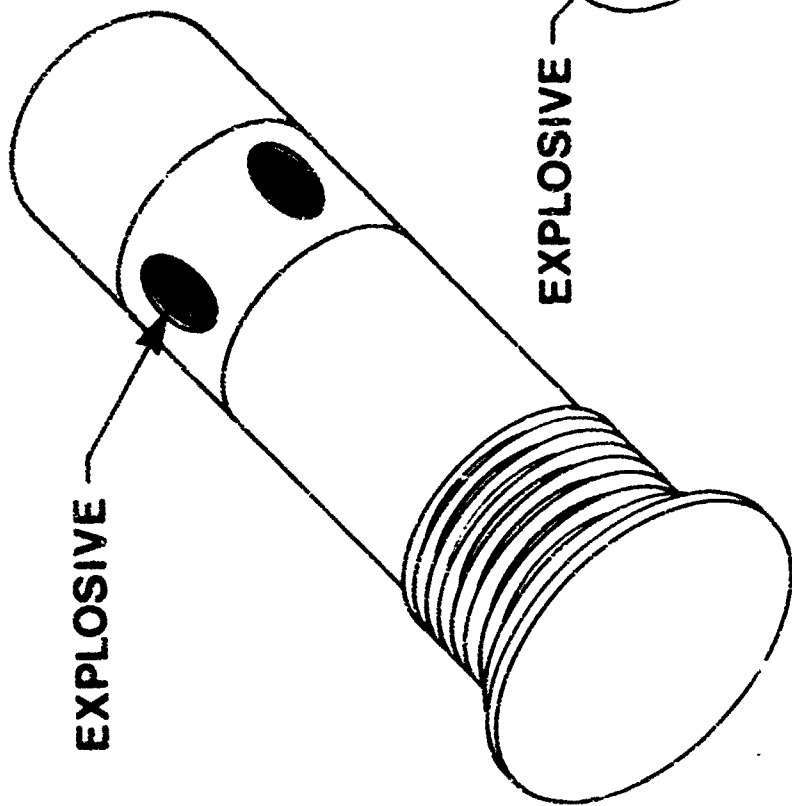
EXPLOSIVE
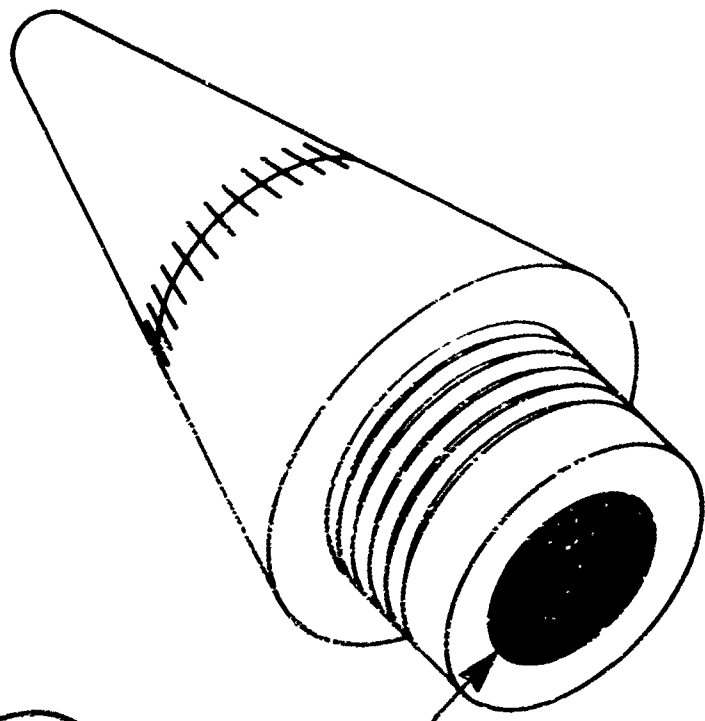
5" PROJECTILE
NOSE FUZE
(MECH. TIME)

EXPLOSIVE

5" PROJECTILE
BASE FUZE
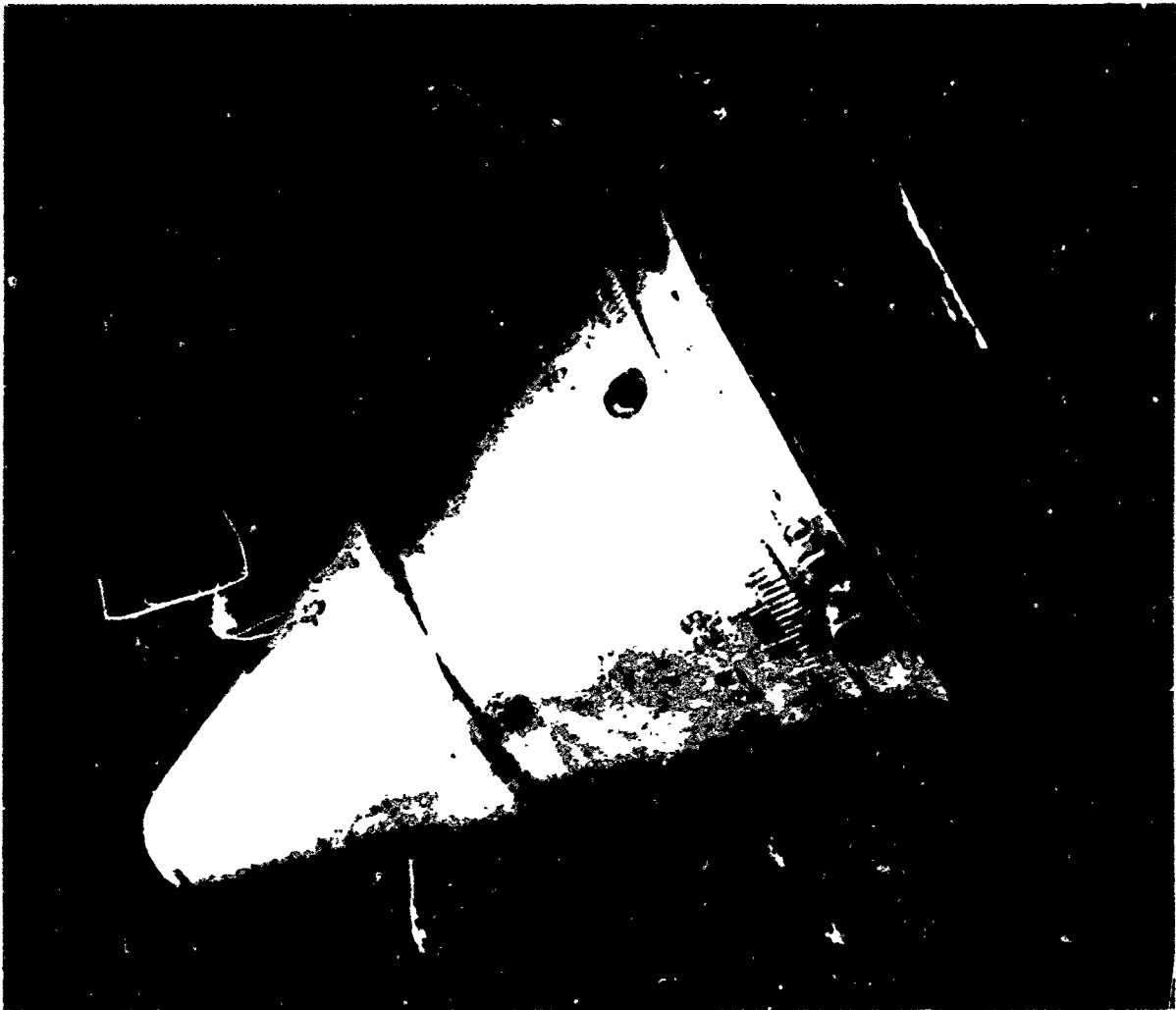
SLIDE NO. 12

MK 50-0

SLIDE NO. 13
5" PROJECTILE NOSE FUZE

MK 28 - 17

GAS GENERATING
ENERGETIC MATERIAL

CARTRIDGE CASE

PRIMER
INITIATOR
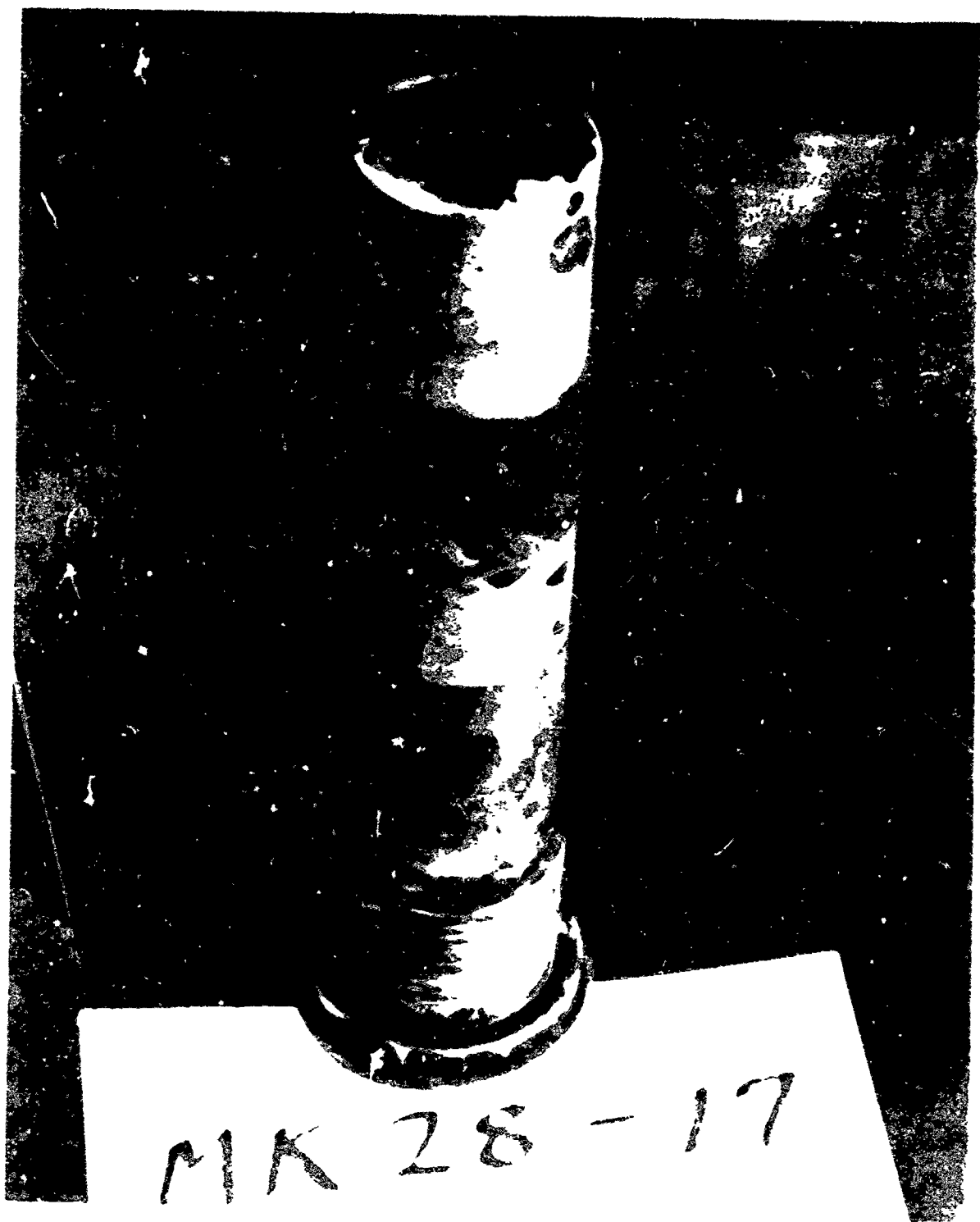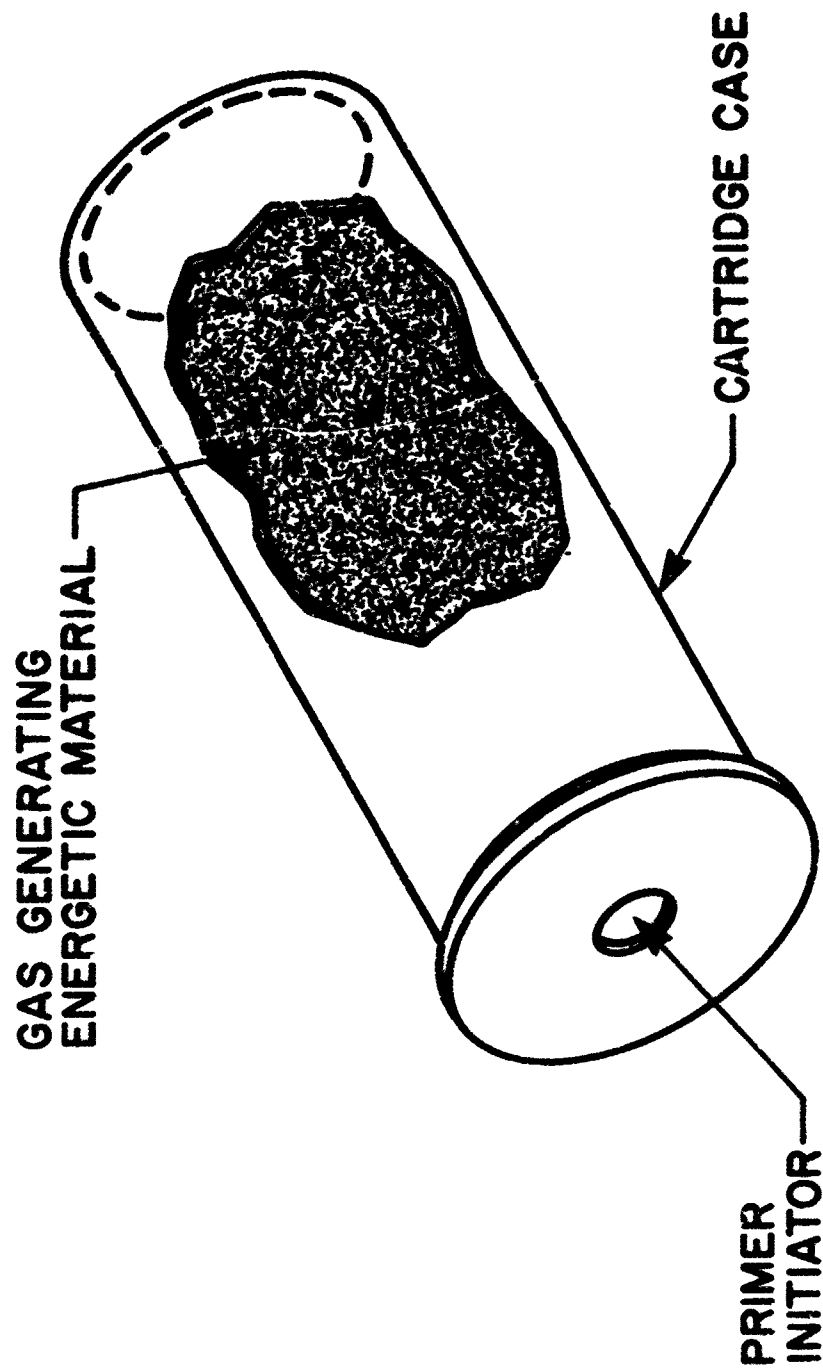
TYPICAL CARTRIDGE ACTUATING DEVICE

SLIDE NO. 15
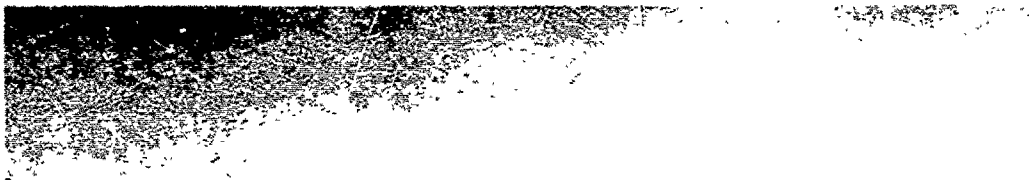
SLIDE NO. 16
CARTRIDGE ACTUATED DEVICE (CAD)

FUZE DELAY IGNITER

PULL WIRE

FLARE MATERIAL (PYROTECHNIC MIX)

ALUMINUM CASE
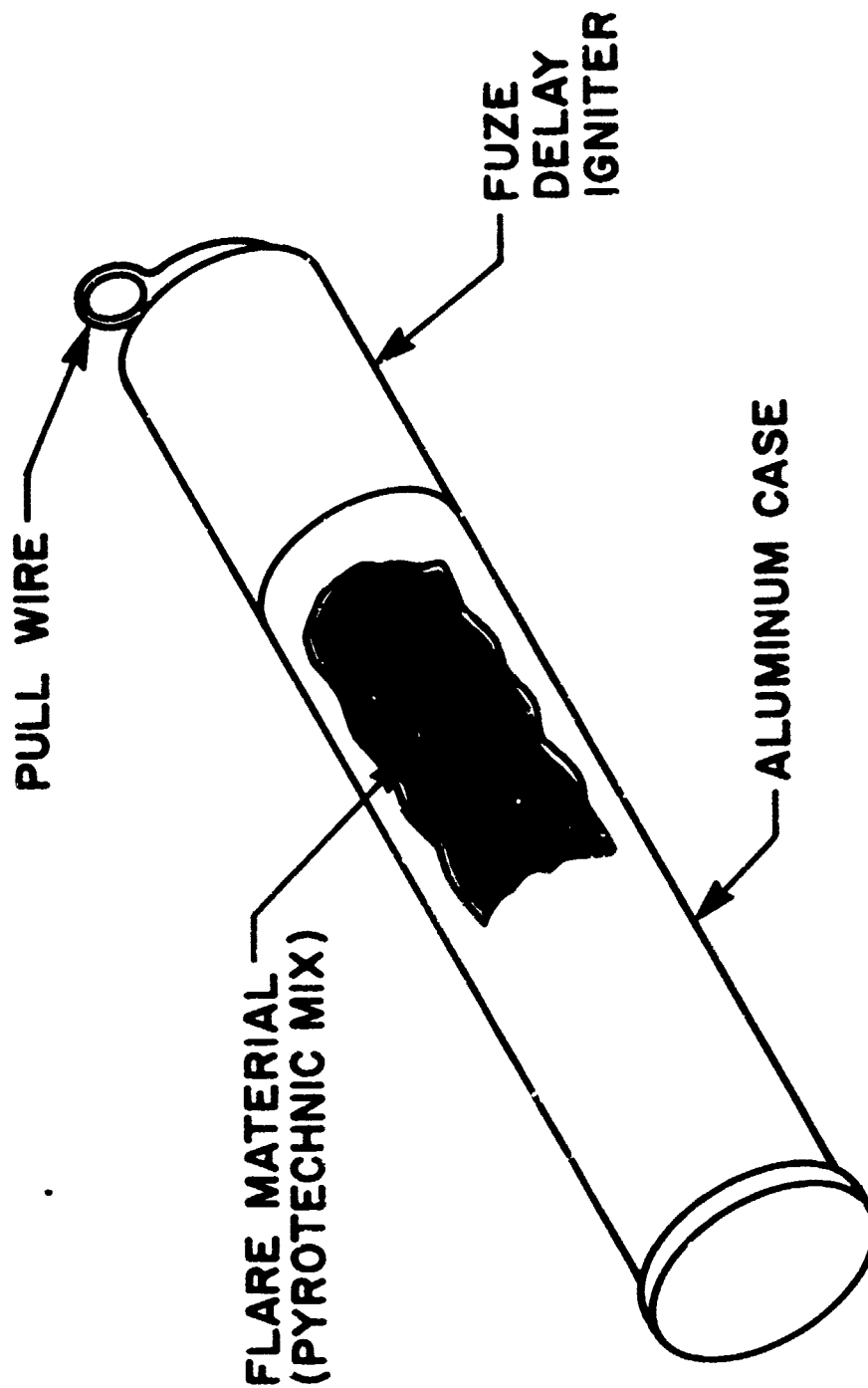
TYPICAL ILLUMINATING SIGNAL

SLIDE NO. 17

849
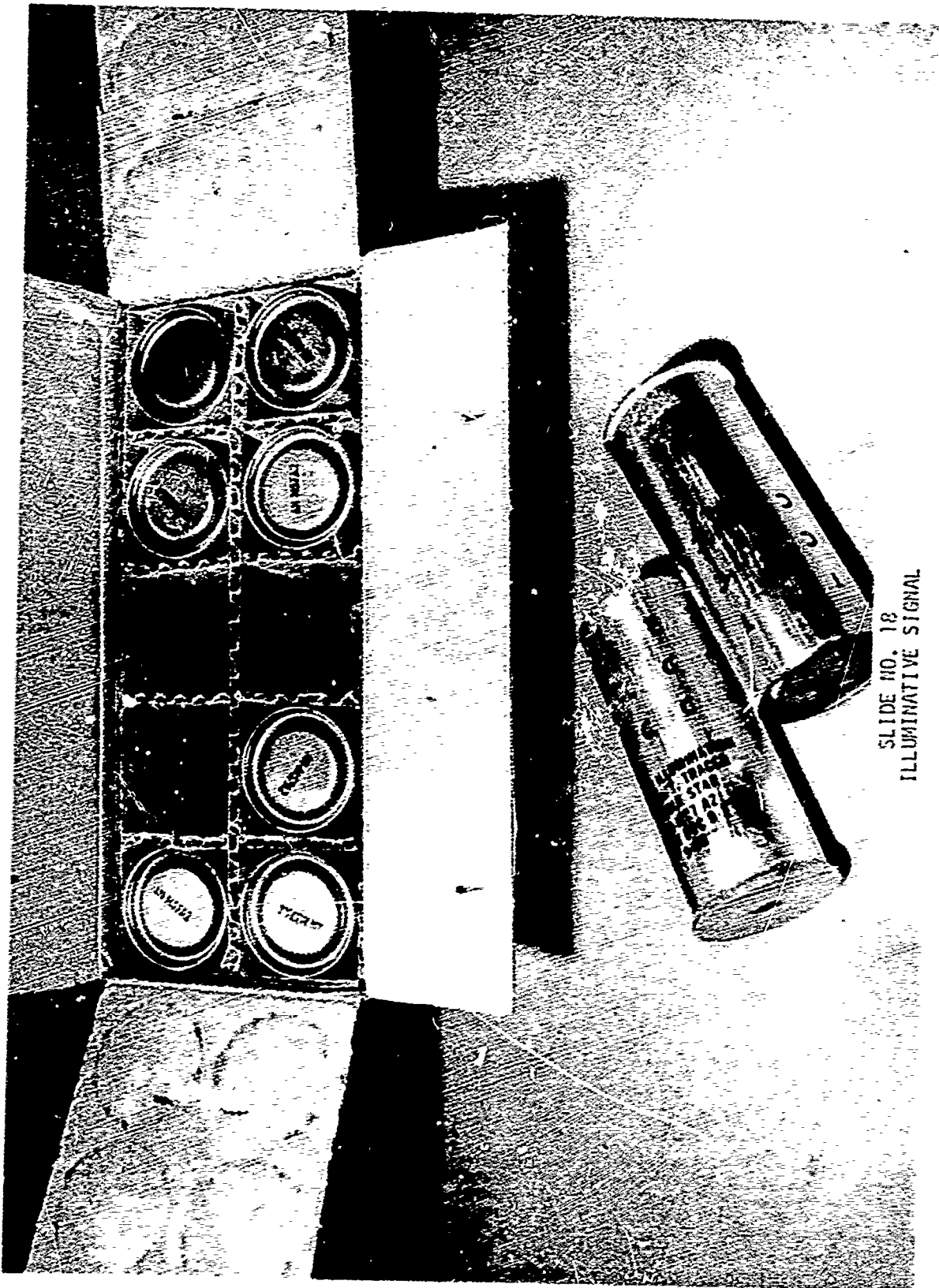
SLIDE NO. 18
ILLUMINATIVE SIGNAL

AMMUNITION COMPONENT BREAKDOWN FOR DEMILITARIZATION/DISPOSAL

NWO-NADC (Single Printing 9/72)

FSN 1305-484-1392

LOT 289C42   ASSY DWG NO 962"21   REV.

FUZE 8 TOTAL WEIGHT	COMPONENT	EXPLOSIVE TYPE	WEIGHT GRAMS	%	INERT MATERIALS		WT (GRAMS)	% OF TOTAL WT
20 MM HEI MK 106 MOD 0	Projectile Mk 12 Mod 0	Incendiary Charge	1.7697	0.661	Projectile, Mk 12	Steel	84.11	31.45
		Mg-Al Alloy	0.814	0.304	Cart Case Mk 5	Steel	115.40	42.40
Total Weight 267.48 GM with the following components		Ba(NO3)2	0.848	0.317	Fuze, Mk 78 Mod 0			
		Abrasive Alum	0.069	0.023	Windshield	Al Alloy	0.26	0.10
		Graphite	0.018	0.007		2s,3s		
Proj., Mk 12 Mod 0		Burster Charge			Firing Pin	Al Alloy	0.19	0.07
Cart. Case, Mk 5 Mod 0		Tetryl	5.280T	1.973		24st		
Fuze, Mk 78 Mod 0			5.174	1.934	Snap Ring	Steel	0.01	Neg
Primer, Mk 47 Mod 0		Binder	0.105T	0.039		ASTM 228-41		
		Graphite	0.013	0.003	Rotor Housing	Al Alloy	4.22	1.58
		Ba,Ca Stearates	0.092	0.034	Rotor	Brass	1.93	0.72
	Cartridge Case Mk 5 Mod 0	Nitrocellulose	40.993	15.325		Fed QQ-B-637 Hard, Alloy 485		
		Basic PbCO3	0.307	0.115				
		K2SO4	0.410	0.153	Set-Back Block	Brass	0.58	0.22
		Diphenylamine	0.410	0.153		1/2 Hard ASTM B16, B21		
	Fuze Mk 78 Mod 0 Booster	Tetryl	0.352	0.132	Lead Disc	Brass	1.34	0.50
						1/2 Hard ASTM B16, B21		
	Lead Detonator Mk 56 Mod 0	Tetryl	0.037	0.014	Lead Cup	Copper	0.03	0.01
		Lead Azide	0.046	0.017		ASTM B152 Type ETP, OHP		
		Tetryl	0.023	0.009				
		Lead Azide	0.024T	0.009T				
		KClO3	0.008	0.003				
		Sb2S3	0.008	0.003	Magazine	Brass	10.12	3.78
		Lead Azide	0.007	0.003		Fed QQ-B-637		
		Carborundum	0.001	Neg		Alloy 464		
	Primer Mk 47 Mod 0	Lead Styphnate	0.065	0.024				
		Barium Nitrate	0.070	0.026				
		Calcium Silicide	0.023	0.009				

SLIDE NO. 19

851

AMMUNITION COMPONENT BREAKDOWN FOR DEMILITARIZATION/DISPOSAL

FSN 1305-494-1392

9ND-NADC (Single Printing 9/72)

LD# 3'9(\42

ASSY DWG. NO. 982121   REV.

FUZE 6 TOTAL WEIGHT	EXPLOSIVE			INERT MATERIALS	WT (GRAMS)	% OF TOTAL WT
COMPONENT	TYPE	WEIGHT GRAMS	%			
	Acetylene Black	0.002	0.001	Fuze Mk 78 Mod 0 (cont.)		
	Gum Arabic	0.002	0.001	Disc Hard	10.12	3.78
	Trinitro-Resorcinol	0.002	0.001	Shear Wire Paper	Neg.	
				Coating Comp. MIL-C-450	Neg.	
				Sealing Comp. MIL-S-22473		
				Ink Fed TT-I-558		
				Pettman Cem. JAN-C-99		
				Paint JAN-P-450		
				Detonator Mk 56		
				Cup Al Alloy 2s, 3s	0.04	0.02
				Disc Al Alloy 2s, 3s	Neg.	
				Varnish MIL-V-16399		
				Primer Mk 47 Mod 0		
				Cup Brass Sheet Fed QQ-B-613 Comp 2	0.53	0.20
				Button Brass 1/4 Hard MIL-B-50	0.51	0.15
				Cup Support Gliding Metal JAN-G-439	0.36	0.14
				Insulator inyl Chloride Polymer	0.02	0.01
				Disc Foil	Neg.	
				Shellac Fed TT-S-271		

SLIDE NO. 20

852

AMMUNITION COMPONENT BREAKDOWN FOR DEMILITARIZATION/DISPOSAL

NWC-NAOC (Single Printing 9/72)

FSN 1305-484-1392

LD# 2890048

ASSY DWG. NO. 962521   REV.

FUZE & TOTAL WEIGHT	EXPLOSIVE			INERT MATERIALS	WT (GRAMS)	% OF TOTAL WT
COMPONENT	TYPE	WEIGHT GRAMS	%			
		TOTAL WEIGHTS AND PERCENTAGES OF MATERIALS USED IN MORE THAN ONE COMPONENT				
	Tetryl	5.586	2.069	Steel	197.52	73.84
	Lead Azide	457	.171	Aluminum	4.71	.77
	Barium Nitrate	.918	.343	Brass	15.01	5.61
	Graphite	.031	.012			

SLIDE NO. 21

853

ENERGETIC MATERIALS CONTAINED IN VARIOUS AMMUNITION ITEMS BURNED IN THE DEMIL FURNACE

- SMOKELESS POWDER (SINGLE & DOUBLE BASE)
- PRIMERS (MERCURY FULMINATE) (LEAD AZIDE)
- TETRYL
- TNT
- COMPOSITION B
- PENTOLITE
- TRACER MIX (ALUMINUM, SODIUM NITRATE, STRONTIUM, ETC.)
- INCENDIARY MIX (MAGNESIUM, SODIUM NITRATE, ETC.)
- LEAD AZIDE (INITIATORS)
- BLACK POWDER

SLIDE NO. 22

EXPECTED/POTENTIAL PRODUCTS OF
COMBUSTION AND REACTION PRODUCTS
RESULTING FROM THERMAL DEACTIVATION/
DEGRADATION IN THE ROTARY DEMIL FURNACE

GASEOUS EMISSIONS:

- NITROGEN OXIDES
- SULPHUR OXIDES
- PHOSGENE GAS
- OZONE
- LEAD VAPOR
- CADMIUM VAPOR
- MERCURY VAPOR
- AMMONIA
- HCL
- H_2SO_4
- HYDRO CARBONS
- HYDROGEN SULFIDE
- CARBON OXIDES

PARTICULATE EMISSIONS:

- OXIDES OF MAGNESIUM
- OXIDES OF ALUMINUM
- OXIDES OF LEAD
- OXIDES OF COPPER
- PHOSPHATES
- POTASSIUM CONTAINING COMPOUNDS
- BARIUM CONTAINING COMPOUNDS
- STRONTIUM CONTAINING COMPOUNDS
- ANTIMONY CONTAINING COMPOUNDS

EPA AMBIENT AIR QUALITY STANDARDS[1]

	PRIMARY	SECONDARY
PARTICULATES		
MICROGRAMS/M^3		
ANNUAL GEO MEAN	75	60
MAX. 24 HR. CONC.*	260	150
SULFUR OXIDES		
MICROGRAMS/M^3		
ANNUAL ARITH. AV.	80 (.03 ppm)	60 (.02 ppm)
MAX. 24-HR. CONC.*	365 (.14 ppm)	260 (.1 ppm)
MAX. 3-HR. CONC.*		1,300 (.5 ppm)
CARBON MONOXIDE		
MILLIGRAMS/M^3		
MAX. 8-HR. CONC.*	10 (9 ppm)	10
MAX. 1-HR. CONC.*	40 (35 ppm)	40
PHOTOCHEMICAL OXIDANTS		
MICROGRAMS/M^3		
ONE-HR. MAX.*	160 (.08 ppm)	160
HYDROCARBONS		
MICROGRAMS/M^3		
MAX. 3-HR. CONC.*		
6-9 AM	160 (.24 ppm)	160
NITROGEN OXIDES		
MICROGRAMS/M^3		
ANNUAL ARITH. AV.	100 (.05 ppm)	100

* Not to be exceeded more than once a year.

1 EPA standards of May 1971. Primary standards to be enforced by summer, 1975; secondary standards have no time limit on enforcement.

EPA SOURCE STANDARDS

STATIONARY SOURCE

POLLUTANT	GENERATOR	INCINERATOR	HNO_3 PLANT	H_2SO_4 PLANT
VISIBLE EMISSIONS, % OPACITY (MAX)	20'	-	10	10
PARTICULATES (MAX 2 HR AV)	0.10 LBS/10^6 BTU	0.080 GR SCF*	-	-
SO_2 (MAX 2 HR AV)				
OIL	0.80 LBS/10^6 BTU	-	-	4 LBS/TON
COAL	1.2 LBS/10^6 BTU			
NO_x (MAX 2 HR AV)				
GAS	0.20 LBS/10^6 BTU	-	3.0 LBS/TON	-
OIL	0.30 LBS/10^6 BTU	-		
COAL	0.70 LBS/10^6 BTU	-		
ACID MIST (MAX 2 HR AV)	-	-	-	0.15 LBS/TON

*40% PERMITTED FOR 2 MIN IN ANY HR

•CORRECTED TO 12% CO_2

SLIDE NO. 25

857

AIR QUALITY CRITERIA

Component	EPA & INDIANA STANDARDS		APSA GUIDELINES
	PRIMARY	SECONDARY	BOUNDARY (ppm)
Particulates, µg/m³	75 (Annual Geometric Mean) 260 (Max. 24 hr conc)[a]	60 150	80 (Process Source) 80 (Incinerator)
Sulfur Oxides, ppm::µg/m³	0.03::80 (Annual Arith Mean) 0.14::365 (Max. 24 hr conc)[a] -- (Max. 3 hr conc)[a]	0.02::60 0.1::260 0.5::1300	0.04[b] (Power Plant) 0.04[b] (Acid Plant)
Carbon Monoxide, ppm::mg/m³	9::10 (Max. 8 hr conc)[a] 35::40 (Max. 1 hr conc)[a]	9 35	0.15
Photochemical Oxidants, ppm... µg/m³	0.08::160 (One hr max.)[a]	0.08	0.04 (Oxidants) 0.03 (Ozone)
Hydrocarbons, p.m.::µg/m³	0.24::160 (Max. 3 hr conc)	0.24	0.20
Nitrogen Oxides, ppm..µg/m³	0.05::100 (Annual Arith Mean)	0.05	0.10[c]

a Not to be exceeded more than 1/yr
b Not to be exceeded over 1% of the time/24 hr sample period
c Not to be exceeded over 1% of time/hr/3 mo.

SLIDE NO. 26

EPA SAMPLING METHODS UTILIZED

- METHOD 1 - VELOCITY TRAVERSE SITE
- METHOD 2 - GAS VOLUME AND VELOCITY
- METHOD 3 - GAS ANALYSIS
- METHOD 4 - MOISTURE
- METHOD 5 - PARTICULATE EMMISIONS
- METHOD 6 - SO_2
- METHOD 7 - NO_x
- METHOD 8 - H_2SO_4
- METHOD 9 - RINGLEMAN OPACITY

SLIDE NO. 27

EPA SAMPLING TRAIN
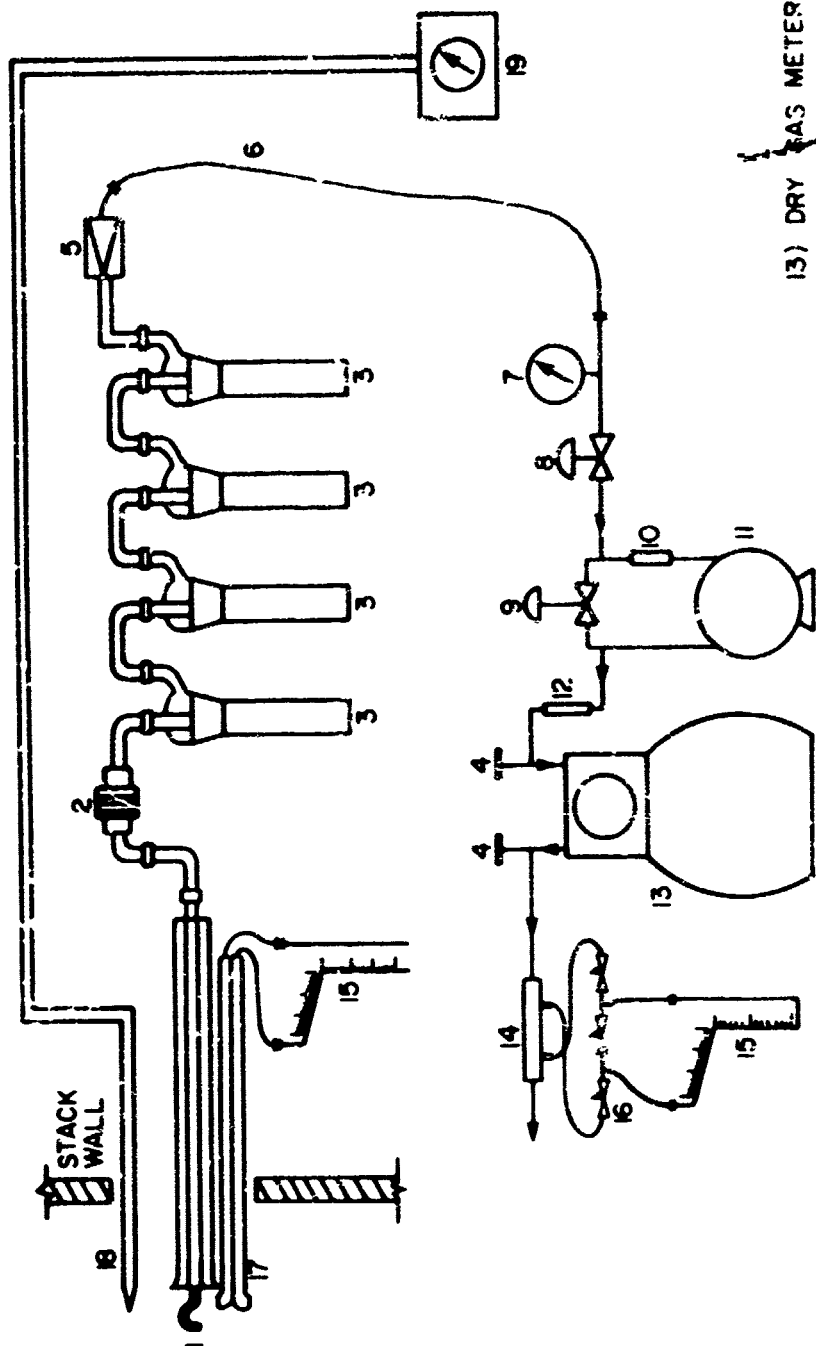
1) PROBE
2) PARTICULATE FILTER
3) IMPINGERS (GREENBURG-SMITH)
4) THERMOMETER
5) CHECK VALVE
6) UMBILICAL CORD
7) VACUUM GAGE

8) COURSE FLOW ADJUST VALVE
9) FINE FLOW ADJUST VALVE
10) OILER
11) VACUUM PUMP
12) FILTER

13) DRY GAS METER
14) ORIFICE TUBE
15) INCLINE MANOMETER
16) SOLENOID VALVES
17) PITOT
18) THERMOCOUPLE
19) PYROMETER

SLIDE NO. 28

860

GAS SAMPLE

RECOVERY & ANALYSIS

GAS BAG NO.3 (12 LITER)
GAS BAG NO.4 (12 LITER)

GAS ANALYSIS -

PHOSGENE GAS
OZONE
LEAD VAPOR
MERCURY VAPOR
AMMONIA
HYDROGEN CHLORIDE
HYDROGEN SULFIDE

GAS BAG NO.1 (70 LITER)

EPA METHOD 3 GAS ANALYSIS
3 REPETITIONS FOR - O_2
CO
CO_2
N_2

1 TEST FOR TOTAL HYDROCARBONS
EPA METHOD 6 SULPHUR DIOXIDE

GAS BAG NO. 2 (70 LITER)

EPA METHOD 7 NITROGEN OXIDE
EPA METHOD 8 SULFURIC ACID MIST
AND SULFUR DIOXIDE

SLIDE NO. 29

861

SAMPLE RECOVERY

TRAIN NO. 1 — CONTAINER NO. 1 – FILTER
CONTAINER NO. 2 – ACETONE WASHINGS – PROBE TIP,
PROBE AND CYCLONE
CONTAINER NO. 3 – SILICA GEL
CONTAINER NO. 4 – CONDENSER WATER

TRAIN NO. 2 — CONTAINER NO. 5 – FILTER
CONTAINER NO. 6 – ACETONE WASHINGS – PROBE TIP,
PROBE AND CYCLONE
CONTAINER NO. 7 – SILICA GEL
CONTAINER NO. 8 – CONDENSER WATER

ANALYSIS — CONTAINER NO. 1 – TOTAL WEIGHT GAIN MG.
SAVE FOR X-RAY DEFRACTION
CONTAINER NO. 2 – TOTAL WEIGHT GAIN MG.
SAVE AS BACK-UP SAMPLE
CONTAINER NO. 3 – TOTAL WEIGHT GAIN MG.
SAVE FOR FUTURE REUSE
CONTAINER NO. 4 – TOTAL WEIGHT GAIN OF CONDENSED
WATER MG.
SAVE AND COMBINE WITH CONTAIN-
ER NO. 8 FOR METALS AA
CONTAINER NO. 5 – TOTAL WEIGHT GAIN MG.
SAVE AND COMBINE WITH CONTAIN-
ER NO. 6 FOR METAL AA
CONTAINER NO. 6 – TOTAL WEIGHT GAIN MG.
SAVE AND COMBINE WITH CONTAIN-
ER NO. 3
CONTAINER NO. 7 – TOTAL WEIGH GAIN MG.
SAVE FOR FUTURE REUSE
CONTAINER NO. 8 – TOTAL WEIGHT GAIN OF CONDENSED
WATER
SAVE AND COMBINE WITH CONTAIN-
ER NO. 6

SLIDE NO. 30

PARTICLE SIZE SAMPLING TRAIN
ANDERSON SIZING HEAD

1 PROBE
2 SIZING HEAD
3 PARTICULATE FILTER
4 IMPINGERS (GREENBURG-SMITH)
5 THERMOMETER
6 CHECK VALVE
7 UMBILICAL CORD
8 VACUUM GAGE
9 COURSE FLOW ADJUST VALVE

10 FINE FLOW ADJUST VALVE
11 OILER
12 VACUUM PUMP
13 FILTER
14 DRY GAS METER
15 ORIFICE TUBE
16 INCLINE MANOMETER
17 SOLENOID VALVES
18 THERMOCOUPLE
19 PYROMETER

STACK WALL

DETAIL A

ANDERSON SIZING HEAD

IMPINGMENT PLATES

THIMBLE

THIMBLE HOLDER

CASING

SLIDE NO. 31

863

SIDE ELEVATION OF STACK SAMPLING ARRANGEMENT

SCAFFOLDING NOT SHOWN

REMOTE CONTROLLED TRAVERSE UNIT

SAMPLING PORT

GAS LINE

26'-0"

12'-0" TO PORT

SLIDE NO. 32

864

SLIDE NO. 33
STACK SCAFFOLDING (SAMPLE PORT PREP)
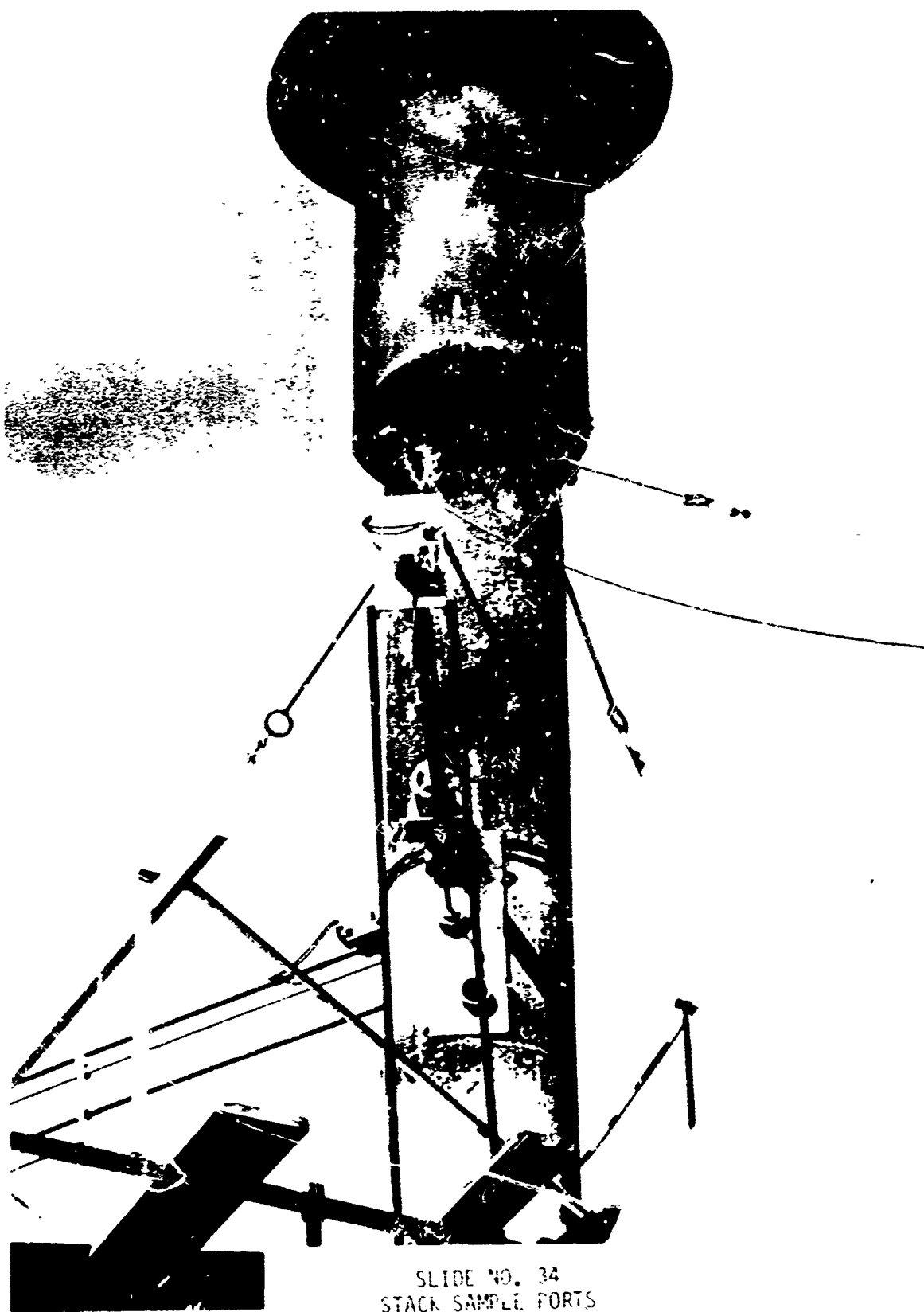
SLIDE NO. 34
STACK SAMPLE PORTS
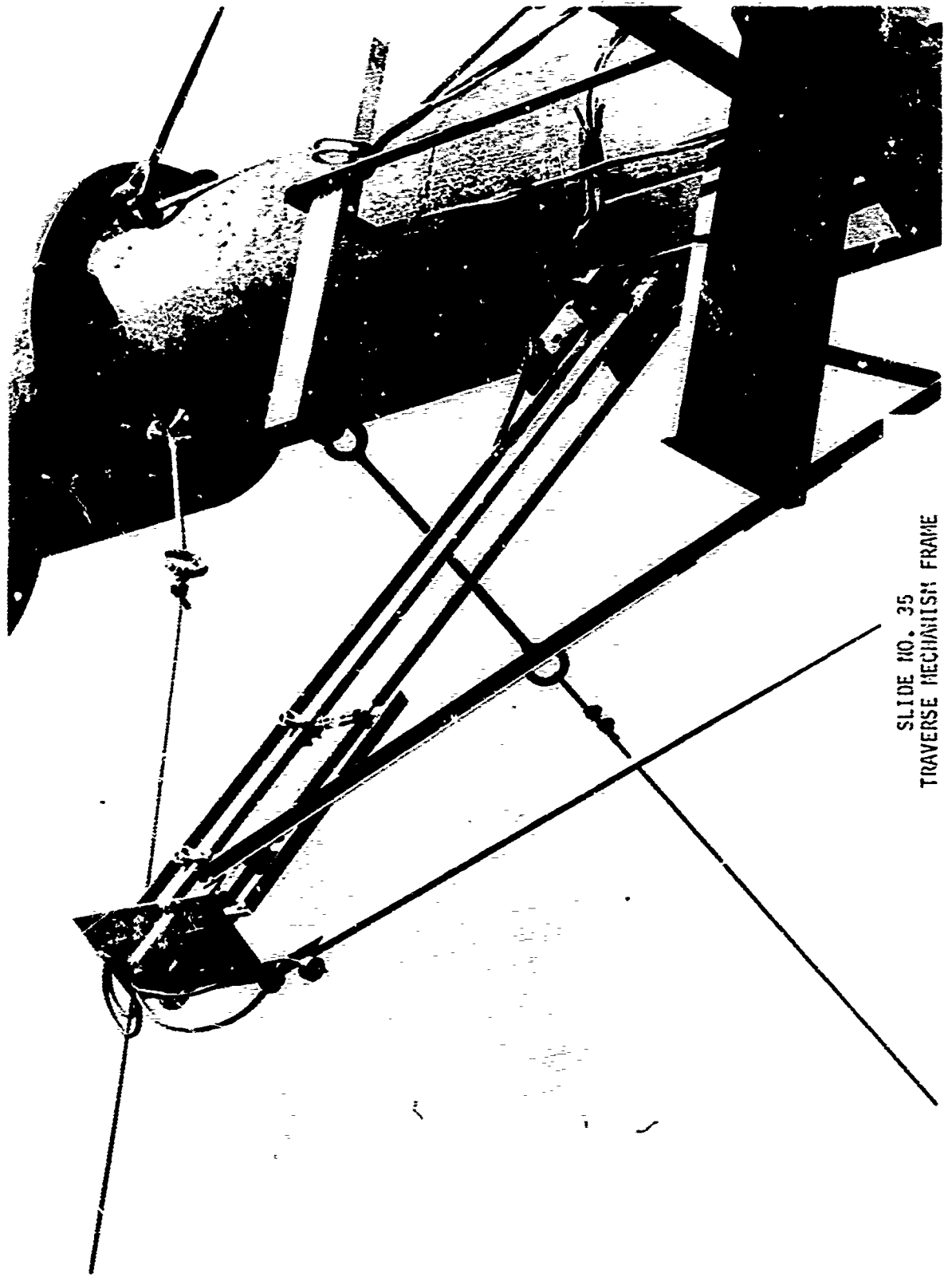
SLIDE NO. 35
TRAVERSE MECHANISM FRAME
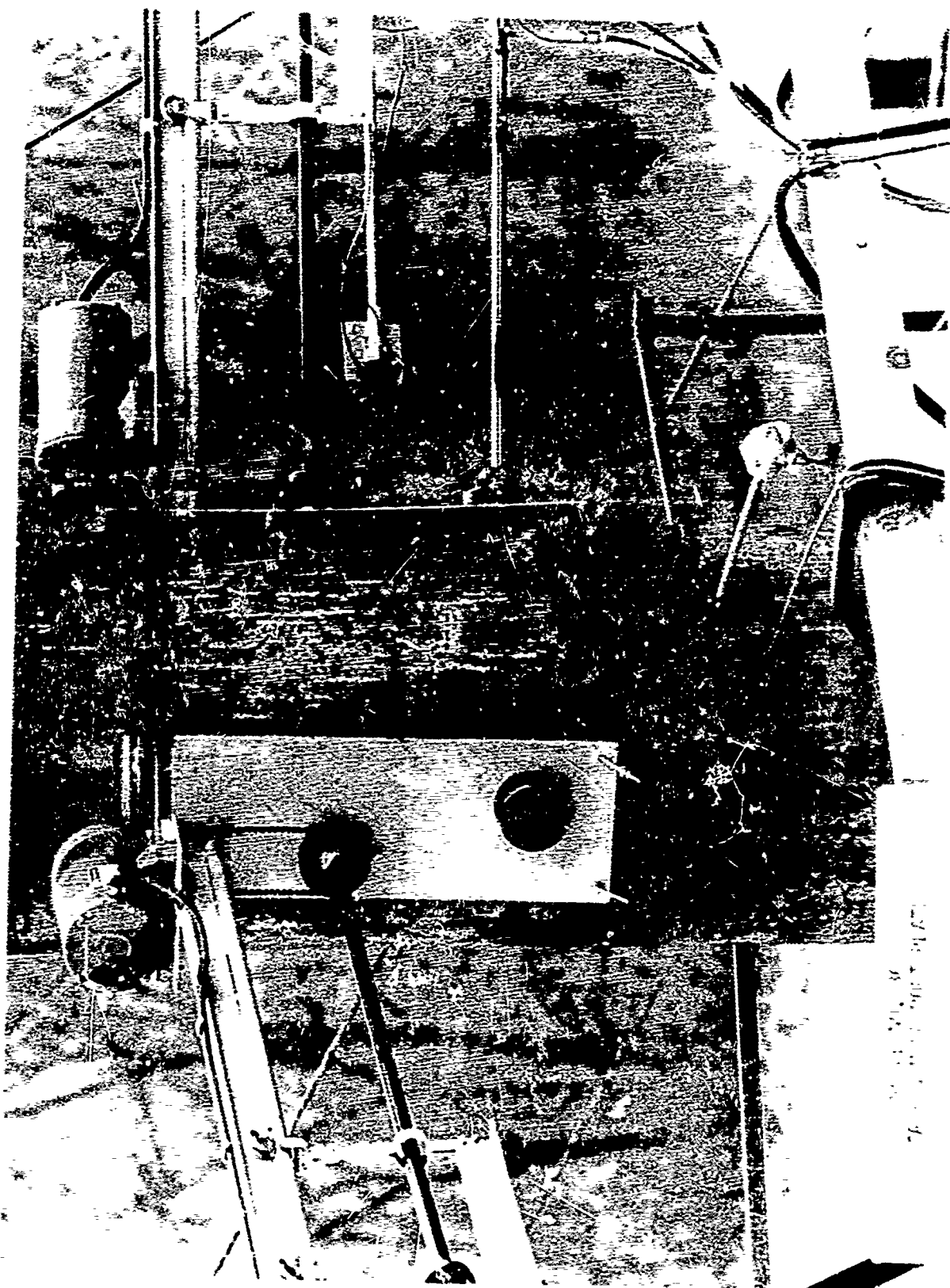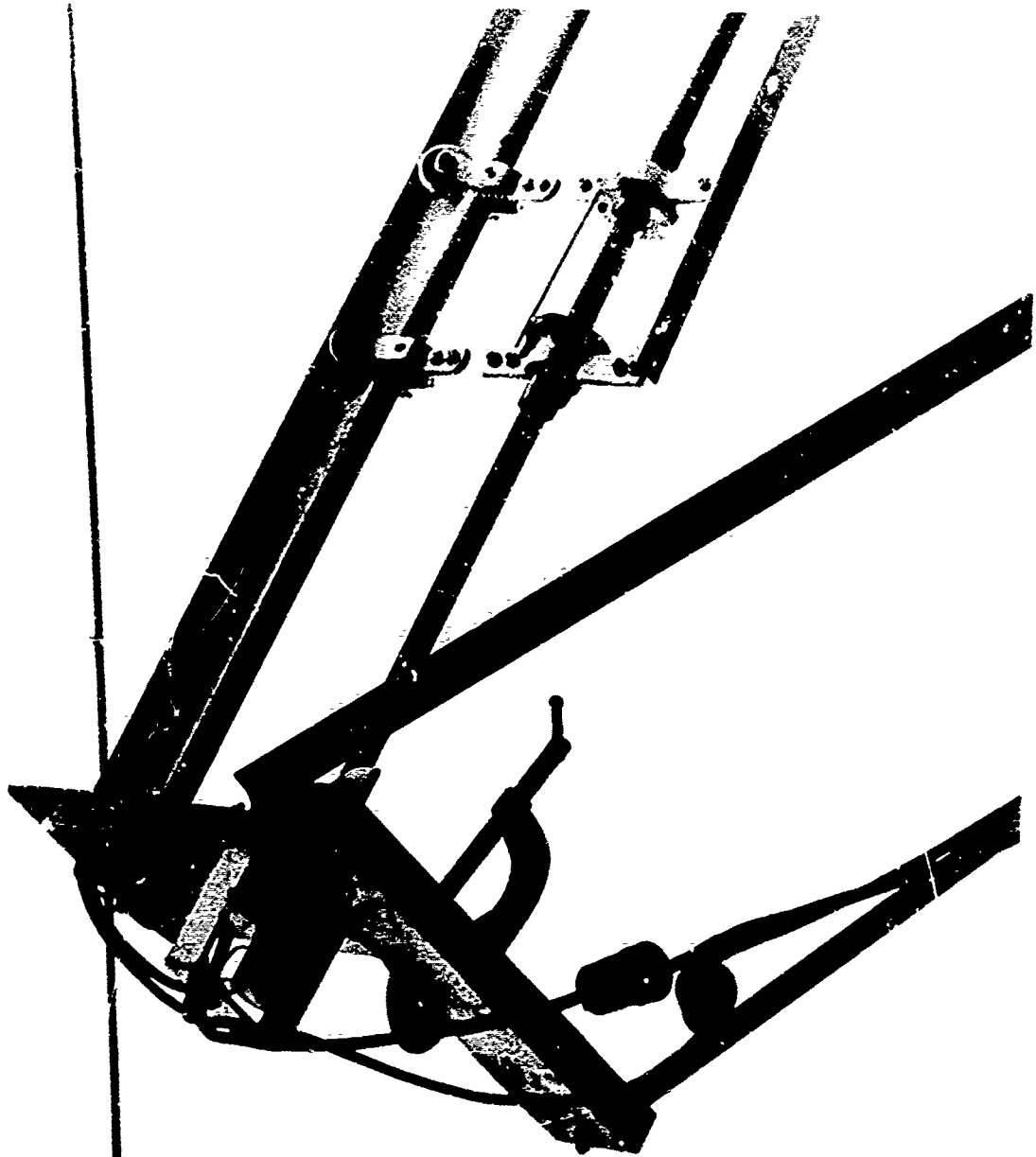
SLIDE NO. 37
TRAVERSE MECHANISM FRAME
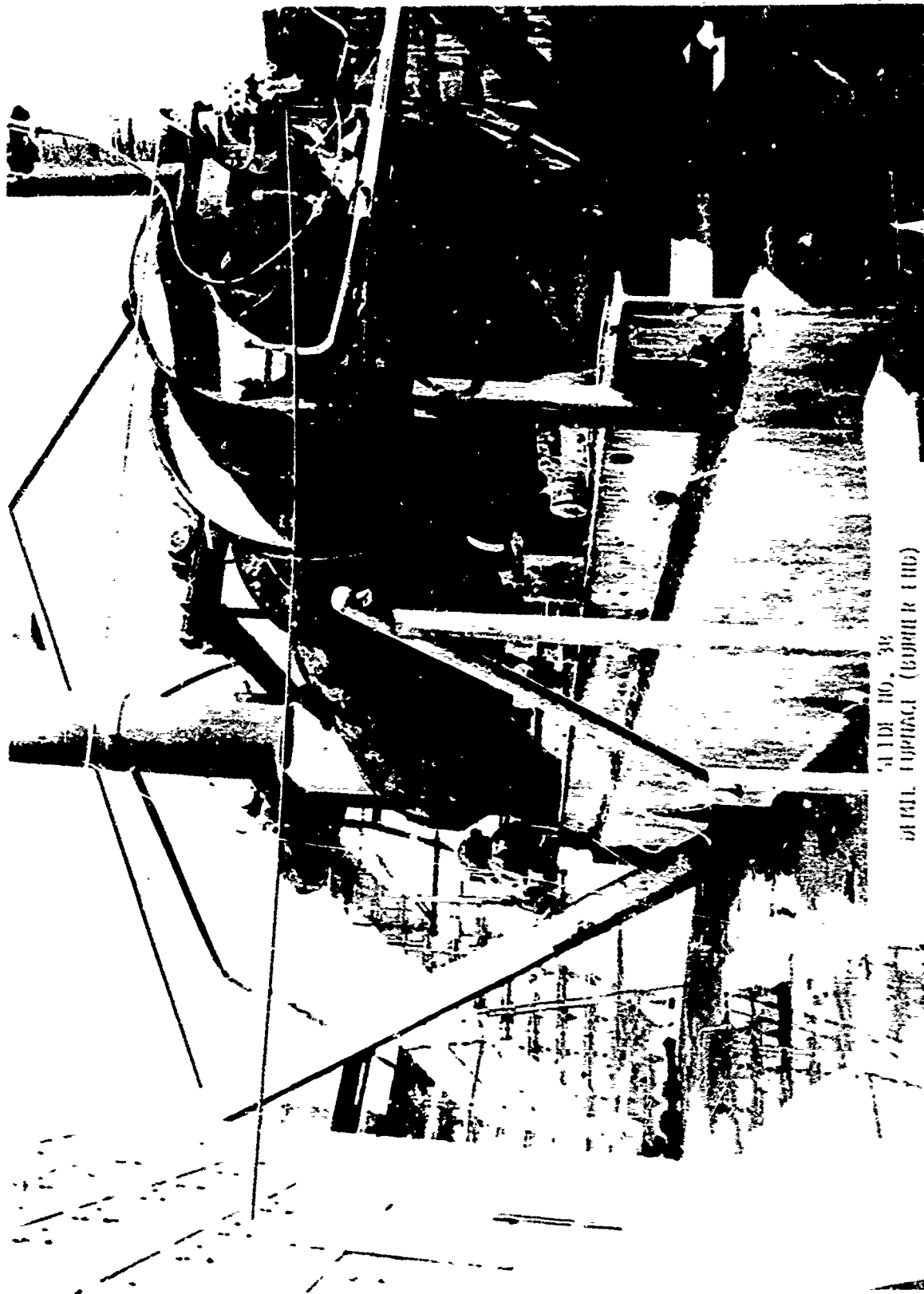
SLIDE NO. 38.
BLAST FURNACE (BURDEN END)

SLIDE NO. 39
DEMIL FURNACE (BURNER EN')

SLIDE NO. 47
PROBE ASSEMBLY

873
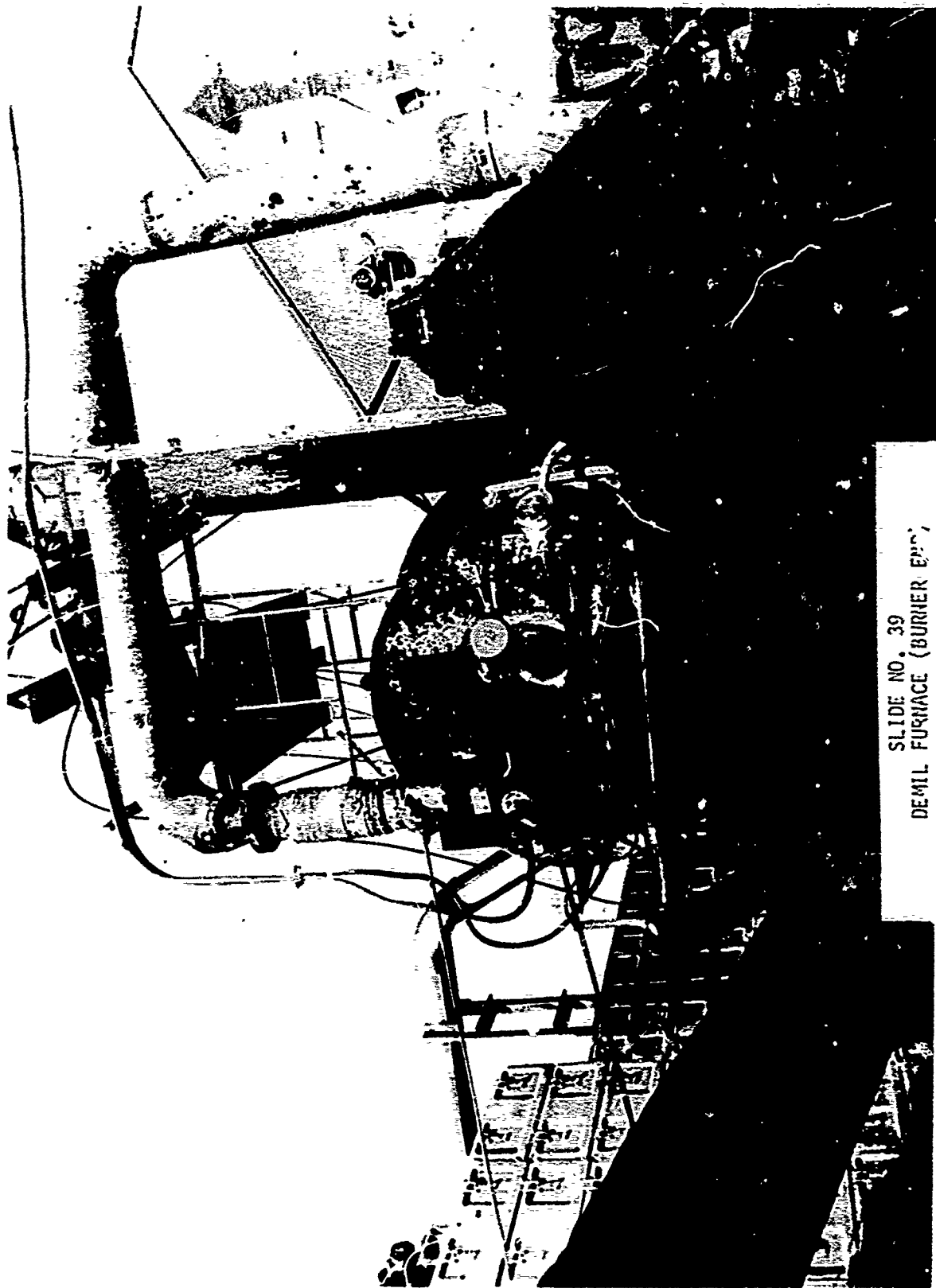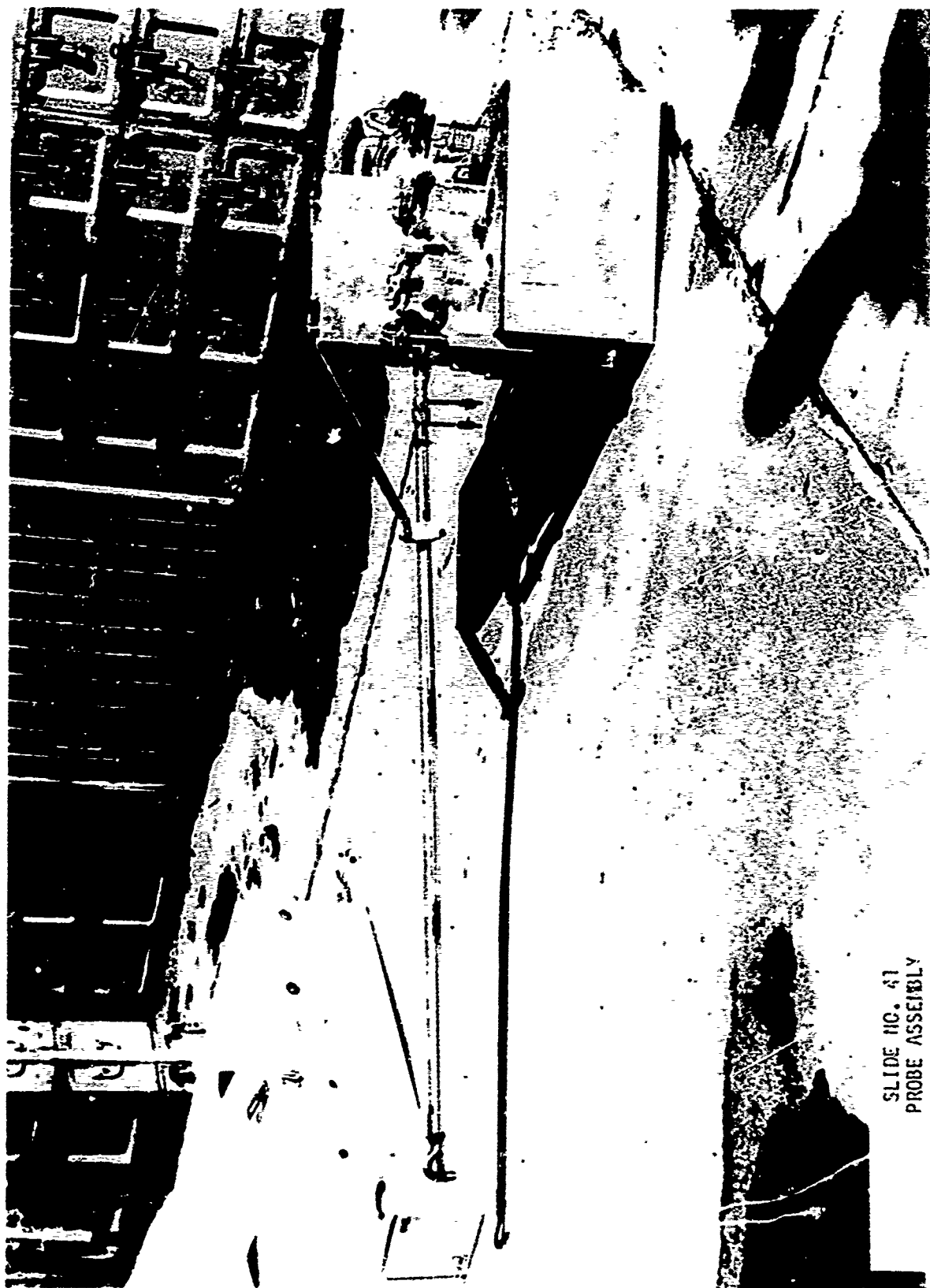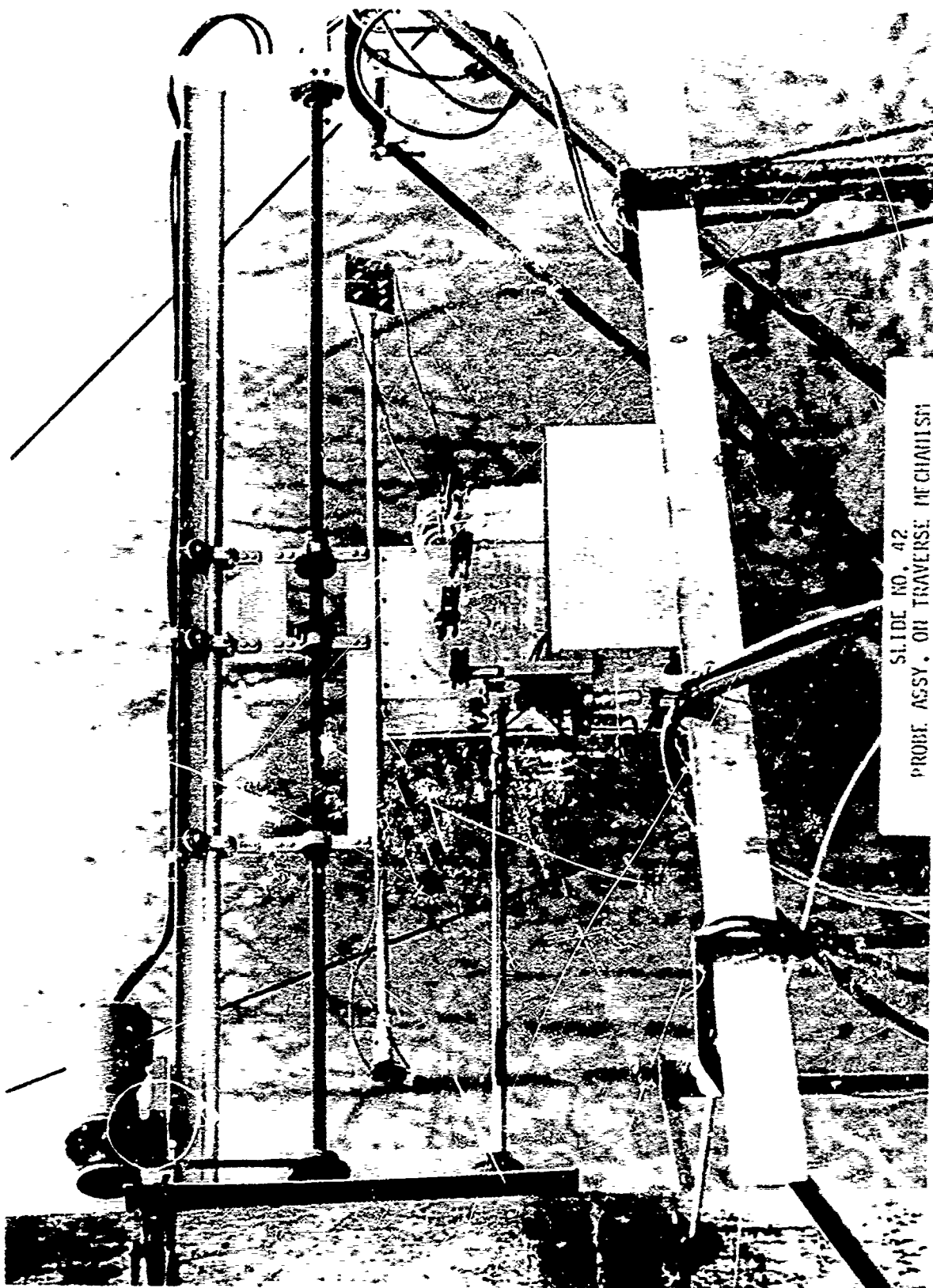
SLIDE NO. 42
PROBE ASSY. ON TRAVERSE MECHANISM
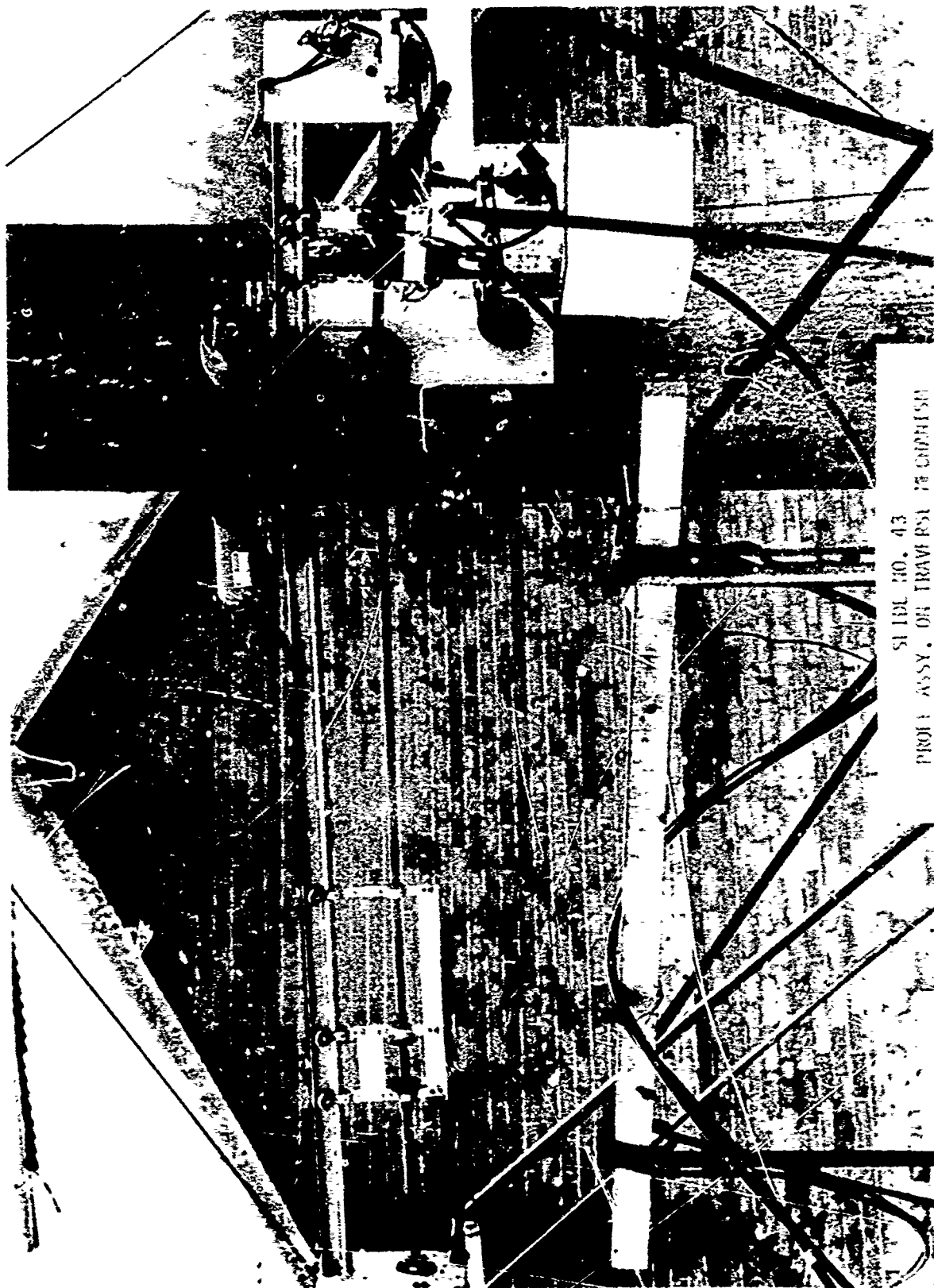
PROBE ASSY. OR TRAVERSE MECHANISM

SLIDE NO. 43

SLIDE NO. 44
PROBE ASSEMBLY ON TRAVERSE ASSY.

876
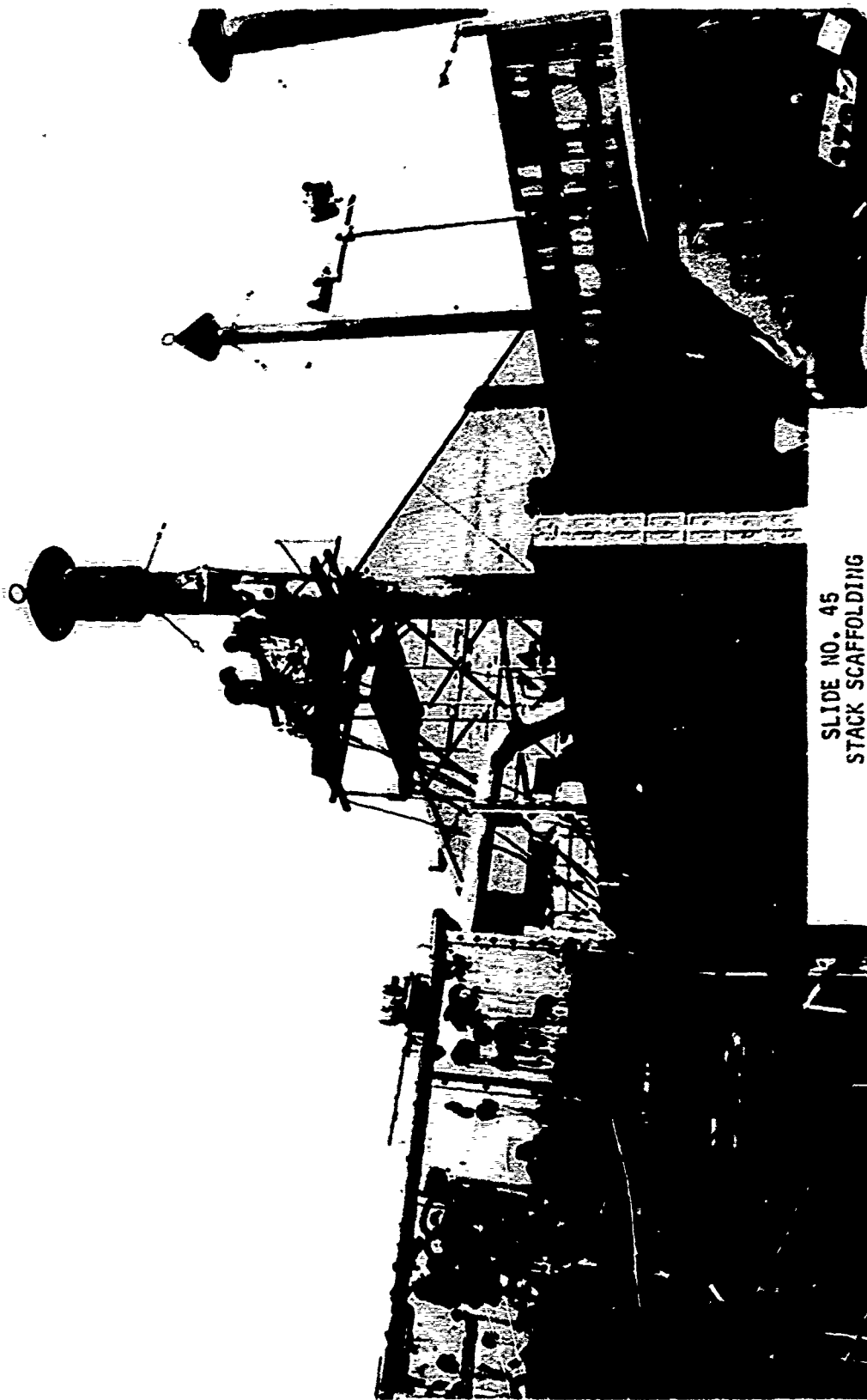
SLIDE NO. 45
STACK SCAFFOLDING

877
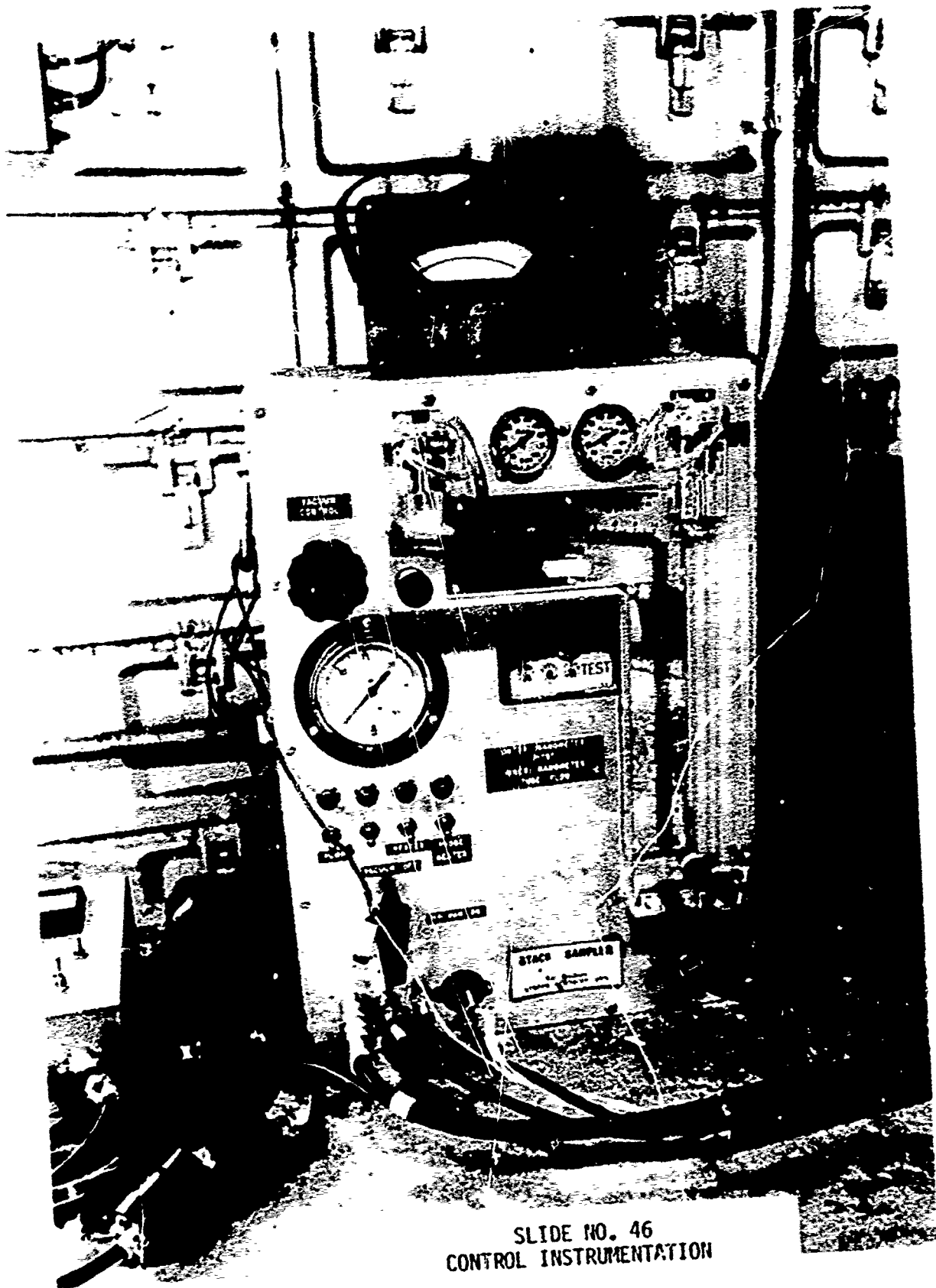
SLIDE NO. 46
CONTROL INSTRUMENTATION

878
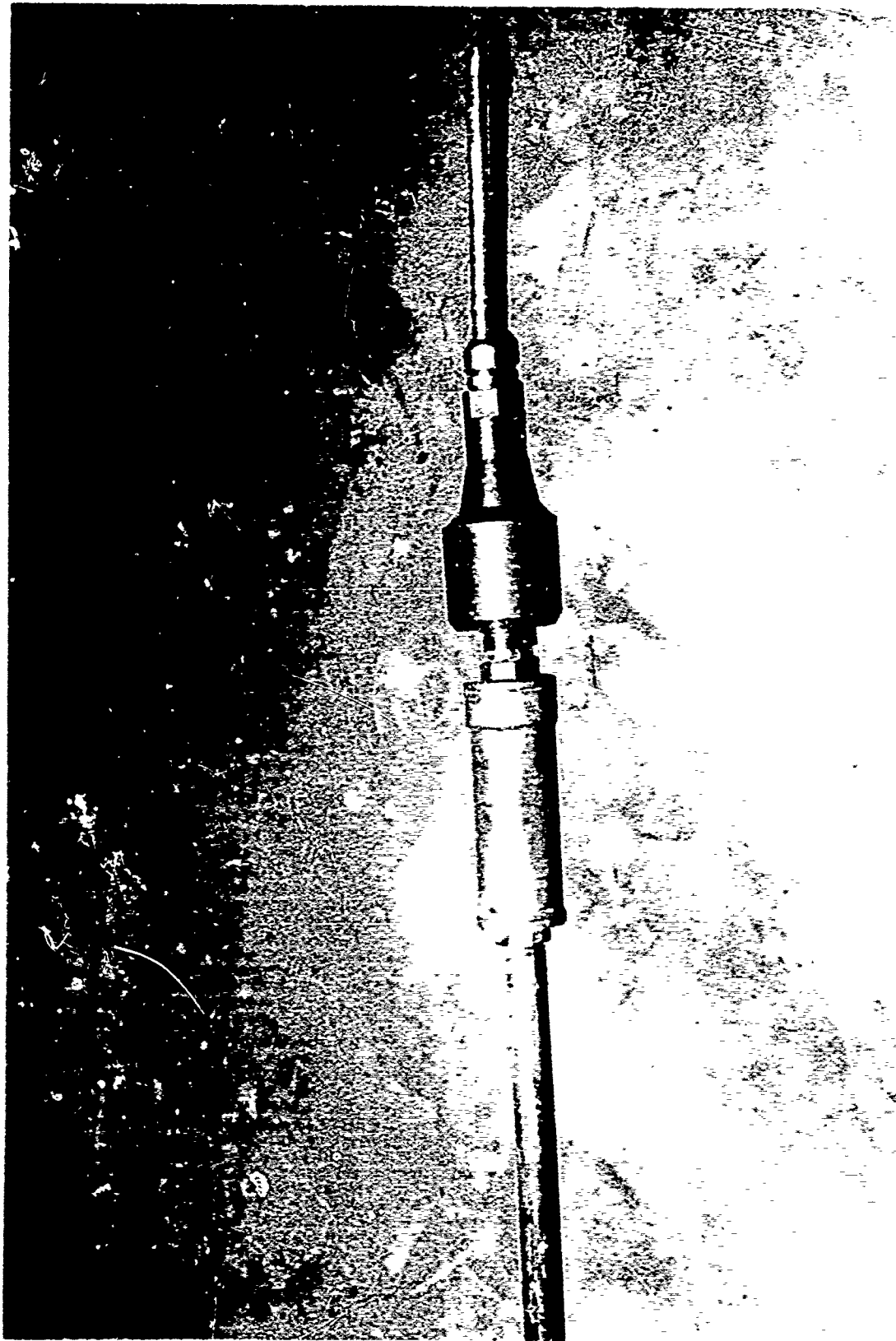
SLIDE NO. 47
ANDERSON SIZING HEAD ASSEMBLY

879
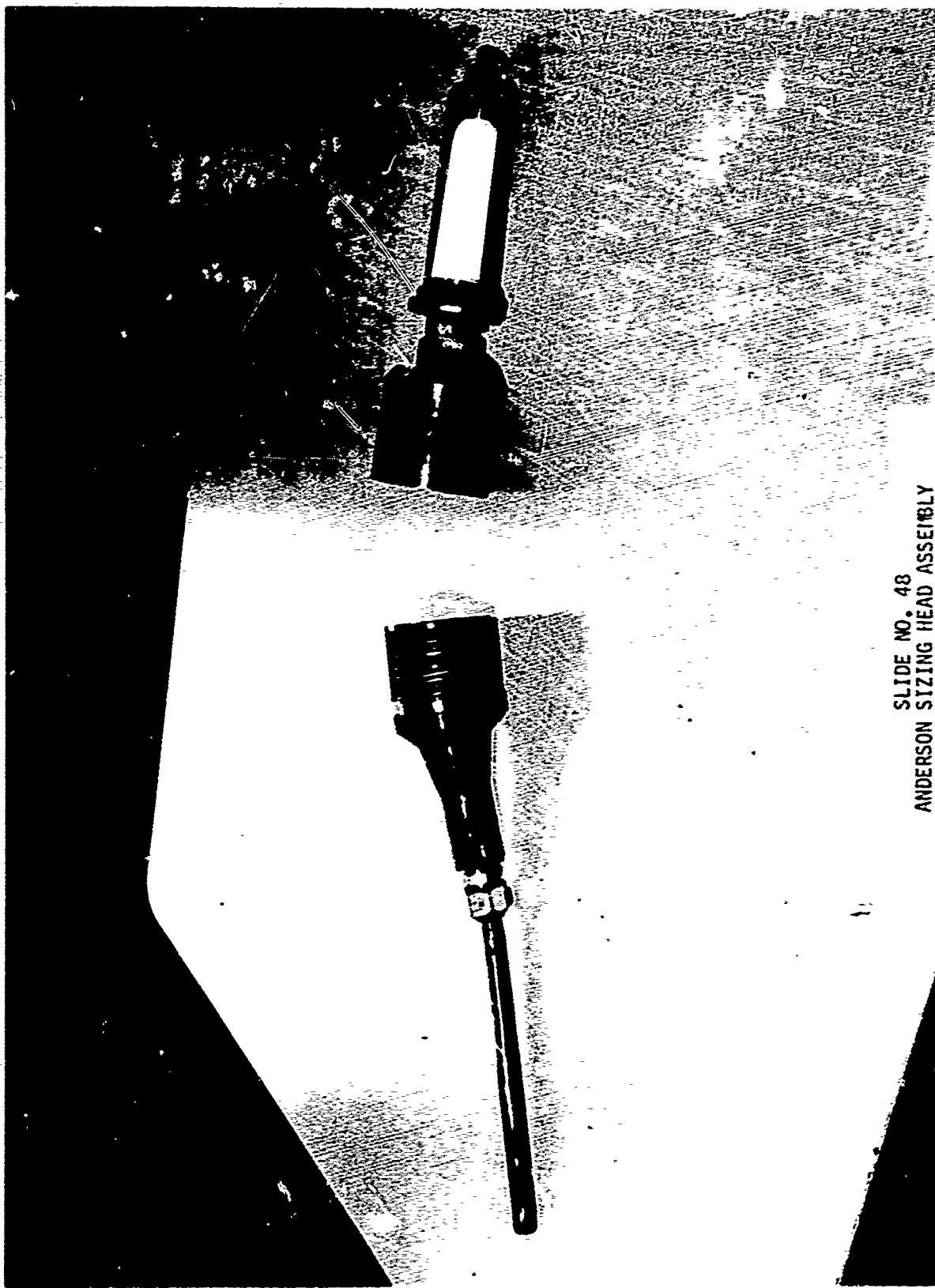
SLIDE NO. 48
ANDERSON SIZING HEAD ASSEMBLY
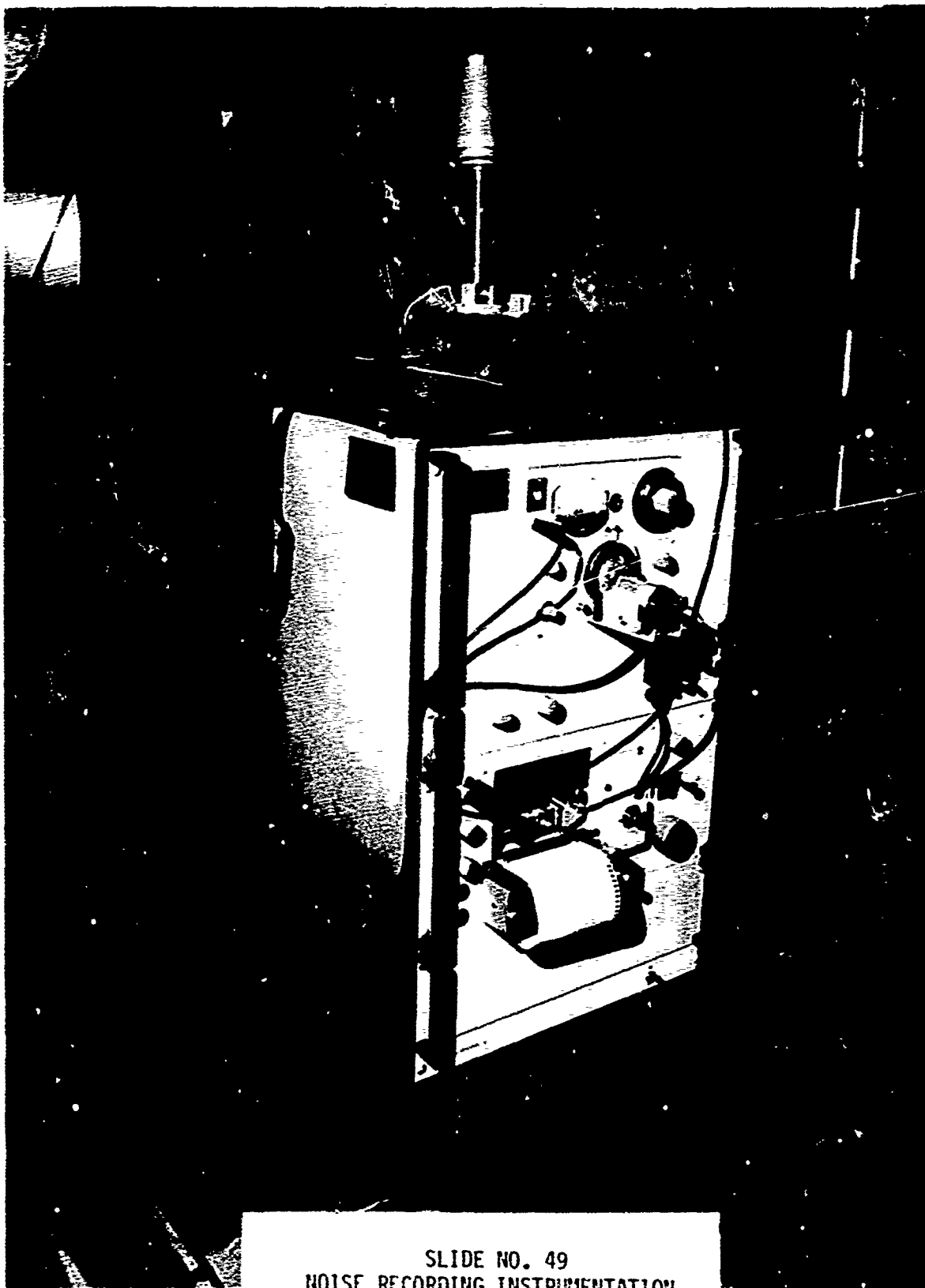
SLIDE NO. 49
NOISE RECORDING INSTRUMENTATION

881
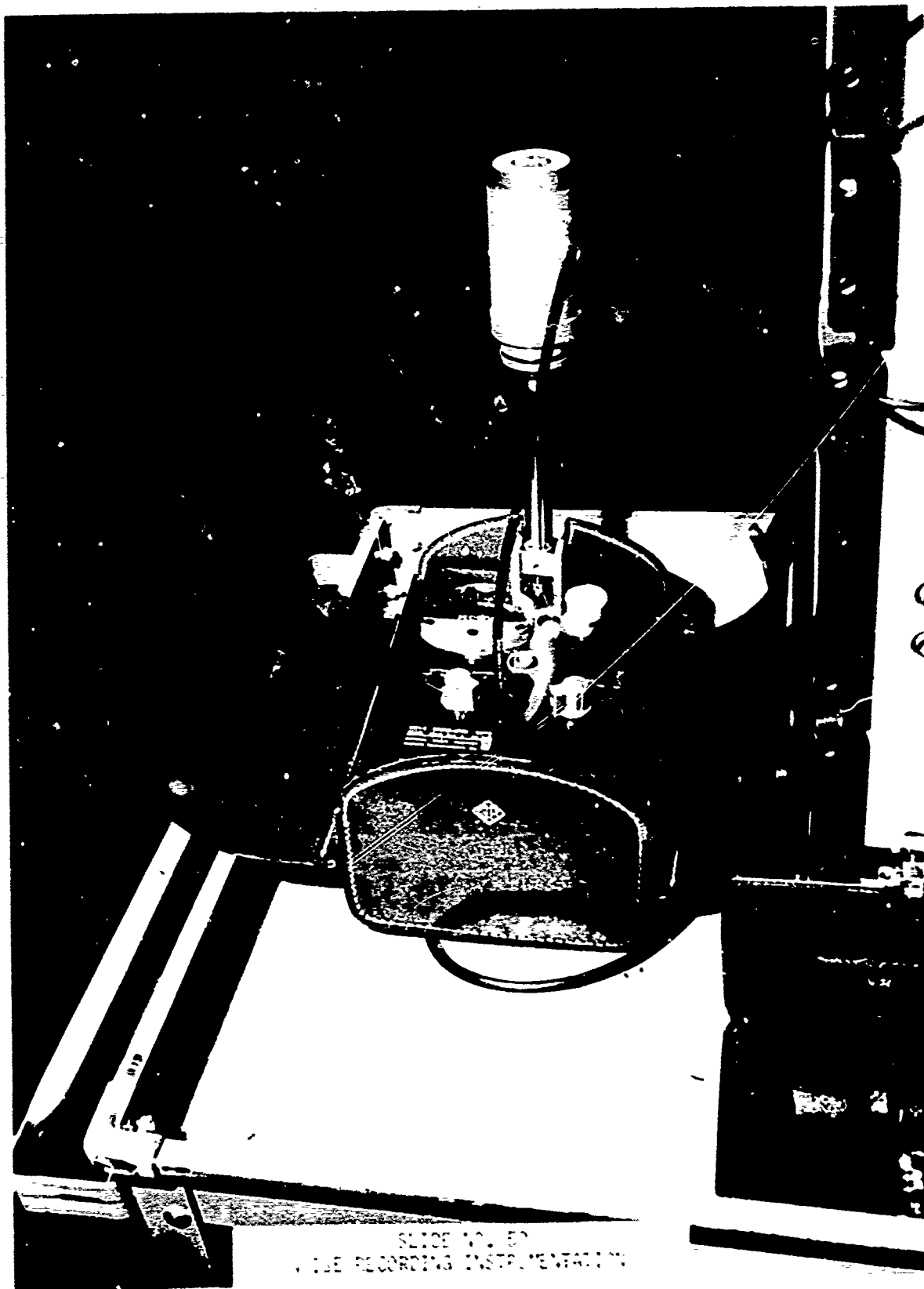
SLIDE NO. 52
THE RECORDING INSTRUMENTATION

NOISE POLLUTION

○ SOUND PRESSURE LEVELS TO BE MEASURED AND RECORDED (IN dB(A), DECIBELS) AT ALL POSITIONS/ LOCATIONS OCCUPIED BY PERSONNEL DURING THE DEMIL OPERATION FOR EACH SPECIFIC MUNITION CHARGED INTO THE FURNACE.

SLIDE NO. 51

SIDE ELEVATION OF STACK SAMPLING ARRANGEMENT

SCAFFOLDING NOT SHOWN

REMOTE CONTROLLED TRAVERSE UNIT

26'-0"

16'-0" TO PORT

SAMPLING PORT

GAS LINE
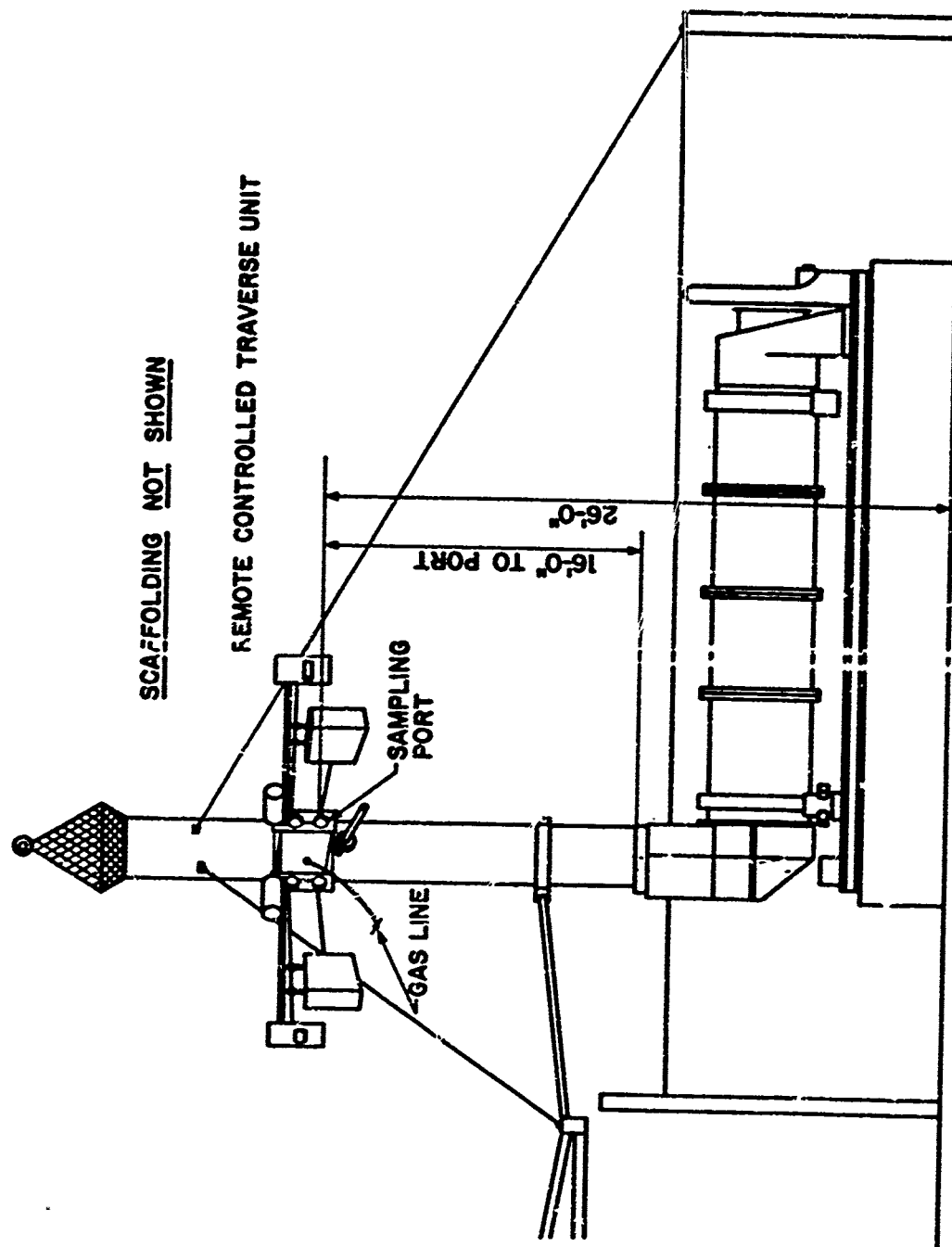
SLIDE NO. 52

THE SPECIFIC SAMPLING PLAN CONSISTED OF

TAKING 6 EMISSION SAMPLES WITH THE FOLLOWING

MATERIAL BEING CHARGED INTO THE FURNACE

SAMPLE	RATE (UNITS/MIN.)
(1.) FURNACE BACKGROUND ONLY (NO AMMUNITION CHARGED)	0
(2.) .50 CAL	175
(3.) 20 mm HE I PROJECTILES	80
(4.) PYRO ILLUMINATING SIGNALS	10
(5.) IMPULSE CARTRIDGES & EXPLOSIVE BOLTS	50
(6.) PROJECTILE FUZES	7

SLIDE NO. 53

885

ACTUAL DATA SHEET FOR METHOD NO.1 TEST
VELOCITY TRAVERSE SITE & GAS VELOCITY

CHARGE - 50 CALIBER
FEED RATE - 175 PER MIN.

<u>VELOCITY TRAVERSE</u>

RUN NO. __4__   DATE __18 DECEMBER 1972__
BAROMETRIC PRESSURE, In. Hg. __29.74__
STATIC PRESSURE IN STACK __(Pg), In Hg. 0.05__
STACK DIAMETER __24 In.__

CROSS SECTION AREA, FT² __3.14__

SEE SKETCH

STACK CROSS SECTION | SCHEMATIC OF STACK ELEVATION VIEW
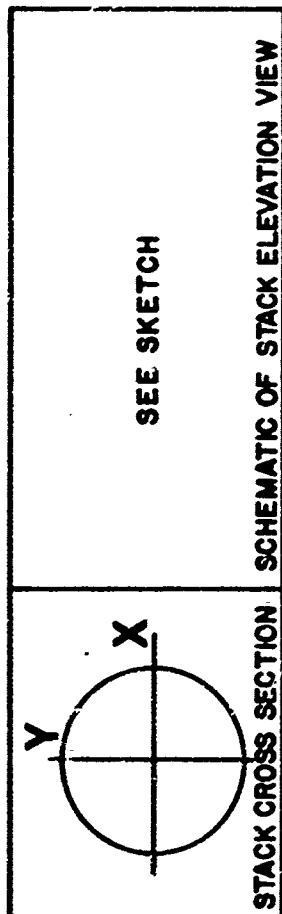
X TRAVERSE (NORTH)

TRA. PT. NO.	VEL. HD. IN. H₂O	√ΔP	STACK TEMP.
1	0.05	.224	280°F
2	0.06	.245	280°F
3	0.06	.245	275°F
4	0.06	.245	280°F
5	0.05	.224	275°F
6	0.05	.224	280°F
		1.407	
AVERAGE		.234	

ΔP AVE. X & Y = .241

Y TRAVERSE (SOUTH)

TRA. PT. NO.	VEL. HD. IN. H₂O	√ΔP	STACK TEMP.
1	0.05	.224	290°F
2	0.06	.245	290°F
3	0.07	.265	300°F
4	0.07	.265	305°F
5	0.06	.245	305°F
6	0.06	.245	300°F
		1.489	
AVERAGE		.248	

SLIDE NO. 54

886

ACTUAL DATA SHEET FOR METHOD NO.1 TEST VELOCITY TRAVERSE SITE & GAS VELOCITY

CHARGE - 50 CALIBER

PARTICULATE TRAVERSE

DATE 18 DECEMBER 1982
RUN NO. 4

AMBIENT TEMPERATURE 25°F
BAROMETRIC PRESSURE 29.74 In. Hg.
ASSUMED MOISTURE % 3
PROBE LENGTH, FT. 4.0
NOZZLE DIAMETER, IN. 0.375

TRAV. PT. NO.	SAMP. TIME (o) min.	STAT. PRESS. (Ps) In. Hg.	STACK TEMP. (Ts) °F	VELOC. HEAD (Ps)	ΔP ORIFICE METER (H) in. H₂O	GAS SAMP. VOL. (Vm) ft.3	GAS SAMP. TEMP. AT DRY GAS MTR. INLET (Tm_in)°F	OUTLET (Tm_out)°F	SAMP. BOX TEMP. °F	TEMP OF GAS LEAVING CONDS. OR LAST IMPING. °F
Y 1	5	0.05	290	0.05	1.02	2.42	60	55	220	70
2	5	0.05	290	0.06	1.23	2.65	63	57	220	70
3	5	0.05	300	0.07	1.42	2.86	66	59	220	70
4	5	0.05	305	0.07	1.42	2.88	69	61	220	70
5	5	0.05	305	0.06	1.23	2.67	72	63	220	70
6	5	0.05	300	0.00	0.23	2.69	75	65	220	70
X 1	5	0.05	280	0.05	1.02	2.40	60	55	220	70
2	5	0.05	280	0.06	1.23	2.87	67	58	220	70
3	5	0.05	275	0.06	1.23	2.64	66	60	220	70
4	5	0.05	280	0.06	1.23	2.69	69	67	220	70
5	5	0.05	275	0.05	1.02	2.71	73	64	220	70
6	5	0.05	280	0.05	1.02	2.40	75	65	220	70
TOTAL	60					31.89	AVG.68	AVG.61		
AVERAGE		0.05	288	0.06	1.19		AVG. 65		220	70

SLIDE NO. 55

887

ACTUAL DATA SHEET FOR METHOD NO.1 TEST
VELOCITY TRAVERSE SITE & GAS VELOCITY

VELOCITY STACK GASES

ACTUAL CONDITIONS   (STACK TEMPERATURE AND PRESSURE)

$$(VS)Ave = KpCp(\sqrt{\Delta P})Ave. \sqrt{\frac{(Ts) Ave}{PsMs}}$$

WHERE:

$(Vs)Ave$ = STACK GAS VELOCITY, FEET PER SECOND, FT/SEC

Kp = 85.48 FT/SEC$(\frac{LB}{LB\ MOLE\ °R})^{1/2}$

Cp = PITOT TUBE COEFFICIENT, DIMENSIONLESS.

= 0.92 IN VELOCITY RANGE OF THIS TEST.

$(Ts)Ave$ = AVERAGE ABSOLUTE STACK GAS TEMPERATURE °R

$(\sqrt{\Delta P}Ave$ = AVERAGE VELOCITY HEAD OF STACK GASES, INCHES H2O.

Ms = MOLECULAR WEIGHT OF STACK GAS (WET BASIS) LB/LB - MOLE

Ps = ABSOLUTE STACK GAS PRESSURE, INCHES HG.

RUN	TYPE OF CHARGE	(Ts) Ave °R	Ps In. HG.	(√ΔP)Ave In. H2O	Ms Lb/Lb Mole	(Vs) Ave Ft/Sec
1	FURNACE BACKGROUND	753	29.84	0.194	28.52	14.33
2	FUSES	765	29.91	0.248	28.55	18.45
3	FLARES	759	29.87	0.248	28.52	18.37
4	50 CALIBER	748	29.79	0.241	28.84	17.63
5	IMPULSE	717	29.88	0.250	28.48	18.03
6	20MM PROJECTILES	733	29.91	0.262	28.78	19.02

SLIDE NO. 56

888

ACTUAL DATA SHEET FOR METHOD NO. 2 TEST

VOLUMETRIC FLOW RATE STACK GASES

STANDARD CONDITIONS (70°F, 29.92 INCHES HG.)

$$Q_s = 3600 \ (1-B_{wo}) \ V_s \ A \ \left(\frac{T_{std}}{(T_s) \ Ave}\right) \left(\frac{P_s}{P_{std}}\right)$$

WHERE:

Q_s = VOLUMETRIC FLOW RATE, DRY BASIS, STANDARD CONDITIONS, FT^3/Hr.

A = CROSS-SECTIONAL AREA OF STACK, Ft^2

B_{wo} = PROPORTION BY VOLUME OF WATER VAPOR IN THE GAS STREAM, DIMENSIONLESS.

V_s = STACK GAS VELOCITY, FEET PER SECOND, Ft/SEC.

(T_s) Ave. = AVERAGE ABSOLUTE STACK GAS TEMPERATURE, °R

P_s = ABSOLUTE TEMPERATURE AT STANDARD CONDITIONS, 530 °R.

P_{std} = ABSOLUTE PRESSURE AT STANDARD CONDITIONS, 29.92 INCHES HG.

RUN NO.	FURNACE TYPE OF CHARGE	V_s Ft/Sec	(T_s)Ave °R	P_s In. HG.	B_{wo}	A	Q_s Ft^3/Hr.
1	FURNACE BACKGROUND	14.33	753	29.54	.049	3.14	1.142×10^5
2	FUSES	18.45	765	29.91	.034	3.14	1.376×10^5
3	FLARES	18.37	759	29.87	.036	3.14	1.402×10^5
4	50 CALIBER	17.63	748	29.79	.036	3.14	1.364×10^5
5	IMPULSE	18.03	717	29.88	.047	3.14	1.437×10^5
6	20 MM PROJECTILE	19.02	735	29.91	.039	3.14	1.492×10^5

SLIDE NO. 57

889

ACTUAL DATA SHEET FOR METHOD NO. 3 TEST

GAS ANALYSIS -- ORSAT & EPA METHODS USING TRAIN AND GAS COLLECTION BAGS FOR LAB ANALYSIS.

ORSAT ANALYSIS

RUN NO.	TYPE OF CHARGE	VOLUME PERCENT DRY BASES (Ave. 3 Runs)			
		NITROGEN	OXYGEN	CARBON DIOXIDE	CARBON MONOXIDE
1	FURNACE BACKGROUND	80.60	16.80	2.40	0.20
2	FUSES	79.90	18.96	1.00	0.14
3	FLARES	79.30	19.90	0.73	0.07
4	50 CALIBER	79.67	16.30	3.70	0.33
5	IMPULSE	80.47	17.53	1.87	0.13
6	20 MM PROJECTILE	80.55	15.55	3.75	0.15

DRY MOLECULAR WEIGHT (LB/LB-Mole)

$$M_D = 0.44(\%CO_2) + 0.32\ (\%O_2) + 0.28(\%N_2 + \%CO)$$

WHERE:

- M_D = DRY MOLECULAR WEIGHT, Lb/Lb-Mole
- $\%CO_2$ = PERCENT CARBON DIOXIDE BY VOLUME
- $\%CO$ = PERCENT CARBON MONOXIDE BY VOLUME
- $\%O_2$ = PERCENT OXYGEN BY VOLUME
- $\%N_2$ = PERCENT NITROGEN BY VOLUME
- 0.44 = MOLECULAR WEIGHT CARBON DIOXIDE DIVIDED BY 100
- 0.32 = MOLECULAR WEIGHT OF OXYGEN DIVIDED BY 100
- 0.28 = MOLECULAR WEIGHT OF NITROGEN AND CARBON MONOXIDE DIVIDED BY 100

RUN NO.	TYPE OF CHARGE	M_D DRY MOLECULAR WEIGHT
1	FURNACE BLANK	29.06
2	FUSES	28.92
3	FLARES	28.91
4	50 CALIBER	29.24
5	IMPULSE	29.00
6	20 MM PROJECTILE	29.22

ACTUAL DATA SHEET FOR METHOD NO.4 TEST

MOISTURE CONTENT

STANDARD CONDITIONS   (70° F, 29.92 INCHES HG.)

$$B_{wo} = \frac{Vw_{std}}{Vm_{std} + Vw_{std}}$$

WHERE:

B_{wo} = PROPORTION BY VOLUME OF WATER VAPOR IN THE GAS STREAM, DIMENSIONLESS.

Vw_{std} = VOLUME OF WATER IN THE GAS SAMPLE (STANDARD CONDITIONS), Ft^3.

Vm_{std} = VOLUME OF GAS SAMPLE THROUGH THE DRY GAS METER (STANDARD CONDITIONS), Ft^3.

RUN NO.	TYPE OF CHARGE	Vw_{std} Ft^3	Vm_{std} Ft^3	B_{wo}
1	FURNACE BACKGROUND	1.31	25.51	.049
2	FUSES	1.15	32.45	.034
3	FLARES	1.21	32.14	.036
4	50 CALIBER	1.18	31.88	.036
5	IMPULSE	1.59	32.48	.047
6	20 MM PROJECTILE	1.41	34.50	.039

SLIDE NO. 59

ACTUAL DATA SHEET FOR METHOD NO.4 TEST

VOLUME WATER VAPOR

STANDARD CONDITIONS   (70°F, 29.92 INCHES HG.)

$$Vw_{std} = V_{i_c} \frac{(P_{H2O})(RT_{std})}{(M_{H2O})(P_{std})}$$

$$= 0.0474 \ V_{i_c}$$

WHERE:

Vw_{std} = VOLUME OF WATER VAPOR IN THE GAS SAMPLE (STANDARD CONDITIONS), FT^3.

V_{i_c} = TOTAL VOLUME OF LIQUID COLLECTED IN INPIN- GERS AND SILICA GEL, ML.

RUN NO.	TYPE OF CHARGE	V_{i_c} ML	Vw_{std} FT^3
1	FURNACE BACKGROUND	27.7	1.31
2	FUSES	24.3	1.15
3	FLARES	25.5	1.21
4	50 CALIBER	25.0	1.18
5	IMPULSE	33.6	1.59
6	20 MM PROJECTILE	29.8	1.41

SLIDE NO. 60

ACTUAL DATA SHEET FOR METHOD NO. 5 TEST
PARTICULATE CONCENTRATION (STSP)(LB/SCF)

PARTICULATE CONCENTRATION STACK GASES

STANDARD CONDITION (70°F, 29.92 INCHES HG)

$$C_s = \frac{\left(\frac{1}{453600} \frac{LB}{MG}\right) Mn}{Vm_{std}}$$

$$= 2.205 \times 10^{-6} \frac{Mn}{Vm_{std}}$$

WHERE:

C_s = CONCENTRATION OF PARTICULATE MATTER IN STACK GAS, LB/SCF, DRY BASIS.

Mn = TOTAL AMOUNT OF PARTICULATE MATTER COLLECTED, MG.

Vm_{std} = VOLUME OF GAS SAMPLE THROUGH DRY GAS METER (STANDARD CONDITIONS) FT^3.

RUN NO.	TYPE OF CHARGE	Mn MG	Vm std FT³	Cs LB/SCF
1	FURNACE BACKGROUND	10.5	25.21	0.0916×10^{-5}
2	FUSES	687.2	32.45	4.67×10^{-5}
3	FLARES	725.0	32.14	4.97×10^{-5}
4	50 CALIBER	1401.6	31.88	9.69×10^{-5}
5	IMPULSE	800.7	32.48	5.43×10^{-5}
6	20 MM PROJECTILE	1346.7	34.50	8.61×10^{-5}

SLIDE NO. 61

ACTUAL DATA SHEET FOR METHOD NO. 5 TEST
PARTICULATE CONCENTRATION
(LBS/1000LB DRY AIR)

PARTICULATE CONCENTRATION OF STACK GASES

(POUNDS / 1000 POUNDS OF DRY AIR)

RUN NO.	TYPE OF CHARGE	C_s LB/1000 LBS. OF DRY AIR
1	FURNACE BACKGROUND	1.221×10^{-2}
2	FUSES	6.227×10^{-1}
3	FLARES	6.627×10^{-1}
4	.50 CALIBER	1.292
5	IMPULSE	7.24×10^{-1}
	20 MM PROJECTILES	1.148

SLIDE NO. 62

ACTUAL DATA SHEET FOR METHOD NO.5 TEST

PROCESS EMISSION RATE (LB/SCF)

EMISSION RATE $= C_s Q_s$

WHERE:

EMISSION RATE = TOTAL PARTICULATE MATTER DIS-
CHARGED FROM STACK INTO ATMOSPHERE, LB/HR.

C_s = CONCENTRATION OF PARTICULATE MATTER IN
STACK GAS, LB/SCF, DRY BASES.

Q_s = VOLUMETRIC FLOW RATE, DRY BASES, STANDARD
CONDITIONS, Ft^3/HR.

RUN NO.	TYPE OF CHARGE	C_s LB/SCF	Q_s Ft^3/HR	EMISSION RATE LB/HR
1	FURNACE BACKGROUND	0.0916×10^{-5}	1.142×10^5	0.105
2	FUSES	4.67×10^{-5}	1.376×10^5	6.43
3	FLARES	4.97×10^{-5}	1.402×10^5	3.97
4	50 CALIBER	9.69×10^{-5}	1.364×10^5	13.22
5	IMPULSE	5.43×10^{-5}	1.437×10^5	7.80
6	20 MM PROJECTILE	8.61×10^{-5}	1.492×10^5	12.85

SLIDE NO. 63

ACTUAL DATA SHEET FOR METHOD NO.5 TEST

PARTICULATE EMISSIONS

50 CALIBER

CONTAINER NUMBER 1 — FILTER

CONTAINER NUMBER 2 — PARTICULATE MATTER AND ACETONE WASHINGS FROM ALL SAMPLE-EXPOSED SURFACES AHEAD OF THE FILTER.

CONTAINER NUMBER	WEIGHT OF PARTICULATE COLLECTED mg		
	FINAL WEIGHT	TARE WEIGHT	WEIGHT GAIN
1			986.8
2			414.8
TOTAL			1401.6

SLIDE NO. 64

896

PARTICULATE DATA TABULATION (PPM)WT.

PARTS PER MILLION (BY WEIGHT)

RUN	TYPE OF CHARGE	CADMIUM	MAGNESIUM	ALUMINUM	LEAD	COPPER	POTASSIUM	BARIUM	STRONTIUM	ANTIMONY
1	FURNACE BACKGROUND	0.0361	.0058	0	0.016	.00011	0	0	.00023	0
2	FUSES	0.410	0.329	0.876	3.760	0.373	0.068	0	.00615	0.012
3	FLARES	0.735	1.89	0.039	0.073	.0066	0.726	0.814	0.119	0
4	50 CALIBER	0.608	0.747	2.337	0.456	0.329	2.660	2.002	0.367	0.329
5	IMPULSE	0.173	.0288	0.0216	.137	.0072	0.620	0	0	0.0144
6	20MM PROJECTILE	1.088	0.669	1.553	1.552	1.157	0.397	1.031	0.023	0.113

SLIDE NO. 65

897

PARTICULATE DATA TABULATION
(PPM)WT.

PARTICULATE CHEMICAL ANALYSIS
(PPM BY WEIGHT)

RUN	TYPE OF CHARGE	OXIDES OF MAGNESIUM	OXIDES OF ALUMINUM	OXIDES OF LEAD	OXIDES OF COPPER	PHOSPHATES	POTASSIUM CONTAINING COMPOUNDS	BARIUM CONTAINING COMPOUNDS	STRONTIUM CONTAINING COMPOUNDS	ANTIMONY CONTAINING COMPOUNDS	LEAD CONTAINING COMPOUNDS	METAL POWDER PARTICULATE MATERIAL
1	FURNACE BACKGROUND	0	0	0	0	0.006	0	0	0	0	0	0.056
2	FUSES	0	0	0	0	0.006	0	0	0	0	0	5.826
3	FLARES	3.140	0		0	0	1.384	0	0	0	0	6.313
4	50 - CALIBER	1.255	0		0	0	0	3.746	0	0	0	12.514
5	IMPULSE	0	0		0	0	0	0	0	0	0	0.976
6	20-MM PROJECTILE	0	0		0	0	0	0	0	0	0	7.558

SLIDE NO. 66

WATER CHEMICAL ANALYSIS (PPM) WT.

WATER CHEMICAL ANALYSIS
(PPM BY WEIGHT)

RUN	TYPE OF CHARGE	CADMIUM	MAGNESIUM	ALUMINUM	LEAD	COPPER	POTASSIUM	BARIUM	STRONTIUM	ANTIMONY	PHOSPHATES	ACIDS IN AEROSOL FORM (AS HCl)
1	FURNACE BACKGROUND	.207	.001	<.001	<.001	<.001	.003	.697	<.001	.014	<.001	.122
2	FUSES	.197	<.001	<.001	.002	<.001	<.001	.005	<.001	.011	<.001	.042
3	FLARES	.002	<.001	<.001	<.001	0	<.001	.208	<.001	.005	<.001	0
4	50 - CALIBER	.002	<.001	<.001	.002	<.001	.002	.460	<.001	.017	<.001	.646
5	IMPULSE	<.001	<.001	<.001	.001	<.001	<.001	.224	<.001	.004	<.001	.025
6	20-MM PROJECTILE	.009	.002	<.001	<.001	<.001	.003	.306	<.001	.003	<.001	0

SLIDE NO. 67

GASEOUS EMISSION DATA TABULATION

(LB/SCF)

GASEOUS EMISSIONS

RUN NO.	TYPE OF CHARGE	NITROGEN OXIDES (AS NO$_2$) LB/SCF	SULPHUR OXIDES LB/SCF	PHOSGENE GAS PPM (VOLUME)	OZONE PPM (VOLUME)	LEAD VAPOR MG/M^3	MERCURY VAPOR MG/M^3	AMMONIA PPM (VOLUME)	HCL PPM (VOLUME)	H$_2$SO$_4$ LB/SCF	HYDRO CARBONS PPM (VOLUME)	HYDROGEN SULFIDE PPM (VOLUME)
1	FURNACE BLANK	2.7×10^{-5}	2.29×10^{-7}	<0.010	<0.005	<0.050	<0.005	0	<0.200	1.32×10^{-7}	38	<0.300
2	FUSES	1.7×10^{-5}	5.08×10^{-7}	<0.010	0.100	<0.050	0.100	0	<0.200	3.02×10^{-7}	<0.1	<0.300
3	FLARES	8.0×10^{-7}	4.76×10^{-6}	<0.010	0.100	<0.050	0.070	0	<0.200	1.71×10^{-5}	<0.1	<0.300
4	50 CALIBER	1.0×10^{-3}	1.85×10^{-6}	<0.010	0.009	<0.050	1.500	0	0.600	4.74×10^{-6}	0.7	<0.300
5	IMPULSE	2.3×10^{-5}	6.83×10^{-7}	<0.010	<0.005	<0.050	<0.005	0	<0.200	9.52×10^{-7}	1.0	<0.300
6	20 MM PROJECTILE	3.5×10^{-5}	3.59×10^{-6}	<0.010	<0.005	<0.050	3.005	0	<0.200	6.20×10^{-7}	0.5	<0.300

SLIDE NO. 68

900

GASEOUS EMISSION DATA TABULATION
(PPM-VOL)

GASEOUS EMISSIONS (IN PPM-VOL)

RUN NO.	TYPE OF CHARGE	NITROGEN OXIDES (AS NO_2) PPM (VOLUME)	SULPHUR OXIDES PPM (VOLUME)	PHOSGENE GAS PPM (VOLUME)	OZONE PPM (VOLUME)	LEAD VAPOR PPM (VOLUME)	MERCURY VAPOR PPM (VOLUME)	AMMONIA PPM (VOLUME)	HCL PPM (VOLUME)	H_2SO_4 PPM (VOLUME)	HYDRO CARBONS PPM (VOLUME)	HYDROGEM SULFIDE PPM (VOLUME)
1	FURNACE BLANK	2.26×10^2	1.376	<0.010	<0.005	<0.005	<0.001	0	<0.200	5.183×10^{-1}	38	<0.300
2	FUSES	1.423×10^2	3.054	<0.010	0.100	<0.006	0.012	0	<0.200	1.186	<0.1	<0.300
3	FLARES	6.897	2.873×10^1	<0.010	0.100	<0.006	0.008	0	<0.200	6.714×10^1	<0.1	<0.300
4	50 CALIBER	8.371×10^3	1.112×10^1	<0.010	0.009	<0.005	0.18	0	0.600	1.861×10^1	0.7	<0.300
5	IMPULSE	1.923×10^2	4.106	<0.010	<0.005	<0.006	<0.001	0	<0.200	3.738	1.0	<0.300
6	20 MM PROJECTILE	2.93×10^2	2.156×10^1	<0.010	<0.005	<0.005	0.001	0	<0.200	2.434	0.5	<0.300

SLIDE NO. 69

RUN	TYPE CHARGE	FEED RATE - No./min.	MAXIMUM STACK TEMPERATURE - °F.	VOLUMETRIC FLOW RATE STACK GASES - ft³/min.	PARTICULATE EMISSION RATE - LB/Hr.	PARTICULATE CONCENTRATION - LB/1000 Lbs. of DRY AIR	GASEOUS EMISSIONS (PPM-Vol.)										
							NITROGEN OXIDES	SULPHUR OXIDES	PHOSGENE GAS	OZONE	LEAD VAPOR	MERCURY VAPOR	AMMONIA	HCL	H_2SO_4	HYDRO CARBONS	HYDROGEN SULFIDE
1	FURNACE BACKGROUND	–	295	1905	0.105	0.01221	226	1.376	<0.010	<0.005	<0.006	<0.001	0	<0.200	.5183	38	<0.300
2	FUSES	7	305	2295	6.43	0.6227	142.3	3.054	<0.010	0.100	<0.006	0.012	0	<0.200	1.186	<0.1	<0.300
3	FLARES	10	305	2340	6.97	0.6627	6.697	28.73	<0.010	0.155	<0.006	0.006	0	<0.200	67.14	<0.1	<0.300
4	50 CALIBER	175	305	2275	13.22	1.292	8371	11.12	<0.010	0.009	<0.006	0.18	0	0.600	18.61	0.7	<0.300
5	IMPULSE	50	260	2390	7.60	0.724	192.5	4.106	<0.010	<0.005	<0.006	<0.001	0	<0.200	3.738	1.0	<0.300
6	20 MM	80	280	2490	12.85	1.148	293	21.154	<0.010	<0.005	<0.006	0.001	0	<0.200	2.434	0.5	<0.300

SLIDE NO. 70

ACTUAL DATA SHEET FOR NOISE POLLUTION

SLIDE NO. 71

903
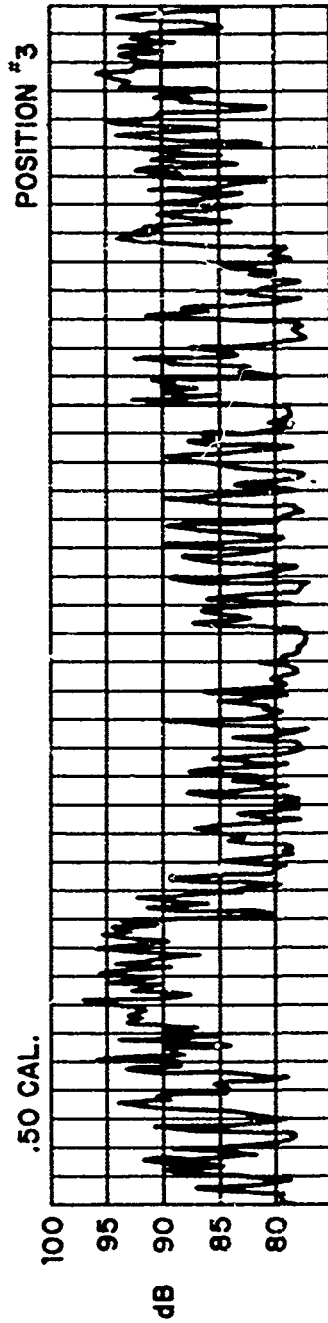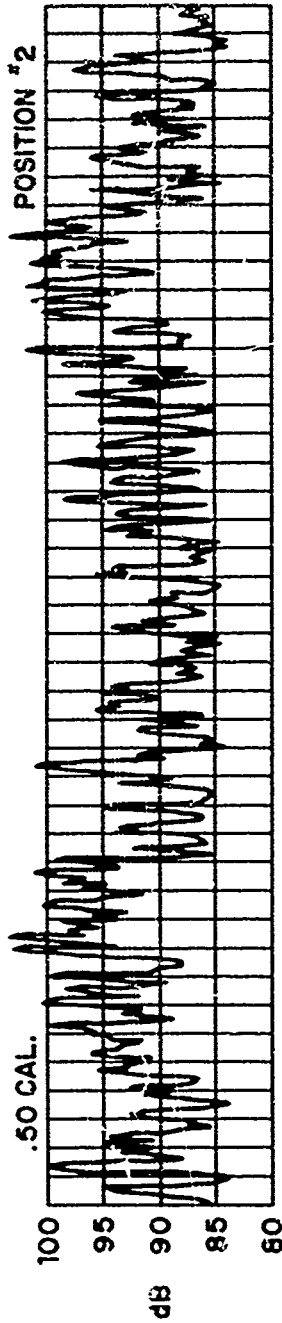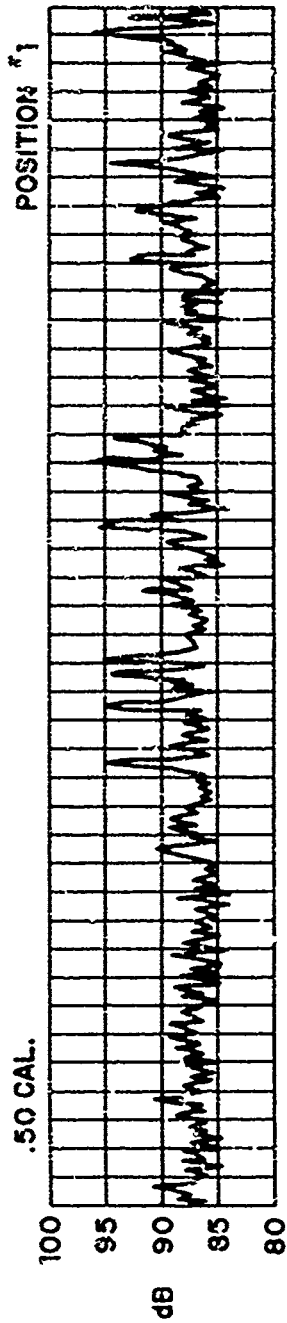
SUMMARY OF PERTINENT DATA GATHERED BY

THIS STACK SAMPLING

- MAX. VOLUMETRIC FLOW RATE OF GASES – 2490 CFM

- MAX. STACK TEMPERATURE – 305F (FUZES, FLARES, .50 CAL.)

- MAX. PARTICULATE EMISSION RATE – 13.22 $^{LB}/_{HR}$ (.50 CAL.)

- MAX. PARTICULATE CONCENTRATION – 9.69 x 10^{-5} $^{LB}/_{SCF}$ ($^{.68 gr}/_{SCF}$)

- PARTICLE SIZE – SEE PARTICLE SIZE & DIST. ANALYSIS

- RINGLEMAN OBSERVATIONS – NONE HIGHER THAN NO.2

- OBSERVATION – NOT ALL EMISSIONS WENT UP STACK – ESTIMATED AS MUCH AS 50% ESCAPING THROUGH OPENINGS IN SYSTEM.

SLIDE NO. 72

PARTICLE SIZE AND DISTRIBUTION AS MEASURED FROM THE ANDERSON SIZING HEAD

PARTICLE SIZE MICRON (μ) →
AMMUNITION TYPE ↓

Ammunition Type	Row	μ / CUM.%									TOTAL
.50 CALIBER	μ	15.06	9.42	6.25	4.71	2.74	1.41	.86	.59		<.59 μ
	%	13.26	3.03	3.46	3.72	7.32	16.24	5.71	17.41	29.85	47.26
	CUM. %	100	86.74	83.71	80.25	76.53	69.21	52.97	47.26	29.85	%
20 MM	μ	13.94	9.65	6.43	4.44	2.81	1.45	.88	.59		<.59 μ
	%	18.59	9.34	7.60	10.60	11.74	10.74	9.75	4.42	17.22	21.64
	CUM. %	100	81.41	72.07	64.47	53.87	42.13	31.39	21.64	17.22	%
FUZES	μ	13.50	8.50	5.67	3.73	2.43	1.27	.76	.55		<.55 μ
	%	17.18	6.43	5.84	7.47	6.19	9.81	10.29	7.24	29.55	36.79
	CUM. %	100	82.82	76.39	70.55	63.08	56.89	47.08	36.79	29.55	%
CARTRIDGE ACTUATED DEVICES	μ	12.70	8.79	5.69	3.99	2.50	1.30	.77	.52		<.52 μ
	%	23.68	9.34	11.83	14.73	12.07	4.84	3.13		13.59	26.72
	CUM. %	100	76.32	67.53	58.19	46.36	31.63	21.56	16.72	13.59	%
ILLUMINATING SIGNALS	μ	13.64	8.68	5.67	3.96	2.58	1.30	.76	.53		<.53 μ
	%	16.48	4.49	4.67	5.24	17.11	10.25	9.38	7.11	25.47	32.58
	CUM. %	100	83.52	79.03	74.36	69.32	52.21	41.96	32.58	25.47	%

● Largest particle   15.06 μ (.50 caliber)

● Smallest particle 0.52 μ (C.A.D.)

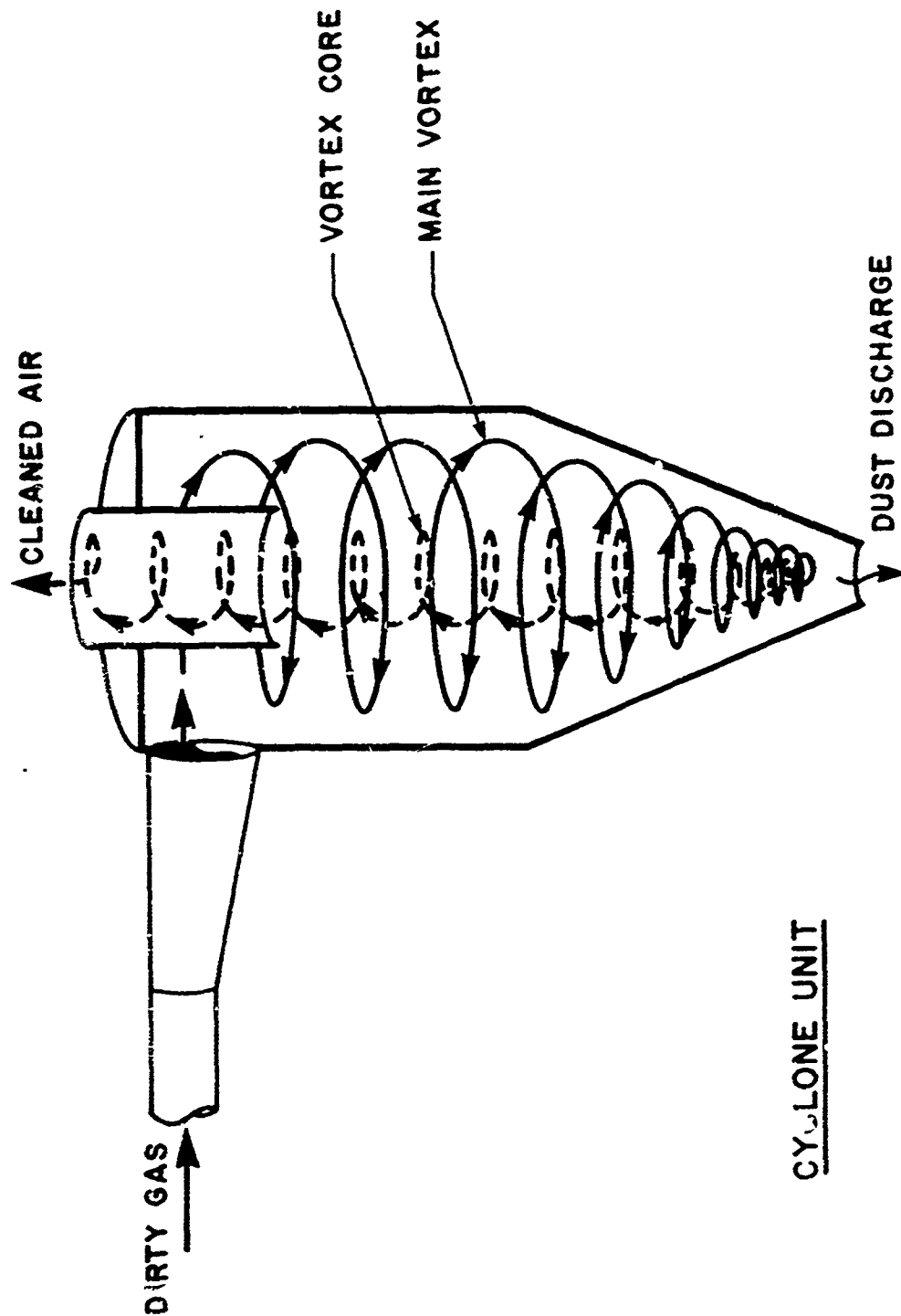● 47.26% of particulate material from .50 caliber is below .59 μ

905

SLIDE NO. 73

B-34256

POLLUTION ABATEMENT/CONTROL ALTERNATIVES

FOR PARTICULATES
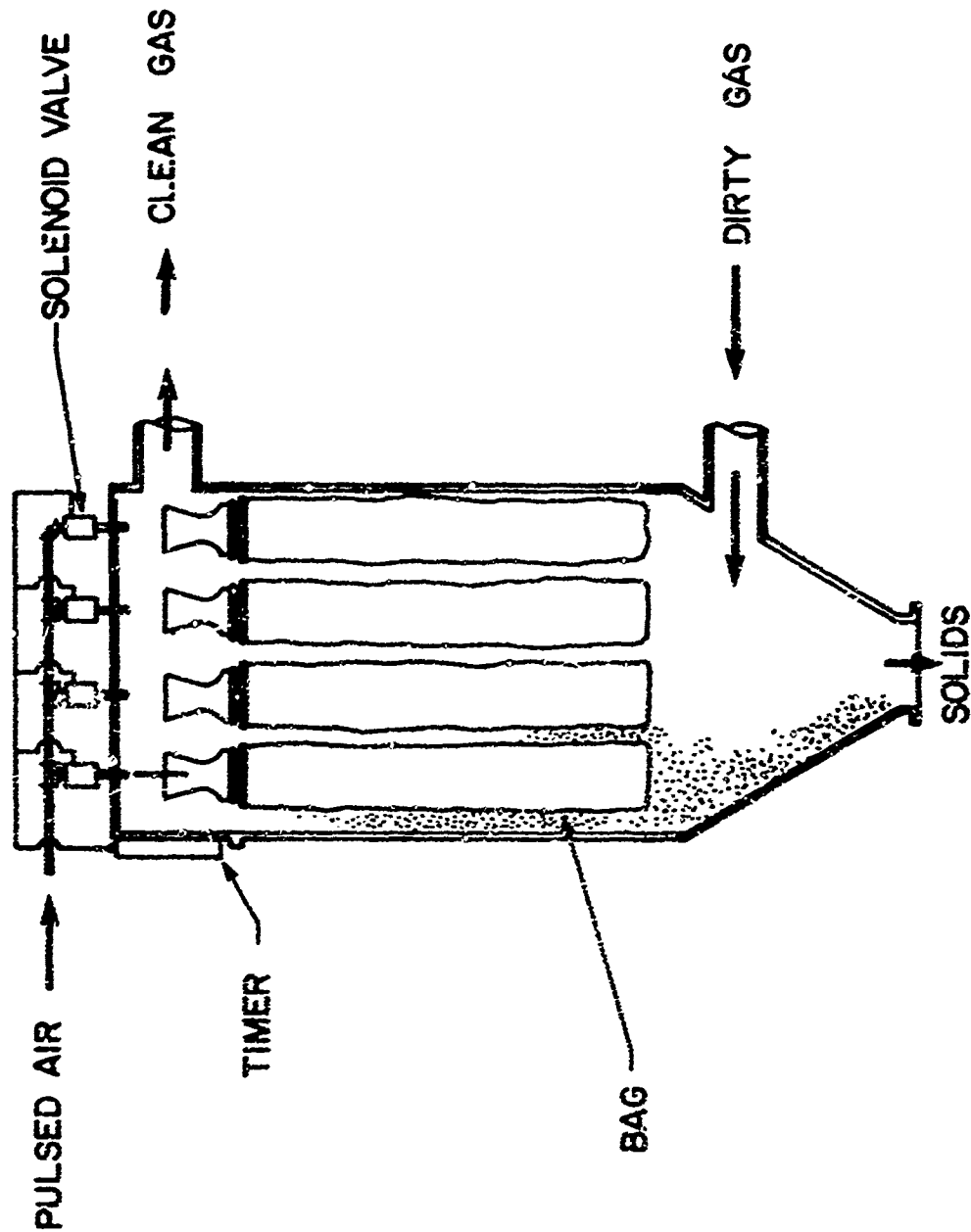
- MECHANICAL COLLECTORS

- FILTERS (BAGHOUSE)

- WET SCRUBBERS

- ELECTROSTATIC PRECIPITATORS

SLIDE NO. 74

906

SCHEMATIC OF A MECHANICAL COLLECTOR

CLEANED AIR

VORTEX CORE

MAIN VORTEX

DIRTY GAS

DUST DISCHARGE

SLIDE NO. 75

CYCLONE UNIT

SCHEMATIC OF A FILTER (BAGHOUSE) COLLECTOR

SOLENOID VALVE

CLEAN GAS

DIRTY GAS

PULSED AIR

TIMER

BAG

SOLIDS

SLIDE NO. 76

908

SCHEMATIC OF A WET COLLECTOR (SCRUBBER)
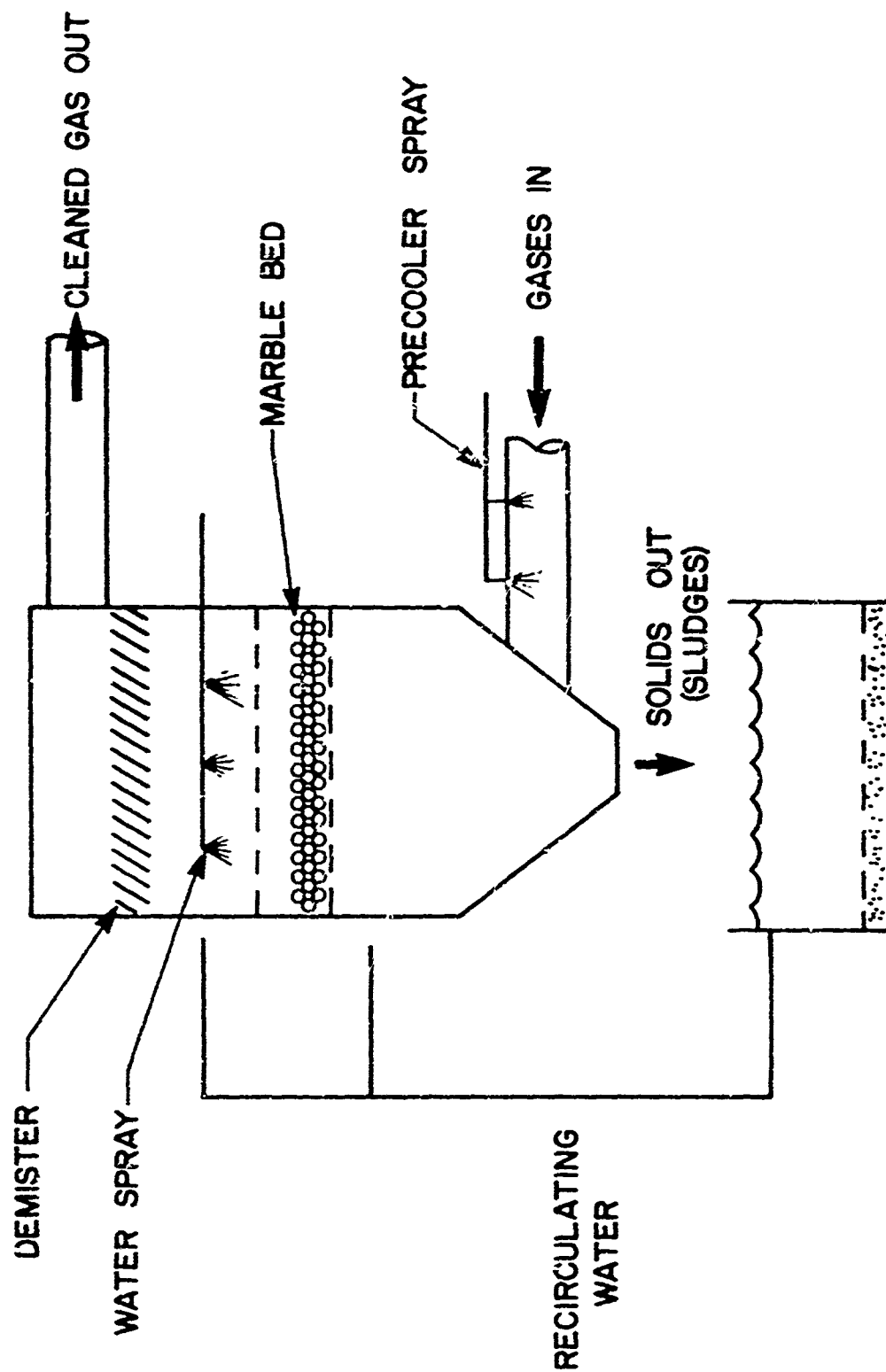
CLEANED GAS OUT

MARBLE BED

PRECOOLER SPRAY

GASES IN

DEMISTER

WATER SPRAY

SOLIDS OUT
(SLUDGES)

RECIRCULATING
WATER

SLIDE NO. 77

909

SCHEMATIC OF AN ELECTRO STATIC PRECIPITATOR

GAS INLET

INSULATOR COMPARTMENT

HIGH VOLTAGE SYSTEM SUPPORT INSULATOR

WATER SPRAYS

DISCHARGE ELECTRODE SUPPORT FRAME

WEIR PONDS

TUBULAR COLLECTING SURFACES

DISCHARGE ELECTRODES

CASING

WEIGHTS

DISCHARGE SEAL

GAS OUTLET

HIGH VOLTAGE CONDUCTOR

ELECTRIC HEATER

DIFFUSER VANES

SLIDE NO. 78

910
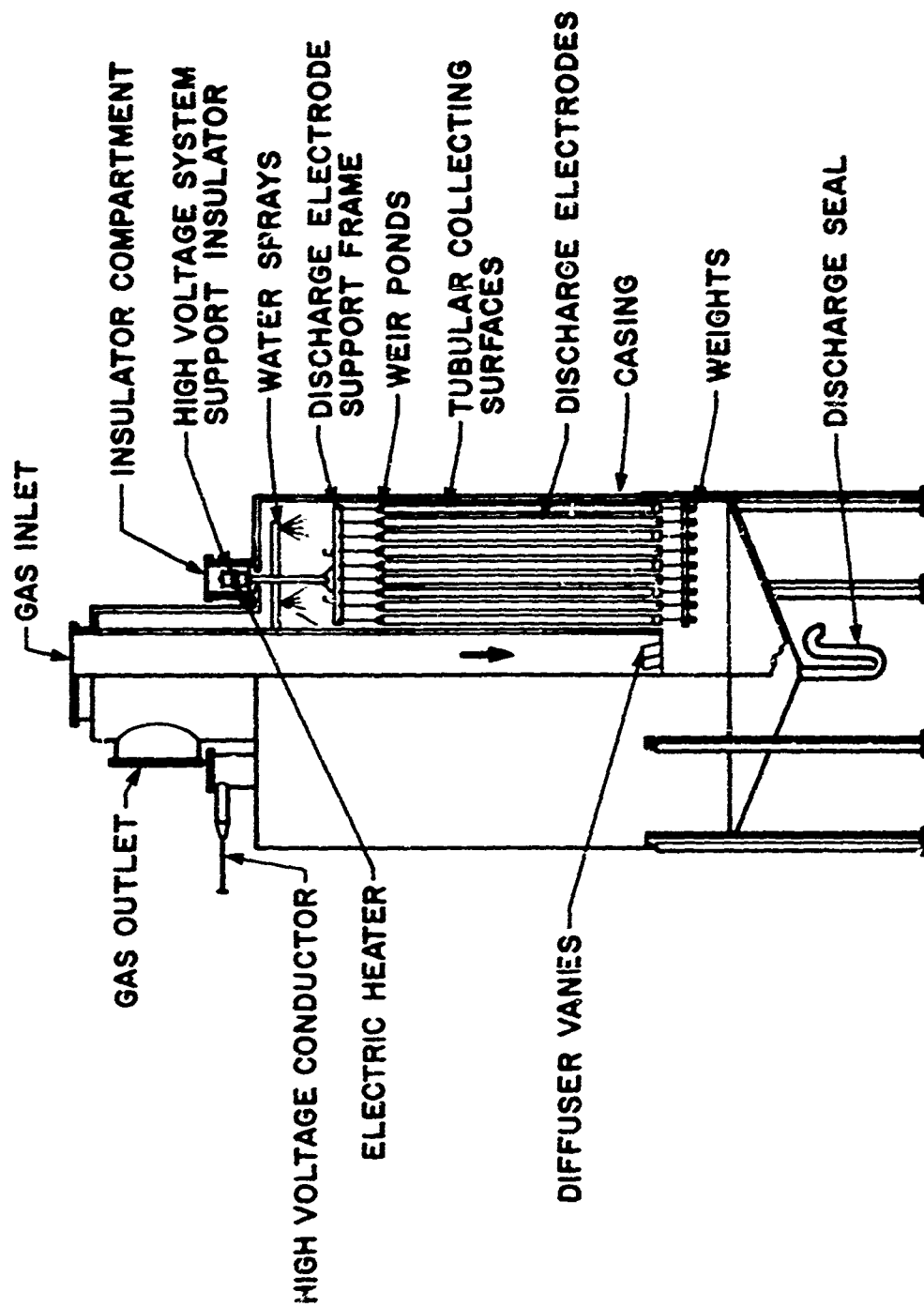
POLLUTION ABATEMENT/CONTROL

EQUIPMENT ALTERNATIVES FOR
ADSORPTION OF GASEOUS
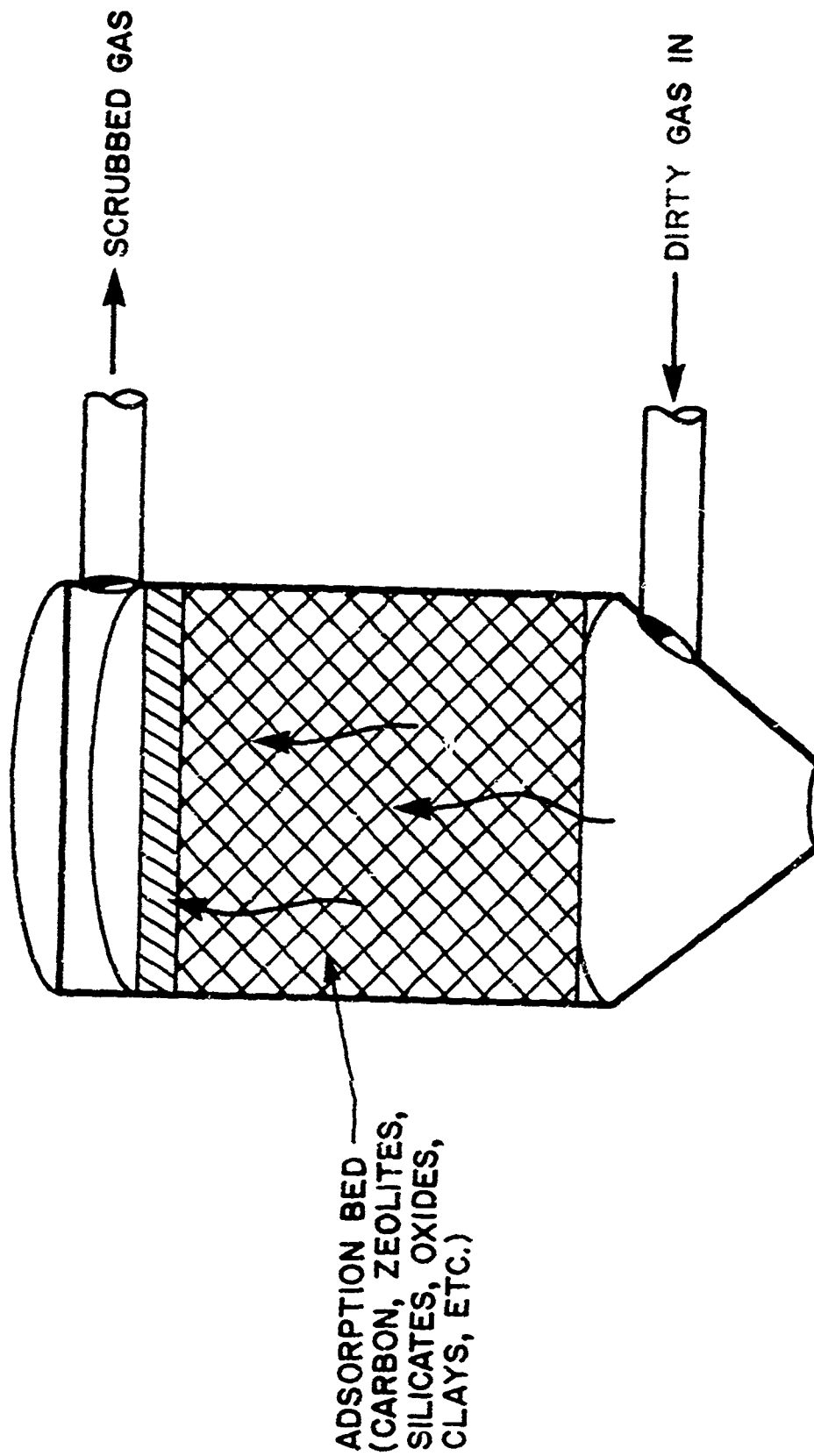## POLLUTANTS

- ADSORPTION SYSTEMS (FILTERS)

- WET SCRUBBER (PACKED TOWER)

- SPRAY CHAMBER

- VENTURI

- AFTERBURNER

- CATALYTIC CONVERTER

SLIDE NO. 79

911

SCHEMATIC OF AN ADSORPTION SYSTEM

SCRUBBED GAS

DIRTY GAS IN

ADSORPTION BED
(CARBON, ZEOLITES, SILICATES, OXIDES, CLAYS, ETC.)

SLIDE NO. 80

912

SCHEMATIC OF A PACKED TOWER (WET SCRUBBER)

CLEANED GAS OUT

DIRTY GAS

PACKING
(MARBLES, PALL RINGS,
RASCHIG RINGS,
INTALOX SADDLES,
TELLERETTES, ETC.)

DEMISTER

SLIDE NO. 81

913

SCHEMATIC OF A SPRAY CHAMBER

CLEAN GAS OUT

DIRTY GAS IN

EFFLUENT OUT

DEMISTER

WATER SPRAY
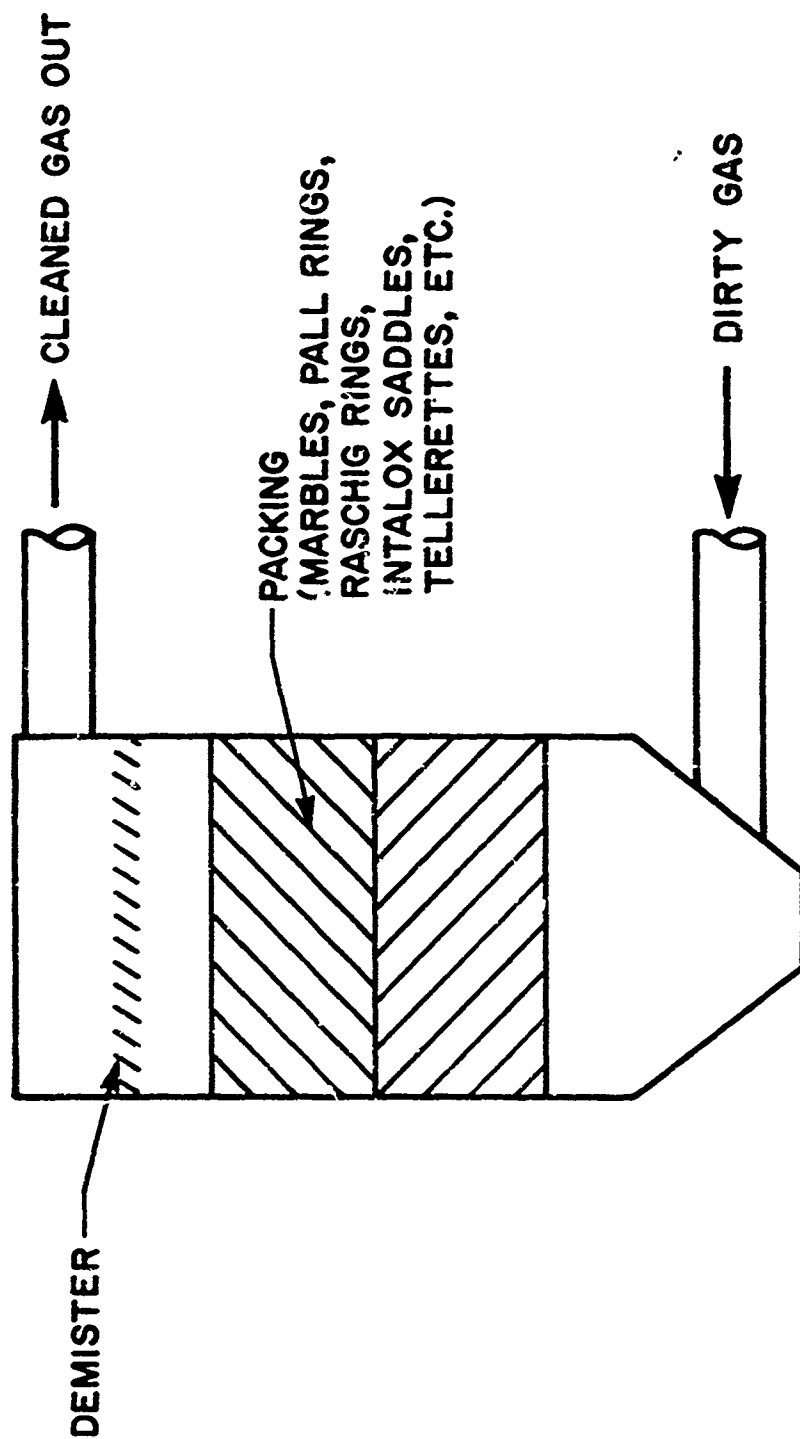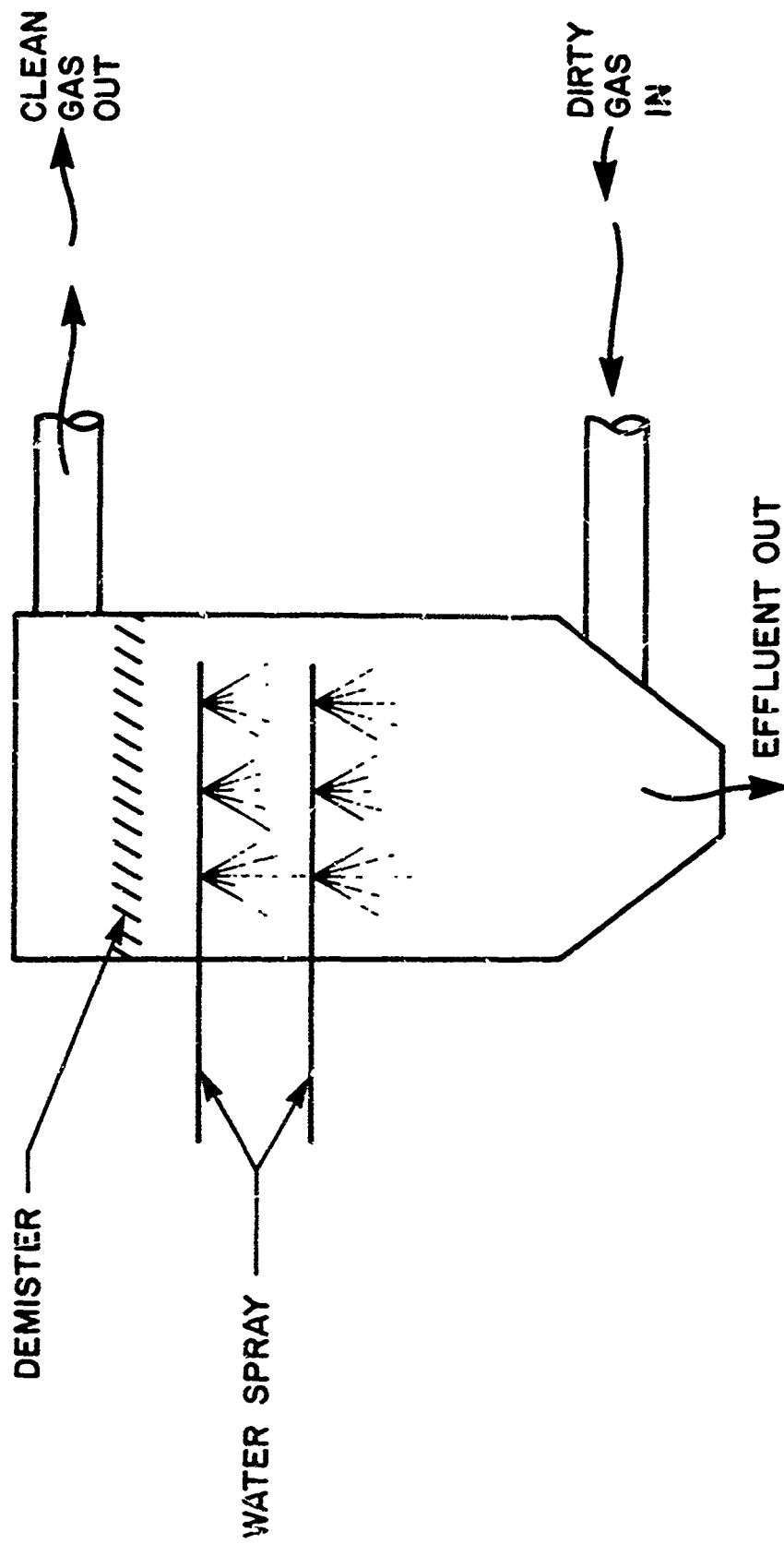
SLIDE NO. 82

SCHEMATIC OF A VENTURI
CHAMBER SCRUBBER

WATER

GAS

SEPARATOR
BOX

CLEAN AIR

SEPARATING
ELEMENT

WATER

SLIDE NO. 83

915
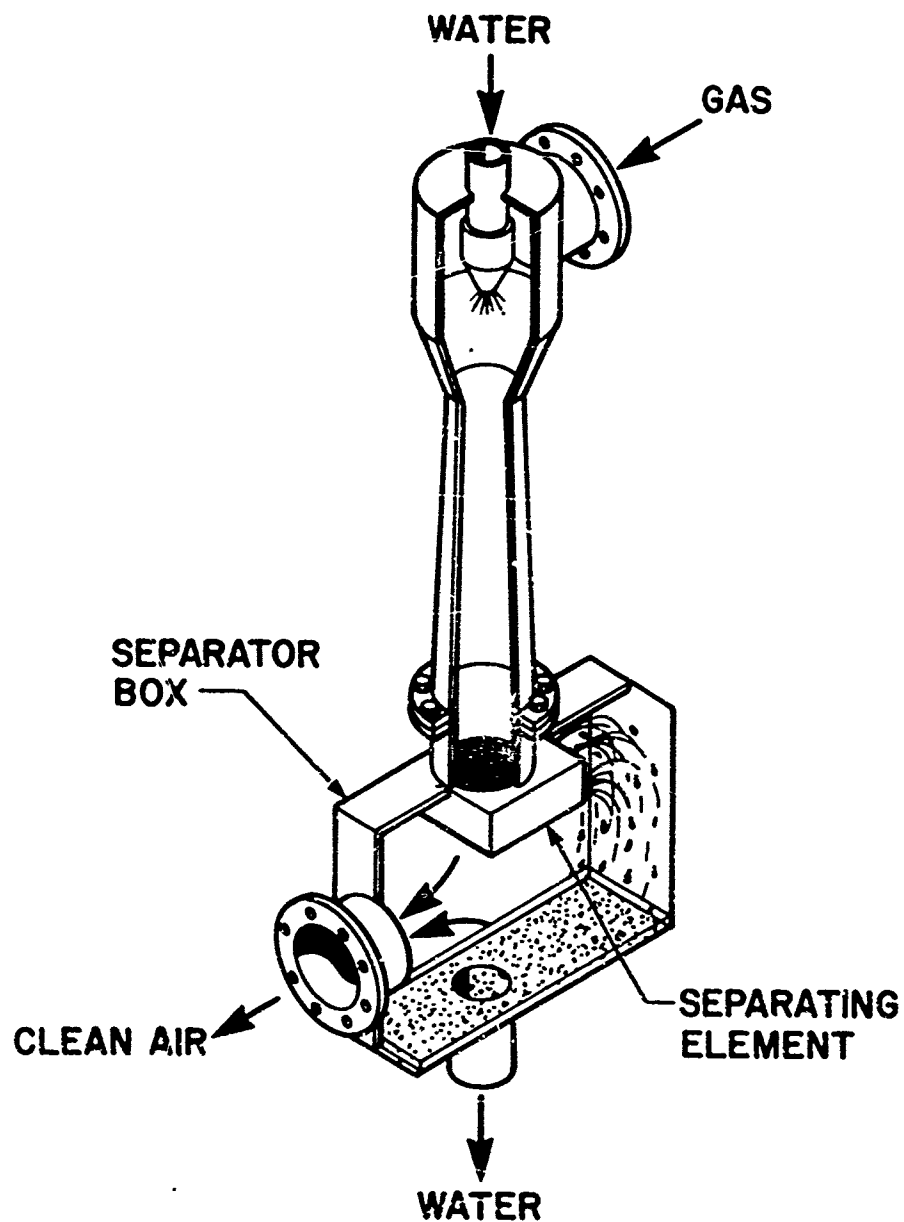
SCHEMATIC OF AN AFTERBURNER

DIRTY GAS IN

FUEL BURNER

CLEANED GAS OUT

WITH OR WITHOUT A CATALYTIC ELEMENT

FAN

MOTOR

SLIDE NO. 84

916
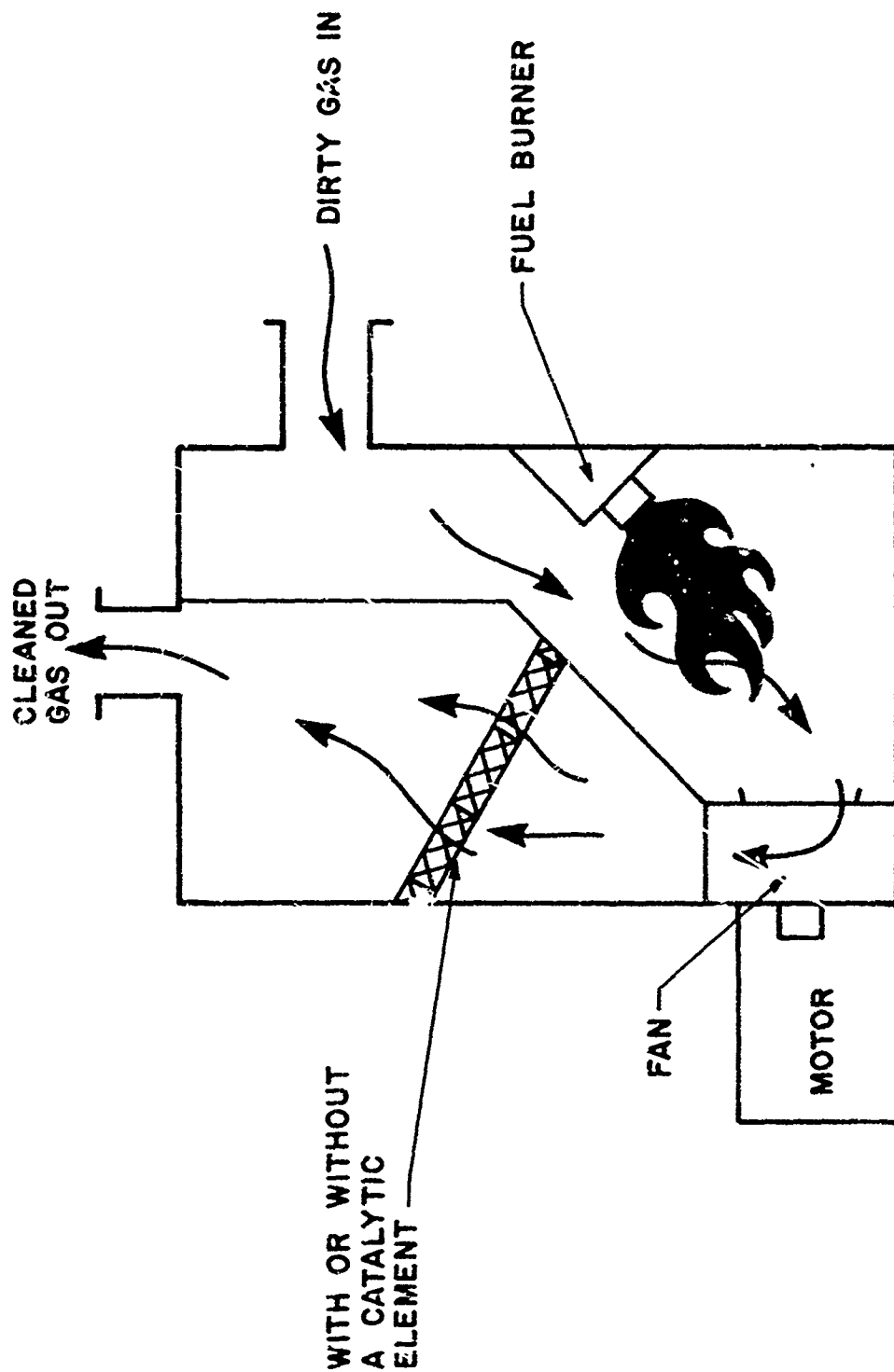
POLLUTION ABATEMENT/CONTROL EQUIPMENT
SELECTED FOR THE 4 BARREL
ROTARY DEMIL FURNACE

SLIDE NO. 85

917
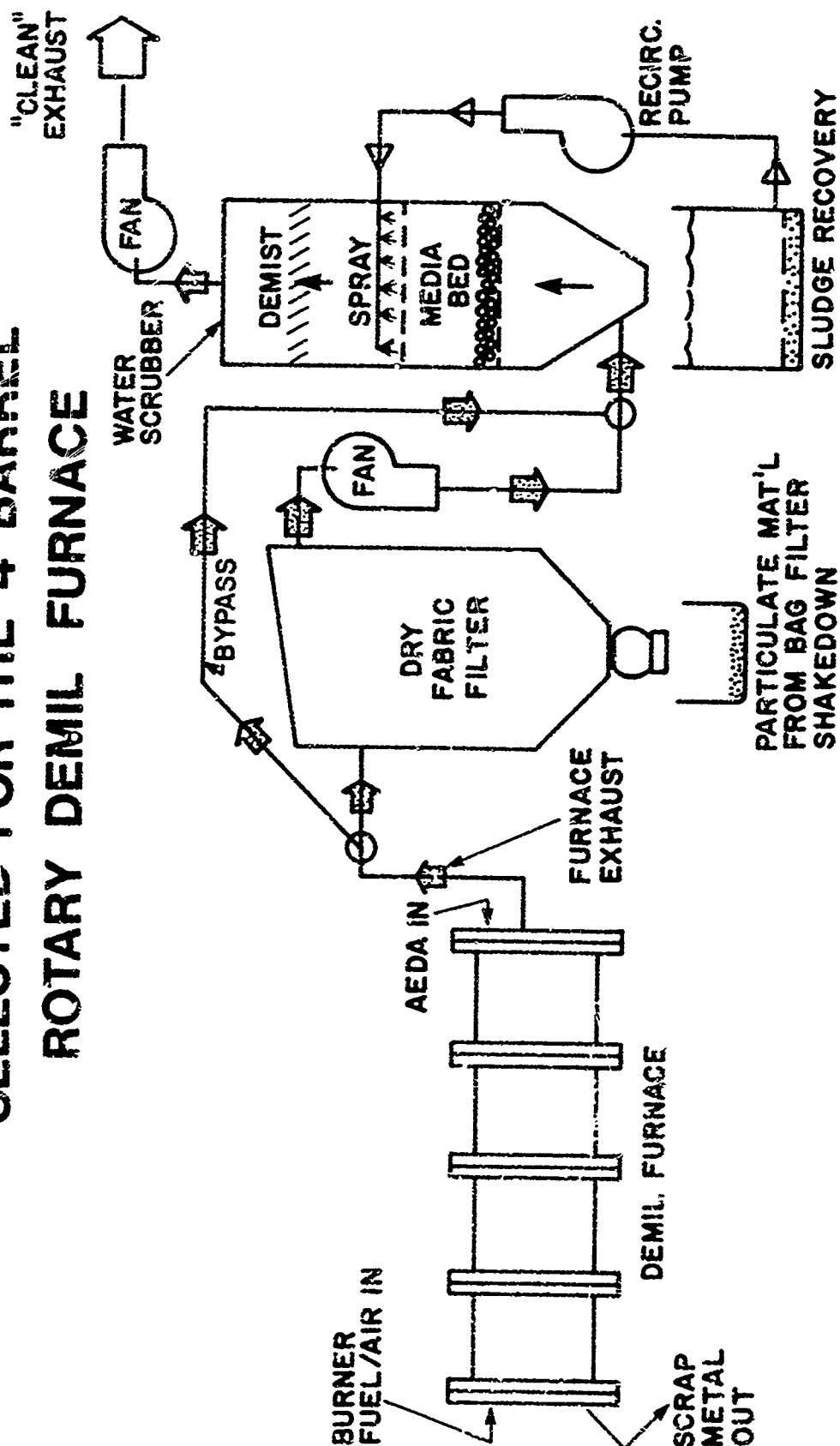
ACKNOWLEDGEMENTS

Appreciation and recognition are in order to the
following for their effort on this project.

- Mr. J. Novak (NAPEC)

  - Developed test plan and monitored the
    actual stack sampling.

- Biagi-Hannan & Associates, Inc., Evansville, Ind.

  - Prime contractor for the Project Cost Estimate
    (Contract N62472-72-C-1147)

- Environmental Consultants, Inc., Clarksville, Ind.

  - Subcontractor who performed the actual EPA
    approved stack sampling.

- Mr. M. Brown (NAVFAC, Northern Div., Philadelphia, Pa.)

  - NAVFAC Project Engineer

DEMILITARIZATION OF OBSOLETE CHEMICAL AGENTS AND MUNITIONS
AT ROCKY MOUNTAIN ARSENAL

Robert K. Hurt
Rocky Mountain Arsenal, Denver, Colo.

GENTLEMEN, THE PURPOSE OF THIS PRESENTATION IS TO DESCRIBE TO
YOU TWO MAJOR DEMILITARIZATION PROJECTS THAT ARE NOW IN PROGRESS
AT THE ROCKY MOUNTAIN ARSENAL IN DENVER, COLORADO. THE FIRST PRO-
JECT, WHICH IS APPROXIMATELY 75 PER CENT COMPLETE, IS THE DISPOSAL
OF BULK MUSTARD AGENT BY INCINERATION. THE SECOND PROJECT IS THE
DESTRUCTION OF THE M34, ONE-THOUSAND POUND, GB-FILLED, AIR FORCE
CLUSTER BOMB. THE FACILITY FOR THIS PROJECT HAS BEEN COMPLETED,
AND OPERATIONS ARE SCHEDULED TO BEGIN IN THE FALL OF THIS YEAR.
THIS CLUSTER BOMB HAS BECOME OBSOLETE, AS IT CANNOT BE DEPLOYED
FROM THE PRESENT DAY, HIGH-PERFORMANCE JET AIRCRAFT.

THIS ARSENAL HAS BEEN DEMILITARIZING OBSOLETE, OR UNSERVICE-
ABLE, AGENT-FILLED MUNITIONS OFF AND ON SINCE 194   MANY INNO-
VATIONS HAVE BEEN MADE IN THE DESIGN AND OPERATION OF THESE TWO
DEMILITARIZATION PROGRAMS TO COMPLY WITH RIGID SAFETY REQUIREMENTS
AND WITH STATE AND FEDERAL ENVIRONMENTAL STANDARDS.

IN 1969, PLANS WERE DEVELOPED TO DISPOSE OF BOTH THE MUSTARD
AGENT AND THE M34 CLUSTER BOMBS IN A "SEA DUMP" OPERATION CALLED
"CHASE." THESE PLANS CREATED CONSIDERABLE CONTROVERSY; AND UPON A
RECOMMENDATION OF THE NATIONAL ACADEMY OF SCIENCES, THE DECISION
WAS MADE TO DEMILITARIZATION THE MUNITIONS AND MUSTARD AGENT AT
ROCKY MOUNTAIN ARSENAL WHERE A VAST AMOUNT OF EXPERTISE AND EX-
PERIENCE, IN THE HANDLING OF TOXIC AGENTS AND MUNITIONS, WAS
AVAILABLE.

919

STRINGENT GUIDELINES WERE ESTABLISHED, FOR THE DESIGN AND OPER-
ATION OF THESE PLANTS, TO INSURE ABSOLUTE SAFETY FOR THE OPERATING
PERSONNEL AT THE ARSENAL, AS WELL AS THE POPULACE IN THE AREAS
ADJACENT TO ROCKY MOUNTAIN ARSENAL. TIME AND COST BECAME A CON-
SIDERATION ONLY AFTER ALL SAFETY FEATURES WERE ACHIEVED.

THE FACILITY FOR THE DESTRUCTION OF THE MUSTARD AGENT WAS
COMPLETED AND TESTED IN JULY 1972, AND OPERATIONS ON A FULL TIME
BASIS WERE INITIATED THE FOLLOWING MONTH.

AT THIS TIME, I WOULD LIKE TO GIVE YOU A BRIEF DESCRIPTION OF
THE LAYOUT OF THE ARSENAL AND HOW IT IS LOCATED IN RESPECT TO THE
SURROUNDING COMMUNITIES.

1. THE ROCKY MOUNTAIN ARSENAL EXTENDS FOR SIX (6) MILES IN AN
EAST-WEST DIRECTION AND FIVE (5) MILES IN A NORTH-SOUTH DIRECTION.
THE CITY OF DENVER HAS EXPANDED UNTIL IT NOW BORDERS ALONG THE
ENTIRE SOUTH BOUNDARY OF THE ARSENAL WITH THE RUNWAYS FROM THE
STAPLETON INTERNATIONAL AIRPORT PRESENTLY TERMINATING AT THE
SOUTHERN BORDER. PLANS ARE NOW UNDER WAY TO EXTEND A NEW RUNWAY
A FULL MILE INTO THE ARSENAL. THE LAND FOR THIS EXTENSION HAS
BEEN DEEDED TO THE CITY AND COUNTY OF DENVER FOR THIS PURPOSE.

2. COMMERCE CITY ABUTS THE FULL WESTERN BOUNDARY AND INCLUDES
BOTH RESIDENTIAL AND INDUSTRIAL AREAS. THE AREAS TO THE NORTH AND

EAST OF THE ARSENAL ARE OPEN COUNTRY AND SPARSELY POPULATED WITH
FARMLANDS.

3. THE ARSENAL WAS BUILT IN 1942 TO PRODUCE MUSTARD AND LEWI-
SITE AND, LATER, TO PRODUCE INCENDIARY MUNITIONS. THESE FACILITIES
ARE LOCATED IN THE SOUTH CENTER SECTION OF THE ARSENAL. THIS IS
ALSO THE AREA WHERE THE MUSTARD AGENT IS NOW BEING DESTROYED BY
INCINERATION.

4. IN 1951, A PLANT WAS BUILT IN THE NORTH CENTRAL SECTION OF
THE ARSENAL TO PRODUCE NERVE AGENT "GB" AND AGENT-FILLED MUNITIONS.
THE "GB" AGENT WAS PRODUCED UNTIL 1957 WHEN THE PLANT WAS CLOSED,
AND IT HAS NOT OPERATED SINCE THAT TIME. THE MUNITION FILLING
PLANTS WERE OPERATED UNTIL 1969 WHEN THEY ALSO WERE CLOSED DOWN.
A FEW OF THE MUNITIONS, AND A PORTION OF THE BULK AGENT, ARE PRE-
SENTLY STORED AT ROCKY MOUNTAIN ARSENAL ALONG WITH THE M34 CLUSTERS
SCHEDULED FOR DEMILITARIZATION.

THE MUSTARD AGENT IS STORED IN HEAVY-WALLED TON CONTAINERS OF
THE SAME TYPE THAT IS USED FOR THE STORAGE AND SHIPMENT OF CHLORINE
BY PRIVATE INDUSTRY. THE SIDES OF THE CONTAINERS ARE CONSTRUCTED
OF SEVEN-SIXTEENTH INCH STEEL, AND THE CONCAVE ENDS ARE THREE-QUAR-
TERS INCH THICK. THE VALVES, FOR LOADING OR UNLOADING, ARE PRO-
TECTED BY A STEEL BONNET DURING TRANSPORT. EACH TON CONTAINER
HOLD FROM 1,700 TO 1,800 POUNDS OF MUSTARD AGENT.

THE AGENT STOCKPILE AT ROCKY MOUNTAIN ARSENAL ORIGINALLY CON-
TAINED 2,451 CONTAINERS OF LEVINSTEIN MUSTARD WHICH IS IN THE
UNPURIFIED STATE WITH APPROXIMATELY 30 PER CENT IMPURITIES, MAINLY,
SULFUR. THERE ARE 956 CONTAINERS OF DISTILLED MUSTARD, MAKING A
TOTAL OF 3,407 CONTAINERS TO BE PROCESSED, AND AMOUNTING TO 3,071
TONS OF MUSTARD AGENT OR APPROXIMATELY 600,000 GALLONS.

THE PROCESS FOR DEMILITARIZATION INCLUDES THE INTRA-ARSENAL
TRANSPORTATION OF THE FILLED CONTAINERS FROM THE TOXIC STORAGE YARD,
OVER APPROXIMATELY TWO AND ONE-HALF MILES OF HARD SURFACED ROADWAY,
TO THE PLANT WHERE THE CONTAINERS ARE PLACED IN A LARGE THAW ROOM.
THE TEMPERATURE IN THIS THAW ROOM IS MAINTAINED BETWEEN 120 AND 140
DEGREES FAHRENHEIT TO FLUIDIZE THE MUSTARD AND FACILITATE THE RE-
MOVAL FROM THE CONTAINER. THIS IS NECESSARY, AS THE AGENT FREEZES
AT A TEMPERATURE OF APPROXIMATELY 50 DEGREES FAHRENHEIT.

THE HEATED CONTAINERS ARE TAKEN TO AN UNLOAD BOOTH WHERE THE
AGENT IS TRANSFERRED TO AN AGENT HOLD TANK. FROM THE AGENT HOLD
TANK, IT IS PUMPED BY A SUBMERGED CENTRIFUGAL PUMP TO A GAS-FIRED
FURNACE WHERE THE MUSTARD AGENT IS INCINERATED. AS THE MUSTARD
AGENT IS HIGHLY COMBUSTIBLE, IT IS ONLY NECESSARY TO MAINTAIN A
GAS PILOT FLAME DURING THE BURNING OPERATION.

THE EXHAUST GASES FROM THE FURNACE, CONTAINING SO_2, HCl AND NO_2,
ARE PASSED THROUGH A SCRUBBER AND THEN THROUGH AN ELECTROSTATIC

PRECIPITATOR TO REDUCE PARTICULATES INTO THE AIR WELL BELOW THE
FEDERAL, STATE AND LOCAL STANDARDS. THE BRINE, RESULTING FROM
THE SCRUBBER OPERATION, IS SPRAY DRIED, AND THE SALTS ARE COL-
LECTED INTO BARRELS FOR LATER DISPOSAL.

THE TON CYLINDER CONTAINS SOME RESIDUE AFTER DRAINING AND IS,
THEREFORE, MOVED INTO A SEPARATE FURNACE WHERE IT IS HEATED TO 1,200
TO 1,400 DEGREES FAHRENHEIT TO BURN OUT THE MUSTARD AND SULFUR. THE
CYLINDERS, WHEN CHECKED OUT BY QUALITY ASSURANCE PERSONNEL AS SAT-
ISFACTORILY DECONTAMINATED, WILL BE OFFERED ON BID AS SALVAGE STEEL.

PRIOR TO REMOVING THE CONTAINERS FROM THE STORAGE AREA, EACH
CYLINDER IS CHECKED FOP 'EAKAGE BY PERSONNEL FULLY DRESSED IN PRO-
TECTIVE CLOTHING, INCLUDING MASK. THE CONTAINERS ARE LOADED INTO
METAL SADDLES, INSTALLED IN TWO AND ONE-HALF TON TRUCKS, BY A
CRANE COMMONLY CALLED A "CHERRY PICKER." THE BODY OF THE TRUCK
HAS A HEAVY METAL PAN BOTTOM, WITH METAL SIDE PANELS, TO PREVENT
MUSTARD FROM GETTING OUT OF THE TRUCK IN THE EVENT OF A MAJOR LEAK
DEVELOPING IN THE CONTAINER DURING TRANSIT.

THE AGENT IS TRANSPORTED IN A CONVOY, CONSISTING OF TWO AGENT
TRUCKS, EACH WITH THREE (3) AGENT CYLINDERS, PLUS A DECONTAMIN-
ATION TRUCK IN FRONT AND A SECURITY VEHICLE FOLLOWING. RADIOS ARE
AVAILABLE IN THE CONVOY TO ALERT PERSONNEL IN THE EVENT THAT AN
ACCIDENT OCCURS IN ROUTE. PRIOR TO THIS PROGRAM, SUCH EXPENSIVE

SAFETY AND SECURITY MEASURES WERE NOT EMPLOYED IN THE PROGRAMS CONDUCTED AT THE ARSENAL.

THE TON CONTAINERS ARE UNLOADED BY AN ELECTRICALLY OPERATED, OVERHEAD CRANE AND MOVED INTO THE THAW ROOM. THE PLANT OPERATION IS PERMITTED TO HOLD ONE-HUNDRED CONTAINERS IN THIS STEAM-HEATED THAW ROOM TO ALLOW A MINIMUM OF FORTY-EIGHT (48) HOURS THAW TIME, THIS THAW ROOM IS CONSTRUCTED WITH INSULATION ON ALL SIDES AND TOP AND IS MAINTAINED UNDER NEGATIVE PRESSURE. MECHANICALLY OPER- ATED, OVERHEAD DOORS ARE INSTALLED AT EACH END OF THE THAW ROOM AND REMAIN CLOSED EXCEPT DURING THE MOVEMENT OF CONTAINERS IN OR OUT OF THE ROOM. THE CYLINDERS ARE STORED ON METAL RAILS, AND A TRENCH EXTENDS THE LENGTH OF THE ROOM TO HOLD ANY MUSTARD IN THE EVENT A LEAK DEVELOPS DURING THE THAWING PROCESS.

THE HEATED CYLINDERS ARE BROUGHT OUT OF THE THAW ROOM, BY A SECOND SET OF OVERHEAD CRANES, AND PLACED IN A MOVABLE CART SET ON RAILS. THIS CART IS DESIGNED SO THAT THE CONTAINER CAN BE TILTED OR ROTATED TO.FACILITATE UNLOADING. AT THE START OF THIS PROGRAM, A DOOR WAS BUILT AT THE FRONT PART OF THE CART. AS THE CART IS MOVED INTO THE UNLOADING BOOTH, THE DOOR SEALS AGAINST THE FRONT OF THE BOOTH SERVING TO FURNISH A PROTECTION FOR THE OPERATOR.

REACHING THROUGH GLOVE PORTS, THE OPERATOR CONNECTS UNLOADING AND VENTING HOSES TO THE VALVES IN THE CONTAINER. THE VALVES ARE THEN OPENED, AND THE AGENT IS DRAWN INTO UNDERGROUND HOLDING TANKS BY VACUUM FROM A NASH HYTOR VACUUM PUMP. THE AMOUNT OF AGENT DRAINED OFF IS MEASURED BY THE SCALES AT THE SIDE OF EACH BOOTH. THE UNDERGROUND STORAGE ROOM, CONTAINING TWO 2,500 GALLON TANKS, IS MAINTAINED UNDER A NEGATIVE PRESSURE. THE AIR DRAWN FROM THIS ROOM IS EXHAUSTED PARTIALLY INTO THE FURNACE BURNING THE AGENT AND PARTIALLY THROUGH CHARCOAL FILTERS.

A NEW BOOTH HAS BEEN BUILT WHERE THE OPERATOR WORKS THROUGH GLOVE PORTS INSTALLED IN THE REAR END, OR SOLID WALL, OF THE BOOTH. THE OPENING, THROUGH WHICH THE TON CONTAINER ENTERS THE BOOTH, IS THEN CLOSED BY A GUILOTINE-TYPE DOOR WITH HERMETICALLY SEALED GASKETS. THIS COMPLETELY SEALS THE TON CONTAINER FROM THE OPERATOR AND GIVES HIM ABSOLUTE PROTECTION IN THE EVENT THE TRANSFER HOSE BREAKS UNDER PRESSURE CREATING A SPRAY OF MUSTARD WITHIN THE BOOTH. THIS BOOTH IS NOW IN OPERATION AND WORKS EXTREMELY WELL WITH FULL APPRECIATION OF THE OPERATORS UN-LOADING THE MUSTARD AGENT.

THE DRAINED CONTAINERS ARE TRANSPORTED TO A SEPARATE ROOM AND INTO A LARGE GAS-FIRED FURNACE. PRIOR TO INSERTING INTO THE FURNACE, A HOLE IS PUNCHED AT EACH END OF THE CONTAINER TO AID

IN THE BURNING AND TO AVOID EXPLOSIVE-TYPE ACTION. THE CONTAINER
REMAINS IN THE FURNACE, AT 1,200 TO 1,400 DEGREES FAHRENHEIT,
UNTIL NO FURTHER FLAMING IS N⁵ ABOVE THE HOLES INDICATING
THAT THE BURNING IS COMPLETE. THE LENGTH OF TIME THAT THE CON-
TAINER REMAINS IN THIS FURNACE IS DEPENDENT UPON THE AMOUNT,
AND CHARACTERISTICS, OF THE RESIDUE REMAINING IN THE CYLINDER.

WHEN THE CONTAINER IS REMOVED FROM THE FURNACE AND COOLED
SUFFICIENTLY FOR TESTING, IT IS CHECKED BY QUALITY ASSURANCE
PERSONNEL. IN THE EVENT IT STILL INDICATES THE PRESENCE OF
MUSTARD, IT IS RETURNED TO THE FURNACE FOR REBURNING; OTHER-
WISE, IT IS DETERMINED SATISFACTORY FOR PROCESSING FOR SALVAGE.
THESE CYLINDERS WILL BE CUT IN HALF WITH A WELDING TORCH, AND
THE SMALL AMOUNT OF ASH REMOVED FROM THE CONTAINER BEFORE SHIP-
PING TO SALVAGE.

THE LIQUID AGENT IS PUMPED FROM THE UNDERGROUND TANKS, BY
A SUBMERGED CENTRIFUGAL PUMP AT APPROXIMATELY 70 PSI, THROUGH AN
ATOMIZING NOZZLE AND INTO A GAS-FIRED FURNACE. THE MUSTARD IGNITES
IMMEDIATELY AND BURNS AND, AS STATED PREVIOUSLY, WILL SUPPORT ITS
OWN COMBUSTION. THE AGENT IS FED INTO THIS FURNACE AT APPROXI-
MATELY TWO (2) GALLONS PER MINUTE, AND THE TEMPERATURE IN THIS
FURNACE APPROACHES 2,000 DEGREES FAHRENHEIT. A CONTROL PANEL,

ALONGSIDE OF THE FURNACE, IS UTILIZED TO CONTROL THE FLOW OF MUS-
TARD, GAS AND AIR INTO THE FURNACE TO MAINTAIN THE DESIRED BURN
RATE AND FURNACE TEMPERATURE.

THE EXHAUST GASES, FROM BOTH THE BULK AGENT AND TON CONTAINER
FURNACES, ARE PASSED THROUGH A QUENCH TANK TO COOL THE GASES WITH
BRINE SPRAYS. THE GASES THEN PASS THROUGH A SCRUBBER COLUMN,
PACKED WITH ONE-INCH GLASS RASCHIG RINGS, AND ARE SCRUBBED WITH
A CAUSTIC SOLUTION WHICH IS CIRCULATED THROUGH A HEAT EXCHANGER
FOR COOLING. THE GASES, EXHAUSTING FROM THE SCRUBBER, ARE PASSED
THROUGH A FIVE-STAGE ELECTROSTATIC PRECIPITATOR TO REMOVE PAR-
TICULATES FROM THE AIR. THESE CONSIST, MAINLY, OF IRON OXIDE.
THE STATE STANDARDS FOR OPACITY ARE SET AT 20 PER CENT. THE
PRECIPITATOR, WITH ONLY TWO UNITS OPERATING, REDUCES THE OPACITY
TO 5 PER CENT; AND WITH THREE UNITS OPERATING, THE OPACITY DROPS
TO 3 PER CENT.

THE BRINE GENERATED FROM THE QUENCH TANK AND SCRUBBER SYSTEM,
ALONG WITH PLANT WASHDOWN WATER, IS PUMPED TO A SPRAY DRYER UNIT
WHERE THE WATER IS EVAPORATED. THE DRIED SALTS ARE COLLECTED
INTO FIFTY (50) GALLON STEEL DRUMS AND STORED IN WAREHOUSES ON
THE ARSENAL FOR LATER DISPOSAL. THESE SALTS CONTAIN MOSTLY
SODIUM CHLORIDE AND SODIUM SULFITE WITH SOME IRON OXIDE AND
SODIUM CARBONATE.

IN THE MUSTARD DEMILITARIZATION OPERATION, THE INPUT INTO THE SYSTEM INCLUDES MUSTARD AGENT, AIR, WATER, SODIUM HYDROXIDE AND NATURAL GAS. EXITING FROM THE PLANT INTO THE ATMOSPHERE INCLUDES AIR FILTERED THROUGH CHARCOAL FILTERS AND SCRUBBED AIR CONTAINING WATER VAPOR. THERE ARE NO LIQUIDS EXPELLED FROM THIS PLANT, AND AS PREVIOUSLY STATED, THE SOLIDS COLLECTED INCLUDE MAINLY SODIUM CHLORIDE AND SODIUM SULFITE.

IN PAST PROGRAMS, WHERE MUSTARD AGENT OR MUNITIONS WERE DESTROYED, THE VAPORS FROM THE INCINERATOR WERE NOT SUBJECTED TO SCRUBBING OR PARTICULATE REMOVAL. DISPERSION, BY PASSING OUT A TWO-HUNDRED FOOT STACK, WAS DEPENDED UPON TO REDUCE LEVELS OF CONTAMINATION TO MEET THE AMBIENT AIR QUALITY STANDARDS.

THE INSTRUMENTATION, MONITORING THE OPERATIONAL AREAS OF THE MUSTARD DEMILITARIZATION PLANT AND THE EXHAUST STACKS, WILL BE TOUCHED UPON LATER IN THE PRESENTATION.

THE NEXT PORTION OF THIS PRESENTATION DESCRIBES THE M34 AIR FORCE CLUSTER BOMB AND THE OPERATIONS INVOLVED IN ITS DEMILITARIZATION.

THE M34 AIR FORCE CLUSTER BOMBS ARE PRESENTLY STORED UNDER METAL, TRANSITORY-TYPE SHELTERS TO PREVENT THE DIRECT SUNRAYS FROM STRIKING AND OVERHEATING THE BOMB CLUSTERS. TO FURTHER PROTECT THESE BOMB CLUSTERS, TEN (10) FOOT HIGH EARTHEN REVETMENTS HAVE BEEN RAISED TO COMPLETELY SURROUND THE BOMB CLUSTERS AND SEPARATE THEM INTO SMALLER GROUPS.

THE STOCKPILE CONSISTS OF 21,115 M34 BOMB CLUSTERS, EACH OF WHICH CONTAIN 76 INDIVIDUAL BOMBLETS, FOR A TOTAL OF 1.6 MILLION BOMBLETS. THESE BOMB CLUSTERS CONTAIN A TOTAL OF 4.2 MILLION POUNDS OF AGENT AND 900,000 POUNDS OF EXPLOSIVES IN THE BURSTERS AND FUZES. THE BOMBLETS ARE CLUSTERED IN FOUR (4) BANKS OF NINETEEN (19) BOMBLETS PER BANK. THE INDIVIDUAL BOMBLET WEIGHS TEN (10) POUNDS AND CONTAINS 2.6 POUNDS OF AGENT AND ONE-HALF POUND TETRYL BURSTER.

IN ORDER TO INSURE THE ABSOLUTE SAFETY ASPECTS, A FACILITY WAS REDESIGNED AND EQUIPMENT DESIGNED TO ACCOMPLISH THE DEMILITARIZATION OF THE BOMB CLUSTER IN A TOTALLY CON- TAINED BUILDING. ALL HAZARDOUS OPERATIONS ARE HANDLED BY REMOTE CONTROL.

THE PROCEDURE FOR THIS DEMILITARIZATION WAS ESTABLISHED FOLLOWING THE REQUIRED GUIDELINES AND INCLUDED THE FOLLOWING OPERATIONS WHICH WILL BE DESCRIBED IN A MORE DETAILED MANNER DURING THE PRESENTATION.

THE M34 BOMB CLUSTERS WILL BE TRANSPORTED IN THE SAME MANNER AS THE MUSTARD TON CONTAINERS, INCLUDING THE CONVOY WITH DECONTAMINATION APPARATUS AND SECURITY VEHICLE.

THE BOMB CLUSTERS ARE TAKEN TO A HOLDING AREA IN THE DEMIL-ITARIZATION FACILITY WHERE THE ROLLING, OR SHIPPING, RINGS ARE REMOVED. THE BOMB CLUSTERS ARE THEN TRANSFERRED TO A DECLUS-TERING CUBICLE AND DISMANTLED. EACH BOMBLET IS PUNCHED AND DRAINED, AND THE EMPTY BOMBLET PASSES ON THROUGH A CAUSTIC BATH AND IS CONVEYED TO A MACHINE WHERE THE BURSTER IS SEP-ARATED FROM THE FUZE. THE BOMBLET IS THEN DROPPED INTO A ROTARY KILN IN WHICH THE BURSTER AND FUZE ARE DESTROYED BY INCINERATION. FINAL DECONTAMINATION IS ACCOMPLISHED IN A SECOND FURNACE, AND THE BOMBLETS ARE THEN READY FOR DISPOSAL AS SCRAP STEEL.

THE OTHER CLUSTER COMPONENTS, OR INERT PARTS, ARE CONVEYED TO A THIRD FURNACE WHERE THEY ARE, ALSO, DECONTAMINATED BY HEAT.

THE LIQUID AGENT FROM THE BOMBLETS DRAINS INTO A HOLD TANK
AND IS PUMPED TO THE ORIGINAL "GB" MANUFACTURING PLANT WHERE IT
IS NEUTRALIZED WITH CAUSTIC. THE RESULTING BRINE IS SPRAY DRIED
IN A FACILITY IDENTICAL TO THAT UTILIZED IN THE MUSTARD DEMIL-
ITARIZATION PROGRAM. THE SALTS PRODUCED, WHICH CONTAIN SODIUM
FLORIDE, ARE COMPACTED AND STORED IN SEALED DRUMS FOR LATER
DISPOSITION.

THE HOLDING ROOM HAS PERSONNEL AIR LOCKS FOR THE ENTRANCE
AND EXIT OF THE PERSONNEL AND BOMB CLUSTERS IN ORDER TO EFFECT
A NEGATIVE PRESSURE IN THE HOLD ROOM. THE BOMB CLUSTERS ARE
STORED ON RAILS, OVER A DUCT COVERED WITH STEEL GRATING, THROUGH
WHICH THE ROOM AIR IS DRAWN AND EXHAUSTED THROUGH VENTURI-
TYPE SCRUBBERS UP A ONE-HUNDRED FOOT STACK.

THE BOMB CLUSTERS ARE TRANSPORTED THROUGH INTERLOCKING
GUILOTINE-TYPE BLAST DOORS INTO THE DECLUSTERING CUBICLES
BY MEANS OF AN OVERHEAD TRAVELING CRANE. THE BOMB CLUSTER
ENTERS THE CUBICLE AND IS PLACED INTO A DECLUSTERING CRADLE.
THIS ROOM IS MONITORED BY A CLOSED-CIRCUIT TELEVISION SYSTEM,
AND NO ONE ENTERS THIS CUBICLE EXCEPT TO CONDUCT MAINTENANCE
OPERATIONS.

THE CLUSTER CASING IS REMOVED MECHANICALLY ALONG WITH THE
METAL HOLDING BANDS AND CLUSTER BARS. THE INDIVIDUAL BOMBLETS

ARE REMOVED BY A COMPUTERIZED AND PROGRAMMED MANIPULATOR. THE
BOMBLETS ARE PICKED UP BY A VACUUM HEAD AND TRANSFERRED TO A
STATION WHERE THE FUZE IS SAFED BY STAKING. THE PARACHUTE CAP
IS PREVENTED FROM FALLING OFF BY CRIMPING THE METAL.

THE BOMBLETS THEN MOVE DOWN A CONVEYOR CHUTE TO A STATION
WHERE HOLES ARE PUNCHED THROUGH THE BOMBLET, AND THE AGENT IS
DRAINED, BY GRAVITY, INTO A PIPE LEADING TO AN UNDERGROUND
TANK.

NEXT, THE BOMBLETS ARE TRANSFERRED, BY A HANGER-TYPE CON-
VEYOR SYSTEM THROUGH A CAUSTIC BATH, TO THE NEXT STATION
WHERE A GUILOTINE-TYPE BLADE CUTS THROUGH THE BOMBLET TO
CUT THE BURSTER AWAY FROM THE FUZE. THIS PREVENTS THE BUR-
STER FROM EXPLODING IN THE ROTARY KILN IN THE DEACTIVATION
PROCESS. THE BOMBLETS PASS THROUGH A SERIES OF TWO BALL-
TYPE BLAST VALVES INTO THE DEACTIVATION FURNACE. ONE VALVE
OPENING ALLOWS THE BOMBLET TO PASS THROUGH, THEN CLOSES,
AND THE SECOND BLAST VALVE OPENS TO ALLOW THE BOMBLET TO
DROP INTO THE FURNACE. THE GASES FROM THIS BURNING OPER-
ATION ARE EXHAUSTED THROUGH A SECOND FURNACE AND THEN THROUGH
A SCRUBBING SYSTEM.

THE ROTARY KILN TURNS AT ABOUT .7 REVOLUTIONS PER MINUTE,
AND THE TEMPERATURE IS MAINTAINED AT 1,000 DEGREES AT THE FIRE

INLET AND 600 DEGREES FAHRENHEIT AT THE OTHER END. THE BOMBLETS ARE MOVED THROUGH THE FURNACE BY MEANS OF A SCROLL ON THE INNER SHELL. WHEN THE BOMBLET EMERGES FROM THE END OF THE FURNACE, THE BURSTER HAS BURNED AND THE ALUMINUM FUZE IS MELTED AND DESTROYED.

THE BOMBLET RECEIVES ITS FINAL DECONTAMINATION BY PASSING THROUGH A SECOND FURNACE ON A HIGH HEAT TYPE METAL CONVEYOR BELT WITH THE TEMPERATURE MAINTAINED AT 1,200 TO 1,400 DEGREES FAHRENHEIT. THE BURNED BOMBLETS ARE FINALLY CONVEYED INTO DUMP TRUCKS FOR MOVEMENT TO A STEEL SALVAGE SCRAP PILE.

THE ENTIRE DECLUSTERING AND DECONTAMINATION PROCESS IS OPERATED FROM A CENTRAL CONTROL ROOM. ALL OPERATIONS CAN BE VIEWED BY CLOSED-CIRCUIT TELEVISION UNITS, AS WELL AS ANY MAINTENANCE THAT IS BEING ACCOMPLISHED. ALL OPERATIONS ARE INTERLOCKED SO THAT ANY MAJOR MALFUNCTION WILL SHUT DOWN THE ENTIRE OPERATIONS UNTIL CORRECTED.

THE AGENT FROM THE DRAINED BOMBLETS WILL BE PUMPED THROUGH DOUBLE-WALLED STEEL PIPE TO THE AGENT NEUTRALIZING FACILITY. THIS BUILDING WAS THE FACILITY IN WHICH ALL OF THE NERVE AGENT "GB" WAS ORIGINALLY PRODUCED. IT IS A SIX-STORY, WINDOWLESS STRUCTURE IN WHICH CONDITIONED AIR ENTERS FROM THE ROOF, PASSES

DOWN THROUGH ALL OPERATING BAYS AND EXITS THROUGH AN UNDERGROUND DUCT TO A SERIES OF TWO VENTURI-TYPE SCRUBBERS.

THE AGENT IS INTERMIXED WITH AN 18 PER CENT CAUSTIC SOLUTION IN A MIXING TEE, AND THE NEUTRALIZED LIQUID DROPS INTO A REACTION TANK. THIS TANK CONTAINS AN AGITATOR WHICH MIXES THE LIQUID UNTIL THE NEUTRALIZATION REACTION IS COMPLETE.

THE NEUTRALIZED BRINE IS TRANSFERRED TO THE SPRAY DRYER, AND AS PREVIOUSLY DESCRIBED, THE BRINE SOLUTION IS REDUCED TO STEAM, WHICH IS EXHAUSTED TO THE ATMOSPHERE, AND A SOLID SALT WHICH IS DRUMMED FOR LATER DISPOSITION.

THE NEUTRALIZATION PROCESS IS CONTROLLED FROM A PANEL IN THE CONTROL ROC .. THIS PANEL INDICATES PRESSURES, TEMPERATURES, STORAGE TANK LEVELS AND CONTROLS THE FLOW OF AGENT AND CAUSTIC THROUGH THE SYSTEM.

THE FINAL PHASE OF MY PRESENTATION COVERS THE INSTRUMENTATION UTILIZED IN THE MONITORING SYSTEM IN THE DEMILITARIZATION PROGRAMS.

THE GOVERNMENT HAS GONE TO THE FOREFRONT IN THE PREVENTION OF AIR POLLUTION FROM THE DEMILITARIZATION PROGRAMS AND TO THE PRE-VENTION OF ANY ESCAPE OF TOXIC CHEMICALS, EITHER LIQUID OR VAPORS, FROM THE DEMILITARIZATION PLANTS. WE HAVE WHAT WE CONSIDER THREE CONCENTRIC MONITORING CAPABILITIES AT THIS ARSENAL WHICH WILL GIVE INSTANT ALARMS IF THE PRESENCE OF ANY SIGNIFICANT AMOUNTS OF TOXIC, OR OBNOXIOUS, VAPORS ARE BEING EXHAUSTED.

934

IN THE MUSTARD PLANT, THE FIRST MONITORING CIRCLE MAINTAINS
CONTINUAL ANALYSIS OF THE AIR IN THE THAW ROOM, UNLOADING BOOTH
AND AROUND THE STORAGE AND PUMP TANKS. THIS MONITORING IS AC-
COMPLISHED BY A TITRILOG II MUSTARD DETECTING INSTRUMENT, WHICH
GIVES A CONTINUAL ANALYSIS OF THE AIR, AND WILL ALARM IF MUSTARD
AGENT IS DETECTED AT A LEVEL OF .8 MILLIGRAMS PER CUBIC METER.
FURTHER MONITORING INCLUDES THE PICKUP OF AIR THROUGH A BUBBLER
SYSTEM. THESE BUBBLER SAMPLES ARE PICKED UP ON AN HOURLY BASIS
AND, WHEN ANALYZED, ARE UTILIZED TO VERIFY THAT MUSTARD CONCENTRA-
TIONS IN THE OPERATING AREAS ARE CONTROLLED BELOW THE THRESHOLD
LIMIT VALUE OF .0042 MILLIGRAMS PER CUBIC METER.

IN THE M34 DEMILITARIZATION PROGRAM, THE FIRST CIRCLE OF
MONITORING AGAIN SURVEYS THE OPERATIONAL AREAS OF BOTH THE DE-
CLUSTERING FACILITY AND THE AGENT NEUTRALIZING BUILDING. THIS
MONITORING IS ACCOMPLISHED BY MEANS OF MECHANICAL AND CHEMICAL
DETECTORS WHICH WILL DETECT "GB" AGENT AT CONCENTRATIONS OF .1
MILLIGRAMS PER CUBIC METER. THE AREAS WILL, ALSO, BE MONITORED
USING THE BUBBLER SYSTEM WITH THE SAMPLES BEING COLLECTED ON AN
HOURLY BASIS. THIS MONITORING SYSTEM WILL DETECT "GB" AGENT AT
A CONCENTRATION OF 3×10^{-4} MILLIGRAMS PER CUBIC METER.

THE SECOND MONITORING CIRCLE INCLUDES THE MONITORING OF ALL
STACK EMISSIONS IN BOTH DEMILITARIZATION FACILITIES. IN THE
MUSTARD PLANT, THE STACK EXHAUSTS ARE MONITORED FOR THE PRESENCE

OF MUSTARD, SULFUR DIOXIDE AND PARTICULATES. THE DYNASCIENCE IN-
STRUMENT ANALYZES FOR SO_2 AND WILL ALARM IF THE CONCENTRATION
EXCEEDS 475 PARTS PER MILLION. THE TRACOR DETECTOR MONITORS FOR
MUSTARD AGENT AND WILL ALARM IF THE MUSTARD CONCENTRATION EXCEEDS
.5 MILLIGRAMS PER CUBIC METER. A BUBBLER SAMPLING DEVICE, FROM
WHICH SAMPLES ARE PICKED UP HOURLY, WILL INDICATE UNACCEPTABLE
MUSTARD LEVELS IF THE CONCENTRATION EXCEEDS 0.03 MILLIGRAMS PER
CUBIC METER.

THE AMOUNT OF PARTICULATES IN THE EXHAUST STACKS IS DETERMINED
VISUALLY BY THE PER CENT OPACITY. CERTAIN PERSONNEL ARE TRAINED
TO GIVE THEM THE CAPABILITY OF READING THE OPACITY PERCENTAGE IN
THE STACK EMISSION.

AT THE M34 CLUSTER DEMILITARIZATION FACILITY, THE STACK EMIS-
SIONS ARE CHECKED BOTH BY THE M5 OR M8 ALARMS, AS WELL AS CONTINUOUS
BUBBLER SAMPLES, AND THE LEVEL OF CONCENTRATION DETECTED IS THE
SAME AS IN THE OPERATIONAL AREAS.

THE THIRD CONCENTRIC MONITORING CIRCLE IS AT THE NINE MONITOR-
ING STATIONS WHICH ARE STRATEGICALLY PLACED AROUND THE PERIMETER
OF THE ARSENAL. EACH OF THESE MONITORING STATIONS HAVE THE CAPA-
BILITY OF DETERMINING THE AMOUNT OF MUSTARD, SULFUR DIOXIDE, ACID
MIST (HCl), NERVE AGENT "GB," AS WELL AS THE SPEED AND DIRECTION
OF THE WIND AT THAT STATION.

IN THE EVENT THAT THE CONCENTRATION OF SULFUR DIOXIDE REACHES
THE LEVEL OF .05 PARTS PER MILLION FOR TEN CONSECUTIVE MINUTES,
AND THE WIND IS FROM THE DIRECTION OF THE MUSTARD FACILITY, AN
ALARM CONDITION WILL BE IN EFFECT. THE QUALITY ASSURANCE LABOR-
ATORY WILL VERIFY THE CONDITION AND, IF VERIFIED, WILL ALERT THE
MUSTARD PLANT SUPERVISION. THE MUSTARD DEMILITARIZATION OPERATION
WILL BE STOPPED AND WILL BE RESUMED ONLY WHEN THE PROBLEM IS RE-
SOLVED AND THE ALARM CONDITION NO LONGER EXISTS.

THE INFORMATION FROM THE MONITORING STATIONS IS AUTOMATICALLY
TRANSMITTED TO THE ARSENAL INSPECTION LABORATORY TELEMETRICALLY
AND IS DISPLAYED ON A MONITORING BOARD. THIS MONITORING PANEL-
BOARD WILL SHOW WIND SPEED AND DIRECTION, AS WELL AS THE EXTENT
OF THE AIR POLLUTION, SO THAT IMMEDIATE ACTION CAN BE TAKEN AND
THE PLANT SHUT DOWN IF NECESSARY.

A TWELVE MONTHS' AVERAGE OF THE RESULTING DATA, FROM THE NINE
STATIONS, INDICATES THAT THE LEVELS OF SO_2, NO_2 AND ACID MIST ARE
FAR BELOW THE ACCEPTABLE STANDARDS. THE ACTUAL AVERAGE VALUES,
FROM THE STACK AT THE MUSTARD DEMILITARIZATION PLANT, SHOW THE
SO_2 AT A LEVEL ONE-HUNDRED TIMES LESS THAN THE STANDARD. THE
LEVEL OF MUSTARD IN THE STACK EMISSION IS RARELY HIGH ENOUGH TO
EVEN BE DETECTED BY THE BUBBLER SAMPLERS WHICH ARE THE MOST SEN-
SITIVE OF THE MONITORING DEVICES.

GENTLEMEN, THIS COMPLETES MY PRESENTATION, AND I WILL BE
GLAD TO ANSWER ANY QUESTIONS YOU MAY HAVE ON THESE OPERATIONS
IF THEY ARE WITHIN MY CAPABILITY OR AUTHORITY TO DO SO.

SUPPRESSIVE SHIELDING OF HAZARDOUS AMMUNITION OPERATIONS

William P. Junkin
Edgewood Arsenal, Aberdeen Proving Ground, Md.

IN 1971, A REQUIREMENT AROSE FOR EDGEWOOD ARSENAL TO PROVIDE AN

OPERATIONAL SHIELD FOR AN OPERATION ON A 4.2" WHITE PHOSPHOROUS FILLED

MORTAR ROUND ASSEMBLY LINE AT PINE BLUFF ARSENAL. A MAJOR CONSIDERATION

IN THE DESIGN OF THE SHIELD WAS THE NEED TO CONSTRAIN THE THICKNESS TO A

MAXIMUM OF 3 INCHES. FOR THIS PROJECT, STEEL VENTED SHIELDS WERE DE-

SIGNED TO PROTECT AGAINST THE EXPLOSIVE EFFECTS. THE BARRIER WAS TO

CONTAIN ALL THE FRAGMENTS, AND SUPPRESS THE HIGH BLAST PRESSURES, FIRE

BALL, AND WHITE PHOSPHOROUS PARTICLES SPRAY WHICH WOULD RESULT FROM THE

DETONATION.

VIEW GRAPH 1 ON

THIS ILLUSTRATES THE MULTI-LAYERED VENTED OR SUPPRESSIVE SHIELD

CONCEPT. THE INTERIOR LAYERS OF LOUVERED AND PERFORATED STEEL SHEET,

STOP DETONATION FRAGMENTS AND FIREBRANDS. ALL LAYERS OF STEEL PERFORATED

SHEET AND THE OUTER LOUVERED SHEET, ACT TO REDUCE BLAST OVERPRESSURE.

THE WIRE SCREENING DISSIPATES THE HEAT FROM THE EXPLOSION. SHIELDS CAN

BE "TAILOR-MADE" TO SUIT THE HAZARD SITUATION; FOR EXAMPLE, PROVIDE

FRAGMENT PROTECTION - BOTH FROM WITHIN AND WITHOUT, AND PROTECT AGAINST

COMBINATIONS OF HAZARDS SUCH AS HIGH BLAST-MINOR FRAGMENT OR MAJOR

FRAGMENT AND LOW BLAST.

VIEW GRAPH 1 OFF

THE MODEL SET BEFORE YOU IS A PARTIAL SECTION OF THE STEEL SUPPRES-

SIVE SHIELD DESIGNED TO CONTAIN THE DETONATION OF THE 4.2-INCH WP MORTAR

ROUND. THE STANDARD EXPANDED METAL GRATING WAS THE LAYER NEXT TO THE

ROUND, AND WITH THE ADJACENT PERFORATED SHEET, STOPPED ALL FRAGMENTS.

THE MATERIALS USED ARE STANDARD STEEL, MILL RUN PRODUCTS. THE MULTIPLE

SUPPRESSIVE LAYERS ARE WELDED INTO PANELS WHICH ARE BOLTED INTO A STURDY

FRAME WORK TO COMPLETELY ENCLOSE THE MUNITION. THE SHIELD DID PERFORM

AS DESIRED; THE RESULTS ARE SHOWN HERE.* ACTUALLY THE WP FIREBALL WAS

LIMITED TO 18' BEYOND THE OUTER SHIELD SURFACE.

VIEW GRAPH 2 ON*/OFF

THE FOLLOWING FILM CLIP CONTAINS SEQUENCES OF SIMULATIONS AND SOME

FULL SCALE TESTS DEMONSTRATING THE OPERATION OF SUPPRESSIVE SHIELDS.

FIRST, MINIATURE MODEL CUBICLES ARE USED TO ILLUSTRATE SHOCK WAVE

EFFECTS AND RELATIVE DAMAGE CAUSED BY EXPLOSIONS IN THEM.

NEXT, USING THE 4.2-INCH WP MORTAR ROUND AS THE TEST MUNITION,

WE'LL SEE THE SUPPRESSIVE SHIELD CONTAINS THE FRAGMENTS AND REDUCE THE

BLAST OVERPRESSURE AND FIRE BALL SO THAT THE LIGHT-WEIGHT ENCLOSURES

IN WHICH THEY ARE PLACED ARE UNDAMAGED. LAST, IN A COMPLETELY DIFFER-

ENT APPLICATION OF SUPPRESSIVE SHIELDING, WE'LL SEE HOW THE DAMAGE

EFFECTS OF DETONATION OF A SINGLE PRIMER IN A SIMPLE TRANSPORT TRAY,

ARE MODIFIED BY THE SUBSTITUTION OF A VENTED SCREEN FOR THE SOLID COVER

OF THE TRAY.

SHOW THE FILM

SCENE 1 - SHOCK WAVE DEVELOPMENT HARD WALL

THIS IS A TWO-DIMENSIONAL SIMULATION OF SHOCK WAVE REACTIONS IN A

THREE-SIDED HARD WALL CUBICLE. NOTE THE SHOCK FRONT MOVING OUT TO THE

941

WALLS AND THE INTENSIFIED REFLECTED SHOCK FRONT AT THE WALL AND THE

CORNERS OF THE CUBE. WHEN THE EVENT IS REPEATED, OBSERVE THE PRESSURE

FRONT LEAKING OUT THE FRONT AND AROUND THE SIDES OF THE CUBICLE.

STIFLING THESE FORCES REQUIRES HEAVILY REINFORCED CONSTRUCTION FOR

BLAST RESISTANT WALLS OF OPERATING CUBICLES AND CAUSES FAILURE OF WEAK

WALLS AND ROOF.

THIS IS A VENTED WALL CUBICLE SIMULATION. NOTE THE PRESSURE FRONT

DIFFUSING THROUGH THE WALLS AND THE ATTENDANT REDUCTION IN THE REFLEC-

TIONS.

THIS INDICATES WHY IT IS POSSIBLE TO CONSTRUCT THESE SHIELDS WITH

THINNER WALLS THAN IS POSSIBLE IN CONVENTIONAL HARD WALL BARRICADES.

SCENE 2 - THE CUBES

THIS IS A SIMULATED SOLID WALLED CUBICLE. THE 135 POUNDS PER SQUARE

INCH OVERPRESSURE PRODUCED BY THE SMALL INITIATOR, WAS SUFFICIENT TO

CAUSE ITS DESTRUCTION.

THIS IS THE SAME TEST USING SCREENS TO SIMULATE VENTED SUPPRESSIVE

WALLS, WITH THE SAME INITIATOR. AS WE SEE IT AGAIN, THE EFFECTS OF THE

INCREASED DEGREE OF VENTING ARE OBVIOUS.

SCENE 3 - FULL SCALE TESTS

WHEN THIS 4.2-INCH WHITE PHOSPHOROUS MORTAR SHELL DETONATES, WHITE

PHOSPHOROUS IS SCATTERED OVER A 60-FOOT DIAMETER AREA, AND FRAGMENTS

ARE THROWN 1,000 FEET FROM THE ROUND. THESE ARE TYPICAL.

SCENE 4 - WP ROUND FIRING IN SUPPRESSIVE SHIELD.

THIS IS A TEST WITH THE 4.2-INCH IN A SUPPRESSIVE SHIELD. THE

SHIELDS REDUCED THE FIRE BALL TO LESS THAN 20 FEET IN DIAMETER; AND

ALL FRAGMENTS AND LARGE PHOSPHOROUS PARTICLES ARE CONTAINED WITHIN THE

SHIELD.

SCENE 5 - FIRING WITHIN THE SHACK

THIS IS A TEST TO ILLUSTRATE THE POSSIBLE USE OF CONVENTIONAL

LIGHT-WEIGHT WEATHER PROTECTION STRUCTURES WITH SUPPRESSIVE SHIELDS.

THE PLYWOOD STRUCTURE SIMULATES A 16-FOOT EXPLOSIVE PROCESSING CUBICLE.

THE SHIELD CONTAINED ALL SHELL FRAGMENTS AND EFFECTIVELY REDUCED BLAST

PRESSURES PREVENTING SIGNIFICANT DAMAGE TO THE STRUCTURE.

SCENE 6

NEXT, THE 4.2-INCH IS DETONATED IN THE STRUCTURE WITHOUT THE SHIELD.

SCENE 7 -- PRIMER TRAY

NOW WE'LL SEE THE APPLICATION OF THE SUPPRESSIVE CONCEPT TO A TRAY

USED TO TRANSPORT 1,400 HIGH EXPLOSIVE PRIMERS SIDE BY SIDE IN A 5.56

MILLIMETER CARTRIDGE MANUFACTURING PLANT. ON THE LEFT SIDE IS THE

SOLID PLASTIC COVER OF THE TRAY. ON THE RIGHT IS THE BASE OF THE TRAY.

IN THE EDGE VIEW, WE CAN SEE THE HIGH DEGREE OF CONFINEMENT OF

THE PRIMERS.

THIS TEST INDICATES THE VIOLENCE WITH WHICH THIS TRAY BREAKS UP

WHEN A SINGLE PRIMER IN A FULL TRAY IS DETONATED. THE RISK OF THE

OCCURRENCE COULD NOT BE TOLERATED IN THE NEW LINES BEING ESTABLISHED TO

PRODUCE THIS CARTRIDGE WHERE THE TRAY IS USED TO FEED PRIMERS INTO THE

LOADING MACHINE. WHEN THE COVER IS REPLACED BY A PERFORATED SHEET,

DETONATION OF A SINGLE PRIMER IN A FULL TRAY CAUSES ONLY TWO MORE TO

DETONATE, THE TRAY DOES NOT RUPTURE. EVEN WHEN FIVE PRIMERS ARE

DETONATED SIMULTANEOUSLY, THE TRAY STILL STAYS TOGETHER. THIS TRAY

WITH THE SUPPRESSIVE COVER IS NOW IN USE AT TWIN CITY, LAKE CITY, AND

FRANKFORD ARSENALS.

END OF FILM

SINCE THE DEVELOPMENT OF THIS VENTED SHIELD WAS REPORTED AT THE

1972 SEMINAR, CONSIDERABLY MORE WORK HAS BEEN DONE, AND BY THE END OF

OCTOBER THIS YEAR, SEVERAL FULL SCALE SUPPRESSIVE SYSTEMS WILL HAVE

BEEN FABRICATED AND TESTED.

OUR CURRENT ACTIVE SUPPRESSIVE SHIELD APPLICATION ENGINEERING

PROGRAMS INCLUDE THREE PROJECTS.

VIEW GRAPH 3 ON

THE MOST COMPLEX OF THESE INVOLVES THE DESIGN, FABRICATION AND

TEST OF A FULL SCALE PROTOTYPE SYSTEM TEST FACILITY SIZED TO HOUSE

THE HAZARDOUS DISASSEMBLY OPERATIONS INVOLVED IN CHEMICAL AMMUNITION

DISPOSAL.

THE THREE MAJOR SYSTEM COMPONENTS ARE THE SHIELD ENCLOSURE, THE

PLENUM CHAMBER, AND THE OUTER WEATHER STRUCTURE. THE SHIELD IS

INSTALLED IN THE SEALED PLENUM. THE OUTER ENCLOSURE PROVIDES A DEAD

AIR SPACE AROUND THE PLENUM FOR LEAK TESTING IT DURING SYSTEM EVALUATION

TESTS AND PROVIDES WEATHER PROTECTION.

THE CRITICAL DESIGN REQUIREMENT OF THIS SYSTEM IS THAT IT MUST

PROVIDE COMPLETE CONFIDENCE THAT IF A DETONATION OCCURS, NO TOXIC

MATERIALS WILL BE RELEASED OUTSIDE THE DISPOSAL FACILITY. THE

GUARANTEE OF LEAKPROOFNESS IS PROVIDED BY THIS LARGE 100,000 CUBIC FOOT

PLENUM CHAMBER AND THE SHIELD. THIS PLENUM IS TIGHTLY SEALED AND

VENTILATED BY A HIGH CAPACITY SYSTEM WHICH PREVENTS ANY EXCESSIVE

PRESSURE BUILD UP IN THE EVENT OF A DETONATION, AND ASSURES A SLIGHT

NEGATIVE PRESSURE WITHIN THE PLENUM DURING NORMAL OPERATION. IT IN-

CLUDES FILTERS TO PURGE ALL TOXIC MATERIALS. THE FUNCTION OF THE

SUPPRESSIVE SHIELD IS TO PROVIDE ASSURANCE THAT THE PLENUM CHAMBER IS

NOT BREACHED AND CRITICAL AUXILIARY SYSTEMS, AND SEALS AGAINST GAS

LEAKAGE ARE PROVIDED A REASONABLE ENVIRONMENT IN WHICH TO PERFORM THEIR

FUNCTIONS.

VIEW GRAPH 3 OFF

VIEW GRAPH 4 ON

THIS IS THE FULL SCALE PROTOTYPE TEST SHIELD. AN OPERATIONAL

SYSTEM WOULD CONTAIN FOUR SUPPRESSIVE ENCLOSURES; HOWEVER, ONLY ONE

IS BEING BUILT FOR TEST TO REDUCE THE COSTS OF THE EVALUATION PROGRAM.

IT IS CONSTRUCTED ENTIRELY OF STEEL AND IS APPROXIMATELY 11 FEET

WIDE, 13 FEET HIGH, AND 23 FEET LONG TO HOUSE THE AUTOMATIC EQUIPMENT

THAT WILL BE REQUIRED. IT ACCOMMODATES 57 MODULAR SUPPRESSIVE PANELS

APPROXIMATELY 4 FEET BY 3 FEET IN SIZE BY 8" THICK.

THE PROTOTYPE FRAMEWORK STRUCTURE IS PURPOSELY OVERDESIGNED TO

ASSURE THAT IT IS STRONG ENOUGH TO WITHSTAND THE REPETITIVE TESTS TO

BE PERFORMED IN THIS OPERATIONAL EVALUATION AND FOR USE IN TESTING

OTHER SYSTEMS FOR DIFFERENT APPLICATIONS.

VIEW GRAPH 4 OFF

THE BLAST SUPPRESSIVE EFFECTS OF THE SHIELD WERE USED TO

MINIMIZE THE STRUCTURAL STRENGTH OF THE PLENUM. WE ACHIEVED A

PRESSURE DROP ACROSS THE SHIELD WALL WHICH RESULTED IN A 2 PSI SIDE-

ON LOAD AT THE NEAREST PLENUM WALL SURFACE; THE PLENUM STATIC PRESSURE

AFTER A DETONATION WILL NOT EXCEED 1/2 PSI.   THIS TEST FACILITY WILL

BE COMPLETED IN SEPTEMBER AND WILL BE TESTED IN OCTOBER.

VIEW GRAPH 5 ON

THE SECOND PROJECT INVOLVES A SUPPRESSIVE ENCLOSURE FOR SHIELDING

OPERATIONS ON 81MM MORTAR LINES BEING INSTALLED AT TWO AMMUNITION

PLANTS.   IT IS DESIGNED FOR THE WORST CASE SITUATION; I.E., SIMULTANEOUS

DETONATION OF 6 ROUNDS CONTAINING A TOTAL OF 12-1/2 POUNDS OF EXPLOSIVE.

IT ASSURES THAT OPERATORS AT ADJACENT STATIONS WILL BE PROTECTED

WITHIN 5 FEET OF THE SHIELD.   NOTE THAT THE THICKNESS OF THE

SUPPRESSIVE WALL IS ONLY 2-1/2 INCHES.   THIS SYSTEM WILL ALSO BE

TESTED IN OCTOBER.

VIEW GRAPH 5 OFF.

VIEW GRAPH 6 ON.

THIS ILLUSTRATES A TRAILER MOUNTED 7' LONG, 7' DIAMETER SUPPRESSIVE

SHIELD CAPABLE OF SAFELY CONTAINING THE EFFECTS OF DETONATION OF A

CLANDESTINE DEVICE CONTAINING 5 POUNDS OF HIGH EXPLOSIVE. THE SHIELD

IS TRANSPORTABLE SO THAT EXPLOSIVE ORDNANCE DISPOSAL PERSONNEL CAN

MOVE IT TO THE DEVICE AND SAFELY REMOVE IT THROUGH POPULATED AREAS

WITHOUT ENDANGERING THE INHABITANTS. THE SYSTEM IS BEING FABRICATED

NOW AND WILL BE TESTED IN OCTOBER OF THIS YEAR. IT WILL THEN BE

PROVIDED TO THE NAVAL EXPLOSIVE ORDNANCE DISPOSAL CENTER IN INDIAN

HEAD, MD., FOR OPERATIONAL EVALUATION.

VIEW GRAPH 6 OFF

THE SHIELD TESTING PROGRAM HAS INCLUDED TOXIC CHEMICAL-SIMULANTS,

INCENDIARY, AND HIGH EXPLOSIVE AMMUNITION. THE EXPLOSIVE CONTENT OF

THE TEST MUNITIONS TO DATE HAS RANGED FROM FRACTIONS OF A POUND TO

POUNDS. EVERY INDICATION IS THAT AS THE CHARGE IS INCREASED, THE

SUPPRESSIVE EFFECTS OF THE SHIELD ARE MORE PRONOUNCED. SCALING COMPU-

TATIONS HAVE BEEN CONFIRMED AS WE PROCEEDED FROM SUBSCALE TO FULL SCALE

TESTING. FOUR-INCH THICK SUPPRESSIVE SHIELDS HAVE STOOD BLAST PRESSURES

IN EXCESS OF 1000 PSI.

VIEW GRAPH 7 ON

THIS SUMMARIZES THE SUPPRESSIVE SHIELD FUNCTIONAL CHARACTERISTICS

BASED ON TESTS TO DATE.

THIS YEAR WE WILL FABRICATE AND TEST SHIELDS AGAINST BLAST

PRESSURES OF 1500 - 2000 PSI - WHICH WOULD BE REPRESENTATIVE OF

PRESSURES TO BE EXPECTED IN A MELT-POUR OPERATION EXPLOSION.

VIEW GRAPH 7 OFF

I WOULD LIKE NOW TO CONSIDER THE GENERAL APPLICATION OF THE

SUPPRESSIVE SHIELD TO AMMUNITION PROCESSING FACILITIES SPACE REQUIRE-

MENTS AND SAFETY.

VIEW GRAPH 8 ON

AS YOU KNOW, WHEN AN EXPLOSION OCCURS IN A THREE-SIDED REINFORCED

HARDWALL CUBICLE, THE HIGH BLAST PRESSURES ARE RELIEVED WHEN THE ROOF

AND ENTRANCE FRACTURE AND BLOW OUT. THESE CHUNKS OF DEBRIS ADD TO

THE FRAGMENT AND BLAST HAZARDS.

VIEW GRAPH 8 OFF

WHEN AN EXPLOSION OCCURS IN A SUPPRESSIVE ENCLOSURE THERE IS NO
FRAGMENT HAZARD. BLAST OVERPRESSURES AND FIRE BALL ARE SIGNIFICANTLY
REDUCED OUTSIDE IT.

OUR CONCEPT OF THE OPTIMUM USE OF SUPPRESSIVE SHIELDING ENCLOSURES
IS TO PLACE THEM IN LIGHTWEIGHT OUTER STRUCTURES WHICH PROVIDE THE
ESSENTIAL WORK ENVIRONMENTAL CONDITIONS - OF WEATHER PROTECTION,
SECURITY, MATERIAL STORAGE, OFFICE SPACE, ETC.

VIEW GRAPH 9 ON

THIS USE IS INDICATED IN THIS ARTIST'S CONCEPT OF A MUNITION
PROCESS LINE. THIS CONVEYOR MOVES MUNITIONS TO AND THROUGH THE
SUPPRESSIVE ENCLOSURES THROUGH DOORS WHICH ARE CLOSED DURING THE
PERFORMANCE OF AUTOMATIC HAZARDOUS OPERATIONS. THE SHIELDS PROVIDE
ADEQUATE PROTECTION TO PERSONNEL NEAR THEM, PREVENT DAMAGE TO MUNITIONS
ON THE CONVEYOR, AND TO THE BUILDING IN WHICH THE LINE IS ESTABLISHED.

VIEW GRAPH 9 OFF

THIS DIAGRAM ILLUSTRATES THE RELATIVE MAGNITUDE OF THE DANGER

AREAS ASSOCIATED WITH THE DETONATION OF A CONFINED 15-POUND HIGH

EXPLOSIVE CHARGE. THE ORANGE AND YELLOW AREAS REPRESENT THE DANGER

AREAS ASSOCIATED WITH A CONVENTIONAL THREE-WALLED CUBICLE (2,000,000

SQUARE FEET), THE YELLOW AREA IS BASED ON BALLISTIC FRAGMENT DISPERSAL

DISTANCE AND DISTRIBUTION. FOR THIS CHARGE SIZE THE RADIUS OF THE

ORANGE AREA (35,000 SQUARE FEET) REPRESENTS THE REQUIRED DISTANCE

WHICH THE BUILDING CONTAINING THE EXPLOSIVE OPERATION MUST BE

SEPARATED FROM ANOTHER INHABITED BUILDING, BECAUSE OF CURRENT

QUANTITY DISTANCE REQUIREMENTS. THE SMALL RED CIRCLE (1,900 SQUARE

FEET) IN THE CENTER OF THE DIAGRAM ILLUSTRATES THE TOTAL HAZARD AREA

APPROPRIATE TO A SUPPRESSIVE SHIELD DESIGNED TO CONTAIN THE 15-POUND

CHARGE. THE ONLY HAZARD IS FROM BLAST, AND AT THIS RADIUS IT IS

SUFFICIENTLY ATTENUATED TO PRECLUDE INJURY TO EARDRUMS. BASED ON

THIS, IF SUPPRESSIVE SHIELDS WERE THE BASIS FOR THE DESIGN OF A PLANT

ENGAGED IN EXPLOSIVES OR AMMUNITION PROCESSING THE SEPARATION

DISTANCES TO OTHER INHABITED BUILDINGS AND SAFE SEPARATION DISTANCES

FOR RELATED PROCESS STEPS COULD BE GREATLY REDUCED.

VIEW GRAPH 10 OFF

VIEW GRAPH 11 ON

FOR EXAMPLE, THIS REPRESENTS A TYPICAL PLANT BUILDING ARRANGE-

MENT WITH SPACING AS REQUIRED BY PRESENT EXPLOSIVES QUANTITY DISTANCE

STANDARDS, AND CONSTRUCTED FROM LACED REINFORCED CONCRETE AS SPECIFIED

IN THE NEWEST DESIGN MANUALS. THE SCALLOPED BORDER REPRESENTS THE

MINIMUM SEPARATION DISTANCE REQUIRED FOR ADJACENT FACILITIES.

VIEW GRAPH 11 OFF

VIEW GRAPH 12 ON

THIS IS THE SAME PLANT, LAID OUT ON THE BASIS OF SUPPRESSIVE

SHIELDING OF ALL HAZARDS OPERATIONS. THE TOTAL AREA REQUIREMENT FOR

THIS PLANT HAS BEEN REDUCED BY MORE THAN 90% WITHOUT ANY COMPROMISE OF

SAFETY.

VIEW GRAPH 12 OFF

VIEW GRAPH 13 ON

THIS SUMMARIZES THE POTENTIAL OF SHIELDS IN NEW PLANTS BASED ON

OUR ENGINEERING STUDIES. THEY OFFER SIGNIFICANT REDUCTIONS IN BULK,

WEIGHT. SPACE, AND COST WITH GREATER ASSURANCE OF PERSONNEL PROTECTION,

IMPROVED PLANT PROTECTION DUE TO ELIMINATION OF DEBRIS AND FRAGMENT

HAZARDS, AND EASIER PLANT CONVERSION, SINCE THE SHIELDS CAN BE READILY

DISASSEMBLED FOR RELOCATION, REPLACEMENT, AND MODIFICATION, WITHOUT

REQUIRING MAJOR BRICK AND MORTAR CHANGES.

THE CONCEPT HAS APPLICATION WHEREVER REAL ESTATE IS AT A PREMIUM,

WHEREVER AUXILIARY SYSTEMS ARE REQUIRED WHICH HAVE OPERATIONAL

LIMITATIONS UNDER CONDITIONS OF HIGH BLAST PRESSURES; WHEREVER

MATERIALS WHICH ARE SENSITIVE TO INITIATION BY IMPACT OR CONTACT WITH

FIREBRANDS, ARE STORED IN THE IMMEDIATE HAZARD AREA, AND WHEREVER

PERSONNEL MUST WORK 'NEAR IN' TO THE POTENTIAL HAZARD.

VIEW GRAPH 13 OFF.

954

TO GAIN FULL UTILIZATION OF THE CONCEPT, NEW APPROACHES MUST BE

TAKEN TO ESTABLISHING SAFE SEPARATION DISTANCES FOR STRUCTURES, PER-

SONNEL, ETC. SINCE PRESENT STRUCTURE DESIGNS DO NOT PRECLUDE THEIR

FAILURE IN AN EXPLOSION, THE SAFETY MANUALS NOW PROJECT THESE

DISTANCES BASED ON THE WEIGHT AND TYPE OF EXPLOSIVES OR PYROTECHNIC

MATERIALS WITHIN A GIVEN OPERATION OR BUILDING TO MINIMIZE THE

POTENTIAL FOR PROPAGATION OF THE EXPLOSION DUE TO BLAST, OR FRAGMENT

AND FIREBRAND CONTACT TO OTHER QUANTITIES OF EXPLOSIVE MATERIAL.

HOWEVER WITH THE SUPPRESSIVE SHIELD, SAFETY SEPARATION DISTANCES

CAN BE BASED SOLELY ON THE ATTENUATED BLAST EFFECTS. TAKING THIS

APPROACH, IT WILL BE POSSIBLE TO GREATLY REDUCE THE REAL ESTATE

REQUIRED FOR AMMUNITION PLANTS WHILE IMPROVING SAFETY OF PERSONNEL

AND FACILITIES.

VIEW GRAPH 14 ON

IN SUMMARY, EDGEWOOD ARSENAL IS DESIGNATED AS THE FOCAL POINT

FOR SUPPRESSIVE SHIELDING ENGINEERING. DURING THE PAST YEAR, WE HAVE

PROGRESSED FROM THE "INTERESTING CONCEPT" PHASE TO FULL SCALE TEST

DEMONSTRATIONS OF THE CONCEPT AS PRODUCTION PLANT OPERATIONAL SHIELDS

EOD PROTECTIVE ENCLOSURES AND AS TOTAL CONTAINMENT FACILITIES FOR

HAZARDOUS OPERATIONS INVOLVING CHEMICAL AMMUNITION DISPOSAL. TESTS

OF THESE FACILITIES WILL BE CONDUCTED WITHIN THE NEXT 60 DAYS. IN

PERFORMING THESE PROGRAMS WE HAVE CONDUCTED SUB-SCALE TESTS WHICH HAVE

CLOSELY CONFIRMED PERFORMANCE PREDICTED USING LONG ESTABLISHED

EXPLOSIVES EFFECTS DATA. THIS YEAR WE WILL CONDUCT ENGINEERING STUDIES

AND TESTS THAT WILL DEMONSTRATE THE CAPABILITY OF THESE SHIELDS TO

PROTECT OPERATIONS INVOLVING LARGE AMOUNTS OF HIGH EXPLOSIVES SUCH AS,

MELT-POUR OPERATIONS, AND PYROTECHNIC AND PROPELLANT MANUFACTURING

OPERATIONS WHERE THE HAZARDS OF PROPAGATIVE REACTIONS EXIST. THE

ARMY IS EMPHASIZING EXPANSION OF SUPPRESSIVE SHIELDING TECHNOLOGY TO

ACCELERATE ITS APPLICATION TO ITS MODERNIZATION AND AMMUNITION DISPOSAL

PROGRAMS AND THUS ACHIEVE THE POTENTIALLY GREAT SAVINGS POSSIBLE FROM
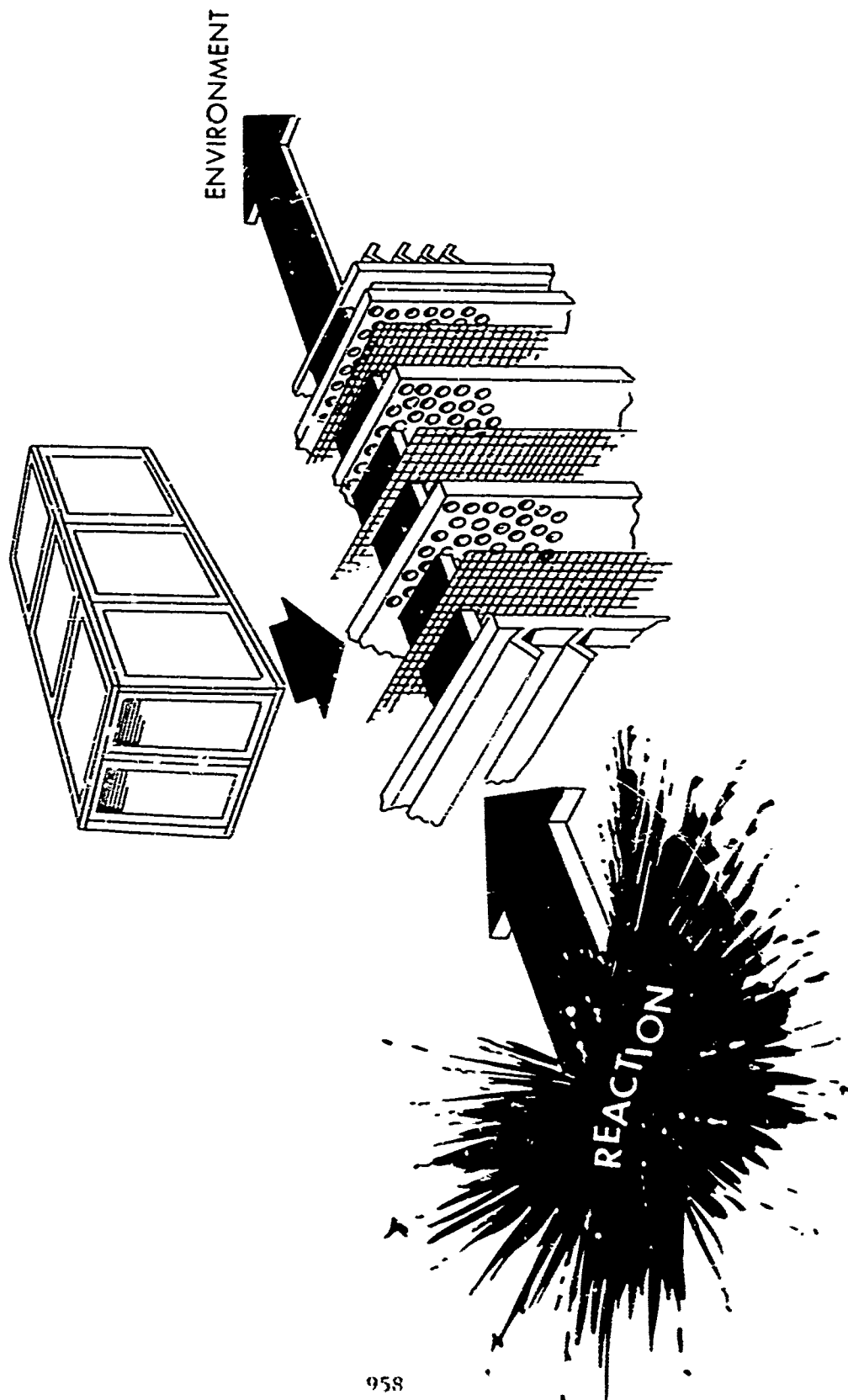
ITS USE.

VIEW GRAPH 14 OFF.

Reports on the testing program are available at Edgewood -

if you wish any, write to:

Commander
Edgewood Arsenal
Attn: SAREA-MT-H
Aberdeen Proving Ground, MD 21010

OPERATIONAL SHIELDING APPLICATION

ENVIRONMENT

REACTION

PERFORMANCE SUMMARY

SUPPRESSIVE SHIELD FOR 4.2" WP MORTAR ROUND

- 100% OF FRAGMENTS RETAINED

- 90% REDUCTION IN FIRE BALL

- 95% REDUCTION IN GLOW BALL

- 68% REDUCTION IN BLAST OVERPRESSURE

- 100% RETENTION OF WP PARTICLES

959

2

CHEMICAL AMMUNITION DISPOSAL SYSTEM (CAMDS) TEST PROTOTYPE

OUTER WEATHER STRUCTURE
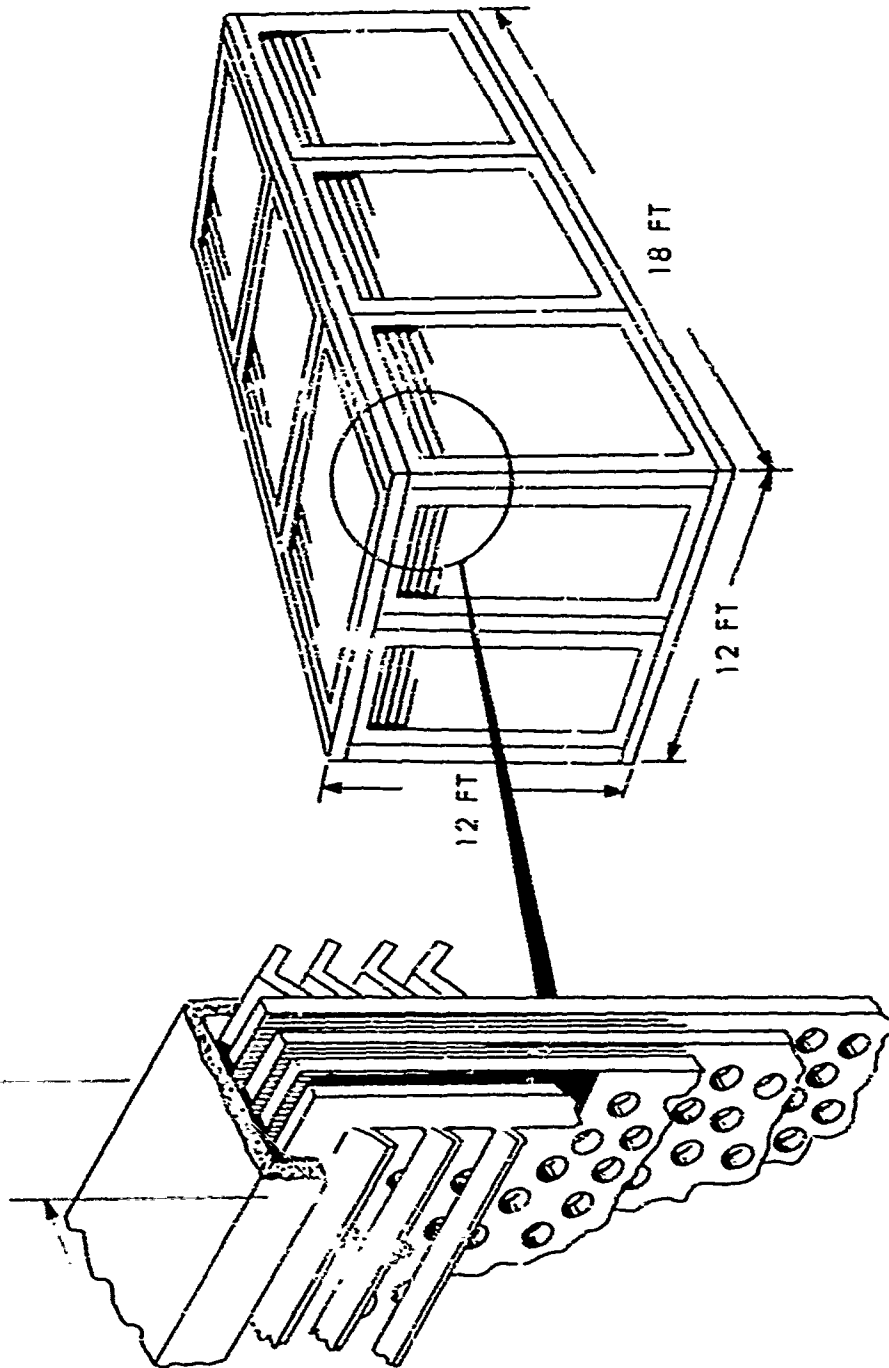
SHIELD

PLENUM

50 FT

24 FT

960

3
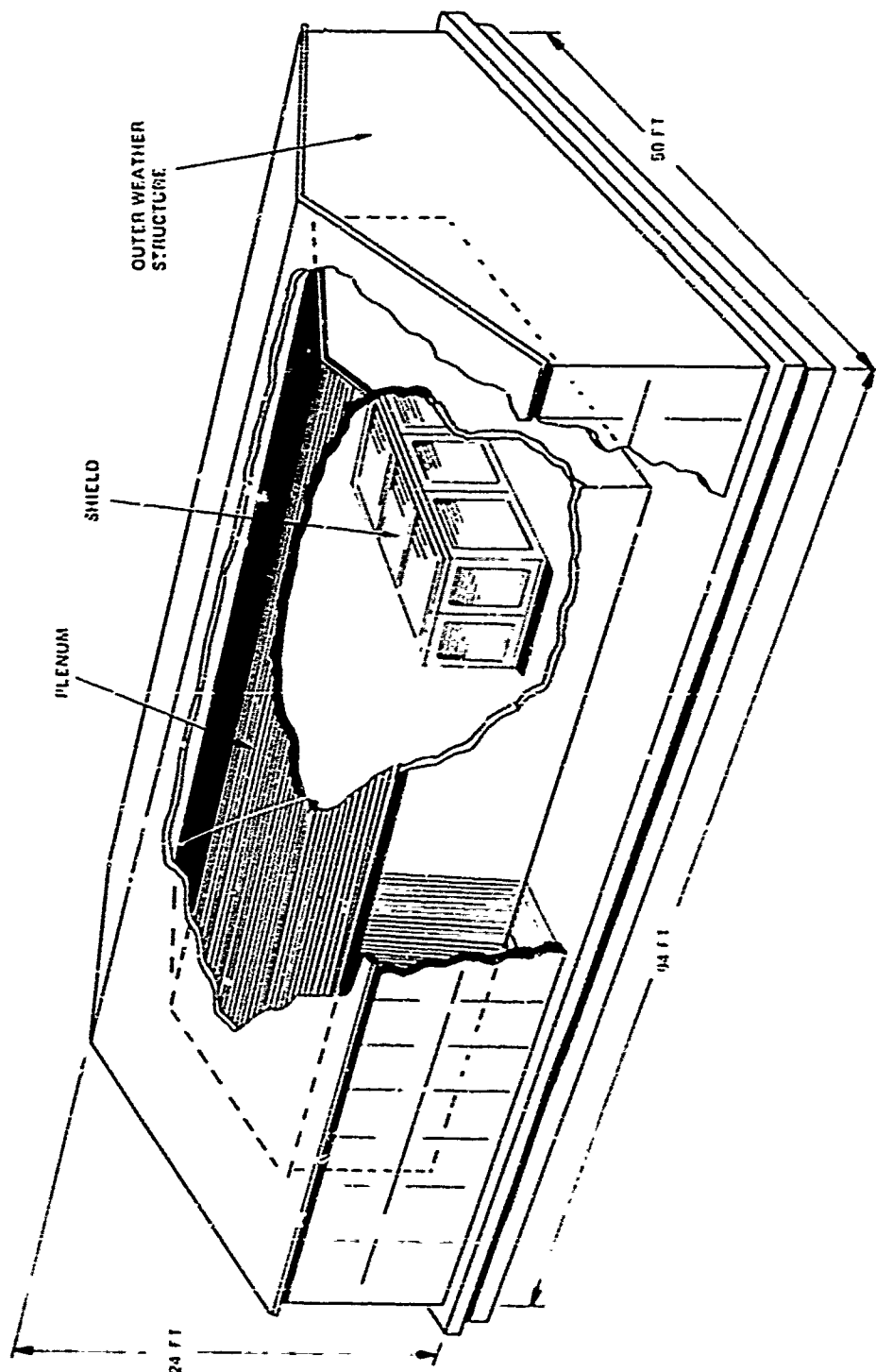
CHEMICAL AMMUNITION DISPOSAL SYSTEM

SUPPRESSIVE ENCLOSURE
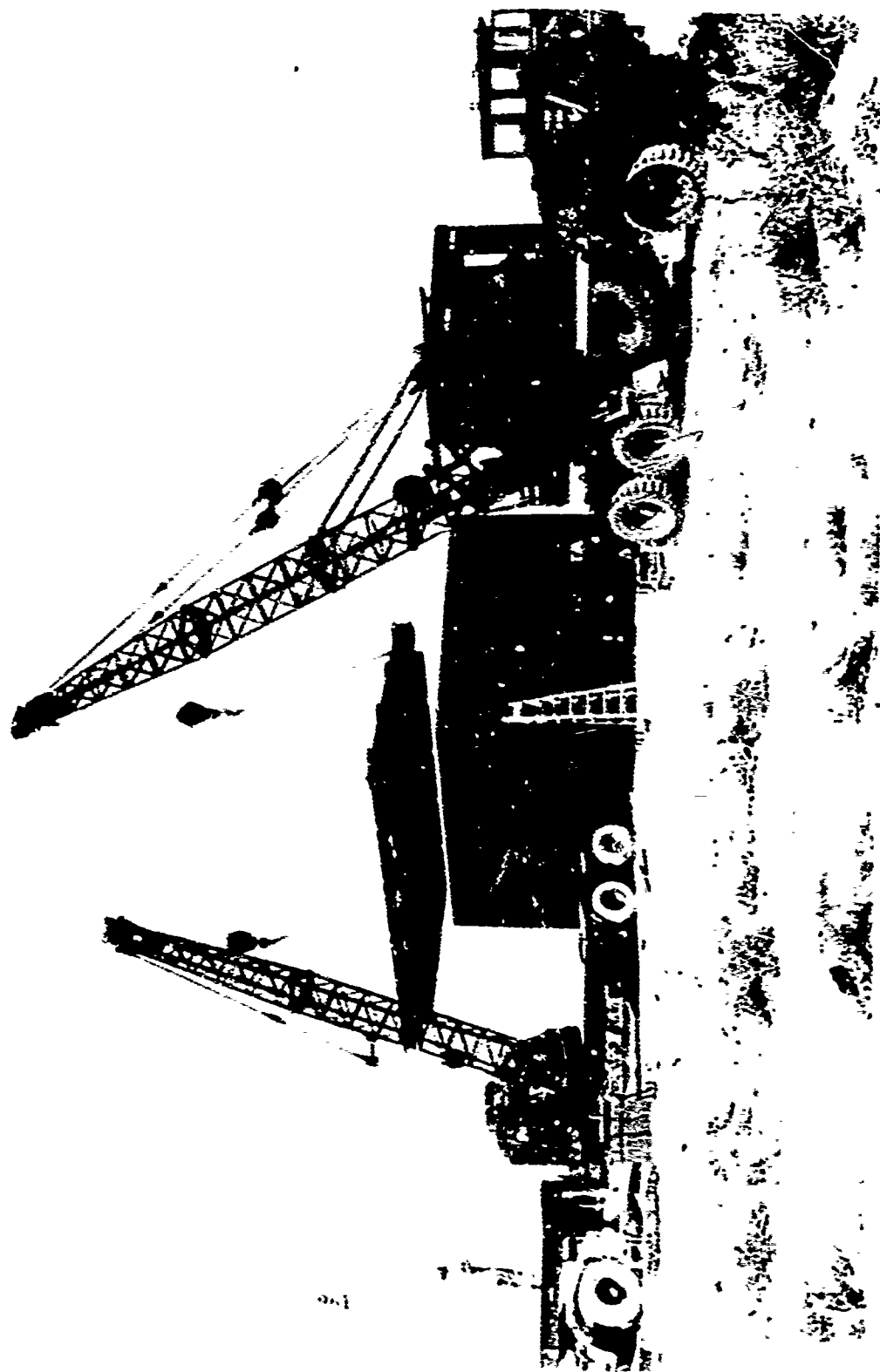
81MM MORTAR LINE SUPPRESSIVE SHIELD
(CAPACITY 6 ROUNDS)

PANEL THICKNESS APPROX. 2½"

18 FT

12 FT

12 FT

5

EXPLOSIVE ORDNANCE DISPOSAL TRAILER

(CAPACITY 1 TO 5 LB. HE IN CLANDESTINE DEVICES)
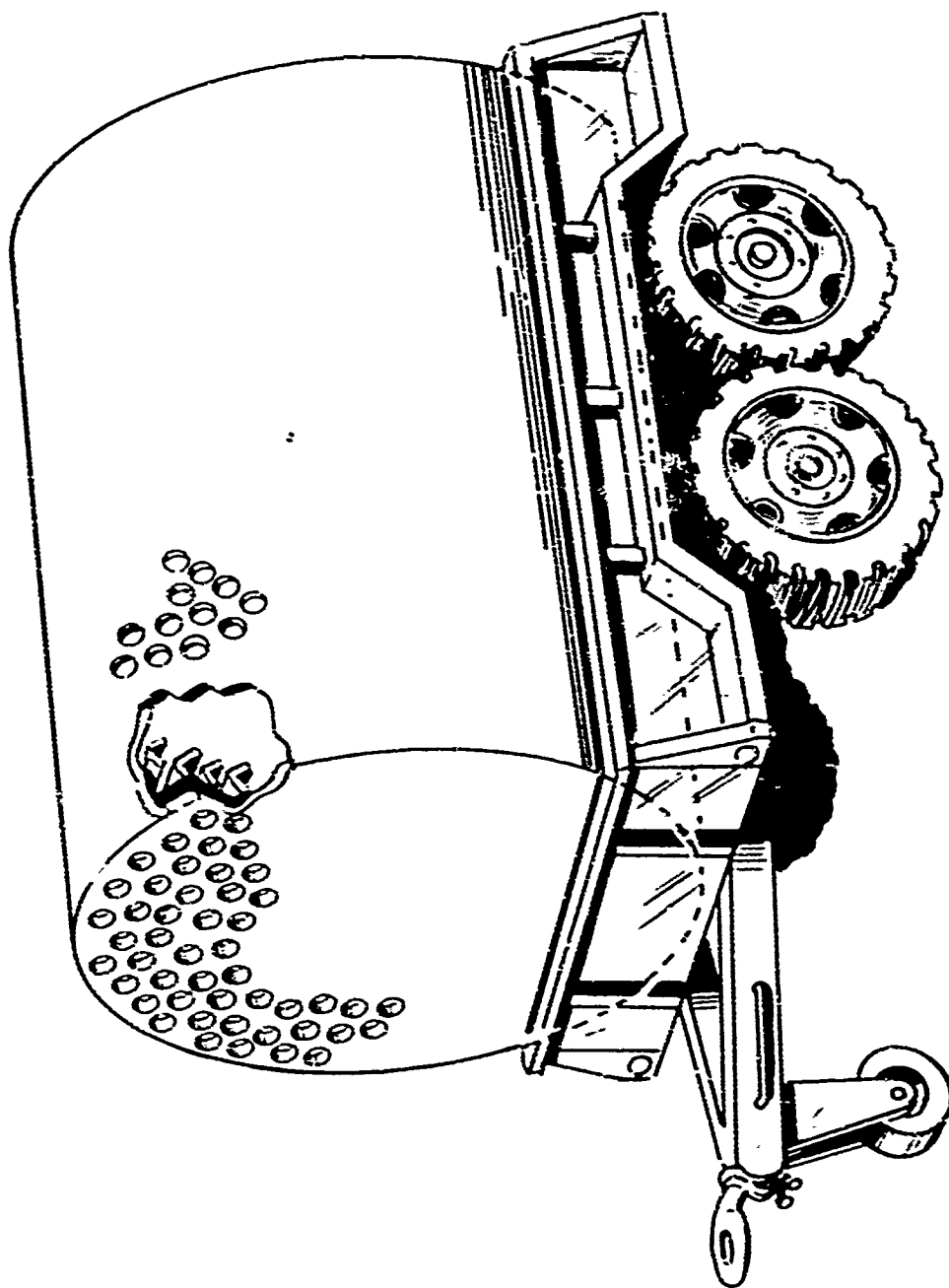
SUPPRESSIVE STRUCTURE
FUNCTIONAL CHARACTERISTICS

HAZARDS PARAMETER	DEGREE OF ATTENUATION/CONTROL
FRAGMENTATION (AND FIREBRANDS)	100%
BLAST OVERPRESSURE (PSI, SIDE ON)	60-80%
IMPULSE PSI/M SEC	60-80%
SHOCK WAVE ARRIVAL	DELAYED BY 50%
FIRE BALL DIAMETER	70-90%
TOXICANT DISPERSION	APPROXIMATELY 90%

964

7
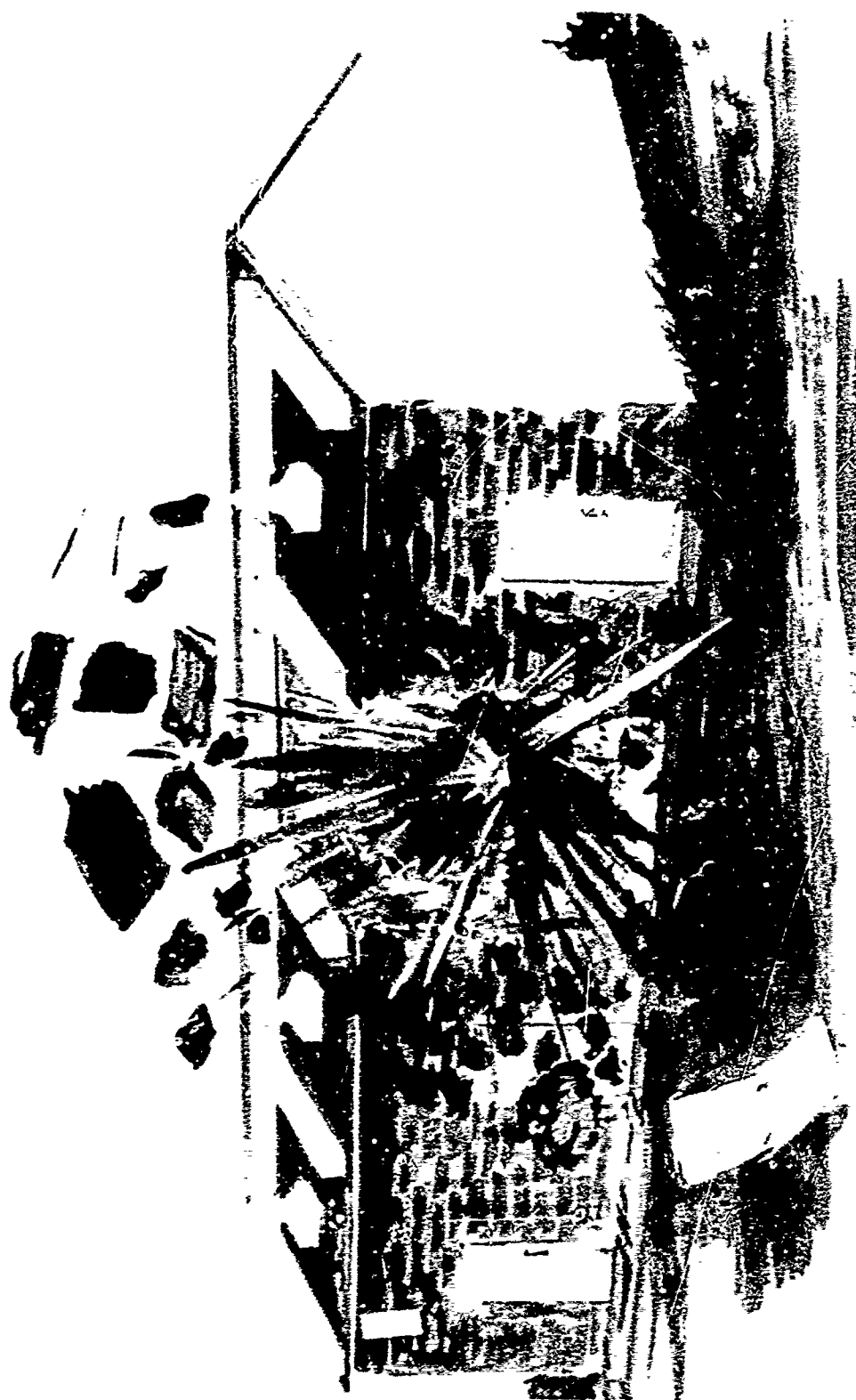
REPRESENTATIVE DANGER AREAS
(15 LB HIGH EXPLOSIVE)

HARDWALL STRUCTURE
DANGER AREA
FRAGMENTS
(yellow)

SUPPRESSIVE STRUCTURE
DANGER AREA (BLAST)
(red)

DEBRIS
(orange)

10
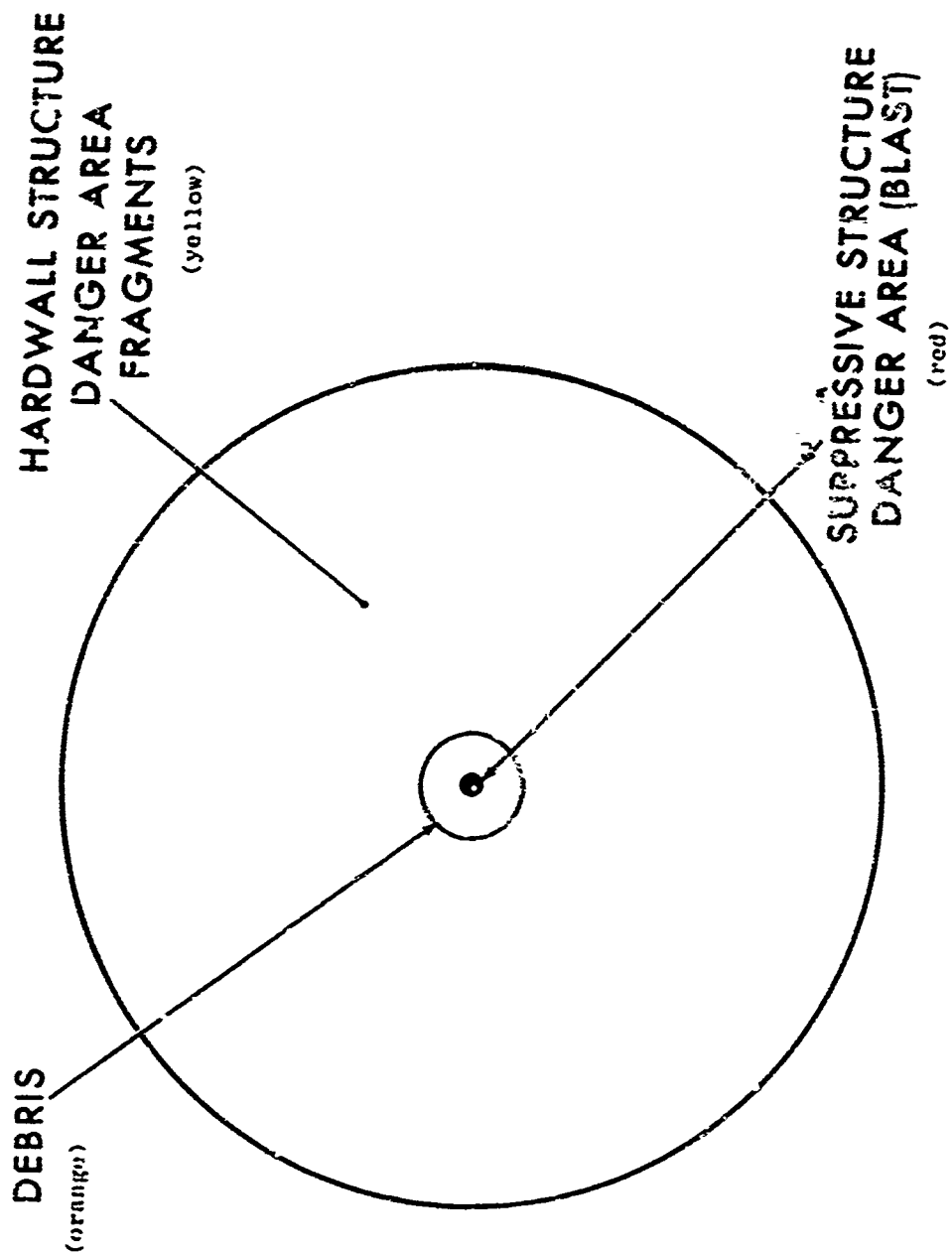
MANUFACTURING AREA WITH HARDWALL CONSTRUCTION
(TM 5-1300, NAVFAC P-397, AFM 88-22)
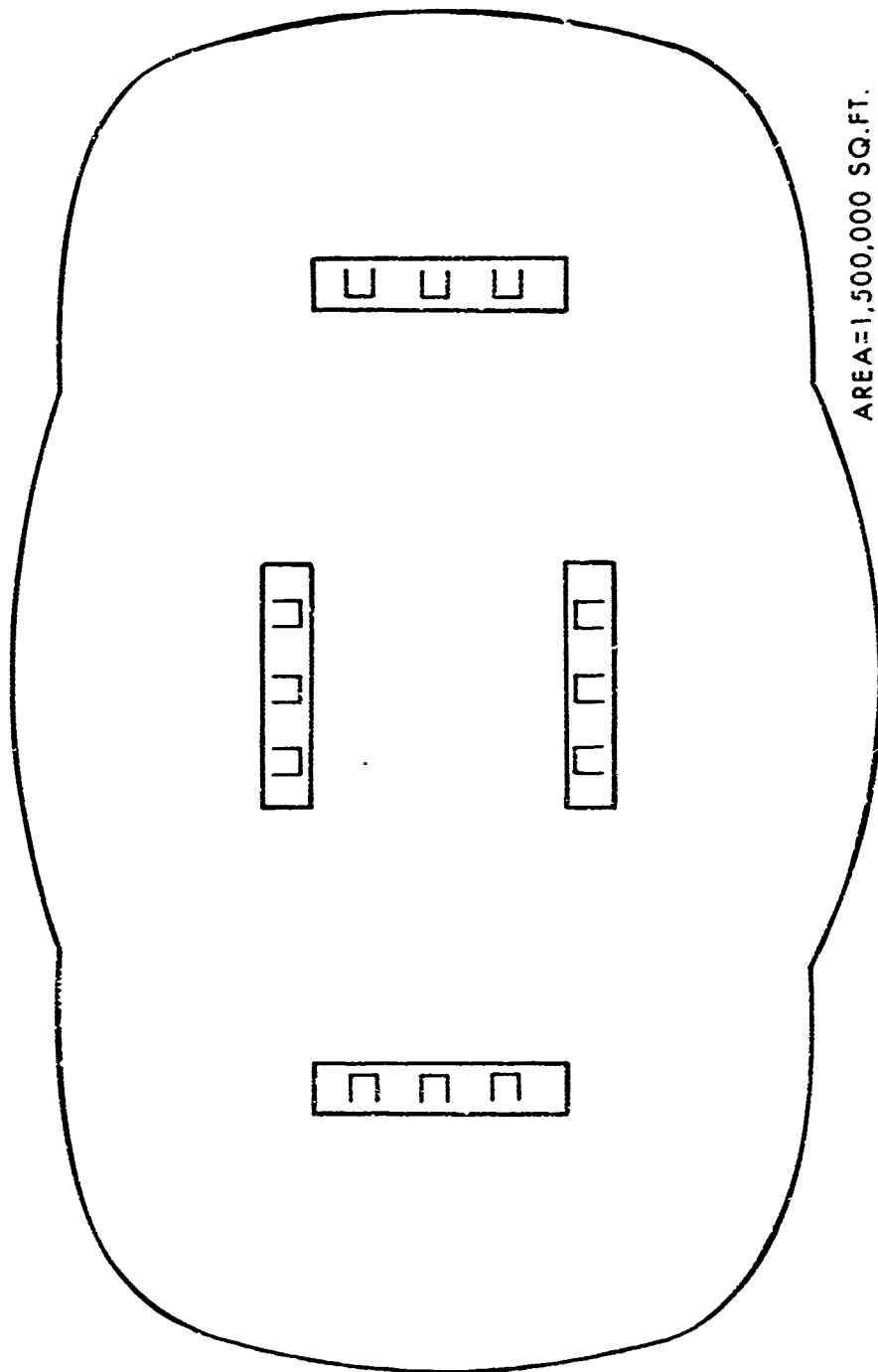
AREA=1,500,000 SQ.FT.
FOUR MUNITIONS LINES
500 LB. HE/BLDG.
INHABITED BLDG. DISTANCE.320FT

TYPICAL MANUFACTURING AREA WITH SUPPRESSIVE SHIELDING
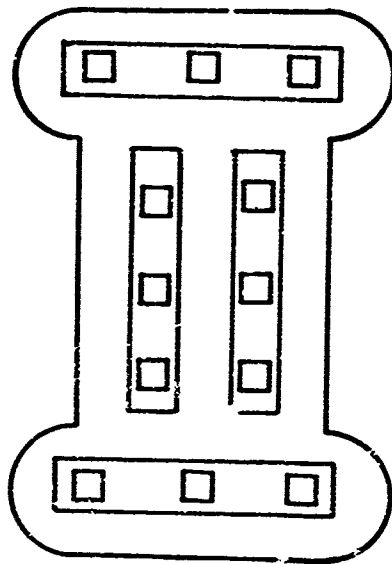
AREA-132,000SQ. FT.
500 LB. HE/BLDG.
FOUR MUNITIONS LINES
BLDG. SEPARATION DISTANCE 61 FT.

12

OPERATIONAL PROTECTION COMPARISON

SUPPRESSIVE SHIELDING vs CONVENTIONAL CONSTRUCTION

- 80% LESS BULK

- 80% LESS WEIGHT

- 95% LESS REAL ESTATE

- 30% LESS COST

- IMPROVED PERSONNEL SAFETY

- COMPLETE FRAGMENT CONTAINMENT

- RAPID PLANT CONVERSION

970

13

SUMMARY SUPPRESSIVE SHIELDING

- EDGEWOOD ARSENAL PROGRAM LEADER

- DEMONSTRATED IMPROVED PROTECTION

- APPLICABLE TO LARGE-SCALE AMMUNITION PROCESSES

- ARMY APPLICATION EFFORT EXPANDING

971

APPRAISING ENERGY HAZARD POTENTIALS BY
ASTM E27'S COMPUTER PROGRAM "CHETAH"

Eli Freedman
USA Ballistic Research Labs
Aberdeen Proving Ground, Md. 21005

Dale N. Treweek and Charles Claydon
Battelle Columbus Lab, Columbus, Ohio

and

William H. Seaton
Tennessee Eastman Co.
Kingsport, Tennessee

ASTM Committee E27 was established about 7 years ago to handle
problems arising from the hazard potential of chemicals. One of its
goals was to develop a computer program that could predict the hazard
potential from a knowledge of only the structure of the material. It is
this program that I am going to discuss here today.

But before starting, I want to emphasize strongly the difference
between what this program tries to do, and what is one of the major
interests of the attendees at this seminar. Most of you are interested
in the problem of defining and predicting the hazard associated with a
given quantity of a known explosive. This goal of this computer code
is quite different.

Approximately 100,000 new organic compounds are synthesized each
year in the United States alone. There is a real need for a quick and
inexpensive method of screening these compounds for explosive hazard
with a minimum of experimental input. That is the aim of the present
program, which is named CHETAH, for Chemical Thermodynamic Estimation and
Hazard Appraisal.

CHETAH has two parts (Figure 1). Part 1 produces an estimate of
the chemical thermodynamic properties of a substance from a knowledge of
only its chemical structure. It carries out this estimation by means of
what is called a second order estimation method. Time does not permit
me to discuss this method, but Figure 2 shows the quality of the results
achieved.

Once the chemical thermodynamic data have been estimated, CHETAH
then proceeds to estimate the hazard potential. There are currently four
different hazard criteria built into the program, as shown in Figure 2.
Let us discuss them in detail.

Preceding page blank

The maximum enthalpy of decomposition is the greatest possible amount of heat that can be liberated by the compound if it were to decompose to the most stable possible products. In reality, these products are not always formed; and if they are, not in the amounts calculated by CHETAH. But that is not significant in this case. Empirically it has been found that there is a good correlation between the hypothetical maximum enthalpy and shock sensitivity. This forms the basis of criterion 1. If the maximum possible enthalpy of decomposition is more negative than -0.7 kcal/gram, the program declares the hazard potential to be HIGH; between -0.7 and -0.3, MEDIUM; and algebraically larger than -0.3, LOW. As with all of the other criteria, only these three levels are recognized by the program.

The second criterion is based on the difference between the maximum enthalpy of decomposition and the heat of combustion. Since a compound that contains sufficient oxygen to enable it to be completely oxidized without the need of outside oxygen is more hazardous than those with either too much or too little oxygen, it follows that the hazard will be greatest when the difference between the maximum heat of decomposition and the heat of combustion is smallest. It is not sufficient, however, just to look at the difference, because this difference is also zero for some non-hazardous compounds, like CCl_4. Hence the difference must be compared with the maximum enthalpy of decomposition, which is never very negative for such non-hazardous compounds. The resultant comparison is shown in Figure 3, which gives the limits for the three degrees of hazard.

Clearly the oxygen balance itself can be used as an indicator of hazard, as has been known for a long time. The oxygen balance for a compound $C_x H_y O_z$ is defined as

$$O.B. = -1600 (2x + 0.5y - z)/\text{mole. wt.}$$

Figure 4 shows the hazard limits associated with the oxygen balance as used in the program.

Criterion 4 is totally empirical. It is defined in Figure 5, and the limits associated with it are given in Figure 6. Experience has shown that this criterion is not useful.

The main problem in using a program like this one is to decide how to set the limits of the various criteria so that few if any hazardous materials escape the screening, even if some non-hazardous ones are erroneously included. These possibilities correspond to the statisticians' type II and type I errors, respectively.

Figure 7 shows that if only criterion 1 is used, and its limits are set at -0.7 kcal/gram for a HIGH hazard, then too many hazardous materials will escape the screen. On the other hand, if the limit is set at -0.3 kcal/gram, then too many non-hazardous materials will be included, and it is obvious that the program will not be used.

If, however, the limit for criterion 1 is set back at -0.7 kcal/gram, and all three criteria are used, then no hazardous material from a sample of 218 compounds will be missed, and only about 12% of the non-hazardous will be mistakenly included.

This program will be made available to the public in January, 1974 by ASTM.

In conclusion, I want to emphasize that the work I have discussed here was done mainly by the co-authors, especially Dr. William H. Seaton of Tennessee Eastman Company, and that my role here today has been mainly one of committee spokesman.

CHETAH

CHETA
ESTIMATION OF CHEMICAL
THERMODYNAMIC DATA

CHTA 2
ENERGY HAZARD POTENTIAL
APPRAISAL

1. MAXIMUM ENTHALPY OF DECOMPOSITION
2. HEAT OF COMBUSTION – HEAT OF DECOMPOSITION
3. OXYGEN BALANCE
4. $y = 10 \, \Delta H_{max}^2 \, w/n$
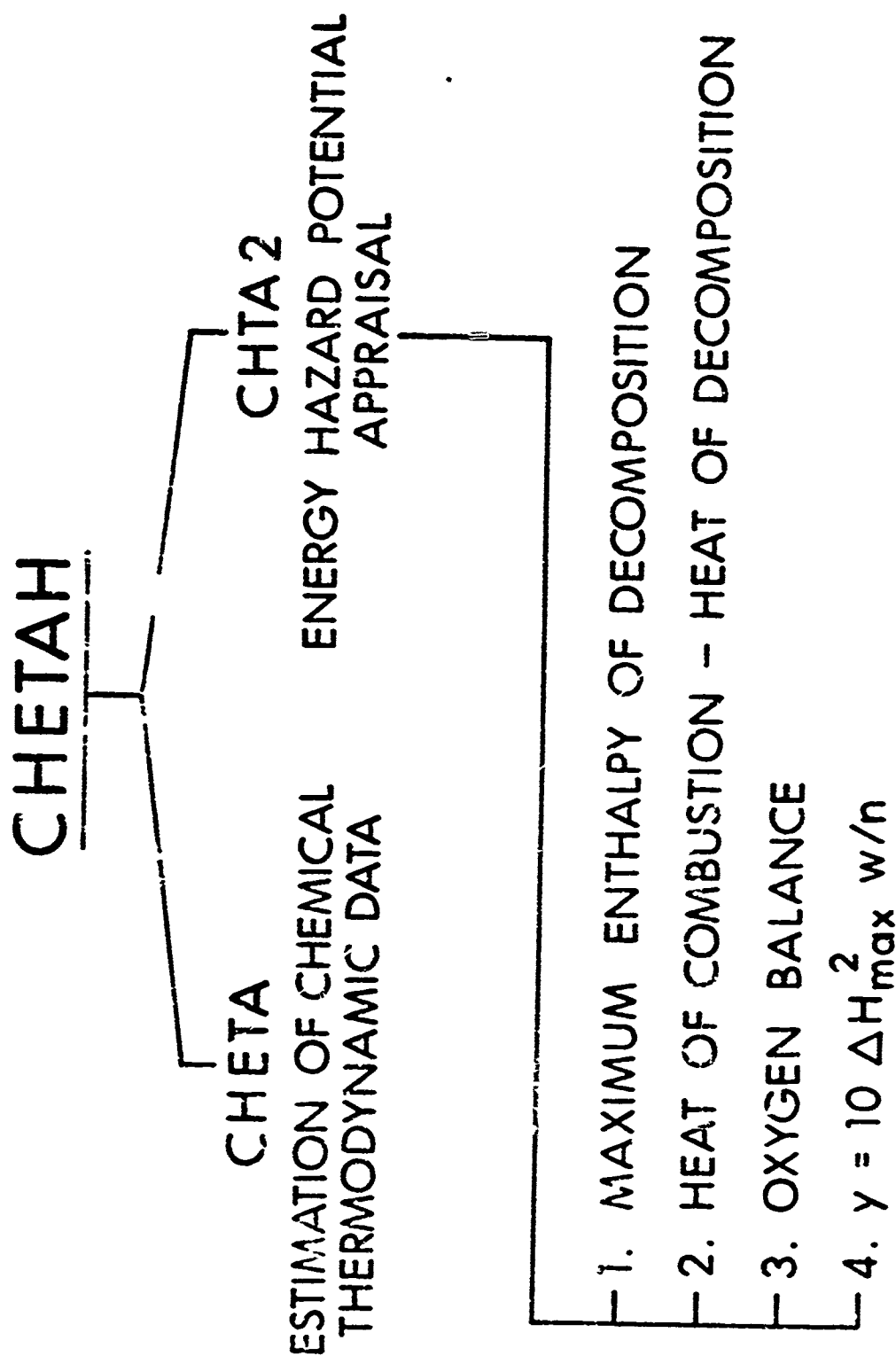
Figure 1.

ESTIMATION ERRORS IN ΔH_f° FOR 25 C,H,O COMPOUNDS

METHOD	MEAN ERROR	STD DEV	95% CONF. LIMITS
ZERO ORDER	-42.6%	77.6%	± 155%
1st ORDER	1.2	9.3	± 18.6
2nd ORDER	-0.3	3.6	± 7.2

Figure 2.

MAXIMUM ENTHALPY OF DECOMPOSITION

HAZARD APPRAISAL

$\Delta H_{max} \leq 0.7$ kcal/g : HIGH

$-0.3 \leq \Delta H_{max} < -0.7$: MEDIUM

$\Delta H_{max} > 0.3$: LOW
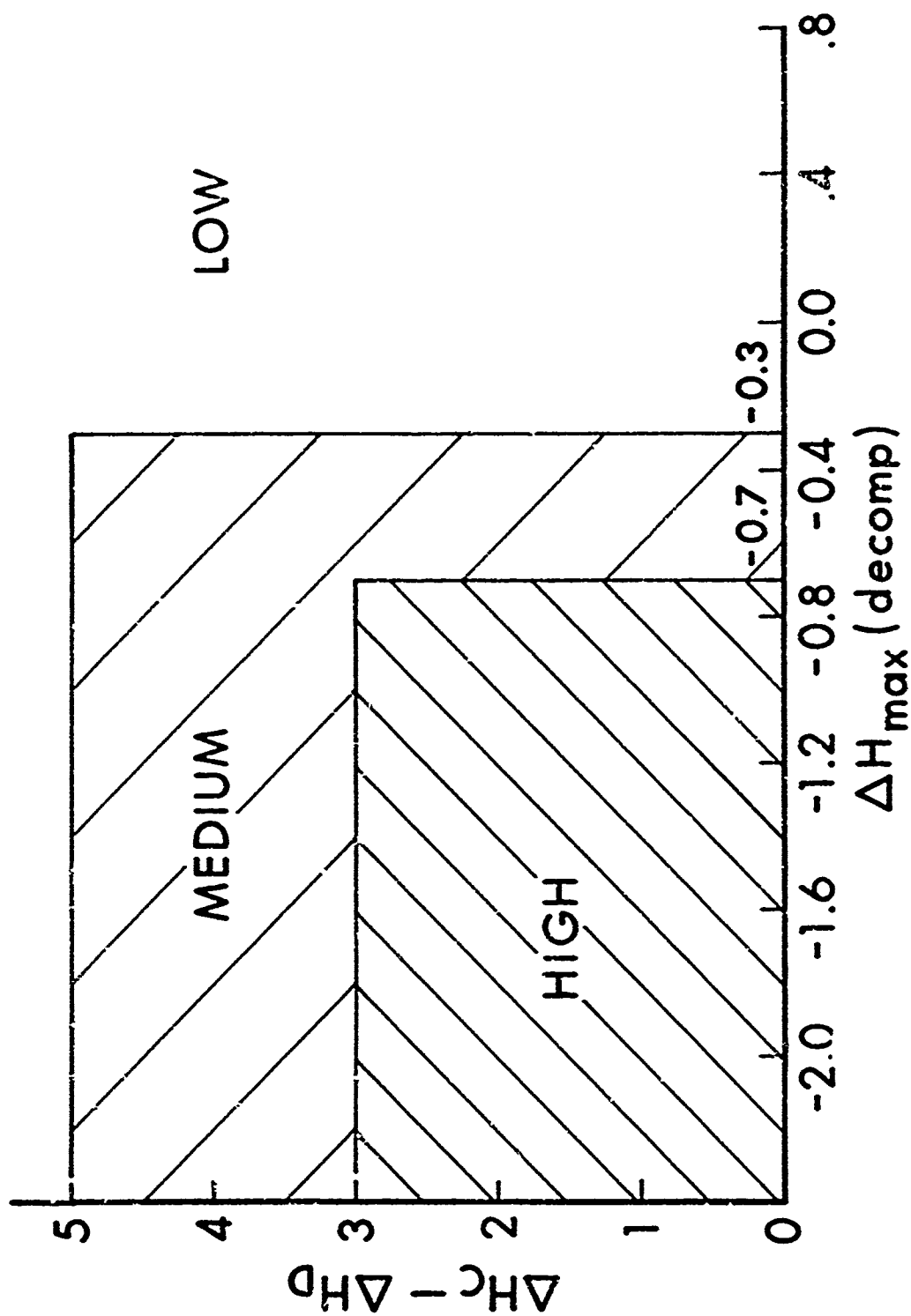
Figure 3.

Figure 4.

OXYGEN BALANCE

HAZARD CRITERION

LOW	MEDIUM	HIGH	MEDIUM	LOW
-160	-80	120	240	

Figure 5.

CRITERION 4

$$y = 10 \; \Delta H_{max}^2 \; w/n$$

w = WEIGHT (grams)

n = NUMBER OF MOLES IN COMPOSITION

$$y \geq 110 : \text{HIGH}$$

$$30 \leq y < 110 : \text{MEDIUM}$$

$$y < 30 : \text{LOW}$$

Figure 6.

RESULTS FOR 218 COMPOUNDS

CRITERION	CRITICAL POINT	TYPE II ERROR	TYPE I ERROR
1	-0.7 kcal/g	27%	12%
1	-0.3	2	75%
1,2,& 3	-0.7	nil	12%

Figure 7.

PROCESS OPTIMIZATION OF A MECHANIZED ROLL:

PRODUCTION AND FIRE FREQUENCY

P. D. Hoffman
W. L. Walker
R. A. Knudsen

Allegany Ballistics Laboratory
Cumberland, Maryland

INTRODUCTION AND SUMMARY

The optimization of the operation of a mechanized roll is a part of the hazards analysis performed by Hercules Incorporated, Allegany Ballistics Laboratory, on a mechanized roll complex. This Army modernization project is being designed and built at Sunflower Army Ammunition Plant. The results of the entire completed hazards analysis, in satisfaction USAMUCOM Regulation 385-22, have been recently reported to Sunflower.

The development of this process optimization application resulted from the need to express the thermal initiation event in probabilistic terms. The general philosophy of a quantitative assessment of risk by the probabilistic approach has been previously presented.[1] The mathematical technique developed in this paper has a general applicability to any assessment of risk due to variance of the in-process potential.

The average production rate of propellant sheet from the mechanized roll is optimized. This includes lost production time due to occasional thermal initiation and fire of the propellant sheet during processing. A mathematical

model is developed that relates the frequency of such fires to the final temperature of the propellant sheet and, in turn, to the operating parameters.

The mathematical model quantifies the level of risk (fire) accompanying any chosen set of roll operating conditions. The optimum cycle time and other parameters are calculated for several nominal moisture contents. In addition, attention is focused on the fact that any major reduction in fire frequency cannot be obtained by tighter control of the roll operation but must be obtained through other measures. In particular, the analysis shows that the major route to reducing fire frequency while maintaining production is through tighter control of the properties of the paste feed to the roll and/or through measurement of those properties for each paste charge and simultaneous adjustment of the roll operating parameters.

DESCRIPTION OF THE PROCESS

The charge of N-5 propellant paste is worked on the 4-roll, Z-type mechanized roll to produce a colloided sheet of propellant. The roll is part of the mechanized roll complex shown in Figure 1 and is labeled calender No. 1 in the figure. Additional conveyors and a carpet roll winding machine, not illustrated, are downstream of the single-pass, even-speed calender No. 2

The schematic of the mechanized roll is shown in Figure 2. The paste is on roll #2 for one-half of the cycle time and passes through two nips formed with rolls #1 and #3. The second nip is maintained at 0.005 inch less than the first nip, which is nominally at 0.050 inch. During the second half of the cycle time, the sheet is worked on roll #4 and passes through a single

nip with roll #3. The rate of work during the second half of the cycle time is 55% of the first half work rate. The nominal setting for gap is ~0.040 inch.

The attainment of the objective, to produce a suitable sheet of colloided propellant, entails some degree of risk. The risk is the thermal initiation of the propellant due to working the paste on the roll. The subsequent loss, for this relatively common occurrence, is essentially only the loss of production time required for clean-up and restart. The risk cannot be eliminated completely and, indeed, within the defined operational situation, minimizing fire frequency will increase cycle time and decrease productivity.

PROCESS MODEL FORMULATION

Since no serious hazard or additional costs occur due to the propellant fire on the rolls, and since ingredient and utility costs are small, the loss is only in production time required for clean-up. Thus the function to be optimized is the production rate. Production rate can be expressed as:

$$P = \frac{a\,(1-x_w)\,W}{\dfrac{t_c}{2} + Af}$$

where

P = production rate, lb/day,

a = conversion factor - 86,400 sec/day,

x_w = weight fraction of moisture in charge, dimensionless,

W = charge weight, lb/cycle,

t_c = total cycle time, sec/cycle,

A = downtime per roll fire, sec/incident,

and f = frequency of roll fires, incidents/cycle.

The factor of two in the equation accounts for the fact that two charges are worked on the roll concurrently so that the cycle time of the roll is one-half that of a single paste charge.

Four parameters are important to the sheet final temperature. The parameters are heat generated by working of the paste on the roll (G), temperature of the roll (T_{roll}), initial paste temperature (T_{paste}), and an initial water content of the paste (x_w). The effect of these parameters on the propellant sheet temperature was evaluated by modeling the roll process on the heat transfer computer program called HETRAN II. Eight cases were run at each of four cycle times for a total of 32 cases, which represent one-half of a 2^4 factorial design at any one cycle time.

The heat generation term for the computer runs consisted of a "shear work" term and a "self heating" term due to nitrate decomposition in the N-5 propellant. The heating rate for the shear work term was calculated for one pass through the first and second nips from the basic equation $G = \tau D$, where τ is the shear strength of the propellant (psi), and D is the shear rate (sec^{-1}) and is defined as the differential velocity, ΔV, divided by gap size, ΔX. This value of G was then normalized with respect to charge weight (W) and averaged over the time it takes for the sheet to make one revolution around the roll. These calculations can be combined into a single term for determining the heat generation in the N-5 sheet. A typical thermal history from one of the computer runs is shown in Figure 3. The shear work heat generation is approximately half during the last half of the cycle. The heat generation due to the decomposition does not become important, relative to the shear work, until about $350^\circ F$.

The value of τ, the effective shear strength of the paste while being worked on the roll, is not known. The value of this parameter for the computer runs was developed by matching an experimental pyrometer temperature history from the original mechanized roll and its associated operating parameters.

From the results of the HETRAN II cases, a predictive equation was developed via the Statistical Analysis System (SAS) stepwise method to select the "best" multiple linear regression equation (cf. Reference 2, Chapter 6).

The resulting equation has the form

$$T_{final} = b_0 + b_1 (T_{roll} + T_{paste}) + b_2 \frac{G}{x_w} + b_3 Gt_c + b_4 G^2 t_c^2 + \frac{b_5}{t_c^2}$$

where T_{final} = final temperature of propellant sheet leaving roll #4, $^\circ$F,

G = heat generated by shear work of the paste on roll #2, Btu/ft^{3}hr,

T_{roll} = initial temperature of the rolls, $^\circ$F,

T_{paste} = initial temperature of paste, $^\circ$F,

t_c = cycle time, sec,

x_w = initial water content of paste, %,

b_0, b_1, b_2, b_3, b_4, b_5 = constants from the regression fit.

The values of the regression coefficients to fit the results of the HETRAN II computer analysis are given in Table I.

A fire results when the final temperature of the propellant sheet exceeds the critical temperature. Nominally, the sheet final temperature is 245°F,

compared to critical temperature of $332^{\circ}F$. The value of the critical temperature was experimentally determined and is for a sheet with ambient air boundary conditions. Theoretical calculations of the critical temperature were also made with kinetic data from similar double-base propellants and the results bracketed the experimentally determined critical temperature.

Although the mean predicted sheet final temperature for the operating situation does not exceed the critical temperature of the sheet, there are variances around the means of the roll operating parameters and waste properties that give a corresponding variance in the sheet final temperature. The probability of the sheet final temperature exceeding the critical temperature in a given operating situation due to this variance is the fire frequency. A graphical representation of the above statement is that the fire frequency is the fractional area under the normal distribution curve above the critical temperature, where the curve is centered on the predicted final temperature. This concept is illustrated in Figure 4. The equivalent mathematical statement is that

$$f = \int_{T_{cr}}^{\infty} \phi \ (T) \ dT = \int_{n_{\sigma T}}^{\infty} \phi \ (n) \ dn$$

where $n_{\sigma T}$ is the number of standard deviations defined by

$$n_{\sigma_{T_{final}}} = \frac{T_{critical} - T_{final}}{\sigma_{T_{final}}}$$

The variance of the sheet final temperature is determined from the standard variance of a function relation (Reference 3, p. 137-145).

$$\sigma^2_{T_{final}} = \sum \left(\frac{\partial T_{final}}{\partial x_i} \right)^2 \ \sigma^2_{x_i}$$

The value of the partial derivatives of T_{final} with respect to the parameters T_{roll} and T_{paste}, is simply the regression coefficient b_1. The partial derivatives on the other independent parameters are functions that must be evaluated for each set of operating values. The shear work term G is a complex function of gap size, ΔX, a direct function of shear strength, τ, differential velocity, ΔV, and charge weight, W.

The derived expression is:

$$G = \frac{\tau \Delta V}{W} \left[\sqrt{0.88 - 8\,(\Delta X_1)} \left(\frac{(K_1 - 0.005\,K_2)}{(\Delta X_1)} + K_2 \right) + \sqrt{0.92 - 8\,(\Delta X_1)} \left(\frac{K_1}{(\Delta X_1) - 0.005} + K_2 \right) \right]$$

where: τ = effective shear strength of the paste, psi,

ΔV = differential velocity between rolls #1 and #2, ft/min,

and ΔX_1 = gap between rolls #1 and #2, inches.

It has been determined that a certain minimum amount of work per pound, E, must be done on the paste to adequately colloid the propellant and mix the ballistic modifiers. Thus, the work rate times the cycle time must satisfy this requirement.

$$G t_c \geq E$$

This is the main mathematical constraint that determines the optimization results. An additional constraint is that the sheet final moisture content must be less than .5%. For the thermal model used, this is equivalent to the constraint that

$$T_{final} \geq 242°F$$

989

A computer program was written to optimize production rate, P, as a function of cycle time t_c. This involved the determination of the parameters G, ΔV, ΔX, T_{final}, σ_T, $n\sigma_{Tfinal}$, and f in satisfaction the above equations and constraints. The constraint $Gt_c \geq E$; i.e., total work done on the propellant, is the factor that produces the results shown in the accompanying figures. The final moisture content constraint of $T_{final} \geq 242°F$ was not encountered for the range of variables studied. The original design values which were based on a cycle time of 150 seconds and standard deviations of the independent variables are shown in Table II.

DISCUSSION OF RESULTS

As cycle time is reduced, the work rate is increased proportionately to satisfy the constraint to maintain the same total work input. This work is manifested as heat energy. Consequently, as cycle time is reduced, there is less time for this fixed total amount of heat to be lost from the sheet and the sheet final temperature for a particular moisture content is higher as the cycle time is reduced. The sheet final temperature as a function of cycle time and moisture content is shown in Figure 5.

As cycle time is reduced with the fixed total work input, the higher value and increased variance of the sheet final temperature gives a higher fire frequency. The fire frequency as a function of cycle time and moisture content is shown in Figure 6.

As cycle time is reduced, the production rate increases initially as a hyperbolic function. The fire frequency is also increasing, but the term Af

990

in the denominator of the production equation is insignificant compared to the roll cycle time, $t_c/2$. As cycle time is further reduced, the down time due to fires becomes significant and the production rate reaches a maximum value and then decreases with further reduction in cycle time. Figure 7 shows the production rate versus cycle time results for a range of moisture contents. The higher moisture content, by providing additional heat removal, allows the paste to be worked more vigorously over a shorter cycle time and results in a higher production rate.

For this study, it has been found that the gap setting has virtually no influence on temperature variance or sheet final temperature as long as the differential velocity is adjusted to maintain a constant work rate, G. The necessary relationship to give the constant work rate for the three optimum points are shown in Figure 8. The values of the parameters for the optimum production rate for the three moisture contents is given in Table III. The optimum gap setting of 0.063 inch was used to calculate the requisite value of the differential velocity, ΔV. The HETRAN thermal analysis did not include the effect of propellant sheet thickness so that sheet final temperature is apparently independent of sheet thickness. This may not be true. Also, the sheet thickness is not freely variable, but is constrained in a qualitative manner for realization of a satisfactory product.

Of the nine independent variables, the variance due to the moisture content, x_w, and effective shear strength, τ, accounted for 99.8% of the variance in the sheet final temperature, T_{final}, with τ responsible for 75 to 85% of the total variance. Thus the variance of the properties of the

991

paste charged to the mechanized roll is the overwhelming contributor to the variance of sheet final temperature and resultant fire frequency.

The standard deviation of the effective shear strength, σ_T, is not actually known. The value of 30 psi is the standard deviation of sheet tensile strength after final rolling. The actual value of σ_T may be greater or smaller which would shift the optimum points. However, the general conclusion of the importance of τ and σ_T in contributing to the fire frequency would not be changed.

The optimum production rates for several initial moisture contents of the N-5 paste, have been calculated. These optimum points are for processing charges with average moisture contents of 5, 8 or 10% water. The standard deviation of 1.3% around those average values still contributes to the fire frequency. A significant improvement in production rate and/or fire frequency would be realized if the moisture content of each paste charge to the roll were measured, and simultaneous adjustment made to the parameters of gap, ΔX, differential velocity, ΔV, and cycle time, t_c, to maintain optimum production rate. In addition, the variance in the moisture content value, which is now known, would be reduced to the variance inherent in the measurement by the moisture analyzer system. As a result, the optimum points for the nominal moisture contents would also shift to lower cycle times and higher production rates.

The fire frequency at the optimum production rate for 8% water, is 0.0032. This is equivalent to 160 fires per million pounds processed when charge weight is 20 pounds. This is a relatively high fire frequency level compared to historical fire frequency data. However, attempts to reduce fire frequency

992

level by increasing cycle time or reducing total work input will lead to lowered production, nonquality product or both. A management decision can be made to reduce the fire frequency and the decrease in production rate relative to the optimum can be assessed. For instance, if cycle time is increased to 113 seconds from 98 seconds, the fire frequency is reduced by about 72% at the cost of a 5% decrease in the production rate from the optimum rate.

CONCLUSIONS

Three specific accomplishments of the optimization study are:

1. The optimum cycle time to maximize production has been determined for the design of 8% moisture.

2. The optimum cycle time and associated operating parameters for the mechanized roll are developed for moisture contents of the paste that are nominal values of 6 and 10%.

3. The relationships developed show that the major contributors to the variance in sheet final temperature are the variance in the effective propellant shear strength and variance in the moisture content.

Furthermore, the technique developed has a more general applicability within the risk analysis field. The variance and functional relationship of any in-process potential (in this case the temperature) to a set of independent parameters and their variance can be determined. The relationship can be a predictive model that is fitted to data generated by experimental measurements or computer modeling, or a functional model developed from

fundamental physical laws The probability of the undesired event can be found by comparison of the in-process potential to the measured material response with the accompanying variances. With these relationships expressed mathematically, then the desired objective function (production rate in this example) can be optimized.

REFERENCES

(1) R. H. Richardson and J. M. Sutton, "Risk Analysis," Minutes of the Fourteenth Annual Explosives Safety Seminar, November 8-10, 1972, p. 467-489.

(2) Draper, N. R. and Smith, H., *Applied Regression Analysis*, John Wiley and Sons, Inc., New York 1966.

(3) Volk, W., *Applied Statistics for Engineers*, McGraw-Hill Book Co., New York, 1953.

TABLE I

REGRESSION COEFFICIENTS AND FIT STATISTICS

$$b_0 = 101.79$$

$$b_1 = .45962$$

$$b_2 = 7.0394 \times 10^{-4}$$

$$b_3 = -2.3333 \times 10^{-6}$$

$$b_4 = 2.5919 \times 10^{-14}$$

$$b_5 = -1.4013 \times 10^{5}$$

$$r^2 = .9711$$

$$F = 154.7$$

TABLE II

DESIGN VALUES AND STANDARD DEVIATIONS
FOR EACH PARAMETER

Variable	Nominal Value	Standard Deviation	Coefficient of Variation
T_{roll}	190°F	0.7	0.37%
T_{paste}	150°F	1.6	1.07
x_w	8%	1.3	16.25
τ	185 psi	30	16.22
$\bar{W}$	20 lb.	0.05	0.25
ΔV	40 ft/min.	0.001	0.0025
ΔX	0.050 inch	0.0005	1.00
t_c	150 sec	0.1	0.067

TABLE III

OPTIMUM POINT PARAMETERS

	Water Content, X_{H_2O}		
	6%	8%	10%
t_c, sec	144	98	64
G, Btu/ft^3 hr	468,750	688,780	1,054,700
ΔX, inches	0.063	0.063	0.063
ΔV, ft/min	53.5	78.6	120.3
T_{final}, °F	266.9	264.7	259.0
σ_T, °F	24.8	24.7	26.7
f, fires/cycle	0.0043	0.0032	0.0031
P, lb/day	20,370	29,030	41,500

CHARGING CARRIAGE

CALENDER No. 2

FOLDING CHUTE

DIELECTRIC HEATER

CALENDER No. 1

METAL REJECTOR

MOISTURE ANALYZER

METAL DETECTOR
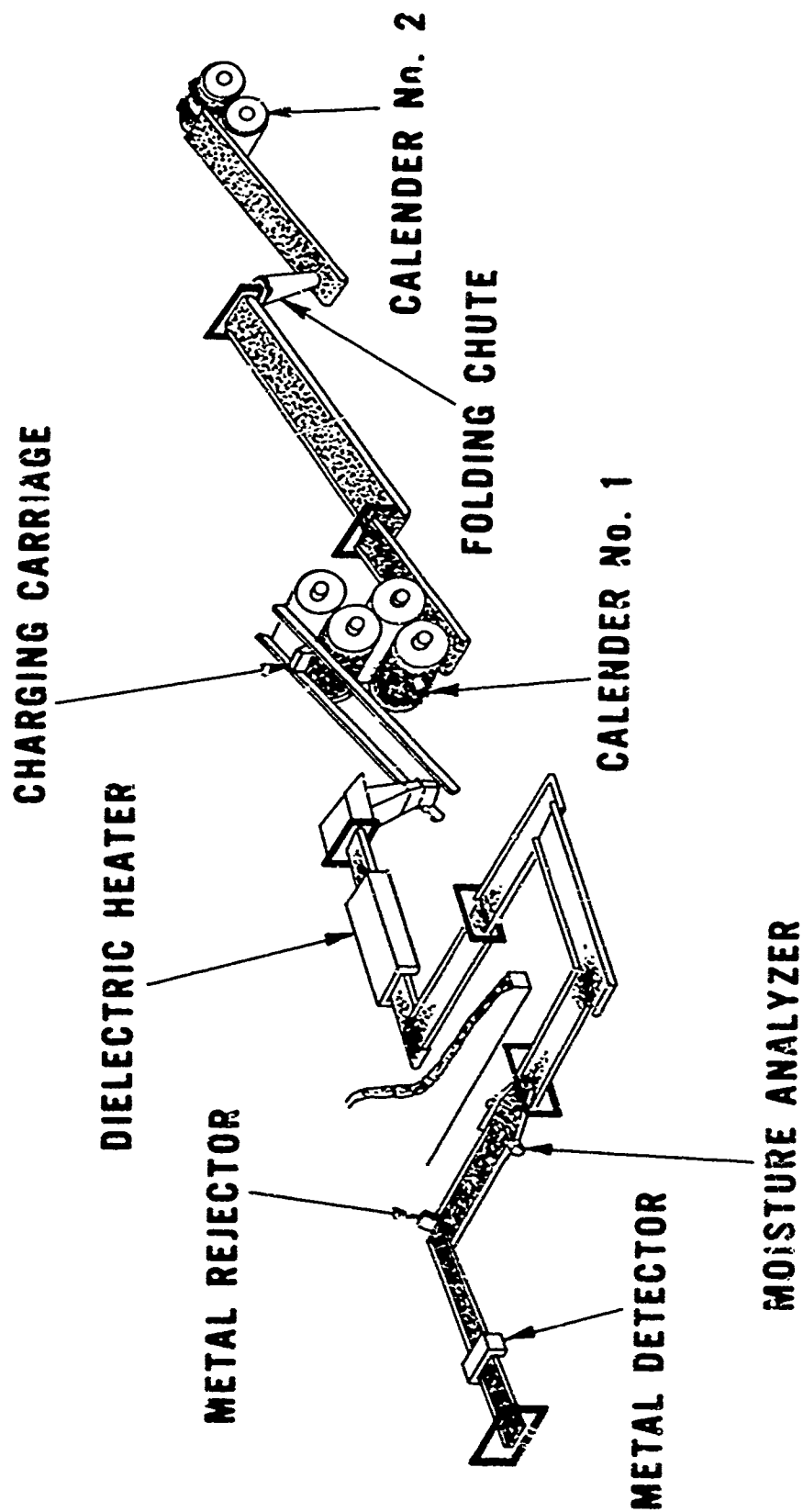
FIGURE 1
Mechanized Roll Complex

SHEET THICKNESS
EXAGGERATED

No. 1

No. 2

No. 3

No. 4
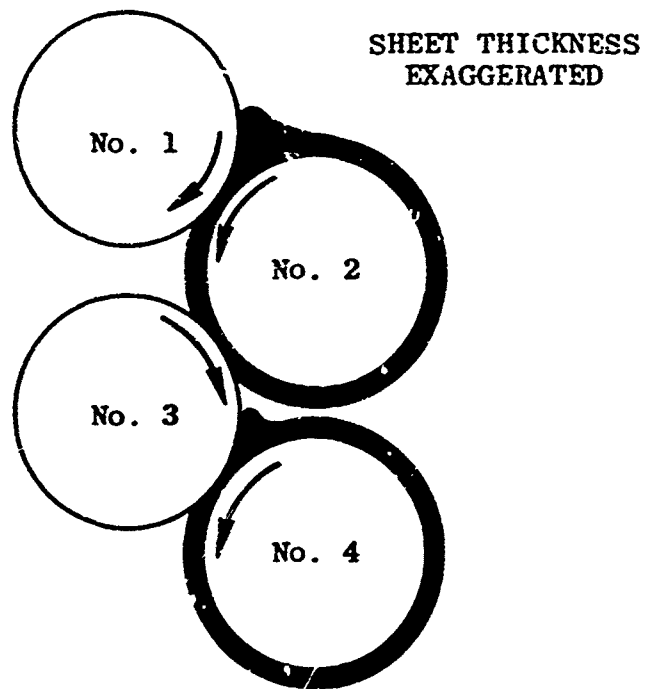
FIGURE 2

Geometry of Four-Roll Z-Type Mechanized Roll

1000
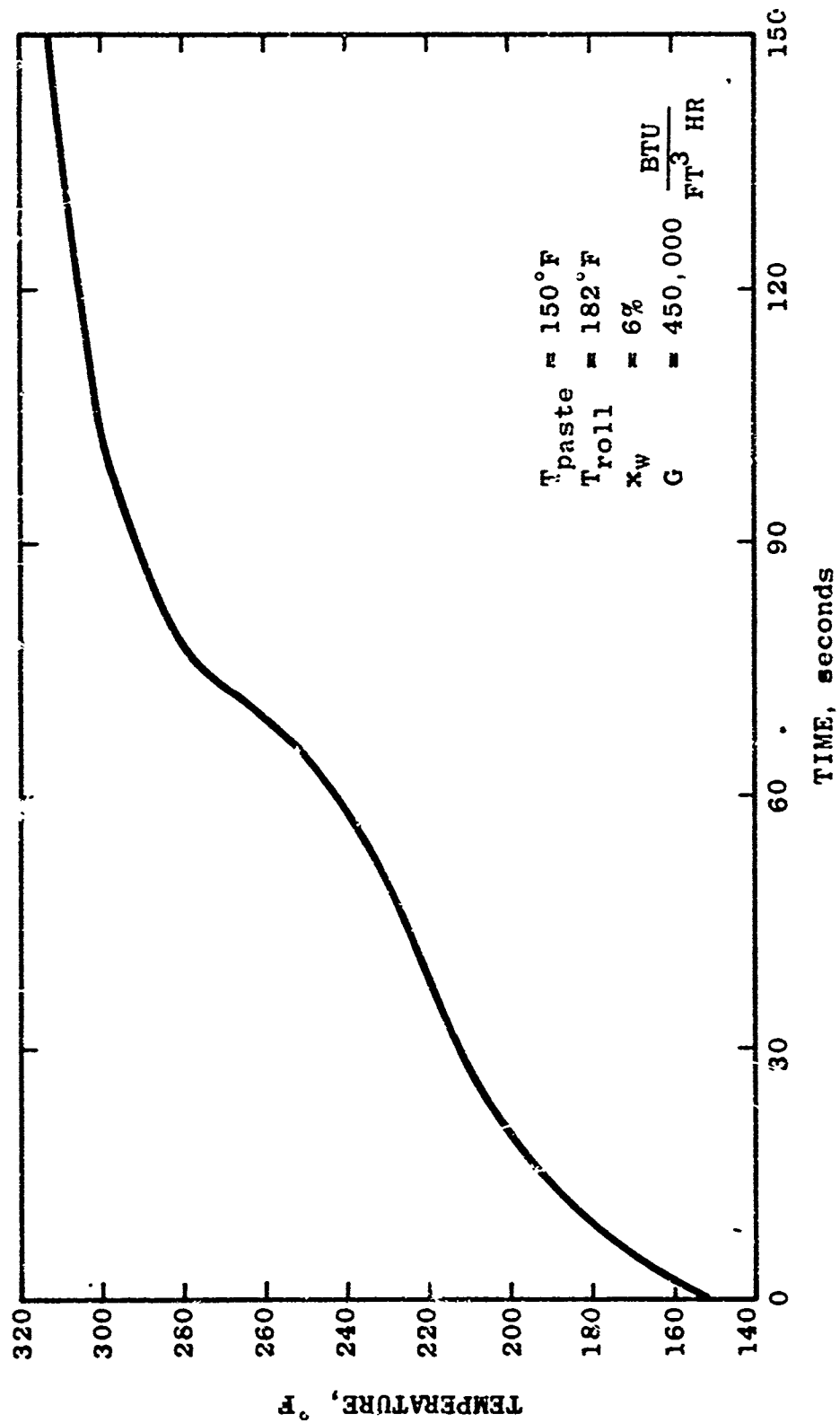
FIGURE 3

Typical Paste Temperature History

TEMPERATURE

f = FIRE FREQUENCY = 0.0067

T_{final}

T_{cr}

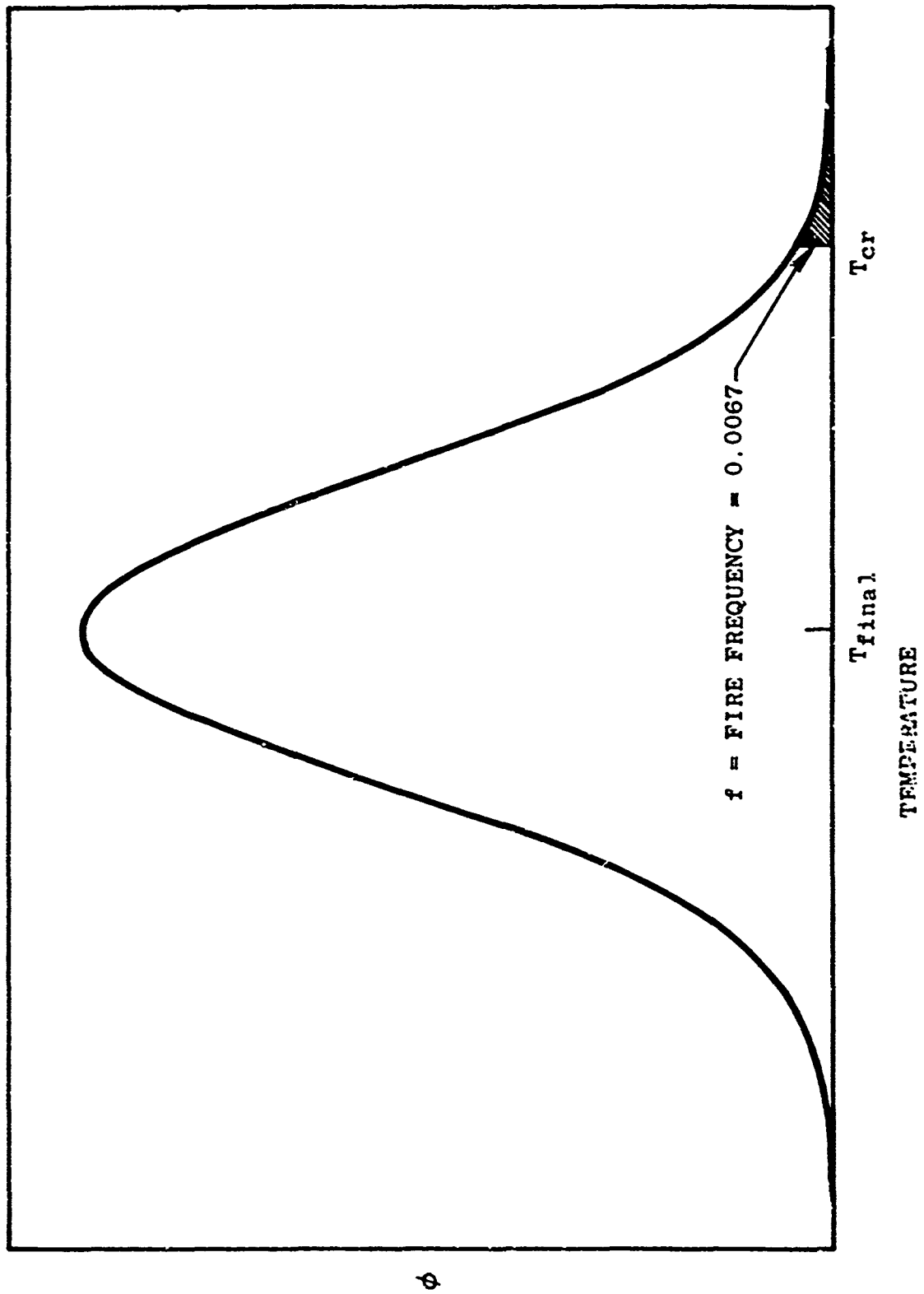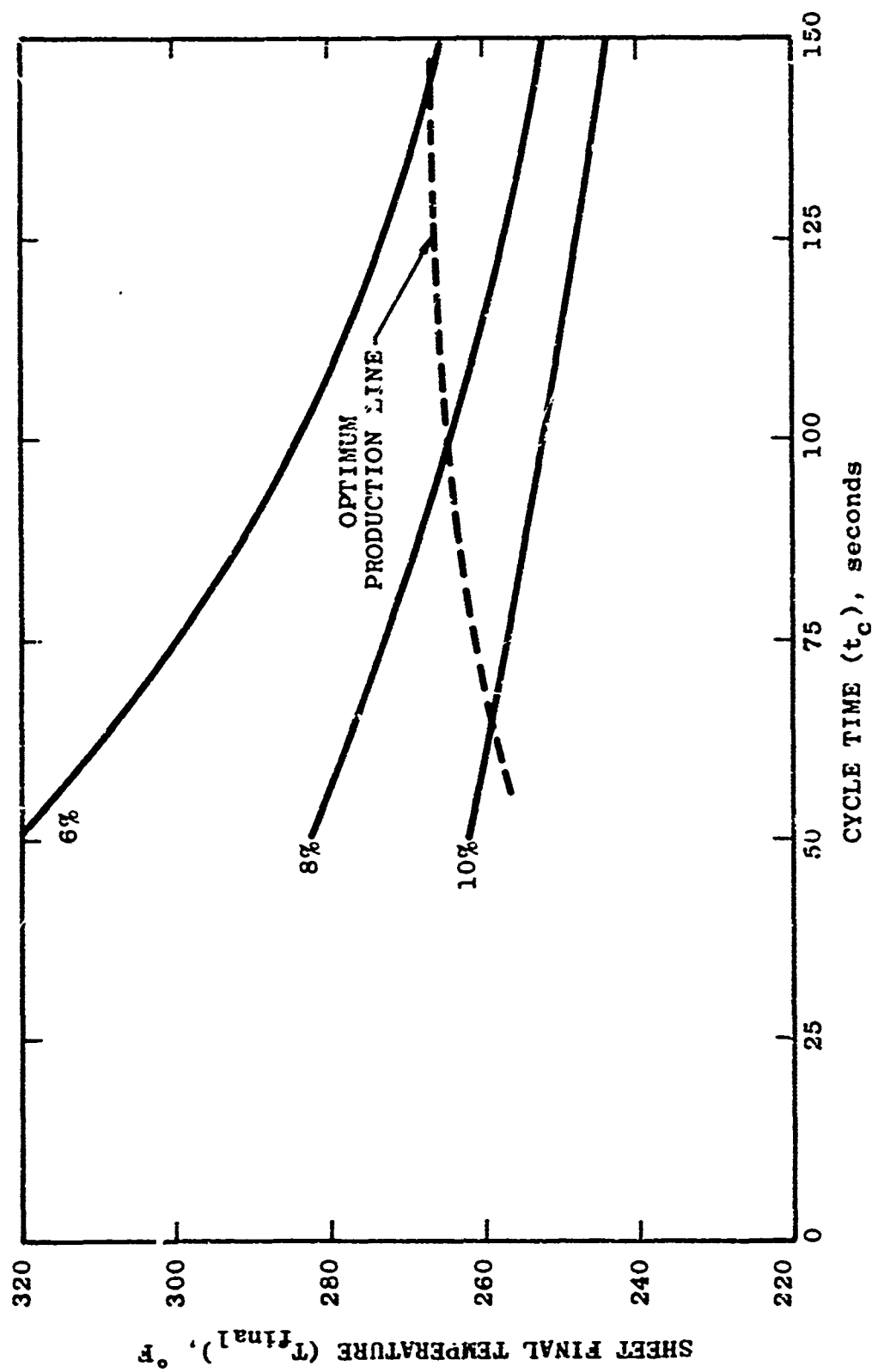Φ

FIGURE 4

Typical Distribution of Sheet Final Temperature

FIGURE 5

Propellant Sheet Final Temperature vs. Cycle Time

FIGURE 6

Fire Frequency vs Cycle Time
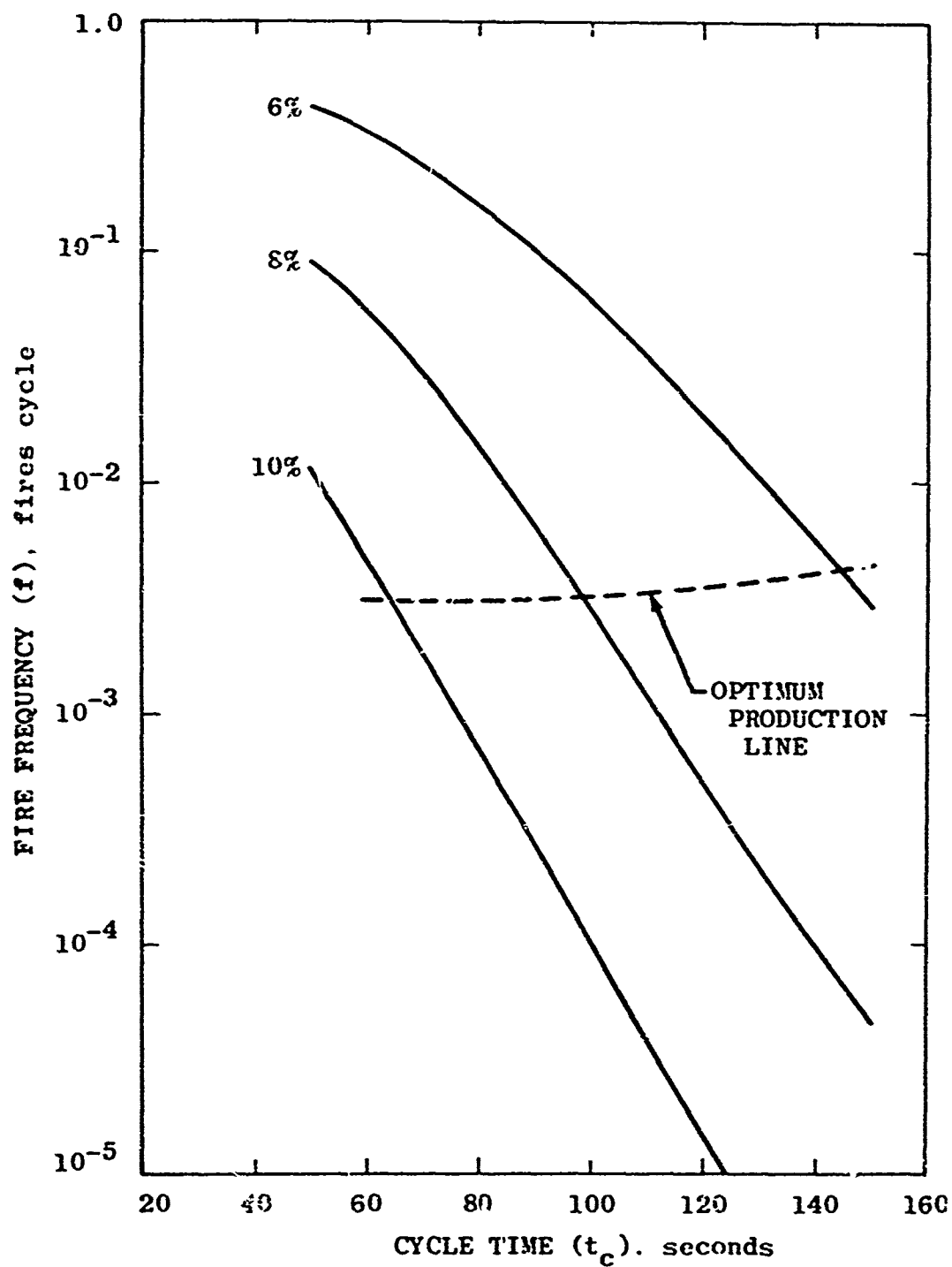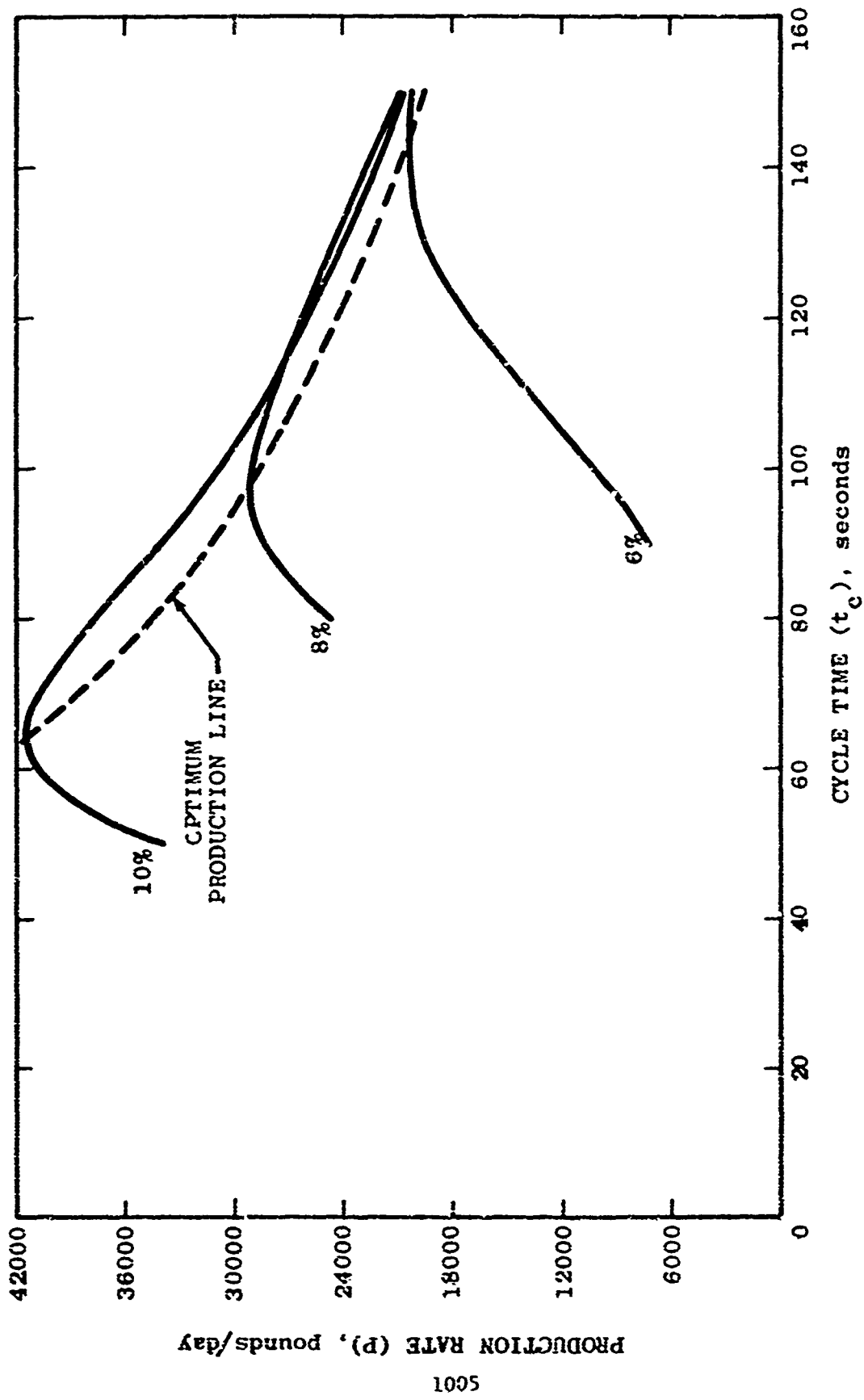
CYCLE TIME (t_c), seconds
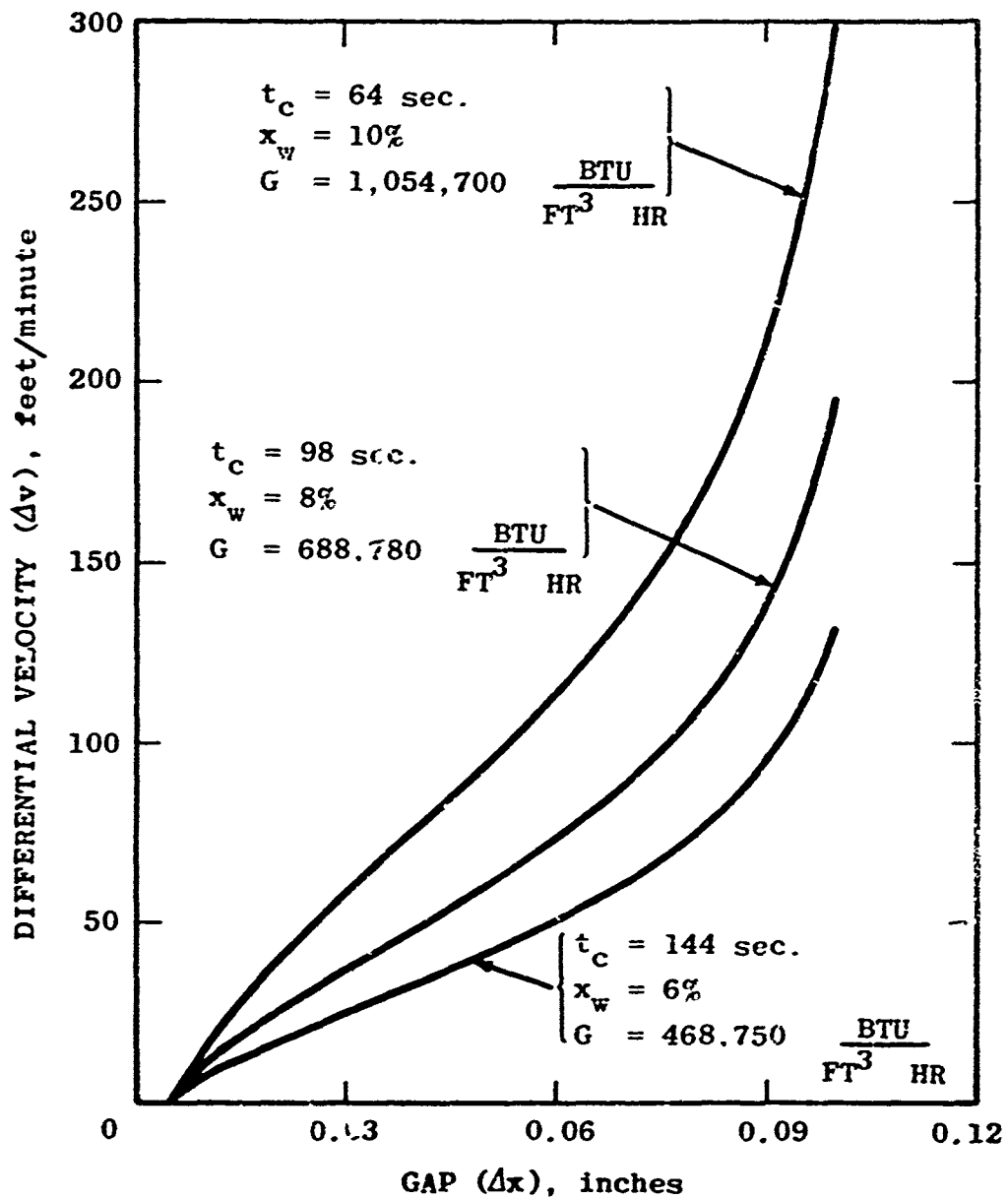
FIGURE 7

Production Rate vs Cycle Time

FIGURE 8

Relation of Differential Velocity and Gap

A RECOMMENDED APPROACH
FOR IMPLEMENTING
MIL-STD-882

Donald Smith
Hercules Incorporated
Magna, Utah

INTRODUCTION

The Department of Defense (DOD) has long recognized the importance of safety, operational effectiveness, procurement time, and costs in implementing weapon systems. Difficulties with making various complex weapon systems fully operational have forced expensive retrofit actions which have led to unacceptable delays in system procurement. Therefore, in 1969 DOD instituted MIL-STD-882 "to provide uniform requirements and criteria for implementing system safety programs."

Much of the early criticism[1] of the standard was directed toward two key factors: (1) the apparent lack of a clear definition of areas of responsibility between the safety function and other engineering support disciplines, and (2) the absence of criteria and/or methods for determining the degree of application or relative emphasis to be placed on a particular system safety program. The latter item often leads to extreme difficulties in implementing the standard since, unless both the procuring agency and the supplier share a common understanding of methods and depth of analysis to be pursued, lost motion and serious cost impacts must be expected.

This paper proposes a systematic approach to implementing MIL-STD-882 based on the groundwork established by the following documents:

- USAMUCOM Reg. 385-22[2]

- NAVORD OD 44942[3]

- SAMSO 68-8[4]

The fundamentals of this approach were presented by the American Ordnance Association Safety Division in 1971.[5]

TECHNICAL APPROACH

A. PRELIMINARY SCREENING

The approach recommended for implementing the standard is based on providing the following:

> (1) A clear and unified technique which will be applicable to all procurements

(2) The methods for deciding the depth of analysis required in specific procurements

(3) The analytical tools for ac~omplishing the tasks

The first step of the recommended approach is shown in Figure 1. A preliminary screening technique is employed to determine if a qualitative or quantitative method of analysis is to be pursued. The criteria for this decision are the hazard categories specified by MIL-STD-882. Task A (Figure 1) is, therefore, a preliminary hazard analysis (PHA) to (1) identify all credible hazards in the analyzed system and (2) rank these hazards by MIL-STD-882 categories. For Category I and II hazards, a qualitative method is recommended and can be carried out by an expansion of the PHA into a failure mode and hazardous effects analysis (FMHEA). Recommendations for overcoming the hazards are then made, together with an assessment of the costs and probable effectiveness of these recommendations.

Figure 2 shows a tabular format for conducting the preliminary hazards analysis. Basically, it records (1) the system or component under investigation, (2) the environment the system or component is to be operated in, (3) the failure mode of the system or component in this environment, (4) the effect on the system or component if the failure or hazard occurs (i.e., what is lost by the occurrence of the hazard), and (5) the MIL-STD-882 categories.

B. SECONDARY SCREENING

Figure 1, Task B shows the recommended approach for Category III and IV hazards. MIL-STD-882 indicates (Paragraph 5.9) that a probability-of-occurrence determination is to be made for all Category III and IV hazards. Therefore, the recommended method is to conduct a quantitative secondary screening using available historical data banks, failure data on similar systems, or worst-case calculations to determine the probability of occurrence of each Category III and IV hazard.

Under Task B those hazards having a probability of occurrence of less than 10^{-12} are to be screened or deleted from further analysis.-- Such a deletion can be made on the grounds of the extreme unlikelihood of the hazard occurring. (Note that NAVORD OD 44942 would recommend the acceptance of a 10^{-11} probability of occurrence for the loss of a large weapon system such as an aircraft carrier.)

Figure 3 shows how this secondary screening can be accomplished using a tabular format. First, the frequency with which the hazardous event occurs must be determined. This is accomplished by statistical methods.[6] From these data, the probability of exposure to a hazardous environment is computed. Next, the probability of hazardous environment

is computed. Finally, the probability of hazardous occurrence is determined from the event frequency and the hazardous environment probability. Thus, this approach assumes that the probability of occurrence of a hazard is dependent not only on the probability of a potentially hazardous event occurring but also on the probability that the system will respond in such a way as to risk personnel or system.

The hazard of a weapon system exposed to elevated temperatures is an example of this method of probability determination. From an analysis of the mission environment, a probability of exposure to high temperature (event frequency) may be determined. Thus, from a test of the explosive component, the probability of reaction may be computed.[2,6] Finally, the probability of occurrence of the reaction for a given mission may be computed from the exposure and the reaction probabilities (Reference 3, Vol. 4).

The last column of Figure 3 is the expected loss as determined by combining the probability of occurrence of the hazard and the loss as assessed in Figure 2.

C. FINAL SCREENING

Figure 1, Task C shows the final screening portion of the recommended approach. Where the probability of occurrence is greater than 10^{-12}, the risk to the system justifies the increased depth of analysis, especially for a large system such as the aircraft carrier.

At this stage of the total system safety analysis, all probability-of-occurrence data are based on historical failure rate data and/or computed values. If there is sufficient doubt that the existing data are applicable to the system being analyzed, the only recourse is to produce the required data in a testing program. The recommended testing program utilizes the capabilities versus requirements technique[2,6,7] to compute the actual probability of occurrence from measurements of the energy capabilities of the system environment and the energy requirements for the system to respond with a hazardous effect.

Where the probability of occurrence is between 10^{-12} and 10^{-6}, a tabular format such as a failure mode effects and criticality analysis is generally sufficient. However, where the probability of occurrence is equal to or less than 10^{-6}, the potential risk is of sufficient magnitude to justify a greater depth of analysis utilizing the fault tree analysis (FTA) approach. The FTA can account for all credible cause-and-effect relationships; whereas the tabular formats can consider only single cause-to-effect hazards. In large complex systems involving automatic controls with the possibility of sequential (interaction between subsystems) hazards, the FTA approach would be the only acceptable technique or method because it is capable of handling these interaction terms.

Figure 4 shows the recommended tabular format for determining probability of occurrence from measurement data. This determination begins with a measurement of the energy capabilities of the environment to which the system is exposed; this could be the stress imposed on the wings of a high-performance aircraft or the temperature to which explosive ordnance is exposed. Next, the energy required to cause a hazardous event is determined by test: e.g., aircraft wings are tested to determine stress levels necessary to cause failure, or the ordnance is tested by an auto-ignition test to determine cookoff temperatures-time requirements. The capabilities measurements and the requirements data are treated by statistical techniques, such as Monte Carlo, to determine risk probability. At this final screening, the data are based on actual operating environments and the response of the analyzed system to these environments; thus, the hazards are accurately defined.

Design and operating criteria must be established to reduce or eliminate unacceptable hazards. No attempt is made in this paper to discuss techniques of criteria establishment. However, Figure 1, Task C shows the outcome of this implementation procedure. First, the probability of occurrence (risk) necessary to satisfy MIL-STD-882 (Paragraph 5.9) is determin d. Next, using the FTA approach and the production of applicable failure probability data by mee surement and testing, the data are made available for conducting tradeoff studies. The studies will establish whether or not system modifications recommended to reduce or eliminate hazards can be justified on the bases of effectiveness in reducing hazards and the costs to implement the changes. Finally, design and operating criteria can be established on a quantitative basis since the capability exists for determining accurate probability of occurrence, costs of system modifications, and the effectiveness of these modifications in reducing hazards.

SUMMATION

Figure 1 shows the total approach to implementing MIL-STD-882. Task A provides the criteria for deciding if a qualitative or quantitative approach should be used. Task B provides a criterion for utilizing historical safety data most efficiently. Task C illustrates a method for selecting those identified hazards requiring a greater depth of analysis. This greater depth of analysis is provided through a measurement and testing program already recognized by service regulations (MUCOM 385-22 and NAVORD OD 44942).

The recommended approach provides a logical means of determining when an FTA approach should be used and, therefore, allows the system safety manager to allocate safety funding in the most effective manner by selecting the analytical methods commensurate with the criticality of a given hazard.

REFERENCES

(1) Bailey, P. G., and Christie, E. R., MIL-STD-882, System Safety Program for Systems and Associated Subsystems and Equipment, "Review of Standards and Specifications," Journal of Quality Technology, Vol. 2, No. 4, October 1970.

(2) Safety - Hazard Analysis, USAMUCOM Regulation Number 385-22, Headquarters United States Army Munitions Command, Dover, New Jersey, 9 August 1971.

(3) Weapon System Safety Guidelines Handbook, NAVORD OD 44942, Naval Ordnance Systems Command.

(4) Weapon System Safety Analysis Requirements, SAMSO 68-8, Department of the Air Force, Space and Missile Systems Organization, Air Force Systems Command, 15 November 1968.

(5) Recommendations for Hazards Analysis and Risk Management, American Ordnance Association, May 1971, AOA Safety Division Executive Board.

(6) Richardson, R. H., and Sutton, J. M., "Risk Analysis," 14th Explosive Safety Seminary, Department of Defense Explosive Safety Board, New Orleans, La., November 1972.

(7) Jones, M. L., and Sutton, J. M., Hazard Evaluation and Risk Control Study for a Nigroguanidine Facility, Prepared for U. S. Army Corp of Engineers Contract DACA 45-73-C-0015, AMC Project 5742632, May 1973.
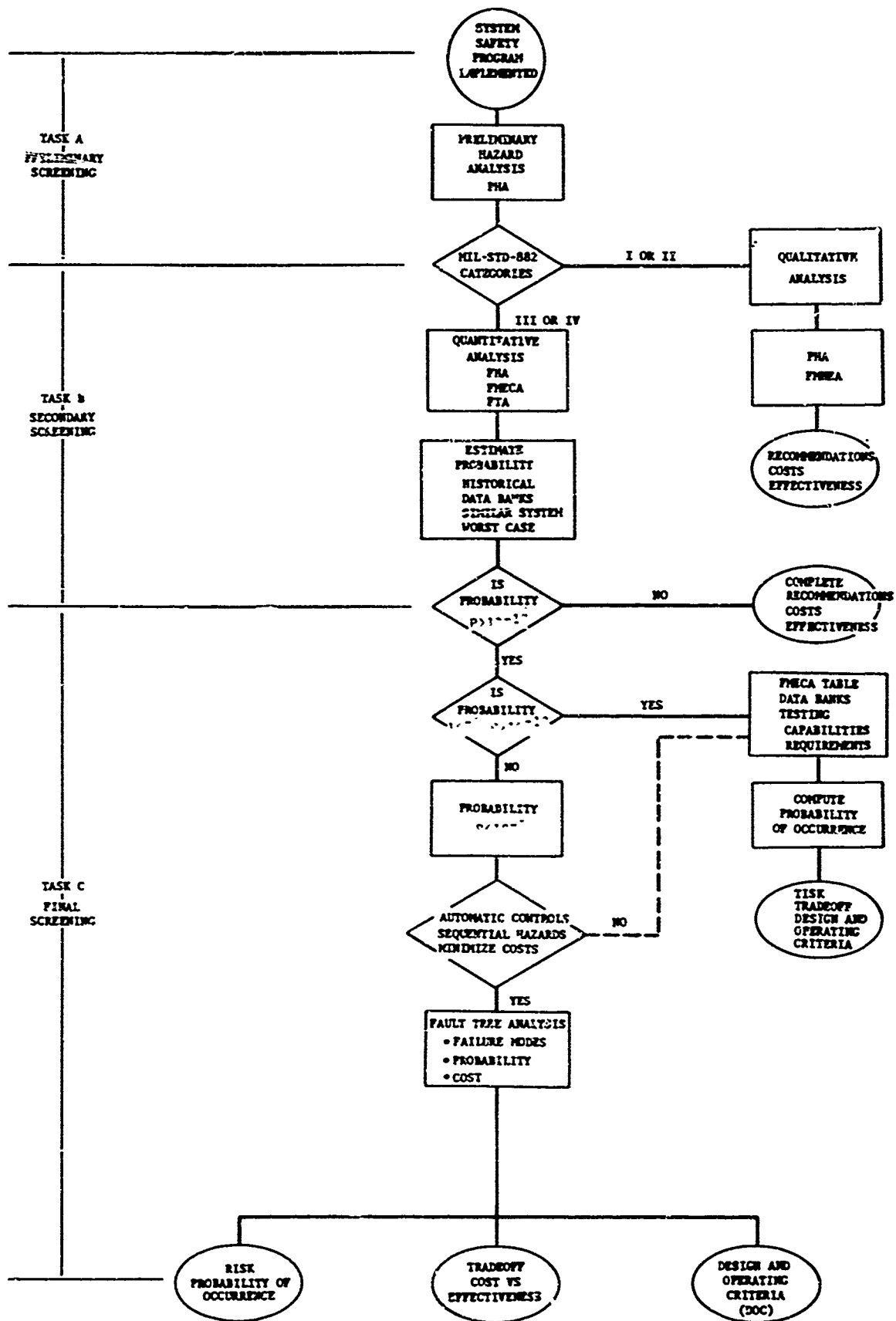
Figure 1. Recommended Procedure for Implementing MIL-STD-882

SYSTEM/ COMPONENT	MISSION/ ENVIRONMENT	FAILURE/FAULT/ HAZARD EVENT	WHAT IS LOST BY HAZARD OCCURRENCE	MIL-STD-882 I II III IV

Figure 2. Preliminary Hazards Analysis Tabulation

Figure 3. Secondary Screening Tabulation

ENERGY CAPABILITY	ENERGY REQUIREMENTS	RISK PROBABILITY	DESIGN AND/OR OPERATING CRITERIA

Figure 4. Probability of Occurrence Tabulation

HUMAN FACTORS IN EXPLOSIVES ACCIDENTS

Dr. A. F. Zeller
Directorate of Aerospace Safety, Norton AFB, California

If there is one point of universal agreement in the safety field, it is that explosives are dangerous. This is borne out by the fact that during 1972 in the United States Air Force (USAF) there were 228 accidents and an additional 358 lesser mishaps designated as incidents. It would seem reasonable to expect that this large number of explosives mishaps would result in a large number of injuries and fatalities. This would seem particularly probable when it is noted that during the same period, of 214 USAF aircraft accidents, 65 resulted in fatalities, and that there were 327 USAF persons killed in the seemingly safe environment of their own private automobiles. These statistics provoke at least two questions: (1) What are explosives people doing wrong that produces 586 mishaps in one year, and (2) what are they doing right that keeps those accidents which involve fatalities to two during a year? A corollary question is why were any fatalities experienced? This evaluation is an attempt to provide some information pertaining to these questions by examining the 1972 accidents in some detail, particularly those which produced injury or death.

During the period studied there were, as indicated, 586 mishaps recorded by the USAF, 228 of which were severe

enough to be defined as accidents. By far the greater number of these occurrences involved general purpose bombs (104); 54 involved aircraft impulse ejector cartridges; 45, unguided aircraft rockets; and 42, 20mm cartridges. Ten other agents were involved in 10 or more mishaps each. Others were in lesser number (Table I). Although the rank order of involvement is changed somewhat, accident experience closely parallels the total numbers. When incidents only are considered, aircraft egress initiators and practice bombs assume greater prominence.

By far the greater number, 321 of the 586 mishaps, occurred in conjunction with an aircraft flight at some phase from taxiing to parking. The process of loading and unloading accounted for the second greatest involvement, with 77 recorded cases. Maintenance and servicing mishaps (50) were third in order. Other activities involved fewer explosives mishaps (Table II).

Accidents have become so synonymous with human error that it is no surprise to note that over half of the mishaps are attributed to this cause (Table III). Most of these errors involved the simple failure to comply with regulations. Of the 312 mishaps in which any human error occurred, 84 or 27 percent were the result of this failure. Three other errors, two of commission (inadvertent actuation or

jettisoning—57, and the related error of improperly set-
ting switches or controls—49) and one error of omission
(failure to check or inspect—51) accounted for most of the
remaining errors (Table IV). How totally unnecessary these
occurrences were is indicated by the simplicity of the
errors committed. Review of the actual mishaps reinforces
this observation. Greater care in adherence to simple,
previously defined procedures would have obviated most, if
not all, of these mishaps. In 311 occurrences there were
no unsafe conditions. The most frequent failure in the
remaining 275 occurrences was simply reported as materiel
failure, with the second most frequent category being fail-
ure of associated equipment. Defective electrical equip-
ment and design deficiency are the other categories with
substantial numbers (Table V).

Of the 586 occurrences, two resulted in fatalities.
Nine involved temporary total injury and one, a permanent
partial injury. Fifteen, of which 14 were in the incident
category, resulted in minor first-aid cases. In 559
instances there were no injuries reported (Table VI). One
of these fatal mishaps was attributed to materiel failure;
the other one was attributed to personnel error. In the
one attributed to materiel failure, a bomb navigation sys-
tem analyst was in the rear cockpit. As he closed the

canopy, the ejection system activated and the mechanic was catapulted into the air. The primary cause was a materiel design deficiency in that there was inadequate clearance between the rear canopy safety strut stop and the seat-mounted initiator. When the rear canopy closed, the safety strut stop contacted the seat-mounted initiator. The initiator mounting bracket severed, causing the initiator to pull free, which fully activated the rear cockpit escape system. Even though the primary cause was considered to be a design deficiency, had the technician complied with technical order procedures and assured that the egress system safety pins were installed, no accident would have occurred. It is somewhat surprising that maintenance of egress systems so consistently accounts for a major portion of the fatalities in the explosives area. A recent summary[1] points out that during a 5-year period (which included 1972) there had been one death per year and serious injuries to three persons, all related to maintenance or check of egress systems. In every instance, personnel error was involved.

The second of the fatal accidents in 1972 resulted from a photoflash cartridge which functioned shortly after two men ascended the work stand. The activation was the result of personnel error in that the assistant test

---

[1] "It's Loaded and It's Lethal," Aerospace Safety, Aug 1973

director was performing ejector rack reset functions with
the cartridges installed in the ejector rack, which was in
conflict with technical orders developed for this operation.

The nonfatal injuries resulted from a variety of causes
in relation to a variety of pieces of equipment.

Excluding first-aid cases, of the 12 accidents involv-
ing greater injury, only two were attributed to materiel
failure; the remaining 10 were considered the direct result
of human failure.

Review of the material so far presented indicates
that the most noteworthy feature is its remarkable simi-
larity to many papers which have preceded it and possibly
to some which will follow it. The onus is placed on the
human for errors committed, with a disproportionate number
of the injuries which accrue resulting from these personnel
errors. The question which immediately and forcefully
presents itself is why must this pattern be repeated and
what, if anything, can be done to reduce the magnitude if
not the relationships involved. In examining the errors
committed, it was noted that failure to follow directives
was by far the most prevalent single cause of explosives
accidents. By implication, the remaining prominent errors
could, with little modification, have been included under
a broader category, failure to comply with established

procedures. The question then arises, how are people persuaded to follow established and tested procedures? The first solution that comes to mind is that they be trained so that these procedures are well known. Examination of the accidents would indicate some few individuals did not know what the procedures were or that the procedures involved were not in accordance with regulations, but in most instances the individuals did know. Relegating to training that small portion due to ignorance, the question still remains as to why those who knew the procedures did not follow them. Review of the reports suggests a number of possibilities. In some, the regulations were not available, or, if abstractly available, they were not readily enough available to be of real use. Some, although available, were couched in terms which the individual could not readily follow, so that while readable, they were not understandable. On occasion, time was of such a premium that the individuals did not feel that the task could be accomplished in the allotted span if time were taken to read the regulations. One possibility is that the individuals failed to comprehend the hazards involved. Another is that this lack of respect for the problem was born and nutured in the obvious lack of regard which those in authority had for these obvious procedures and by the knowledge that careful

inspection and checks would not be forthcoming. All of
these might well be subsumed under two headings: first,
faulty attitude, and second, poor supervision. If an indi-
vidual knows and does not perform, this is essentially an
attitude problem. On the other hand, if he does not know,
this is a supervisory problem. If the material presented
for his use is not available or is not readable or usable,
this is a supervisory problem. If examples of faulty
behavior are set by supervisors, this too is a supervisory
problem. If the work is not checked, this is a supervisory
problem. Improved accident prevention in the explosives
area, then, seems to reduce itself to, (1) the development
of improved attitude on the part of the individual worker,
and (2) to improved supervision, particularly by his imme-
diate supervisors.

It should be noted that the individuals involved in
explosives accidents are the same kinds of USAF individuals
who in their off-duty time operate their own private motor
vehicles. For the most part, they are young, males, and
faced with the same problems as their peer group in the
civilian society, with the additional difficulties which
may arise from being a part of a regimented subportion of
the American culture. In spite of the high number of
traffic fatalities which were cited (327 in 1972), it

should be noted that this number is in marked favorable contrast to that immediately preceding the introduction of a concentrated remedial program (437 in 1964). It should also be noted that in many ways the operation of a private motor vehicle involves the same kinds of attitudes and the same kinds of problems as are faced by the airman in his on-job activities. The high private motor vehicle accident rate of eight years ago resulted in a major program by the Air Force to reduce this unnecessary attrition. For this purpose a carefully devised driver training program, based on a series of concepts which accepted the young airman as a rational being whose attitude would change in direct proportion to the reasonableness of the information which was given to him documenting that a change was necessary, was developed. At no time was the individual himself either told implicitly or explicitly that it was his attitudes that were the focal point of the program. As far as he was concerned, it was a training program oriented toward the imparting of usable information in an interesting way. This program, defined as the Air Force's Multimedia Program, was initiated, and within five years after its initiation had resulted in a 23-percent drop in traffic fatalities. During the same period of time, fatalities for the nation

as a whole were rising. The utilization of comparable
philosophies, even of comparable programs, should have a
salutary effect in the explosives area.

Because of the success of the driver training program,
the USAF is currently embarked upon the development of a
similar program to be directed at supervisors in the ground
area. This, like the preceding program, is based on the
philosophy of rationality and is aimed directly at improv-
ing the attitudes and interests of the first-line super-
visor. It appears a reasonable expectation that such a
program should be conducive to reduced accidents. Because
the program is oriented toward safety supervisors and staff,
some fallout in the explosives area within the Air Force is
expected. What is more pertinent, however, is that the
same approach taken in programs aimed directly to super-
visors in the explosives area should be of benefit.

If, as is suggested, the problems are individual atti-
tudes and supervision, then programs directed toward these
areas should be beneficial.

When an explosives accident is envisioned, one sees
visual images of huge billows of smoke and overtowering
tongues of fire accompanied by recurring blasts of varying
magnitudes. Review of explosives accidents indicates,
however, that such occurrences are extremely rare. In

most instances, damage is restricted to the item which is involved and an injury does not occur. The possibility that any one of these occurrences may result in major destruction or death is, however, always high. The prevention of holocausts, therefore, rests not so much in their direct preclusion, but in the recognition that it is the mundane "little accident" which is the day to day problem in the explosives field. If these are prevented, the holocausts will not occur. On the basis of the rationality of the human and the appeals which can be made to this as demonstrated by the Air Force's driver training program, it is advanced as an article of faith that a program aimed at improving the attitude of the individual in the explosives area, together with programs aimed at improving supervision, particularly the attitudes of supervisors, can result in a marked decrease in the number of explosives mishaps which occur each year. There is no reason to believe that what is a good program cannot be made markedly better by the application of relatively simple measures assiduously developed and rigorously pursued.

TABLE I

USAF EXPLOSIVES MISHAPS BY AGENCY INVOLVED

1 Jan 1972 - 31 Dec 1972

Agency Involved	Total Acdnts	Total Incdts	Total
Bomb, General Purpose	31	73	104
Acft Impulse Ejector Cartridge	37	17	54
Aircraft Rocket (Unguided)	28	17	45
20mm Cartridge	32	10	42
Aircraft Egress Initiator	8	28	36
Flare or Signal Device	16	11	27
Bomb, Practice	8	19	27
Other	68	183	251
TOTAL	228	358	586

TABLE II

USAF EXPLOSIVES MISHAPS SUMMARY ACTIVITY
1972

Activity	Total Acdnts	Total Incdts	Total
Flight	186	135	321
Loading/Unloading	8	69	77
Maintenance/Repair/Service	8	42	50
Inspecting Acft or Equipment	8	39	47
Test/Check	9	22	31
Arm/Dearm	4	22	26
Other	5	29	34
TOTAL	228	358	586

TABLE III

USAF EXPLOSIVES MISHAPS - PRIMARY CAUSE

1972

Primary Cause	Total Acdnts	Total Incdts	Total
Unsafe Condition--Undetermined	1	3	4
USAF Personnel	78	205	283
USAF Civ Personnel	0	5	5
Non-AF Personnel	2	6	8
Materiel Failure	134	117	251
Supervision	3	13	16
Unsafe Condition/Other	10	9	19
TOTAL	228	358	586

TABLE IV

USAF EXPLOSIVES MISHAPS – UNSAFE ACTS

1972

Unsafe Acts	Total Acdnts	Total Incdts	Total
No Unsafe Act	143	130	273
Failed to Comply with Regs	18	66	84
Inadvertent Actuation/Jettison	26	31	57
Failed to Check/Inspect/Warn	8	43	51
Set Switch/Control Improperly	18	31	49
Failed to Note Obvious Hazard	2	7	9
Improper Handling of Firearms	2	6	8
Handling/Loading-Other	1	6	7
Stacking Materials Unsafely	0	6	6
Vehicle Operation-Other	0	6	6
Applied/Allowed Improper Force	3	1	4
Failed to Note Improper Setup	2	2	4
Failed to Properly Secure Load	0	4	4
Failed to Secure Equipment	0	4	4
Inadequate Supervision	1	3	4
Failed to Use Safety Cautions	1	2	3
Incorrect Use of Control	1	2	3
Use of Defective Tools	1	2	3
Stacking Materials Too High	0	2	2
Failed to Secure Fifth Wheel	0	1	1
Failed to Secure Trlr Tow Bar Ar	0	1	1
Improper Adjustment of Equipment	1	0	1
Improper Use of Tool or Equipment	0	1	1
Oper Unsafe Act NEC	0	1	1
TOTAL	**228**	**358**	**586**

TABLE V

USAF EXPLOSIVES MISHAPS – UNSAFE CONDITIONS

1972

Unsafe Condition	Total Acdnts	Total Incdts	Total
No Unsafe Condition	85	226	311
Materiel Failure	39	43	82
Failure of Associated Equipment	42	25	67
Acft/Msl Equip Defective-Electrical	32	26	58
Design Deficiency	20	20	40
Acft/Msl Equip Defective Other Than Electrical	4	7	11
Expl/Armament Equip Defective-Nonelectrical	3	2	5
Extreme Weather Conditions	2	2	4
Internal Part Defective	0	3	3
Defective Mach/Equip-General	0	2	2
Defective Mech Equip Other Than Brakes	0	1	1
Hazardous Arrangement	1	0	1
Inadequately Tied Down	0	1	1
TOTAL	228	358	586

TABLE VI

USAF EXPLOSIVES MISHAPS - PRIMARY CAUSE & INJURY CLASS
1972

Injury Class	AF Mil	AF Civ	Oth Civ	Mat Fail	Supv	WX Surf	WX Oth	Haz Area	Oth Cond	Und	Total
Temp Total	7			1	1						9
Perm Partial	1										1
Fatal	1			1							2
First Aid	6	1	1	6			1				15
No Injuries	271	4	7	242	15		3		15	2	559
TOTAL	286	5	8	250	16		4		15	2	586

SYSTEM TO ESTABLISH PRIORITIES FOR ATTENTION TO EXPLOSIVE HAZARDS

By:

WILLIAM T. FINE
Chief of Safety Department
Naval Ordnance Laboratory
Silver Spring, Maryland 20910

ABSTRACT

A problem frequently facing the head of any
safety organization is to determine just how serious
each known hazard is, and to decide to what extent
he should concentrate his resources and strive to
get each situation corrected. Normal safety routines
such as inspections and investigations usually produce
varying list of hazards which cannot all be corrected
at once. Decisions must be made as to which ones are
the most urgent. Since budgets are limited, there is
necessity to assign priorities for costly projects to
eliminate hazards. Therefore there is a great need
for a method to quantitatively determine the relative
seriousness of each hazard.

To supply this need, a formula has been devised
which weighs the controlling factors and "calculates the
risk" of a hazardous situation, giving a numerical
evaluation to the urgency for remedial attention to the
hazard. Calculated Risk Scores are then used to establish
priorities for corrective effort.

I. INTRODUCTION

    1. In every organization, there usually exists many hazardous situations at any one time. Additional hazards are continually being noted, all of which demand the attention of the person responsible for safety. But it's a rare case when SAFETY is able to get action started on everything at once. Time, facilities and money available just do not permit it. Safety needs a method to determine just how serious each hazard is, and what proportion of available time, effort and resources should be devoted to each situation. If there are many work orders in for safety projects, the maintenance people would no doubt like to know <u>which</u> orders are the most important and should be done first.

    As another reason to know just how serious each hazard is, we must realize that there is <u>some</u> risk in everything we do. We cannot attain absolute safety in any operation unless we close it down. Someone must decide whether the degree of risk in any operation is acceptable. If it's acceptable, we don't worry about it. But if we do not wish to accept the degree of risk, we must act to eliminate it. <u>Therefore our basic need is for a method to calculate the amount of risk in each so-called hazardous situation first so that we can decide whether it actually does require our attention, and next, to establish priorities based on the amount of risk in each situation.</u>

    2. In this report, I am presenting an easy way to "calculate the risk" due to a hazard. By using a simple formula, we can come up with a numerical rating for the <u>relative severity</u> or importance of each hazard. This rating will establish a priority for each situation, and give us guidance as to where to concentrate our efforts. This formula uses simple, down to earth terms, <u>without</u> any high powered mathematics, so it can be easily used by anyone.

II. RISK SCORE FORMULA

    The formula for calculating the seriousness of the risk due to a recognized hazard is called the "Risk Score Formula."

    1. A numerical evaluation is determined by considering three factors, the <u>consequences</u> of a possible accident due to the hazard, the <u>exposure</u>, and the <u>probability</u> that th consequences will occur.

    2. THE RISK SCORE FORMULA is as follows:

    Risk Score = Consequences x Exposure x Probability

It is pointed out that the numerical ratings or weights assigned to each factor are arbitrarily assigned and flexible, based on the judgment and experience of the investigator making the calculation. Now let us review the elements of this formula.

    3. The first element, <u>CONSEQUENCES</u>, is defined as the most probable result of an accident due to the hazard we are concerned with (injuries and property damage). Numerical ratings are assigned for the most likely

consequences of an accident, from 100 points for a catastrophe down through various degrees of severity to one point for a minor cut or bruise.

SEVERITY OF CONSEQUENCES	RATING
a. Catastrophe: numerous fatalities; extensive damage (over $1,000,000); major disruption...................	100
b. Several fatalities; damage $500,000 to $1,000,000	50
c. Fatality; damage $100,000 to $500,000.............	25
d. Extremely serious injury; (amputation, permanent disability); damage $1,000 to $100,000........................	15
e. Disabling injuries; damage up to $1,000...........	5
f. Minor cuts, bruises, bumps, minor damage.........	1

4. The next factor, EXPOSURE, is defined as the frequency of occurrence of the hazard-event, (the hazard-event being the first undesired event that could start the accident sequence). We rate the frequency at which the hazard-event occurs, from continuously with 10 points, through various lesser degrees down to 0.5 for extremely remote.

The hazard-event occurs:	RATING
a. Continuously (or many times daily)................	10
b. Frequently (approximately once daily).............	6
c. Occasionally (from once per week to once per month	3
d. Unusually (from once per month to once per year)	2
e. Rarely (it has been known to occur).... . ..,.....	1
f. Very Rarely (not known to have occurred, but considered remotely possible)...............................	0.5

5. The third factor, PROBABILITY, is defined as the likelihood that, once the hazard-event occurs, the complete accident-sequence of events will follow with the necessary timing and coincidence to result in the accident and consequences. The ratings go from 10 points if the complete accident-sequence is most likely and expected, down to 0.1 for the "one in a million" or practically impossible chance.

The accident-sequence, including the consequences:

  a. Is the most likely and expected result if
the hazard-event takes place................................. 10

  b. Is quite possible, would not be unusual, has
an even 50/50 chance.. 6

  c. Would be an unusual sequence of coincidence...... 3

  d. Would be a remotely possible coincidence (it has
happened here)... 1

  e. Extremely remote but conceivably possible (has
never happened after many years of exposure)................ 0.5

  f. Practically impossible sequence or coincidence; a
"one in a million" possibility (has never happened in spite of
exposure over many years).................................. 0.1

 6. Now, let us take a few examples. For demonstration, we have selected
a variety of situations.

  a. EXAMPLE #1:

    (1) Problem. Building No. 303 at the Naval Ordnance Laboratory
contains a number of ovens which are used for environmental testing (heating)
of explosive material with up to five pounds of high explosive material
in an oven. One side of the building is made of "blow-out panels" so
that in case of an accident most of the blast will be expended out the
blow-out panels rather than demolish the building. This type of oven has
been known to heat excessively due to faulty heat controls and thereby
cause the explosives in the oven to detonate. People walk past the out-
side of this building. The potential hazard considered here for which we
are calculating the risk, is the endangering of persons who occasionally
walk near the building.

    (2) The first step in calculating the risk is to study the
situation and list the most probable sequence of events for an accident.
Here is our hypothetical accident sequence, step by step:

      (a) Several ovens are in use, each containing explosives.
This is normal.

      (b) Persons are present in the area outside the building.
This is a normal and accepted condition.

      (c) Now something goes wrong. The thermostat of one
oven fails and the oven temperature rises above the proper operating range.
(This is the hazard-event).

(d) The secondary emergency shutoff control also fails to function.

(e) The oven overheats.

(f) The explosive detonates.

(g) A passerby near the building is fatally injured by flying debris.

(3) Now we consider the formula use:

Risk Score = Consequences x Exposure x Probability

(a) CONSEQUENCES. We decided that a fatality was most likely. That is item "c" on the rating chart, with a rating of 25. Therefore CONSEQUENCES = 25.

(b) EXPOSURE. The hazard-event is the failure of the thermostat. Investigation shows that this has happened before, but very "rarely." That would be "e" on the rating chart. Therefore EXPOSURE = 1.

(c) PROBABILITY. This has to be a careful opinion based on judgment and experience. We must decide on the likelihood that the complete accident-sequence will follow the hazard-event. Very briefly stated, we consider that all ovens have been equipped with secondary shutoff controls. Maintenance is very thorough and does ensure the proper functioning of the emergency shutoff controls. We would therefore consider that their failure at any time is quite unlikely. For a set of emergency shutoff controls to fail at the same time and on the same oven where a thermostat has happened to have failed, would be a remotely possible coincidence. It would also take somewhat of a further coincidence to place a person in a vulnerable position outside the building at the same time. Thus we arrive at an opinion that the net or total Probability is remotely possible, (fourth item down the list). So PROBABILITY = 1.

(d) Substituting in the formula:

Risk Score = 25 x 1 x 1 = 25

There is no particular significance to this Risk Score of 25 until we compute the Risk Scores for other hazards using the exact same criteria and judgment and have a basis for comparison.

b. EXAMPLE #2:

(1) Problem. Six compressed oxygen cylinders are standing unsupported on a pallet in the shop next to a busy aisle; caps are on securely. In this case, we consider that there are two hazards:

Hazard 1.): A cylinder could topple and cause a foot injury.

Hazard 2): A cylinder could topple, rupture and become a missile.

(2) Since there are two hazards, each one is evaluated separately and their Risk Scores added.

(3) Evaluating Risk Score for Hazard No. 1, the foot injury hazard:

(a) The accident sequence is:

1 Condition as stated above.

2 Shop trucks, carts and pedestrians pass close by many times daily, often brushing against cylinders. This is the hazard-event.

3 A person bumps a cylinder hard enough to cause it to topple over.

4 Cylinder falls on the man's foot.

5 A disabling injury results: fractured bones in the foot.

(b) We now apply the formula:

1 CONSEQUENCES are a disabling injury, "e" on the rating chart. C = 5 points.

2 For the EXPOSURE or the Frequency of the hazard-event: persons brushing against or bumping a cylinder occurs many times per day. That is "a" on the rating chart. Therefore E = 10.

3 For PROBABILITY, we estimate the likelihood, step by step, of all events occurring to include the fractured foot. Our reasoning follows: once a cylinder has been bumped, it is quite possible that one will topple over: ("b" on the rating chart). It is also possible, but slightly unusual that it would land on a man's foot: that would be "b" to "c" on the rating chart. But if it did land on his foot, a fracture is most likely. That is "a." Putting these together, we consider that the net likelihood of this series of events occurring as being "quite possible," but somewhat unusual, somewhere between "b" and "c" on the rating chart. Therefore, we interpolate and say P = 4.

(c) Now we substitute in the formula. The calculation for the Risk Score for the oxygen cylinders, foot hazard is:

Risk Score = 5 x 10 x 4 = 200

1038

(4) Next we evaluate the Risk Score for Hazard No. 2, the missile hazard.

      (a) Accident sequence:

         <u>1</u> Condition is as stated above.

         <u>2</u> Shop trucks, carts and pedestrians pass close by many times daily, <u>often</u> brushing against cylinders. That is the hazard-event.

         <u>3</u> A person bumps a cylinder and it topples over.

         <u>4</u> A cylinder ruptures or the valve is broken off, escaping compressed gas causes missile action.

         <u>5</u> Very serious injury occurs.

      (b) Use of the formula:

         <u>1</u> First consider the CONSEQUENCES. We would expect a <u>very seriou. injury</u>, "d" on the chart. So <u>C = 15</u>.

         <u>2</u> Next the EXPOSURE. This is the same as for the foot hazard: the hazard-event, bumping a cylinder occurs several times daily. <u>E = 10</u>.

         <u>3</u> Next, consider the PROBABILITY that a missile and <u>very serious injury</u> will result. Toppling over is quite possible, but a topple should not ordinarily cause a rupture, and cylinders have protective caps. So the tank rupturing is <u>remotely possible</u>, or "d" on the rating chart. But in event of a rupture, missile action and a very serious injury could easil: follow 'b". Therefore we consider the net probability that the serious injury will occur is "remotely possible." <u>P = 1</u>.

         <u>4</u> Substituting in the formula:

         Risk Score = 15 x 10 x 1 = 150

         <u>5</u> Adding the Risk Scores of the two hazards, Total Risk Score = 200 + 150 = 350.

     c. EXAMPLE #3.

      (1) <u>Problem</u>. A 12,000 gallon propane storage tank is located close to operations involving ultra-highly compressed air lines and equipment: Air and nitrogen at 15,000 psi. A high pressure pipeline explosion could result from a malfunctioning safety valve, a human error in operating the equipment, or damage to a pipeline. Blast or flying debris could then strike the propane storage tank, rupture it and cause it to explode with the consequences of several fatalities and building damage up to $500,000.00.

(2) Sequence of events:

    (a) _Normal activities_ involve operation of equipment and pressurizing of pipelines in the vicinity of the propane storage tank.

    (b) A 3000 psi pipeline 30 feet away from the storage tank becomes damaged and unnoticed. (This is the hazard-event.)

    (c) The pipeline bursts.

    (d) Metal debris from the blast strikes the propane tank with such force that the tank is ruptured.

    (e) Propane leaks out of the tank.

    (f) A spark ignites the propane fumes.

    (g) The propane and air mixture explodes.

    (h) Building damage is $500,000 and two men are killed.

(3) Next we determine values and substitute in the formula.

    (a) CONSEQUENCES: Two fatalities and damage loss of $500,000. $\underline{C = 5}$.

    (b) EXPOSURE: High pressure air lines have been known to have been neglected or damaged. Frequency of such occurrences is "unusual." This is "d" on the rating chart. Therefore $\underline{E = 2}$.

    (c) PROBABILITY: Now we estimate the likelihood that a damaged pipeline will explode and the explosion will occur close enough and with enough blast to throw debris and strike the propane tank with such force as to complete the accident sequence. Several pipeline bursts have occurred in past years, but none have damaged the propane tank. Just a few of the pipelines are considered close enough to endanger the tank. After careful observation, the complete accident sequence is considered _very remotely possible_. This is "e" on the rating chart, and the rating is placed at $\underline{P = 0.5}$.

    (d) Substituting into the formula:

$$R = 50 \times 2 \times 0.5 = 50$$

7. SUMMARIZING RISK SCORES. In the same manner as demonstrated, the Risk Scores for other hazardous situations have been calculated. These cases are now _listed in order of their Risk Scores_, or we can say – in order of the _relative seriousness of their risks_, on a "Risk Score Summary and Action Sheet."

(See Illustration: Risk Score Summary and Action Sheet)

Note the two horizontal lines on the right side of the chart. Above the upper horizontal line are the hazards with the highest Risk Scores, down to a Risk Score of 200. The line was drawn here because it was adjudged that for these risks, corrective action was required immediately, and any operation must be stopped until the score was lowered. The middle section of the chart contains the hazards considered somewhat less urgent but still requiring attention as soon as possible. The hazards listed below the lower horizontal line are lesser ordinary hazards that should be eliminated without undue delay, but not as emergency situations.

8. RESULTS AND USES OF SUMMARY OF RISK SCORES.

a. The Risk Score Summary and Action Sheet is now a very useful device. It:

(1) Establishes priorities for attention by both Safety and Management since hazards are listed in order of their importance. The position on the list of any item can be lowered by corrective action which will decrease any one of the factors; Consequences, Exposure, or Probability.

(2) Provides guidance to indicate urgency of newly discovered hazards. For each new hazardous situation, compute the Risk Score. Its urgency is indicated by the ACTION area in which its Risk Score falls. For example, when a highly hazardous situation is noted in a highly essential operation, the location on the chart would serve as backing if it is felt that the operation must be stopped until the hazard is reduced.

(3) Can become a valid method of evaluating a safety program, more realistic than using accident statistics: at any given time the complete chart for a plant represents the actual status of safety. i.e., let us say the chart shows seven "immediate actions" or emergency items; six items in the "urgent" category; and 12 "minor" hazards. Accomplishment of the safety program over a period of time will then be demonstrated by reducing risk scores and moving items downward on the chart, from the high risk categories into lower risk areas. For example, it would be progress to reduce our "emergency action" items from seven to two, and our "urgent" items from six to four, or to lower the overall average Risk Score from 92 to 74, etc.

ESTABLISH A SAFETY PROFILE FOR YOUR PRODUCT

Walter M. Cinibulk
817 Silver Spring Avenue
Silver Spring, MD 20910

ABSTRACT

The answer to the question "how safe is this product" is becoming more essential for making the proper management decision for future profitability. This paper describes the concept and methods developed for performing a safety analysis by quantitatively assessing the consequences of hardware generated hazards. The objective of this safety analysis is to provide a systematic, measurable and efficient method of determining the safety profile of an equipment (product) design. The fundamental basis for the hazard assessment techniques described is the recognition that product safety is three dimensional:

- Injury Potential
- Frequency of Occurrence
- Hazard Index

In addition to discussing methods for assessing the injury potential, the frequency of occurrence and the hazard index, a graphical presentation "Safety Profile" of the interaction of these safety parameters is described.

BACKGROUND

The dictionary defines safety as "freedom from danger, risk, or injury". In actual practice, the term safety has assumed several different meanings and covers different concepts.

To many, safety is a statistic, expressed as an accident rate - such as fatalities per million passenger miles, or man hours lost per man year. In engineering, safety has traditionally been associated with reserve strength, expressed as safety margins or safety factor. With respect to recognized, potentially hazardous activities or situations, safety is associated with providing safeguards such as lifeguards, fire extinguishers, life preservers, etc. Often, safety is simple a list of rules and procedures to be observed in order to reduce exposure to danger, remove risks, and to protect against injury.

With respect to equipments which we produce, use and are exposed to, safety must start with a management policy and a committment to the design of the product. The technology involved is determined by the type of product, and the approach utilized in the overall process of bringing a "safe" product to market will differ from company to company. This process involves design, manufacturing, quality control, marketing and advertising, product service and maintenance, legal, insurance and the full participation of management. The process, however, starts with design and engineering, provided that there is a means to specify, measure and analyze. To achieve the objective of a "safe" design requires the ability to specify what is required and a means to analyze so that achievement can be measured and verified. The fundamental question which this paper addresses is not "Is this design safe?", but rather "How safe is this design?".

DISCUSSION

The analysis is designed to identify and define all potential hazard events, their cause, the effect on equipment operation and personnel safety. In this context, hazard event is an equipment failure or fault caused by a malfunction or operator error. Each event is categorized by estimating the injury potential frequency of occurrence and calculating the hazard index. This index defines the level of hazard of each event in terms of the effect on equipment (product) safety - i.e., hazard to personnel. The combination of these important characteristics recognizes that the utlimate aim and objective of the analysis is:

    a. Identify, in measurable terms, the inherent, potential safety hazards of the equipment design

    b. Quantitatively specify safety requirements in equipment specifications and verify the status of the design with respect to these safety requirements.

    c. Provide a logical listing of recommended corrective actions arranged by priority of importance.

    d. Construct an easily understood, meaningful safety profile.

To this end, it is recognized that the Frequency of Occurrence (a probabilistic estimate) by itself is not a complete measure. The Injury Potential or the Level of Hazard by themselves are also incomplete measures. The true impact of an event (failure or fault) on the safety of an equipment is best defined by the combination of Injury Potential, Frequency of Occurrence and Level of Hazard. It is significant to recognize that both Frequency of Occurrence and the Level of Hazard (Hazard Index) are expressed in quantitative terms. The only subjective judgment required is the assessment of the Injury Potential of a postulated event.

There are several valid techniques available for estimating and assessing frequency of occurrence or probability of failure. The key problem, therefore, is to develop a meaningful numerical index for defining various levels of safety hazards. Such an index has to be based on a measurable quantity. It was recognized that the degree of safety hazard, generated by a failure or fault event, is related to the time that is available to implement corrective action to avoid injury. The less time there is to mitigate the injury, the higher the degree of hazard. The level of hazard, therefore, is defined as an inverse exponential of this "time available to take action".

Once the level of hazard (criticality to safety) of each event can be defined, this characteristic can be combined with the level of injury potential and frequency of occurrence to produce a measure of the true impact on equipment safety. A method, called Safety Profile, was therefore devised whereby potential failures and faults (hazard events) are "ranked" in order of importance by plotting the probability vs. level of hazard, so that decisions can be made on a logical basis. This plot can then be used to 1) judge compliance of the equipment against safety objectives, and 2) identify failure modes in order of priority for recommending and implementing corrective actions.

ANALYSIS PROCEDURES

A systematic, organized approach is essential for performing the Analysis in order to assure that all potential failures are identified, evaluated and assessed as to their impact on safety. An overall view of one type of analysis procedure

indicating the sequence of required tasks for performing the Analysis for safety assessment is shown in Figure 1. To facilitate the Analysis and to provide a ready means of checking that all functions and modes of operation have been considered, a worksheet is used whose headings correspond to the individual tasks shown in Figure 1. The procedure shown in Figure 1 is based upon the Failure Mode Effects Analysis technique. Other analysis methods, which serve to identify and define failure and fault event, are equally applicable, such as the Fault Tree Analysis technique. The actual analysis technique utilized will depend upon the product being analyzed, the projected use environment, utlimate objective and ayalyst preference. It is emphasized that the validity of the measurement - frequency of occurrence, injury potential and hazard index - is dependent of the actual analysis technique utilized to identify the hazard events.

The tasks shown in Figure 1 are summarized as follows:

TASK 1 - <u>SYSTEM DESCRIPTION (BLOCK DIAGRAMS: DRAWINGS)</u>

Establish clear and precise definition of system operation and function. Develop functional and logic block diagrams.

TASK 2 - <u>FAILURE MODE</u>   .

All realistically possible failure modes at the outputs of each of the elements composing the functional block diagrams are listed and identified.

TASK 3 - <u>FAILURE MODE CAUSES</u>

The probable causes, in terms of failures of malfunctions, are identified and listed for each failure mode.

TASK 4 - <u>EVALUATION OF EFFECT</u>

The effects of symptoms of each failure are defined.

TASK 5 - <u>COMPENSATING PROVISIONS</u>

Any provision which permits continued, safe operation in the presence of a failure is noted.

TASK 6 - <u>INJURY POTENTIAL</u>

Based upon application and use environment, the effect of each failure mode is categorized as to its injury potential.

QRC
INCORPORATED

TYPICAL SCHEMATIC FLOW DIAGRAM OF ANALYSIS TASKS

1   SYSTEM/EQUIPMENT DESCRIPTION

2   FAILURE MODE IDENTIFICATION

3   FAILURE MODE CAUSES

4   EVALUATION OF EFFECT

5   COMPENSATING PROVISIONS

6   INJURY POTENTIAL

7   FREQUENCY OF OCCURRENCE
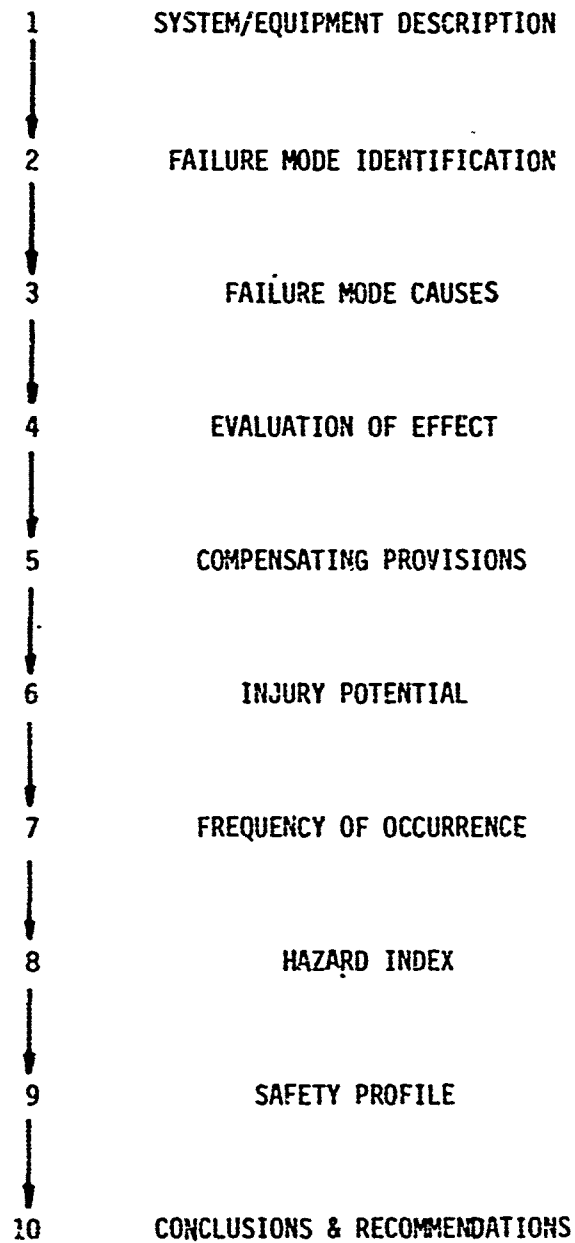
8   HAZARD INDEX

9   SAFETY PROFILE

10   CONCLUSIONS & RECOMMENDATIONS

FIGURE 1

TASK 7 - FREQUENCY OF OCCURRENCE

Frequency of occurrence of each postulated failure mode cause is estimated.

TASK 8 - HAZARD INDEX

A level of hazard, which is descriptive of the criticality of the safety hazard, is calculated for each failure mode. The calculation uses the time (T) available to take action which will avoid injury. Hazard Index $= e^{-T}$.

TASK 9 - SAFETY PROFILE

Develop priority listing by plotting a matrix of hazard level vs. probability of occurrence.

TASK 10- CONCLUSIONS & RECOMMENDATIONS

Develop necessary corrective actions to resolve problems. Relative urgencies are defined by the Safety Profile. Use the Profile to judge compliance with safety objectives.

The key tasks which are the essential elements for a safety oriented analysis are Tasks 6, 7, 8 and 9 and, therefore, merit further elaboration.

INJURY POTENTIAL (TASK 6)

For each identified failure mode, the analysis describes and defines the effect on product performance and capability. This effect is translated into categories or ranks of injury potential, so that this information becomes one scale for measuring safety. These "ranks" should reflect the intended equipment application and use environment. An example for level of severity ranks, which at the same time indicate broadly applicable definitions, is shown in Figure 2.

RANK	INJURY POTENTIAL
1	Failure will not result in personnel injury.
2	Failure will cause personnel injury.
3	Failure will cause major injury and death.
4	Failure will cause multiple major injury and multiple death.

FIGURE 2

The injury potential definitions for each rank should be expanded and refined as appropriate to accurately reflect the type of product, the intended applications and use environment.

FREQUENCY OF OCCURRENCE (TASK 7)

Frequency of occurrence for each postulated identified event (failure or fault) is estimated by means of an analysis of the equipment element associated with the function that has been assumed to have failed and is assessed in quantitative terms.

This probability provides a measure of the expected number of occurrences of each identified event during the specific period of equipment life under consideration.

Regardless of the assessment technique or data base used, the objective is to derive the most valid failure probability estimate possible (consistent with available data). In addition to estimating individual numerical failure probabilities for each failure, a system of frequency of occurrence ranks is established, with each rank identified and defined to fit the particular equipment being evaluated. Assignment of individual failures into a specific level is based on its estimated contribution to the overall equipment failure probability.

The number of levels to be defined and established will depend upon the equipment, its application and use environment since the depth of analysis is a function of the number of frequency of occurrence levels that can be logically defined and established in a meaningful manner. The fewer the number of defined levels, the coarser the analysis will be. Discrimination between failures increases almost exponentially with the number of individual levels that can be established, defined and utilized.

It is recommended that at least four frequency of occurrence ranks be establihsed

Rank 1 - Failure probability (frequency of occurrence) very low. Any single probability of occurrence less than 0.01 of the overall probability of failure.

Rank 2 - Failure probability low. Any single failure probability of occurrence more than 0.01 but less than 0.05 of the overall probability of failure.

Rank 3 - Failure probability medium. Any single failure probability of occurrence more than 0.05 but less than 0.1 of the overall probability of failure.

Rank 4 - Failure probability high. Any single failure probability of occurrence more than 0.1 of the overall probability of failure. If equipment failure should occur, chances are that the failure will be the one postulated.

These recommended definitions can be modified or expanded as necessary, depending on the equipment being analyzed and the amount of failure data available for the type of hardware involved.

The value of the overall analysis and utilization of its results is not limited by the availability of failure data. Where information is sparse or suspect, relative probability of individual failure and the contribution that each failure would make to overall system or equipment probability of failure can still be estimated, based on engineering judgments and prior experience.

Since a consistent, logical judgment base has been defined, the only requirement is the ability to make a realistic, valid judgment of the <u>relative</u> probability of individual failure modes in terms of overall equipment failure.

EVALUATION OF EFFECT AND HAZARD INDEX (TASK 8)

The effect of individual events is evaluated and a hazard index calculated from the point of view of impact on hazard to personnel (safety).

It is recognized that a specific event (failure or fault) may have a significant effect on both safety and function. It should also be recognized that a specific failure may have a very different impact on safety than on function. The assessment of the hazard index for safety analysis purposes requires concentration on the ultimate effect on personnel rather than on equipment function.

The degree of safety hazard generated by an event is related to the time (T) that is available to implement corrective action to avoid injury. The less time there is to mitigate injury, the higher the degree of hazard. The event that causes injury without warning, where the time available for taking corrective action approaches zero, it identified as "1.0", the highest level of hazard. On the other end of the spectrum is the event that is of such a nature that correction is not necessary to avoid injury, and safe operation is maintained throughout the life cycle of the equipment. This event is classified "0", the lowest level of hazard.

The hazard index, which is the measure of the degree of the safety hazard, is expressed as e^{-T}, where T is the actual time available to implement correction to avoid injury.

The determination of the actual available time requires the evaluation and analysis of the following time intervals:

    a. T_C - Time available to implement corrective action (time interval from occurrence of failure mode until injury occurs).

b. T_R - The time required to recognize the existence or presence of a hazard condition, or the time required for an automatic safety device to react and mitigate resultant injury.

c. T - Actual time available to take action; $T = T_C - T_R$.

The other important factor to be recognized in determining the available time T, is the presence (or absence) of built-in instrumentation or warning devices which present an indication that a failure has occurred. The time required to recognize a hazardous condition is less if it is indicated by a built-in instrument or warning device. The hazard in such a case is less than if detection must depend upon the experience of alertness of the operator.

It is evident that the Hazard Index (degree of safety hazard) can be evaluated and described in terms of a simple, meaningful numerical value. The measurable base utilized for establishing the Hazard Index is time. The time factor T is established with the assistance of the equipment designer by analyzing available test information, experience with similar equipments, or an analytically derived estimate of the time available to take action which will avoid injury.

SAFETY PROFILE (TASK 9)

The "Safety Profile" is a convenient, practical means of identifying and comparing each hazard event to all other hazard events with respect to their criticality to equipment safety. This is achieved by a graphic presentation of the three significant characteristics: Injury Potential, Frequency of Occurence and Hazard Index. By plotting these three values for each failure mode in a matrix (figure 3), the priority for initiating corrective measures and a graphic representation of the "safety profile" of the analyzed equipment is established. Such a matrix of the three hazard event characteristics recognizes that the ultimate aim of the Analysis is to:

a. Verify the status of the design with respect to safety requirement.

b. Provide a logical listing of recommended corrective actions arranged by priority of importance (criticality).

The Profile, graphically presented, also recognizes that the true impact of a hazard event (failure or fault) on the safety of a product is best defined by the combined evaluation of all three characteristics. For instance: a specific failure with a low level of injury potential, a high frequency of occurrence, may have a low hazard index. This means that a low priority is assigned in the Profile.

Another failure with a low level of injury potential and an extremely low frequency of occurrence may have a high hazard index. This failure mode is again identified with a relatively low priority in the Profile.

Since each hazard event is assigned a serial number which uniquely and conveniently identifies it and the associated equipment element, the overall equipment safety profile is constructed by inserting that event serial number in the matrix square representing the frequency of occurrence and hazard level for the hazard event.

As clearly indicated in the Profile, Figure 3, the further the square in which the hazard event is recorded is from the origin, the greater the impact of system safety, the greater the hazard, and the more urgent is the need for implementing corrective actions.

It is readily apparent that the graphical display of the Criticality Matrix of all hazard events provides an instrument for clearly defining not only the product safety profile, but also indicating the relative importance and priority of recommended corrective actions. This method of presentation also facilitates in clearly communicating these facts to all disciplines (technical and management) that have to be involved in the corrective action decision-making process.
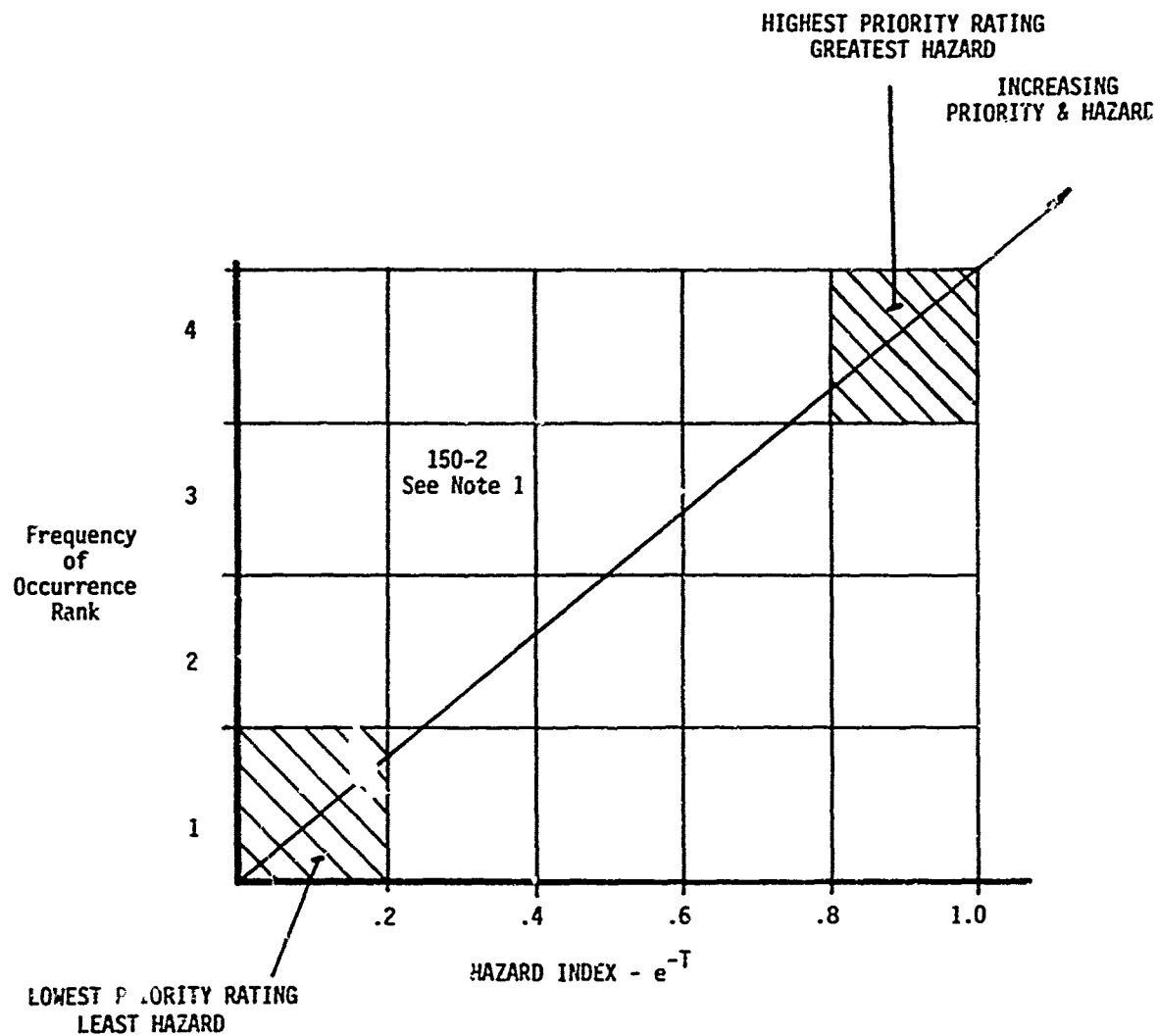
SAFETY PROFILE

FIGURE 4

Note 1: Example of plotting Hazard Event with SN 150 - Injury Potential - 2
Probability   - 3
Hazard Index - .2 to .4

1054

Experience has shown that the completed Safety Profile display very character-
istic failure event distributions that can be effectively used as a management
decision tool to, for instance, select the best equipment design from 2 or
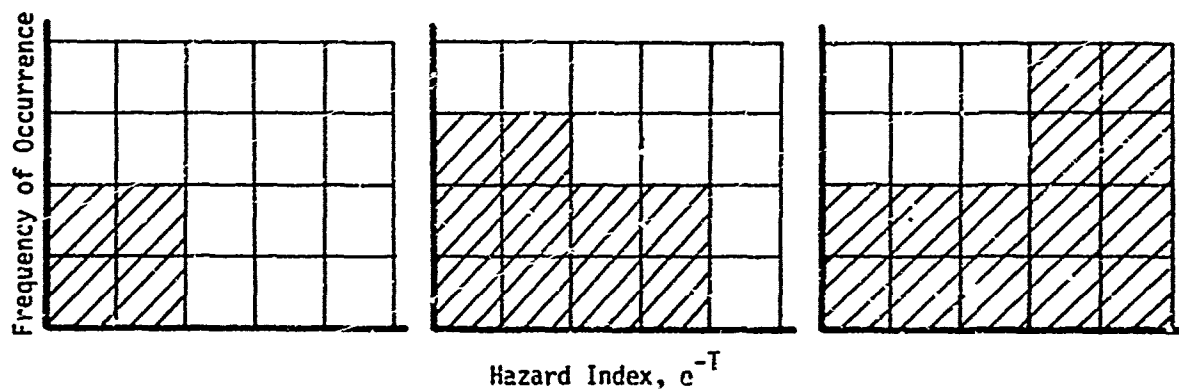more submissions. Three Typical Profiles are shown in Figure 5.

Hazard Index, e^{-T}

FIGURE 5. Typical safety profiles, showing, left to right,
ideal, adequate, and unacceptable products.

SOME RECENT APPROACHES IN HAZARDS CLASSIFICATIONS

S. Fleischnick
Picatinny Arsenal, Dover, N. J.

INTRODUCTION

WITHIN THE PAST YEAR, I HAVE BEEN INTIMATELY INVOLVED IN A
NUMBER OF PROGRAMS RELATING TO PROBLEMS IN SAFETY AND IN HAZARDS
CLASSIFICATIONS. I HAVE HAD AN OPPORTUNITY TO DELVE INTO
(1) THE DETAILS OF TEST PROCEDURES AND TECHNIQUES BEING UTILIZED
FOR HAZARDS CLASSIFICATIONS, AND (2) THE INTERPRETATION OF THE
RESULTS OF SUCH TESTS.

IN MY CONTACTS, I HAVE ENCOUNTERED WHAT I CONSIDERED AT
THE TIME TO BE MISUNDERSTANDINGS OR MISINTERPRETATIONS RELATING
TO HAZARDS CLASSIFICATIONS, SOME LEADING TO OVERCLASSIFICATION
AND SOME TO UNDERCLASSIFICATION. THE IMPLICATIONS OF SUCH MIS-
CLASSIFICATIONS ARE OBVIOUS, AS THEY RELATE TO PROTECTION OF
PERSONNEL AND PROPERTY, TO FACILITIES COSTS, TO PRODUCTION
AND SHIPPING COSTS.

I HAVE, HOWEVER, RECONSIDERED THE USE OF THE PHRASE,
"MISUNDERSTANDING IN HAZARDS CLASSIFICATIONS," SINCE THE TECH-
NIQUE OR SUGGESTIONS WERE, IN FACT, NEW APPROACHES TO HAZARDS
CLASSIFICATION. ACCORDINGLY, I HAVE CHANGED THE TITLE OF MY
PRESENTATION TO "SOME RECENT APPROACHES IN HAZARDS CLASSIFI-
CATION."

DISCUSSION

PART A

LET ME START WITH PERHAPS SOME ELEMENTARY STATEMENTS CONCERNING HAZARDS CLASSIFICATION AND THEIR RELATED QUANTITY-DISTANCE STANDARDS. AND I SHALL BE REFERRING TO DOD CONTRACTORS SAFETY MANUAL FOR AMMUNITION, EXPLOSIVES AND RELATED DANGEROUS MATERIALS, DOD 4145.26M DATED OCTOBER 1968, AND TO TB 700-2, EXPLOSIVES HAZARD CLASSIFICATION PROCEDURES DATED 19 MAY 1967.

PARAGRAPH 700 OF DOD 4145.26M, RELATING TO QUANTITY-DISTANCE REQUIREMENTS APPLICABLE TO STORAGE, PROCESSING AND HANDLING OF AMMUNITION AND EXPLOSIVES, STATES THAT HAZARDS CLASSIFICATION OF ITEMS WILL BE ASSIGNED IN ACCORDANCE WITH TB 700-2.

THE DOD MANUAL PROVIDES QUANTITY-DISTANCE STANDARDS FOR SEVEN CLASSES OF MATERIALS. I SHOULD LIKE TO REFER ONLY TO CLASSES 7, 2 AND 1. CLASS 7 MATERIAL IS DESIGNATED AS MASS DETONATING, AND CLASSES 2 AND 1 AS FIRE HAZARDS.

FOR CLASS 7, MAGAZINE AND INTRALINE DISTANCES ARE SPECIFIED WITHIN WHICH MAJOR PROPERTY DAMAGE CAN BE EXPECTED FROM OVER-PRESSURES, AND MAJOR HAZARDS TO PERSONNEL EXIST. BUT EVEN TO INHABITED BUILDING DISTANCES, SEVERE STRUCTURAL DAMAGE MAY OCCUR AND THERE MAY BE LOSS OF LIFE OR SEVERE INJURIES FROM PARTIAL COLLAPSE OF BUILDINGS AND FROM FRAGMENTS. THE LIMITATIONS OF QUANTITY-DISTANCE REQUIREMENTS IN PROTECTION OF FACILITIES AND PERSONNEL ARE CLEARLY DEFINED, AND MUST BE RECOGNIZED.

CLASS 2 MATERIALS, EVEN THOUGH NOT MASS DETONATING AS DEFINED BY TB 700-2, DO PRESENT HAZARDS SIMILAR TO THOSE FOR CLASS 7 MATERIALS, INCLUDING HAZARDS DUE TO OVERPRESSURES. OVERPRESSURES ARE IMPLICIT IN THE QUANTITY-DISTANCE REQUIREMENTS WHICH APPROXIMATE A CUBE-ROOT SCALING FORMULA (FIGURE 1).

FIGURE 1 - CLASS 2 QUANTITY-DISTANCE REQUIREMENTS

PART B

THE LIMITATIONS OF OUR HAZARDS CLASSIFICATION SYSTEM AS IT RELATES TO PROTECTION OF PERSONNEL NOT ONLY FROM BLAST, BUT ALSO FROM FRAGMENTS AND FIRE, HAS BEEN RECOGNIZED BEFORE. IN AN ARTICLE IN THE ANNALS OF THE NEW YORK ACADEMY OF SCIENCES, (VOLUME 1, ART. 1, OCT 28, 1968, PP 199), SETTLES DISCUSSES THE CARD GAP TEST OF THE TB 700-2 AND ITS UTILIZATION IN DIFFERENTIATION BETWEEN DETONATING AND NON-DETONATING REACTIVE MATERIALS, AND QUESTIONS THE ACCEPTANCE BY THE GOVERNMENT AND BY INDUSTRY OF A TWO-HAZARD SYSTEM BASED ON THIS TEST METHOD: DETONATING MATERIALS OR CLASS 7, AND FIRE HAZARD MATERIALS OR CLASS 2. HE STATES THAT NON-DETONATING MATERIALS CAN CAUSE INJURIES, DEATH AND MAJOR PROPERTY DAMAGE.

FIGURE 2 - EXPLOSIVES HAZARDS SPECTRUM - ACCORDING TO SETTLES

SETTLES PROPOSES TO REDEFINE CLASS 2 MATERIALS TO ESSENTIALLY A CLASS 1 MATERIAL WITH NO HAZARDS TO BE EXPECTED FROM OVERPRESSURES OR FROM FLYING FRAGMENTS AND MISSILES. (FIGURE 3)

FIGURE 3 - COMPLETE HAZARDS SPECTRUM - ACCORDING TO
SETTLES

THE PROPOSAL IS AN INTERESTING ONE, IF WE GO ONE STEP FURTHER, NAMELY, INTRODUCE THE CONCEPT OF TNT EQUIVALENCIES IN THE EVALUATION OF HAZARDS POTENTIAL FROM BLAST FOR ALL MATERIALS WHICH MAY PRODUCE SIGNIFICANT OVERPRESSURES. TNT EQUIVALENCIES PERMIT A FINER BREAKDOWN OF OVERPRESSURE POTENTIALS AND PROVIDES IN ESSENCE AN INFINITE NUMBER OF QUANTITY-DISTANCE REQUIREMENTS. I WILL DISCUSS TNT EQUIVALENCIES SHORTLY.

UNLESS THE CONCEPT OF TNT EQUIVALENCY IS EMPLOYED, THE PRESENT CLASSIFICATIONS OF 7, 2 AND 1 SHOULD BE RETAINED IN PREFERENCE TO THE CLASSIFICATION PROPOSED BY SETTLES, SINCE THEY DO TAKE ADVANTAGE OF MAJOR DIFFERENCES IN OVERPRESSURES.

BUT THE USE OF ANY CLASSIFICATION SYSTEM MUST NOT RELAX EITHER THE NEED FOR PROTECTION OF PERSONNEL INVOLVED WITH REACTIVE MATERIALS OR THE NEED TO LIMIT THE NUMBERS OF PEOPLE EXPOSED TO SUCH HAZARDOUS MATERIALS.

PART C

I SHOULD NOW LIKE TO DISCUSS THE MORE RECENT APPROACH TO HAZARDS CLASSIFICATION, NAMELY, THE UTILIZATION OF MAXIMUM TNT EQUIVALENCY. IN THIS TEST, THE REACTIVE MATERIAL IS SUBJECTED TO THE SHOCK OF A HIGH EXPLOSIVE BOOSTER CHARGE, AND MEASUREMENTS MADE OF THE PRESSURE WAVES PRODUCED. THE PRESSURE WAVES OBTAINED ARE

CORRELATED WITH THOSE OBTAINABLE FROM VARIOUS WEIGHTS OF TNT AND THE EQUIVALENT WEIGHT OF TNT ESTABLISHED. THE BOOSTER CHARGE WEIGHT IS THEN INCREASED UNTIL NO FURTHER INCREASE IN TNT EQUIVALENCY IS OBTAINED FOR THE TEST MATERIALS. THE MAXIMUM TNT EQUIVALENCY VALUE IS UTILIZED IN DESIGN OR STRUCTURES AND IN QUANTITY-DISTANCE DETERMINATIONS.

HOWEVER, SOME MATERIALS SUCH AS PROPELLANTS AND PYROTECHNICS ARE VERY SENSITIVE TO THE AMOUNT OF BOOSTER USED, AND THE USE OF A MAXIMUM TNT EQUIVALENCY VALUE CAN LEAD TO OVERCLASSIFICATION.

I SHOULD LIKE TO REVIEW DATA OBTAINED FOR SMALL WEB SINGLE-BASE PROPELLANT, NAMELY, THE 8" M1 PROPELLING CHARGE WHEN PACKAGED IN ITS SHIPPING CONTAINER (REFERENCE IITRI FINAL REPORT J6265-2 AND IITRI LETTER DATED 18 JANUARY 1973). FIGURE 4)

FIGURE 4 - 8" M1 PROPELLING CHARGE IN M18A2 SHIPPING CONTAINER

THE M1 PROPELLING CHARGE CONTAINS 13.1 LBS OF M1 SINGLE PERFORATED GRAINS WITH A NOMINAL WEB OF 0.016 IN. THE CHARGE ASSEMBLY CONSISTS OF 5 INCREMENTS OF PROPELLANT - EACH IN A CLOTH BAG. THE PROPELLANT IS INITIATED BY 5 OUNCES OF CLASS 1 BLACK POWDER LOCATED AT THE BASE OF THE CHARGE. THE CHARGE IS PACKAGED IN A METAL CAN, THE M18A2 SHIPPING CONTAINER, USING CORRUGATED PAPER, WOOD AND OTHER FILLER MATERIAL TO OBTAIN A TIGHT PACK.

THIS CHARGE WAS SUBMITTED TO A SERIES OF TESTS INCLUDING THOSE PRESCRIBED IN TB700-2 DROP TESTS AND TNT EQUIVALENCY TESTS USING A VARIETY OF INITIATORS.

FOR THE TNT EQUIVALENCY TESTS, THE FOLLOWING TEST CONFIGURATIONS WERE USED:

FIGURE 5 - BOOSTER CONFIGURATION FOR TNT EQUIVALENCY TESTS

FIGURE 6/6A - TNT EQUIVALENCY TESTS SETUPS FOR SINGLE AND MULTIPLE CHARGE CONFIGURATIONS

FIGURE 7 - TNT EQUIVALENCY TEST AREA

THE DATA OBTAINED IN THE TNT EQUIVALENCY TESTS USING A SINGLE PROPELLING CHARGE IS SHOWN IN FIGURE 8.

FIGURE 8 - PRESSURE EQUIVALENCY VS. BOOSTER SIZE FOR ONE M1 PROPELLING CHARGE

WHEN A ONE OZ. TETRYL BOOSTER WAS USED, TNT EQUIVALENCIES OF 10 PERCENT WERE OBTAINED IN SINGLE CHARGE DETONATION TESTS. HIGHER TNT EQUIVALENCIES (UP TO 140 PERCENT) WERE OBTAINED WITH LARGER BOOSTERS (4 TO 32 OZS. OF COMPOSITION C-4). THE 140 PERCENT EQUIVALENCIES WERE OBTAINED WITH A BOOSTER EQUIVALENT TO 5 PERCENT OR MORE OF THE WEIGHT OF PROPELLANT.

IN OTHER TESTS (FIGURE 9), A LOWER TNT EQUIVALENCY OF 2.5 PERCENT FOR A SINGLE CANISTER WAS OBTAINED WHEN USING A SQUIB TO INITIATE THE BLACK POWDER BASE PAD. AND IN MULTIPLE (15 AND 50) CHARGE TESTS, TNT EQUIVALENCIES OF 1 PERCENT WERE OBTAINED.

SYMPATHETIC DETONATION DID NOT OCCUR WHEN A ONE OZ. TETRYL BOOSTER WAS USED AS REQUIRED BY TB 700-2. WITH LARGER COMPOSITION C-4 BOOSTERS, SYMPATHETIC DETONATION WAS OBTAINED.

IN THE EXTERNAL HEAT TESTS PRESCRIBED BY TB 700-2, DETONATION DID NOT OCCUR. THE SHIPPING CONTAINERS WERE FOUND INTACT ALTHOUGH THEIR LIDS WERE BLOWN OFF AND RECOVERED AT DISTANCES UP TO 100 FEET.

NO IGNITIONS WERE OBTAINED IN THE DROP TESTS FROM HEIGHTS OF 4 FEET AND 40 FEET.

IN THE CARD GAP TEST FOR THE PROPELLANT, AS DETERMINED BY TB 700-2, A VALUE OF 63 CARDS WAS OBTAINED. A VALUE OF LESS THAN 70 CARDS IS ONE OF THE CLASSIFICATION CRITERIA FOR CLASS 2.

RATES OF PROPAGATION OBTAINED IN THE CARD GAP TESTS WERE: 5000 METERS/SEC WITH ZERO CARDS, 3300 METERS/SEC FOR 63 CARDS, 1400 METERS/SEC FOR 128 CARDS.

BASED ON THIS DATA, HOW SHOULD WE CLASSIFY THE PROPELLING CHARGE IN ITS PACKAGED FORM?

IN THE STANDARD TESTS OF TB 700-2, THERE WAS NO EVIDENCE OF SYMPATHETIC DETONATION EVEN WHEN THE CHARGE WAS INITIATED BY ONE OUNCE OF TETRYL; AND WITH NO EVIDENCE OF DETONATION IN THE FIRE TEST AND IN THE DROP TEST, A CLASS 2 HAZARD CLASSIFICATION WOULD APPEAR TO BE IN ORDER. AND THE CARD GAP TEST CONFIRMS THIS FOR THE PROPELLANT, ASSUMING THAT WE AGREE WITH THE CARD GAP TEST CRITERIA FOR CLASSIFICATION.

But what about the information developed that very high outputs are obtainable when the propellant charge is subjected to the shock of a large high explosive booster?

This high output is not unexpected. The high explosive must certainly affect the burning characteristics of the black powder base charge as well as the propellant. At the least, detonation of the explosive will cause break up of the grains and provide for a much faster burning. That such interactions can occur is taken into consideration when materials of different classes are mixed. DOD 4145.26M (para 704b) states:

"Where items of different classes are stored together in the same building or location, applicable explosive weight for the total number of items in each explosive class will be added together to determine the total explosive weight. This total explosives weight and the tables applicable to the most hazardous class shall be used to determine proper safety distances."

The relative weights of different classes is not important; the possible interaction is. Where mixing can be shown not to cause a change in characteristics, such mixing can be allowed, for example, the presence of a coarse granulation black powder in close proximity to the propellant charge in the 8" M1 Propelling Charge.

SIMILAR PROBLEMS IN HAZARDS CLASSIFICATION BASED ON TNT
EQUIVALENCY TESTS HAVE BEEN ENCOUNTERED WITH OTHER MATERIALS SUCH
AS PYROTECHNIC COMPOSITIONS. IT HAS BEEN PROPOSED THAT WHEN
OUTPUT VARIES WITH BOOSTER CHARGE, THE MAXIMUM OUTPUT SHOULD BE
UTILIZED TO ASSURE THAT UNDER ANY CIRCUMSTANCES SAFETY FACTORS
WILL NOT BE EXCEEDED. TO DESIGN TO THIS WORST SITUATION,
REGARDLESS OF WHETHER SUCH A SITUATION COULD EVER ARISE, I FEEL
TO BE UNREALISTIC, LEADING TO OVERCLASSIFICATION AND OVERDESIGN.

PART D

WHAT RECOMMENDATIONS DO WE HAVE FOR IMPROVING ON OUR METHODS
FOR HAZARDS CLASSIFICATION?

THE BASIC RECOMMENDATION THAT CAN BE MADE IS THAT ANY TEST
FOR HAZARDS CLASSIFICATION MUST ATTEMPT TO SIMULATE THE CONFIGURA-
TION OF THE ITEM BEING EVALUATED AND THE ENVIRONMENT AND STIMULI
TO WHICH THAT ITEM MAY BE SUBJECTED.

SOME OF THE TESTS IN TB 700-2 ATTEMPT TO DO THIS. FOR EXAMPLE,
THOSE LISTED IN CHAPTER 4, "MINIMUM TEST CRITERIA FOR DETERMINING
HAZARDS CLASSIFICATION OF GUN TYPE PROPELLANTS FOR CANNON, GUN
TANK, MORTAR AND ROCKET MOTORS UP TO 8 INCH DIAMETER." (FIGURE 9)

FIGURE 10 - TABLE 4 OF TB 700-2

INCLUDED ARE TESTS FOR SINGLE CHARGE DETONATION, SYMPATHETIC
DETONATION AND EXTERNAL HEAT TEST. I COULD QUIBBLE WITH THE
DETONATION TEST PROCEDURE IN WHICH THE CHARGE IS INITIATED BY A
ONE OUNCE TETRYL BOOSTER AND A BLASTING CAP. A MORE APPROPRIATE
INITIATOR WOULD BE A SQUIB.

OTHER TESTS IN TB 700-2, SUCH AS THOSE WHICH MIGHT BE USED FOR
BULK REACTIVE MATERIALS AS LISTED IN CHAPTER 3, ARE OF LIMITED VALUE
BUT ARE USEFUL IN SCREENING OUT THE MORE SENSITIVE AND UNSTABLE
MATERIALS.

THE TNT EQUIVALENCY TEST IS AN IMPORTANT TEST, BUT CARE MUST
BE EXERCISED IN INTERPRETATION OF THE DATA AS RELATED TO REAL
LIFE SITUATIONS.

IT IS STRONGLY RECOMMENDED THAT TB 700-2 BE REVIEWED IN DEPTH,
AND AMENDED TO ASSURE PROPER INTERPRETATION OF THE TEST RESULTS
AND TO ASSURE MORE REALISTIC SIMULATION OF THE CONFIGURATION OF
THE ITEM (OR SYSTEM) BEING EVALUATED, AND OF THE ENVIRONMENT AND
STIMULI TO WHICH THAT ITEM MAY BE SUBJECTED.

PART E

THERE IS ONE ADDITIONAL AREA OF ACTIVITY WHICH REQUIRES MUCH
MORE ATTENTION, AND THAT IS ATTEMPTING TO REDUCE THE HAZARDS
CLASSIFICATION OF ITEMS BY REDESIGN, BY REPACKAGING, OR BY
RECONFIGURATION IN STORAGE AND SHIPMENT. IT IS IMPORTANT NOT
ONLY TO DETERMINE THE HAZARDS CLASSIFICATION OF AN ITEM, BUT ALSO
TO ATTEMPT TO REDUCE ITS CLASSIFICATION. WHILE THIS IS IMPLIED
IN SEVERAL LOCATIONS OF THE TB 700-2 AND IN THE DOD 4145.26M,

ONLY RECENTLY HAVE WE MADE SOME PROGRESS - ONLY BECAUSE OF NECESSITY. THE TESTS DESCRIBED ABOVE ON THE 8" M1 PROPELLING CHARGE, AND WORK ON A TRIPLE-BASE PROPELLANT CHARGE, HAVE PERMITTED DOWNGRADING FROM CLASS 7 TO CLASS 2. AND WE HAVE RE-PACKAGED DETONATORS SO THAT IF ONE GOES OFF, WE DO NOT GET MASS DETONATION. THERE MUST BE MANY OTHER FRUITFUL AREAS FOR THIS KIND OF ACTIVITY. NOT ONLY IS SAFETY ENHANCED BUT MAJOR SAVINGS IN DOLLARS CAN BE REALIZED.

SUMMARY

1. THERE ARE SIGNIFICANT LIMITATIONS IN PRESENT QUANTITY-DISTANCE REQUIREMENTS IN THE DEGREE OF PROTECTION AFFORDED TO PERSONNEL AND FACILITIES WITHIN INTRALINE AND WITHIN INHABITED BUILDING DISTANCES. THESE LIMITATIONS MUST NOT BE OVERLOOKED IN PROVIDING SPECIAL PROTECTION TO PERSONNEL AND TO FACILITIES HANDLING REACTIVE MATERIALS, AND TO LIMITING THE NUMBER OF PEOPLE EXPOSED.

2. THE CONCEPT OF TNT EQUIVALENCY IS VERY USEFUL IN AVOIDIN OVERCLASSIFICATION, IF SUCH EQUIVALENCY IS DETERMINED BY TESTS APPROXIMATELY THE "REAL LIFE" CONFIGURATION OF THE ITEM BEING EVALUATED AND THE ENVIRONMENT AND STIMULI THAT THE ITEM CAN BE EXPECTED TO SEE.

3. ANY TEST PROCEDURES FOR HAZARDS CLASSIFICATION SHOULD TAKE INTO CONSIDERATION "REAL LIFE" CONDITIONS. TB 700-2 SHOULD BE RE-EVALUATED TO THESE CRITERIA.

4. MORE EMPHASIS MUST BE PLACED ON REDUCING THE HAZARDS CLASSIFICATION OF END ITEMS.

CLASS 2 DISTANCE REQUIREMENTS

Figure 1

QUANTITY

DISTANCE IN FEET

POUNDS (OVER)	POUNDS (NOT OVER)	INHABIT BLDG DIST (1)	PUBLIC RR & HWAY DIST (1)	ABVGD MAG & INTRALINE (1)	EARTH COVERED MAGS (2)
0	1000	75	75	50	
1000	5000	115	115	75	
5000	10000	150	150	100	
10000	20000	190	190	125	
20000	30000	215	215	145	
30000	40000	235	235	155	
40000	50000	250	250	165	
50000	60000	260	260	175	
60000	70000	270	270	185	

FOR DETERMINING DISTANCES TO BE USED IN EVENT SPECIAL REQUIREMENTS EXIST FOR AMOUNTS ABOVE 1,000,000 POUNDS, THE VALUES GIVEN ABOVE WILL BE EXTRAPOLATED BY MEANS OF CUBE-ROOT SCALING AS FOLLOWS:

FOR INHABITED BUILDINGS, PUBLIC RAILROADS AND PUBLIC HWYS   D   8W 1/3

FOR ABOVEGROUND MAGAZINE AND INTRALINE SEPARATIONS D   5W 1/3

1069

Figure 2

EXPLOSIVES HAZARDS SPECTRUM

EXTENT OF HAZARDS	REACTION VIOLENCE	HAZARDS CLASSIFICATIONS
	HIGH VELOCITY DETONATION HAZARD > 16,000 FT/SEC IN MILD STEEL	MASS DETONATING CLASS 7
	MEDIUM VELOCITY DETONATION HAZARD < 16,000 FT/SEC IN MILD STEEL	
	LOW VELOCITY DETONATION HAZARD	
	HIGH RATE EXPLOSION HAZARD	
	MEDIUM RATE EXPLOSION HAZARD	
	LOW RATE EXPLOSION HAZARD	FIRE HAZARD CLASS 2
	LARGE FIRE BALL FIRE HAZARD	
	SMALL FIRE BALL FIRE HAZARD	

HAZARDS OF BLAST OVER-PRESSURES

HAZARDS OF FLYING FRAGMENTS AND MISSILES

HAZARDS OF RADIANT HEAT AND FIRE

1070

Figure 3

COMPLETE HAZARDS SPECTRUM

HAZARDS CLASSIFICATIONS

REACTION VIOLENCE

EXTENT OF HAZARDS

EXPLOSION HAZARD

CLASS 7

HIGH VELOCITY DETONATION HAZARD
>16,000 FT/SEC IN MILD STEEL

MEDIUM VELOCITY DETONATION HAZARD
<16,000 FT/SEC IN MILD STEEL

LOW VELOCITY DETONATION HAZARD

HIGH RATE EXPLOSION HAZARD

MEDIUM RATE EXPLOSION HAZARD

FIRE HAZARD

CLASS 2

LOW RATE EXPLOSION HAZARD

LARGE FIRE BALL FIRE HAZARD

SMALL FIRE BALL FIRE HAZARD

HAZARDS OF BLAST OVER-PRESSURES

HAZARDS OF FLYING FRAGMENTS AND MISSILES

HAZARDS OF RADIANT HEAT AND FIRE

1071

Figure 5

BOOSTER CONFIGURATION FOR TNT EQUIVALENCY TESTS

M18A2 CANISTER

BLACK POWDER BAG

NUMBER 6 DUPONT CAP LEADS

STEEL PLATE

M1 PROPELLING CHARGE IN CLOTH BAGS

C4, 120° CONE BOOSTER

STYROFOAM

NUMBER 6 DUPONT CAP

Figure 6

TNT EQUIVALENCY TEST SETUPS FOR SINGLE & FIVE CHARGE CONFIGURATIONS

DONOR CANISTER

BLAST PAD

STEEL BANDS

SAND SURFACE

STEEL PLATE

BLAST PAD

1073
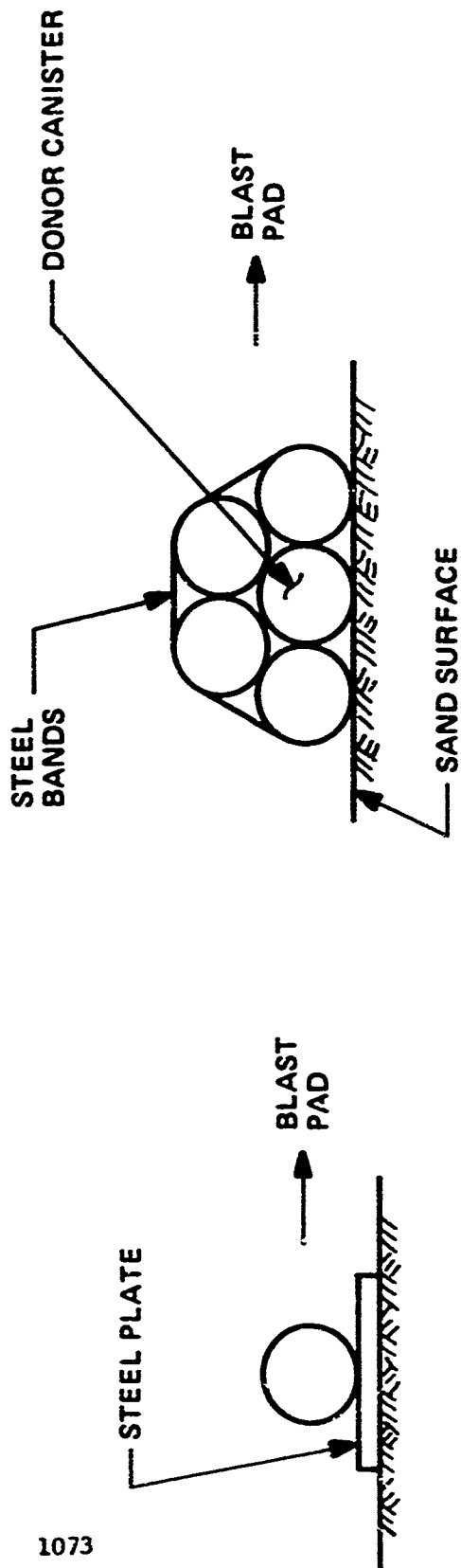
MULTIPLE CHARGE TEST
CONFIGURATION EXAMPLE
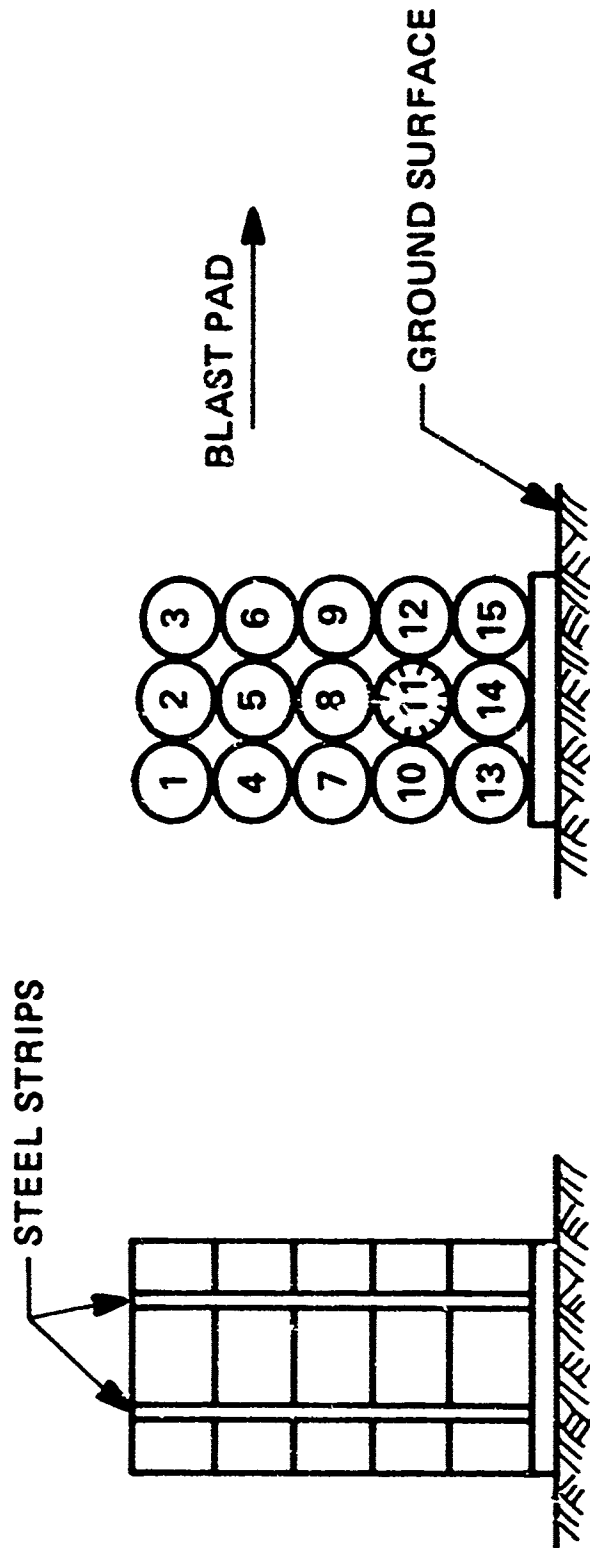
Figure 6A

Figure 7

TNT EQUIVALENCY TEST AREA

FASTAX CAMERA →

6E

5E
4E
3E
2E
1E

0

← DISTANCE TO
FIRST GAGE →

CHARGE LOCATION

PRESSURE
GAGE
LOCATIONS

SECOND BLAST
PAD NOT USED
DURING THESE TESTS
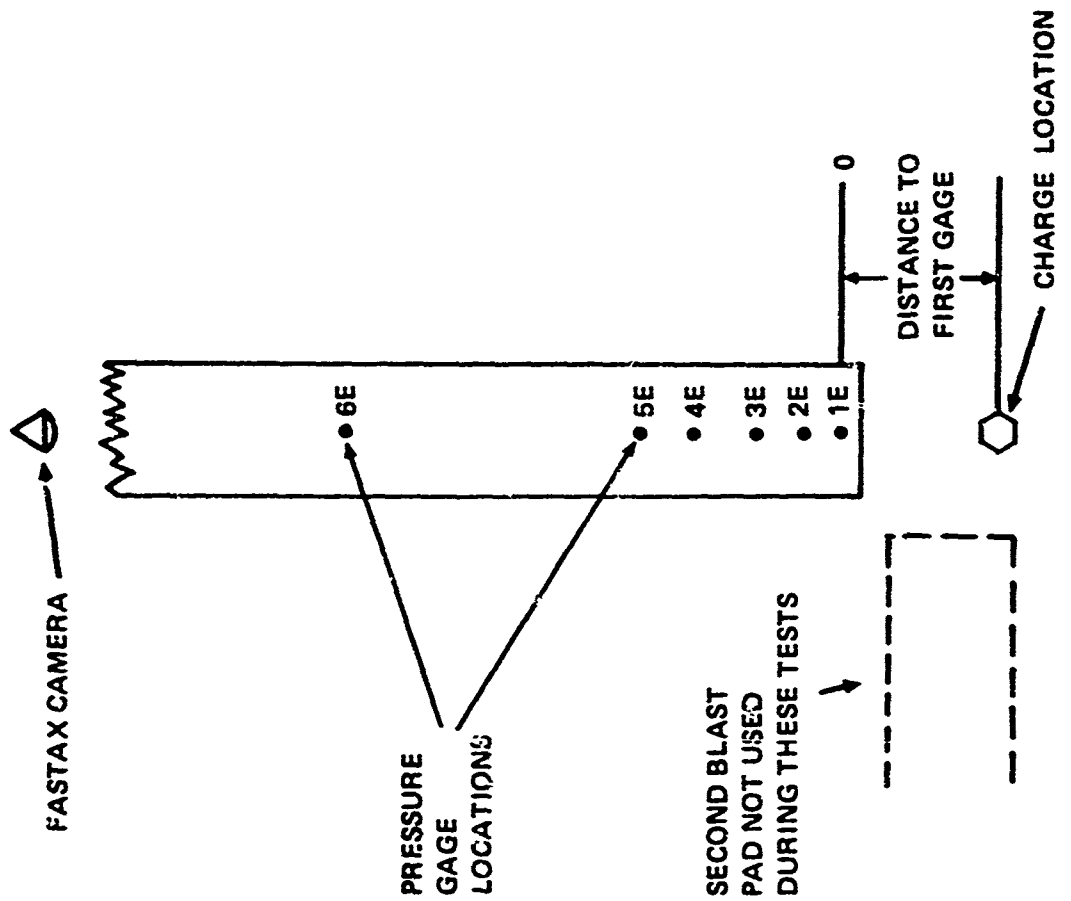
Figure 8

PRESSURE EQUIVALENCY VS BOOSTER SIZE

Figure C
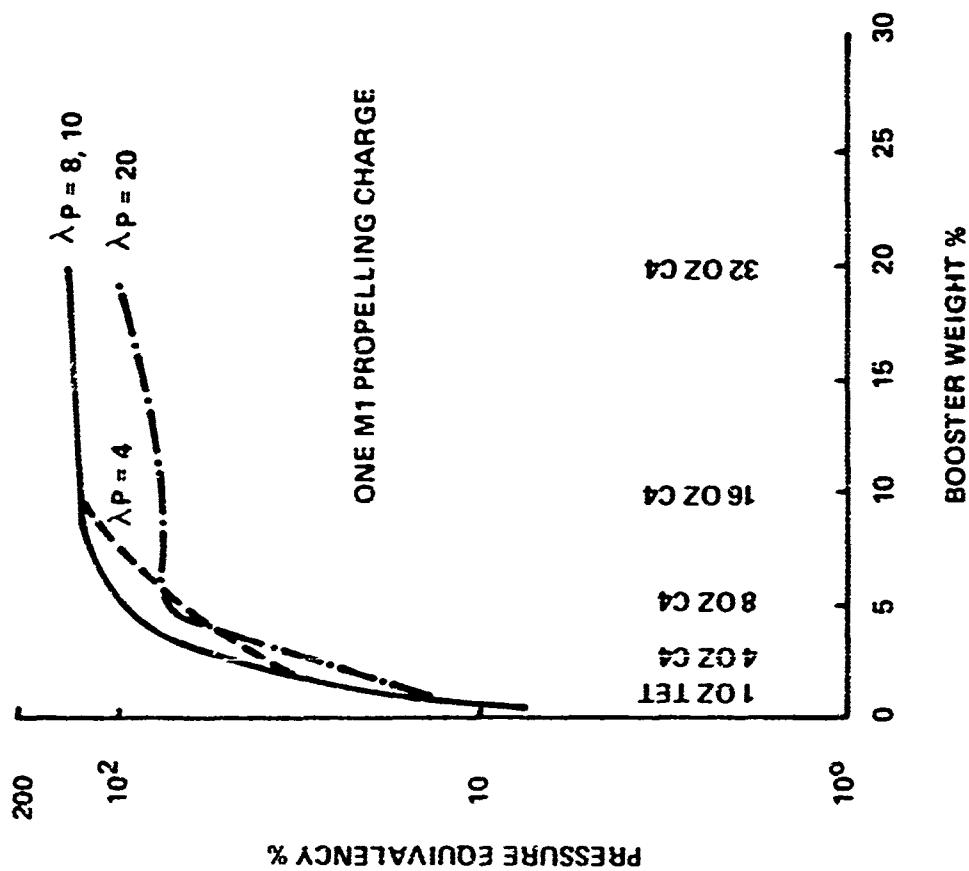
OTHER TESTS ON M1 PROPELLING CHARGE AND ON THE PROPELLANT

TEST	TEST CONFIGURATION	RESULTS OF TEST
TNT EQUIVALENCY	SINGLE CANISTER - SQUIB INITIATOR (15 AND 50)	2.5% TNT EQUIV (PRESSURE)
TNT EQUIVALENCY	MULTIPLE CANISTERS - 1 OZ TETRYL BOOSTER INITIATOR FOR 1 CAN	1% TNT EQUIV (PRESSURE)
SYMPATHETIC DETON	TB 700-2 - 1 OZ TETRYL INITIATOR	NO SYMPATHETIC DETONATION
SYMPATHETIC DETON	TB 700-2 EXCEPT LARGER C-4 INITIATORS	SYMPATHETIC DETONATION
EXTERNAL HEAT	TB 700-2	NO DETONATIONS. ALL CHARGES IGNITED. SOME UNBURNED PROPELLANT FOUND AFTER TESTS
DROP	4 FOOT, 40 FT IN CANISTER	NO IGNITIONS
CARD GAP	TB 700-2, PROPELLANT	63 CARDS

RATES OF PROPAGATION

0 CARDS - 5000 METER/SEC
63 CARDS - 3300 METER/SEC
128 CARDS - 1400 METER/SEC

Figure 10

MINIMUM TEST CRITERIA

TYPE TEST	NUMBER ITEMS PER TEST	NUMBER OF TESTS	PRIMING	BOOSTER	CONFINEMENT
TEST A. DETONATION	2 SHIPPING CONTAINERS	5 – OR UNTIL FIRST DETONATION OF BOTH	BLASTING CAP	30 GRAM TETRYL	NONE
TEST B. DETONATION	2 SHIPPING CONTAINERS	3 DET OF PRIMED CONTAINER ONLY	BLASTING CAP	30 GRAM TETRYL	NONE
TEST C. EXTERNAL HEAT	2 SHIPPING CONTAINERS	1	NONE	NONE	STEEL BANDED

1078

METHODS OF REDUCING THE VULNERABILITY OF AMMUNITION STORES

Mr. Harry Reeves
Ballistic Research Laboratories
Aberdeen Proving Ground, MD

I. INTRODUCTION

In the logistic process from arsenal to user, it becomes necessary for the Army to accumulate large quantities of ammunition at various distribution points. While individual rounds of ammunition are inherently hazardous, when stored in large quantities, the propagation of damage by fire or detonation greatly magnifies the problem. Procedures had to be developed for safe handling and storage even under ideal conditions. In general, these involve segregation by categories which essentially recognize hazard differences between munitions. Packaging and stacking can also be regulated to minimize propagation risk. As storage points move closer to the enemy, they become increasingly attractive targets to saboteurs, "sappers," snipers, and attack by mortars, artillery, and aircraft weapons. Passive defense techniques such as revetments, sandbagging, and stack separation have been devised, but at best offer only limited protection.

The problem of ammunition stores vulnerability may be defined in terms of the availability of land areas and the combustible packaging materials as well as the ammunition itself. Stack separation, a general procedure for decreasing total losses for all types of ammunition, is the only means available for minimizing losses when storing mass-detonating ammunition in unprotected open-field storage. In many situations in combat theaters, adequate land areas and security forces for the proper protection and storage of ammunition are not available. During the period January 1966 through September 1971, the value of the combined USARV and ARVN ammunition dump and ammunition supply point (ASP) losses exceeded $146,000,000. This figure does not include:

 a. ammunition losses suffered by other U.S. Forces (the value of the combined Air Force-Marine Corps ammunition losses at DaNang, 27 April 1969, was in excess of $123,000,000).

 b. losses suffered by other allies in Southeast Asia.

 c. losses suffered after the ammunition leaves a supply point, and

 d. other materiel losses associated with the storage and transportation of ammunition (buildings, trucks, barges, etc.).

Accurate comprehensive statistics on the overall dollar value associated with all U.S. ammunition losses are not available, but such losses appear to be staggering.

Conventional ammunition comprises a large variety of bombs, bulk explosives, projectiles, propellants, grenades, pyrotechnics, etc. For most Army "dumps," however, the largest amounts probably fall in the general category of artillery munitions. These may be of a fixed, semi-fixed or separate loading type design in a variety of sizes from 76mm to 8-inch. However, from a vulnerability point of view the materials fall into two general classes: propellant (cased or uncased) and high explosive projectiles.

When a stack of mass-detonating ammunition, Quantity Distance Class 6 and 7[1*], is subjected to attack, and one round in the stack detonates, the detonation en masse of the entire stack may follow. Round-to-round damage is propagated by blast and fragmentation. The packaging material, if present, usually has little or no effect on either the extent or the rate of propagation of damage. Fortunately, however, high explosive (HE) projectiles are relatively insensitive to fragment or bullet impact. Tests at the Ballistic Research Laboratories[2] (BRL) and elsewhere, indicate that relatively high striking energies on a projectile wall are required to initiate a high order detonation which in turn is necessary before damage in the form of sympathetic detonations can be propagated to any adjacent projectiles.

In contrast, tests have been conducted and data[3,4,5] are available showing that solid propellants are quite vulnerable to fragment or bullet impact. Compared to HE projectiles, relatively low striking energies will ignite the propellant charge of conventional munitions, which in turn will ignite combustible packaging material, which suggests that such impacts are the most likely initial cause of serious fires.

These findings are at least partially confirmed by observations on actual ammunition dump fires in Southeast Asia. When ammunition stores came under attack, damage was usually propagated by burning packaging material and ammunition cook-off.** The extent of damage and the rate of propagation seemed related to the type of ammunition and the flammability of the packaging material. Some fires burned for days... hazardous for firefighters to approach because of the risk of high order detonations. Yet, detonations en masse seldom occurred.

Without a doubt, the ammunition dump vulnerability problem is complex. However, the above observations indicate that the hazards

---

*References can be found on Page 1086
**Cook-off is defined as the deflagration or detonation of ammunition caused by the absorption of heat from its environment.

associated with stacked, boxed artillery ammunition is most significant to the Army in terms of actual and potential losses.

Other than changes in the design of ammunition or changes in storage procedures, modifications of packaging to reduce its combustibility is the only means available for reducing losses. If non-combustible or fire retardant packaging materials could be employed to maintain the temperature of undamaged ammunition below cook-off temperature range, the damage within a stack could be limited to a small area with a significant reduction in overall losses. To evaluate the effectiveness of fire-retardant treatments in reducing the vulnerability of stacked ammunition, a series of tests was conducted. In these tests, stacks of both treated and untreated packing boxes of either 81mm Mortar, 90mm TP-T, or 105mm HE Semi-Fixed Ammunition were subjected to both small arms projectile and steel fragment impact. Fire-retardant treatments included: (1) painting the surfaces of the packing boxes with fire-retardant paints, (2) impregnating water solutions of chemicals into the wood boxes under pressure to reduce their flammability, (3) painting the exterior surface of fiber shipping containers with fire-retardant paint, and (4) replacing the fiber shipping containers with a fire-resistant kraft paper covered with aluminum foil. The effectiveness of these techniques were evaluated by contrasting test results.

II. SCOPE OF STUDY

The cost and time necessary to test the effectiveness of all types of possible vulnerability reduction techniques for all types of damage mechanisms is prohibitive and unnecessary. Testing the effectiveness of a technique, using one sample of a class of ammunition, can be used to provide information on the effectiveness of the technique for the whole class. If the damage mechanism used to evaluate the effectiveness of a successful vulnerability reduction technique is selected on the basis of its ability to maximize the probability of damage, then the effectiveness of the technique can be evaluated for other (less effective) damage mechanisms.

A. Packaging Material

The boxes used to package the ammunition, used in these tests, are constructed of either pine or spruce boards nailed together. They are of a double-end construction type with two vertical cleats on each end, three cleats, hinge and hasp hardware and either hemp or polyproplene rope handles. The individual rounds of ammunition are encased in treated cylindrical fiber containers and packed either two or three to a box. The materials used to package 81mm, 90mm and 105mm ammunition (wooden boxes and fiber containers) are similar to those used for packaging a wide variety of artillery ammunition (57mm-152mm). Any changes in the packaging materials, or their characteristics, that are successful in reducing the vulnerability of stacked 81mm, 90mm, and

1081

105mm ammunition, should also reduce the vulnerability of other ammunition in the same classes.

B. Propellant Hazard

When stacked ammunition is subjected to attack by fragmenting projectiles or small arms fire and the propellant charge in one or more rounds reacts (burns), then the combustible packaging material may be ignited. .The probability that a propellant fire will ignite the packaging material is related to the charge weights per round, the number of rounds that burn and the duration of the fire. The minimum amount of burning propellant required to consistently ignite a "standard wooden box" or fiber container is unknown. Nevertheless, tests conducted at BRL* in 1965 show that if the propellant charge in a single round of 90mm (nine pounds of M17 propellant) burns, both the fiber container and wooden box used for packaging that round will likely be ignited.

C. High Explosive Hazard

All types of explosively filled projectiles are vulnerable to combat induced damage. The level of response (High Order detonation, Low Order detonation or Burning) of a projectile to attack, and the probability of inducing a particular response are, in general, a function of the magnitude of the threat, projectile wall thickness and the sensitivity of the explosive filler. The more violent reactions can ignite propellant charges of any rounds adjacent to it which can, in turn, ignite the packaging material. Burning HE reactions can ignite the packaging material directly as a consequence of long duration burning.

D. Damage Mechanism

The selection of the damage mechanisms, used in this series of tests, was based on their ability to initiate packaging material fires as a consequence of propellant and explosive filler reactions. Additional requirements were that test-to-test impact parameters be reproducible and that the stack of target ammunition remain as intact as possible, i.e., limit the spread of ammunition about the target area as a result of attack or target ammunition response.

E. Other Related Tests

The effectiveness of fire-retardant paints in reducing the flammability of stacked wooden boxes (105mm) has been demonstrated in a series of tests conducted at Edgewood Arsenal[6]. The report on that work

---

Unpublished ad hoc data. Boxes of 90mm ammunition were subjected to impact by 120 grain steel fragments at 1700 mps.

concludes; "The fire hazard of preservative-treated packing boxes can be considerably reduced by applying an adequate thickness of fire-retardant paint coating to the exterior surfaces".

Since the Edgewood Arsenal tests used empty 105mm packing boxes and a propane burner ignition source, the tests do not adequately portray a "combat-damage" type situation. The effects of fragment/projectile impacts and blast will break up the wooden packing boxes and expose untreated surfaces. In this report, a fire-retardant treatment is evaluated under more realistic combat conditions.

III. APPROACH AND TEST PROCEDURES

To evaluate the effectiveness of new packaging techniques and materials, in reducing the vulnerability of stacked ammunition, a series of tests were conducted wherein stacks of 81mm mortar, 90mm TP-T and 105mm HE ammunition were subjected to projectile and fragment impact. Details of these tests are discussed in the following sections.

A. Preparation of Target Material

Standard wooden packing boxes containing either three rounds of fuzed 81mm mortar, two rounds of 90mm TP-T, or two rounds of 105mm HE semi-fixed ammunition were chemically treated to reduce their flammability. Treatments included either painting all surfaces with a fire-retardant paint or impregnating water solutions of chemicals into the wood under pressure. The fiber shipping containers were either painted with a fire-retardant paint or replaced by wrapping the ammunition in several layers of fire-resistant kraft paper and aluminum foil. Any combustible padding material found inside the box and the external carrying handles were removed. In addition, a limited number of tests were conducted to evaluate the effectiveness of fusible closing plugs for the 105mm HE-ammunition. These low melting point plugs were designed to induce a burning cook-off reaction in lieu of an explosive cook-off reaction.

B. Target Configuration

The cost of testing large stacks of ammunition (multiple pallet configurations) would be prohibitive. Stack sizes and configurations were selected (a single or modified pallet) to provide meaningful data economically and allow for both vertical and horizontal propagation of fire as it would occur in field storage.

C. Damage Mechanisms

A preliminary firing program, exploratory in nature, lead to the selection of the following mechanisms.

1. A caliber 0.50 API versus boxed 81mm mortar rounds. Impacts on the center of a projectile initiated burning HE reactions.

2. A 20mm API versus boxed 90mm TP-T rounds. Impacts on the cartridge cases produced long duration propellant fires.

3. Fragment sidespray from a detonating HE-filled projectile versus boxed 105mm HE ammunition. Multiple fragment impacts ignited the propellant charges in more than one round.

D. Test Procedures

Fires were initiated by subjecting the target ammunition to ballistic impact (see section 3 above). For the gunfire tests (81mm and 90mm), the gun-to-target distance was varied from 15 to 35 meters. All impacting projectiles were fired at service velocity. For the 105mm tests, the donar-to-target distance was 4 meters. Tests were scheduled on those days when wind velocities were low (0-16 km/hr) so that the influence of this parameter was negligible.

IV. RESULTS AND CONCLUSIONS

Detailed test data, in the form of Firing Records, will not be presented at this time. These data will be made available in a Ballistic Research Laboratories report when testing is completed.

However, the following conclusions have been reached, based on the test data now available.

a. Both the fire-retardant paint and impregnation treatment, of the wooden boxes, can be used to retard the rate at which fire propagates through a stack. This can extend cook-off times and reduce firefighting hazards.

b. Both surface paint and impregnation treatments will eventually fail if subjected to a high-temperature environment over a long period of time.

c. Impregnation treatments are more effective than surface paint treatments. Propellant and explosive-filler reactions can splinter wooden boxes and shred fiber containers, exposing untreated surfaces that can be ignited.

d. Treating wooden boxes and ignoring the fiber containers is a waste of time.

e. Undamaged boxes and fiber containers provide excellent thermal insulation.

f. Controlling the response of ammunition components, through design, can enhance the effectiveness of both treatments. That is, design ammunition components so that when they react to impact, they react violently. In most cases, burning HE and relatively long duration propellant fires are more hazardous than violent short duration reactions.

g. Both the treated and substitute fiber containers tested are unacceptable. Improved fiber containers, with built-in fire-retardant features, are under development.

h. The fusible plugs, used in the 105mm tests, have an unacceptable failure rate, i.e., explosive cook-off reactions were observed. A redesigned plug will be tested.

i. In general, the more effective a treatment, the greater the cost.

V. SUMMARY

The vulnerability problems associated with each type of ammunition are in many cases unique, and to address them on an individual basis is beyond the scope of this presentation. However, if solutions to these problems are to be realized, then a reordering of priorities will be required. That is, the survivability/safety characteristics of ammunition stores must be put in a more competitive position with other design objectives. The design of the ammunition and packaging must be developed jointly. This will require that a liaison, between designers, be maintained throughout the design/development cycle. From this liaison, trade-off's can be established which will provide a product that is both effective and reasonable in cost.

LIST OF REFERENCES

1. Department of the Army Technical Manual, "Care, Handling, Preservation, and Destruction of Ammunition," TM9-1300-206, November 1964.

2. H. J. Reeves, "An Empirically Based Analysis on the Response of HE Munitions to Impact by Steel Fragments (U)," Ballistic Research Laboratories Memorandum Report No. 2031, March 1970, CONFIDENTIAL.

3. "Vulnerability of Propellant-Filled Munitions to Impact by Steel Fragments," Ballistic Research Laboratories Contract Report No. 65, March 1972.

4. R. Schumacher, "Vulnerability Testing of Ammunition in a Structural Mock-Up of AH-56A (U)," Ballistic Research Laboratories Memorandum Report No. 1994, July 1969, CONFIDENTIAL.

5. H. J. Reeves, "Vulnerability of Small Caliber HE Ammunition to Projectile Impact (U)," U.S. Army Ballistic Research Laboratories Technical Note No. 1652, April 1967, CONFIDENTIAL.

6. N. Reich and L. Teitell, "Fire Tests of Preservative-Treated Wooden Packing Boxes Used For 155mm Ammunition," Edgewood Arsenal Technical Report No. 4365, April 1970.

PHYSICAL CHARACTERIZATION OF POWDERS:
IMPORTANCE TO THE PRODUCER AND USER OF HIGH ENERGETIC MATERIALS

Lowell D. Haws
Monsanto Research Corporation
Miamisburg, Ohio

For a given solid explosive, propellant, or pyrotechnic composition the majority of bulk handling and explosive performance characteristics are related to one or more physical properties characteristic of the finely divided state of that composition. Manufacturing process variables contribute in large measure to these particulate characteristics. These statements are illustrated pictorially in Figure 1 where the element "Process Variables" is seen to be the central one in the outward migration of cause and effect interfaces; i.e., the process variables in large part cause the resultant powder product to possess certain physical characteristics; the latter in turn influence the mechanical properties and/or the explosive performance. In scanning the literature on explosives it is this writer's impression that the element identified as "Particulate Physical Properties" receives too little attention and yet it interfaces with both the concerns of the manufacturer (Process Variables) and the user (Explosive Performance) of energetic powders whether they be explosives, propellants, or pyrotechnics; hence the analytical chemist or powder technologist responsible for characterizing the powder serves the very important role of <u>bridge scientist</u>. Each of the elements of this circle will be illustrated in turn beginning with "Process Variables". Later in the paper an attempt will be made to clarify some misconceptions concerning "particle size" analysis.

Most particulate explosives and single-base propellants are recrystallized after synthesis either to improve purity or to produce a product that is easier or safer to handle, or both. Entire books have been written on the subject of kinetics of nucleation and growth of crystals from solutions and melts and the resultant effect on particulate properties. Two excellent ones are A. E. Nielsen's book titled "The Kinetics of Precipitation"[1] and a more recent one by Randolph and Larson titled "Theory of Particulate Processes"[2]. The purpose of this paper is not to delve into the subject of crystallization but rather to make more visible the relation between an explosive powder's performance and the control of the variables affecting nucleation and growth. From a practical standpoint the physical characteristics of a precipitate are partially determined by the conditions prevailing at the time of formation. The influence of the factors shown in Figure 2, such as temperature, rate of mixing, concentration, etc., in the reaction environment are variables affecting particulate properties over which the manufacturer has some control; they can be understood by relating them to the supersaturation of the process system. In batch and steady state recrystallization systems at Mound Laboratory we strive to maintain control of each of these variables within 2% in order to eliminate lot-to-lot variability in physical characteristics of resulting products, hence ultimately in explosive performance.

Let's now jump immediately to the periphery of the "correlation circle" and discuss a few mechanical properties (see Figure 3) of powders that are especially important with energetic materials. Such jumps are commonly made in the real world anyway, i.e., from process specification to performance evaluation without much consideration of the physical characteristics. The ease with which a powder flows is related to the size distribution, particle shape, and surface area. The shear strength of a pressed compact is related among other things to the packing arrangement of the component particles which in turn is a complicated function of particle shape and size distribution. Pressure-density relationships of powders are affected by the particulate physical characteristics of the powder. In the propellants industry, shape distribution of the product powder is particularly important in dewetting phenomena.

With reference to explosive performance one can identify (see Figure 4) two characteristics that have been demonstrated as being related to the physical characteristics of the finely divided state - these are sensitivity and detonation velocity. A few samples of correlations made by various people are now cited. First, according to Eyring's grain burning theory, the time, τ, for complete reaction of a grain in a detonation is directly proportional to the grain or particle radius; i.e.,

$$\tau = \bar{r}g/k_r\lambda$$

where $\bar{r}_g$ = grain radius,

k_r = specific rate constant for one molecule, and

λ = V/S where

V = specific volume
S = effective cross-sectional area of the molecule.

Indeed Cook[3] and others have demonstrated the validity of this relationship with various explosives - pressed and cast. On the other hand, Malin and co-workers[4] at Los Alamos showed that the presence of a few large crystals in low density, sensitive explosives may lead to infinite diameter velocities greater than those characteristic of fine crystallized material. MacDougall et al.[5] have shown that in low density charges of ammonium picrate the opposite is found; namely, addition of a small percentage of coarse material to fine particles lowered the detonation velocity. Thus, the distribution of the sizes of particles in the product powder is seen to be very important. Another example somewhat related is the burning rate of propellants as a function of oxidizer particle size. This is illustrated in Figure 5 for the stoichiometric mixture of ammonium perchlorate and bitumen at various pressures from the data of N. N. Bakhman.[6] Several laboratories including Mound Laboratory have demonstrated that a rather smooth relationship exists between the <u>specific surface area</u> of an explosive powder and the explosion

time of that explosive initiated by an exploding wire. A generalized curve illustrating that relationship is shown in Figure 6 (solid line). Reference to this illustration will also be made later in this paper. The effect of particle size and initial density of pressed TNT charges on sensitivity to shock initiation was reported by Campbell and co-workers[7] using a wedge technique and smear camera records. Their data presented in Figure 7 suggest that at intermediate densities the particle size is more important - fine-grained TNT was more sensitive than coarse grained material - than is the density, whereas at densities approaching the limiting value, density becomes more important. Initiation behavior probably gradually changes from one of a heterogeneous explosive to that of a homogeneous one. On the other hand Dinegar and co-workers at Los Alamos, in a paper entitled "The Effect of Interstitial Gases on the Shock Sensitivity of Granular PETN",[8] described a special small-scale gap sensitivity test and showed that the shock sensitivity of PETN increased with a decrease in surface area - or in effect, with an _increase_ in coarseness of the particulates. This is illustrated in Figure 8; note that an increase in brass thickness corresponds to an increase in sensitivity. With reference to spark sensitivity the magnitude of electrostatic charge buildup normally increases with an increase in _specific surface_. An excellent discussion of the generation of electrostatic charge by powders

with emphasis on the potential hazards of sparks was presented at the International Conference on Powders in 1968.[9] No further comments are needed at a meeting of explosive experts on the undesirability of electrostatic charge buildup nor the difficult task involved in the experimental investigation of the electrostatic properties of explosives.

The point being made thus far in this paper is that except for liquid explosives and blasting gelatin, every explosive, solid propellant, and pyrotechnic composition in common use today is composed of material whose state of subdivision and properties associated therewith have a bearing on that material's handling and ultimate use properties, e.g., combustion and/or detonation properties. And yet the physical characteristics of the subdivided state are oftimes ignored, or in some cases the most appropriate particle characteristic is not even measured. Furthermore, as suggested in some of the examples, there appears to be much conflicting "evidence" relating some physical characteristic of the finely divided state to explosive performance characteristics. Some of this dichotomy is probably real; however, in many instances this author feels that much of the contradiction is founded in the confusion surrounding the interpretation of powder characterization data. In subsequent discussions, Particulate Physical Properties suggested in Figure 1 will refer to dimensional and geometric attributes of the finely divided state.

Even today some people suffer from the impression that all that is required for complete physical characterization of a powder is a set of sieves. Determining the size distribution through sieve analysis many times may provide irrelevant cr inadequate information. It cannot be overstressed that it is _all_ of the relevant characteristics of the product powder that the user should seek to know. Unfortunately powder characterization is a complex technology. We are in trouble at the start in attempting to reach commonality even in our definitions of the size of three-dimensional macroscopec objects let alone microscopic species in one-dimensional terms. There is no single classification that meets all purposes. Describing particles or particle size is an effort somewhat analagous to that of the three blind men who were told to describe an elephant with one touch: one grabbed the tail, another the trunk, and another felt the side of the elephant - obviously they all reported different things. The same is true of particles; many people measure different dimensional attributes but wind up calling them all "particle size" without elaboration as to how the results were obtained. This is one possible reason that different investigators draw different conclusions in correlating powder performance with particle "size".

A simple thought-provoking exercise focusing on the complexity of the definition of size is hopefully afforded by the following example: If the question arose as to which of the two "bricks"

illustrated in Figure 9 was larger, how would you respond? The answer obviously depends on the criterion laid down. For instance, if the bricks are to be used as edging for a path, the dimension that matters is the overall length; the width of the brick is essentially unimportant. If, on the other hand, the bricks are to be laid flat to form a pillar, then the height of the brick is the most relevant feature. The volume or weight of the top brick in Figure 9 is also greater than that of the bottom one, but the solid diagonal is less. Obviously the parameter to be used depends on the purposes for which the brick is intended. All too often the analytical chemist or powder technologist is asked to determine the particle size of a powder sample without further elaboration as to what dimensional characteristic is being sought or the intended use of the information. There are many methods with varying degrees of sophistication for measuring particle size or size distribution. The analyst can expect a high degree of accuracy and precision with each of these methods for powders comprised of particles that are hard, smooth, non-friable spheres. Unfortunately not many real-world powders, especially explosives, exhibit these attributes, and the problems begin to mount resulting in as many particle size distributions for a single powder as there are methods to measure them. Not the least of these problems is the degree of dispersion of the powder itself. Should one measure some characteristic property of the individual or ultimate particle? Or is the

performance parameter rather a function of the size of the aggregates of individual particles or agglomerates? Examples of particles in various states of aggregation are illustrated in Figure 10. In answer to the last query, one should make measurements if at all possible on that state of aggregation in which the powder finds itself during performance testing.

Let us now look at some of the powder particulate physical characteristics that are helpful in differentiating one powder population from another of the same composition. One classification that this author finds helpful is shown in Figure 11. The physical features of a particle are either readily measurable or are recognizable but not readily measurable - analogous in some respects to quantitative and qualitative chemical analysis. In many instances the manufacturer and user of the powder product is reluctant to make inquiries concerning these recognitive characteristics because numbers are not often associated with particle shape and surface morphology; yet these may be as important or even more relevant in correlating performance properties as the more quantitative characteristics. For example, the electrostatic sensitivity of needle-shaped PETN may be different from that of fat hexagonal-shaped species of similar length.

The remaining comments are restricted primarily to evaluations of surface area and recognitive properties; particle size distribution measuring techniques are discussed at length in several books.[10]

Some of the methods used for determining surface area are useful for measuring exterior surfaces, whereas others indicate the totality of surface area available for the support of a single layer of gas molecules. Thus, as with particle size, the proper definition depends on the kind of surface area with which we ourselves wish to contend. As illustrated in the cross-sections of particles in Figure 12, not all materials nor all particles of a specific material are alike with regard to either their external or their internal surface structure. A single pure crystal grown slowly from solution or a melt normally has flat impervious surfaces, this is usually not the case however with shock crystallized powders. An aggregate of crystals may or may not permit a gas to diffuse through the layers in contact with each other.

A classification of surface area measurement techniques is shown in Figure 13. The most common techniques used employ either the principles of adsorption or fluid flow; the latter (designated as permeametry) normally provides a measure of external surfaces, whereas adsorption techniques provide a means of measuring the total surface - internal as well as external. Therefore, surface area values of powders

determined via permeametric techniques are usually considerably lower than those determined by adsorption, especially for particles containing microcapillary connections to the interior.

As suggested earlier, certain measurement methods are more appropriate than others for determining a specific powder characteristic. The correlation that follows serves as an example. Previously (see Figure 6), mention was made that the explosion time of an explosive pressed in an exploding bridgewire detonator is readily predicted from the permeametrically measured specific surface; predictions of explosion time based upon B.E.T. (adsorption) surface area measurements are tenuous. And yet adsorption techniques are based on reasonably solid theoretical grounds, whereas permeametry has no sophisticated theory to "justify" its use as a surface area measuring technique. Why then the better correlation with permeametry? The reason presumably lies in the fact that the method for determining surface area (permeametry in this case) is more closely related to the conditions existing during performance testing. i.e., propagation of a shock wave through a similar density compact of explosive material. Most of the powders we deal with are friable, and therefore measurement of the surface area of the bulk powder via B.E.T. methods, for example, provides little meaningful information whereas correlation of results obtained in a compacted state are appropriate.

Returning now to the recognitive characteristics, examples can readily be found where high energy powders of identical chemical composition and purity and of similar measured specific surface and particle "size" had different explosive performance characteristics. Sometimes, a clue to such differences can be gleaned simply by peering through an optical microscope or preferably a scanning electron microscope to make an assessment of the particle shape distribution and surface morphologies. Examples of PETN crystals with similar average sieve size made by small variations in the recrystallization process are shown in Figure 14.

The burning surface of an explosive, propellant, or pyrotechnic powder is a complex region of activity involving many chemical and physical processes which relate to product performance. Because various chemical and physical conditions (see Figure 15 for example) alter the surfaces of many explosive powders, a detailed evaluation of the recognitive characteristics of the particles comprising the explosive product is necessary in order to better appreciate the nature and magnitude of such changes. Recall a previous illustration (dotted curve of Figure 6) showing the effect of heating on the surface area of certain high explosive materials. A combination of such quantitative data with visual evidence such as presented in Figure 16 provides one with a more comfortable feeling in making

interpretations concerning the mechanism of surface alteration.
Notice the annealing effects to the PETN caused by the thermal
environment. In addition to surface annealing, particle disinte-
gration caused by decomposition of certain metal perchlorate complex
explosives have also been followed with the aid of SEM photomicro-
graphs.

Particle shape is also important in the solid propellants industry
as well. Summerfield and Parker[11] point out that some of the
parameters needed for a complete description of propellants are
seldom reported. Included among these is particle shape distri-
bution which is particularly important in the question of dewetting
and of microscopic flame structure.

In summary, an attempt was made in this paper to make visible some
of the inconsistancies in the literature with regard to correlation
of explosive propellant and pyrotechnic performance characteristics
with physical properties such as particle "size". It should be
re-emphasized that some of these inconsistancies and reversals are
probably real. However, a plea is made for more complete physical
characterization or at least critical evaluation of the appropriate-
ness of the methods employed in order to increase our knowledge in
the following areas: (1) the nature of sensitivity of high energetic
powder to various types of stimuli, (2) the various performance

effects based on rates of combustion and/or detonation, and (3) the nature of effects of manufacturing process variations on product performance.

REFERENCES

1. A. E. Nielsen, "The Kinetics of Precipitation" (The Macmillan Company, New York, 1964).

2. A. D. Randolph and M. A. Larson, "Theory of Particulate Processes" (Academic Press, New York, 1971).

3. M. A. Cook, "The Science of High Explosives" (Reinhold Publishing Corporation, New York, 1958) especially Chapter 6.

4. M. E. Malin, A. W. Campbell and C. W. Mantz, $\underline{J}$. $\underline{Appl}$. $\underline{Phys}$. $\underline{28}$, 63 (1957).

5. MacDougall et al. - see $\underline{Chem}$. $\underline{Rev}$. 45, 69 (1949).

6. N. N. Bakhman, $\underline{Combustion\ and\ Flame}$, $\underline{17}$, 383 (1971).

7. A. W. Campbell, et al., $\underline{The\ Physics\ of\ Fluids}$, $\underline{4}$, 511 (1961).

8. R. H. Dinegar, et al., "The Effect of Interstitial Gases on the Shock Sensitivity of Granular PETN," LA-5036, October, 1972.

9. H. F. Eden (Arthur D. Little, Inc.), "Aspects of Electrostatic Charging of Powders," presented at International Conference on Powders, Chicago, 1968.

10. R. R. Irani and C. F. Callis, "Particle Size: Measurement, Interpretation, and Application" (John Wiley and Sons, New York, 1963); C. Orr, Jr., and J. M. Dallavalle, "Fine Particle Measurement" (The Macmillan Company, New York, 1960); R. D. Cadle, "Particle Size" (Reinhold Publishing Corp., New York, 1965).

11. M. Summerfield and K. H. Parker, "Interrelations Between Combustion Phenomena and Mechanical Properties in Solid Propellant Rocket Motors," in "Mechanics and Chemistry of Solid Propellants" ed. by A. C. Eringen, et al. (Pergamon Press, London, 1967).

FIGURE 1
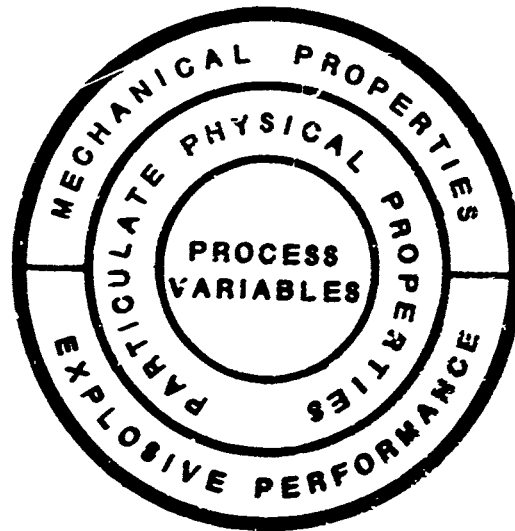
CORRELATION DIAGRAM

FIGURE 2

PROCESS VARIABLES

- CHEMICAL COMPOSITION OF "REACTANTS"

- TEMPERATURES

- CONCENTRATIONS

- RATES OF ADDITION (FOR BATCHWISE PROCESSES)

- AGITATOR DESIGN AND SPEED

- SOLUBLE ADMIXTURES

FIGURE 3

MECHANICAL PROPERTIES

- FLOWABILITY
- SHEAR STRENGTH
- COMPACTION CHARACTERISTICS
- DISFERSIBILITY

FIGURE 4

EXPLOSIVE PERFORMANCE

- SENSITIVITY

  - SHOCK
  - IMPACT
  - ELECTROSTATIC
  - FRICTION

- DETONATION VELOCITY

FIGURE 5

BURNING RATE AS A FUNCTION OF PARTICLE SIZE FOR STOICHIOMETRIC MIXTURE AP + BITUMEN AT VARIOUS PRESSURES
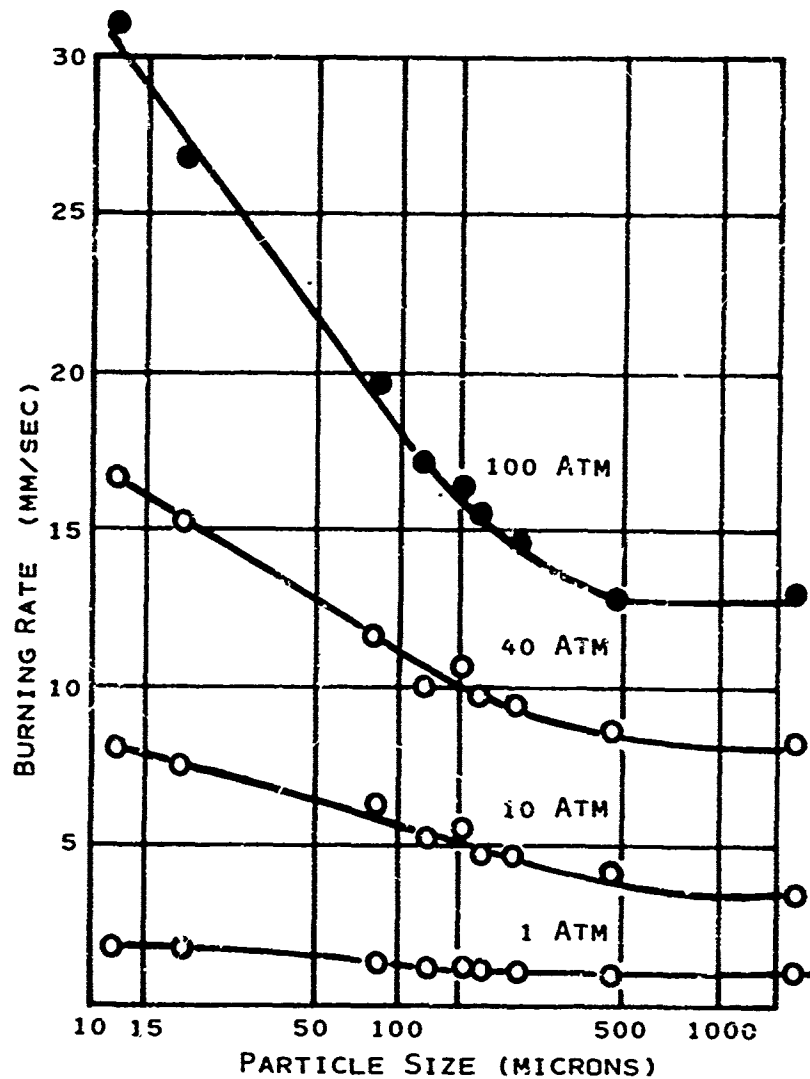
FIGURE 6

EXPLOSIVE POWDER SURFACE AREA EFFECTS
(GENERALIZED)
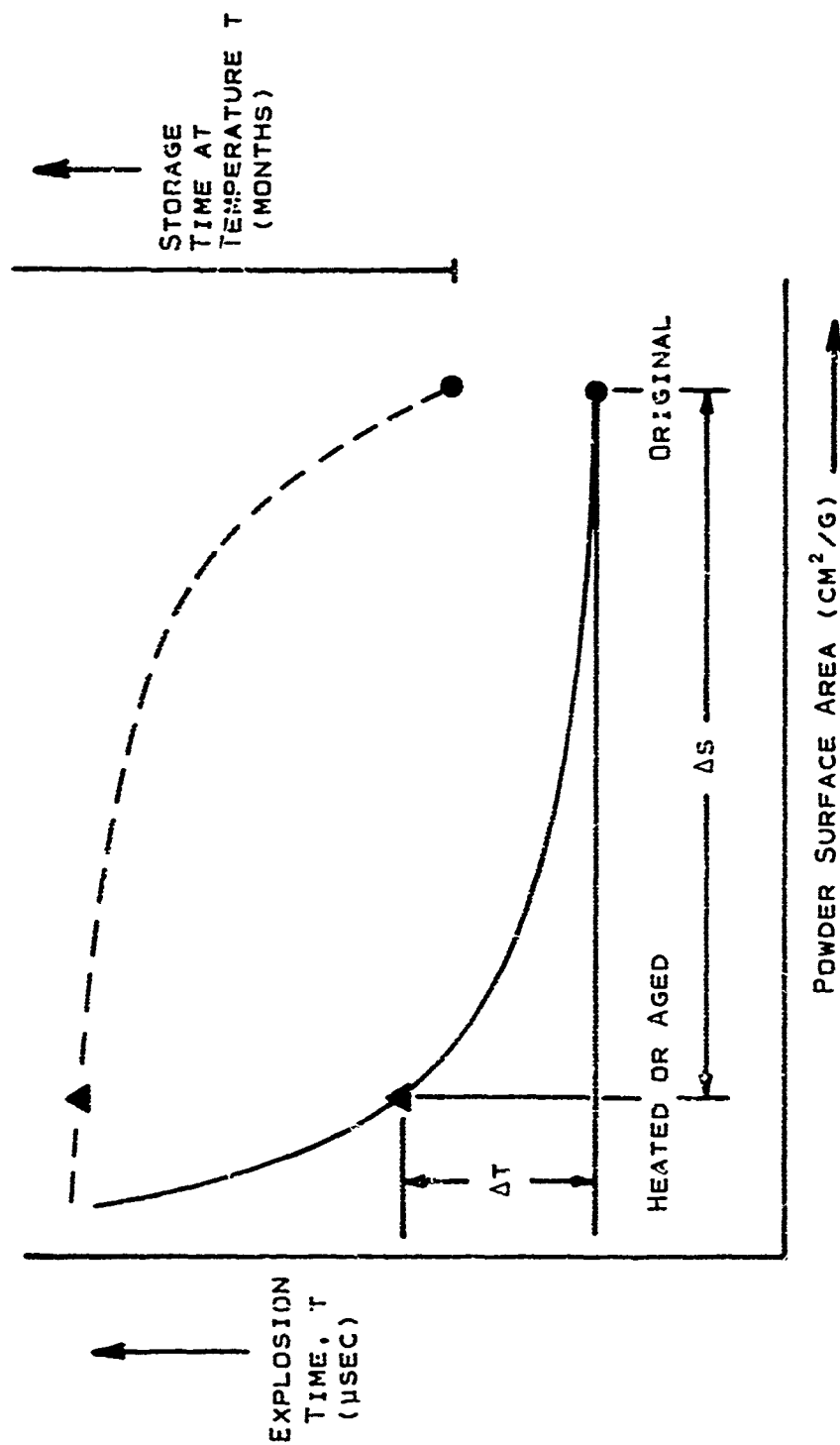
FIGURE 7

EFFECTS OF INITIAL DENSITY AND PARTICLE
SIZE ON THE SENSITIVITY OF PRESSED
TNT CHARGES
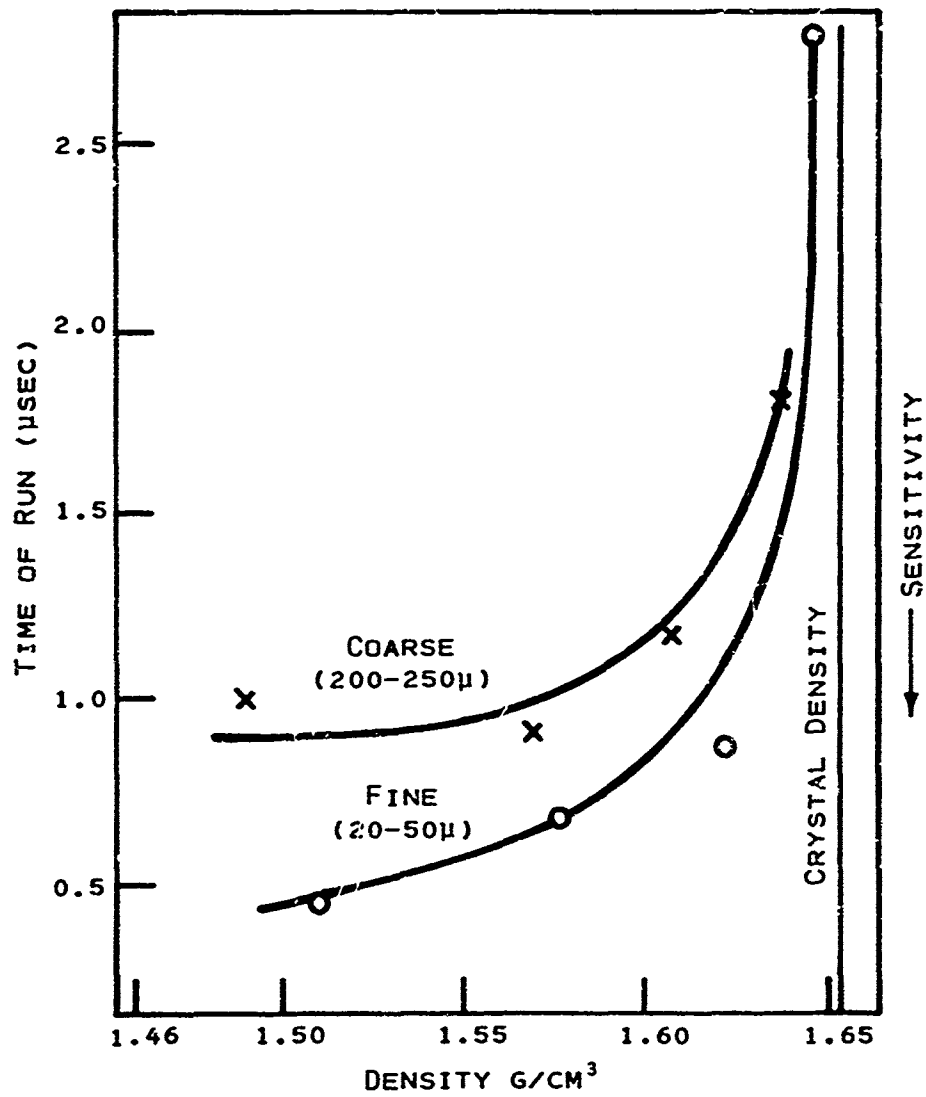
FIGURE 8

EFFECT OF PETN SURFACE AREA
AND OXYGEN CONTENT ON
SMALL-SCALE GAP-TEST SENSITIVITY
TOTAL GAS PRESSURE = 500 PSIG.

O PETN SPECIFIC SURFACE = 3300 CM^2/G
● PETN SPECIFIC SURFACE = 15000 CM^2/G

AIR VALUES

BRASS ATTENUATOR THICKNESS IN INCHES (T.5)

PERCENT O_2 IN O_2/N_2
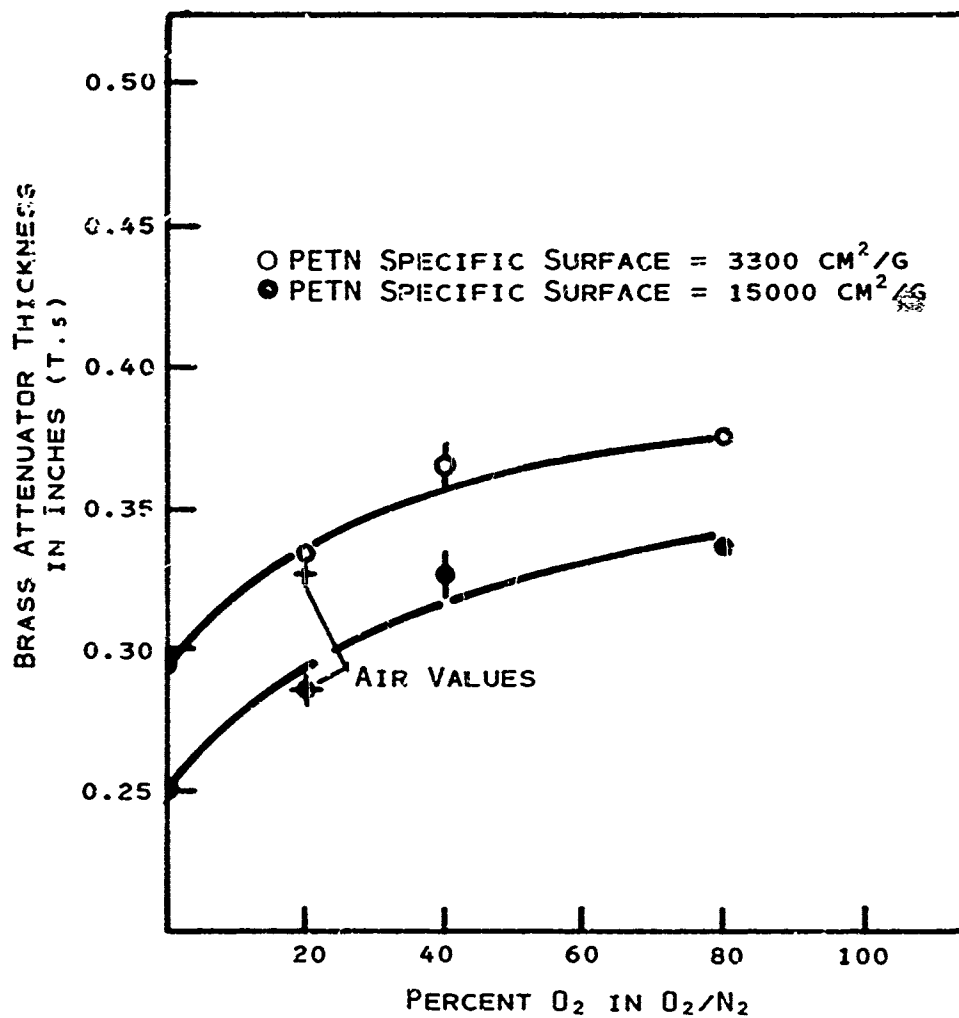
FIGURE 9

WHICH IS LARGER?
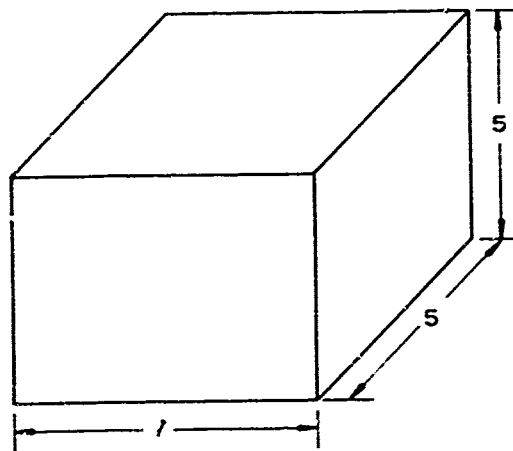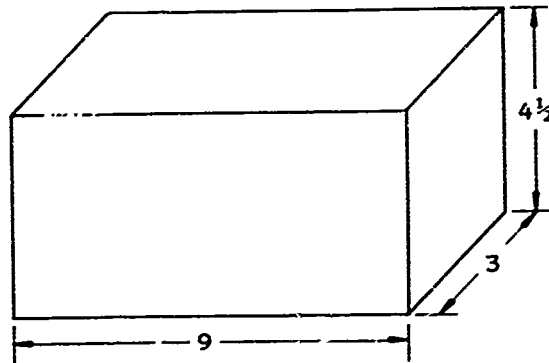
FIGURE 10

DEFINITIONS   EXAMPLES

INDIVIDUAL OR
PRIMARY PARTICLE

AGGREGATE

AGGLOMERATE

1111

FIGURE 11

PARTICULATE PHYSICAL PROPERTIES

MEASUREABLE

- PARTICLE SIZE (AVERAGE)
- PARTICLE SIZE DISTRIBUTION
- SURFACE AREA
- PORE VOLUME

RECOGNITIVE

- PARTICLE SHAPE
- SURFACE MORPHOLOGY

FIGURE 12

CROSS SECTIONS OF PARTICLES
EXHIBITING VARIOUS STRUCTURES
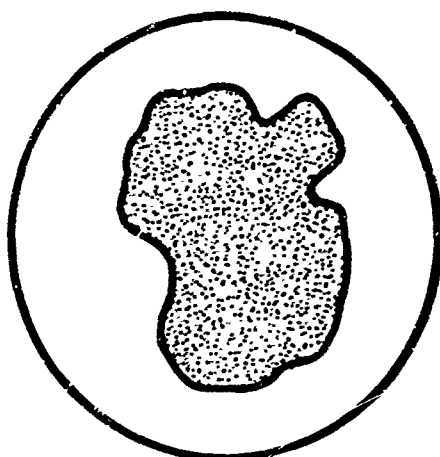
No INTERIOR CONNECTIONS
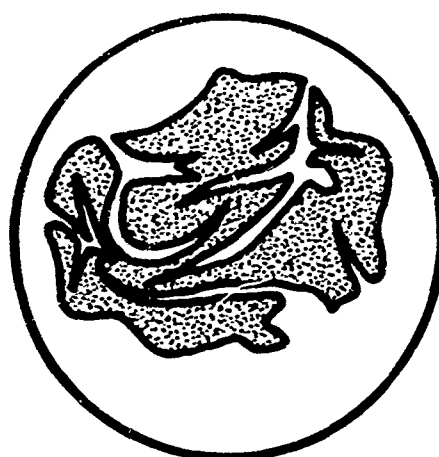
MICROCAPILLARY CONNECTIONS
TO THE INTERIOR
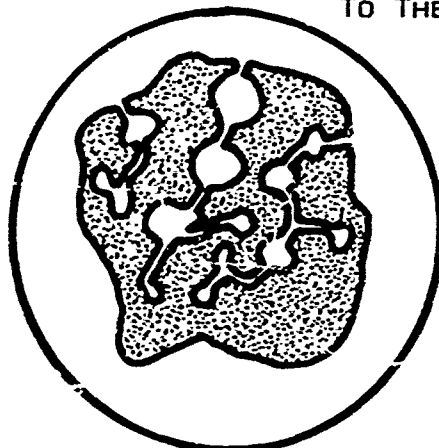
INTERIOR PORES AND INTERCONNECTING
MICROCAPILLARIES

FIGURE 13

MEASUREMENT OF SURFACE

● PERMEABILITY OF FLUID FLOW:

    LIQUID FLOW
    GAS FLOW

● ADSORPTION:

    STATIC
    DYNAMIC

● ABSORPTION OF RADIATION

● OPTICAL MEASUREMENT

● HG INTRUSION POROSIMETRY

FIGURE 14

MORPHOLOGICAL FEATURES OF SELECTED
PETN BATCHES
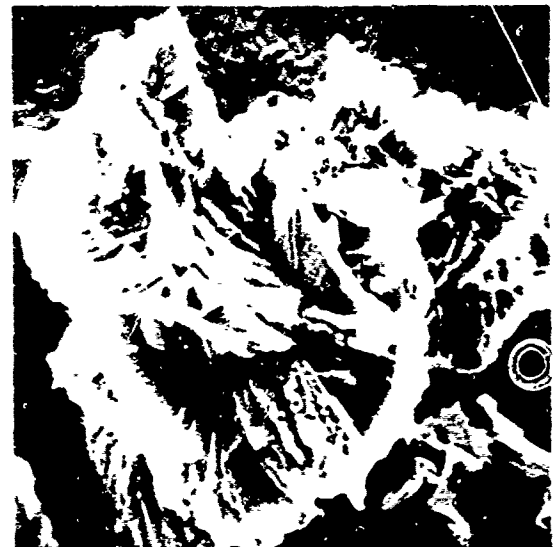
FIGURE 15

CONDITIONS AFFECTING
EXPLOSIVE PARTICULATE SURFACES

1. PROCESS VARIABLES

2. HEAT (THERMAL)

3. ADDITIVES (CHEMICAL)

4. COMPACTION (MECHANICAL)

FIGURE 16

SEM PHOTOMICROGRAPHS
ILLUSTRATING THERMAL EFFECTS ON PETN MORPHOLOGY
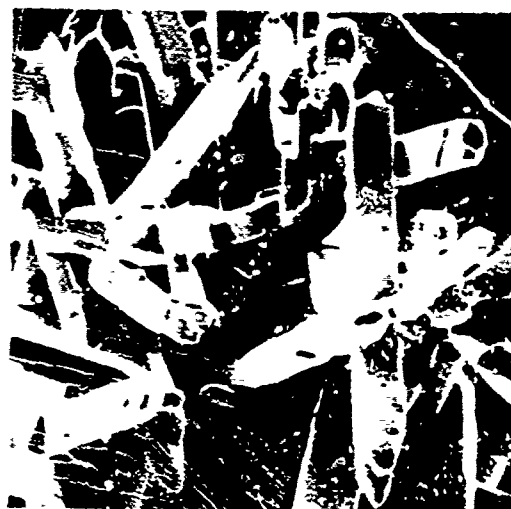
UNHEATED |◄———►| HEATED 1 DAY AT 97°C

10µM

THE NEED FOR REVISION OF TB 700-2

(Explosives Hazard Classification Procedures)

Dr. Billings Brown
Hercules Incorporated, Magna, Utah

ABSTRACT

The subject Procedures is in need of further revision. The current edition applies only to storage of explosives and solid propellants. Its scope should be broadened to include all military explosive materials in all life cycle environments. The current edition is preoccupied with detonations. The revision should include all explosive hazards such as fragments and firebrands as well as blast. Some tests in the current revision are not applicable to all materials. These tests should be updated. The current edition often leads to misclassification. To remedy this fault, new tests and a modified test interpretation are proposed. End item classification should be delayed until full scale tests have been performed. The DODESB is urged to solicit suggestions from appropriate experts and begin work on the revision.

INTRODUCTION

The subject Explosives Classification Procedures (TB 700-2) is in need of revision. The objective is to develop a procedure which will enable us to establish the Q/D classification for all explosive materials in each of their several life cycle environments.

Revisions were made in 1959, 1962 and 1967. I will discuss very briefly why another revision is necessary and what needs to be accomplished.

This paper is presented at the request of DODESB. This does not in any way imply DODESB endorsement of the contents. The ideas presented herein were collected from the Services, NASA, DOT, and Contractors. The assistance of the various contributors is acknowledged.

WHY IS A REVISION NEEDED?

Four reasons are immediately apparent.

1. The current procedures applies only to the storage environments.

2. Continuing trends toward novel and higher energy propel'ants and explosives makes it imperative that the hazards classification procedure change to keep pace with these developments.

Preceding page blank

3. Some of the specified tests do not apply to all of the explosive materials of current interest. Two examples are pyrotechnics and slurry blasting agents.

4. Many explosive materials are currently misclassified. Some materials are precluded from use in weapons systems not because they are unmanageably hazardous, but rather because they are misclassified as hazardous by the current Procedures. An example of this overclassification is an aluminum hydride fueled solid propellant which exhibited extreme sensitivity in the currently accepted impact test but which, when scaled up, remained intact through a 32 foot drop test (Figure 1).

Other materials are classified as harmless by these Procedures when they should not be. One example is composite solid propellant which is represented as being Class 2 (Fire Hazard) when in fact large motors containing it explode upon impact (Figure 2). Another example is gelled slurry blasting agent which is Class 2 in the small tests but which cooks off to a detonation in a large scale bonfire test.

Thus, revision of the subject Procedures is necessary.

WHAT NEEDS TO BE DONE?

Four things. Let me list them first, then discuss each in more detail.

First, we need to extend the scope of the Procedure in three different directions. Second, we need to revise the application and interpretation of some tests. Third, we need to add some tests. Fourth, we need to revise the classification scheme.

EXTEND THE SCOPE

The scope must be extended in three different dimensions to apply to all types of hazard from all types of potentially explosive material in all their life cycle environments.

1. The present Procedure applies only to storage. Although it states "data is required in order to determine that these compositions are safe to handle, transport, and store" in fact none of the specified tests will ensure safety during transportation or handling. The Procedure should be revised to be equally applicable during concept formulation, contract definition, development, testing, production, shipment, operation and disposal.

Manufacture should be included because the military is ultimately responsible for paying the bill should an incident occur. Further, if DOD shirks the responsibility for production, DOL (OSHA) will certainly move in and assume the authority to protect the manufacturing personnel.

1120

End use of an item should also be included because DOD is responsible if a shell explodes prematurely or an initiating device fails or an errant rocket falls into a suburb after launch.

2.   The current Procedure determines "the reaction of ammunition, explosives, and solid propellants". The scope should be extended to include all military potentially explosive materials. Certainly pyrotechnics should be included. Certainly slurry blasting agents should be included. Perhaps initiating devices should be included, and certainly so if they contain primary explosives. Perhaps liquid propellants should be considered at this time, as they are being developed for use in guns.

3.   The present Procedure is preoccupied with the results of a detonation. The scope must be extended to recognize all hazards due to an explosion. Fragments and firebrands which are propelled to great distances by an explosion are ignored.

TEST CONSTRAINTS

Tests must be made on a scale that provides meaningful information from which a decision can be made. The Procedure claims that "The sample weights or dimensions listed are the minimum upon which conclusions may be drawn;". However, I do not get a warm, secure feeling when the sample weight used in the only impact type test is only 10 mg.

It is certainly true that at least the initial screening tests must be on a sufficiently small scale so that even the smallest manufacturer can perform them in his facility. The next scale of testing must be small enough so that samples can be shipped legally between laboratories.

But large weapon systems call for large decisions, and large decisions ought to have the benefit of being reached based on large scale tests. The revised procedure should reinstitute the four phases of testing stated in the 1962 edition. The scale of testing in each phase should match the corresponding scale of weapon development. Laboratory tests should precede preliminary development. Subscale tests should precede engineering development. Full scale tests should precede production. Tests employing a pallet load or a truckload or a boxcar full of items (as appropriate) must precede deployment.

It would be preferable if results from all tests were scaleable. Then, as experience provided assurance, large scale tests could be minimized.

Tests must simulate all the credible initiating stimuli to be found in the several life cycle environments. These external stimuli can be summarized into about five types. Impact, friction, shock, electrostatic and thermal. Then you can look at the details: How hard, how long, how hot, how much.

TEST REVISION

Many tests now specified in the Procedure need to be changed in order to make them relevant to the life cycle environments seen by an explosive or propellant. Some recently developed tests need to be added. To list all the specific problems would require too much time. One example is the requirement in several tests to provide a 2-inch cube. But how do you proceed when testing a powder such as smokeless powder or a pyrotechnic, or a soft gel such as a slurry blasting agent? Another example concerns the Bureau of Mines Impact machine. Hercules has had to make 12 major changes to the design of this machine in order to achieve adequate repeatability. Has everybody made the _same_ changes? As a third example, the thermal stability test could easily double as a materials compatibility test, if the explosive cube was heated in contact with the material which would ultimately contain the explosive, in the weapon system.

OLD TESTS REVISITED

Some relevant tests which were specified in earlier editions of the Procedures should be reinstituted. The bullet impact test is becoming important again as sportsmen take aim on trucks hauling rocket motors. The critical diameter test is important in determining on what scale a shock initiation test must be conducted in order to be of any value.

NEW TESTS

Several small scale tests have been developed in recent years which give results relevant to the various life cycle environments. Dr. Donna Price at NOL has reported on a practical confined burning test or closed pipe test designed to simulate in small scale the confinement of a large mass of explosive. Impact type tests which appear to scale up include the flying plate impact test developed at IITRI, the Susan test developed at Lawrence Livermore Laboratories and the shotgun test developed at Hercules.

These and other tests should be critically evaluated for relevance, scaleability and wide ranging applicability, and the best tests incorporated into the Procedures revision.

CLASSIFICATION SCHEME REVISION

We should make the U. S. military classification consistent and compatible with other schemes. The U. N. is currently meditating on a hazards classification scheme, concerned primarily with transportation. The U. N. scheme offers only _one_ classification for explosives. Therefore, I want to define an explosion as any event causing damage at a distance, and an explosive as any material potentially able to cause damage at a distance, whether from blast, fragments or firebrands. The U. N. calls this last hazard (firebrands) a "superfire" hazard.

Chapter 3 of the current Procedures, dealing with bulk compositions, has a section on Interpretation of Results which enables conversion of test results into a classification. Neither Chapter 4, dealing with end items of ammunition and explosives, nor Chapter 5, dealing with solid propellant rocket motors, have Interpretation sections. Chapter 5 designates rocket motors as Class 2 or Class 7 before performing the tests, based on behavior of the propellant in Chapter 3.

Needed is an Interpretation of Results scheme which will properly assess the hazard of the full scale item. What I propose is a classification based on probability and severity, as is at least implied by the requirements of MIL-STD-882.

Diagraming the Interpretation of Results section in Chapter 3 of the Procedures (Figure 3) helps to emphasize the need for revision. First, the BuEx impact test, which currently gives the only indication of a transportation hazard, uses only a 10 mg sample. Impact results are considered separately from other test results. Second, the No. 8 Cap test and NOL Card Gap test are redundant. No matter what the results of the Cap test, we are directed to proceed to the Card Gap test. Third, no data on explosions or subdetonation reactions are obtained. The incorrect conclusion is reached by implication that if a detonation is not recorded, the material is safe to handle. This conclusion is false.

On a positive note, there are two examples of combining test results to reach a decision on classification. To be Military Class 2, a material must pass the Thermal Stability test AND the Ignition test AND the Card Gap test.

The suggested revised classification scheme is diagramed next (Figure 4) and is shown divided into Phase I and Phase II. These phases deal with bulk materials. Phases III and IV are concerned with the assembled weapons and are omitted here for brevity.

Phase I is performed at the inventor's facility and testing is simple but adequate to assign a DOT classification for shipping samples to other facilities for further testing. The No. 8 Cap test (0.70 g) would be replaced by a Type A Cap (0.05 g), since we need to know only whether the material is hypersensitive to shock.

Phase II tests larger samples. The Confined Burning test substitutes the confinement of a steel pipe for the self-confinement of a large sample. The U. S. BuMines Impact test would be modified to use a 1/4 inch thick sample. This larger size is chosen to minimize effects of nonhomogeneous samples. It has also been tentatively established that results from relatively thick samples tested in this apparatus will scaleup to predict results in one-lbm size impact tests such as the Flying Plate and Susan tests.

Samples of certain sensitive materials are entirely consumed in this impact test, indicating propagation is occurring in this small test size. This should provide cause to proceed only with utmost caution.

The NOL Card Gap test would be modified to determine reaction velocity and to provide information on fragments and firebrands.

All of the Phase II tests are arranged in an AND sequence. Final classification depends on the result of the Subscale Impact test, emphasizing the importance of the handling and transportation environments.

Assignment of a classification should be made only after Phase IV, full scale testing is complete.
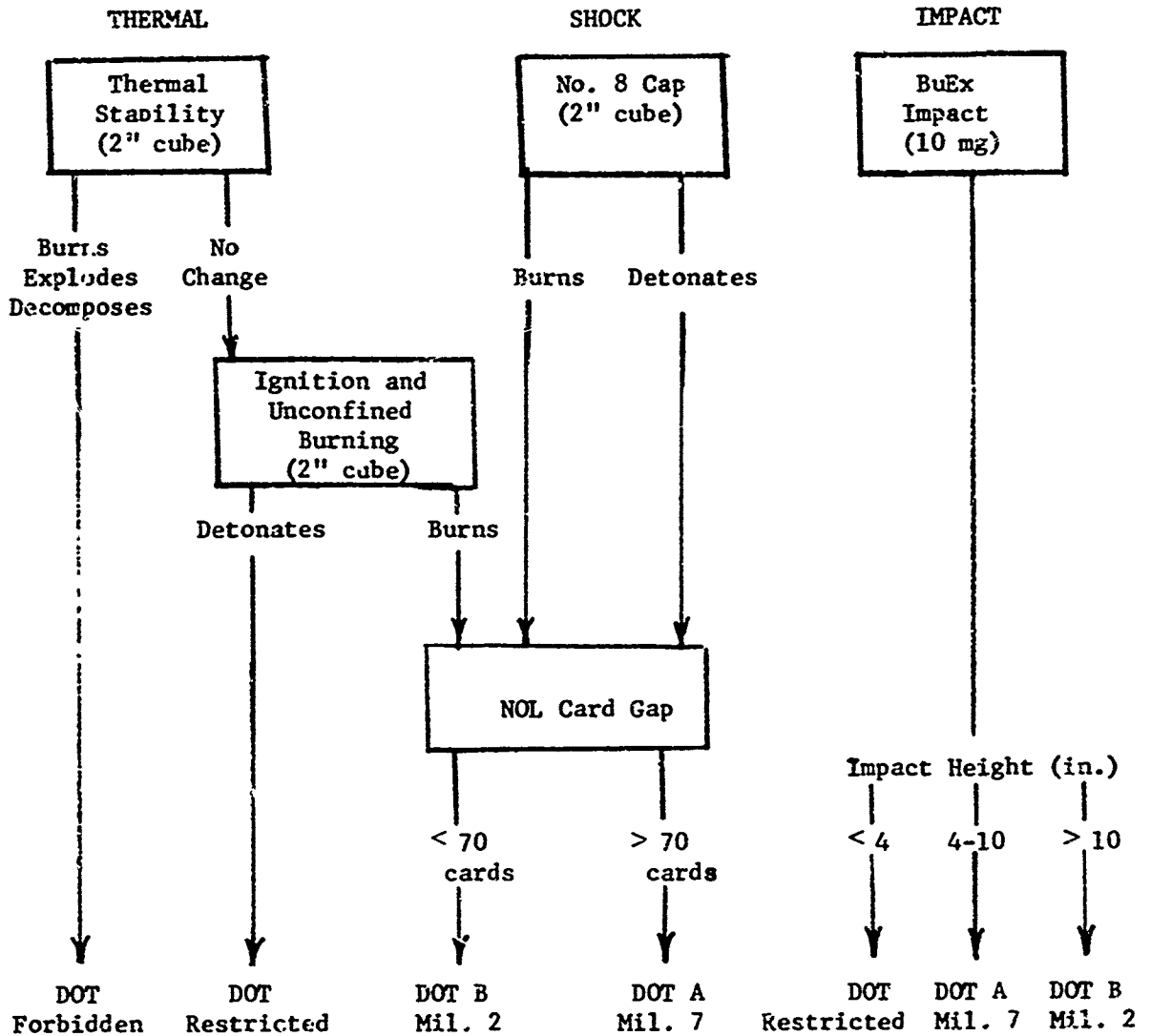
CONCLUSIONS

The current edition of the Explosives Hazard Classification Procedures is again in need of revision because:

1. Its limited scope should be extended to cover more environments.

2. Tests relevant to the environmental stimuli should be added.

3. The hazard classification resulting from application of the Procedures must be correct for all explosives materials in all life cycle environments. The classification scheme as a practical matter must fit within the U. N. scheme, and be modified to fully cover the explosives industry in the U. S. as it relates to military propellants, explosives and pyrotechnics.

RECOMMENDATIONS

1. The DODESB should begin immediately to expedite a major revision on the Procedures.

2. The DODESB should invite comments and suggestions from experts, including the JANNAF Hazards Evaluation Committee and the various Service consultants as appropriate.

3. The DODESB should demonstrate that hazards tests are relevant to the environment and applicable to all military explosive materials.
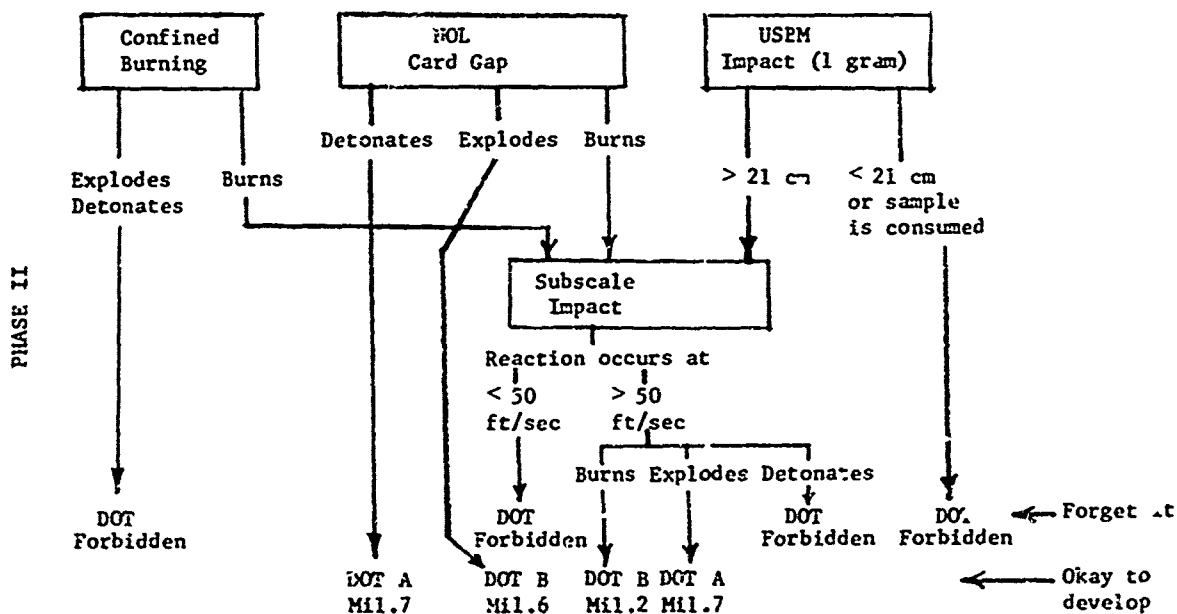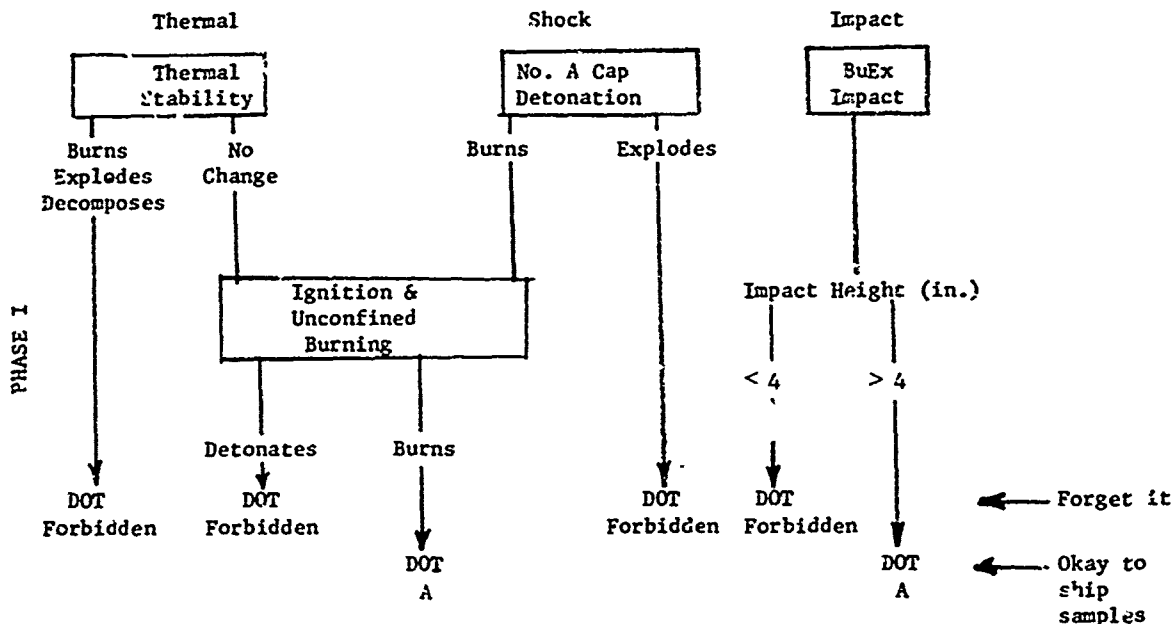
CURRENT BULK COMPOSITION TEST INTERPRETATION SCHEME
(1967 Revision of Procedure)

THERMAL | SHOCK | IMPACT

Thermal Stability (2" cube)

No. 8 Cap (2" cube)

BuEx Impact (10 mg)

Burns Explodes Decomposes | No Change

Burns | Detonates

Ignition and Unconfined Burning (2" cube)

Detonates | Burns

NOL Card Gap

< 70 cards | > 70 cards

Impact Height (in.)

< 4 | 4-10 | > 10

DOT Forbidden | DOT Restricted | DOT B Mil. 2 | DOT A Mil. 7 | DOT Restricted | DOT A Mil. 7 | DOT B Mil. 2

NOTE THAT:

- Transportation and handling (impact) safety is based on results of testing 10 mg sample only

- No fragment or firebrand data are obtained

1125

SUGGESTED REVISED CLASSIFICATION SCHEME

PHASE I

Thermal

Thermal Stability

Burns Explodes Decomposes

No Change

Ignition & Unconfined Burning

DOT Forbidden

Detonates

DOT Forbidden

Burns

DOT A

Shock

No. A Cap Detonation

Burns

Explodes

DOT Forbidden

Impact

BuEx Impact

Impact Height (in.)

< 4

> 4

DOT Forbidden

DOT A

◄— Forget it

◄— Okay to ship samples

PHASE II

Confined Burning

Explodes Detonates

Burns

DOT Forbidden

HOL Card Gap

Detonates Explodes Burns

USBM Impact (1 gram)

> 21 cm

< 21 cm or sample is consumed

Subscale Impact

Reaction occurs at

< 50 ft/sec

> 50 ft/sec

Burns Explodes Detonates

DOT Forbidden

DOT Forbidden

DOT Forbidden

◄— Forget it

DOT A Mil.7

DOT B Mil.6

DOT B Mil.2

DOT A Mil.7

◄— Okay to develop

1126

EFFECT OF EARTH COVER ON FAR-FIELD
FRAGMENT DISTRIBUTIONS*

L. E. Fugelso
C. E. Rathmann
General American Research Division
General American Transportation Corporation

Abstract

The effect of earth cover on the far-field fragment density expected
from the accidental detonation of stored munitions was estimated by
preparing three models of fragment-cover interaction. Comparison of the
theoretical calculations with limited experimental data show that the
model wherein the crown of the earth cover does not retard any fragments
gives the best agreement. Models for fragment-fragment interaction which
effectively account for stack configuration lead to a simplified model
for the effective number of munitions contributing to the far-field frag-
ment density. Parametric studies of the effect of altered mass distribu-
tions and fragment shape were conducted to assess possible differences
between accidental detonation source parameters and arena data source
parameters. Tentative quantity-distance relationships for the fragment
hazard were prepared.

Introduction

Munitions, such as bombs and shells, are generally stored in large
rectangular stacks containing up to 200,000 pounds of explosive filler.
These stores are in the open, within earth revetments, within earth-
covered igloos, or within steel or reinforced concrete structures. The

---

present design of the revetment or igloo, with regard to fragment retardation, prevents the fragments from striking an adjacent munition store and detonating it by impact. During the accidental detonation of munition store, fragments will be hurled to large distances. A theoretical examination of the far-field fragment distribution from the accidental detonation of stored munitions was undertaken to define and illustrate the dependence of the fragment hazard on the many parameters that define the munition store. The effect of an igloo structure on the far-field fragment patterns is the primary interest in this study; however, in the systematic development of the far-field fragment density calculation, it became necessary to include the effect of the stack size and shape as well as the influence of altered mass distributions, initial velocities and fragment shapes that may occur during accidental detonation.

Summary of Main Results

The model which most adequately describes the effect of the igloo is that the crown of the igloo is blown off. Only fragments with initial elevation angles less than 10° are retarded (these are completely stopped). About a 10% reduction in fragment densities in the far-field is effected by the presence of an igloo. The model for the stack shows that only the munitions in the surface layers contribute significantly to the far-field fragment density.

The initial velocity for the fragments should be taken as the highest value from the arena data. The fragments that are thrown to the far-field must have a higher effective ballistic density than the mean value given in the arena data; i.e., the fragments that reach far distances tend to be elongated with the long axis aligned with the trajectory. Since these

projectiles have a high mass/presented-area ratio the injury criterion may be well below the 11 or 58 foot-pound criterion.

Because there is very little data on far-field fragment measurements and because the experiments were not systematically planned to measure the dependence of the far-field fragments on the several parameters of the typical munition storage configuration, an extensive experimental program to determine this is highly recommended. Until experimental verification of the predicted parameter dependence is obtained, the analytical predictions given here must remain hypothetical.

Method of Approach

The prediction of the far-field fragment density is decomposed into two problems. The first is, given a distribution of fragments and initial velocities on a unit hemisphere centered at the munition store (the distance at which the fragment hazards are evaluated are large compared to the store dimensions and this dependence of the source dimensions may be neglected) determine the far-field fragment density. The second problem is to determine the parameter distributions on the unit hemisphere which adequately represent the munition store. A summary of the computational procedure to effect a solution to the first problem is given below. The remainder of the paper is devoted to the second problem.

Evaluation of the Far-Field Fragment Density

Consider a unit hemisphere whose center is at the origin of a spherical coordinate system, (R, α_0, ϕ), where R is the range, α_0 is the elevation angle above the (flat) surface, and ϕ is an azimuth angle, measured from some arbitrary reference line in the surface (Fig. 1). The initial velocities of the fragments are defined as a function of α_0 and ϕ. At each value of α_0 and ϕ, there is a probability density function $f(m, \alpha_0, \phi)$ such that

$f(m,\alpha_0,\phi)$ dm represents the number of fragments per unit solid angle with mass between m and m + dm.

The cumulative distribution function

$$F(m,\alpha_0,\phi) = \int_m^\infty f(\bar{m},\alpha_0,\phi)\, d\bar{m},$$

defines the number of fragments per unit solid angle with mass greater than m.

In an infinitesimal element of azimuth, $\Delta\phi$, the number of fragments, $N(R,\phi)$, that fall beyond R is calculated by integrating over a slice of the unit hemisphere.

$$N(R,\phi) = \int_0^{\pi/2} \cos\alpha_0\, d\alpha_0 \int_{m_1(R,\alpha_0,\phi)}^\infty f(\bar{m})\, d\bar{m}\ \Delta\phi$$

The lower limit, $m_1(R,\alpha_0,\phi)$, is the mass of the fragment that just reaches R given the elevation angle α_0 and the initial fragment velocity at α_0 and ϕ. All fragments (with the same ϕ and α_0) which have masses larger than $m_1(R,\alpha_0,\phi)$ will fall at larger ranges than R. By considering $N(R,\phi)$ and $N(R + \Delta R, \phi)$ for an infinitesimal ΔR, the fragment density at (R,ϕ) is

$$q(R,\phi) = -\frac{1}{R}\left(\frac{\partial N}{\partial R}\right)_\phi = \frac{1}{R}\int_0^{\pi/2} \cos\alpha_0\, d\alpha_0 [m_1(R,\alpha_0,\phi)]\left(\frac{\partial m}{\partial R}\right)_{\alpha_0,\phi}$$

The partial derivative $\left(\frac{\partial m}{\partial R}\right)_{\alpha_0,\phi}$ can be evaluated from the expression for the range, which is obtained as an approximation to the numerical solution to the ballistic trajectory equations, assuming drag forces (constant drag coefficient) and gravity only,

$$R = \frac{m}{\beta}^{1/3} h(\xi)\ \{.5140 - 1.0358 \ln \frac{m}{V_0}^{1/6} (\frac{g}{\beta})^{1/2} \}$$

$$h(\xi) = \frac{3\sqrt{3}}{2}\ \sqrt{\xi}\ (1-\xi)[1+a(\xi - \frac{1}{3})^2]$$

with

$$a = 3.25, \quad \xi < \frac{1}{3}$$

$$a = 2.00, \quad \xi > \frac{1}{3}$$

$$\xi = \sin \alpha_o$$

Let

$$\beta = \frac{\rho C_D}{2 \kappa^{2/3}}$$

where m is the mass of the fragment

C_D is the drag coefficient

κ is the ballistic density

ρ is the air density

g is the gravitational acceleration

A is the cross section area of the fragment normal
   to the trajectory

The presented area, A, is a function of the fragment mass through

$$A = \left(\frac{m}{\kappa}\right)^{2/3}$$

For a tumbling fragment, this area A is taken as the mean presented area.

This approximation for the range is within 1% for $7.5° \leq \alpha_o \leq 40°$ and for the fragment masses and velocities of interest. To evaluate the integral, an approximation for $F(m, \alpha_o, \phi)$ is required. A reasonable approximation to the arena data is the Thomas (1944) approximation

$$F(m, \alpha_o, \phi) = N_o(\alpha_o, \phi) \exp \{- (m/\mu(\alpha_o, \phi))^{1/3}\}$$

where $N_o(\alpha_o, \phi)$ and $\mu(\alpha_o, \phi)$ are parameters indicating, respectively, the total number of fragements per unit solid angle at α_o and ϕ_o and one-sixth the mean fragment mass is the direction given by α_o and ϕ.

Then, with $\xi = \sin \alpha_0$ as the integration variable,

$$q(R,\phi) = \frac{\beta}{R} \int_0^1 \frac{d\xi N_0(\alpha_0,\phi)}{\{\mu(\alpha_0,\phi)\}^{1/3} h(\xi)} \frac{\exp \{ -[m_1(R,\alpha_0,\phi)/\mu(\alpha_0,\phi)]^{1/3} \}}{\{-.0039 - 1.0358 \ln (\frac{m}{V_0}^{1/6}(\frac{g}{\beta})^{1/2})\}}$$

The far-field fragment density in the side spray direction for a single munition with its axis horizontal is calculated. The values of μ and V_0 were obtained from the arena data(JMEM 1970) by averaging these numbers in the range $60° < \psi < 120°$, where ψ is measured from the axis of the munition extended, $\psi = 0°$ denoting the nose end of the munition. The value of q for M117 750 pound bomb is shown in Figure 2. The value of the initial parameters are, $N_0 = 6000$ fragments per steradian, $V_0 = 8000$ feet per second, $\mu = 30$ grains $\psi = 590$ grains per cubic inch. Feinstein's (1972a) calculated value of q in the direction $\psi = 90°$, obtained by numerical interation of the arena data over the unit hemisphere is also shown. Both calculations agree throughout the range 500 ft-2000 ft to with a factor of 2.

Effect of Stack Configuration

When a single munition detonates under the influence of a proper fuze, the initial fragment mass distribution, mean shape and initial fragment velocities are well known through physical measurements. With these initial conditions and some reasonable assumptions on the ballistic trajectory equations, the fragment density at large ranges can be readily calculated. When a stack of munitions is detonated with each munition simultaneously detonated, these initial fragment parameters from the stack (seen from the far-field where the stack may be viewed as a point source) are altered in that the initial velocities may be changed and a certain number of fragments will be retarded or stopped by the adjacent munitions. In the case where the stack is ignited at a single munition and the remaining

munitions detonate sympathetically, induced by either blast or fragment impact, the initial mass distributions, shape factors, and velocity distributions may be further drastically altered.

The starting point for building a model for the stack is to consider the fragment interaction from two adjacent munitions. Since the largest number of fragments from a munition are ejected approximately normal to the axis of the munition, we consider only this side-spray and idealize each munition to an infinite cylinder and assume their axes parallel. (Figure 3) When a single munition detonates, the initial velocity of the fragments and the mass distribution are independent of angle and are known. First, we consider the simultaneous detonation. If no collisions between fragments occur, the effect initial fragment parameters would be the sum of those of the two individual munitions. However, there will be a great number of such collisions if the munitions are fairly close. The motion of a typical fragment (mass m_1 ejected from munition 1 to angle α_1) is altered slightly if (under conditions of perfectly inelastic impact, appropriate to the initial fragment velocities) it strikes a smaller fragment from the other munition, while it will be stopped completely if it strikes a larger fragment. Using typical fragment distributions (we use the Mott distribution (Thomas 1944) throughout for our calculations), there are many more smaller fragments, so that the probability of interacting smaller fragments will be large, while the probability of interacting with a larger fragment is quite small. The number density of fragments from the second munition was calculated from the ballistic equations (ignoring gravity) as a function of distance and time along rays from the center of the second munition. Figure 4 shows a typical fragment number density versus distance for an M117 750 lb bomb. The density curve shows a

slow rise from the arrival of the first and largest fragment followed by a very rapid rise near the propagation of fragments with the mean fragment mass. Effectively then fragments propagate outwards as an expanding shell. Hot, condensed combustion products from the detonation of the explosive are contained within this shell and at early times, have not expanded much and have nearly the density of the solid explosive material. Now if the test fragment is ejected at such an angle that it misses the shell of fragments from the second munition the probability of it colliding with any fragment is small, whereas, if it intersects the shell the probability of collision is large. In this latter case the test fragment must effectively perforate a steel shell of approximately the thickness of the original munition and then, further must penetrate a mass of hot, highly condensed explosive products. Using a drag model for the perforation of the shell and gas products we find the velocity of the test fragment to be significantly reduced, up to 40% for a 1 pound fragment for the case of the 750 lb bomb with a 0.5 ft. spacing.

We are interested in test fragments that will be thrown to large distances from the munitions and need consider only fragments with mass larger than the mean fragment mass. A convenient and quite adequate approximation (for intermunition spacings of the order cf the radius of the munition) is that all fragments ejected with $-\frac{\pi}{4} \leq \alpha_1 \leq \frac{\pi}{4}$ are stopped by the adjacent munition. Fragments ejected outside this angle will not be significantly affected.

It is a straightforward procedure to build up a model for a large stack by adding a third munition to these first two and calculating which fragments are stopped and which are not, and then adding a fourth, etc.

1134

It suffices to note that no fragments will escape if a munition is completely surrounded. The fragments from a surface layer can be thrown to the far-field. Thus a very simple model to account for the stack configuration is generated. Let N_S be the number of munitions in the side layer nearest the observer and let N_T be the number of munitions on the top layer. The unit hemisphere source then has N_S effective munitions ejecting fragments from the horizontal up to an elevation of 45° and N_T from 45° to vertical. An approximation to the integral for the far-field fragment density (assuming both layers have the same munition orientation relative to the normals of the respective surfaces) yields the following expression for the number of effective munitions in the stack, N_{eff}

$$N_{eff} = 0.9\ N_S + 0.1\ N_T$$

The far-field fragment density, q, is related to the fragment density from a single munition, q_1, through

$$q \approx N_{eff}\ q_1$$

Effect of Cover

The effect of the igloo structure on the fragments is now examined. Assume that the fragment properties from the stack is known and that they can be represented on a unit hemisphere located within the confining structure. The cover, however, will retard or stop some or all of the fragments. The typical earth-covered igloo structure is cylindrical steel arch, with a rectangular floor plan; the front and rear wall are vertical. The rear wall and the cylindrical portions are covered with earth, (Figure 5 shows the cross section through the cylindrical arch); the earth cover has a minimum of two feet at the crown. The front wall is concrete, possibly reinforced and has heavy steel doors.

When the stack detonates, a fraction of the energy goes into breaking up the munition cases, a fraction into kinetic energy and the fragments to be thrown out, and a fraction remains in the blast wave. This last fraction, which remains in the air blast, can be estimated by the Fano formula. The blast will interact with cover and cause it to deflect and break up. A certain fraction of this blast energy will be absorbed in the breakup of the cover and in the kinetic energy of the cover fragments, (which will consist of steel arch fragments, earth cloos, concrete fragments and pieces of the door). From the studies of the blast that is propagated to large distances from explosions within igloos this fraction of energy absorbed by the cover is quite small, being of the order of 10% of the blast energy released from the open stack (Fugelso, Weiner and Schiffman, 1973). If all of this absorbed energy shows up as kinetic energy of the earth cover, the typical earth cover fragment velocity will be of the order of 1000-2000 ft/sec.

Consider a cylindrical shell contained within a semi-cylindrical earth cover. When the munition is detonated, the resulting blast wave creates an overpressure on the inside of the earth cover, causing it to move radially outwards, see Figure 6. The earth cover is considered to have no strength in the tangential direction. As the earth cover moves out, it breaks up into small fragments which are contained between an inner and an outer radius. If gravity is neglected, all interactions between fragments and the earth cover occur along radii and the only result of a fragment-cover interaction is to alter the magnitude of a fragment's velocity, not its direction.

Three models developed to account for the earth cover are:

MODEL 1. The earth cover moves out very slowly compared with the fragments from the stack and the fragments from the stack must perforate an earth layer which is essentially intact. The earth cover, is however broken up and behaves essentially as a fluid. The main effect of the cover is increased drag on the fragments. Experiments by Allen et. al. (1957) on the retardation of steel spheres by sand show, that, for high fragment velocities, the main retardation is essentially of this form.

In this model, the effect of the cover is to reduce the fragment's velocity as it passes through the cover. Since the cover does not move appreciably during the perforation process, assume it is stationary and that the fragment must perforate the original thickness.

Denoting the thickness of the igloo by h (when h is a function of the initial angle and azimuth angle). By comparing the fragment velocity as it emerges from the cover with the fragment velocity in air alone, we define an effective initial velocity. The effect of the earth cover, in this model is to retard the fragment; the magnitude of this effect can be represented as a fictitious lower initial velocity as a function of elevation angle on the unit hemisphere. Using the value of $\rho_{earth} = 100$ lb/ft^3 and the value of h as a function of elevation angle from the center of the igloo, we can readily calculate the far-field fragment density. Figure 7 shows the reduction in far-field fragment density for a typical single munition.

MODEL 2. The second model again assumes the cover doesn't move very far when the fragments overtake it, but the interaction of fragments with the cover is described differently. The cover is assumed to break

up into fragments that have a mass distribution similar to the fragment distribution. If a bomb fragment strikes an earth clod which is larger it is stopped completely. If it strikes a clod which is smaller it is not affected. This model is a simplification of completely inelastic impact in which the velocity of the fragment and clod, upon impact, have the same final velocity.

The effect of this model is to reduce the number of fragments (on the unit hemisphere) t at are thrown out. Mathematically this is represented by an altered mass distribution.

Assuming the probability that a metal fragment will strike at least one earth fragment in $\frac{1}{3}$ foot penetration of the earth cover, and that the earth clod distribution mass distribution is the same as the fragment distribution, we estimate the far-field fragment density. (Shown also on Fig. 7)

This model, with the very optimistic values for a fragment getting through without impact, gives an order of magnitude reduction for the far-field fragment density.

MODEL 3. The third model differs from the other two in that it is assumed that the earth cover breaks up and moves away fast enough so that no interaction between metal fragments and the cover will occur for any initial elevation angle greater than the final crater lip. For lower elevation angles the blast will be trying to move a large amount of earth and will not break it up. For the higher angles, the cover is assumed completely ineffective in stopping fragments and for the lower angles, all fragments are considered to be stopped. Figure 8 schematically illustrates this mode. Estimates of α_m, the angle to the top of the residual cover,

are obtained from the profiles of the craters in the Arco detonations (ANESB 1947) and Eskimo I (Weals 1973). An estimate of $\alpha_m \sim 10^\circ$ is consistent with this data. In this model then, the calculation of the fragment density in the far-field is effected by replacing the lower limit in the integration over α_0 by α_m.

Consistent with our previous model for N_{eff} from a stack, an approximation to the integral for q yields

$$N_{eff} = 0.7\ N_S + 0.1\ N_T$$

Effect of Other Parameters

The effect of the far-field fragment density when two of the initial fragment parameters are altered is now examined. The fragment mass distribution seems to be changed when a stack of munitions is detonated with a single munition primed (Draper and Watson 1970, Feinstein and Nagaoka, 1970, Feinstein 1972b). The observations indicate that more large fragments are generated. There is no available data, however, on the mass distribution that is obtained; therefore, a simple model to examine this effect is used. Assume the altered mass distribution has the same functional form as the arena data but with fewer total fragments and a larger mean fragment mass. The effect of this change is illustrated for fragment densities in the side direction for the M117 750 lb bomb. Figure 9 shows the fragment density versus γ (= μ/μ arena) for $1 \leq \gamma \leq 10$ at selected ranges between 500 ft and 2500 ft. For the smaller range, the fragment density decreases with increasing γ, decreasing about an order of magnitude as γ increase about an order of magnitude. At the other extreme (i.e., ranges of 2000 and 2500 feet), the change in fragment density with γ is very slight, being about 30% over the range of γ presented.

Although there are fewer total fragments for larger γ, there is a larger fraction of large fragments and the larger fragments are hurled to larger distances than smaller fragments.

As far as the far-field fragment hazard is concerned, the effect of changing the mass distribution in a stack detonation is slight.

Now turn to a feature whose effect will not be slight in estimating the far-field fragment hazard. In solving the ballistic trajectory equations, it is normally assumed (in all the theoretical works presented) that the fragments are spinning as they leave the detonation site and that the presented area can be represented (at least over the larger trajectories) as the mean presented area. It would be possible for some fragments to be ejected with no or little spin or, if spinning at the outset, to stabilize with their major axis roughly parallel to the trajectory. In this case the presented area would be minimized and the ballistic density maximized.

For example, look at a fragment with square cross-section and with an aspect ratio of 2:1, aligned with the trajectory. For steel fragments, the ballistic density is 1980 gr/in^3 or three times the mean value.

The far-field fragment density was calculated for various values of the ballistic density, ranging from the mean value given in the arena data to four times the ar·na data (i.e. from ~ 600 gr/in^3 to 2500 gr/in^3). Figure 10 shows the fragment density versus ballistic density at selected ranges from 500 feet to 2500 feet for the M117 750 lb bomb in the side spray direction. At the larger ranges (e.g. 2500 feet) a dramatic increase in the fragment density is noted, increasing by almost two orders of magnitude as the ballistic density changes by a factor of four. It is suggested that this factor is quite important for far-field fragment estimations. Now it is improbable that all fragments will be stabilized

and oriented to the trajectory, but even if only 10% or them are, while the remaining 90% are spinning; the increase of the far-field fragment density will be dramatic.

The effect of increased initial velocity which is observed by Draper and Watson (1970) is less dramatic in increasing the far-field fragment density. An examination of the maximum range of a fragment of mass explains this. The maximum range is

$$R = \beta(\frac{\kappa}{\kappa_A})^{2/3} m^{1/3} [.5140 - 1.0368 \ln (137(\frac{\kappa}{\kappa_A})^{1/3} \frac{m^{1/6}}{V_0})]$$

where κ is the actual ballistic density

κ_A is the arena average ballistic density

V_0 is the initial velocity

The dominant dependence on V_0 is with $\ln V_0$ while the dominant dependence on κ is as $\kappa^{2/3}$.

Note changes in V_0 by a factor of 2 or 3 may be expected, while the value of κ for selected projectiles could range easily up to 5-10 times the arena value.

Open Stack Models - Theory and Experiment

The calculations are compared with the fragment density in the far-field (500 feet to 1500 feet) for the side spray direction from the 2x3 and 5x3 stacks of M117 750 lb bombs tested at NWC (Feinstein and Nagaoka, 1970). In the former $N_T = 2$, and $N_T = 5$ in the latter, while $N_S = 3$ for both. Thus

$$N_{eff} = \begin{cases} 2.9 \text{ for } 2 \times 3 \text{ stack} \\ 3.2 \text{ for } 5 \times 3 \text{ stack} \end{cases}$$

Figure 11 shows the comparison using the arena data approximation. The comparison is quite good.

The next comparison is with the first two events in the Big Papa test. These tests were the detonation in an open revetment of a mixed stack of M117 750 lb bombs and M66A2 2000 lb bombs. The 750 lb and 2000 lb bomb are both tritonal filled and have the same C/M ratio. The arena data for the 2000 lb bomb has the same fragment velocity (within 10%) and the same average fragment mass as the 750 lb bomb with approximately $\frac{8}{3}$ more fragments. Therefore, each 2000 lb bomb is replaced by 2-2/3 750 lbs for the purpose of comparison.

The stacks for these detonations were rectangular. Details of the stack composition are given in Peterson (1968). In the first test, there were 64 750-lb bombs in the top layer and 4 750-lb and 12 2000-lb bombs in the side. For the second test, there were 21 750-lb bombs in the top and 4 750-lb and 8 2000-lb bombs on the side.

Thus N_{eff} = 39 in the first case and 25 in the second. The comparison between theory (using arena data) and measured values is not very good; between 2000 ft and 3000 ft there is roughly a factor of 50 between the two. Schreyer and Romesberg (1970) noted that using arena data and a multiplier, an effective stack of approximately 250 bombs was required to match the data between 2000 and 3000 ft.

Peterson (1968) measured the mass of the smallest fragments at 1800 and 3000 ft. These fragments are much smaller than that predicted from the ballistic equations. The initial velocity required for these fragments is well in excess of 25,000 ft/sec. However, if the effective ballistic density was twice the arena average these small fragments could reach these distances with no increase in initial velocity. Therefore, the fragment densities, were recalculated using N_{eff} and $\kappa = 1200$ grains/in^3.

1142

Figure 12 shows the comparison of the predicted and experimental. The comparison is not great (a factor of $\sim$ 2 at 2000 ft), but probably reasonable. There are very slight changes in q from 500 to 1500 ft. suggesting that the agreement with the NWC 2x3, 5x3 tests remains valid.

A more realistic source model would probably have the smaller fragments starting out with a higher velocity than the larger fragments and would also exhibit dependence of the shape factor on the size. Since there is no data available on this dependence, no attempt to fit any such variation was made.

Igloo Models - Theory and Experiment

There is only one experiment for weapons contained within an igloo that can be compared with the theoretical far-field fragment densities. Fragment densities from the Eskimo I test of 13696 TNT loaded 155mm shells detonated in a standard Army Igloo were measured. The shells were placed in a stack (shown in Figure 13) with the munitions oriented vertically. Figure 14 shows the plan view of the test, and indicates the lines along which fragment measurements were made.

The number of shells on the top layer for considering fragments off either end is 3700; off the side almost half of these are screened by the odd shape of the stack; N_T = 2300 there. Off the end N_S = 240 and off the side N_S = 280. First the far-field fragment densities from this stack model were calculated (using arena data) for each of the three cover models. For the third cover-fragment model, the value of the calculated fragment density was low by at least an order of magnitude and the predicted density has a slope much greater than that measured. The two models with strong cover-fragment interaction deviated further.

Recalling the argument presented above for considering altered initial data to account for the experimental results in Big Papa, we look at the

minimum fragment mass versus range data (Weals, 1973, Feinstein, 1972b).
Figure 15 shows the minimum mass fragment recovered as a function of range
for this experiment. Also plotted is the theoretical minimum mass versus
range using κ = 660 grains/in^3, V_o = 4500 fps; κ = 1200 grains/in^3, V_o =
4500 fps; and κ = 660 grains/in^3, V_o = 40,000 ft/sec. In line with the
previous fit to the Big Papa experiment the velocity increase to account for
the mass is rejected as the prime explanation and the ballistic density
corresponding to the more slender projectile is accepted.

The density calculations were repeated, but a value of κ = 1200 gr/in^3
was used, together with the arena data initial velocity and fragment den-
sities. The model wherein fragments are stopped for low elevation angles,
but otherwise unimpeded, yields values which are in good agreement with the
measurements. The calculated values agree to within a factor of two for
most of the range and the slope is qualitatively in agreement. For fragments
in the direction of the headwall, assume the headwall is destroyed by the
blast and offers no resistance to low elevation angle fragments in that
direction. For this model the N_{eff} are as follows:

Headwall N_{eff} = 0.9 (240) + 0.1 (3700) = 586   600

Side N_{eff} = 0.7 (280) + 0.1 (2300) = 426   425

Back N_{eff} = 0.7 (240) + 0.1 (3700) = 538   550

Figure 16 shows the measured data and the theoretical predictions for this
model. The perforation and collision models for the igloo effect would yield
values lower than these by better than an order of magnitude.

Tentative Quantity-Distance Relations

On the basis of the theory and their limited comparisons with experimental
data, the following model for the calculation of the far-field fragment den-
sity from the accidental detonation of stacks of munitions is tentatively
proposed.

I. Each munition generates an isotropic fragment distribution with the total number of fragments from the arena data distributed uniformly over a unit sphere. These numbers have an upper bound given by the average densities in the arena data in the side direction. The average fragment mass is taken as that of the arena data. The ballistic density used will be taken as twice that given in the arena data.

II. Let N_T denote the number of munitions in the top layer of the stack and N_S the number of munitions in nearest side. The total number of effective munitions is:

1) For an open stack

$$N_{eff} = 0.9 \, N_S + 0.1 \, N_T$$

2) For a stack within a standard earth-covered igloo

$$N_{eff} = 0.7 \, N_S + 0.1 \, N_T$$

In the headwall direction, treat the stack as open.

III. With these numbers as input, the far-field fragment density is calculated by the approximate formula

$$q_{stack} = N_{eff} \, q_{single}$$

IV. All fragments are considered hazardous. This assumption is made for two reasons. First most of the fragments at these distances have a terminal kinetic energy greater than 58 foot-pounds. The smaller fragments that reach these enormous distances most likely have a high mass-to-presented-area ratio and would be much more ballistically effective.

Tentative quantity-distance curves for a typical munition are presented. An assumption on typical stack shapes is required to illustrate the calculations. Let M equal the total number of munitions in the rectangular stack with dimensions 3n x n x n (Fig. 16). This stack shape

is approximately the one that would fit into a standard igloo. For this example

$$N_T = 3n^2$$

and $N_S = 3n^2$ off the end

           $= n^2$ off the side

Thus $N_{eff} = 3n^2$ off the side ⎫
             $= 1.2\ n^2$ off the end ⎬ open store

             $= 2.4\ n^2$ off the side ⎫
             $= n^2$ off the end ⎬ stored in earth-covered igloo

and $M = 3n^3$

The quantity of explosive, W, is

$$W = MW_1$$

where W_1 is the explosive weight in a single munition.

Figure 18 shows the quantity-distance relations for the M117 750 lb bomb. Values of the fragment density of 1/600 square feet and 1/6000 square feet are shown. Also plotted are the inhabited building distance for Class 7 explosives (DOD Manual 4145, 27M, 1971) and the British criterion $R = 515\ W^{1/5}$ for a 10^{-5} probability of being struck by a fragment (Jarrett 1968). The DOD inhabitated building distances are based primarily on blast criteria, nominally, that a critical value of the peak overpressure is not exceeded. This requirement yields an approximate quantity-distance relation of the form $W \propto R^3$. Safe distances for personnel in the open are some multiple of the inhabitated building distance. It should be noted that the tentative quantity-distances curves for the fragment hazard indicate that the fragment hazard might be the controlling safety feature for stacks with less than 100,000 to 200,000 lbs of explosive. The

quantity-distance relation for these fragment hazards will increase the required safe distances for the smaller stacks.

Summary

The theoretical predictions for far-field fragment densities for the accidental detonation of stacked munitions and of stacked munitions within igloo magazines compares quite well with the few adequate measurements of the far-field fragment densities.

1. The fragment densities in the far-field are calculated using an approximation to the exact solution to the ballistic trajectory equations. The approximation technique is very good for the fragment masses and initial velocities of interest. The ballistic equations that this approximation represents ignores any yaw effects and any wind conditions. The spin of the fragments is approximated by assuming an effective mean presented area only and no deviations from the spinless trajectory by Magnus and cross forces are considered. This effect of spin on the trajectory was not estimated, but it could be appreciable.

2. The ballistic equations allow the fragment density to be computed at large ranges from the specification of fragment number, mass, initial velocity and ballistic density at any specified azimuth and elevation on the unit hemisphere centered at ground zero. Given a set of arena data for a single munition, the far-field fragment densities may be readily computed.

3. The model for the stacks led to a definition of an effective number of single munitions. Only munitions in the top layer and the side layer nearest the observation point contribute significantly to the far-field fragment density. The bulk of the contribution comes from the side

layer. Fragments from munitions in the interior of the stack are effectively stopped by the fragments, blast, and combustion products from the adjacent munitions.

4. The best model for describing the effect of an earth cover on the retardation of fragments is that the crown of the earth cover is blown apart by the blast and moves out as part of the fragment pattern and does not significantly interact with the munition fragments. At very low elevation angles the cover essentially remains in place and completely stops all fragments with very low elevation angles. The original purpose for the design of the earth cover is the prevention of intermagazine communication of the detonation by fragment impact and blast. As far as fragments are concerned, this objective is met. The cover affords little reduction in the far-field fragment numbers, though.

5. The distribution of fragment masses, total fragment numbers and fragment initial velocities from an accidental detonation in a stack, wherein one of the munitions detonates and the remainder are detonated sympathetically, may differ significantly from the values obtained by detonating a single munition. In particular, larger fragments and higher initial velocities may be expected. The effect of larger fragments (together with its corollary property of fewer of them) do not significantly alter the densities that may be expected in the ranges 1000-3000 feet. Increases in initial velocity affect the fragment densities only slightly. The parametric studies indicate that the fragment densities in the far-field are extremely sensitive to effective ballistic density. A change in this variable by a factor of two leads to increases in the number of fragments observed in the far-field by better than an order of magnitude.

6. Use of arena data could not effect a match between theory and the measured data from the Big Papa and Eskimo I experiments. The detailed measurements of these experiments show that much smaller fragments are ejected to larger distances than could be expected using the initial velocities and the average shape factor from the arena. Modifications of either of these factors could account for the observed data. The velocity increments required are large, being a factor of 3-10 times the maximum arena velocity, while only small changes in the average effective shape factor are required.

7. An additional assumption for use in the theoretical calculations at this stage of development is that the initial hemisphere parameters should be chosen isotropic with the largest values of fragment number and velocity from the arena data chosen. The munitions in an accidental detonation will be tossed about prior to initiation of the sympathetic detonation and the actual orientation will be subject to some sort of statistical distribution. This project is interested in the determination of safe distances and to be conservative it should be assumed that the maximum source is operative in any direction.

It is worth noting that either greatly enhanced initial velocity or an altered ballistic density is required to explain the measured far-field fragment density. We lean toward the latter as the fragment density is extremely sensitive to small changes in the shape factor, while extremely large initial velocity increments are required. If the latter case is descriptive, some thought must be given to the injury criteria. Fugelso (Fugelso, et.al. 1960, 1961, 1966) has shown that perforation limit velocities for thin metallic plates are highly dependent on the mass to presented

area ratio at impact. Sperraza and Kokinakis (1968), and Kokinakis, (1970) have shown similar dependence for perforation limit velocities of skin. Their data yield

$$V_{limit} = a + b \frac{A}{m} \quad a, b, \text{ constants}$$

The trauma data (Bowen et.al.1968) for unilateral and bilateral lung hemorrhage by blunt missile impact also shows somewhat smaller dependence on A/m.

In view of the high possibility of the far-field fragments being highly elongated, it is suggested that the critical velocity requirements be reexamined quite thoroughly. For the present it is suggested that all fragments beyond 1000 feet be treated as potentially lethal.

REFERENCES

Allen, W. P., Mayfield, E. B. and Morrison, H. L., 1957, "Dynamics of a Projectile Penetrating Sand", Jour. Appl. Phys. 28, 370-376.

Army Navy Explosives Safety Board, 1947, "Igloo Tests, Naval Proving Ground, Arco, Idaho, 1945", Tech. Paper No. 3.

Bowen, I. G., Fletcher, E. R., Richmond, D. R., Hirsch, F. G. and White, C. S., 1968, "Biophysical Mechanisms and Scaling Procedures Applicable in Assessing Responses of the Thorax Energized by Air-Blast Overpressures or by Nonpenetrating Missiles", Annals of the New York Academy of Sciences, 152, 118-171.

Draper, E. and Watson, R. R., 1970, "Collated Data on Fragments from Stacks of High Explosive Projectiles", Ministry of Defense, Directorate of Safety (Army Department) Tech Memo, February, 1970.

Feinstein, D. I., and Nagaoka, H. H., 1970, "Fragment Hazards From Munition Stacks", Minutes of the Twelfth Explosive Safety Seminar, 287-309.

Feinstein, D. I., 1972a, "Fragmentation Hazards to Unprotected Personnel", IITRI Final Report J6176, Contract DAHC-04-69-C-0056.

Feinstein, D. I., 1972b, "Fragment Hazard Study Grading and Analysis of 155mm Yuma Test Fragments", IITRI Final Report J6272, Contract DAAB09-72-C-0051.

Fugelso, L. E., Arentz, A. A., and Poczatek, J. J., 1961, "Mechanics of Penetration I, Metallic Plates, Theory and Applications", GARD Final Technical Report 1127, Contract DP-19-129-QM-1542.

Fugelso, L. E., 1962, "Mechanics of Penetration II, Single and Laminated Plates", GARD Final Technical Report 1127, Contract DA-19-129-9M-1542.

Fugelso, L. E. and Bloedow, F. H., 1966, "Studies in the Perforation of Thin Metallic Plates by Projectile Impact: I. Normal Impact of Circular Cylinders", GARD Final Technical Report 1250, Contract DA19-129-AMC-247(N).

Fugelso, L. E., Weiner, L. M., and Schiffman, T. H., 1972, "A Computation Aid for Estimating Blast Damage From Accidental Detonation of Stored Munitions", Minutes of the Fourteenth Explosives Safety Seminar, 1139-1166.

Jarrett, D. E., 1968, "Derivation of the British Explosives Safety Distances", Annals of the New York Academy of Sciences, 152, 18-35.

Joint Munitions Effectiveness Manual, 1970, Air-Surface Weapons Characteristics, (C).

Kokinakis, W., 1971, "A Note on Fragment Injury Criteria", Minutes of the Thirteenth Explosives Safety Seminar, 421-428.

REFERENCES
(CONT'D)

Peterson, F. H., Lemont, C. J., and Vergmothe, R. R. 1968, "High Explosives Storage Test: Big Papa", Final Technical Report, AFWL-TR-67-132.

Schreyer, H. L. and Romesberg, L. E., 1970, "Analytical Model for High Explosive Munitions Storage", Final Technical Report, AFWL-TR-70-20.

Sperraza, J., and Kokinakis, W., 1968, "Ballistic Limits of Tissue and Clothing", Annals of the New York Academy of Science, 152, 163-167.

Thomas, L. H., 1944, "Computing the Effect of Distance on Damage by Fragments", BRL Report 468.

Weals, F. H., 1973, "ESKIMO I Magazine Separation Test", NWC Final Technical Report, NWC TP 5430.

$$N(m,a_o,\phi)$$
$$V(a_o,\phi)$$
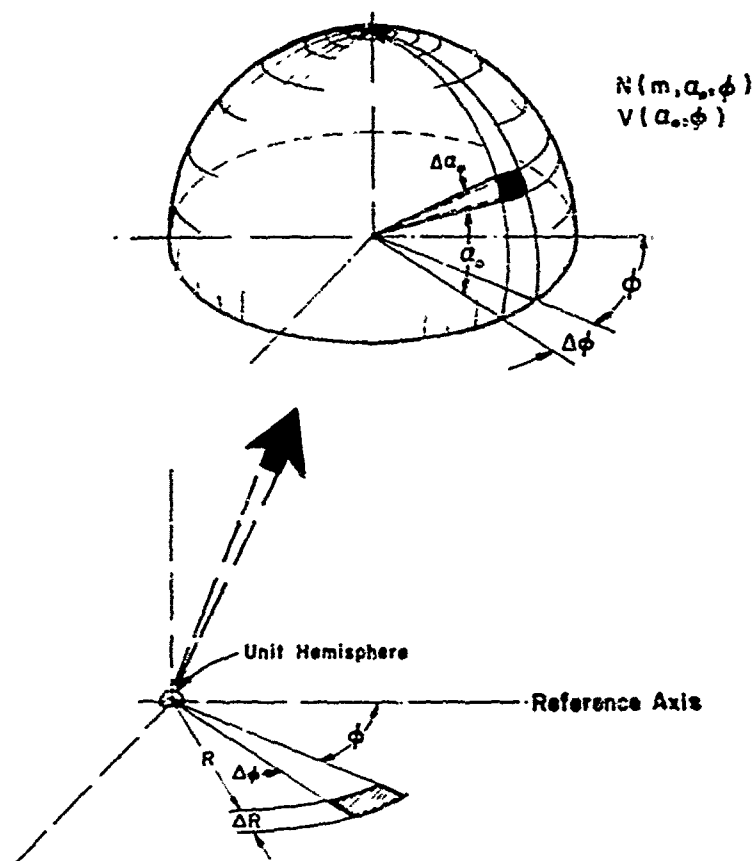
Figure 1, ILLUSTRATION OF COORDINATE SYSTEM AND UNIT
HEMISPHERE USED FOR CALCULATION OF FAR-FIELD FRAGMENT DENSITIES.
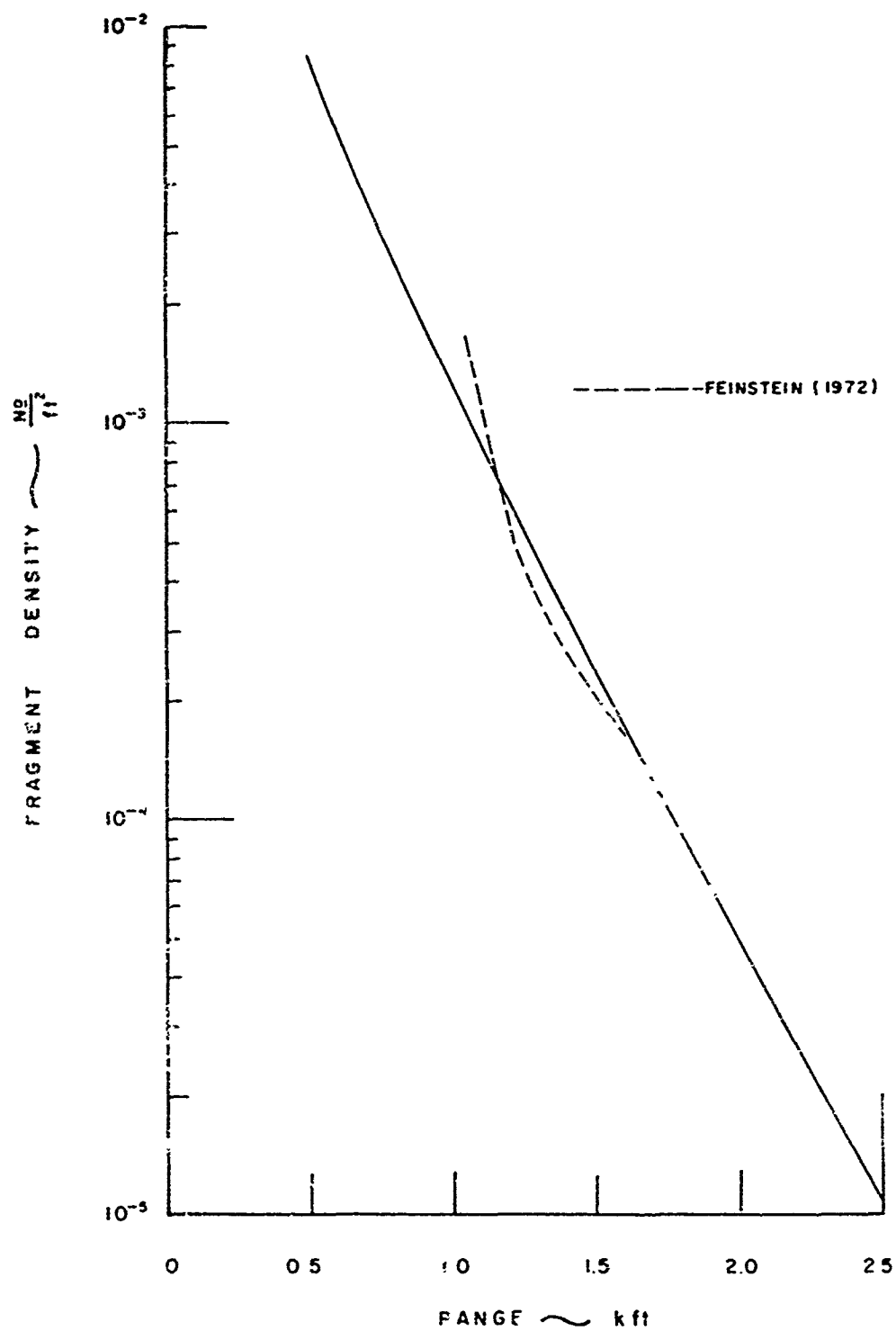
Figure 2. SINGLE MUNITION FRAGMENT DENSITY VERSUS RANGE M117 750-lb. BOMB (SIDE DIRECTION).
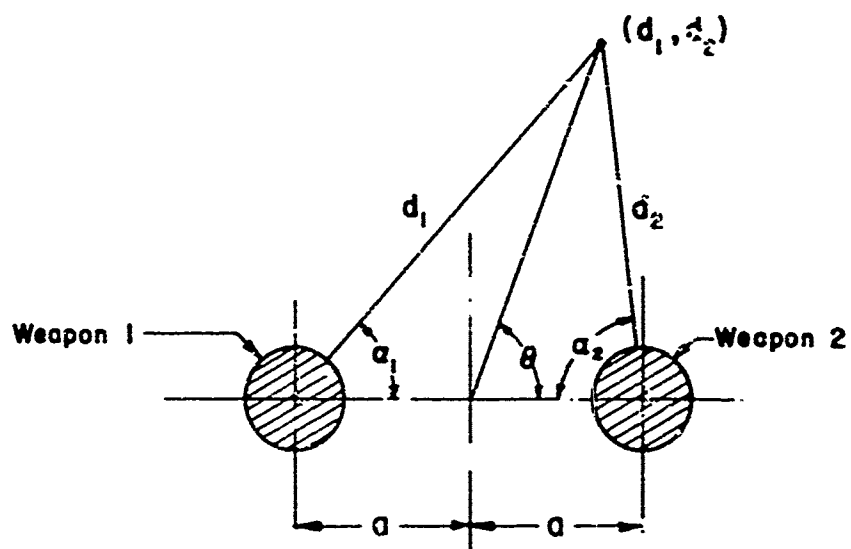
Figure 3, INTERACTION GEOMETRY
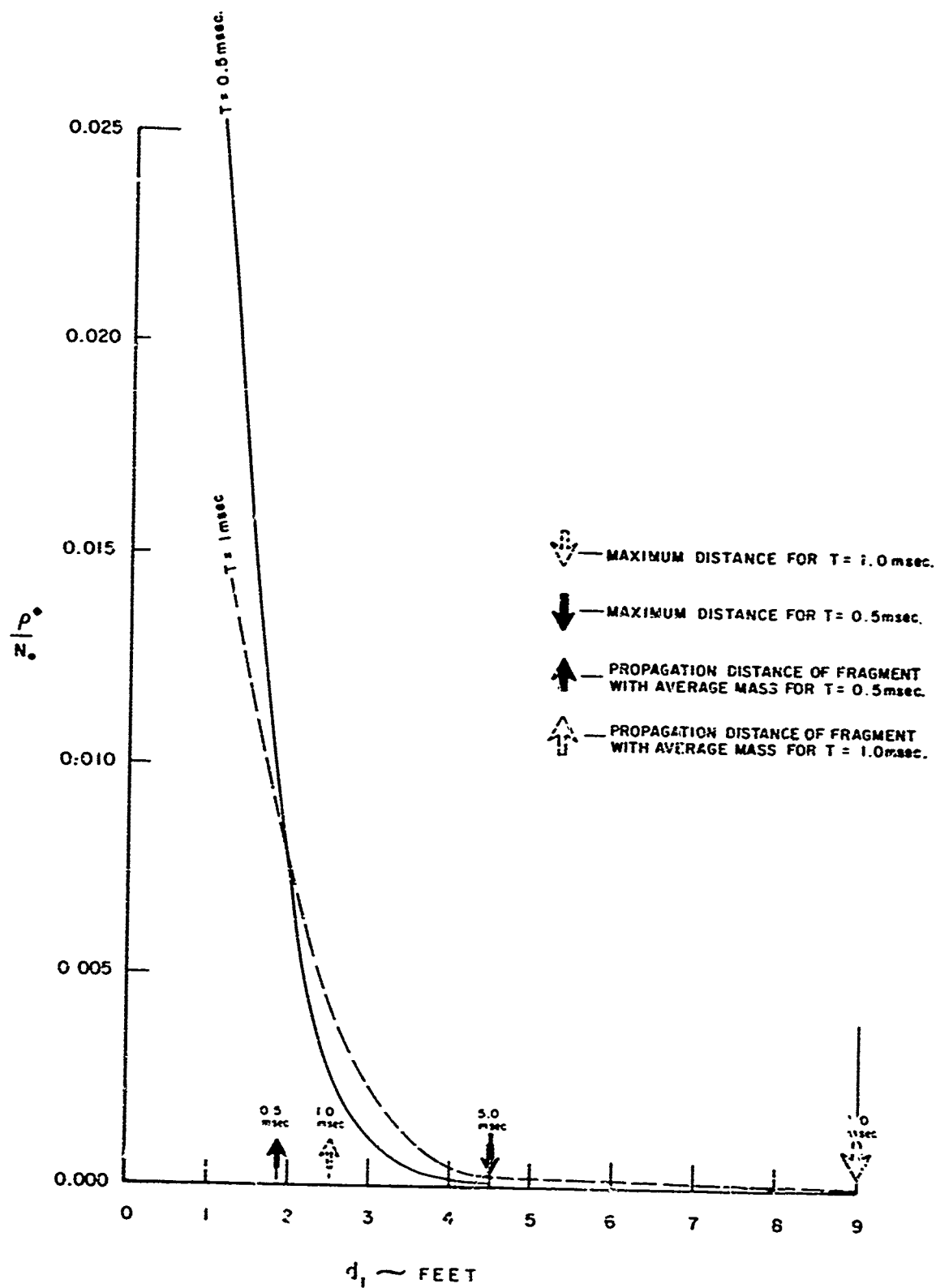
Figure 4. NUMBER DENSITY OF FRAGMENTS FROM A MII7 750-lb BOMB ALONG A RAY.
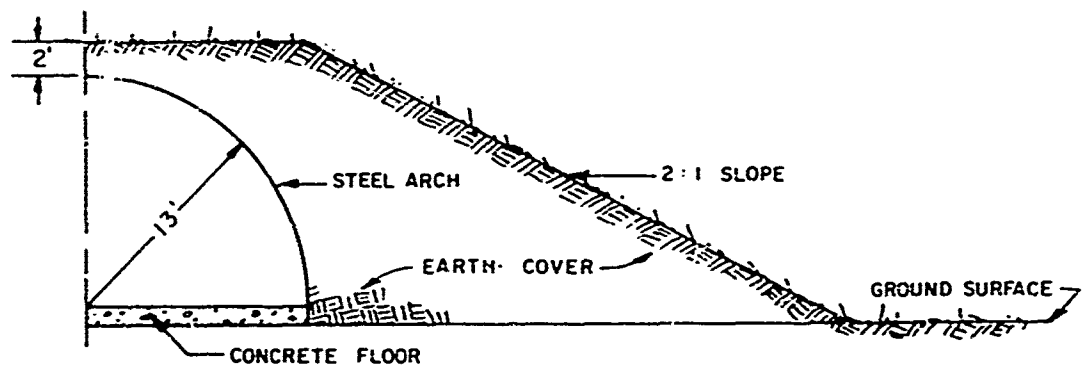
Figure 5,   CROSS SECTION THROUGH ARMY STANDARD IGLOO MAGAZINE
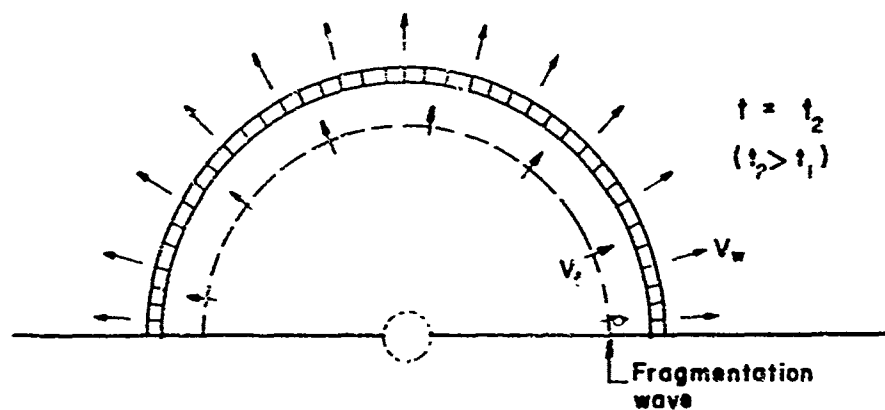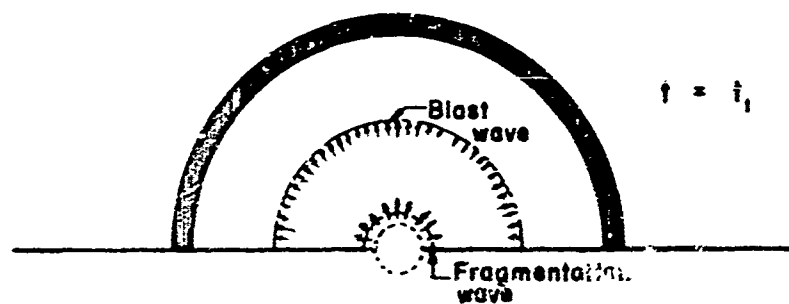
Figure 6. MODEL FOR FRAGMENT-COVER INTERACTIONS (ASSUMING
BLAST WAVE ARRIVES AT COVER BEFORE FRAGMENTATION
WAVE).
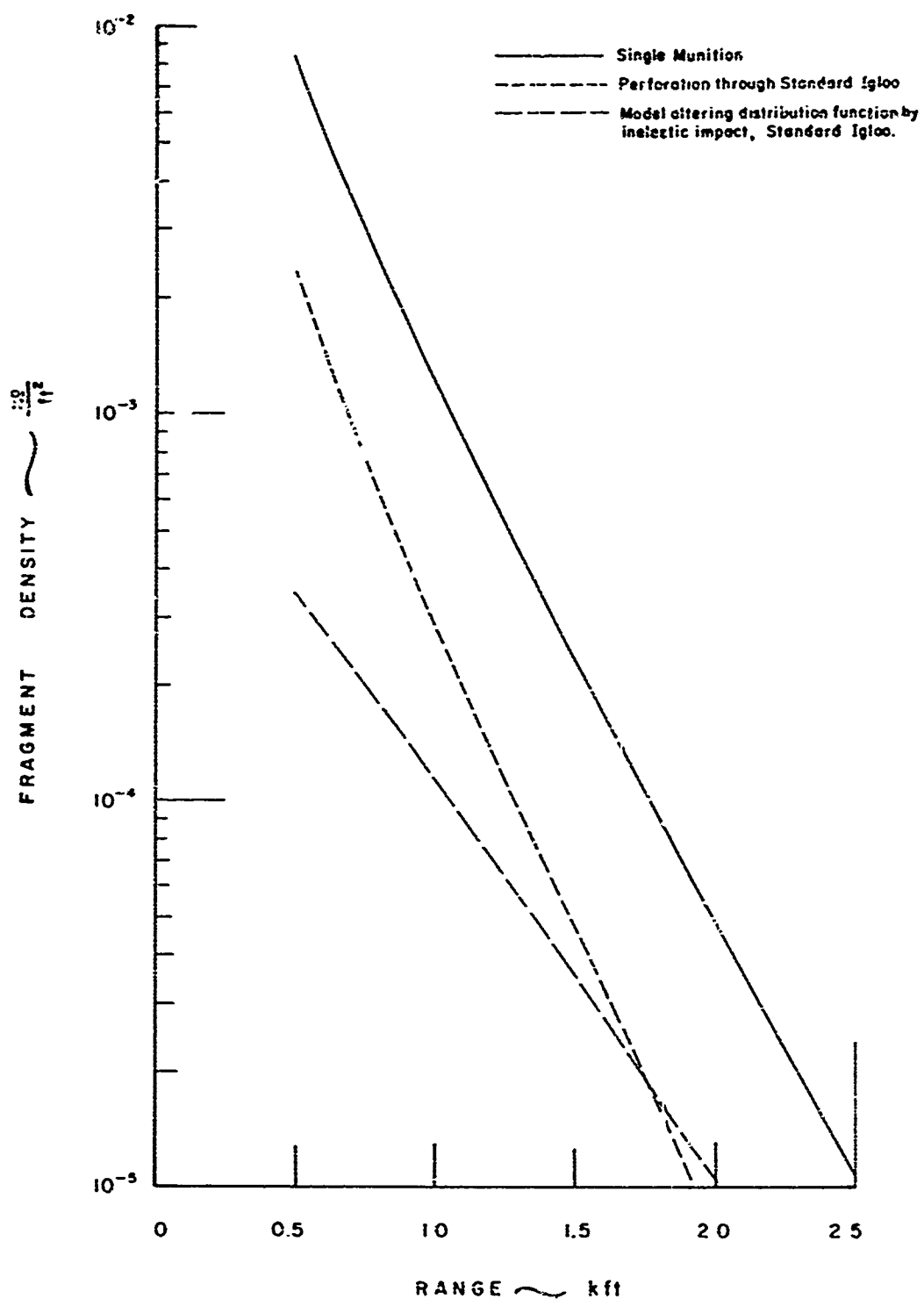
Figure 7. EFFECT OF EARTH COVER ON FRAGMENT DENSITY VERSUS RANGE
M.117 750-lb. BOMB (SIDE DIRECTION)

1159

INITIAL CONFIGURATION — EARTH COVER

— METAL IGLOO

— MUNITIONS STACK

CONFIGURATION AT AN EARLY TIME

EARTH COVER (This portion breaks up under the blast and moves out)

METAL FRAGMENTS

EARTH COVER (This part stays put)

CONFIGURATION AT A LATER TIME

EARTH COVER (All broken up)

METAL FRAGMENTS

REMNANT OF EARTH COVER

FRAGMENTS STOPPED
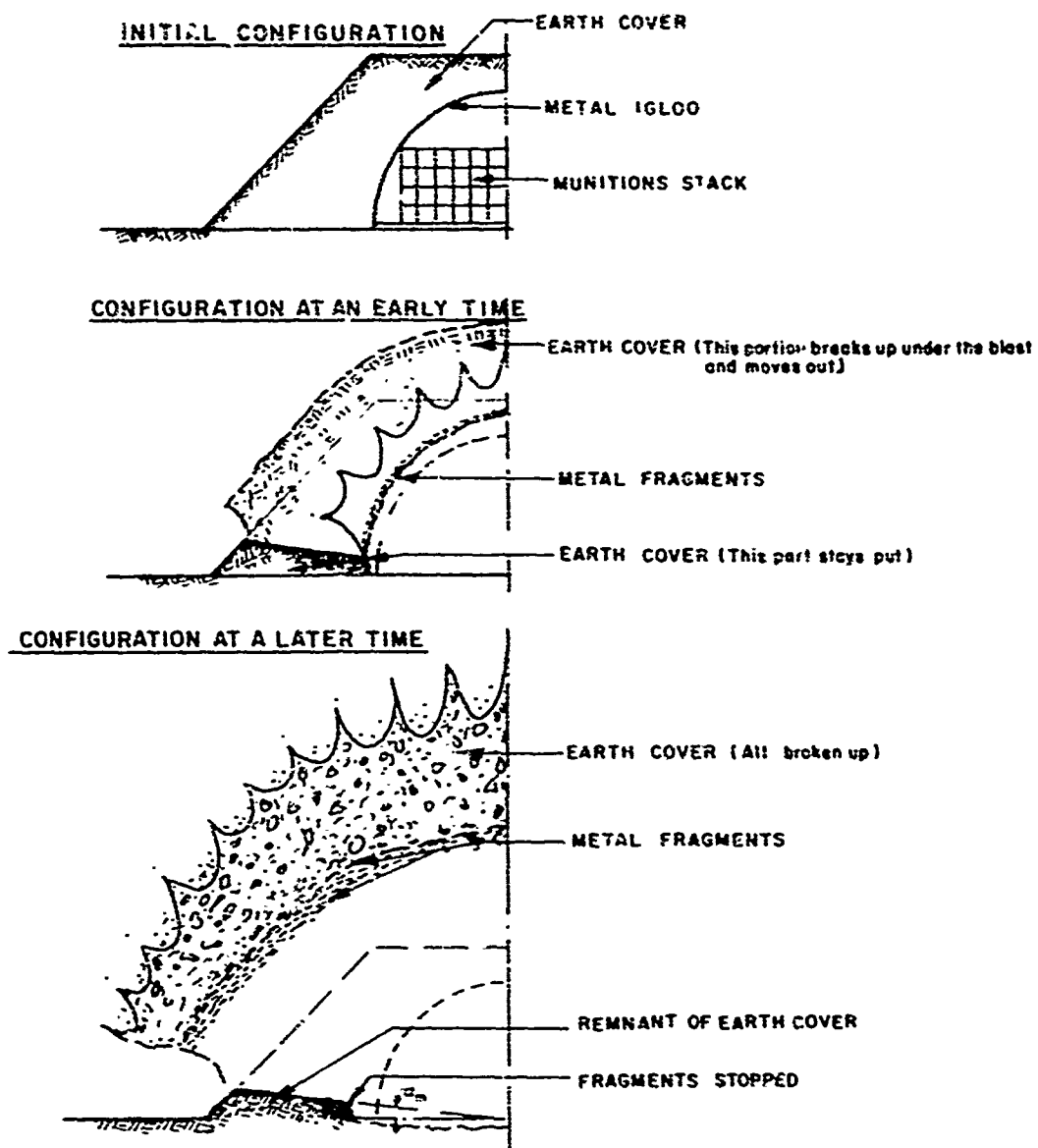
Figure 8. SCHEMATIC DIAGRAM ILLUSTRATING THE THIRD MODEL OF EARTH COVER EFFECT ON FRAGMENTS.
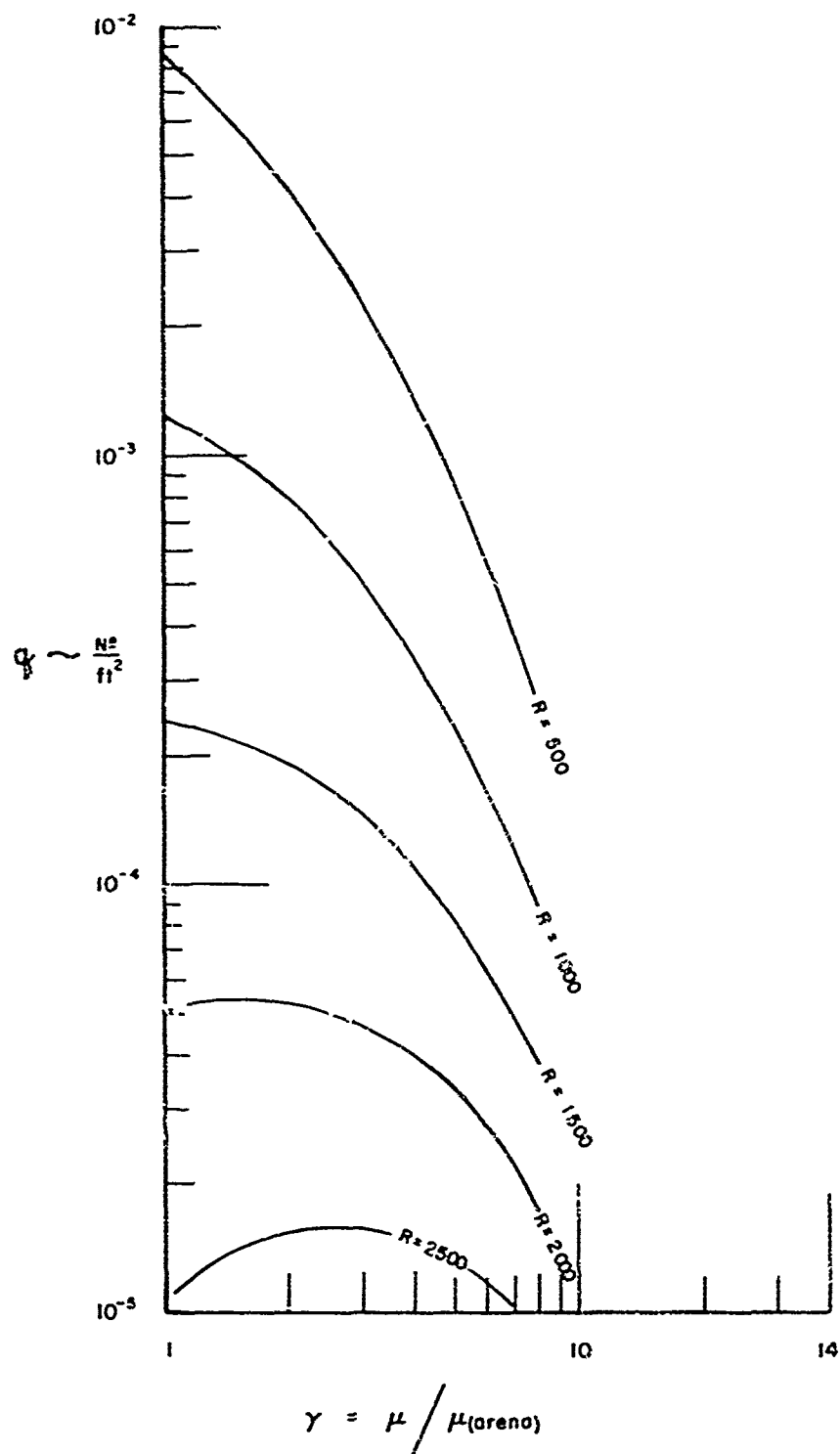
Figure 9. EFFECT ON q FROM CHANGES OF MASS DISTRIBUTION AT VALUES OF R. MII7 750-lb. BOMB (SIDE DIRECTION)

1161
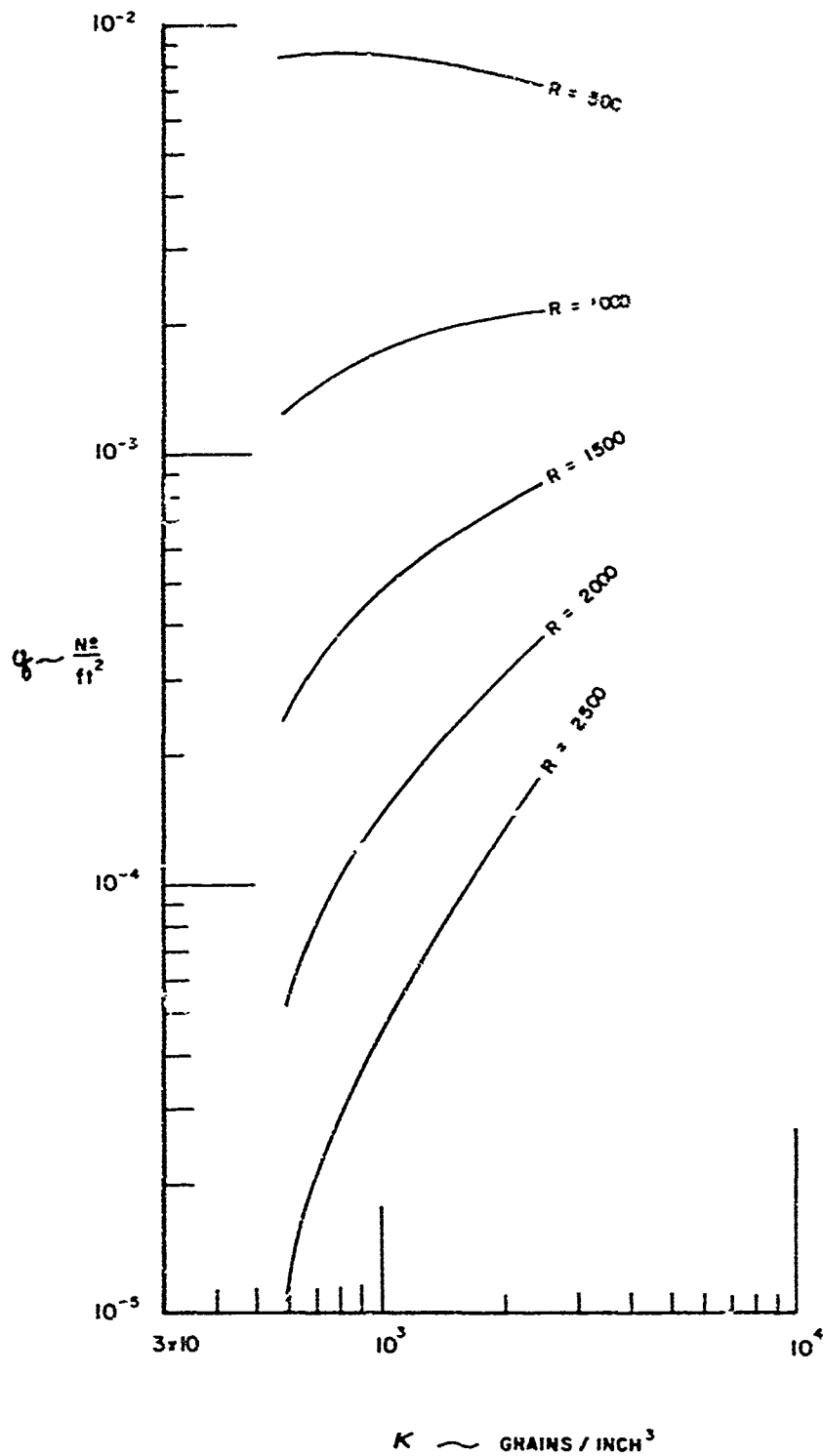
Figure 10. EFFECT ON q FROM CHANGES OF BALLISTIC DENSITY AT
VALUES OF R. M117 750-lb. BOMB (SIDE DIRECTION)

1162
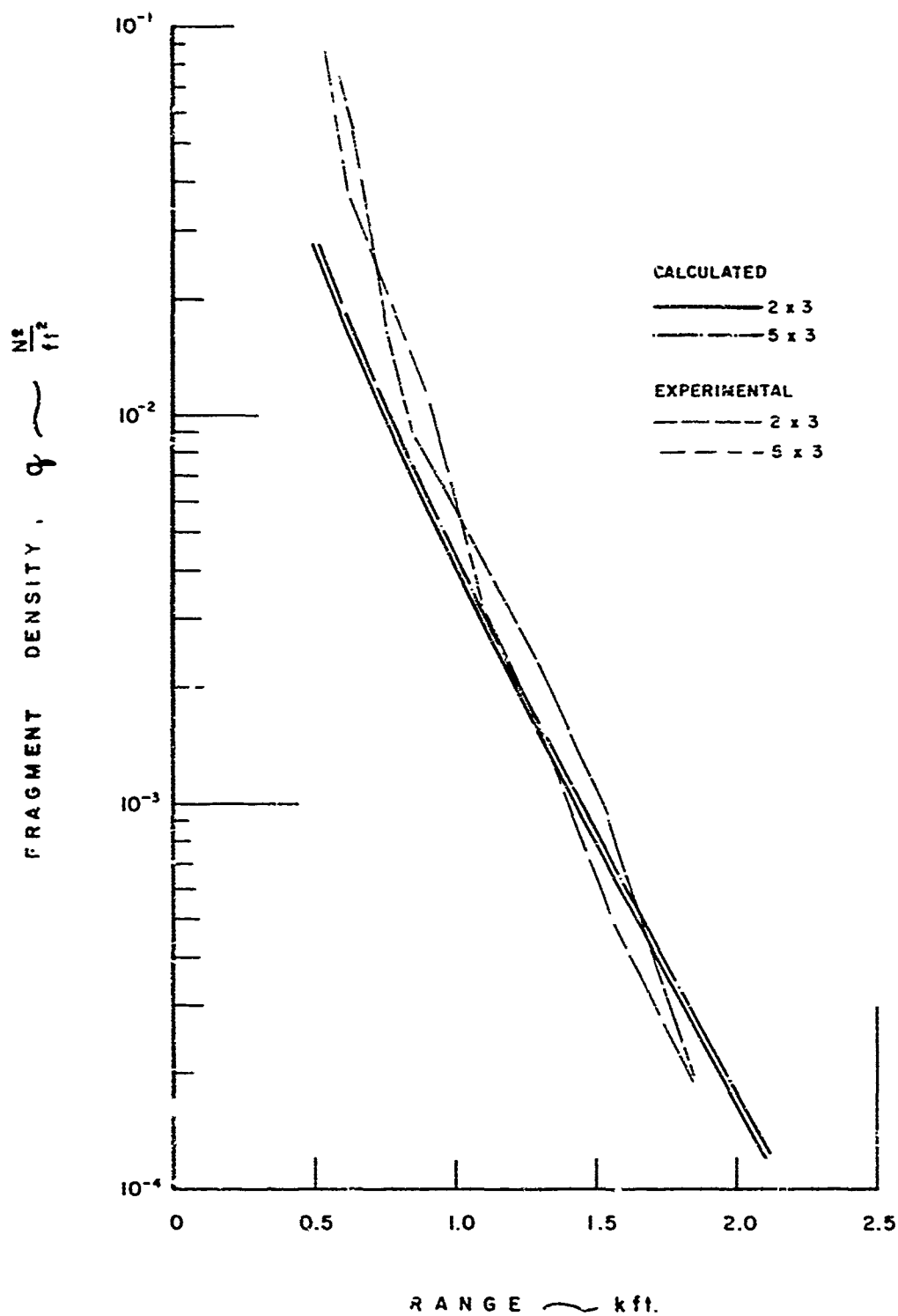
Figure 11. COMPARISON OF CALCULATED FRAGMENT DENSITY VERSUS
RANGE WITH EXPERIMENT-SMALL STACK OF M117 750-lb BOMBS
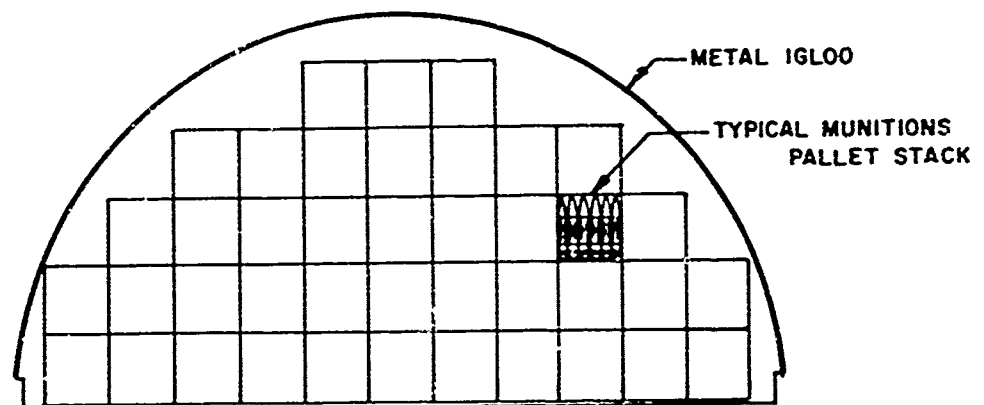(SIDE SPRAY DIRECTION)

1163
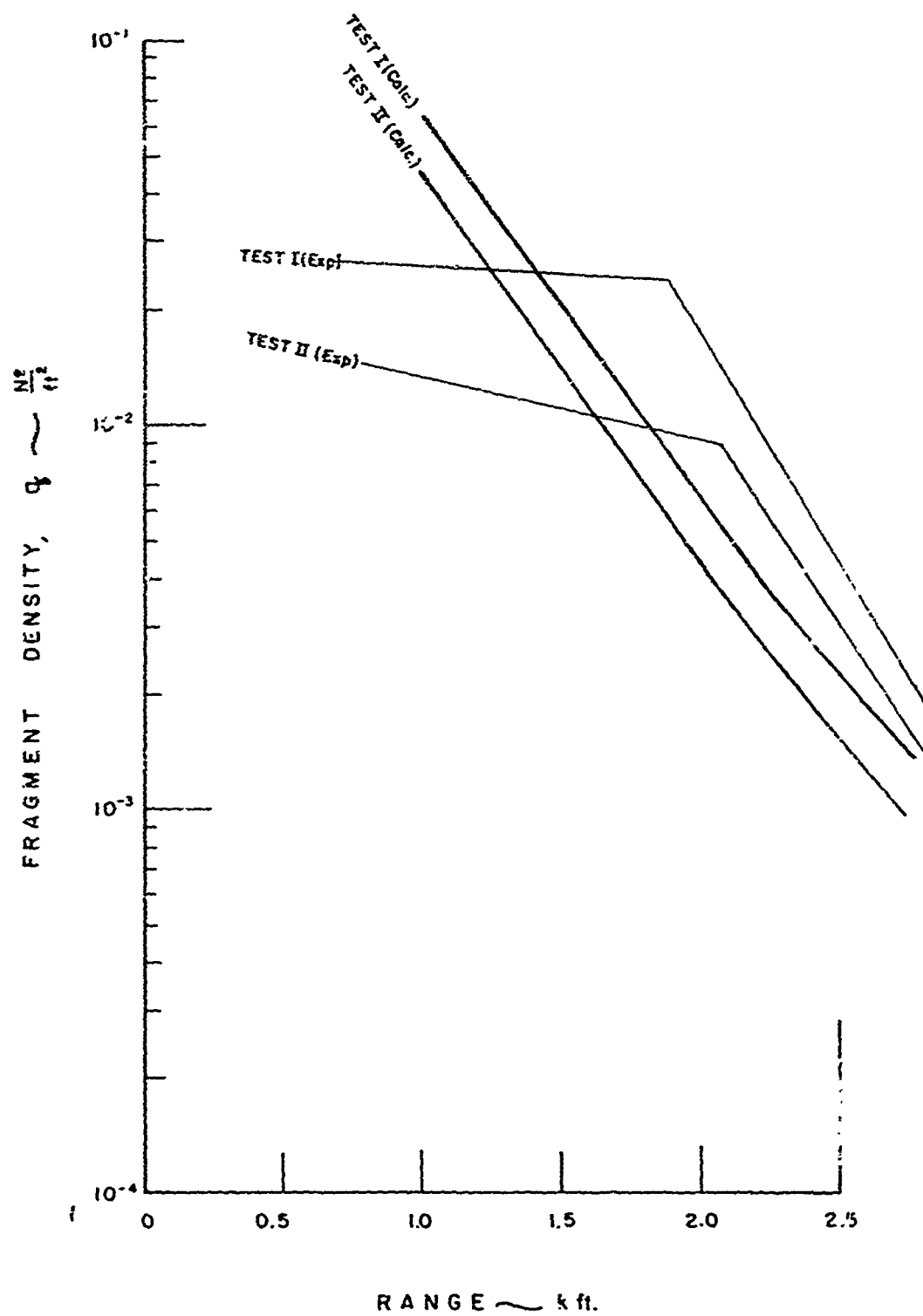
Figure 12. CALCULATED FRAGMENT DENSITY VERSUS RANGE-BIG PAPA

1164

Figure 13, CROSS SECTION OF PALLET STACK IN IGLOO MAGAZINE ESKIMO I.
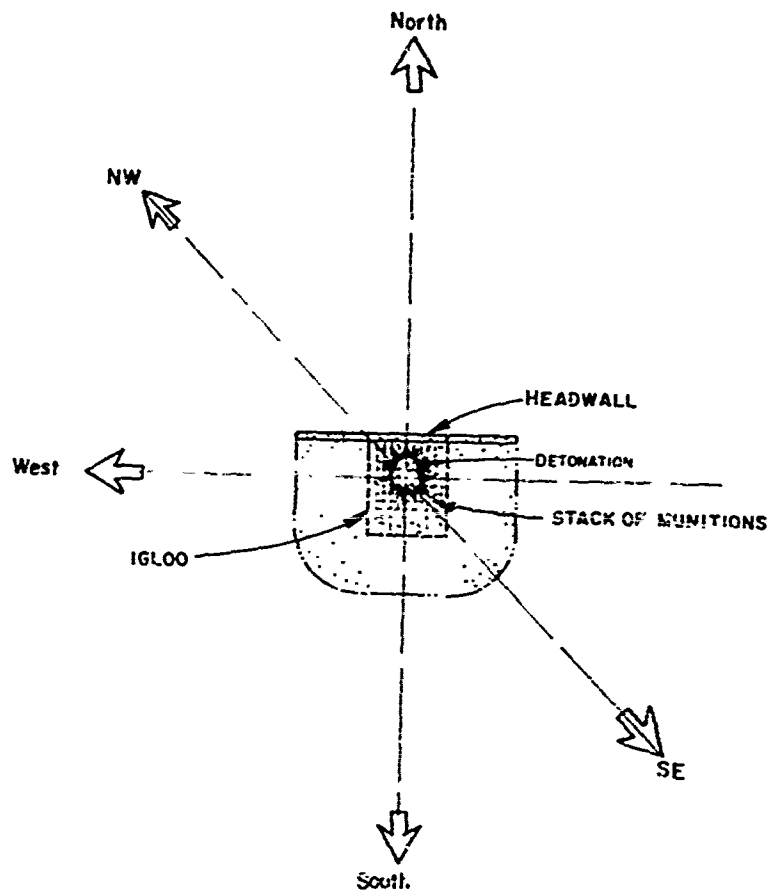
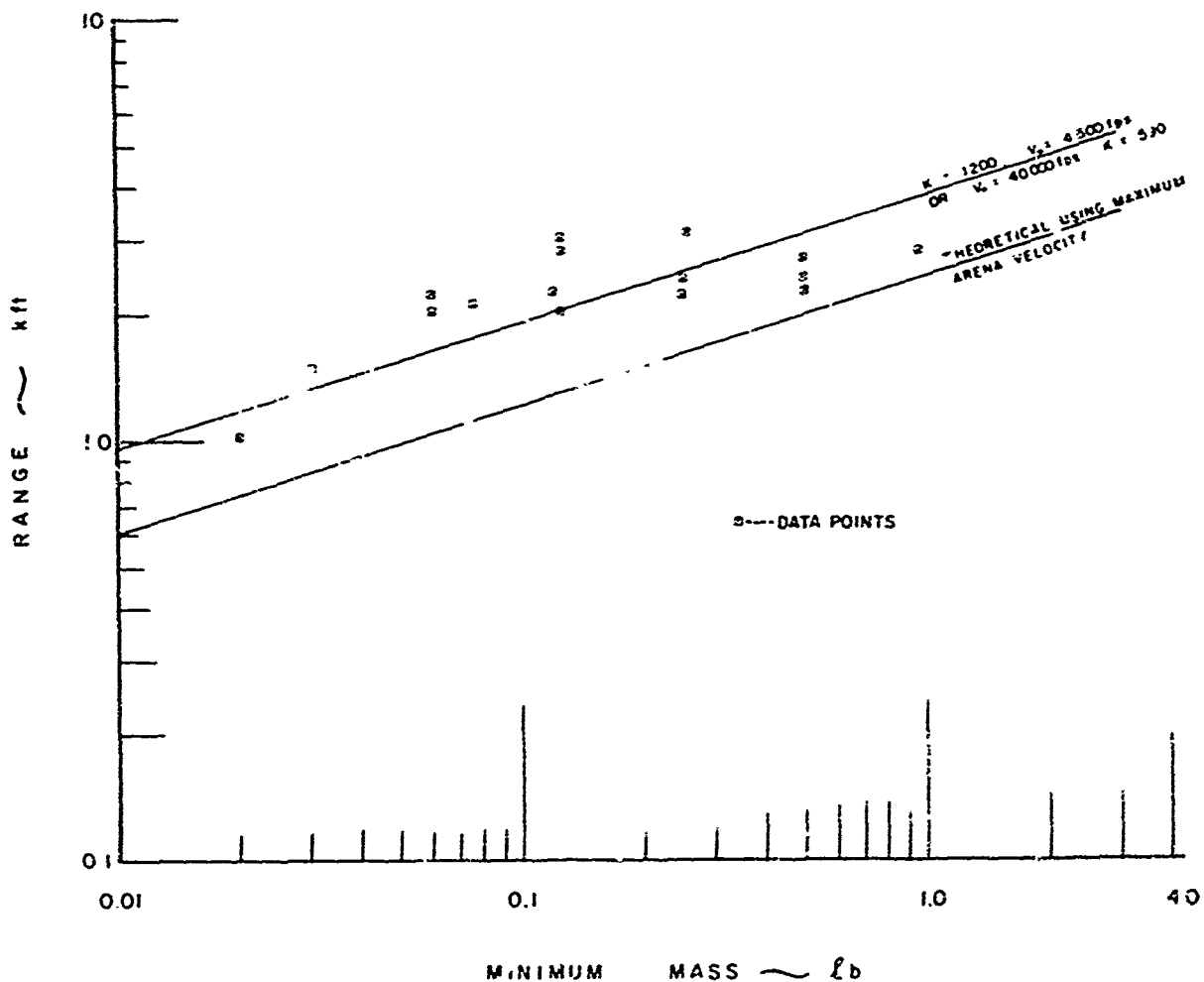Figure 14, PLAN SHOWING RAYS WHERE FRAGMENT DENSITIES WERE MEASURED. (ESKIMO I)

Figure 15, MEASURED MINIMUM MASS FRAGMENTS VERSUS RANGE-
ESKIMO I (EXP. WEALS 1973) COMPARED WITH THEORY-
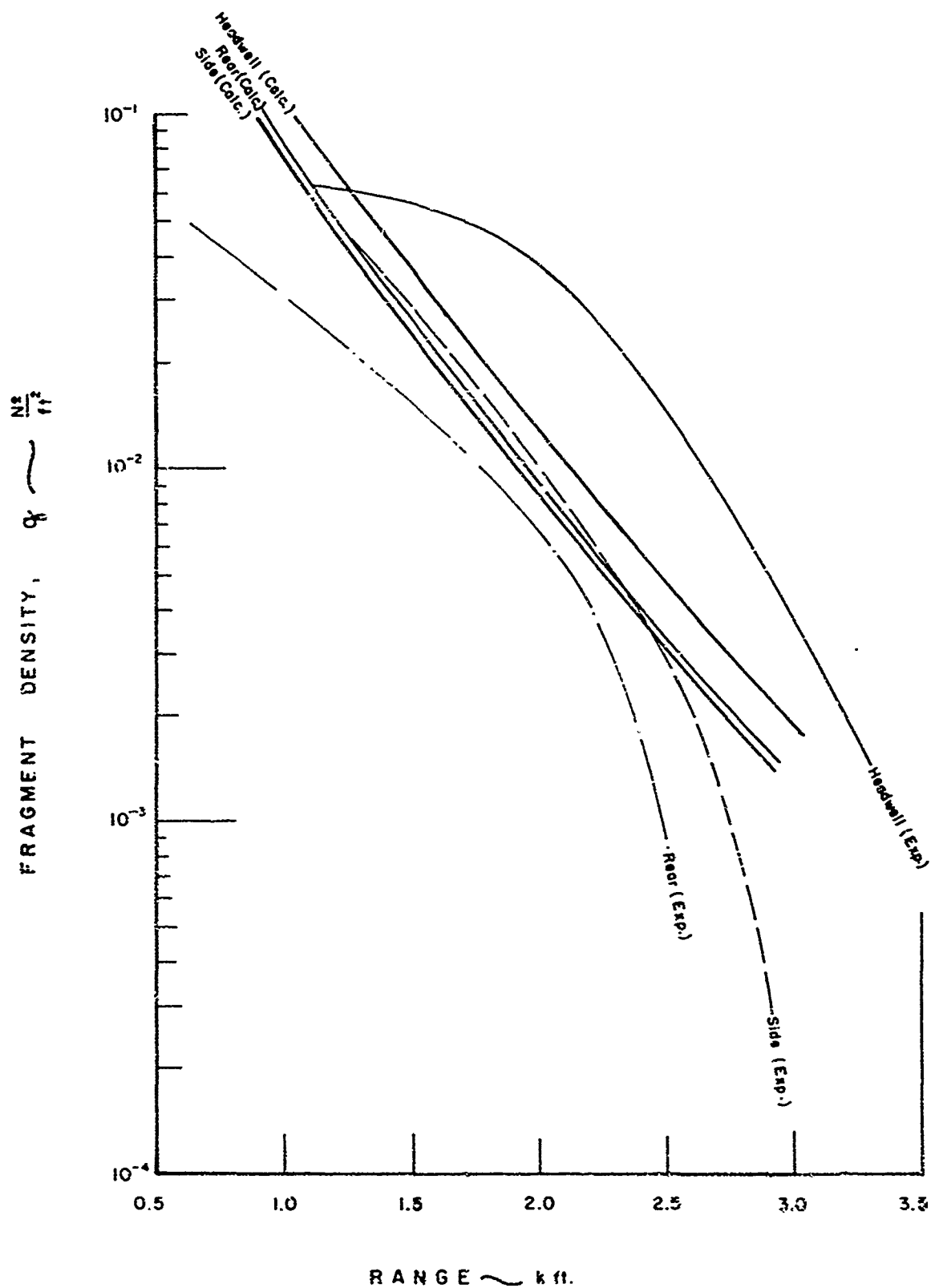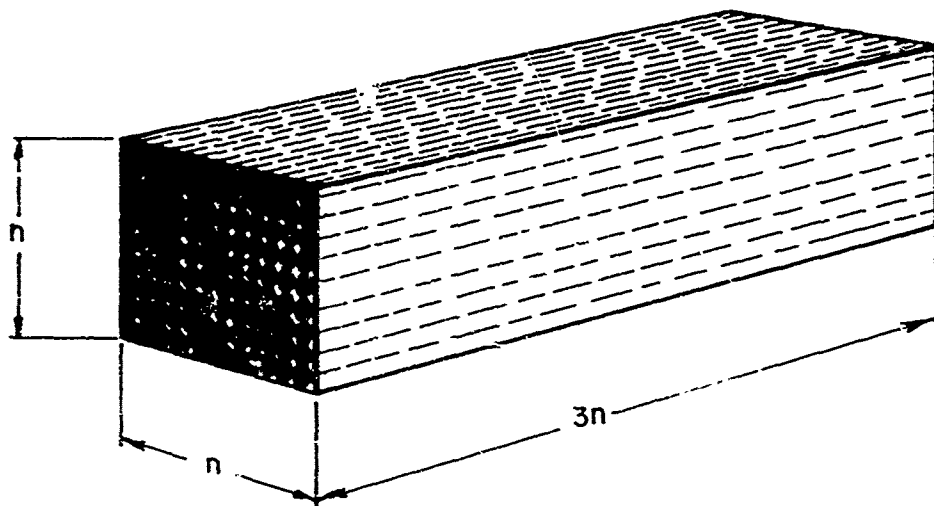FRAGMENTS EJECTED AT OPTIMUM LAUNCH ANGLE.

Figure 16, CALCULATED FRAGMENT DENSITY VERSUS RANGE, ESKIMO I.

n = Number of munitions in a direction

$3n^3$ = Total number of munitions in the stack

Figure 17. SCHEMATIC DIAGRAM OF THE STACK CONFIGURATION FOR THE EXAMPLE QUANTITY – DISTANCE CALCULATIONS.
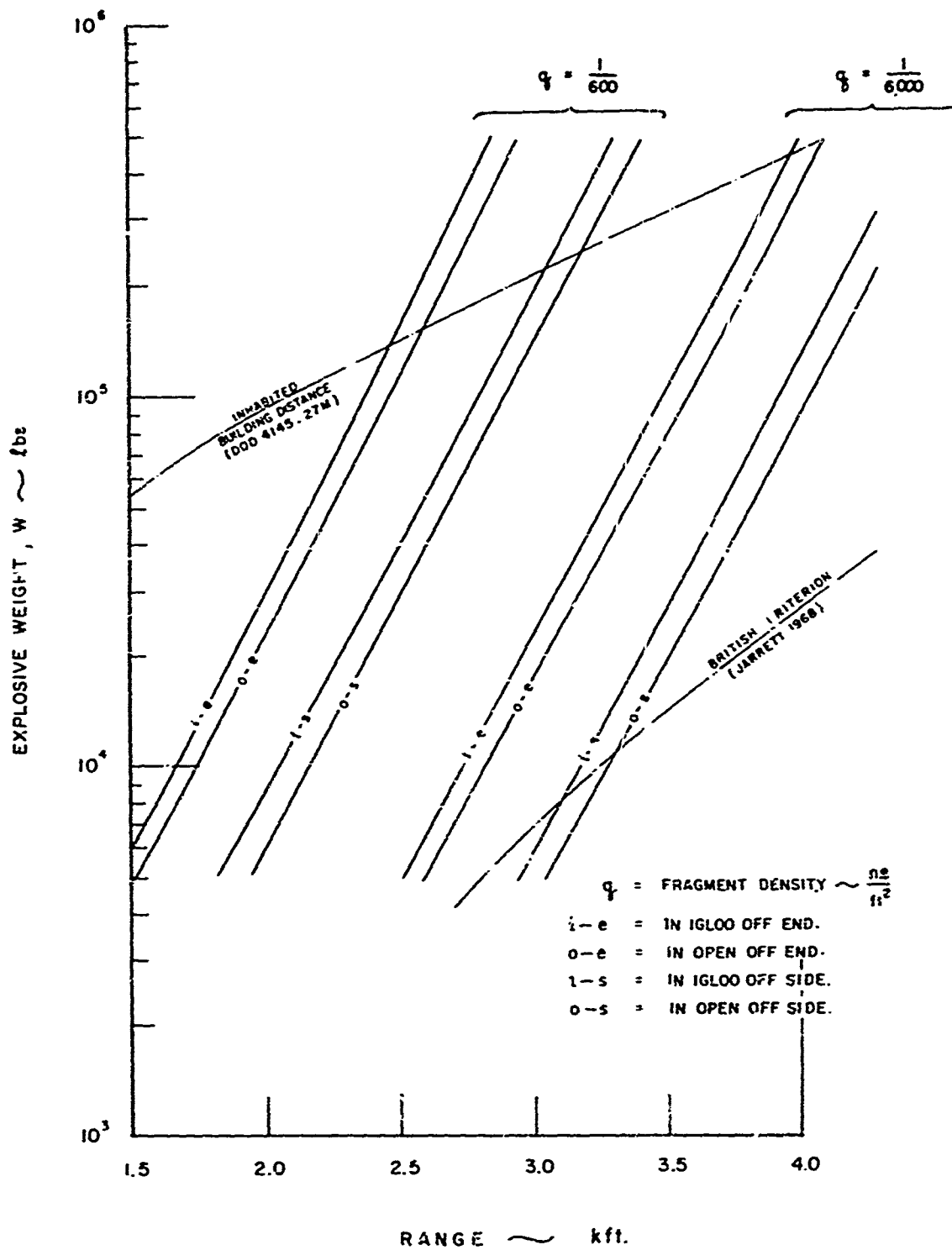
Figure 18. QUANTITY-DISTANCE FOR STACKS OF M117 750-lb. BOMBS.

1170

ASSEMBLY AND ANALYSIS OF FRAGMENTATION DATA FOR LIQUID PROPELLANT VESSELS

W. E. Baker, V. B. Parr, R. L. Bessey and P. A. Cox

Southwest Research Institute
San Antonio, Texas

ABSTRACT

The objective of this work was to assemble and analyze fragmentation data for exploding liquid propellant vessels. These data were to be retrieved from reports of tests and accidents, including measurements or estimates of blast effects, fragment velocities, masses, shapes, and ranges. Correlations were to be made, if possible, of fragmentation effects with type of accident, type and quantity of propellant, blast yield, etc. A significant amount of data was retrieved from a series of tests conducted for measurement of blast and fireball effects of liquid propellant explosions (Project PYRO), a few well-documented accident reports, and a series of tests to determine autoignition properties of mixing liquid propellants. The data were reduced and fitted to various statistical functions. Comparisons were made with methods of prediction for blast yield, initial fragment velocities, and fragment range. Reasonably good correlation was achieved. This work was conducted for the NASA-Lewis Research Center under Contract NAS3-16009.

I. INTRODUCTION

The primary hazard relating to large-scale explosions has been assumed to be the blast wave generated by the explosion; thermal effects to be next, and effects of damaging fragments to be last. The study reported in this paper partially rectifies this assumption by providing a comprehensive analysis of fragmentation effects of bursting liquid propellant vessels.

In assessing fragmentation hazards for any source of fragments, a number of questions must be answered:

- How many fragments are produced?

- Of what sizes, shapes and masses?

- Where do they impact, and with what velocities and orientations?

- How do fragment characteristics relate to explosion parameters such as blast yield?

- What are the terminal ballistics effects of fragment impact on people and other "targets"?

Many experimental studies and supporting analyses have been conducted to answer these questions for cased explosion munitions, but relatively few have been addressed to other explosion hazards which can project damaging fragments. This study addressed all five questions for bursting liquid propellant vessels, but emphasized the first four, with only a cursory look at terminal ballistics effects. This paper is a drastically condensed version of the full report of the study, Ref. 1.

II. BACKGROUND

In storage or in a launch configuration within tankage in a rocket motor, liquid propellants are initially contained within vessels of various sizes, geometries, and strengths. Various modes of vessel failure are possible, from either internal or external stimuli. If the vessel is pressurized with static internal pressure, one mode of failure is fracture, instituted at a critical size flaw and propagated throughout. A similar failure can occur if the vessel is accidentally immersed in a fire, and pressure increases internally because of vaporization of the propellant. Some launch vehicles have the liquid fuel and oxidizer separated by a common bulkhead. Accidental overpressurization of one of these chambers can cause rupture of this bulkhead, and subsequent mixing and explosion of the propellant. External stimuli which can cause vessel failure include high-speed impact by foreign objects, accidental detonation of the missile warhead, dropping a tank (as in toppling of a missile on the launch pad), etc. Vessel failure can result in an immediate release of energy or it can cause later energy release by propellant and oxidizer mixing and subsequent ignition. Other modes of failure which have resulted or could result in violent explosions are fall-back immediately after launch due to loss of thrust, or low-level failure of the guidance system after launch causing an impact into the ground at several hundred feet per second.

Failure of a vessel containing liquid propellants can result in various levels of energy release, ranging from negligible to the full heat value of the combined propellant and oxidizer. Toward the lower end of the scale of

energy release might be the failure of a pressurized vessel caused by crack propagation. Here, the stored pressure energy within the compressed propellant or gas in an ullage volume above the propellant could accelerate fragments of the vessel or generate a weak blast wave. In the intermediate range of energy release could lie vessel failure by external stimulus and ignition, either very rapidly or at very late times, so that only small proportions of mixed propellant and oxidizer contribute to the energy release. At the upper end of the scale could be the explosion of a mixed propellant in a vessel wherein a premixed propellant and oxidizer detonate as a high explosive, and explosions resulting after violent impact with the ground. In studies of possible blast and fragmentation effects from vessel rupture, a critical problem has been to accurately assess the energy release from the accident or incident. A common method of assessment of possible energy release has been on the basis of equivalent pounds of TNT. This method is used because a large body of experimental data and theoretical analyses exist for blast waves generated by TNT or other solid explosives (Refs. 2 and 3). Although the comparison with TNT is convenient, the correlation is far from exact. Specific energies which can be released, i.e., energy per unit volume or mass of reacting material, differ quite widely for TNT and various liquid propellants or mixtures of liquid propellants and oxidizers (Ref. 4).

Dependent on the total energy and violence of this energy release, the sizes and shapes of fragments generated by bursting liquid propellant vessels and their appurtenances cover a very wide spectrum. At one extreme is a vessel bursting because of seam failure or crack propagation from a flaw wherein only one "fragment" is generated, the vessel itself. This fragment can be propelled by releasing the contents of the vessel. At the other extreme is the conversion of the vessel and parts near it into a cloud of small fragments by an explosion of the contents, similar to a TNT explosion (Refs. 5 and 6). For most accidental vessel failures, the distribution of fragment masses and shapes undoubtedly lies between these two extremes. The modes of failure of the vessel may be dependent upon details of construction and the metallurgy of the vessel material. Some of the masses and shapes are dictated by the masses and shapes of attached or nearby appurtenances. In any event, assessment and prediction of these parameters is much more difficult than is true for the better understood phenomenon of shell casing fragmentation.

Once the masses, shapes, and initial velocities of fragments from liquid propellant vessels have been determined, the trajectories of these fragments and their losses in velocity caused by air drag must be computed. This problem is one of exterior ballistics. It differs from conventional exterior ballistic studies of trajectories of projectiles, bombs, or missiles because the body in flight is invariably very irregular and is usually tumbling

violently. Exact trajectories cannot be determined as they can for well-designed projectiles. Only approximate trajectories can be estimated, usually by assuming "equivalent spheres" or other geometric shapes for which exterior ballistics data and techniques exist. But, in some fashion, ranges and impact velocities for fragments which are initially projected in specified directions can be predicted from the bursting vessel with specified initial velocities. Such analysis is given by Ahlers (Ref. 7).

This problem is not complete until one can assess the effect of fragments from the burst propellant vessels on various "targets". For a proper assessment of hazards, one should consider a wide variety of targets, including humans, various classes of buildings, vehicles. and even aircraft. Problems of this nature are exceedingly compi-   not only because of the inherent statistical nature of the characteristics of the impacting fragments but also because the terminal ballistic effects for large irregular objects impacting any of the targets described are not well known. In most studies of fragment damage from accidents, the investigators have been content to simply locate and approximate the size and mass of the fragments in impact areas and have ignored the important problem of the terminal ballistic effect of these fragments.

Extensive studies have been conducted for many years regarding the related problem of potential failure of nuclear reactor vessels from a variety of causes. The source of energy causing a reactor vessel failure can be stored compressive energy in a liquid or gas within the containment vessel, a chemical energy release, or an uncontrolled nuclear energy release. The latter source is, of course, not present in the failure of liquid propellant vessels, but the first two sources are present. Although many of the studies of nuclear reactor vessels have concentrated on the design of the pressure vessel and the attachments to it to obviate failure, many other studies also have been concerned with shock and fragmentation effects if failure occurs. Work which can be related in some respects to fragmentation of liquid propellant vessels is reported in Refs. 8 through 11.

Project PYRO involved many test explosions with liquid propellants. The purpose of Project PYRO (Refs. 12 through 14) was "to develop a reliable philosophy for predicting the damage potential which may be experienced from the accidental explosions of liquid propellants during launch or test operations of military missiles or space vehicles '. Three combinations of propellants and oxidizers were chosen for test and evaluation, and at lease seven agencies were involved in the program. The primary objective was to determine and estimate blast yield and its effects; fragmentation studies were secondary. But Jeffers (Ref. 15) analyzed a small number of the photographic records to determine fragment velocity. (As will be apparent later in this paper, the films from Project PYRO, when studied carefully, provide the primary source of data for initial velocities

for liquid propellant explosions.)

There are a number of experimental studies and analyses of the effects of bursting pressure vessels which fail under the action of internal energy sources other than liquid propellants or runaway nuclear reactors. A number of these can provide useful information. They are reported in Refs. 16 through 22. Usually, the internal energy source was a compressed gas.

III. RETRIEVAL OF FRAGMENTATION DATA

Agencies were contacted to obtain data on fragmentation of bursting liquid propellant vessels and launch vehicles. These included all major NASA centers, several AEC laboratories, the military service ordnance laboratories, missile launch ranges, the Department of Defense Explosive Safety Board, and commercial and other contractors. Visits were made to those agencies which had relevant data, and reports and films of tests or accidents involving vessel fragmentation were obtained. The agencies visited and the type of data obtained are summarized in Ref. 1.

The primary useful sources of data were "missile maps" from several tests and accidental explosions, the reports for Project PYRO (Refs. 12 through 14) and the motion pictures of the PYRO tests. In all, eight "events" were discovered with missile maps giving size, shape and range of fragments which were sufficiently detailed for valid statistical treatment. No reported data were found on initial or final impact velocities of fragments, but the PYRO films provided raw data which were analyzed to obtain initial velocities for some tests. The reported PYRO blast data gave an accurate measure of blast yield for correlation with initial velocities. Only one experiment yielded data for initial velocities, blast yield, and a missile map - a test of a Saturn IV stage during the PYRO series.

IV. MEASUREMENT OF FRAGMENT VELOCITIES

We noted earlier that we found no reported reduced data on either initial or impact velocities from bursting liquid propellant vessels. But, during the PYRO experiments, several motion picture cameras with intermediate to high framing rates (64 to 1000 frames/sec) filmed each test for the primary purpose of obtaining data on fireball size as a function of time. We reviewed all of the PYRO films at the repository for data from these tests (Air Force Rocket Propulsion Laboratory at Edwards Air Force Base, California), and borrowed the films where fragments were visible.

There were 94 PYRO tests which yielded measurable fragment velocity data. For most of these experiments, several camera views of each test were available. Film speeds were accurately determined, with timing marks at known repetition rates impressed on the edges of most films. The tests for which we reduced fragment velocity data represented a spectrum of propellant types, scale of test, and type of simulated accident. In addition, reduced blast data and measured blast yields are known for each experiment and reported in Refs. 12 and 13. Cameras were located during PYRO tests along radial lines at azimuth angles 0°, 240° and 340° and on a tower directly above the event. A few tests were also photographed from airplanes and from the tops of nearby mountains, but these cameras were located too far away to provide fragmentation data. The greatest number of films and the largest amount of data came from cameras located at the azimuth angles of 0° and 240°. These cameras were 420 feet from the center of the test pad, and from these positions, filmed the event with several different focal length lenses and at framing rates ranging from 64 pps to 1,000 pps. Cameras at azimuth position 340° were located radially 1,050 feet from the center of the test site and were mounted 146 feet above it. Only a few tests were photographed from this location and not all of the films provided fragmentation data. Some cameras had a field of view which was so large relative to the size of the fireball that fragments could not be seen. Other cameras with longer focal length lenses provided good film data. Overhead shots from the tower above the test pad provided very little usable data because fragments were obscured by the fireball.

Film data reduction was accomplished using a Vanguard Film Analyzer. Data obtained from the films included the frame number, relative to the initiation of the explosion, the X and Y positions of the fragment referenced to the frame numbers, the spacing of the timing marks, the height to the top and bottom of the tank, the tank diameter and, if in the field of view, the height of the tower above the test pad. If available, the height of the tower was used for computing the scale factor; otherwise, tank dimensions were used. Since each test was viewed from more than one direction (primarily from camera locations at azimuth angles at 0° and 240°), an attempt was made to identify the fragments in camera views from two locations. When available, such data permitted a fairly accurate determination of the flight path of the fragments. If the fragments were identified only in a single view, their flight paths were by necessity assumed to lie in a vertical plane normal to a radial line defining the azimuth position of the camera.

A computer program was written to process the data received in punched card form from the Vanguard Analyzer. Although the details of the program will not be presented here, it solves the equations describing the geometry and prints the results in a usable form. The program also creates a tape file for statistical analysis of the results.

The fragment velocity data measured from the PYRO films are available on punched cards and in computer printouts. A partial summary of the data for one group of tests is shown in Table 1 (a complete summary is available in Ref. 1). The key designator for all data is the PYRO test number, given in the left-hand column. The next five columns are data from Ref. 12, while the last four columns are the reduced fragment velocity data. Yield is the measured blast terminal yield, expressed as a percent of propellant weight in TNT which would produce the observed blast wave characteristics far from the explosion. The last two columns give the mean initial velocities and standard deviations of these means for the number of fragments observed (seventh column) for each test. The third column did not apply to this particular group of tests, but was important for drop and high velocity impact tests.

The data represent a wide spectrum of test conditions, propellant types, and propellant weights, allow some correlation with methods of prediction of initial velocity, and also lend themselves to various types of statistical analysis. A limitation to the data which renders statistical studies difficult is that relatively few fragments could be observed in any one test. Some grouping between tests with different propellants, different blast yields, etc., has proven possible. It was not possible to obtain any reasonable estimates of size, mass or shape of fragments from the films, and only a very few fragments could be identified as the same fragment from more than one camera.

V. FRAGMENT PHYSICAL CHARACTERISTICS AND RANGE

All of the accident and test data retrieved was reviewed for pertinent information on fragment size, weight, distance, and distribution. The criteria for each fragment were that the range, weight and maximum projected area be specified. The nature of the test or accident, blast yield, type of propellants, etc., were also of interest.

From approximately 168 reports and memos reviewed, only eight events, listed in Table II, yielded sufficient information to meet the above criteria. There were many other reports which had partial information, such as distance listed for fragments over 5 pounds, with fragments under 5 pounds listed in number per square yard.

The eight events listed in Table II can be classified in the following three groups:

(1)   Events 1 and 2 were Saturn IV confined by missile (CBM), LO_2/LH_2 explosions.

TABLE I

PARTIAL SUMMARY OF FRAGMENT VELOCITY MEASUREMENTS

(LO_2/RP-1 CONFINEMENT-BY-THE-MISSILE TESTS)

Test No.	Prop. Wt (lb)	Impact Or Drop Velocity (ft/sec)	Ignition Time (msec)	Yield (%)	Tank L/D	No. Of Camera Views	No. Of Fragments Observed	Mean Velocity $\bar{V}$ (fps)	Standard Deviation σ_v (fps)
48	200	---	310	9.8	5.58	2	12	300	263
49	200	---	316	12	5.58	2	16	394	305
58	200	---	200	27	2.14	2	14	434	192
87A	200	---	70	16	2.14	2	15	698	374
88	200	---	60	4	5.58	2	13	291	111
95A	200	---	120	17	2.14	2	13	660	459
192	1000	---	216	14	2.07	2	14	484	246
193	1000	---	222	20	2.07	2	18	621	312
209	1000	---	121	10	2.07	3	15	898	637
237	200	---	127	32	2.14	2	5	608	287
270A	1000	---	225	13	2.07	4	32	515	289
275	25000	---	515	4	2.14	4	20	265	202
278	25000	---	530	13	2.14	3	16	507	451
282	25000	---	540	13	2.14	3	13	976	615
301	94000	---	840	4	---	2	9	962	143

TABLE II

CHART OF EVENTS GIVING FRAGMENT CHARACTERISTICS

Event No.	Ref. No.	Test or Accident Type	Propellant Type	Total Propellant Weight (lb)	Blast Yield Y, (%)
1	13	PYRO Test 62 (SATURN IV)	LO_2/LH_2	91,000	5.0
2	24	S-IV	LO_2/LH_2	101,198	1.1
3	23	J2 Spill Test	$LO_2/LH_2/$ RP-1	1,754	23.0
4	23	J3 Spill Test	$LO_2/LH_2/$ RP-1	1,754	24.4
5	23	J1 Spill Test	$LO_2/LH_2/$ RP-1	4	62.6
6	25	Mixing Test	LO_2/LH_2	240	86.0
7*	--	Mixing Test	LO_2/LH_2	240	70.0
8*	--	Mixing Test	LO_2/LH_2	240	73.0

---

* Data from these tests were furnished by the NASA test director, Mr. J. H. Deese. There is no formal reference.

(2)   Events 3, 4, and 5 were spill tests using three tanks, on 120° radials with $LO_2/LH_2/RP-1$, and mixing on the ground (CBGS).

(3)   Events 6, 7, and 8 were mixing tests using two tanks with LO_2/LH_2 and pouring the contents of one tank into the other.

The data from each of the events were reduced by careful analysis of each fragment to assure that size (maximum projected area), weight, and distance were specified. In some cases, it was possible to fill in missing items by estimating weight and/or size from information supplied by descriptions or photographs. Because of the paucity of fragment data, considerable effort was expended to extract as much fragment data as possible, without undue loss in accuracy of the parameters. Distances for each fragment were determined from fragment maps.

For each event, fragment data by event code, fragment number, distance (R), weight (W), width, length, maximum projected area (A), area divided by weight (A/W), and drag coefficient (CD) were entered on key punch sheets. The drag coefficients were estimated from photographs and descriptions, and subsequent comparison with data from Ref. 26. Cards were keypunched and used in the analyses described below.

Using standard computer programs with a CDC 6500 computer, the data from each event were subjected to the following routines:

(1)   Means and variances were calculated for R, W, A, A/W, CD, Log R, Log W, Log A and Log A/W.

(2)   Histograms were constructed for the parameters listed in (1) above.

(3)   Correlation plots were made for R versus W, R versus A, R versus A/W, R versus Log W, and R versus (A/W) CD.

The output from the correlation routine was studied to determine if there were discernable patterns of correlation between parameters within an event. While there was some general pattern in some cases, as a whole the scatter was so great as to discourage further inquiry along these lines. This result could be explained by not considering the flight angle and initial location of the fragments.

The histograms were studied to relate the parameters R, W, A, and A/W to probability frequency of distributions. Since the sample size

varied from 31 to 1,056, the histograms varied in information content in about the same ratio. However, the form of some of the histograms suggested that a normal probability density function would supply an adequate fit, and others offered the possibility of a good fit by a log normal distribution. The Weibull distribution was also considered, but later results showed that better fits were obtained by the normal and log normal distributions.

In order to equalize the effects of varying sample size, the data for each parameter of interest within an event were sorted in ascending order, and the value for the parameter for the 10th, 20th, 30th, 40th, 50th, 60th, 70th, 80th, and 90th percentile was identified. A plot on normal and log normal probability paper was then made for each parameter for each event. Figure 1 is a plot of distance for event 3 on normal probability paper, while Figure 2 is a plot of the same data on log normal probability paper. Since the points on the normal probability paper lie closer to a straight line than those on the log normal paper, the normal distribution is a better fit. From the plots over all 8 events, the normal distributions adequately fitted the distance (R), and A/W and that log normal distributions best fit the weight (W) and area (A). A complete summary of the fragment data is listed in Table III, giving the estimated standard deviation (S), and mean (M) for the respective distributions for each parameter in each event.

A "W" statistic for goodness of fit for each parameter was calculated using the methods outlined by Hahn and Shapiro (Ref. 27). The approximate probability of obtaining the calculated test statistic, given that the chosen distribution is correct, was then determined. There are thirty-two distributions, one each for R, W, A, and A/W for each of the eight events. The probability of obtaining the calculated value of W is greater than 50% for all except the A/W distributions for events, 3, 4, and 5, indicating adequate fits for all except these three distributions, as it is customary to consider values exceeding 2 to 10% as adequate grounds for not rejecting the hypothesis that the data belong to the chosen distribution. It is interesting to note that each of the parameters is distributed in the same family (i.e., normal or log normal) across all eight events. That is, distance (R) has a normal distribution function in each of the eight events, indicating a repeatable pattern. Estimates for the means and standard deviations for each of the distributions are given in Table III.

A regression analysis was conducted to determine variation of range of fragments with explosive energy. First, the mean distance R in feet versus yield Y in percent was plotted on log-log paper for each of the eight events. The three mixing tests, events 6, 7 and 8, were grouped together and apart from the data for the other five events. A regression equation was then derived to describe a linear fit to the points for events 1 through 5. This equation is
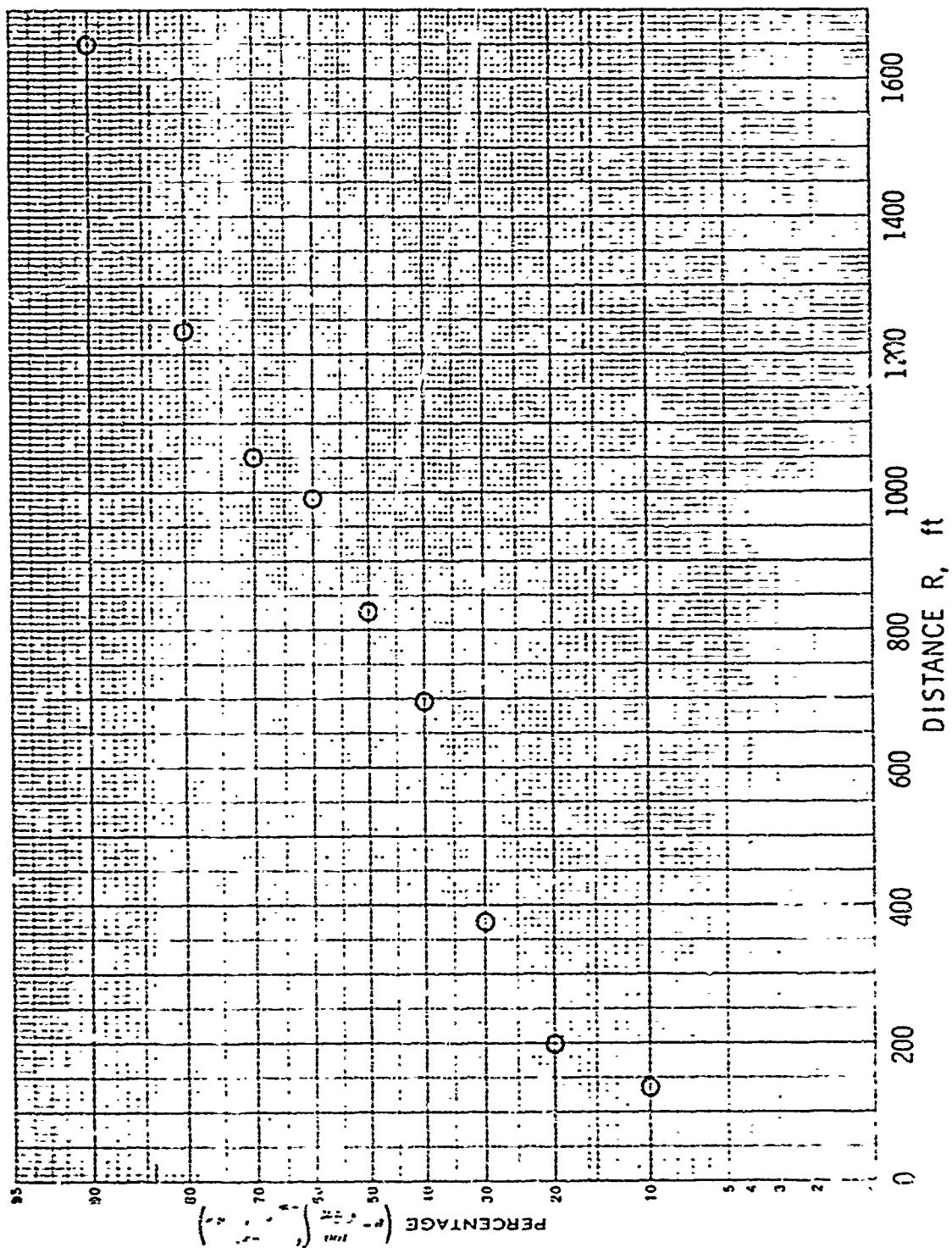
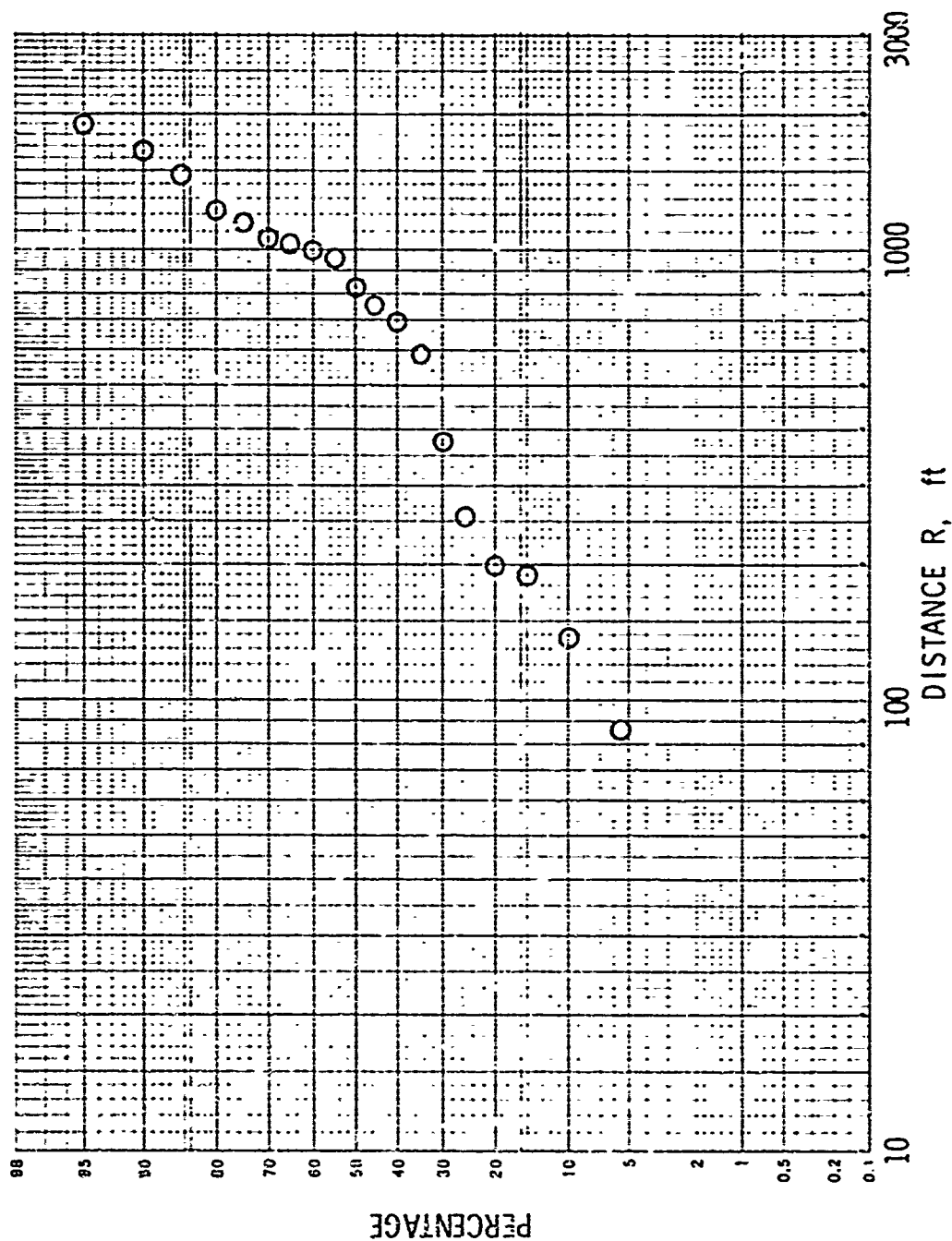FIGURE 1 . EVENT 3 PROBABILITY DISTRIBUTION (NORMAL), DISTANCE R

DISTANCE R, ft

PERCENTAGE

3000

1000

100

10

88
85
80
80
70
60
50
40
30
20
10
5
2
1
0.5
0.2
0.1

FIGURE 2. EVENT 3 PROBABILITY DISTRIBUTION (LOG NORMAL), DISTANCE R

TABLE III

SUMMARY OF FRAGMENT DATA

Event No.	No. Of Fragments	Yield, Y %	Yield, Y lbs TNT	R[1] Range, (ft) Dist	M	S	Weight, W, (lb) Dist	M	S	Area, A, IN² Dist	M	S	Area/Weight Dist	M	S
1	341	5.0	4.55×10^2	N	447	194	L	4.98	2.23	L	344.9	2.8	N	86.9	60.6
2	38	1.1	1.08×10^3	N	377	203	L	26.49	3.14	L	299.5	7.16	N	54.9	46.2
3	105	23.0	4.03×10^2	N	830	557	L	38.82	3.25	L	331.5	4.4	N	22.7	57.6
4	86	24.4	1.35×10^2	N	740	342	L	56.35	2.82	L	667.7	3.98	N	16.2	10.8
5	31	62.6	1.097×10^3	N	986	574	L	51.16	2.42	L	293.5	2.75	N	8.8	9.0
6	1056	86.0	2.06×10^2	N	158	88	L	0.05	6.95	L	3.3	5.2	N	171.3	149.3
7	325	70.0	1.67×10^2	N	152	86	L	0.16	5.04	L	6.9	5.0	N	83.7	233.4
8	252	73.0	1.75×10^2	N	152	79	L	0.17	6.54	L	9.8	5.3	N	99.4	122.7

(1) Dist. is the type of frequency distribution.

N is normal, and

L is log normal

$$R = 315 \, Y^{0.2775}$$

Data points and the regression line are shown in Figure 3.

Figure 3 also shows the estimated distance which should contain at least 95% of the fragments. Needed to make this estimate are the upper 95% confidence limit (CL) on the estimate of the mean (M), and the upper 90% confidence limit on the estimate of the standard deviation. The confidence limit on the mean was calculated using the following formula:

$$CL = M + \frac{S}{\sqrt{n}} \, (t_n \; ; \; 95) \, ,$$

where n is the number of fragments and $(t_n \; ; \; 95)$ is the value of the t distribution with n degrees of freedom at the 95th percentile.

The confidence interval for the standard deviation was calculated using the following formula:

$$CL = \frac{\Sigma X_i^2 - (\Sigma X_i)^2 / n}{X^2_{(n-1) \; ; \; 90}}$$

where X_i is the distance of the ith fragment, n is the number of fragments, and $X^2_{(n-1) \; ; \; 90}$ is the value of a chi square distribution with $n-1$ degrees of freedom at the 90th percentile. Then, using the new upper confidence level values of M and S, the range R_{95} in which 95% of the fragments should fall was calculated as follows:

$$R_{95} = M + S \, (t_n \; ; \; 95)$$

These values formed the upper ends of the vertical bars in Figure 3.

A line was then drawn parallel to the regression line, and just touching the longest bar. Thus, the distances read from this line could be expected to encompass at least 95% of the fragments resulting from a given yield.
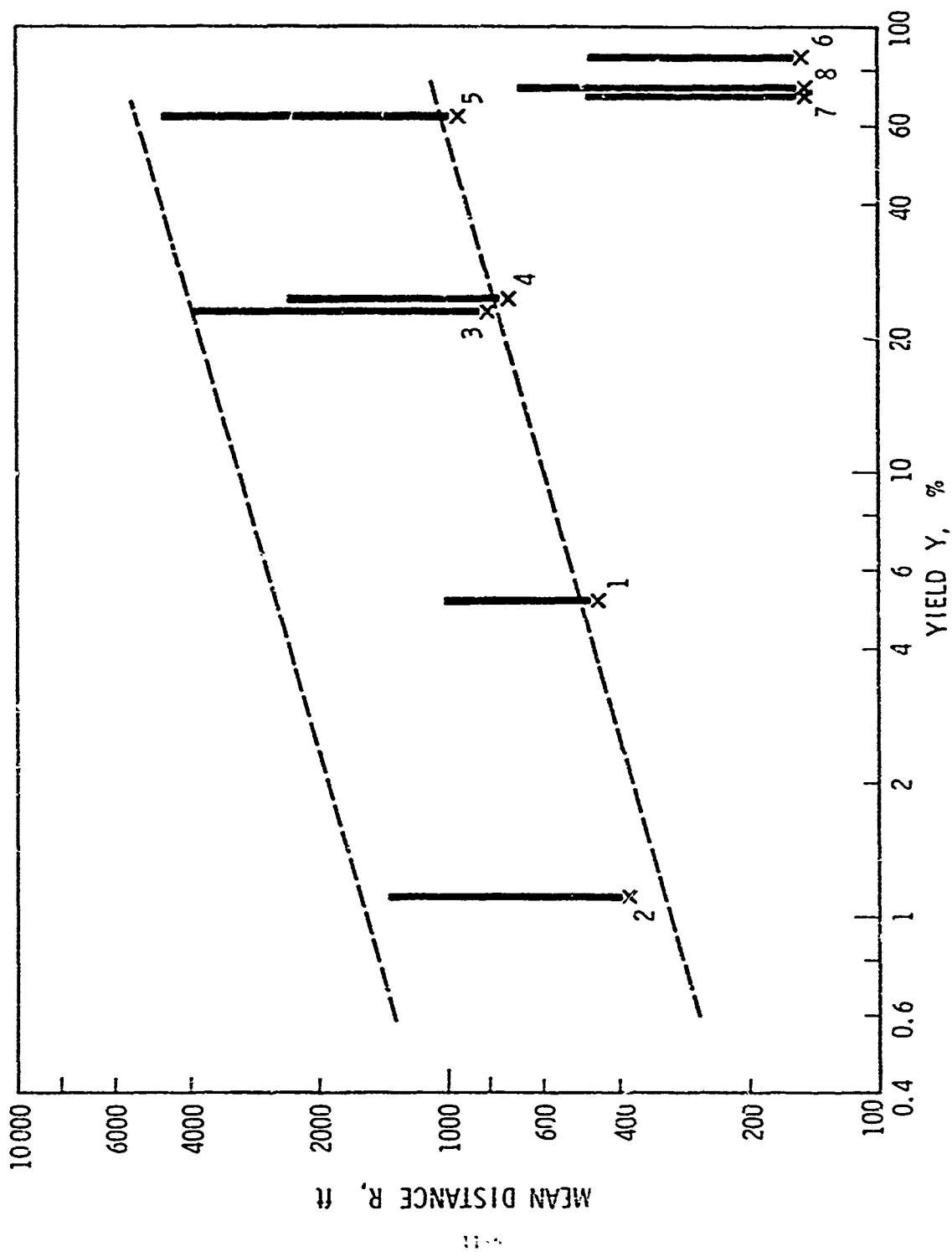
FIGURE 3. MEAN DISTANCE R VS. YIELD Y, WITH ESTIMATED RANGE
(CONTAINMENT) OF THE FRAGMENTS

VI. ESTIMATION OF BLAST YIELD

Although the primary purpose of the study reported here was to analyze and predict fragmentation of liquid propellant vessels, the energy released during liquid propellant explosions usually generates measurable blast waves in air. In the past, primary emphasis has been placed on the measurement or estimation of blast yield (synonymous with blast energy), so that data on blast yield and characteristics of blast waves from propellant explosions are much more voluminous than are data on fragmentation. Furthermore, the blast wave generated by propellant explosions can serve as the "driver" for accelerating fragments from appurtenances located near such explosions. For these reasons, some method of estimating blast yield is required in studies of fragmentation.

Explosive effects are often expressed in safety circles by comparison with blast waves generated by TNT. This has led to expression of blast yields in "equivalent pounds of TNT". But, liquid propellant explosions differ from TNT explosions in a number of ways, so that the concept of "TNT equivalence" is far from exact. Some of the differences are described below:

(1) The specific energies of liquid propellants, mixed in stoichiometric proportions, are significantly greater than for TNT[4] (Specific energy is energy per unit mass)

(2) Although the potential explosive yield is very high for liquid propellants, the actual yield is much lower because propellant and oxidizer are never intimately mixed in the proper proportions before ignition. The yield is very dependent on the mode of mixing of fuel and oxidizer, i.e., on the type of accident which occurs or is simulated. Maximum yields are experienced when intimate mixing is accomplished before ignition.

(3) Blast yield per unit mass of propellant decreases as total propellant mass increases. (This parameter is constant for TNT.)

(4) Confinement of propellant and oxidizer, and subsequent effect on explosive yield, are very different for liquid propellants and TNT. The degree of confinement can seriously affect explosive yield of liquid propellants, but has only a secondary effect on detonation of TNT or any other solid explosive.

(5)   The geometry of the liquid propellant mixture at the time
        of ignition can be quite different than that of the spherical
        or hemispherical geometry of TNT usually used for gener-
        ation of controlled blast waves. The sources of compiled
        data for blast waves from TNT or Pentolite such as Refs.
        2 and 3, invariably rely on measurements of blasts from
        spheres or hemispheres of explosive. The liquid propellant
        mixture can, however, be a shallow pool of large lateral
        extent at the time of detonation.

(6)   Spontaneous ignition can occur early in the process of
        mixing of fuel and oxidizer, even for propellants which
        are not hypergolic. This results in very low blast yield.

(7)   The blast waves from liquid propellant explosions show
        different characteristics as a function of distance from
        the explosion than do waves from TNT explosions. This
        is simply a manifestation of some of the differences dis-
        cussed previously, but it does change the "TNT equiva-
        lence" of a liquid-propellant explosion with distance
        from the explosion. Fletcher (Ref. 28) discusses these
        differences and shows them graphically in Figures 4 and 5.
        These differences are very evident in the results of the
        many blast experiments reported in Project PYRO (Refs.
        12 through 14). They have caused the coinage of the phrase
        "terminal yield", meaning the yield based on blast data
        taken far enough from the explosion for the blast waves
        to be similar to those produced by TNT. At closer dis-
        tances, two yields are usually reported; an overpressure
        yield based on equivalence of side-on peak overpressures,
        and an impulse yield based on equivalence of side-on positive
        impulse.

    We have reviewed the experimental and analytical work in blast
effects of liquid propellant explosions quite thoroughly, and the results of
this review are included in Ref. 1. Significant work other than that of
Project PYRO (Refs. 12 through 14) is reported by Farber and co-workers
in References 29 through 33, Pesante and Nishibazashi in Ref. 34, and
Gayle, et al, in Ref. 35. Several of the references, notably 14 and 29,
include methods of prediction of blast yield. We feel, however, that the
existing methods all have certain limitations and have devised our own
methods, combining parts of the previous methods.

    Our methods are based primarily on PYRO results (Refs. 12 through
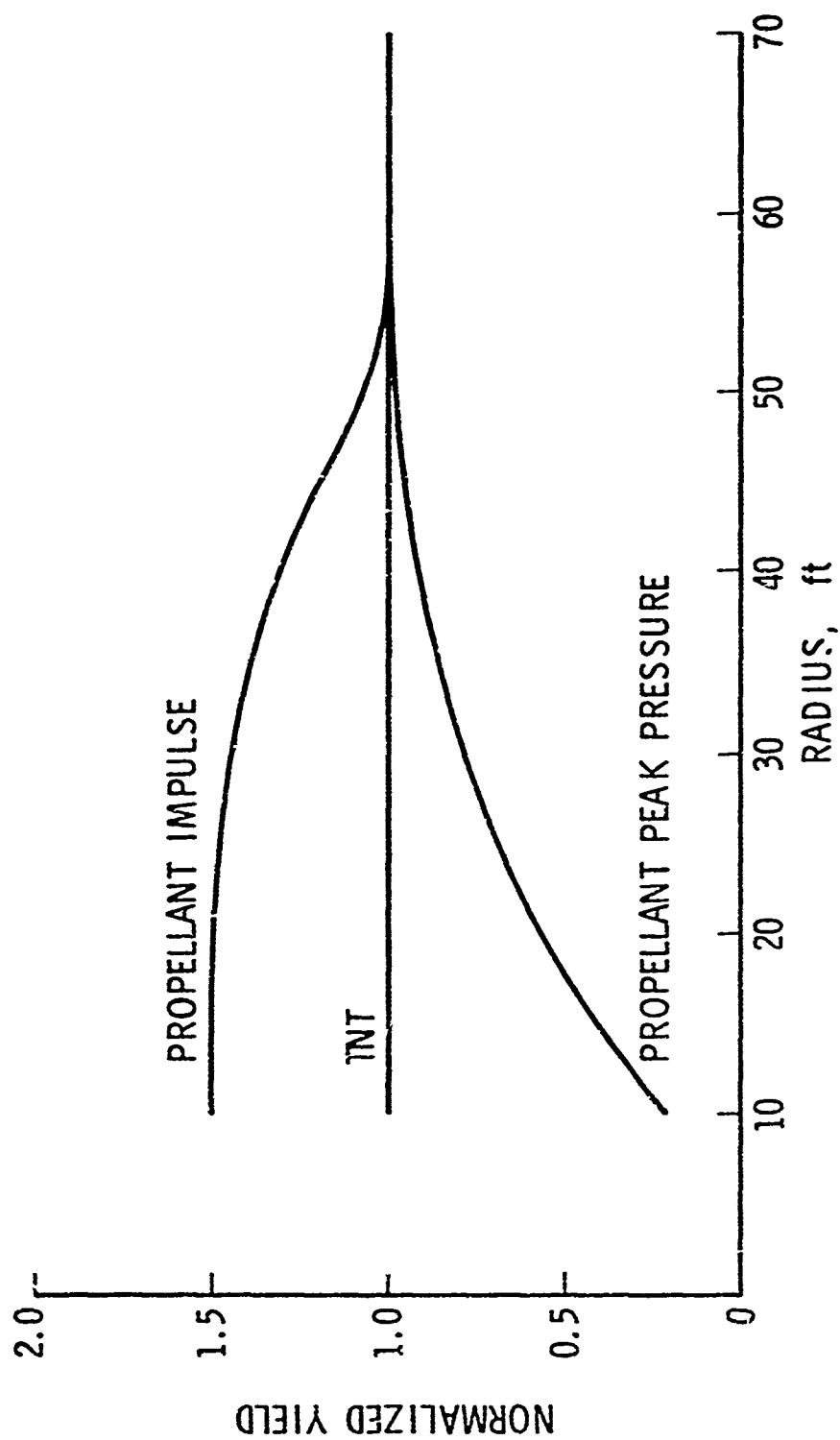14) and on the work of Farber and Deese (Refs. 29 through 33). These

FIGURE 4. NORMALIZED PRESSURE AND IMPULSE YIELDS FROM EXPLOSION OF N_2O_4/AEROZINE 50 (REF. 28)
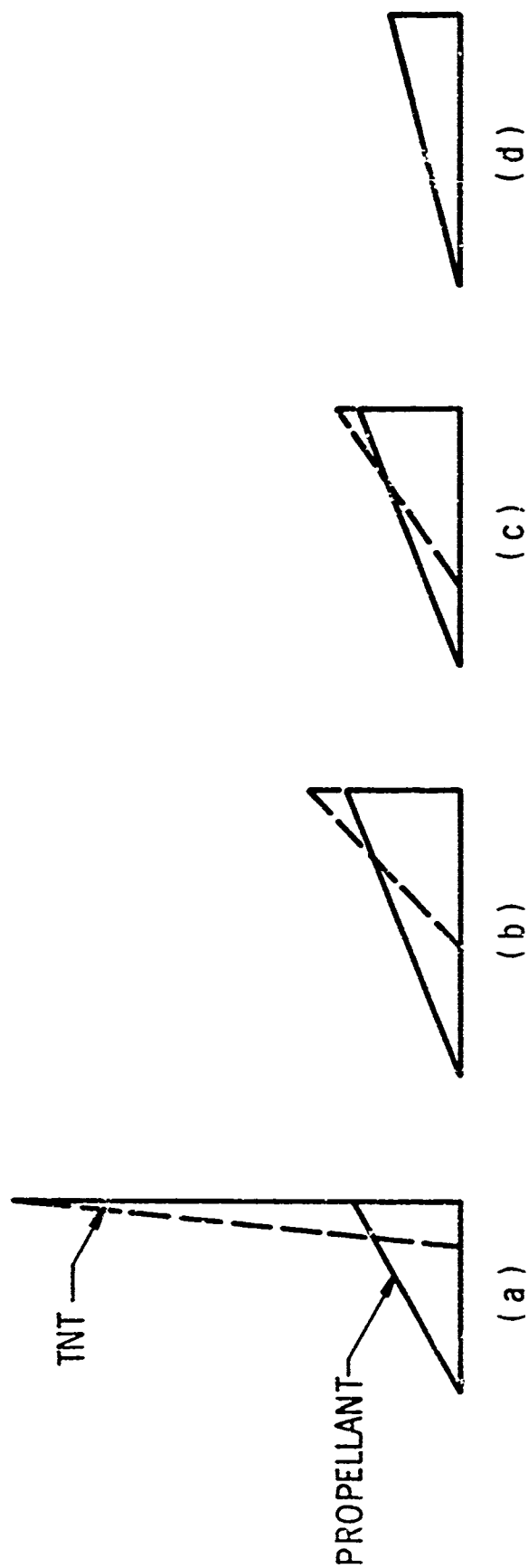
FIGURE 5. REPRESENTATIVE SHOCK IMPULSES SHOWING COALESCENCE OF SHOCK WAVES FROM DISSIMILAR SOURCES (STAGES a) THROUGH d))(REF. 28)

1190

methods retain many of the features of the previous work. Factors which appear to have a secondary effect on blast yield, such as L/D ratio of tankage, are ignored. The concept of "TNT equivalency" is used only to estimate the energy of a liquid propellant explosion and not to predict detailed blast wave characteristics. Blast is strongly dependent on type of propellant, type of simulated accident, impact velocity, and ignition time, so these factors must be accounted for in estimating blast wave characteristics and yield.

Throughout the PYRO work, blast yield is expressed as percent yield, based on an average of pressures and impulses measured at the farthest distance from the source when compared to standard reference curves (Ref. 2) for TNT surface bursts (terminal yield). Hopkinson's blast scaling (Ref. 2) is used when comparing blast data for tests with the same propellants and failure conditions, but different mass of propellant. So the blast parameters P (peak side-on overpressure) and $I/W^{1/3}$ (scaled impulse) are plotted as functions of $R/W^{1/3}$ (scaled distance) after being normalized by the fractional yield. This procedure is equivalent to determining an effective weight of propellant for blast from:

$$W = W_T \times \frac{Y}{100}$$

where W_T is total weight of propellant, Y is terminal blast yield in percent, and W is effective weight of propellant. Because the data are normalized by comparing to TNT blast data, the effective blast energy E can be obtained by multiplying W by the specific detonation energy of TNT, 1.4×10^6 ft lb/lb$_m$. We use smoothed curves through the scaled PYRO blast data, and the equation above, to obtain blast wave properties for any particular combination of propellants and simulated accident. Each propellant combination and type of accident is considered separately in Ref. 1. Following is the procedure for one particular combination.

For the case of mixing and an explosion within the missile tankage (CBM), time for ignition and mass of propellant are the principal determinants of blast wave properties. Because the scaling of ignition time assumed for PYRO is not proven by the PYRO test results, we simply plot a smooth curve through PYRO results for blast yield Y as a function of time t in Figure 6. We also use Farber's physical reasoning in plotting this curve; i.e., for zero time for mixing, yield must be zero, and, for long enough time, yield must decrease. A direct plot against ignition time is used, independent of mass of propellant, because it fits the data as well as scaled time plots and also serves to indicate that scaling ignition time has not yet been verified experimentally. Once blast yield Y has been determined from Figure 6 for an assumed ignition time, effective weight of propellant W is then calculated for known Y and W_T, and blast pressures and impulses are obtained from fits to PYRO data in Figures 7 and 8.
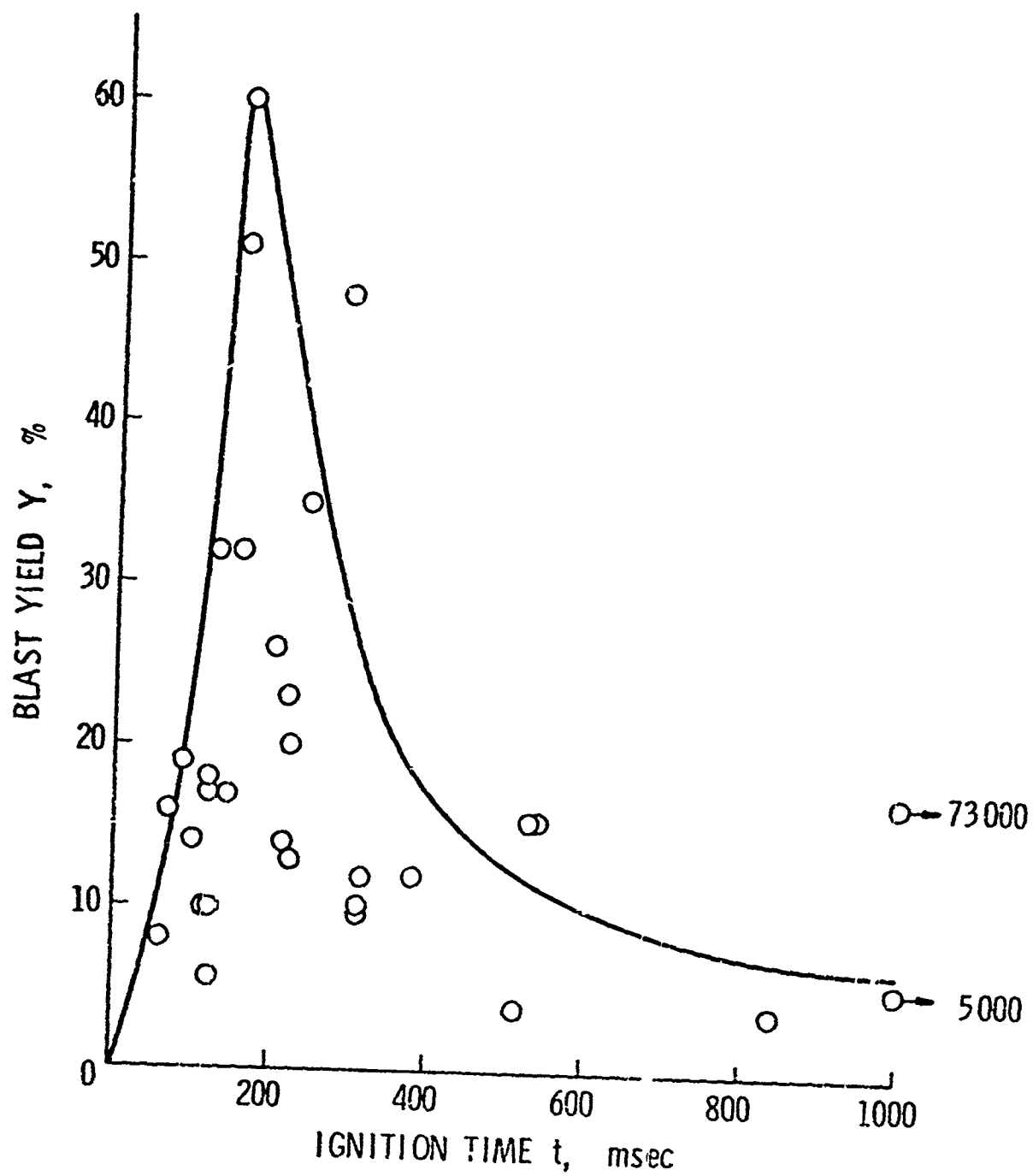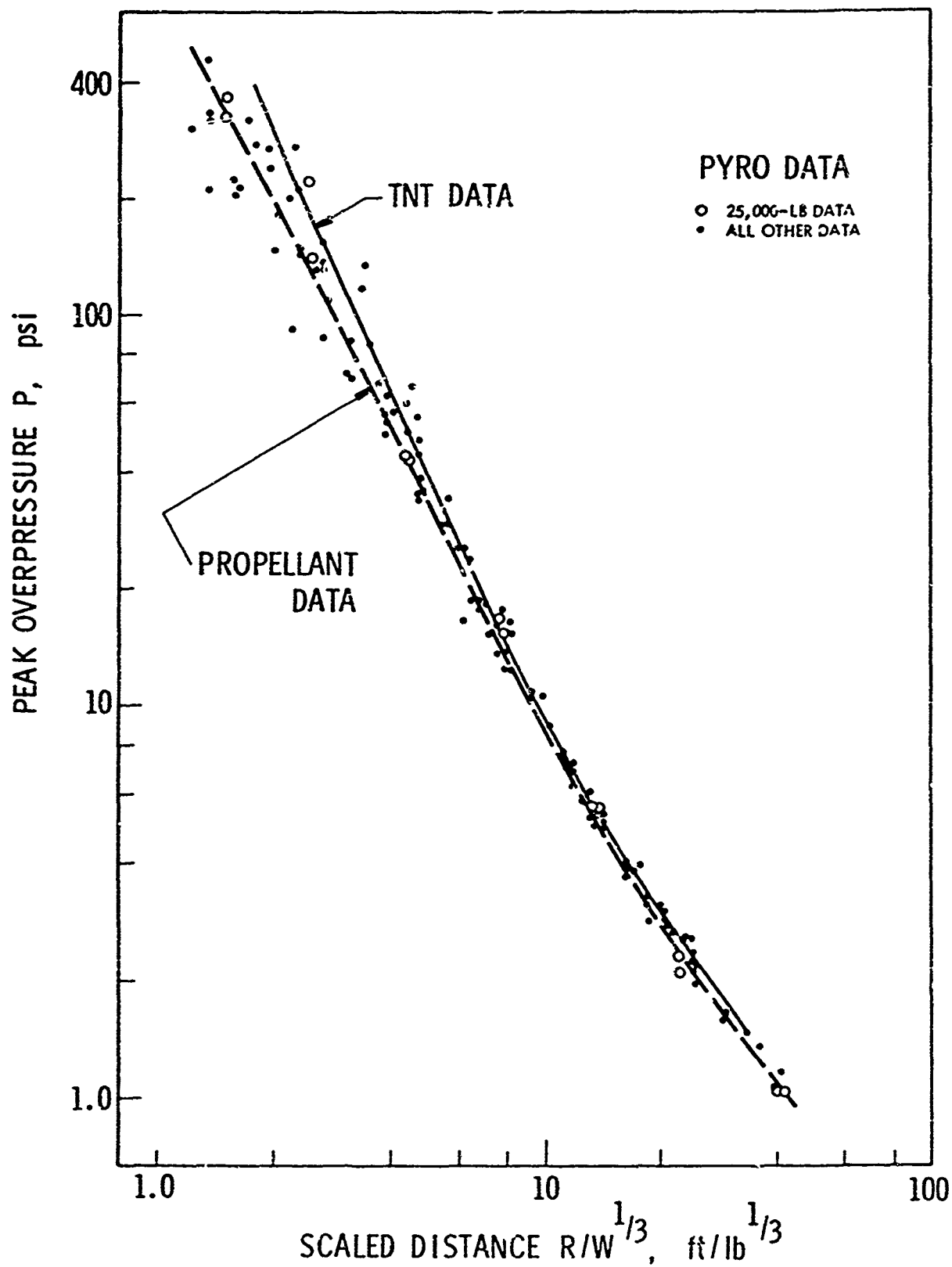
FIGURE 6. IGNITION TIME VS YIELD LO$_2$/RP-1 CBM

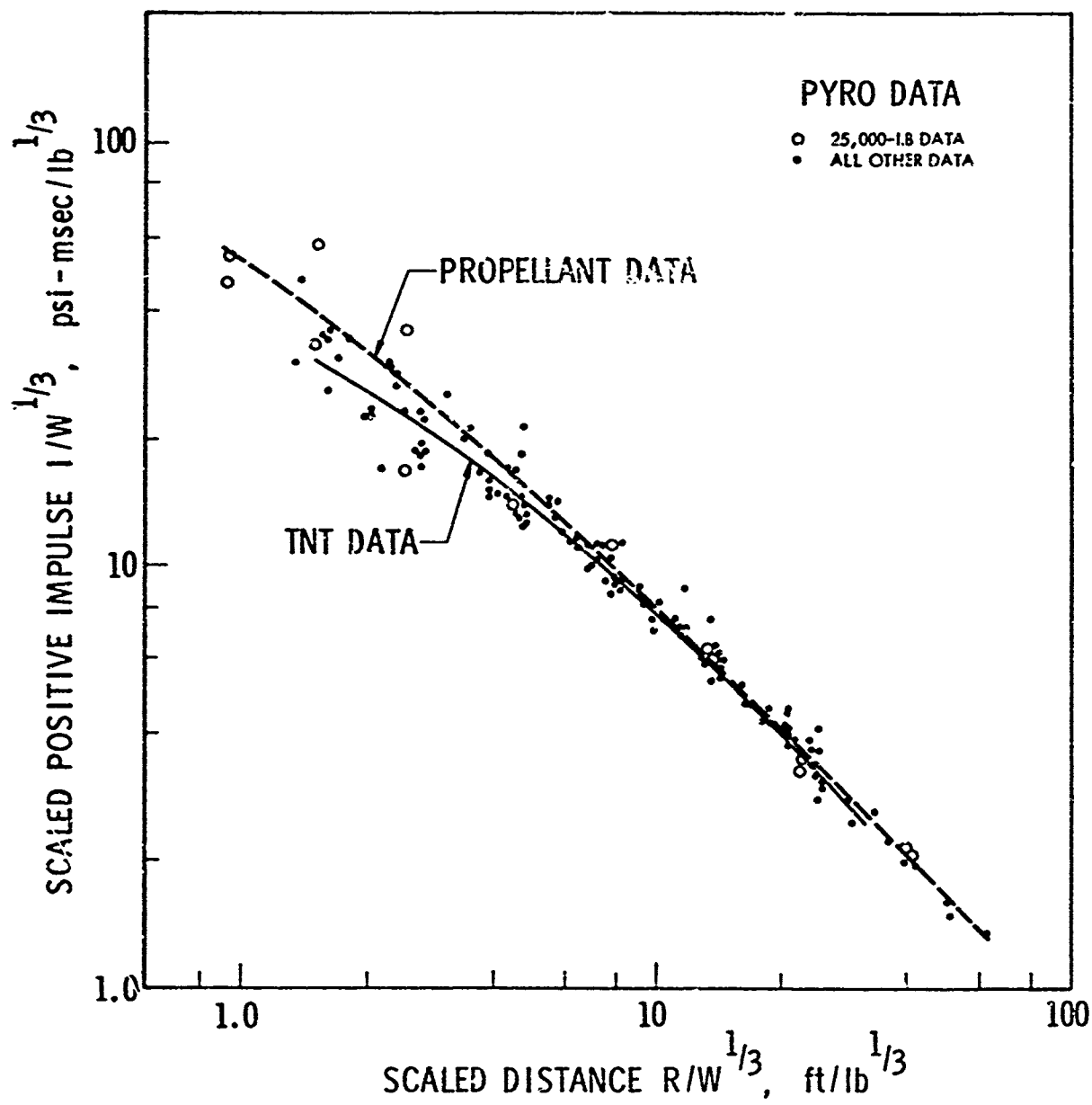FIGURE 7. PRESSURE VS SCALED DISTANCE FOR
LO$_2$/RP-1 CBM CASE

1193

FIGURE   8. SCALED POSITIVE IMPULSE VS SCALED DISTANCE
FOR   LO$_2$/RP-1 CBM CASE

For simulated fall-back on the launch pad (CBGS), impact velocity as well as ignition time are important parameters in estimating blast yield. Methods are given in Ref. 1 for estimation of the effect of impact velocity on blast yield, but are not included here for brevity.

VII. PREDICTION METHODS AND CORRELATIONS

As a part of this study, methods were developed or adapted for prediction of certain fragmentation characteristics for bursting liquid propellant vessels. These included:

(1) Development of a method for prediction of initial fragment velocities for explosions occurring within missile tankage (CBM cases)

(2) Development of a method for predicting initial velocities of appurtenances subjected to propellant blasts

(3) Use of exterior ballistics equations to predict fragment range.

These methods are presented in detail in Ref. 1, and are summarized here, together with such correlations as can be made with fragmentation data.

The method developed for predicting initial velocities of bursting tankage is an extension of the methods reported in Refs. 20 and 21. The earlier work considered bursting, spherical vessels separating into two hemispheres, and an internal high-pressure gas expanding through the time-varying opening between these hemispheres. Motions of the hemispheres were calculated until accelerations approached zero. We extended these methods, assuming that the spherical vessel divided into n equal fragments, and that unreacted liquid propellant was accelerated by the hot, high pressure gas resulting from the explosion along with fragments of the vessel. The method was found to be nearly independent of the number n. Initial properties of the hot gas could be adjusted to match known internal volume of a vessel, and known total energy by comparison with blast yield predictions. Reasonably good correlations were achieved when compared to CBM tests with two different masses of propellant, as can be seen from Figures 9 and 10.

Initial velocities of objects near bursting vessels can be predicted by considering the net transverse pressures on the objects during the diffraction and drag phases of blast traversal, and by assuming that the object translates under this pressure as a rigid body. The time history of
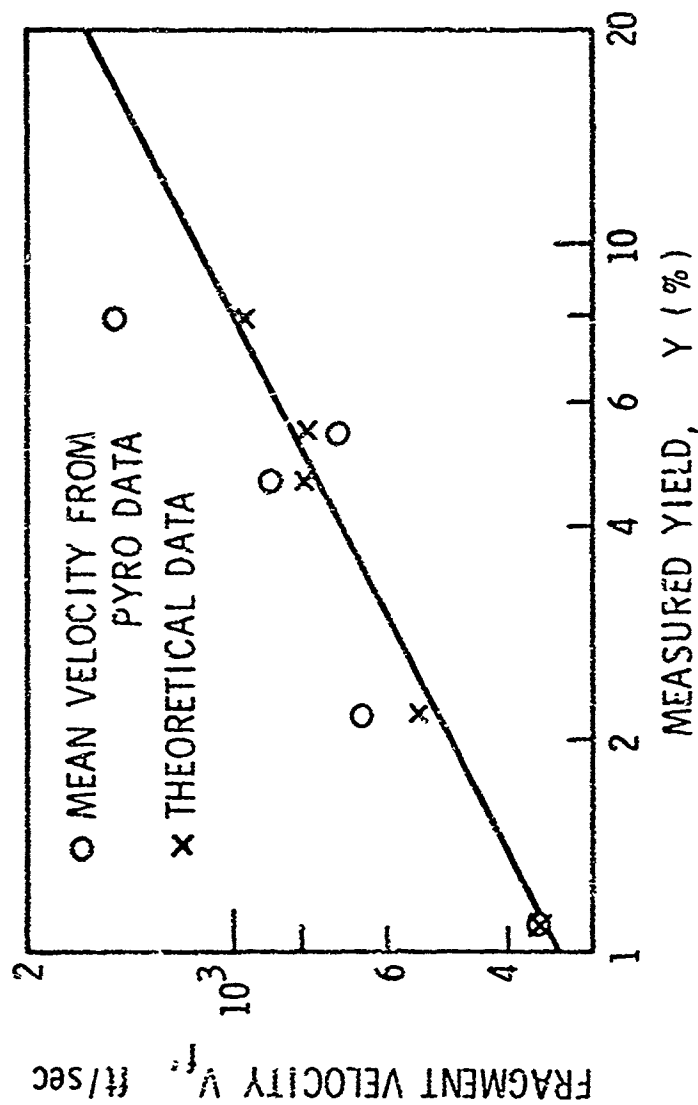
1195

FIGURE 9. FRAGMENT VELOCITY: CORRELATION OF DATA FROM PYRO LH$_2$/LO$_2$ TESTS WITH THEORETICAL VALUES, W$_t$ = 200 LBS
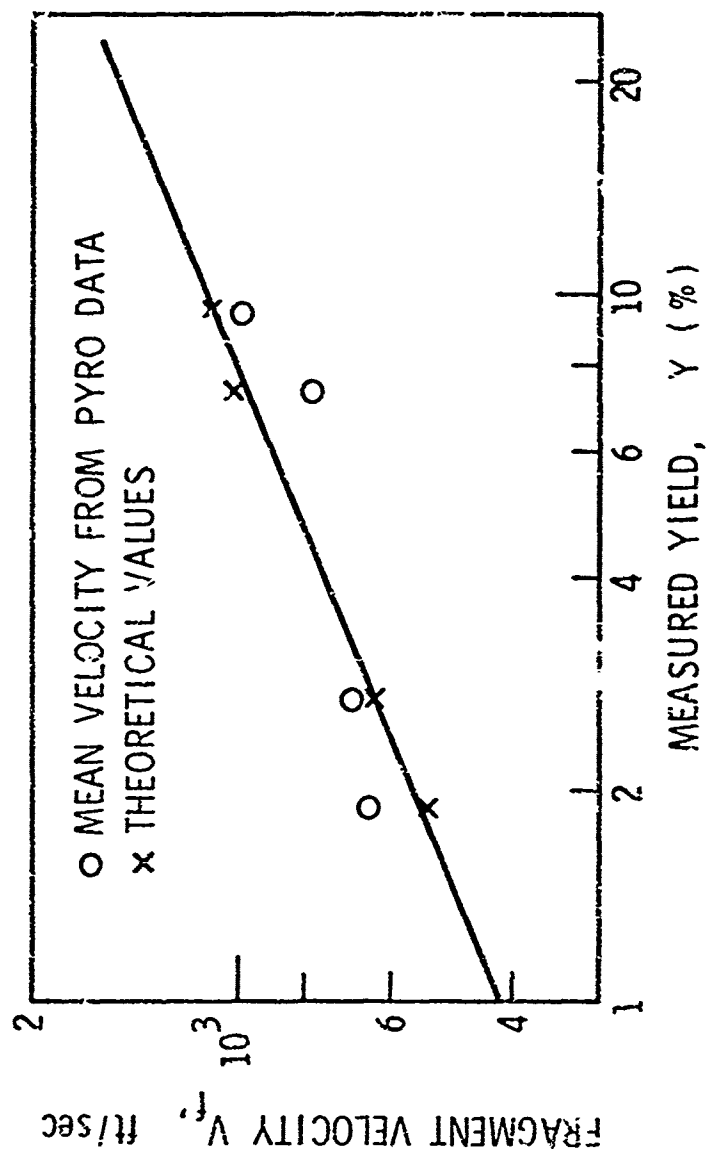
FIGURE 10. FRAGMENT VELOCITY:CORRELATION OF DATA FROM PYRO LH_2/LO_2 TESTS WITH THEORETICAL VALUES, $W_t = 1000^2$ LBS^2

blast overpressure and drag pressure must be well known, as well as the shape and mass of the object. No good correlation could be made with fragment velocities measured from PYRO films because blast measurements were, in most cases, made beyond the distances of objects which become fragments and because geometry of the fragments seen in the films was not known. Approximate values could be assumed for one test, PYRO test 293. The calculated value for the drag method given in Ref. 1 was 745 ft/sec velocity, while the measured average velocity from the films for this test was 461 ± 226 ft/sec. These values are at least of the same order of magnitude, but this very limited comparison does not, of course, validate the prediction method.

One of the oldest problems in ballistics is the prediction of range of a solid object which is launched into the air at some velocity and in some given direction. One must know the object's mass, initial velocity, initial elevation angle, cross-sectional area, and drag coefficient. This, together with air density, allows prediction of range for a body which does not tumble or lift. We utilized the adaptation of solution to exterior ballistics equations which was made by Oslake, et al, in Ref. 36, and drag coefficients from Refs. 37 and 38 to make predictions of fragment range for the one experiment for which both initial velocity and final range data were available. This is identified as Event 1 earlier in this paper, and as the SIV test in PYRO reports. A "mean" fragment could be postulated from statistical averages of data from this test. If this fragment is assumed to be irregular with a drag coefficient of $C_D = 0.75$, then the predicted mean range is $R = 353$ ft. This compares with the observed mean range of $R = 447.4$ ft. Choice of a slightly lower C_D would imply some regularly-shaped fragments mixed with irregular ones, and would result in better agreement.

VIII. DISCUSSION

The review of potential sources of data for fragmentation of liquid propellant vessels yielded limited information on fragment sizes, shapes and range (eight events) and a number of films of Project PYRO tests which were reduced to give data on initial fragment velocities. (For only one test were both types of data available.) The data have been reduced and stored in computer card files.

Statistical fits have been made to such fragment parameters as mass, presented area, mass per unit presented area, initial velocity, etc., as functions of blast yield and range. Prediction equations based on these fits were developed and are presented.

Only limited correlations of deterministic prediction methods with data were possible because of paucity of data or lack of knowledge of needed input parameters for the deterministic methods.

Damage from fragments to humans and other "targets" is discussed briefly in Ref. 1, but not treated in detail because it was essentially beyond the scope of this study.

We believe that the work reported here constitutes the first relatively comprehensive study of fragmentation effects from exploding liquid propellant vessels. Predictions can be made of some of these effects using results from this work. But there are limitations imposed by the limitations in fragmentation data - which have been retrieved from sources in which study of fragmentation effects was secondary or even entirely incidental. There is little doubt that prediction methods could be better tested if one were able to design and conduct experiments with the specific purpose of observing and measuring fragmentation effects.

REFERENCES

1. Baker, W. E., V. B. Parr, R. L. Bessey and P. A. Cox, "Assembly and Analysis of Fragmentation Data for Liquid Propellant Vessels," NASA CR prepared under Contract NAS3-16009 for NASA-Lewis Research Center (in review).

2. Baker. Wilfred E., Explosions in Air, Univ. of Texas Press, Austin, Texas, May 1973.

3. Kingery, C. N. and B. F. Pannill, "Peak Overpressure vs. Scaled Distance for TNT Surface Burst (Hemispherical Charges)", BRL Memo Report No. 1518, Aberdeen Proving Ground, Maryland, April 1964. AD 443102.

4. Carter, P. B., Jr., "A Method for Evaluating Blast Parameters Resulting from Detonation of Rocket Propellants", AEDC-TDR-64-200, Arnold Engineering Dev. Center, Air Force Systems Command, Oct. 1964. AD 450140

5. Gurney, R. W., "The Initial Velocities of Fragments from Bombs, Shells, and Grenades," BRL Report 405, 1943.

6. Henry, I. G., "The Gurney Formula and Related Approximations for the High-Explosive Deployment of Fragments," Hughes Aircraft Company, Report No. PUB-189, Culver City, California, Apr. 1967.

7. Ahlers, E. B., "Fragment Hazard Study," Minutes of the Eleventh Explosives Safety Seminar, September 19t9, pp. 81-107.

8. Gwaltney, R. C., "Missile Generation nd Protection in Light-Water-Cooled Power Reactor Plant." ORNL-NSIC-22, Oak Ridge National Laboratory, September 1968.

9. Gates, R. W., "Containment of Fragmens f. om a Runaway Reactor," Stanford Research Institute, Menlo Park, California, SRIA-117 AEC Research and Development Report UC-8(, Reactor Technology TID-4500 (27th Edition), February 15, 196. Final Report prepared for U. S. Atomic Energy Commission, Contrat No. AT (04-3)-115, Project Agreement No. 2.

10. Proceedings of the Second United Nations International Conference on Peaceful Uses of Atomic Energy, Vol. 11, Reactor Safety and Control, United Nations, Geneva, 1958.

11. Brittan, R. O. and J. C. Heap, "Reactor Containment," pp. 66-78 in Ref. 10.

12. Willoughby, A. B., C. Wilton and J. Mansfield, "Liquid Propellant Explosive Hazards. Final Report - December 1968. Vol. I - Technical Documentary Report," AFRPL-TR-68-92, URS-652-35, URS Research Company, Burlingame, California.

13. Willoughby, A. B., C. Wilton and J. Mansfield, "Liquid Propellant Explosion Hazards, Final Report - December 1968. Vol. II - Test Data," AFRPL-TR-68-92, URS 652-35, URS Research Co., Burlingame, California.

14. Willoughby, A. B., C. Wilton and J. Mansfield, "Liquid Propellant Explosion Hazards. Final Repor: - December 1968. Vol. III - Prediction Methods," AFRPL-TR-68-92, URS 652-35, URS Research Co., Burlingame, California

15. Jeffers, S. L., "Fragment Velocity Measurements from Three Project PYRO Experiments," Report SC-DR-69-329, Aerospace Nuclear Safety Department 9510, Sandia Laboratories, Albuquerque, New Mexico, June 1969.

16. Hunt, D. L., F. J. Walford and F. C. Wood, "An Experimental Investigation into the Failure of a Pressure Vessel Containing High Temperature Pressurized Water," AEEW-R 97, United Kingdom Atomic Energy Authority, Reactor Group, September 1961.

17. Larson, R. J., and W. C. Olson, "Measurements of Air Blast Effects from Simulated Nuclear Reactor Core Excursions," BRL Memorandum Report No. 1102. Aberdeen Proving Ground, Md., September 1957.

18. Muzzall, C. E. (editor), "Compendium of Gas Autoclave Engineering Studies," Report Y-1478, Y-12 Engineering Division, Union Carbide Corporation, Nuclear Division, Oak Ridge, Tennessee, November 1964.

19. Baker, W. E., S. Silverman and T. D. Dunham, "Studies of Explosions in the NASA-MSC Vibration and Acoustic Test Facility (VATF)," Final Report on Contract NAS9-7749, Southwest Research Institute, March 1968.

20. Taylor, D. B. and C. F. Price, "Velocities of Fragment From Bursting Gas Reservoirs," ASME Transactions, Journal of Engineering for Industry, Nov. 1971.

21. Grodzovski, G. L., and F. A. Kukanov, "Motion of Fragments of a Vessel Bursting in a Vacuum," Soviet Engineering Journal, Mar/Apr 1965.

22. Pittman, J. F., "Blast and Fragment Hazards From Bursting High Pressure Tanks," NOLTR 72-102, May 1972.

23. (Anonymous), "Summary Report on a Study of the Blast Effect of a Saturn Vehicle", Report No. C63850, Arthur D. Little, Inc., Cambridge, Massachusetts, February 1962.

24. (Anonymous), SIV All Systems Vehicle Malfunction 24 January 1964, Douglas Missile & Space Division, Santa Monica, California.

25. Deese, J. H., Test Conductors Damage Assessment Report on Auto-Ignition L02/LH2 Mixing Test Experimental Explosion of 2 March 1972, Systems Engineering Division, Kennedy Space Center, NASA.

26. Hoerner, Sighard F., Fluid-Dynamic Drag, Published by the Author, Midland Park, New Jersey, 1958.

27. Hahn, Gerald J. and Shapiro, Samuel S., Statistical Models in Engineering, John Wiley and Sons, Inc., New York, 1967.

23.   Fletcher, R. F., "Liquid-Propellant Explosions", Jour. of Space-craft and Rockets, 5, 10, pp. 1227-1229, October 1968.

29.   Farber, E. A. and Deese, J. H., "A Systematic Approach for the Analytical Analysis and Prediction of the Yield from Liquid Propellant Explosions", Tech. Paper No. 347, Eng. Progress at the Univ. of Florida, XX, 3, Mar. 1966.

30.   Farber, E. A., Klement, F. W. and Bonzon, C. F., "Prediction of Explosive Yield and Other Characteristics of Liquid Propellant Rocket Explosions," Final Report, October 31, 1968, Contract No. NAS 10-1255, Univ. of Florida, Gainesville, Florida.

31.   Farber, E. A., "Characteristics of Liquid Rocket Propellant Explosion Phenomena. No. 448. Part VIII. Prediction of Explosive Yield and Other Characteristics of Liquid Propellant Rocket Explosions," Vol. XXIII, No. 11, Engineering Progress at the Univ. of Florida, Nov., 1969.

32.   Farber, E. A., "Characteristics of Liquid Rocket Propellant Explosion Phenomena Series. Report No. IX. Critical Mass (Hypothesis and Verification) of Liquid Rocket Propellants," Univ. of Florida, Gainesville, Florida, September 1971.

33.   Farber, E. A., Smith, J. H. and Watts, E. H., "Electrostatic Charge Generation and Auto-Ignition Results of Liquid Rocket Propellant Experiments", Report No. X, Univ. of Florida, Gainesville, Florida, October 1972.

34.   Pesante, R. E. and Nishibazashi, M., "Evaluation of the Blast Parameters and Fireball Characteristics of Liquid Oxygen/Liquid Hydrogen Propellant", Report No. 0954-01 (01) FP, Aerojet-General Corporation, Downey, California, April 1967.

35.   Gayle, J. B., Blakewood, C. H., Bransford, J. W., Swindell, W. H. and High, R. W., "Preliminary Investigation of Blast Hazards of RP-1/LOX and LH_2/LOX Propellant Combinations", NASA TM X-53240, George C. Marshall Space Flight Center, Huntsville, Alabama, April 1965.

36.   Oslake, J. J., Getz, R. J., Romine, R. A. and Sooftov, K., "Explosive Hazards of Rocket Launchings," Ford Motor Company Technical Report +-108:98, November 1960, AD253-235.

37.   Heppner, L. D. and Steedman, J. E., "Drag Coefficient for Fragment Simulating Projectiles, 20 MM, Caliber .50, and Caliber .30," APG DPS-286, August 1961, AD 822-489.

38.   Richards, E., "Comparative Dispersion and Drag of Spheres and Light Cylinders," APG BRL TR-717, March 1950.

LIABILITY FOR TORTS ARISING OUT OF THE MANUFACTURE AND
TRANSPORTATION OF EXPLOSIVE OR INCENDIARY ORDNANCE
BY THE U.S. ARMED FORCES

Joseph H. Rouse
U.S. Army Claims Service
Fort Meade, Maryland

I. Types of Tortfeasors Involved

a. GOCO plants categorized as independent contractors.

b. POPO plants categorized as independent   "   .

c. Suppliers of ingredients utilized categorized as subcontractors

of a and b or in some cases contractors of f.

d. Suppliers of machinery utilized categorized as subcontractors of

a and b or in some cases contractors of f.

e. Common carriers categorized as independent contractors.

f. U.S. in its capacity as employer or contractor.

II. Basis for Liability

a. Statutory or common law principles of the state of occurrence

applies to all listed in I above.

b. Legal principles imposing absolute or strict liability concerning

hazardous or dangerous material are generally applicable to all but If

above (U.S.)).

c. U.S. is liable only as set forth in Federal statutes waiving

sovereign immunity principably the Federal Tort Claims Act (28 U.S.C.

2671 et seq.)

1. Decisions interpreting this statute excluded strict liability commencing with the Dalehite decision by the U.S. Supreme Court (346 U.S. 15 (1953)) on the 1948 Texas City explosion and reaffirmed as recently as 1972 (Laird v. Nelms, 92 S. Ct. 1899 (1972)).

2. Few Federal courts have avoided Dalehite rationale by calling strict liability by another name and thus imposing liability on U.S. Examples below.

(a) Florida has non-delegable duty statute for dangerous work. U.S. held liable in spraying contract (Emelewon US, 391 F.2d 9 (5th Cir. 1968 cert. denied 393 U.S. 841)). Recently used in case involving contract for electrical work.

(b) California case based on Restatement of Torts Section 413 subjects employer of independent contractor to liability for unreasonable risks if he does not spell it out in contract or use additional means of minimizing risks. Thorne v. United States, 479 F.2d 804 (9th Cir. 1973).

(c) Wisconsin has Safe Places Act applicable to buildings owned by principal (e.g. U.S. ownership of GOCO plant) which holds building owner liable (American Exchange Bank v. U.S., 257 F.2d 938 (7th Cir. 1958)). Globig v. Greene & Gust Co., 201 F. Supp. 945 (E.D. Wisc. 1962), aff'd 313 F.2d 202 (7th Cir. 1963) involving housing at Badger Army Ammunition Plant. Other states laws e.g. Illinois Scaffolding Act and Kansas Factory Act have provided basis to hold U.S. liable. While U.S. may not be fined for failing to follow state safety law, Federal Tort Claims Act liability can be based on state law as applies to private person.

(d) Unpublished decision upheld by appellate court held Lone Star GOCO plant a joint venture and Day and Zimmerman not an independent contractor (U.S. v. Martin, 354 F.2d 687 (15th Cir. 1966)). See however, Market Insurance v. United States, 415 F.2d 459 (5th Cir. 1969).

3. Great majority of cases have not held U.S. liable on such a specious basis as in 2 above in absence of actual negligence by U.S. employees.

Examples are too numerous to list. Suffice to say that U.S. is not liable:

(1) Landowner (Gowdy v. U.S., 412 F.2d 525 (6th Cir. 1969)).

(2) Because of requiring DOD Safety Manual be followed (Lipka v. U.S., 369, F.2d 288 (2d Cir. 1969) cert. denied 387 U.S. 935 and Page v. U.S. 350 F.2d 28 (10th Cir. 1965) cert. denied 382 U.S. 979) and cases cited therein.

(3) Due to requirement of safety supervision (see cases in (2) above).

(4) Due to attempting to delegate a non-delegable duty (Market Ins. Co. v. U.S. supra).

(5) Due to Good Samaritan Doctrine Roverson v. U.S., 382 F.2d 714.

iII. Essential question is matter of control whether contractor is independent or a U.S. employer (Baum v. U.S., 427 F.2d 219 (5th Cir. 1970), Tort 1. Federal Tort Claims Act limits liability of U.S. to negligence of its employees. Pegs on which U.S. liability may be hung. (List is not intended to be inclusive)   .

a. Actual negligence by U.S. employee at GOCO or POPO plant e.g. where U.S. employee is actual tortfeasor as by repairing or modifying piece of equipment which causes explosion due to faulty repair or modification.

b. Actual negligence by U.S. employees in designing layout for production which causes explosion due to improper design.

c. Waiver by U.S. of preliminary safety tests for new production layout which could have prevented explosion;

d. Design of faulty package by U.S. for explosive ordnance which if designed properly would not have exploded in shipment.

e. Formulation by U.S. of improper safety standards which if properly formulated could have prevented explosion.

f. Supplying from U.S. sources faulty ingredients of which no notice was given to GOCO or POPO plant.

g. Supplying from U.S. sources faulty manufacturing machinery as to which no notice was given to GOCO or POPO plant.

IV. Seeking indemnity from joint tortfeasors where more than one tortfeasor proximately caused loss or injury.

Fact that employer's liability is limited by State Workmen's Compensation law does not preclude U.S. from seeking indemnification of all or part of amount U.S. is required to pay (Seckinger v. U.S., 397 U.S. 203 (1972); Stanley v. U.S., 476 F.2d 606 (6th Cir. 1969)).

1. If GOCO contractor is involved such indemnity generally not sought as contract provides that such is a proper cost thereunder.

2. This generally does not apply to POPO contracts, transportation contracts or supply contracts. U.S. Department of Justice will seek indemnity to extent of the percentage of liability of others.

3. Practical effect of above is that U.S. will be sued even in a "non-liability" case so that employer will be joined in suit and attempt will be made to circumvent local law limiting employer's liability through this route.

1208

HOW A LAWYER FROM INDUSTRY VIEWS
SAFETY ENFORCEMENT AND LITIGATION

David L. Hirsch
Norris Industries
Los Angeles, Calif.

This presentation is an overview of a contractor operator of a Government-Owned-Contractor-Operated plant's knowledge and acceptance of current risks which must be accepted.

"They say a turtle never makes progress unless he sticks his head out of his shell". We contractors who operate GOCO plants may have our heads too far out of our shells. It is my view that the GOCO contractors are currently incurring risks which are more substantial then risks which were assumed during the past 20 years.

These risks are generated by:

1. The public's anti-war sentiments;

2. More aggressive and better qualified plaintiff's counsel;

3. The rapid increase of class and action suits;

4. The necessity for many large companies to be self-insured since the risks involved are greater than are willing to be undertaken by insurance carriers at normally accepted premium rates;

5. Drastic changes in product liability law--primarily created by a more socially oriented judiciary; and

6. More and stronger State and Federal Legislation.

I speak today generally about the following:

   I.   LIABILITY FOR GOVERNMENT-OWNED FACILITIES.

  II.   LIABILITY TO THIRD PARTIES.

 III.   LIABILITY UNDER THE OCCUPATIONAL SAFETY AND HEALTH ACT
        OF 1970 (PUBLIC LAW 91-596).*

  IV.   LIABILITY FOR ENVIRONMENTAL POLLUTION.

   V.   LIABILITY FOR ACTS OF THE PLANT SECURITY FORCE.

   I.   LIABILITY FOR GOVERNMENT-OWNED FACILITIES.

In the past a GOCO contractor was exempted from liability
for facilities unless there was willful misconduct or
lack of good faith on the part of its directors, officers,
managers, superintendents, or other equivalent represen-
tatives who supervise the direction of all or substan-
tially all of the contractor's operations at a GOCO
plant site. In the McDonnell Douglas Corp. Case 68-1
BCA 702 willful misconduct and lack of good faith was
defined as: "a knowing disregard for greatly unreason-
able risks". To my knowledge no contractor has ever
been held liable under these standards.

Today (essentially since September 1970) any contractor
shall be conclusively presumed to be liable for loss or
damage of Government-owned property if the contractor
fails to administer a maintenance program approved by

_____

* Although not discussed in this speech, the Consumer Product
Safety Act of 1972 (Public Law 92-573) may also have a sub-
stantial impact on GOCO contractors. This matter is yet to
be explored since the law is too new to properly analyze.

the contracting officer or the contractor has failed to maintain and administer a property control system in accordance with Appendix B of ASPR. It is my understanding that these changes came about because it was found that contractors were not properly maintaining Government furnished equipment and were not keeping adequate records and making adequate inventories of Government-owned property entrusted to their possession.

Some other sanction should have been used. It is possible that some form of liquidated damages could have been assessed where the Government's equipment was damaged or lost when its property was not adequately maintained or records not adequately kept.

In lieu of this more practical approach, the Government chose to make the contractor liable for loss or damage of Government-owned property in his possession in the event the contractor failed to adequately maintain the property or to keep reasonable property accounting records. I am under the impression that no contractor has been found liable under this new prescription; however, the possibility does exist that in the event of a fire or explosion at a GOCO plant where the contractor's property records or maintenance program have been disapproved, a contractor could be held liable for a substantial sum even though the fire or explosion was not in any way related to property record keeping or to maintenance of Government-owned property.

<u>SUGGESTED CHANGE</u>:

If the Government is to remain self-insured for Government-owned property then a conclusive presumption based on unacceptable maintenance of property record keeping practices should be deleted and some other sanction should be inserted in the contract.

II. <u>LIABILITY TO THIRD PARTIES</u>.

Due to more aggressive Plaintiff's attorneys. Government employees, military personnel and other parties are seeking redress against contractor operators and suppliers of contractor operators for injury received during either wartime or peacetime incurred by explosion of an ammunition item. Plaintiff's attorneys are using product liability. implied warranty. implied contract. and a Government-contractor joint venture as grounds for reaching contractors who operate Government-owned plants or supply Government-owned plants.

We are currently being sued by a former soldier who was injured by our product. Included in the suit are both the loading plant and metal parts plants operators. The soldier is claiming that although he is unclear as to the cause of the explosion the manufacturer should be liable for $3,000,000 since he was injured utilizing (without negligence on his own part) the item supplied to him by the United States Government.

It is high time that the Government indemnify contractors from this type of liability. In the ammunition components manufacturing business many different contractors are involved in producing the parts which result in an end item which is used by a soldier. The item itself may be inherently hazardous, the training a soldier obtained may be faulty, the storage of the item may have been under severe conditions, the handling of the item in transit may not have been in accordance with normal safety standards, etc. Furthermore, it is possible that faulty items do get into the system since there is no practical way to assure 100% quality on every item of ammunition delivered to the field. Only NASA has been able to seek to achieve this quality level in its efforts in reaching the moon and even NASA admits to many small failures.

SUGGESTED CHANGE:

Since ammunition is inherently dangerous, the Government should indemnify the GOCO contractor and his suppliers from any third party liability. This would blunt the efforts on the part of Plaintiff's counsel to reach contractors and would leave open only the Federal Torts Claims Act which involves only the Government's actual negligence and not liability without fault. This is a good time to provide this indemnification since Plaintiff's counsel are just becoming aware of this area of litigation.

III. LIABILITY UNDER THE OCCUPATIONAL SAFETY AND HEALTH ACT OF 1970 (PUBLIC LAW 91-596).

The Government indemnifies the contractor from financial liability where the Government's equipment does not meet OSHA standards. However, where the Government's facilities do not meet OSHA s⁺ ⁻ ⁻ ds, the contractor cannot be indemnified against criminal sanctions which can be imposed under this law. It is my understanding that most contractor operators submit extensive projects for bringing the Government facilities into compliance with OSHA standards; however, most of these projects have not been funded. In the event of a serious injury or death an OSHA investigation would take place and, although the contractor would plead that the Government is responsible, it is quite likely that the contractor could be involved with criminal sanctions since an OSHA judge could easily state that the contractor should have made the changes at his own expense and sought restitution from the Government at a later date. Again, to my knowledge, this has not occurred; however, it is a risk which is unfortunately borne by most contractors.

Where Government-owned property is provided to GOCO and COCO contractors who are not provided the financial indemnification most GOCO operators are provided, the contractor is open for large fines where the Government will not provide funds to bring its equipment up to OSHA standards.

SUGGESTED CHANGES:

1. Either the Government should fund the projects submitted, or

2. The statute should be amended to provide that the Secretary of Defense may exempt specific operations for a specific period from the operation of the statute.

IV. LIABILITY FOR ENVIRONMENTAL POLLUTION.

This problem can best be explained by a set of facts from a specific contractor's experience. The contractor in question was polluting a stream. The State asked the contractor to pay $10,000 a year until such time as the pollution was abated; the Government (United States Attorney's office) defended the contractor in the State court and argued that the State court had no jurisdiction; and the State court continued its process and issued a judgment of $1,700,000 against the company and the Commanding Officer of the plant in his personal capacity. The Federal Government is now seeking to move the case to Federal court and is arguing that the contractor operator was an agent of the Government. This argument may fall on deaf ears in Federal court since there is considerable legal precedent for considering a contractor operator an independent contractor. Most of the cases involved with State taxation of Federal Government operations where a contractor

operator is involved tend to follow the independent

contractor relationship in lieu of the agency.

It is interesting to note that since June of 1973

class actions can be brought against a contractor

under the Federal Clean Air Act of 1971. Here again

it is unlikely that the contractor operator can hide

behind the agency relationship.

To my knowledge most GOCO operators have submitted

pollution control abatement projects to the Government

and many of these projects are still unfunded.

SUGGESTED CHANGE:

The solution to this problem is, of course, to clean

up the plants at a great expense to the Government or

to totally indemnify the contractor so that these

risks will not be borne by the contractor.

V. LIABILITY FOR ACTS OF THE PLANT SECURITY FORCE.

Most GOCO operators either hire their own guard force

or subcontract out for guard force protection. In

the event a guard shoots and injures or kills an in-

truder and this shooting was not in defense of the

guard or in defense of others but only in defense of

Government property, the contractor operator through the

guard as an agent of the contractor operator could be

liable in State court for substantial damages.

It is the DOD's policy that the guard force be equipped

with hand guns; however, there is no protection and r.

1216

insurance which a contractor can carry to protect a contractor from an action by a well meaning guard. The only solution to this problem is to make a guard a deputy sheriff so that the guard will be acting as a public official and will be protected by the State law of the jurisdiction in question. In most jurisdictions the training of a deputy sheriff is a substantial cost. Heretofore the Government has been unable or unwilling to pay these costs; therefore, the contractor operator is open to this specific risk.

SUGGESTED CHANGE:

The contractor operator's guard force should not be required to carry hand guns or the Government should pay the cost of the training of the guard force so that the guards may be deputized.

This was a brief overview of a series of potential risks which a contractor operator may be forced to endure. The one outstanding point is that these risks could be easily absorbed by the Government through rather simple solutions. Clearly most of these problems have not been substantial to date and contractors have not been overly burdened. But now is the time to resolve the problem before the contractor is severely financially burdened.

Until these matters are resolved, I guess we contractors must accept the maxim: "When you get to the end of your rope, tie a knot in it and hang on".

NAVAL WEAPONS COOK-OFF PROGRAM

LCDR R. R. Stoops, USN
Naval Air Systems Command, Washington, D. C.

The presentation for this mornings session deals with the thermal protection of air-launched weapons. This effort, which is conducted under the Naval Weapons Cook-off Program, is specifically directed at reducing the threat to the aircraft carrier.

The term "cook-off" refers to the explosive reaction which occurs when a munition is subjected to a heat source such as an accidental fuel fire aboard a carrier. When a weapon is heated the chemical reaction of the explosive increases to the point where the reaction is self generating and the volume of gas produced opens the case. It is the manner in which the case opens which is of prime interest to us in the Cook-off program. Case opening may be manifested in various ways, from a non-violent rupture to a catastrophic detonation.

In July 1967 while on station in the Gulf of Tonkin, the USS FORRESTAL was conducting routine combat flight operations when an inadvertent ZUNI rocket firing initiated a flight deck fire. Before the ensuing conflagration was extinguished over 100 men had lost their lives and the damage exceeded 72 million dollars. One and one half years later, in January 1969, USS ENTERPRISE was operating off the coast of Hawaii when a similar fire erupted. Again there were numerous deaths and catastrophic damage.

I have a film this morning of these two fires which illustrates the magnitude and intensity that a flight deck conflagration can reach. The film is an extract of the closed circuit video tape taken of the flight deck during all aircraft launches and recoveries. By way of explanation I might mention that aboard ship, flight operations are conducted on a cyclic basis. Aircraft are normally launched and recovered every 1 3/4 hours with the aircraft recovery commencing immediately following the launch. After completion of the launch/recovery sequence, which generally requires 20 to 30 minutes, the aircraft are refueled, rearmed and prepared for the next cycle. Probably the most critical period during this evolution with respect to hazards from a fire, occurs from that point when aircraft engines are started until the launch is complete. It is during this time that all aircraft are fully loaded with fuel and ordnance and the activity on the flight deck is at a peak. The FORRESTAL and ENTERPRISE fires both occurred during this phase.

These, and other flight deck fires which were contained before reaching similar proportions, have provided the thrust behind the Naval Cook-off Program. Our prime objective is to reduce the hazards of air-launched weapons by increasing the delay prior to an explosive reaction and to reduce the consequent damage when exposed to a massive fire. To attain this objective, three individual goals have been established.

(1) The initial objective is to provide a minimum of five minutes cook-off time for all weapons.

(2) The intermediate goal of the program is to extend the cook-off time to a minimum of ten minutes and to reduce the severity of the reaction.

1219

(3) The ultimate objective is to provide naval weapons that will neither detonate nor explode in a fire.

You may have observed in the film that the first weapon reactions occurred within two minutes of fire initiation and that subsequent explosive reactions continued to negate fire suppression efforts. We believe that if the fire-fighter is provided with five minutes of hazard-free time, the conflagration can be controlled.

As the cook-off program evolved, it became apparent that to facilitate and standardize weapon cook-off testing and reporting, practical definitions of reactions were required. To fulfill this need the following definitions were adopted:

1. Detonation. A "detonation" is defined as that reaction which occurs when the munition performs in its design mode. The maximum possible air shock is formed and essentially all of the case is broken into small fragments.

2. Explosion. An "explosion" is classified as a violent pressure rupture and fragmentation of the munition case with resulting air shock occurs. With an explosion, most of the metal case breaks into large pieces which are thrown about with unreacted or burning explosives.

3. Deflagration. A "deflagration" is described as the reaction which occurs when the explosive in the munition burns. The case may rupture or the endplates blow out but there is no fragmentation of the case. The deflagration of a large rigidly confined munition such as a General Purpose Bomb; however, may result in a rather violent case rupture.

These standardized definitions for describing cook-off reactions have assisted in clarifying much of the ambiguity related to cook-off testing.

The Naval Cook-off Program is organized into three major areas which will now be addressed in greater depth. These include:

1. Test programs which characterize cook-off reactions and determine individual weapon survivability in fire.

2. Weapon cook-off improvement program for in-service weapons.

3. The development of new concepts to be incorporated in future weapons.

THE THERMAL PROTECTION OF INSERVICE NAVAL WEAPONS

Richard W. Slyker
Naval Missile Center
Point Mugu, California

The Naval Weapons Cook-Off Improvement Program as discussed previously by the NAVAIR presentation is part of the Naval Weapons Cook-Off Program Plan. The NAVMISCEN (Naval Missile Center) was tasked as the lead Naval field activity in 1969 for the Weapons Cook-Off Improvement Program because of its engineering cognizant function on inservice weapons. As the lead field activity the NAVMISCEN coordinates the efforts of approximately seven participating Navy field activities, other DOD activities and contractors in achieving the program objectives.

The objective of the Naval Weapons Cook-Off Improvement Program is to provide a five minute minimum thermal protection and decrease the explosive reaction of those inservice weapons when subjected to a fuel fire. The fire criteria was designed to simulate the conflagration such as experienced on the USS FORRESTAL and USS ENTERPRISE. The thermal protection systems developed shall withstand all the environments to which the weapon is exposed.

The Weapons Cook-Off Improvement Program has been active since 1969, the initial thrust of the program was to protect the MK 82 500 pound bomb and its associated fuzes due to their high usage rates. Upon completion of the MK 82 bomb program which resulted in the release to production of the MK 82 MOD 2 bomb, M904E4 mechanical nose fuze and M148E1 adapter booster the program's emphasis changed to the other MK 80 series bombs and the five inch Zuni rocket. Having effectively completed the MK 80 series bomb and five inch rocket, the program's current emphasis is on the Rockeye Cluster Bomb Unit and Air Launched Missiles.

The Cook-Off Improvement Program is divided into four major areas: bombs, unguided rockets, missiles and aircraft gun systems. Each of these weapon types present a different set of problems when developing a suitable thermal protection system.

The following Bar charts (Figures 1, 4, and 7) briefly summarize the status of the Cook-Off Program on each inservice Naval weapon.

BOMBS (Figure 1)

With respect to the bombs, the Navy's MK 80 series has been thermally protected, the 500 pound MK 82 is in production and the MK 83 and 84 have been released for production. Cook-Off times for these bombs have been increased from the two to four minute time frame to nine to ten minutes. Over 300,000 thermally protected MK 82's have been produced to date. The thermal concept used was an active external coating possessing ablative characteristics, an increased internal hot melt thickness and a solid internal base pad (Figure 2). The Rockeye II Cluster Bomb Unit is presently the subject of an intensive program which will be discussed in more detail later.

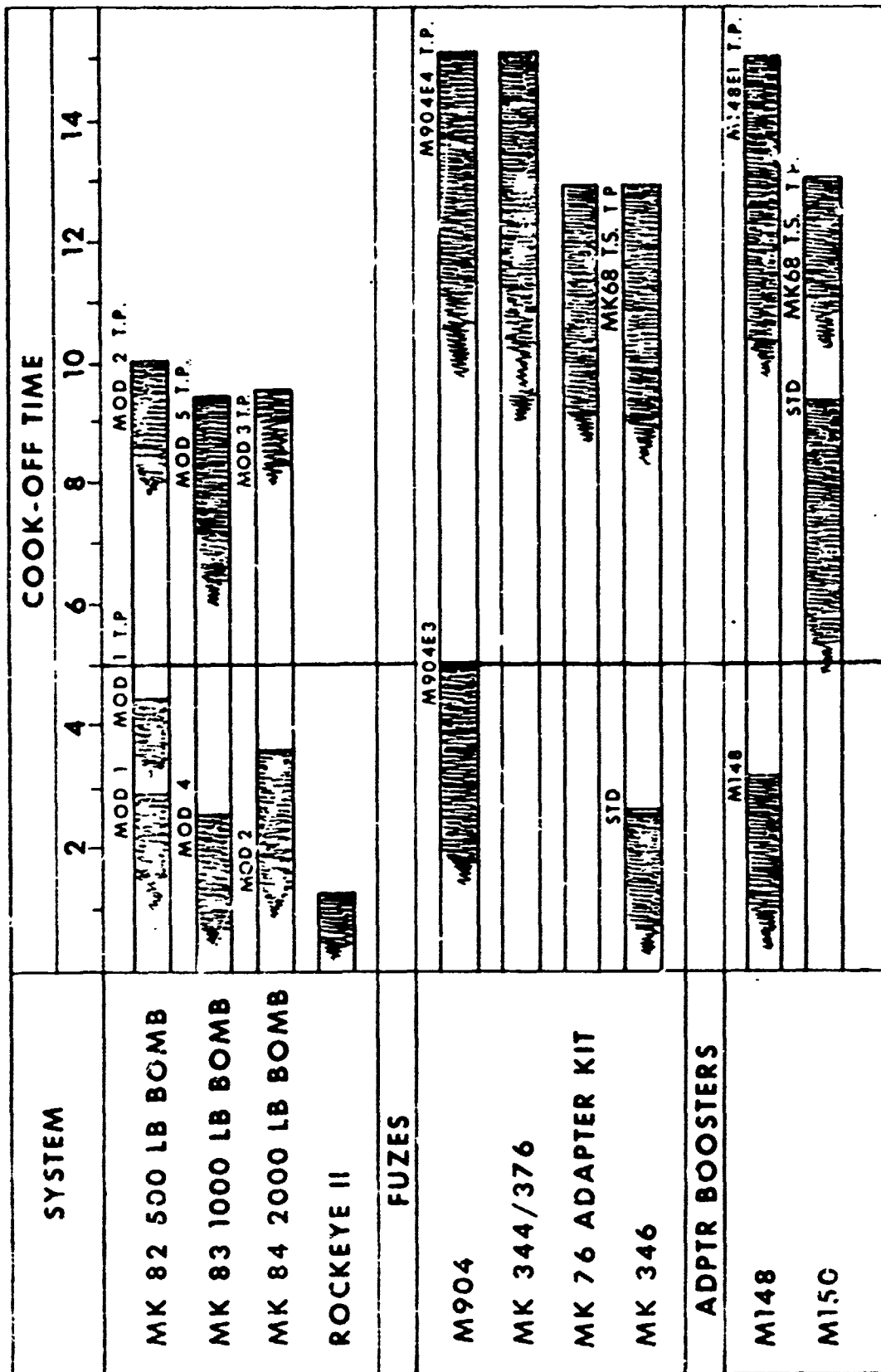# BOMB COOK-OFF IMPROVEMENT PROGRAM STATUS
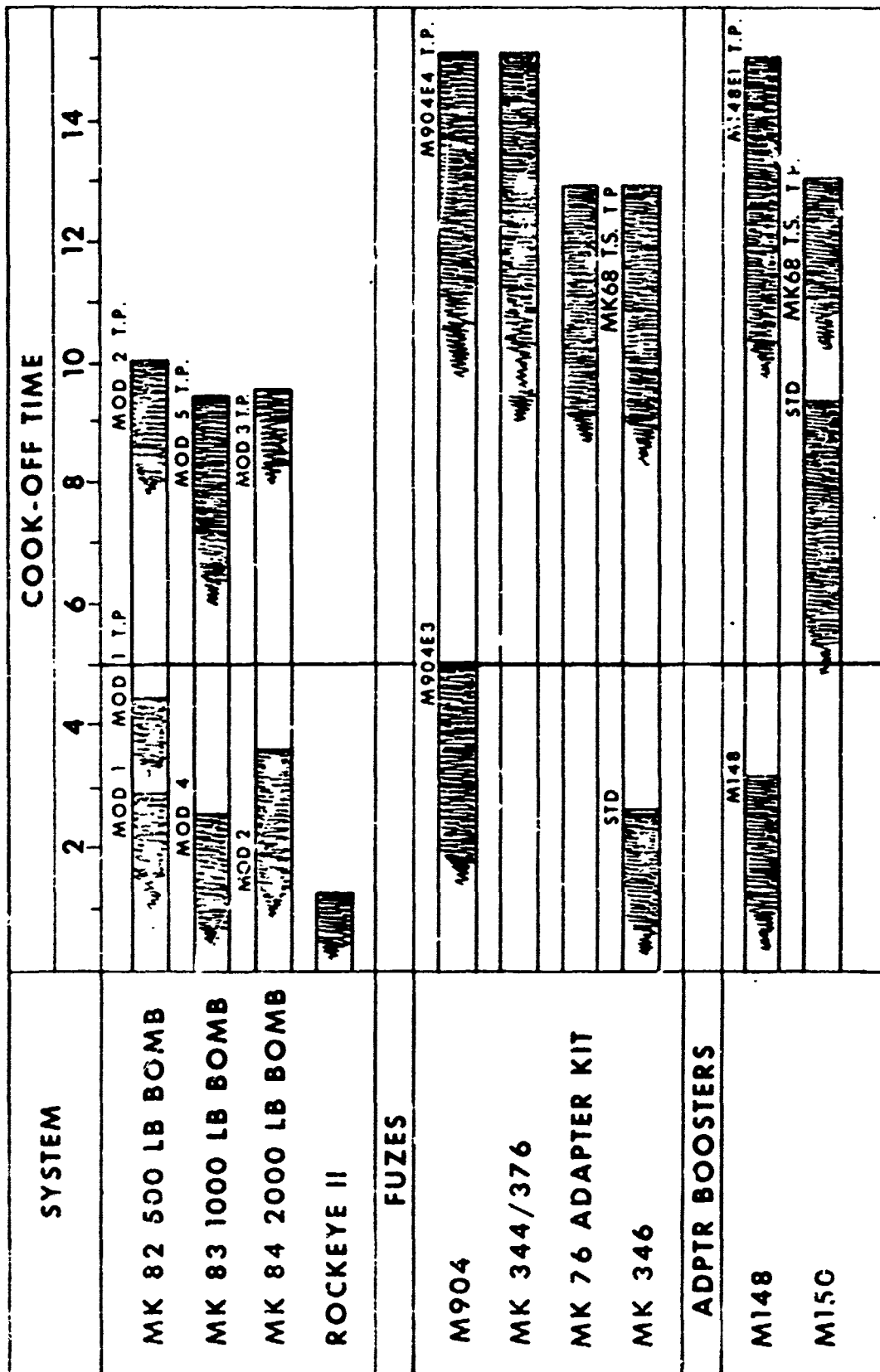

FIGURE 1

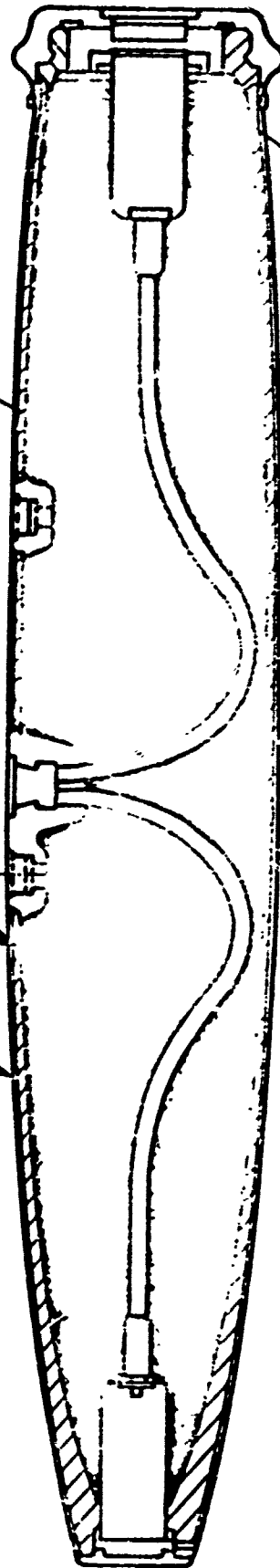# BOMB COOK-OFF IMPROVEMENT PROGRAM STATUS

FIGURE 1

1222

MK 82 MOD 2 THERMALLY PROTECTED BOMB

.150 AVCO FM 26 COATING

¼ INCH WS 12675 HOT MELT

EXPLOSIVE

1½ INCH TUFFSEAL

1223

FIGURE 2

The fuzing systems for these bombs also required thermal protection. In order to ensure a deflagration reaction of the bomb, the fuze system must have a longer Cook-Off time than the bomb itself. For this reason a minimum of 12 minutes has been established for general purpose bomb fuzing systems. The M904 and MK 346 are mechanical fuzes while the MK 344 and MK 75 are electrical. Electrical fuzes inherently possess greater Cook-Off times and as shown in Figure 1 did not require modification as did the M904 or MK 346. Thermal protective sleeves were developed to increase Cook-Off time of the two mechanical fuzes (Figure 3).

The adapter boosters are a part of the fuze explosive train and must meet the same requirements as the fuzes for safety.

ROCKETS (Figure 4)

The approach used on unguided rocket systems was to thermally protect the launcher vice the individual rocket components. The Cook-Off times shown in Figure 4 are for the motors and warheads in a standard and then thermally protected launcher. The Zuni thermally protected LAU-10D/A launcher has been released for production which will commence early in calendar year 1974. A thermal protection system has been developed for the 2.75 inch Rocket system, however qualification for Fleet use is required. The thermal protection system developed for the LAU-10D/A consists of an external launcher intumescent coating, an intumescent painted forward fairing and the addition of the aft thermal shield as shown in Figure 5.

MISSILES (Figure 6)

Figure 6 shows that all of the air launched missile motors and warheads react in under five minute; most of the motor reactions are under two minutes. In order to develop thermal protection systems for the missiles, instrumented Cook-Off tests of unprotected hardware have been conducted to define the critical heat paths, temperature profiles, failure modes, in addition to Cook-Off times and reactions. With this data, thermal protection systems are being developed to increase the time and reduce the severity of reaction.

Presently, the approaches being investigated include external coatings, internal liners, heat path interrupters and warhead design modifications. The air launched missile protection problem differs from other ordnance because of the design requirement limitations and complexities of the systems. External coatings have been tested on SIDEWINDER motors and warheads and have demonstrated that they can increase Cook-Off time, the motor's reaction time was increased from approximately one to five minutes and the warhead from three to nine minutes. The problems which need to be solved with external materials, such as the one shown on the SIDEWINDER prior to actual missile application (Figure 7) include: increased thermal performance to provide for a minimum thickness, thickness control, surface finish, application, adhesion and environmental characteristics.
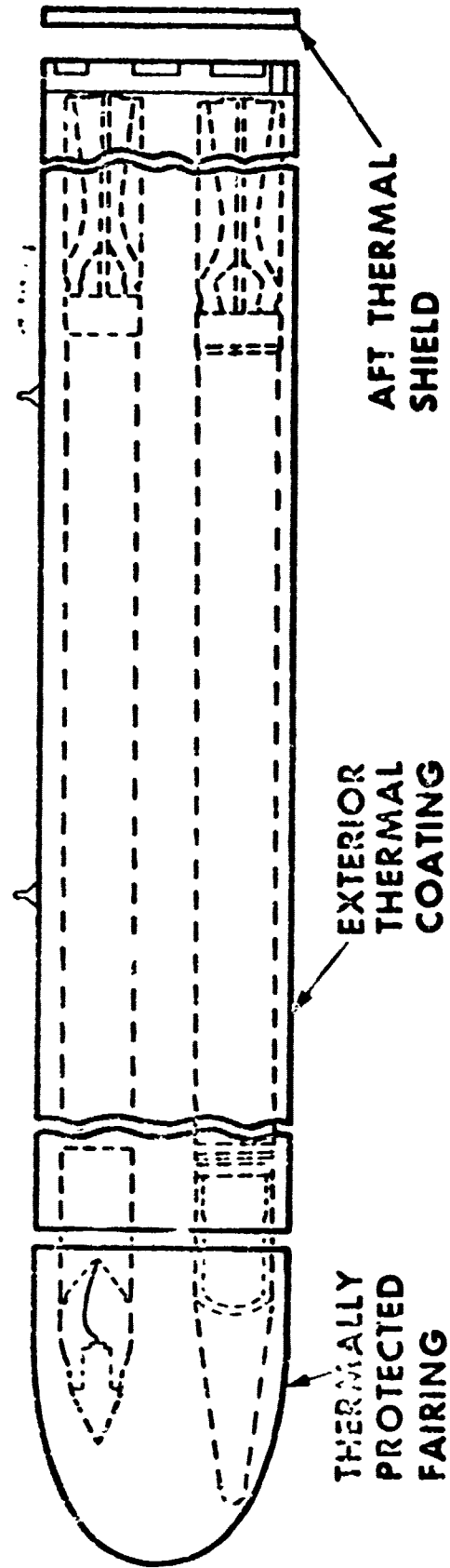
THERMALLY PROTECTED LAU 10 D/A 5" ROCKET

THERMALLY PROTECTED FAIRING

EXTERIOR THERMAL COATING

AFT THERMAL SHIELD

FIGURE 5

1227

MISSILE COOK-OFF IMPROVEMENT PROGRAM

COOK-OFF TIME MINUTES

FIGURE 6

122ª
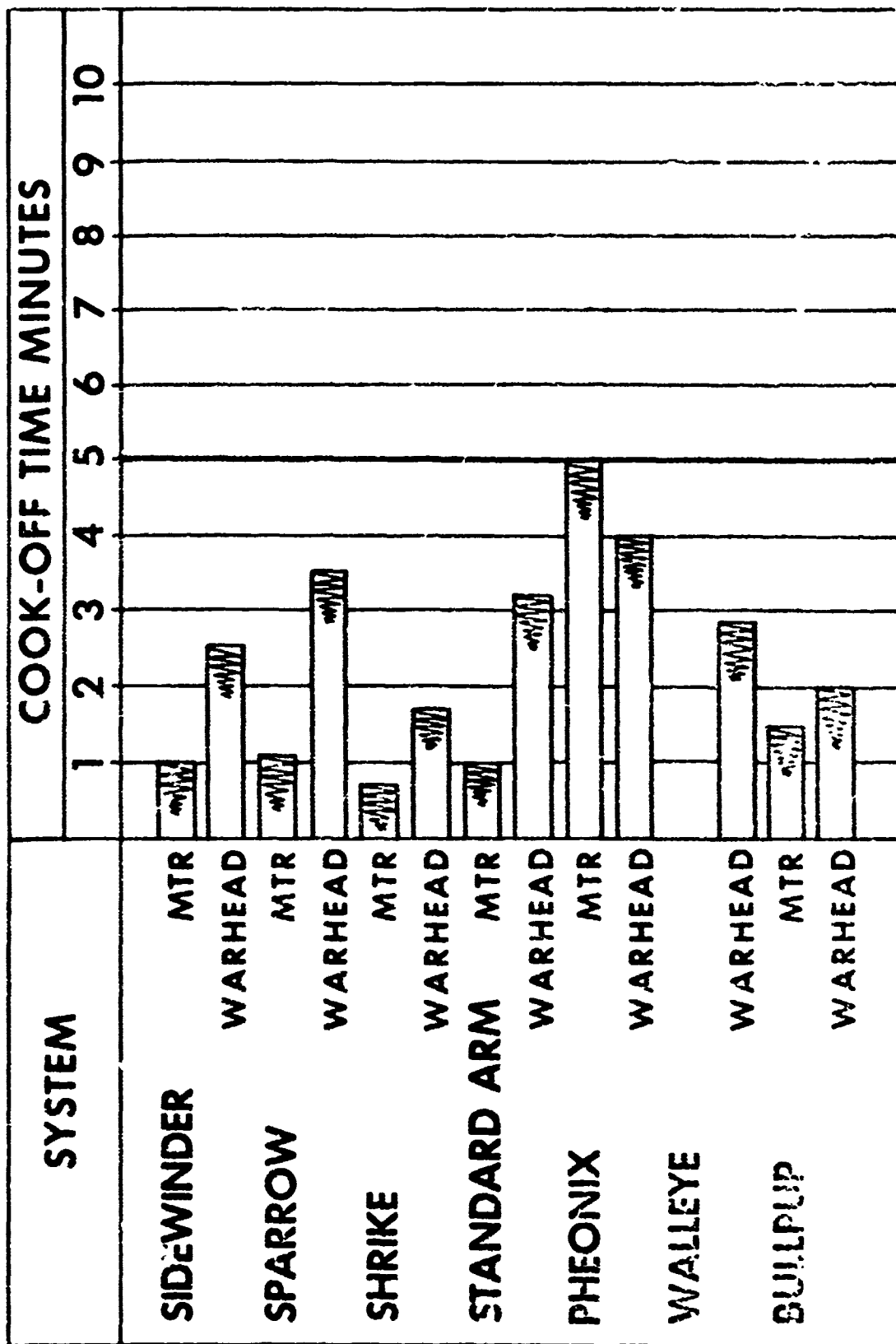
WARHEAD PROTECTION CONCEPTS

REDUCING CRITICAL HEAT PATHS

INTERNAL INSULATORS & DESIGN CHANGES

EXTERNAL THERMAL COATING

EXTERNAL COATING
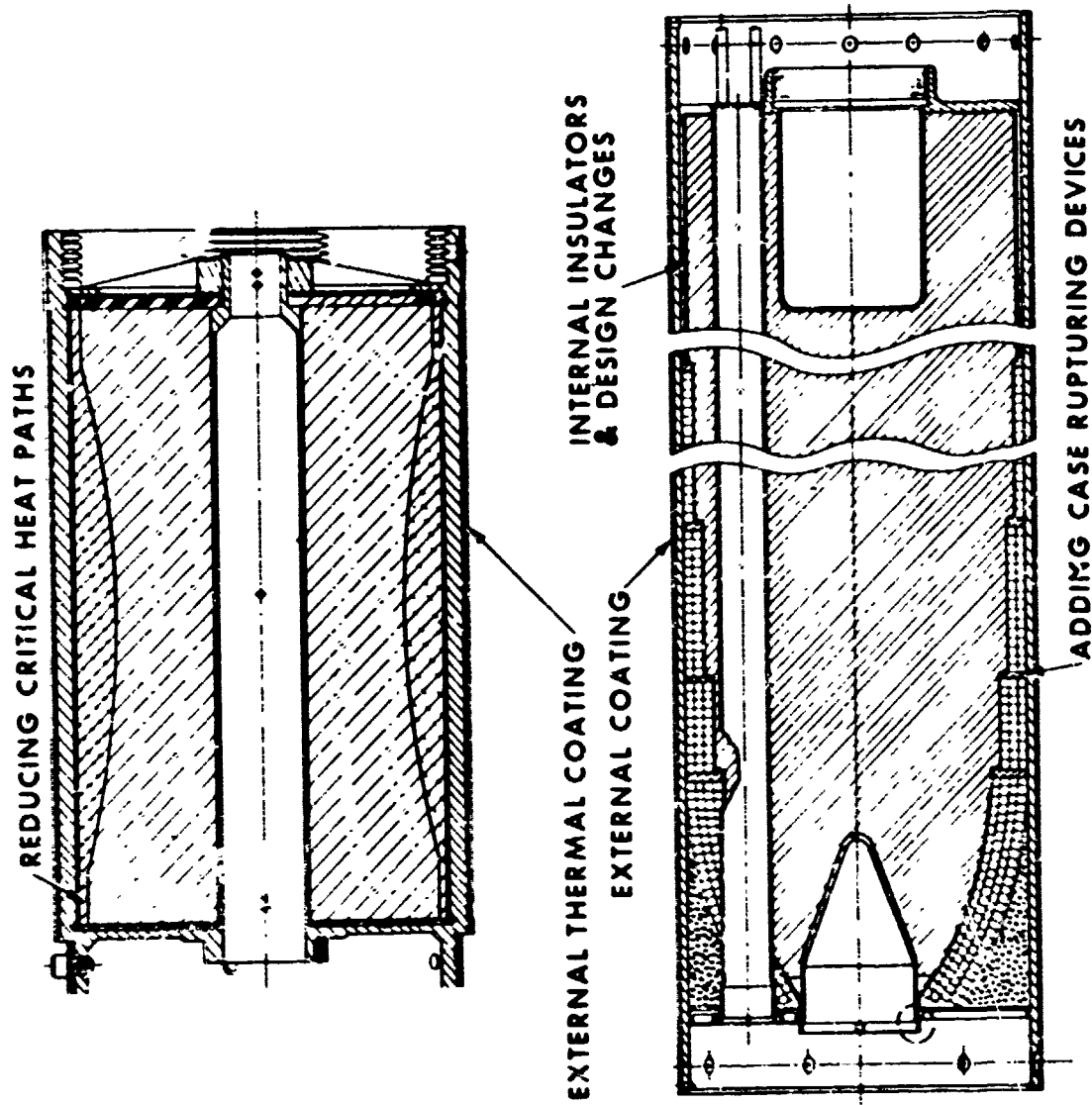
ADDING CASE RUPTURING DEVICES

FIGURE 7

Internal liners are being considered mainly in the missile warheads area (Figure 7). The warhead's liner thickness is being increased in thickness at the ends to improve Cook-Off characteristics; theoretically it should increase time and decrease reaction.

Heat path interrupters are also being considered in the warheads to eliminate the critical heat paths to the explosive.

Current action in the missile program includes completion of the baseline tests; the development of external thermal protection systems for missiles; and the development of internal warhead thermal protection methods.

Another weapon currently being thermally protected is the Cluster Bomb Unit, Rockeye II (Figure 9). The Cook-Off reaction of the weapon ranges from detonation to deflagration with a minimum time of one minute, thirteen seconds.

To meet the objective of the Rockeye Cook-Off program, i.e., extend the Cook-Off time to over five minutes and decrease its reaction, the following approaches were studied.

1. External intumescent coating.

2. Elimination of critical heat paths.

The external thermal materials chosen for initial evaluation were those previously qualified in other Cook-Off programs.

The initial thermal protection system evaluation on Rockeye has been completed. The thermal protection system tested increased the Cook-Off time, however based on the Cook-Off test analysis, additional protection can be obtained. The revised thermal protection system is being defined and will be subjected to the initial qualification tests during September. If the initial qualification tests are successful, approximately 20 weapons will be subjected to environmental, Cook-Off, flight, functional, carrier suitability and safety testing. Qualification will begin in December and program completion is scheduled for fourth quarter Fiscal Year 1974.

Figure 10 briefly reviews the thermal protection concepts which either were implemented or are being tested in Cook-Off Improvement Programs.

During the program approximately 50 external thermal protective materials were evaluated, the materials considered included modified rubbers, ablative coatings, intumescent paints and coatings, filled plastics, metal cloths, inorganic coatings, metal oxides and various combinations. Because of their cost, application, thermal, physical and environmental properties organic coatings which act through ablation and or intumescence have been selected in most cases for final qualification. Figure 11 gives some typical time temperature curves for external materials being considered, the tests were conducted in the Navy's small
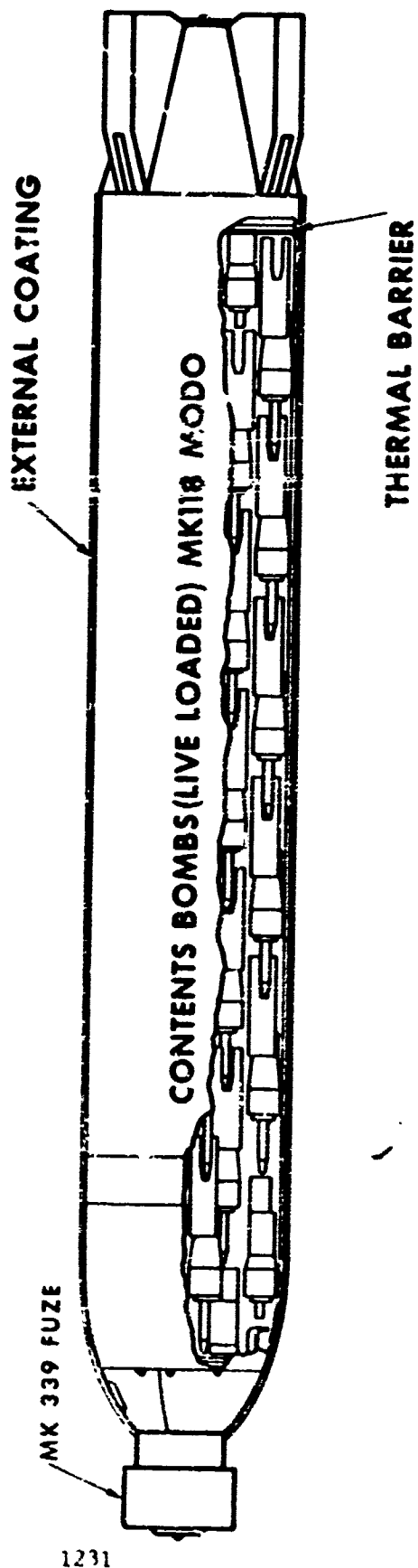
MK 20 ROCKEYE

EXTERNAL COATING

MK 339 FUZE

CONTENTS BOMBS(LIVE LOADED) MK118 MODO

THERMAL BARRIER

1231

FIGURE 9

THERMAL PROTECTION CONCEPTS FOR INSERVICE WEAPONS

CONCEPT	MATERIALS	USED ON
EXTERNAL THERMAL MATERIALS	ABLATIVE COATING	BOMBS
	INTUMESCENT COATING	ROCKETS ROCKEYE
	INTUMESCENT PAINT	MISSILES
INTERNAL MATERIALS	HOT MELTS	BOMBS
	PLASTIC LINERS/FILLERS	MISSILE WARHEADS BOMBS
HEAT INTERRUPTERS	PHENOLIC	ADAPTER BOOSTERS
DESIGN CHANGES	SLEEVES	MECHNICAL BOMB FUZES
	HEAT SHIELDS	ROCKETS & ROCKEYE
	METAL PART CONSTRUCTION	MISSILES ROCKEYE

FIGURE 10

1232

THERMAL PROTECTION CONCEPTS
FOR INSERVICE WEAPONS

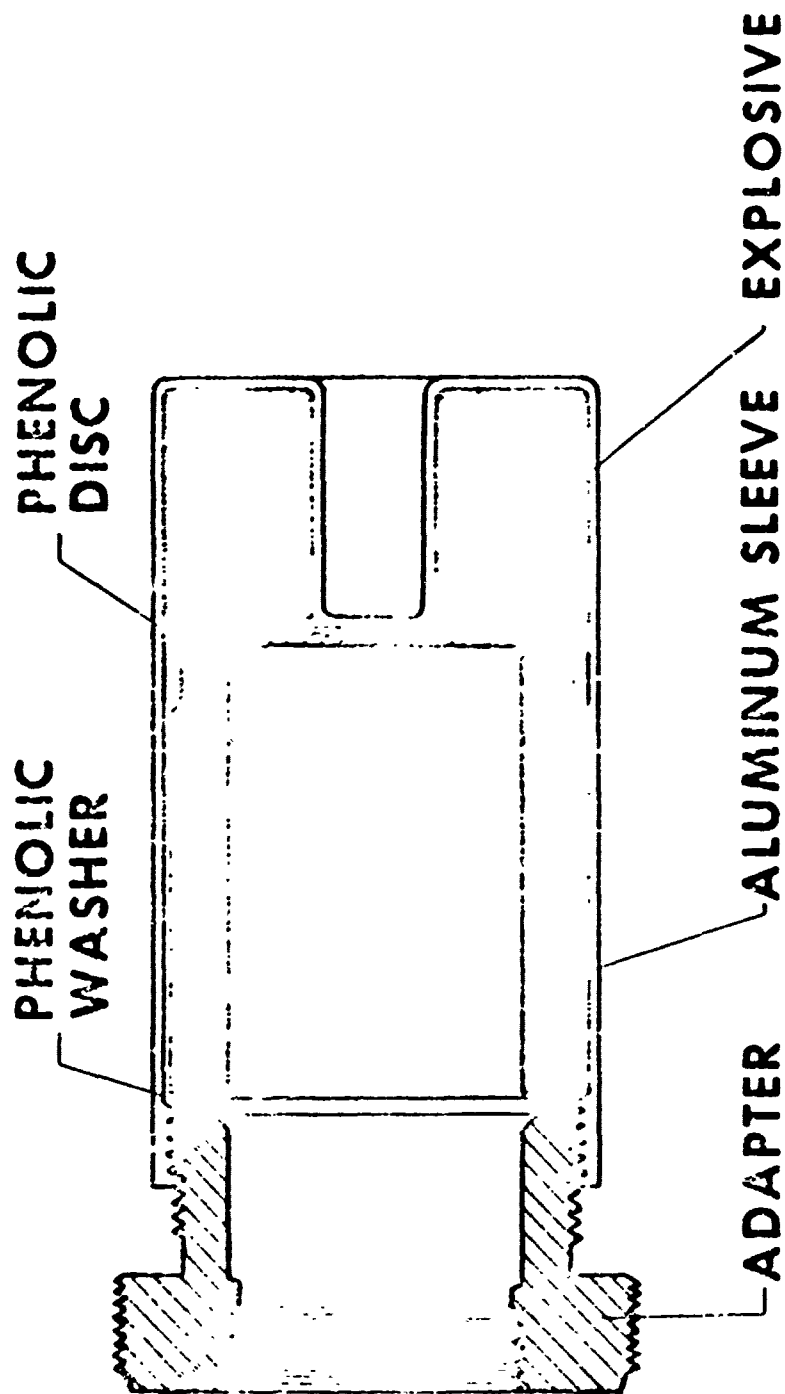| CONCEPT	MATERIALS	USED ON
EXTERNAL THERMAL MATERIALS	ABLATIVE COATING	BOMBS
	INTUMESCENT COATING	ROCKETS ROCKEYE
	INTUMESCENT PAINT	MISSILES
INTERNAL MATERIALS	HOT MELTS	BOMBS
	PLASTIC LINERS/FILLERS	MISSILE WARHEADS BOMBS
HEAT INTERRUPTERS	PHENOLIC	ADAPTER BOOSTERS
DESIGN CHANGES	SLEEVES	MECHNICAL BOMB FUZES
	HEAT SHIELDS	ROCKETS & ROCKEYE
	METAL PART CONSTRUCTION	MISSILES ROCKEYE

FIGURE 10

1232

ROCKET LAUNCHER MATERIALS

.040 ALUMINUM

TIME MINUTES

TEMPERATURE °F

ROCKET
LAUNCHER
MATERIALS

.040 ALUMINUM

TIME MINUTES

TEMPERATURE °F

100
200
300
400
500

M148E1 ADAPTER BOOSTER

PHENOLIC WASHER

PHENOLIC DISC

EXPLOSIVE

ALUMINUM SLEEVE

ADAPTER

FIGURE 12

MK346 AND M150 ADAPTER BOOSTER WITH MK68 THERMAL SHIELD

MK68 THERMAL SHIELD

MK5 GUIDE

MK346 FUZE

M150 ADAPTER BOOSTER

EXPLOSIVE

FIGURE 13

1236
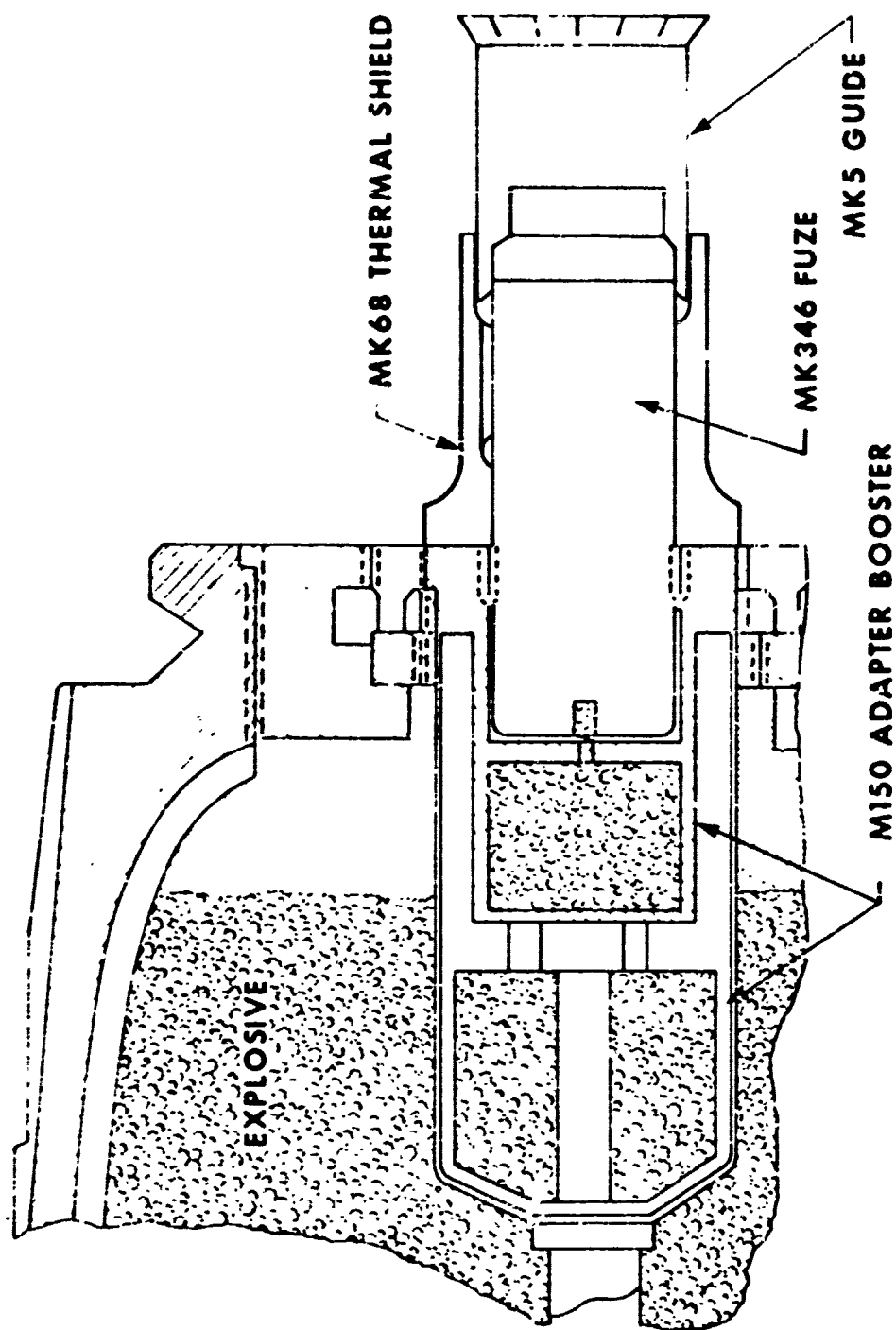
COOK-OFF TESTING

	CURRENT	DECK FIRE
FIRE TEMP	1800°F	0 - 2200°F
DISTANCE FUEL TO TEST ITEM	3 - 4 FT	3 - 4 FT UNTIL RACK FAILS THEN ON DECK
WIND	NO	YES
ENVIRONMENT	FIRE	FIRE & FIRE FIGHTING & REACTING ORDNANCE
OBSTRUCTIONS	NONE	WING - FUSELAGE ETC

1237

FIGURE 14

2

manner many of the weapons which currently deflagrate in the present fast Cook-Off test may actually explode or detonate under less ideal heating conditions.

In order to insure that our weapons do not effect the survivability of our carriers during a fire another test should be establish which tests for "worst case reaction" in addition to "worst case time". With this test we can insure that the fire fighters have time to control a major conflagration and if the conflagration cannot be controlled that the resulting weapon Cook-Offs do not affect the survivability of that carrier.

In conclusion, the Naval Weapons Cook-Off Improvement Program has achieved the establishment of repeatable Cook-Off times for most air launched weapons, and has thoroughly qualified thermally protected bombs and rocket systems in production. In addition, thermal protection is being developed for all inservice weapons which do not satisfy the five minute time, deflagration reaction requirement.

Another disasterious conflagration similar to those aboard USS FORRESTAL and USS ENTERPRISE would inevitably require a reappraisal of attack carrier aviation, and could drastically curtail its future. However, the successful results to date, in this program and others, indicate we can achieve the desired increase in weapon safety.

ORDNANCE RESPONSE TO MASSIVE JET FUEL FIRES

BY

W. D. SMITH, NWL, DAHLGREN, VIRGINIA

INTRODUCTION

The Naval Weapons Laboratory, Dahlgren became involved in the Weapon Survivability in Fire Program, more commonly known as the Cook-off Program, immediately following the FORRESTAL fire. It was the immediate responsibility of NWL to develop baseline safety data on the characteristics of naval air launched weapons when exposed to a jet fuel fire. The secondary goal of the program was to investigate means of improving ordnance resistance to fire.

TEST CONFIGURATIONS AND PROCEDURES

Generally, the ordnance to be tested was suspended in its prelaunch configuration above a fast cook-off test site as shown in Figure 1. The ordnance height above the test site surface was dependent on the height of the ordnance above the flight deck when racked to an aircraft, usually 36 to 66 inches. The test site was constructed to contain both the water used to provide a level fuel surface and the jet aircraft fuel which provided the fire energy source. Two types of test sites were used. Figure 2 shows the test pan which was constructed on the ground surface by building an earthen retaining wall one-foot high and one-foot thick. Polyethelene or steel plate was used to provide a watertight bottom. This test site was suitable for tests with winds up to five knots, an infrequent occurrence at Dahlgren, except very early in the morning. Figure 3 shows the test pit which was constructed to alleviate the wind problem. The pit was constructed with a six-inch thick steel plate bottom and was approximately eight-feet deep. Pipes imbeded in the banks assisted in providing oxygen to the
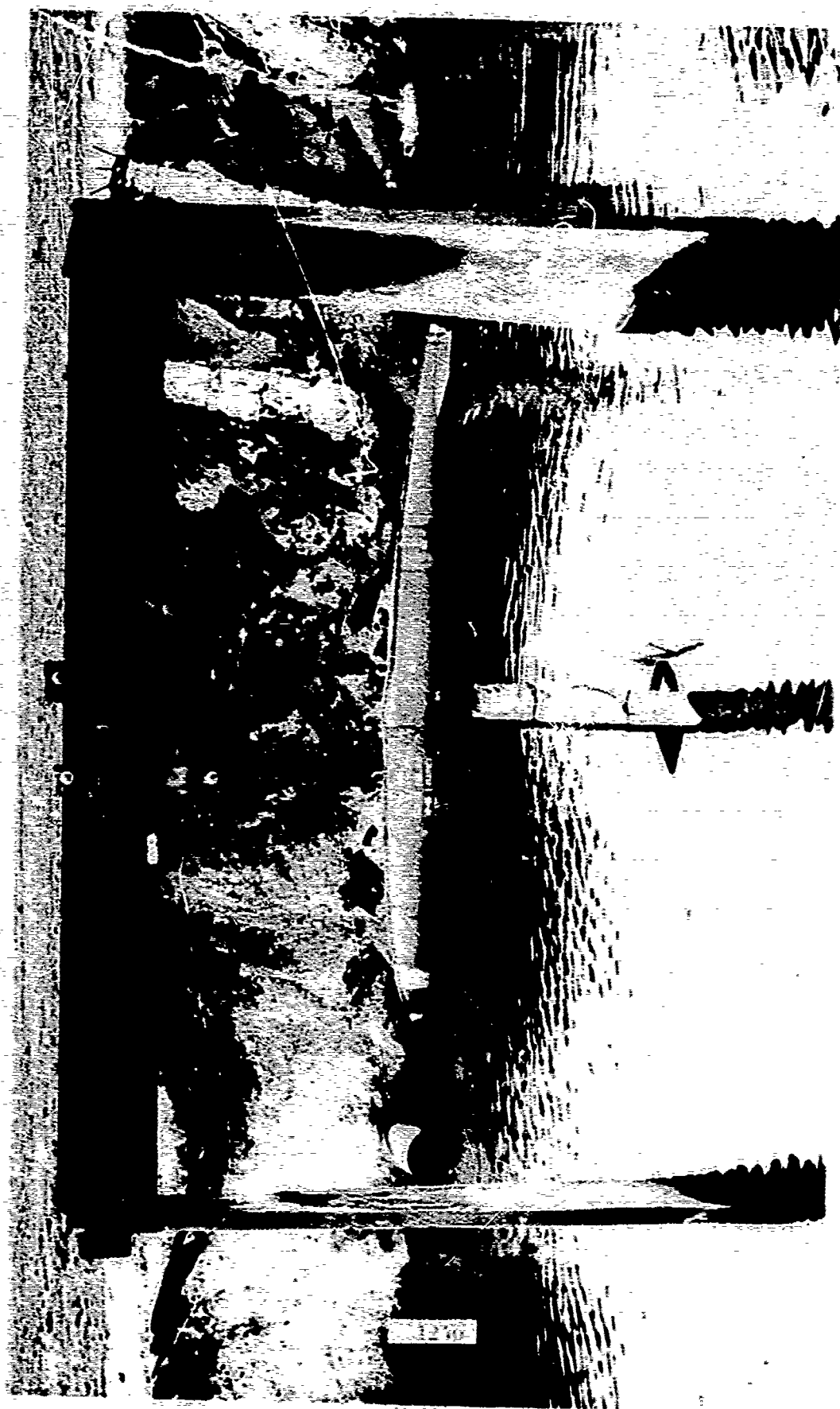
1239

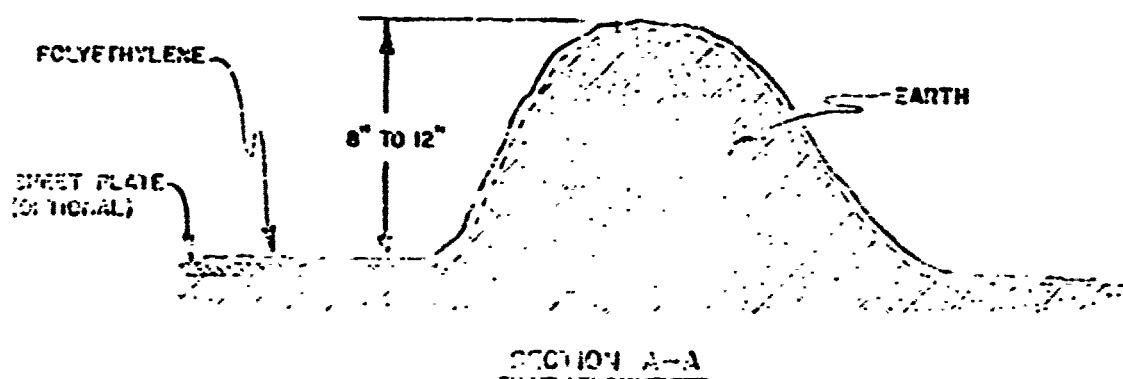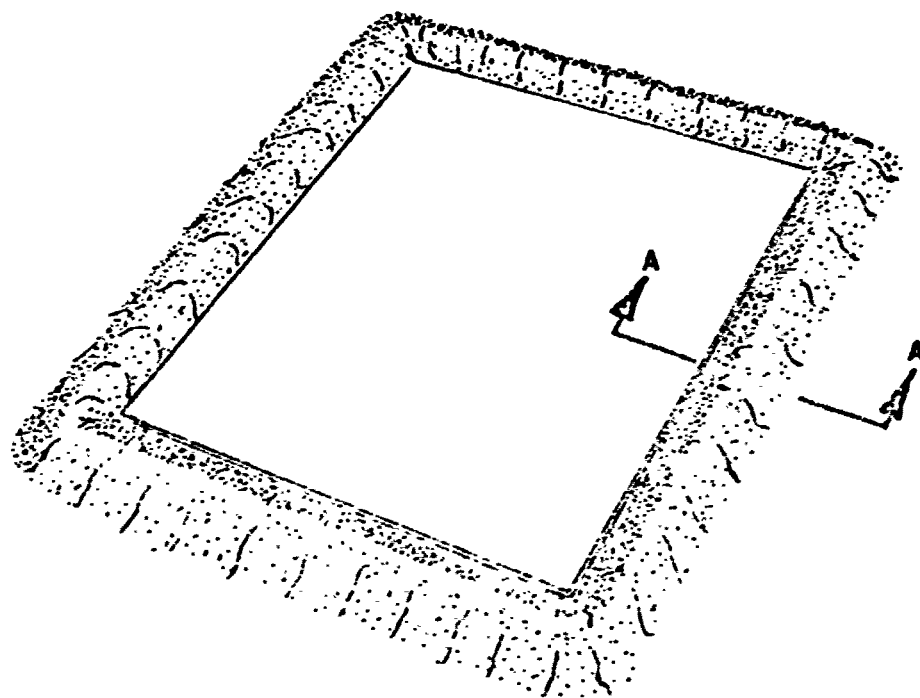Typical fast cook-off test setup. A MARK 82 bomb is suspended 36 inches above the surface of 30-foot square test pit.

Figure 1

POLYETHYLENE

SHEET PLATE
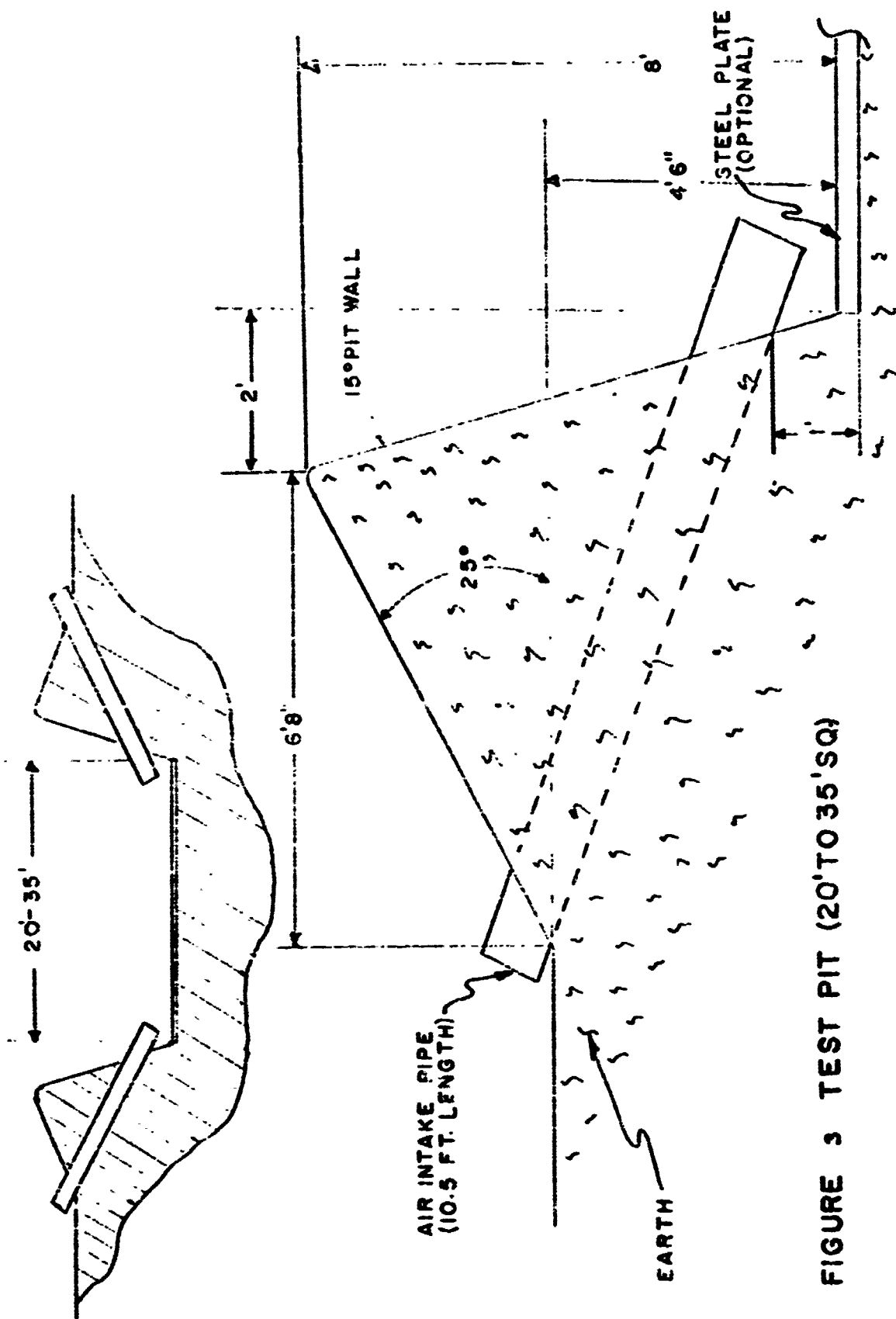(OPTIONAL)

8" TO 12"

EARTH

SECTION A-A

FIGURE 2 TEST PAN (20' TO 45' SQ.)

FIGURE 3 TEST PIT (20' TO 35' SQ)

8'

4'6"

STEEL PLATE
(OPTIONAL)

15° PIT WALL

2'

25°

6'8"

20'-35'

AIR INTAKE PIPE
(10.5 FT. LENGTH)

EARTH

1242

fire. The minimum and maximum sizes for the test sites was 20 feet square and 35 feet square, respectively.

Complete time to event histories were recorded for each test. Thermocouples placed between the ordnance case and explosive load monitored the internal temperature versus time profile of the ordnance. A Closed circuit television-video tape system and motion picture cameras provided a visual record of the tests. Piezoelectric pressure gages recorded the blast overpressure created by the ordnance reaction.

Minimum test specifications were 30 seconds time to fire buildup (1000°F flame temperature) and a minimum average flame temperature of 1650°F.

WEAPONS TESTED

The program was originally divided into nine classes of weapons to be tested. They are:

(1) General Purpose Bombs

(2) Cluster, Fire and Other Bombs

(3) Missiles

(4) Rockets

(5) Pyrotechnics

(6) Aircraft Fuel Tanks

(7) Aircraft Guns

(8) Mines

(9) Torpedoes

BASELINE TEST RESULTS

General Purpose Bombs

The MARK 80 series GP bombs and M117 750 pound bomb caused the most severe damage in the FORRESTAL fire. It was found after extensive testing that Composition-B explosive loaded bombs would detonate in a fire, without

fuze initiation, in approximately two minutes. The damage caused was extensive and the hazard to personnel and equipment was severe. Cook-off tests of H-6 and tritonal loaded bombs resulted in deflagrations in the neighborhood of three minutes. These results lead to the recommendation that Comp-B loaded bombs be restricted from carrier use. Elimination of these bombs greatly reduced the damage from bomb reactions in the ENTERPRISE fire.

As part of the General purpose bomb program, tests were conducted to determine the temperature rise rate and air cooling rate of MARK 80 series bombs during and after their exposure to fire. The internal time-temperature history of an inert, instrumented MARK 82 bomb suspended above a fuel fire was analyzed for varying lengths of fire exposure. The maximum temperature rise rate observed at the explosive/case interface was 3.92°F/sec during fire exposure and the maximum air cooling rate observed was 0.5°F/sec after fire removal.

Tests to investigate possible methods of cooling ordnance while exposed to a fire were also conducted. An inert, instrumented MARK 82 bomb was also used for these tests. Figures 4 and 5 show the Nuclear Biological Chemical (NBC) wash down system which was found to be ineffective in cooling a bomb, even in the most desireable orientations where the water from the flush deck nozzles impinged directly on the bomb. The most effective bomb cooling was obtained using a 1.5 inch diameter hand held hose delivering water (salt or fresh) at 60 to 95 gallons per minute at an angle of ten to 50 degrees to the bomb nose (See Figure 6). It was found that the bomb could be cooled at the rate of 5.0°F/sec to a stabilized internal temperature of 110°F. Similar tests using Light Water (aqueous film forming foam) provided no cooling.

Figure 4

Water from the NBC washdown flush deck nozzle impinging on the bomb case. The bomb is suspended over the center plume of the nozzle.

Figure 5

The bomb is suspended between two flush deck nozzles with water from the side spray imping-
ing on both sides of the bomb.

Figure 6

Fireman applying water to bomb during cooling test.

FIRE, CLUSTER AND OTHER BOMBS

A. ROCKEYE II

The bomblets in the ROCKEYE II cluster bomb began to react in approximately one minute and continued for several minutes. Bomblet reactions varied from deflagration to detonation. The dispenser case melted in approximately 60 seconds allowing direct exposure of the bomblets to the fire.

B. MARK 77 Series Fire Bombs

The MARK 77 series fire bombs were found to melt in one minute releasing the napalm load into the fire, thus increasing the fire fuel supply. The igniters produce considerable local fragmentation hazard when they explode after the bomb case has melted.

C. Photoflash Bombs

The M120 and M120A1 photoflash bombs detonate in little more than a minute of fire exposure. The blast and fragmentation produced are extremely hazardous to aircraft, personnel and equipment on the flight deck.

MISSILES

Separate tests of the rocket motors and warheads of the following missiles were conducted:

(1) AIM-7 SPARROW

(2) AIM-9 SIDEWINDER

(3) AGM-45A SHRIKE

(4) AGM-78A STANDARD ARM

A. Rocket Motors

The rocket motors reacted very quickly, usually within the first minute of flame exposure. The most hazardous motors tested were the

STANDARD ARM motor that exploded and threw pieces up to 200 feet, the BULLPUP motor which went propulsive and the PHOENIX motor which burned violently for an extended time.

B. Warheads

Missile warheads showed no general time to reaction trend, with times ranging from one minute for the SHRIKE warhead to eight minutes for the STANDARD ARM. The reactions of all but the SPARROW warhead, which burned mildly, were hazardous. The most hazardous warhead by far was the MARK 40 BULLPUP warhead which is capable of blowing a large hole in a flight deck when it detonates in a fire.

ROCKETS

The 2"75 FFAR and 5"0 ZUNI rockets were tested in their launchers. Sysmpathetic massive detonations of both the 2"75 FFAR and 5"0 ZUNI rocket warheads occurred in as little as three minutes. Blast and fragmentation damage were severe. No propulsive motor reactions occurred.

PYROTECHNIC DEVICES

The pyrotechnic devices tested included photoflash cartridges, aircraft parachute flares, marine location markers, illumination signals and decoy flares. These devices generally reacted in the design mode. That is, they burn as designed but because of their small size do not create a serious hazard when they react in a fire. The only exception is photoflash car _dges which when reacting in large quantities, such as in a dispenser, create a considerable fragment hazard to personnel and equipment in the immediate area. Most of the pyrotechnic devices react within the first minute of flame exposure.

EXTERNAL AIRCRAFT FUEL TANKS

Aircraft fuel tanks, although not weapons, were considered in the program because they could feed additional fuel to an existing fire and increase the length of time the fire burns. The 300 gallon AERO 1-D and 600 gallon ATP-H4 tanks were tested containing various quantities of fuel (both JP-5 and AV gas). No violent reactions occurred. The time required to melt the tank and release the fuel load depended on the quantity of fuel in the tank. The larger the fuel load, the longer the time to reaction. The reaction time varied from 20 seconds for tanks with 10% fuel loads to eight minutes for tanks with full fuel loads.

AIRCRAFT GUNS

The MARK 4 MOD 0 gun pod was the only gun tested and was loaded with 750 rounds of 20mm HEI ammunition. Reactions began at approximately two minutes, one minute after the aluminum pod body began to melt. The reactions were sporadic and continued for nearly seven minutes. Debris from the pod, mainly cartridge cases and projectiles, were scattered up to a distance of 300 feet. The most common reaction was initiation of the cartridge propelling charge. No more severe projectile reaction than a deflagration was observed. The reactions are hazardous only in that they would tend to scatter fire fighting teams, thus hindering the fire fighting capability of the ship.

MINES AND TORPEDOES

No tests of mines and torpedoes have been conducted due to a lack of funds.

RECENTLY COMPLETED PROGRAMS

The results of the baseline tests and a serious fire related accident with an ejection seat led to the following additional test programs:

(1) Ejection Seats

(2) "All-up" Missiles

(3) Mixed Stores

(4) Close Proximity

These test programs were necessary to develop additional safety data for the fleet.

RESULTS

Ejection Seats

Ejection seat systems used in the majority of naval aircraft were tested in a fire environment to determine: (a) the time to reaction, (b) the type of reaction that occurs and (c) the time-temperature history inside the cockpit. Both the underseat rocket pack system shown in Figure 7 and the rocket catapult system shown in Figure 8, were tested installed in an aircraft fuselage.

The typical sequence of events during the tests was as follows:

(1) Cockpit canopy melts within two minutes after start of fire exposing the seat directly to the fire.

(2) Rocket pack or rocket catapult is ignited by the fire, ejecting the seat from the aircraft at a minimum of three and a half minutes. The maximum distance the seats traveled was 350 feet.

(3) The initiator system (cartridges, initiators, etc.) usually reacted after the rocket pack or rocket catapult had functioned.

The primary heat path to the seat is through the canopy. Pilot survival is impossible after the aircraft has been exposed to the fire for two minutes. The reactions of the ejection seats are hazardous in that they would tend to cause fire fighting personnel to scatter. No blast or fragmentation hazards are produced.

Figure 7   Underseat rocket pack ejection seat system installed on pilot seat for fast cook-off test.
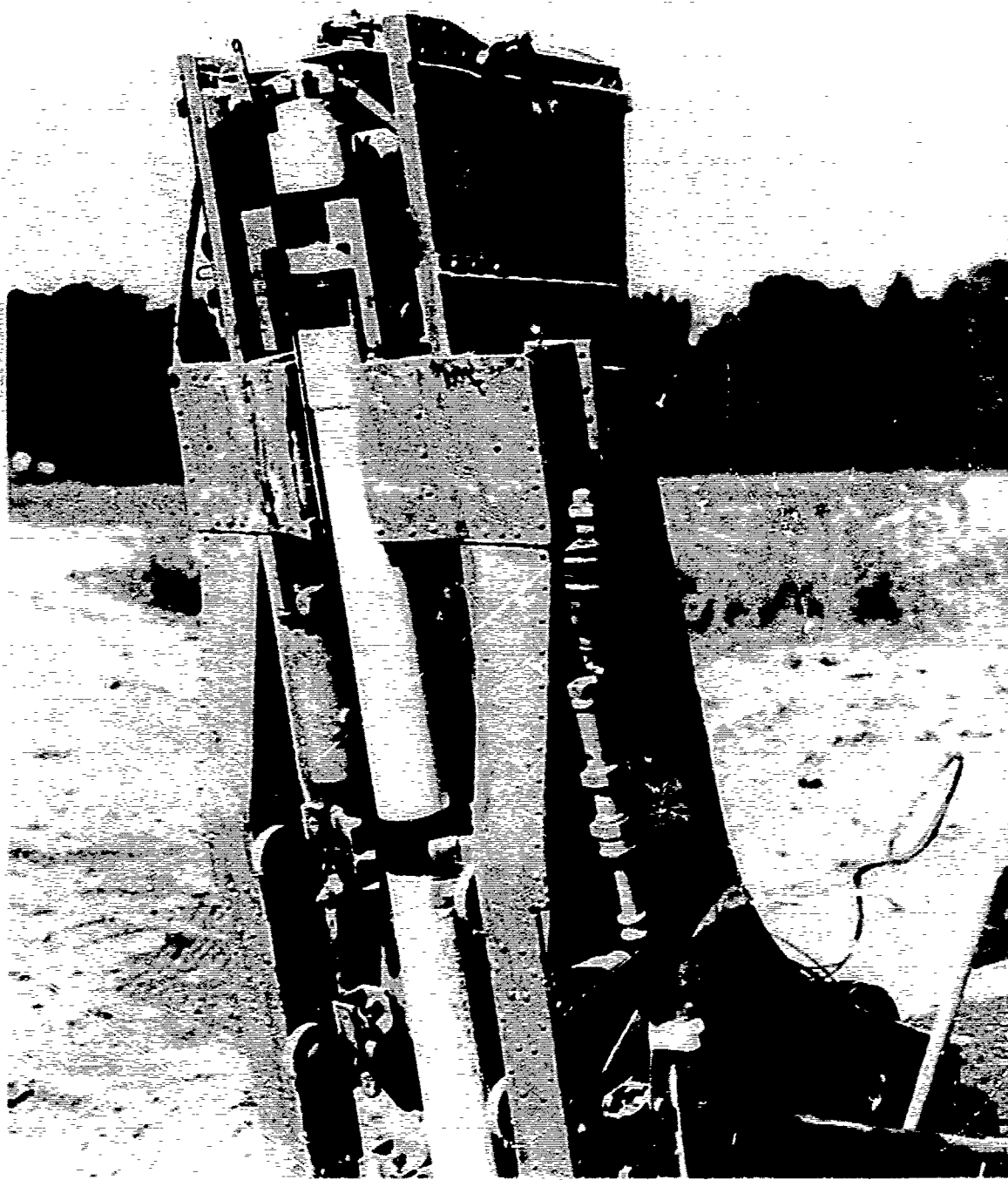
Figure 8

Rocket catapult ejection system installed on pilot seat for fast cook-off test.

"ALL-UP" MISSILES

Since the tests of missile warheads and motors had been conducted separately, it was decided to subject the entire assembled missile to a fire environment to determine if any interaction between the motor and warhead would occur. The following missiles and guided weapon were tested:

(1) AIM-9 SIDEWINDER

(2) AIM-7 SPARROW

(3) AGM-45A SHRIKE

(4) MARK 1 MOD 0 WALLEYE

The test results were very similar to the results of individual warheads and motors. No interaction between the warheads and motors occurred. The most hazardous missile was the SHRIKE where the warhead exploded before the rocket motor deflagrated. The WALLEYE guided bomb was by far the most hazardous weapon tested in this series, partially detonating at six minutes 19 seconds. The blast was extreme with the burning explosive being thrown up to 1200 feet.

MIXED STORES

The mixed stores tests were conducted to determine if the reaction of weapons on one weapon station would cause sympathetic reactions of weapons on an adjacent station. Because of the large numbers of weapons that can be carried by a single aircraft (bombs, rockets, missiles, etc.), it was not possible to test all the possible combinations. The main emphasis was therefore placed on the only two thermally protected weapons which are currently in production, the MARK 82 MOD 2 bomb and LAU-10A/A 5"0 ZUNI rocket launcher. The bomb

and launcher with fuzed "All-Up" rounds were suspended 16 inches apart, simulating their orientation when racked to adjacent weapon stations on the A-7 aircraft. Figure 9 shows a typical pre-test photograph. Also tested were three bombs in a Triple Ejector Rack (TER) configuration shown in Figure 10. These bombs were rigged to drop to the test pit floor at two minutes into the test, the time that the TER melts in a fire.

Sympathetic ZUNI warhead detonations failed to cause the MARK 82 bombs to react. However, the three bombs in the TER test simultaneously detonated at 15 minutes. The crater blown in the pit bottom was 12 feet deep and 15 feet in diameter. Figure 11 shows the damage which was done to a six-inch thick steel plate in the pit bottom. It could not be determined whether the reaction was caused by a fuze initiated bomb detonation or whether a bomb detonated without fuze initiation.

Additional tests of bombs in a TER configuration are planned to evaluate the cause of the massive reaction. The environment at the deck level, the effect of the fall to the steel deck on the fuze and bomb and the time-temperature history of a bomb on the deck will be determined in a test program commencing in October 1973.

CLOSE PROXIMITY

No data exist on the susceptibility of naval air launched weapons to slow cook-off when positioned near to (0 to 90 feet), but not exposed in, a jet fuel fire. Close proximity tests were therefore conducted to answer the following questions:

(1) What is the safe distance from a jet fuel fire for ordnance?

(2) What length of exposure to the environment near to a jet fuel fire will cause a reaction to occur?

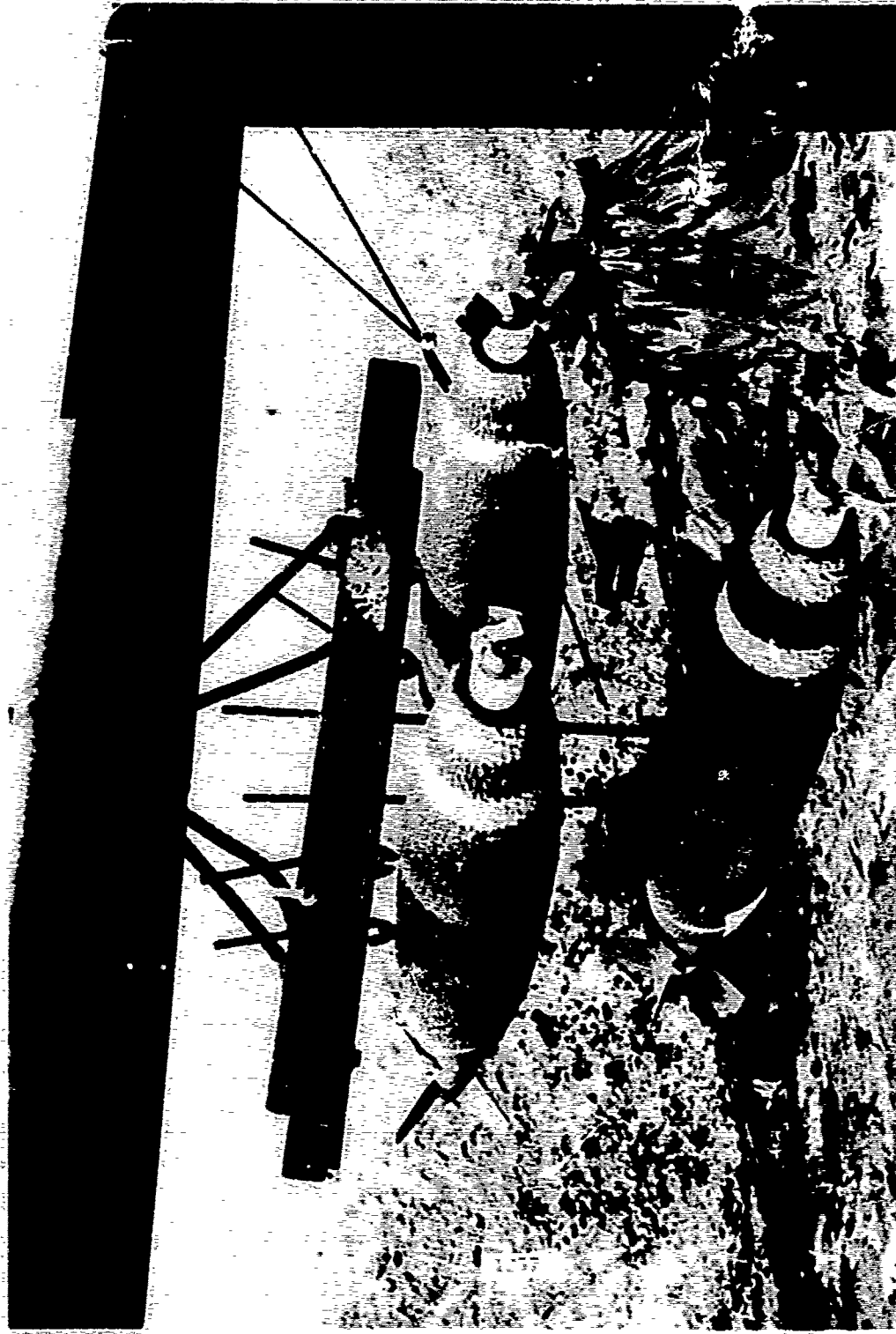(3) How severe are the ordnance reactions that occur?

Figure 4

Figure 10

MARK 82 bombs configured in Triple Ejector Rack orientation for Mixed Stores fast cook-off test.
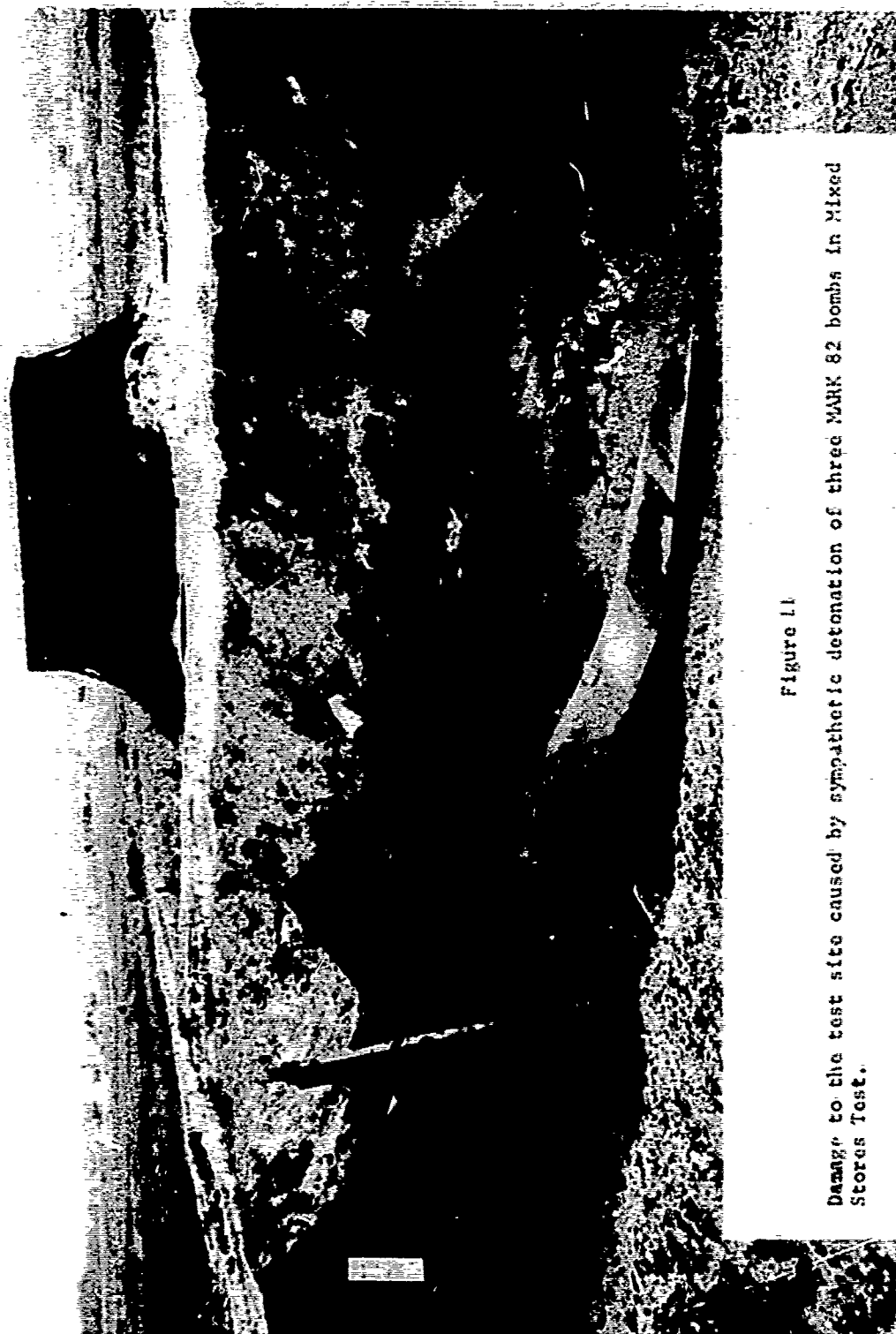
Figure 11

Damage to the test site caused by sympathetic detonation of three MARK 82 bombs in Mixed Stores Test.

All tests were conducted using inert, instrumented ordnance. Funding limitations precluded tests on live ordnance to answer question number (3). The environment from the edge of the fire luminous bondary to 90 feet was evaluated to determine the temperature distribution around the fire and the heat flux that would be incident on a weapon throughout this distance. It was found that the temperature varies from 600°F at the fire edge to 140°F at 20 feet and essentially ambient temperatures thereafter. Maximum radiant heat flux was 0.6 BTU/ft^2 second at the fire edge.

Tests of inert, instrumented MARK 82 MOD 2 bombs, M904E4 bomb nose fuzes, LAU-10A/A ZUNI launchers and MARK 48 MOD 4 SIDEWINDER warheads showed that slow cook-off would occur only within 20 feet of the fire.

Time to reaction is difficult to predict for the weapons tested because the temperature at reaction is dependent on heating rate. The higher the heating rate, the higher the temperature at reaction. No temperature at reaction information is known to exist for the explosives in the weapons tested at the heating rates observed. Therefore the data from these tests will be used in a computer model which is currently being developed at NWL to predict time to reaction for explosives at various heating rates. Data from this program will not be available until near the end of 1973.

COOK-OFF RESERACH

The long range goal of the cook-off program is to develop methods to completely eliminate ordnance reaction in a fire. As a means to accomplish this goal, NWL has been conducting research into an improved internal liner for thick walled ordnance to replace the currently used asphaltic hot melt. The liner would be designed so that when subjected to a fire it would react chemically with the explosive and desensitize it.

RDX based explosives generally exhibit a rapid exothermic decomposition at 500°F. A liner material which would have an endothermic effect (i.e., increase the temperature of the exotherm) would have a significant effect on the ordnance time to reaction. Candidate liners having the following characteristics are being investigated:

(1) does not interact with the explosive below 350°F.

(2) absorbs a substantial quantity of heat between 350°F and 400°F (endothermic process).

(3) releases a thermal desensitizing or diluting agent between 400°F and 500°F.

A combination of thermogravimetric analysis and differential scanning calorimetry was used to select liner materials for small scale bomb cook-offs.

The small scale cook-off tests were conducted electrically with "pipe" bombs. A "pipe" bomb is simply a three-inch diameter water pipe six-inches long loaded with one pound of H-6 explosive. The ends are threaded for caps which provided the pressure seal. The bombs are cooked-off by an electric heating filament which simulates the temperature rise rate at the hot melt/case interface of a MARK 82 bomb in a jet fuel fire.

The results of the small scale tests are presented in Table 1. This table shows four important relationships. First, the addition of the desensitizers-trithiane and increasing the quantity of asphaltic hot melt improves the cook-off time over asphaltic hot melt. Second, comparing the cook-off times for 25% s-trithiane-75% hot melt with 25% s-trithiane-75% RTV 560 shows that the latter cook-off time is longer even though the quantity of liner material was less by 50%. This indicates that asphaltic hot melt sensitizes the explosive. Third, increasing the liner

thickness increases the cook-off time. Finally, incorporation of a
desensitizing agent in the bomb liners increased the cook-off times.

Further small scale chemical and pipe bomb tests are currently being
conducted at NWL on additional promising materials. Data from these
tests will be available late in FY 74.

TABLE 1
NAVAL WEAPONS LABORATORY

SMALL BOMB COOK-OFF TESTS

REACTION DATA		LINER COMPOSITION			
TIME SECONDS	REACTION* MODE	PERCENT DESENSITIZER IN LINER	DESENSITIZER	SUPPORT MATRIX	PERCENT LINER TO EXPLOSIVE
244	E	25	Irganox 565	RTV560	10.2
232	E	25	s-trithiane	RTV560	10.0
208	D	50	s-trithiane	RTV560	9.9
207	D	25	CARSTAB DLTDP	RTV560	10.2
184	D	25	s-trithiane	RTV560	4.4
178	D	25	WYTOX x540	RTV560	3.8
170	B	25	s-trithiane	HOT MELT	19.7
167	D	25	Arkon P115	RTV560	9.9
158	D	25	Irganox 1010	RTV560	9.9
151	D	10	CARSTAB DLTDP	RTV560	3.3
149	D	25	Melamine	RTV560	9.9
148	D	10	s-trithiane	HOT MELT	9.4
146	D	25	CAO-44	RTV560	9.9
145	D	0.0		HOT MELT	7.0
141	D	25	Ammonium Phosphate	RTV560	9.9
135	E	10	Irganox 565	RTV560	3.8
134	D	25	450 Wax	RTV560	9.9
132	B	10	s-trithiane	RTV560	4.2
123	D	25	Diammonium Phosphate	RTV560	9.9

* E = Explosion

D = Deflagration

B = Burning

1262

REDUCTION OF COOK-OFF HAZARDS

Jack M. Pakulak, Jr.
Naval Weapons Center
China Lake, California

Abstract. The continuing objective of this program is to study the chemical and thermal stability of explosives and various liner materials. From this study we can identify means by which the cook-off time of a bomb or warhead in a fuel fire can be extended and the severity of the cook-off reaction can be reduced. The areas that relate to the explosive, internal liner, case and external coating are studied together in relationship to the cook-off problem.

INTRODUCTION

Following the USS FORRESTAL fire in 1967 and, as a result of the RUSSEL Report, work was started to identify cook-off characteristics. The USS ENTERPRISE fire in January 1969 further emphasized the hazards and the urgent need for longer cook-off times and less violent reactions. The basic goal is the development of explosive systems that will eliminate, delay, or minimize the damaging effects of cook-off.

Studies have continued in the three interrelated areas: explosives, liners, and coatings. The explosives considered were the TNT type cased explosives and PBX-type explosives. The liners used with these explosives were none, various cavity paints, hot melts with and without outgassing agents, and Butarez rubber with ammonium oxalate (AO). The coating materials that were studied in part in this report are: Pfizer Firex 39-010, NASA-313, UK-AWRE coating, and AVCO FM-26.

Explosives, Liners and Coatings

The data from the thermal patterns on the selected common explosive and certain mixtures are summarized in Table 1. For the majority of applications, the exothermic onset and peak temperature values are the most important since they are indicative of the relative stability of the explosive or explosive mixture. For example, the use of AP with HMX or RDX lowers the thermal stability of the HMX or RDX.

The evaluation of Composition B with certain liners and coatings has progressed through laboratory study and small-scale testing to full-scale testing using MK 24 Zuni warheads as test vessels. Table 2 summarizes the results of these tests.

The normal heating rate at the inside metal skin of the MK 24 warhead is about 2-3°C per second in the 150°-200°C temperature range. The heating rate is not linear but it is a 1/T function versus log time. This means that this warhead can reach 300°C within 2 minutes from start of the test.

Data from the Mk 24 warhead tests indicated that the cook-offs occurred about the time the explosive melted. The melted TNT probably penetrated the liner material and came in contact with the metal surface. The time to cook-off for the two PBX explosives was about twice that of the Composition B explosive which was in contact with red cavity paint. The cook-off reaction was mild when compared with the Composition B explosive,

under the confinement and short burning distance (the radial distance from the center of the warhead) in the Mk 24 warhead.

Other explosives have been tested in various test vessels (warheads, SCB, etc.) and the data are shown in Table 3. This covers some of the work on different explosives and their reaction under different test conditions and confinement. From the data given in Table 3, the explosives that appear to be less of a problem are PBXN-3, PBXN-102, and H-6.

Those that present more of a problem are Comp. B and PBXN-101. The presence of aluminum in an explosive seems to help in reducing the severity of the reaction on fast cook-off, possibly by controlling the explosive burning rate under pressure.

In the liner development area, Lauryl methacrylate (LM) has been successfully prepolymerized to yield a readily castable liner material containing 50% by weight of ground ammonium oxalate, mean diameter 24 microns, and 0.2% lecithin wetting agent. Thermal analysis shows a clean and complete gaseing reaction at 220°C.

In the coating study, a simple temperature dependent equation has been described for the back side temperature with respect to time for the steel plates (uncoated and coated) heated in a fuel fire. The linear

relationship is shown in an area of interest by Eq. (1) for an uncoated plate.

$$t_o = A_o e^{-B_o/T} \qquad (1)$$

where:

t_o = time for uncoated plate, sec

A_o = equation constant, sec

B_o = material constant, $^\circ K$

T = temperature, $^\circ K$

then for a coated plate:

$$t_x = A_o e^{-B_o/T} e^{CN} = t_o e^{CN} \qquad (2)$$

where:

t_x = time for coated plate, sec

C = coating material constant for a given environment, mils

N = thickness of coating, mils

The value of C has been determined for several coating materials and are listed in Table 4.

They are NASA-313, AVCO-FM26, Pfizer 39-010, UT AWRE and R/M 1776. Once the Eq. (1) is satisfied for a bare warhead or motor in a fire, the amount of coating necessary to give a desired back-side temperature after a given time (t_x) can be estimated from Eq. (2). The value of C is

determined from laboratory tests. For a two layer coating, Eq. (2) is modified to

$$t_x = t_o e^{C_1 N_1} e^{C_2 N_2} \tag{3}$$

where:

$C_1 N_1$ and $C_2 N_2$ correspond to the material constants and thickness of each layer.

Future Plans

The study will continue on explosives, liners, and coatings. Two shock resistant explosive formulations are being studied for thermal stability, reaction severity, and application. Samples of LM loaded with either calcium formate, sodium formate, or orotic acid will be prepared and then thermally analyzed. Evaluation bombs, containing LM loaded with ammonium oxalate as the liner, will be tested. In the coating area of study, consideration will be given to a two or possibly a three layer coating system on missiles to overcome the aerodynamic heating problem.

TABLE 1 Summation of Thermal Data.

No.	Sample	Endotherm, °C	Exothermic onset,[a] °C	Exothermic peak, °C	Wt loss,[b] %
1	TNT	75	262	277	92
2	HMX	188	261	272	99
3	RDX	182	[c]	217	90
4	Tetryl	126	162	188	76
5	Octol	80,183	206[d]	236 (1st) 260 (2nd)	95
6	CH-6	184	[c]	203	96
7	PBXN-3	184	213	226	92
8	PBXN-5	188	257	269	97
9	PBXN-101	184	219	250	94
10	PBXC-303	138	161	169	87
11	H-6	78	167	211 (1st) 300 (2nd)	58[e]
12	AP (200μ)	238	258[d]	284 (1st) 377 (2nd)	99
13	AP/HMX 50/50	181	202	220	72
14	AP/RDX 53/47	185	[c]	192	65
15	PL 6239 (N35)	322	361[d]	450 (1st) 540 (2nd)	43

[a] "Onset" is defined as the first detectable evidence of reaction on the DTA curve

[b] Total weight-loss after major or final exothermic reaction

[c] Detection of onset obscured by melting phase

[d] Onset of first exothermic peak.

[e] Total weight-loss after 2nd exothermic reaction Additional 14% weight-loss from here to end of test run (550°C)

TABLE 2. Fast Cook-Off Tests With Mk 24 Test Vessels.

Explosive load	Liner		Coating		Aft end sealer	Heating rate[a], °C/sec	Time to reaction	Reaction type[b]
	Type	Thickness, in	Type	Thickness, mils				
Composition B	Black cavity paint	0.008-0.010	None		c	2.7	1 min 16 sec	Partial detonation
Composition B	Hot melt	~0.25	None		c	2.6	2 min 47 sec	Deflagration/explosion
Sand	Butarez/AO[d]	0.25	UK[e]	~40	f	0.4	---	---
Composition B	Butarez/AO[d]	0.25	UK[e]	~40	f	0.4	8 min 23 sec	Deflagration/explosion
Composition B	Butarez/AO[d]	0.25	UK[e]	55	g	0.5	8 min 51 sec	Deflagration/explosion
Composition B	Butarez/AO[d]	0.25	Pfizer Firex	120	g	0.4	12 min 50 sec	Explosion
Composition B/5% 20u Al	Black cavity paint	0.008-0.010	None		g	2.2	1 min 46 sec	Partial detonation
Composition B	Hycar/Ca formate	0.25	NASA 313[h]	~45	g	0.4	5 min 18 sec	Explosion
Composition B	Hot melt/Ca formate	0.25	None		g	1.4	3 min 9 sec	Explosion
Composition B	Hot melt/Na formate	0.25	None		g	1.9	3 min 16 sec	Explosion
PBXN-101	Red cavity paint	0.008-0.010	None		g	3.3	2 min 43 sec	Deflagration/explosion
PBXN-102	Red cavity paint	0.006-0.010	None		g	2.7	2 min 48 sec	Deflagration

[a] Heating rate in 150-200°C region at inside metal skin.

[b] As given under Definitions.

[c] Tuffseal

[d] Ammonium oxalate.

[e] United Kingdom coating - AWRE developed intumescent paint. Aldermaston, England.

[f] R45M (ARCO Chemical Company) + MgO.

[g] R45M + Ca formate.

[h] NASA coating containing P-nitroanilinebisulfate.

TABLE 3 Fast Cook-off Data on Selected Explosives.

Test vessel	Explosive	Liner type/ thickness, mils	Cook-off time, sec	Type of reaction.
SCB[a]	Dextex	Black cavity paint/8-10	150, 160	Explosion
	Comp B/D-2	Same	121, 128	Partial detonation
	TNT	None	245	Explosion
	Tritonal	None	305	Explosion
	Comp B	None	112	Detonation
	Comp B	Black cavity paint/8-10	98	Explosion
	H-6	None	105	Deflagration
	H-6	Hot melt/250	222	Deflagration
	H-6	Plastonium-44/250	435	Explosion
	Minol-2	None	177	Explosion
	Amatex-20	None	122	Partial detonation
	PBXN-101	None	112, 141	Deflagration
	PBXN-102	None	130	Deflagration
Mk-24	PBXN-101	Red Cavity paint/ 8-10	163	Explosion
	PBXN-102	Same	168	Deflagration
	Comp B	Black cavity paint/8-10	76	Partial detonation
		Hot melt	167	Explosion
		Butarez/AO/250	770	Explosion
Warhead A	Comp B	Black cavity paint/8-10	...	Detonation
	PBXN-101	Red cavity paint/ 8-10	180	Detonation
	Comp B	Hot melt/~200	160	Deflagration
	Comp B	Black cavity paint/AO/~100	315	Deflagration
Mk-82[b] bomb	H-6	Hot melt/250	1,202	Detonation
Warhead B	PBXN-3 T	Teflon/20	146-330[c]	Deflagration
Warhead C	Dextex	Hot melt/100-200	120-180[d]	Explosion
[b]		Hot melt/formate/[e] 100 and 180	511, 559	Deflagration
[b]		Butarez/AO/ 100 and 150	424, 754	Explosion

[a] SCB is a small-scale cook-off bomb

[b] With external thermal protection

[c] Results of three tests

[d] Results of four tests

[e] 50/40/10 by weight of hot melt, calcium formate and sodium formate

TABLE 4 Coating constant, C, from equation $t_x = t_o e^{CN}$
for several selected materials at a back-side temperature of 400°F

Material	C (mil^{-1})
AVCO FM-26	0.0091
UK	0.027
NASA (313, 45B3) [AVCO Flamarest-1000]	0.022
Pfizer 39-010	0.017
R/M 1776	0.0037

Definitions of Ordnance Explosive Reactions
Obtained by Cook-Off

1. The Naval Ordnance Systems Command establishes the following terminology with definitions which shall be used when reporting ordnance explosive reactions resulting from cook-off. They are listed in decreasing order based on air shock and fragmentations.

   a. Detonation: Munition performs in design mode. Maximum possible air shock formed. Essentially all of case broken into small fragments. Blast and fragment damage is at maximum. Severity of blast causes maximum ground crater or flight-deck hole capable by the munition involved.

   b. Partial Detonation: Only part of total explosive load in munition detonates. Strong air shock and small as well as large case fragments produced. Small fragments are similar to those in normal munition detonation. Extensive blast and fragmentation damage to environment. Amount of damage and extent of breakup of case into small fragments increase with increasing amount of explosive that detonated. Severity of blast could cause large ground crater, or large flight-deck hole on carrier if munition is large bomb; hole size depends on amount of explosive that detonates.

   c. Explosion: Violent pressure rupture and fragmentation of munition case with resulting air shock. Most of metal case breaks into large pieces which are thrown about with unreacted or burning explosive. Some blast and fragmentation damage to environment. Fire and smoke damage as in deflagration. Severity of blast could cause minor ground crater, or small depression on flight-deck of carrier if munition is large bomb.

   d. Deflagration: Explosive in munition burns. Case may rupture or end-plates blow out; however, no fragmentation of the case. No fragments are thrown about. Damage to environment due only to heat and smoke of fire. No discernible damage due to blast or fragmentation.

A SIMPLIFIED METHOD FOR ESTIMATING THE APPROXIMATE TNT EQUIVALENT FROM LIQUID PROPELLANT EXPLOSIONS

By

Louis C. Sutherland

Wyle Laboratories, El Segundo, California

When rocket propellants are mixed together, an explosive release of energy, or detonation, can occur. To represent a significant hazard, at least three elements are required:

1. The quantity of propellant must be substantial.

2. The mixture ratio of fuel-to-oxidizer must fall within a certain restricted range.

3. There must be a source of ignition energy if the propellant mixture is not hypergolic (i.e., self-igniting upon contact).

It is common practice to express the explosion potential in terms of an equivalent weight of TNT.[1] However, the current state-of-the-art allows only empirical estimates to be made of this equivalent weight of TNT based on experimental data.[2-5] For example, the TNT equivalent for liquid oxygen –liquid hydrogen propellants employed in a static engine test stand might be based on the following rules:

● Propellants stored in tanks or unburned in combustion chamber

 – Equivalent TNT weight = 20% of total propellant weight.

● Propellants flowing in fuel lines between fuel storage, tankage and combustor

 – Equivalent TNT weight of propellant flowing in a period of two seconds.

The "two-second" rule for the quantity of propellant in flow lines potentially involved in an explosion is based on industry experience on the maximum time required to close a rocket propellant flow valve.[6] The TNT equivalent, in this case, is taken as 60% of the propellant weight that is spilled by the two-second flow of both propellants. This later percent equivalent is consistent with recommended practice according to Reference 1.

The choice of a 20% TNT equivalent for the stored propellants and a 60% figure for the flow spill appears inconsistent at first. However, a new evaluation of the available data on TNT equivalents from actual LOX/LH$_2$ explosions indicates that these are, in fact, reasonable design figures.

Results of intentional LOX/LH$_2$ propellant explosions from 23 of the Project PYRO tests[2] and three real accidental explosions involving these propellants[1] are summarized in Figure 1. The figure shows the estimated equivalent TNT weight (W_T) based on measured explosion parameters (i.e., overpressure versus distance) as a function of the actual propellant weight (W_p). Data were utilized from Project PYRO for nine tests of LOX/LH$_2$ with W_p = 200 lbs, eight tests with W_p = 1000 lbs, five tests with W_p = 25,000 lbs, and one test with W_p = 91,000 lbs of propellant.

Although there is a wide scatter in the results at the lowest propellant weights, the average values of the equivalent TNT weight (W_T) fall surprisingly close to a simple two-thirds power scaling law. Such a scaling law is, indeed, not unexpected on the basis of the following rationale.

● The weight of propellants (W_p) in tanks (of similar shape) will tend to vary as the cube of a characteristic tank dimension (d) or $W_p \propto d^3$.

● The equivalent TNT weight (W_T) of propellant which participate in a detonation can be expected to vary in direct proportion to a mixing area which in turn should tend to vary as a square of a characteristic tank dimension (d) or $W_T \propto d^2$.

● Combining these two highly simplified relationships leads to the scaling law suggested by the results in Figure 1, namely that:

$$W_T \propto W_p^{2/3}$$

● Other effects, such as the method of propellant confinement, method of tank rupture and ignition delay time, appear to be secondary to this basic scaling trend and are undoubtedly the source of significant variation about the mean trend.

Although only a portion of the Project PYRO results were utilized for Figure 1, they are considered representative of the general trend. This trend permits a reasonable evaluation to be made of conservative estimates of the possible explosion magnitude. With this in mind, the following additional information is obtained from Figure 1.

a. The three actual accidental explosions noted on the figure indicate an average TNT yield which is about a factor of 2.8 below the average trend line for yield from the PYRO tests.

b. The upper bound of the PYRO data, shown by the vertical bars through the data for W_p = 200, 1000 and 25,000 lbs., lies roughly on a similar two-thirds power scaling trend line which indicates a maximum probable yield of about 2.9 times the average yield.

c. Assuming the two-thirds scaling law is valid, the data suggest that the maximum yields observed in the Project PYRO tests were about 2.8 x 2.9 or eight times greater than the average (scaled) yield estimated from the actual accidents.

For comparison, dashed lines which define design rules corresponding to a 20% and 60% yield are shown on the figure. It is clear that the 20% or 60% TNT equivalent rules would lead to very conservative estimates of the TNT equivalency, particularly for large amounts of propellant. More significant, however, is that these constant percentage equivalency rules do not appear to be consistent with available experimental data. The simple two-thirds power law illustrated appears to provide a better empirical model for approximating the TNT equivalence of LOX/LH$_2$ propellants over a wide range of propellant weights. Furthermore, the data suggest than an upper bound estimate of the TNT equivalent for these propellants might be given by $W_T \simeq 4 W_p^{2/3}$. It is suggested that a simple two-thirds power scaling law of this form be considered for evaluation of liquid-propellant explosions. The empirically-determined scaling constant (4) would probably vary substantially for different types of propellants, tank configurations, and failure modes as demonstrated very well by the experimental studies.
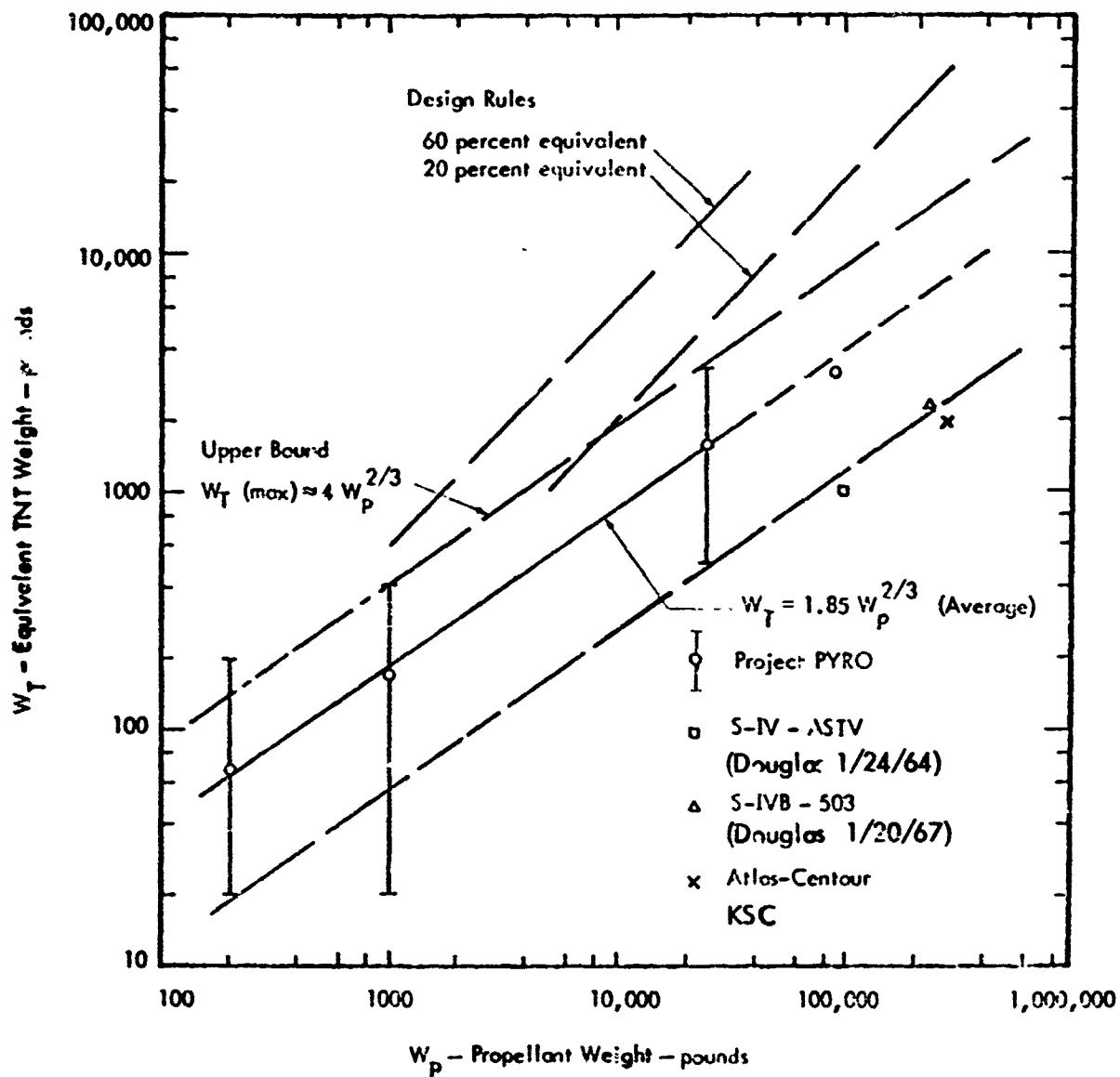
Figure 1. Trend in Measured Equivalent TNT Weight from LOX/LH$_2$ Propellant Explosions Compared to Design Rules

REFERENCES

1. JANNAF Hazards Working Group, "Chemical Rocket/Propellant Hazards –
    Volume I, General Safety Engineering Design Criteria," CPIA Publication
    194, October 1971.

2. "Liquid Propellant Explosive Hazards – Project PYRO," AFRPL TR-68-92,
    Volumes I, II and III, December 1968.

3. "Statistical Analysis of Project PYRO Liquid Propellant Explosion Data,"
    Bellcomm, Inc., 1969.

4. "Solid Propellant Explosive Test Program – Project SOPHY," Aerojet-General
    Corporation, AFRPL-TR-67-211, Volumes I and II, August 1967.

5. "Prediction of Explosive Yield and Other Characteristics of Liquid Propellant
    Rocket Explosions," Erich A. Farber, University of Florida, Gainsville,
    NASA Contract NAS 10-1255, Final Report, 31 October 1968.

6. Personal Communication, H. Weiss, Rocketdyne Division, North American
    Rockwell Corporation, May 1971.

BLAST FROM DETONATION OF A FUEL-IN-AIR DISPERSION

Lloyd H. Smith and Gilbert F. Kinney

Naval Weapons Center
China Lake, California

Introduction. Fuels such as ethylene oxide, propylene oxide, or a mixture of the hydrocarbons methyacetylene, propadiene, and propane (MAPP) when dispersed in air can be made to detonate. These explosions are described in Reference 1. These explosions are of the distributed energy type and these characteristics in some respects may differ significantly from those of a condensed explosive such as TNT. Thus the close-in explosiion effects of the fuel-in-air dispersion are less intense than those for the condensed explosive. The far-field effects for the dispersion however can be greater, and for two reasons. One is that the less intense center may show reduced losses through irreversibilities associated with localized energy dissipation. More important however is that the energy release per unit mass of dispersed fuel can well exceed that per unit mass of a condensed explosive because in the former part of its reaction oxygen is supplied by external air.

TNT Equivalence. The TNT equivalence of a mass of explosive can be defined as the mass of TNT required to produce the same explosion effect. This ordinarily is expressed as an equivalence ratio or factor, the ratio of the two masses. Equivalence factors depend strongly on the effect selected as a basis for comparison; that is on the method of computation. Here we first compute equivalence factors theoretically from thermodynamic considerations, and then ones as obtained from representative blast wave configurations.

Theoretical Energy Considerations. From a thermodynamic viewpoint the pertinent energy index for an explosion reaction is the Helmholtz free energy function (Reference 2). This is defined as the internal energy relative to an arbitrary datum minus the temperature-entropy product. It is possible to make a reasonable estimate for this index using conventional methods provided that the chemistry involved in the detonation portion is fully described. This procedure as follows:

Let us select ethylene oxide, formula C_2H_4O, as a representative fuel, and assume that its carbon component forms carbon monoxide and its hydrogen component forms water. Then the internal energy change for the detonation reaction at ordinary pressures and temperatures can be calculated as about -14,320 joules per gram of ethylene oxide. (This is obtained from published values for enthalpy of formation when corrected to internal energy by subtracting the pressure-volume product.)

Values for the entropy for all components of this detonation reaction are

available except that for ethylene oxide itself. This latter can reasonably be estimated as about 110 joules per mole-Kelvin. Then a computed entropy change for the detonation reaction (allowing for the entropy of mixing) is +6.7 joules per gram-Kelvin. The corresponding Helmholtz free energy change, at 298K, becomes -14,920-298 × 6.7 = -16,920 j/g for the dispersed fuel.

The corresponding Helmholtz free energy value for detonation of TNT is known to be about -4,830 j/g. Thus the TNT equivalence factor for detonation of dispersed ethylene oxide becomes 14,920/4,830, or 3.5 closely.

The above equivalence factor presumes carbon monoxide as a detonation product. Had carbon dioxide been assumed, the corresponding values are -27,720 j/g, +2.5 j/g-K, and a free energy change of -28,470 j/g. The associated equivalence factor then becomes 28,470/4,820, or about 5.9, compared with 3.5 for carbon monoxide.

Fuel-Air Ratios. These two computed TNT equivalence factors presume different amounts of oxygen consumed in detonation reactions; that is, they presume different fuel-air ratios. From chemistry of the reactions it may be calculated that detonation of ethylene oxide to carbon monoxide requires 1.5 moles of oxygen per mole of fuel, or 7.14 moles of air. This respresents 12.3 volume percent of fuel vapor dispersed in the air. Corresponding values for detonation to carbon dioxide are 2.5 moles of oxygen, 11.9 moles of air, and 7.8 volume percent fuel in air.

These computed fuel-air ratios are each within the detonation zone, known to be about 6 to 24 volume percent (Reference 3). Hence it appears that either of the two TNT equivalence ratios 3.5 or 5.9 or perhaps some intermediate value, might well apply to a particular explosion circumstance. In any event these calculations confirm the observation that a fuel dispersed in air can give a more extensive far-field explosion effect than can the explosion of the same mass of TNT.

Experimental. For experimental fuel-in-air detonations the fuel, usually liquid ethylene oxide, was dispersed explosively by a central cylindrical charge, as illustrated schematically in Figure 1. (As noted in Reference 3, the fuel in liquid form does not detonate.) The resulting cloud was reasonably well defined and approximately cylindrical in shape. Its detonation was obtained by auxillary detonators positioned within the cloud. Pressure-time measurements were made with dynamic gauges at the ground surface, both outside the cloud and also immediately below it at various locations. The results presented here represent averaged smoothed values all as normalized to unit mass of fuel.

Representative Blast Wave Configurations. A typical pressure-time history as observed beneath a detonating fuel-in-air dispersion is shown in Figure 2. For comparison a similar curve for detonation of a hemispherical charge of the same mass of TNT positioned at ground zero is also shown. Several aspects merit comment.

For these blast waves, the one for the fuel-in-air detonation shows a peak overpressure lower than that for TNT. However the duration is appreciably longer. Also, the impulse per unit area, as given by the area under the pressure-time curve is substantially greater for the fuel-in-air detonation. These observations have implications with regard to damage potential; thus for impulse-sensitive targets the fuel-in-air detonation may be the more damaging, but for hard targets that require a high peak overpressure it may be less damaging.

Corresponding configurations for the blast wave beyond the dispersion cloud are shown in Figure 3. It is evident that at such distances, where the peak overpressure is considerably less, that the fuel-in-air dispersion exceeds TNT with regard to both peak overpressure and impulse per unit area. The theoretical energy calculations above for TNT equivalence are thus at least partially validated.

TNT Equivalence From Blast Wave Measurements. Blast waves from a fuel-in-air dispersion and from a hemispherical surface charge of TNT are compared in Figure 4 for distances selected so that the two peak overpressures are identical. In this circumstance it becomes possible to estimate a corresponding TNT equivalence factor. Thus this particular overpressure extends some forty percent further from the explosion center of the fuel-in-air dispersion than from TNT. Hence the TNT equivalence factor becomes $(1.40)^3 = 2.7$ closely. Based on impulse however, the impulse per unit area for the fuel-in-air detonation is some seventy-five percent greater than that for TNT. Hence here the equivalence factor becomes $(1.75)^3 = 5.0$, These factors 2.7 and 5.0, although differing substantially, are not greatly inconsistent with those obtained from the energy calculations above, or 3.5 and 5.9 as shown.

It should be emphasized that all such blast equivalence factors depend strongly on the particular blast waves selected for comparison, and a substantial range in values is to be expected.

Summary. The TNT equivalence for the blast from a fuel-in-air detonation has been estimated as ranging from 3.5 to 5.9 when based on energy considerations, and from 2.7 to 5.0 when based on typical blast wave configruations. It is pointed out that such a range of values is well to be expected because of the differing geometrical natures of fuel-in-air detonations and TNT detonations.

REFERENCES

1. Robinson, Clarence A., Jr. "Fuel-Air Explosives," Aviation Week & Space Technology, Feb. 1973, p. 41.

2. Kinney, G. F., "Explosive Shocks in Air," McMillan 1962.

3. Bowen, James A., "Hazard Considerations Relating to Fuel-Air Explosive Weapons," Fourteenth Annual Explosives Safety Seminar Minutes, Nov. 1972.
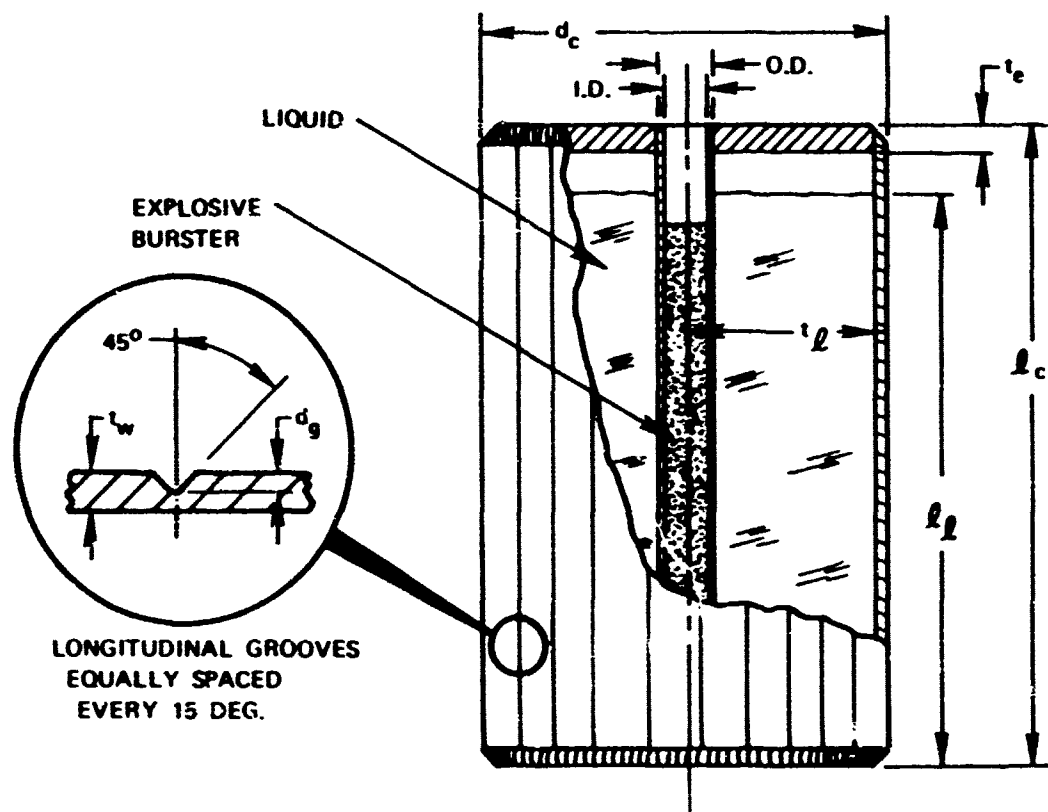
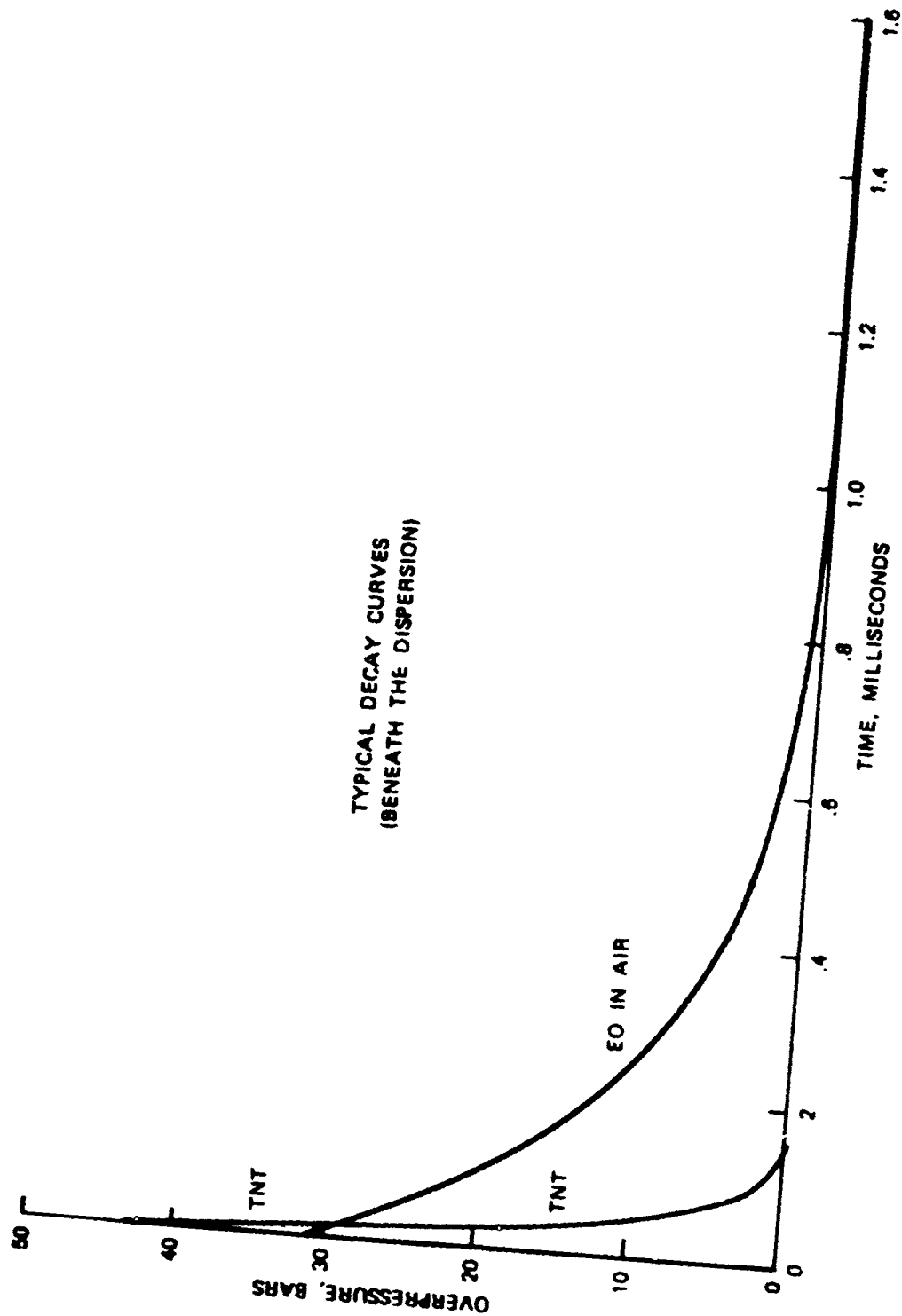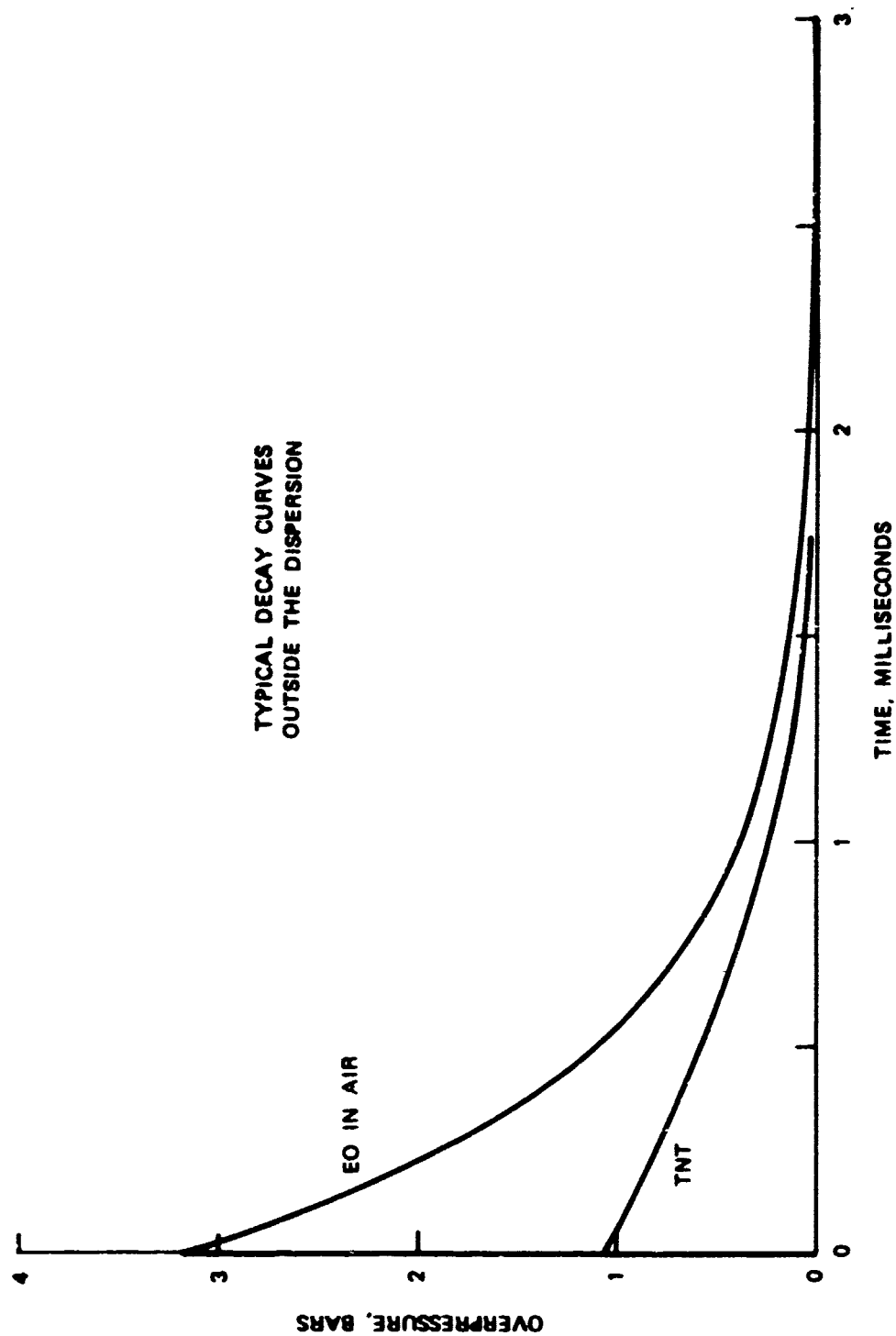FIG. 1. Configuration of Typical Scaled Fuel Air Explosive Warhead.

TYPICAL DECAY CURVES
(BENEATH THE DISPERSION)

FIG. 2. A Typical Pressure-Time History.

FIG. 3. Corresponding Configurations For The Blast Wave Beyond The Dispersion Cloud.

OVERPRESSURE DECAY CURVES
(FOR SAME PEAK OVERPRESSURE)

FUEL-IN-AIR

TNT

TIME, MILLISECONDS

OVERPRESSURE, BARS
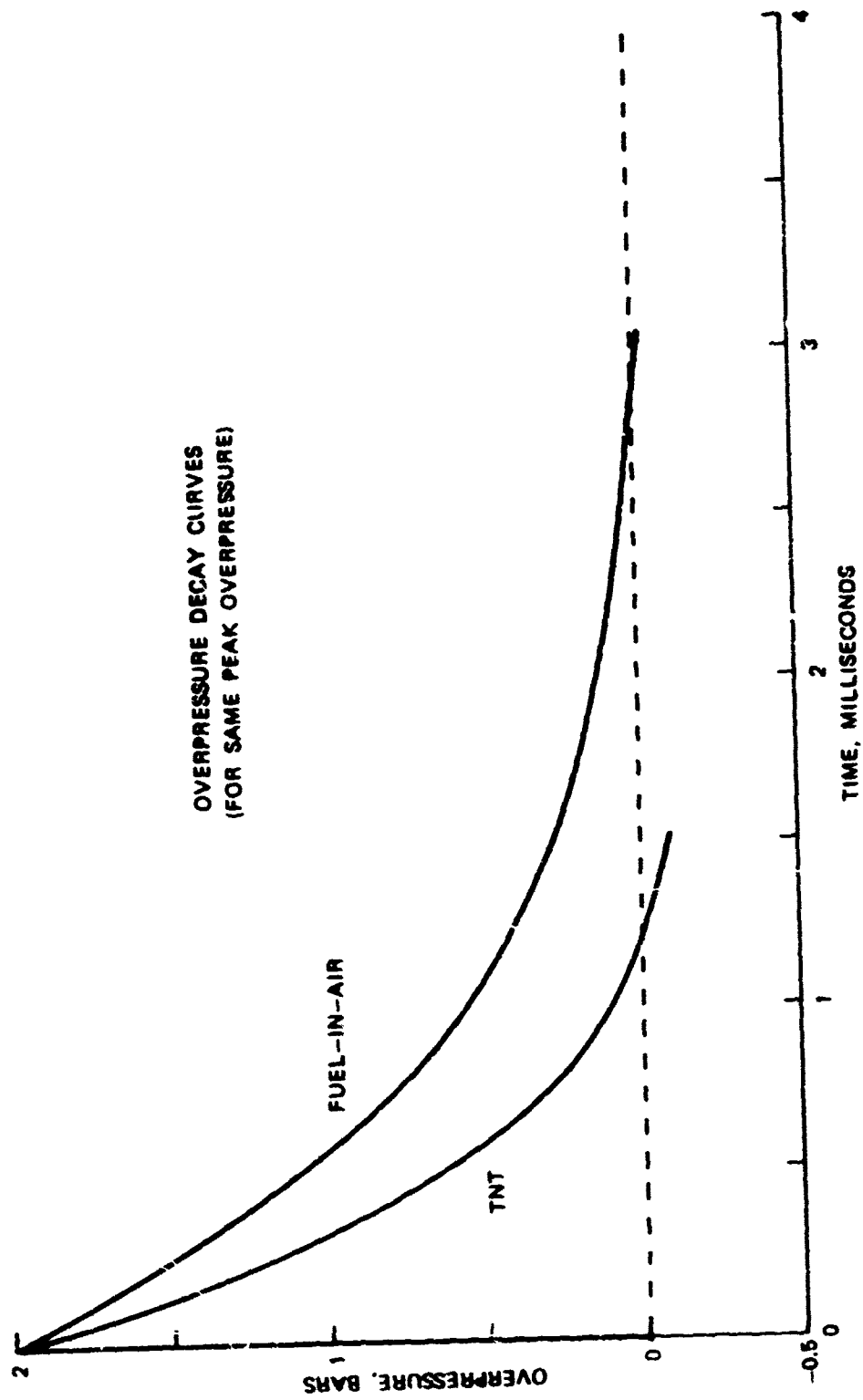
FIG. 4. Comparison of Blast Waves From a Fuel-in-Air Dispersion and From a Hemispherical Surface Charge of TNT.

Explosive Yield Limiting Self-Ignition Phenomena
in LO_2/LH_2 and LO_2/RP-1 Mixtures

Dr. Erich A. Farber
University of Florida
Gainesville, Fla.

Abstract

This paper is intended to present a brief summary of the work of
Dr. Farber's group at the University of Florida in arriving at credible
explosive yield values for liquid rocket propellants.

The results are based upon logical methods which have been well worked
out theoretically and verified through experimental procedures.

The three independant methods developed for this purpose are:

I.   The Mathematical Model

II.   The Seven Chart Approach

III. The Critical Mass Method

The material has been published in about two dozen reports and papers
by Dr. Farber and his group in such places as the Annals of the New York
Academy of Sciences, various Space Congress Proceedings, Transactions of
the International Cryogenic Engineering Society, Department of Defense
Explosive Safety Board Annual Meeting Proceedings, The International Fire
Institute Bi-Annual Reports, etc.

In addition, some of the material has been presented both formally
and informally to NASA groups at Kennedy Space Center, Marshall Space Flight
Center, to groups at the Air Force Rocket Propulsion Laboratory, at Edwards
Air Force Base, to members of the Aerospace Corporation, to the Ballistics
Research Laboratory at Aberdeen Proving Grounds, and others.

This work presents a rational approach to predict explosive yield
values of liquid rocket propellants and other characteristics.

Introduction

In the early days when liquid propellant rockets were of small size it was not difficult to locate personnel and equipment at a safe distance so that in case of an accidental failure no great damage was done. As the size of these rockets increased, however, safety became a serious problem since the distances required for safety became so large that not enough land was available. Furthermore, since remote control became necessary, technical and economic problems were encountered.

For the above reasons another look had to be taken of what the hazards really are and what the basic characteristics of liquid propellants are so that better understanding might allow control of them.
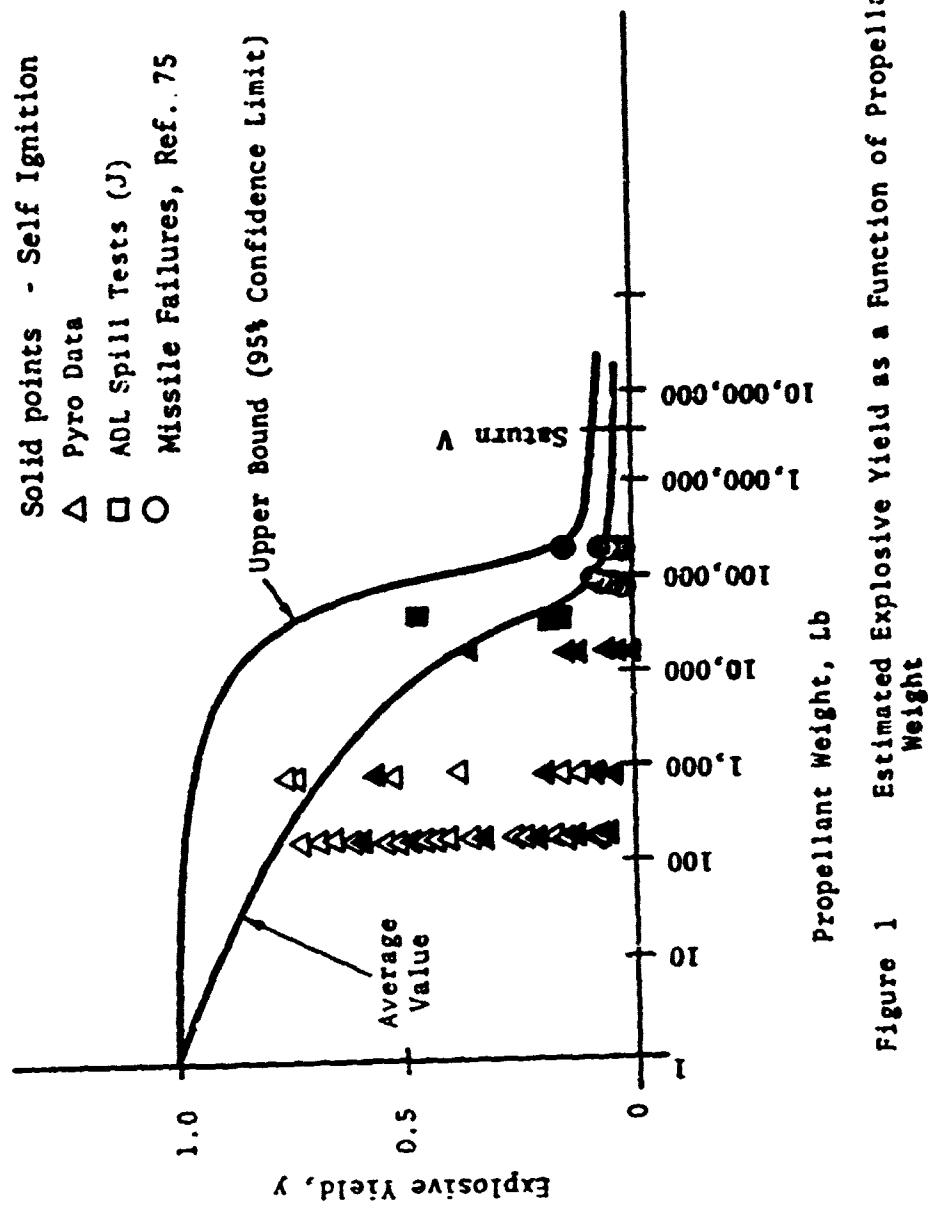
The Mathematical Model

In 1964 Dr. Farber's group developed a Mathematical Model with a minimum of information available which described the behavior of liquid rocket propellants. It was based on very limited information but described the explosive behavior on a statistical basis indicating that, at small quantities high explosive yields could be expected, but with large quantities of liquid rocket propellants the explosive yields expected are quite low.

Figure 1 of this paper gives the results from the Mathematical Model and also many actual data points which became available after the model was developed. It shows that the predictions, which were not the initial intent of use for this model, are in very good agreement with the experimental results.

It was observed that with small quantities of liquid rocket propellants the explosive yield could be controlled since in most cases the mixture had to be ignited and thus, if done at the right time, the maximum yield was obtained.

With quantities above 10,000 the experiments could not be controlled and something always set them off before very large quantities of the propellants

Figure 1   Estimated Explosive Yield as a Function of Propellant Weight

could mix. This was also true for the actual rocket failures which occurred.

Thus the difference in behavior of large and small quantities was recognized and, as will be shown later, was explained.

The Seven Chart Approach

The Mathematical Model did not give detailed information as to what brought the explosive yield about; it only gave the over-all behavior. So another approach was developed which looked at the actual phenomena in the mixing of the propellants in much greater detail.

For this purpose the problem was broken up into three parts. The yield potential was the maximum amount of explosive yield which could theoretically be obtained because of the presence of propellants. This varied with time due to evaporation and other losses. The mixing function indicated which constituents were mixed and how much of them as a function of time. Obviously when none of the fuels and oxidizers are mixed an explosion is not possible even though the quantities present may be very large. This was done both theoretically and experimentally both in the laboratory with inert or non-explosive mixtures as well as with explosive mixtures in the field.

Four methods for determining the mixing of propellants had to be developed to analyze the processes. They were the high speed photographic analysis, the wax cast analysis, the vibration mixing analysis, and the thermocouple analysis.

These methods were used first several at the same time on the same experiment so as to evaluate their correlation and then the thermocouple analysis was used on the actual explosive field experiments. In addition to the mixing phenomena this analysis also established the ignition point location, the shock and reaction front propagation characteristics. They, it is believed, represented the first measurements of this kind in an actually exploding mixture.

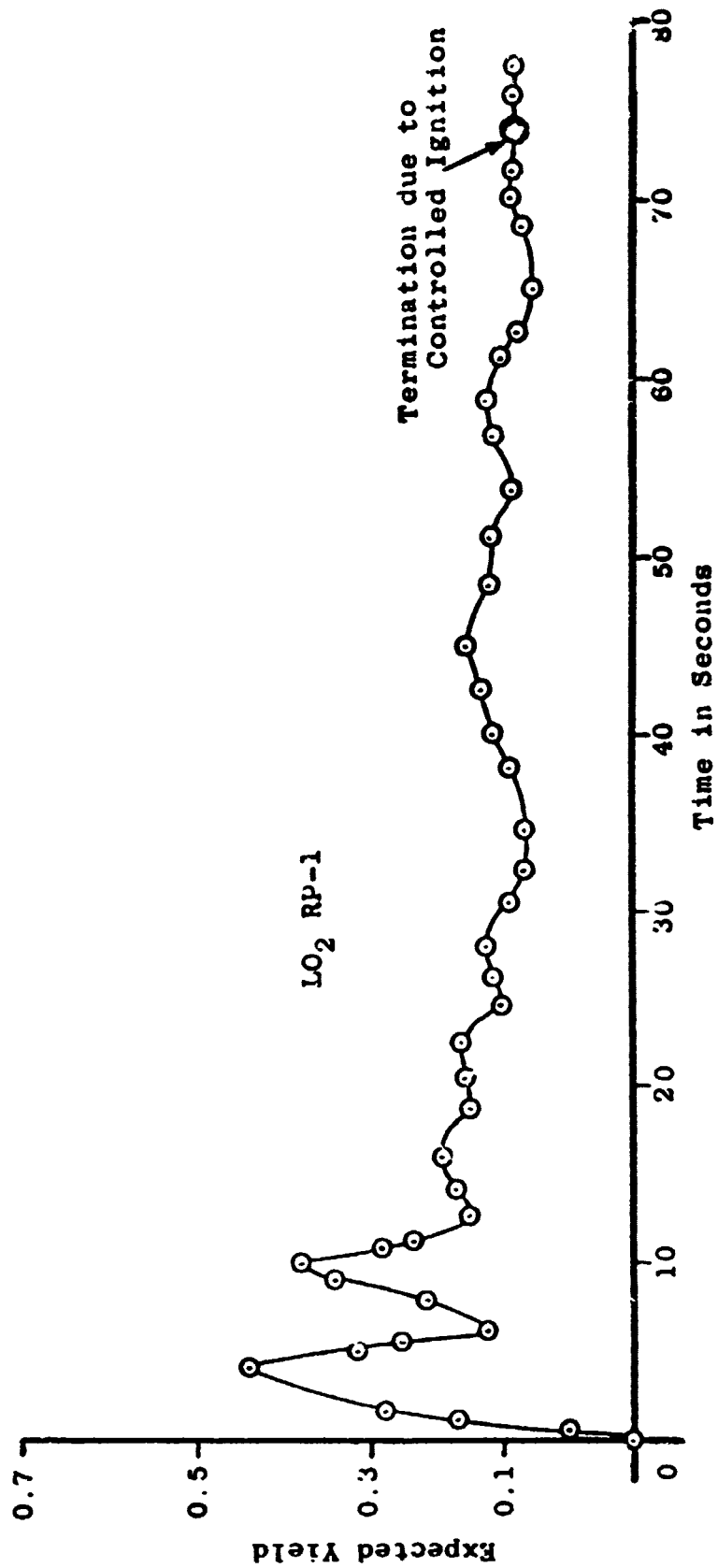Results from this work are presented in Figure 2 which was a 200 lb

Termination due to
Controlled Ignition

LO_2 RP-1

Expected Yield

Time in Seconds

Figure 2   Expected Yield as a Time Function
(200 lb Cold Flow and Explosion Experiment)

LO$_2$/RP-1 experiment carried out at the Air Force Rocket Propulsion Laboratory, Edwards Air Force Base, California. The mixing function was actually determined and then the mixture was initiated when all the mixing had subsided. Laboratory simulation agreed well with actual measurement.

For the larger experiments, the 25,000 lb, and the S-IVB tests, laboratory simulations were used for prediction purposes. From Figures 3 and 4 it can be seen that the mixing curve was determined giving the explosive yield which can be expected at any time after failure. All that needs to be done is super-imposing the actual ignition time to get the actual explosive yield.

The ignition time with small quantities of propellants which can be con-trolled can be accurately predicted. With large quantities which ignite of their accord, this ignition time prediction is not quite so easy. For this reason work had to be done on searching for the reason that the larger mixtures self-ignited. Many possible sources could be cited but the most likely one was the self generation of electrostatic charges and voltages which when built up to a certain value would produce a discharge and ignite the mixture. This investigation led to the Critical Mass Concept which sets the upper limit to the explosive yield which can be produced by liquid propellants.

The Critical Mass

As was mentioned in the above section, the mixing function gives the amounts of propellants mixed at any time and thus the explosive yield which can be expected at any time after failure.

It was shown through laboratory experiments that with the mixing phenomena, electrostatic charges and voltages are always produced when the constituents are dielectrics. The details of this work are given in the various reports and papers covering this work and listed in the bibliography.

From the laboratory experiments it was noticed that the charge and voltage buildup was proportional to the quantities involved and it was also noticed that
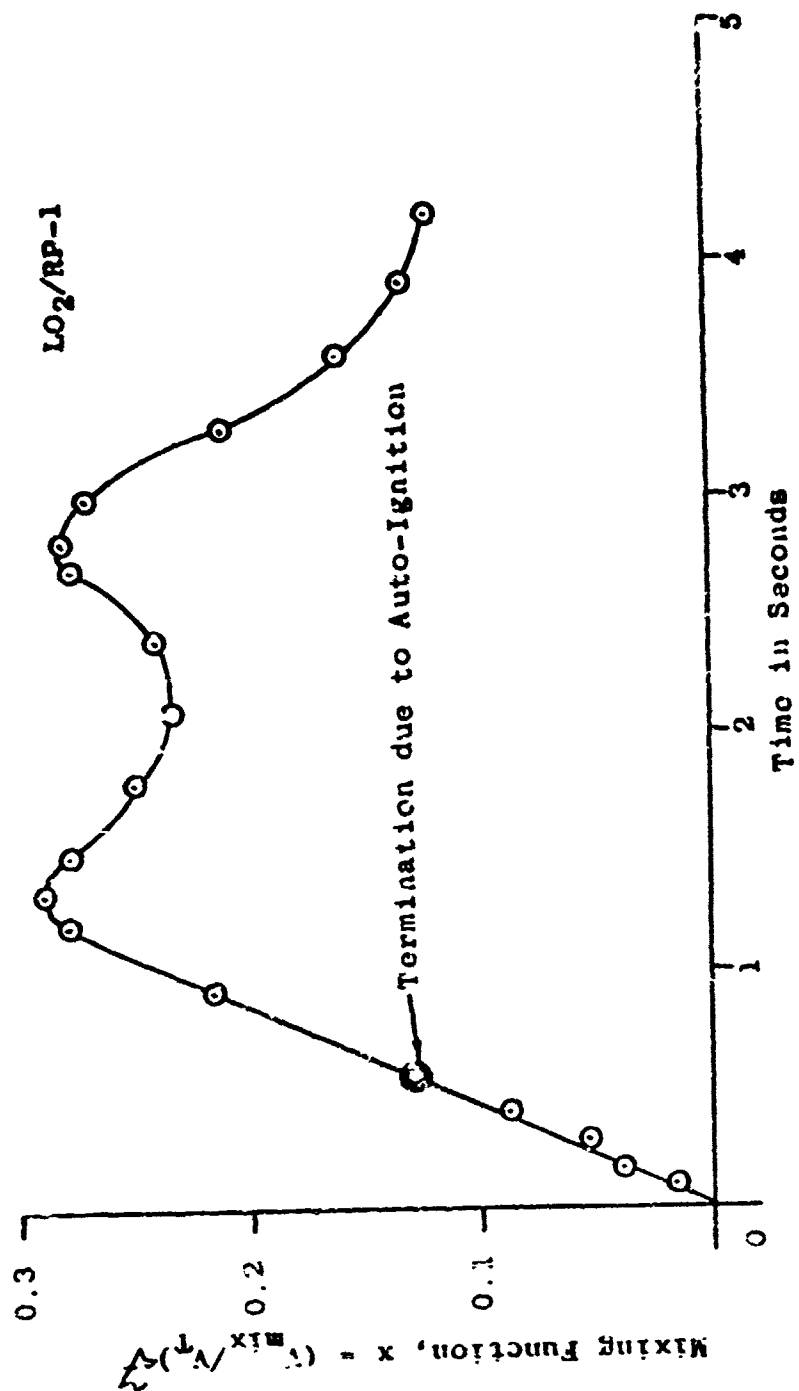
Figure 3 — Mixing Function, 25,000 lb Explosion Experiment (Based Upon 3" Diameter Simulated Experiment)
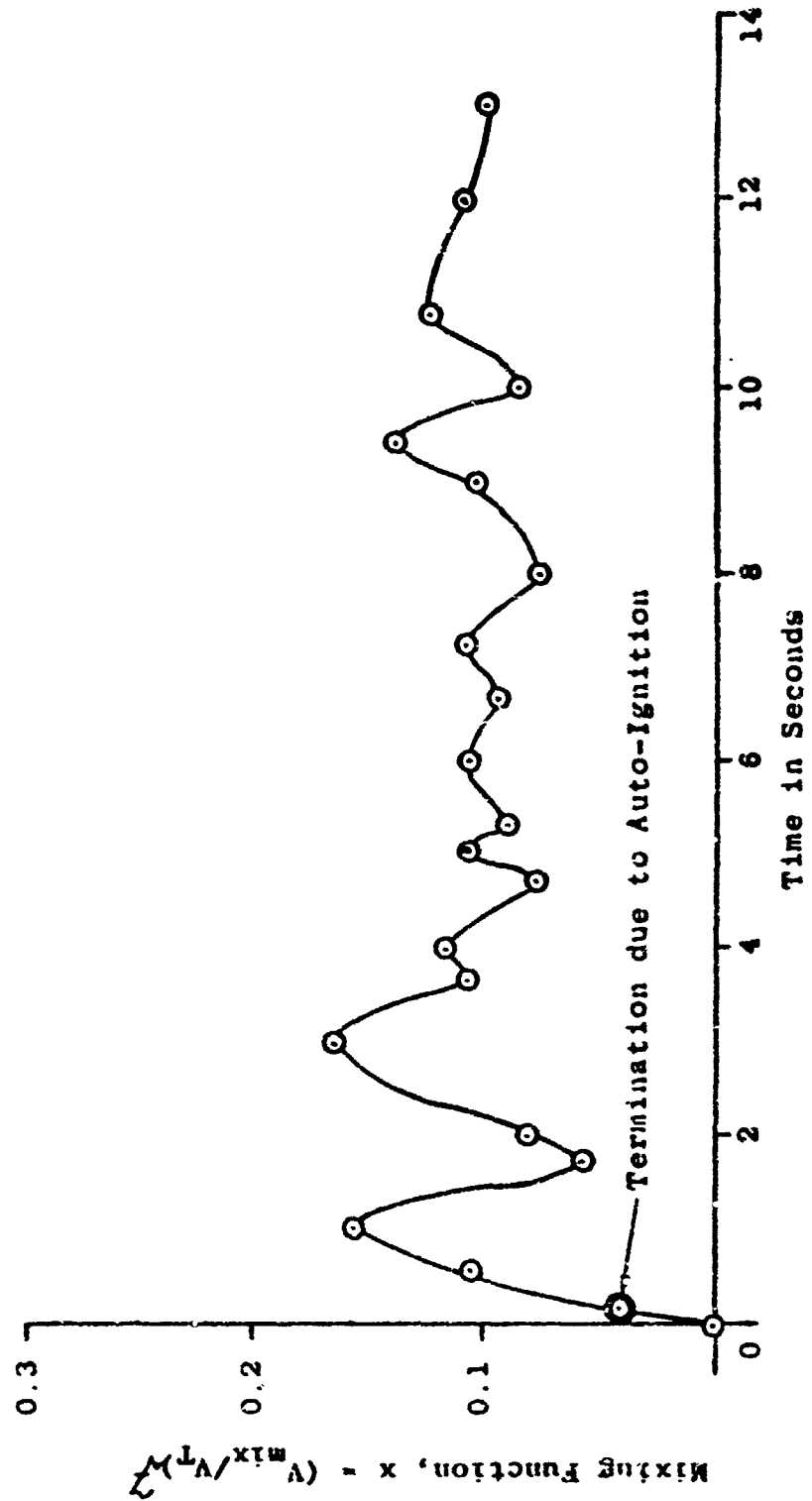
LO$_2$/RP-1

Termination due to Auto-Ignition

Time in Seconds

Mixing Function, x = $(r_{mix}/v_T)^2$

Figure 4 Mixing Function, S-IV LO$_2$/LH$_2$ (Based upon 3" Diameter Simulated Experiment)

the average bubble size produced by the heat transfer between the constituents was about ¼ inch in diameter. These observations lead to the prediction of critical quantities which would produce high enough voltages for discharge to occur. These predictions indicated that ignition would be a certainty with quantities of about 3000 lb mixed, when the mixing was done relatively gently, with the boiling process providing most of the mixing energy. When external energy is available to bring the propellants together such as dropping, impact or explosive mixing, the critical quantities become larger.

Figure 5 gives these critical quantities later named the "Critical Mass" meaning that as soon as this quantity is mixed ignition will occur and larger quantities cannot be mixed without explosion.

The predictions were later verified by actual failures as well as very carefully carried out field tests. The critical mass is the upper limit indicating that no larger quantities can be mixed but smaller quantities may under some conditions self-ignite. All actual liquid propellant explosions must lie below the critical mass curve.

Self-Ignition Field Experiments

To measure the electrostatic charges and voltages produced during the mixing process actual explosive mixtures were employed, some time after the predictions were made based on inert laboratory tests.

For this purpose both LO_2/LH_2 and $LO_2/RP-1$ were chosen. Basically two tanks were located excentricly above each other and one propellant was poured into the other. Liquid level probes controlled the quantities in the tanks and screens monitored the charges and voltages generated. The quantities employed were 6 lb, 60 lb, and 240 lb.

No explosions were obtained with the 6 lb series since the voltages obtained were too small to produce discharge. The same was observed with the 60 lb experiments even though the voltages were considerably higner. With the
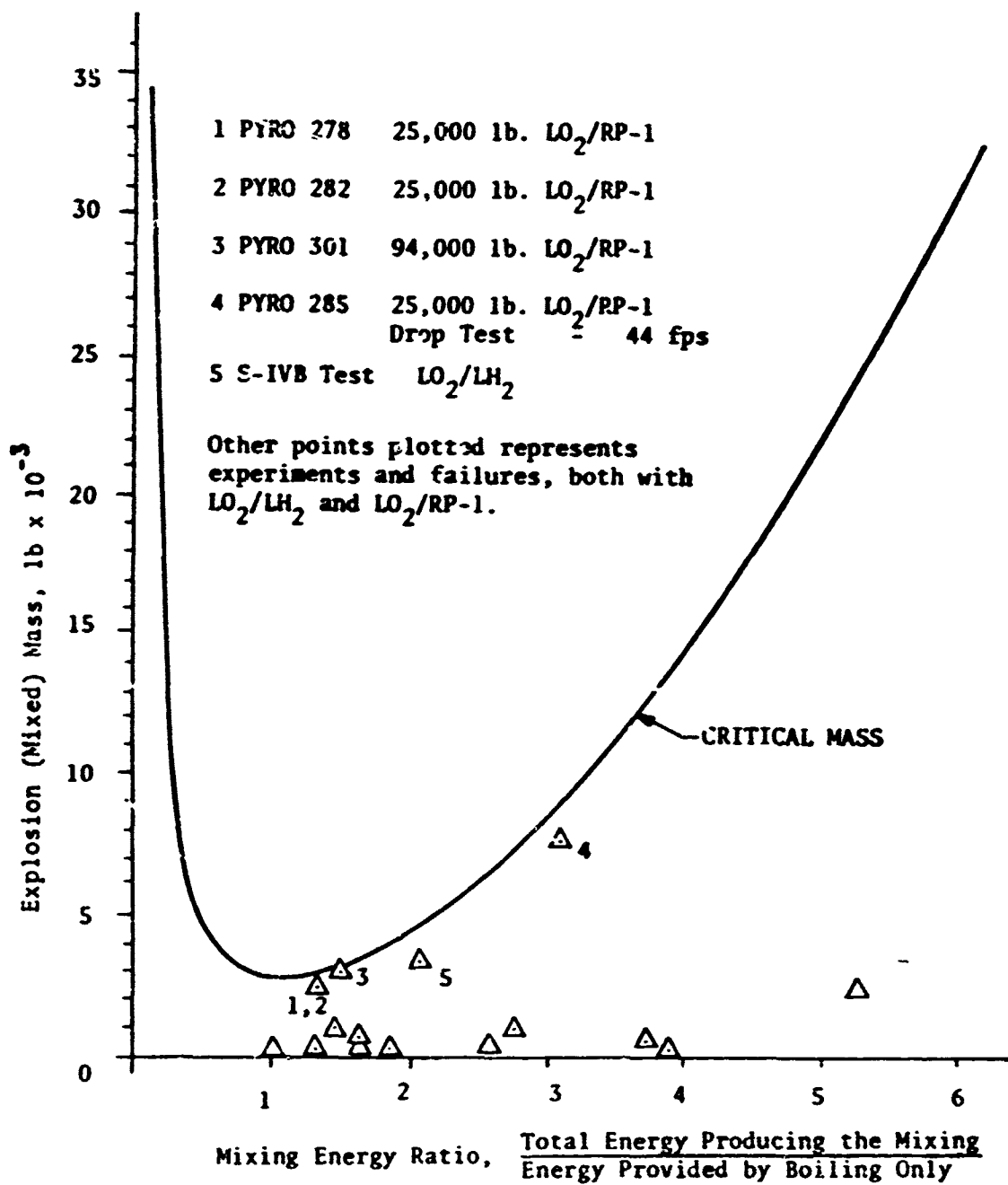
35

1 PYRO 278   25,000 lb. LO_2/RP-1

30

2 PYRO 282   25,000 lb. LO_2/RP-1

3 PYRO 301   94,000 lb. LO_2/RP-1

4 PYRO 285   25,000 lb. LO_2/RP-1
              Drop Test - 44 fps

25

5 S-IVB Test LO_2/LH_2

Other points plotted represents
experiments and failures, both with
LO_2/LH_2 and LO_2/RP-1.

CRITICAL MASS

Explosion (Mixed) Mass, lb × 10^{-3}

Mixing Energy Ratio, $\dfrac{\text{Total Energy Producing the Mixing}}{\text{Energy Provided by Boiling Only}}$

Fig. 5   Explosion Mass - Mixing Energy Relationship

1296

240 lb experiments discharge was produced in the 10th experiment with LO_2/LH_2 and the results for all the tests are presented in Figure 6.

It can be seen from this Figure that the critical mass, predicted several years earlier, is the intersection of the lower charges and voltages produced thus indicating that at that quantity explosion initiation will occur every time. Also, the average value of each of the series of experiments intersects at that point indicating that the average value becomes the minimum value and the ignition value when critical values are reached.

Figure 7 is a similar graphical presentation for $LO_2/RP-1$. In these experiments the charges and voltages necessary for self-ignition were never reached with 240 lb of propellants in the number of experiments carried out.

It might be mentioned that to make certain that the instrumentation in the tanks did not influence the test results some experiments were carried out without any instrumentation and the self-ignition was produced even earlier. as was expected. The screens in the tank have a diluting effect since they spread the charges out over a larger region. Also, experiments were carried out with thermocouple grids in the tank to establish the location of the ignition point and the shock front and reaction front propagation characteristics.

It seems that the systematically laid out procedures, throughout an eight year period, resulted in a much better understanding of the basic phenomena, brought out a number of new concepts and information and resulted further in a logical approach for the analysis and prediction of liquid rocket propellant explosion hazards.

The results obtained were further used in analyzing the Saturn V destruct system, and various early Space Shuttle configurations under differnet modes of failure.
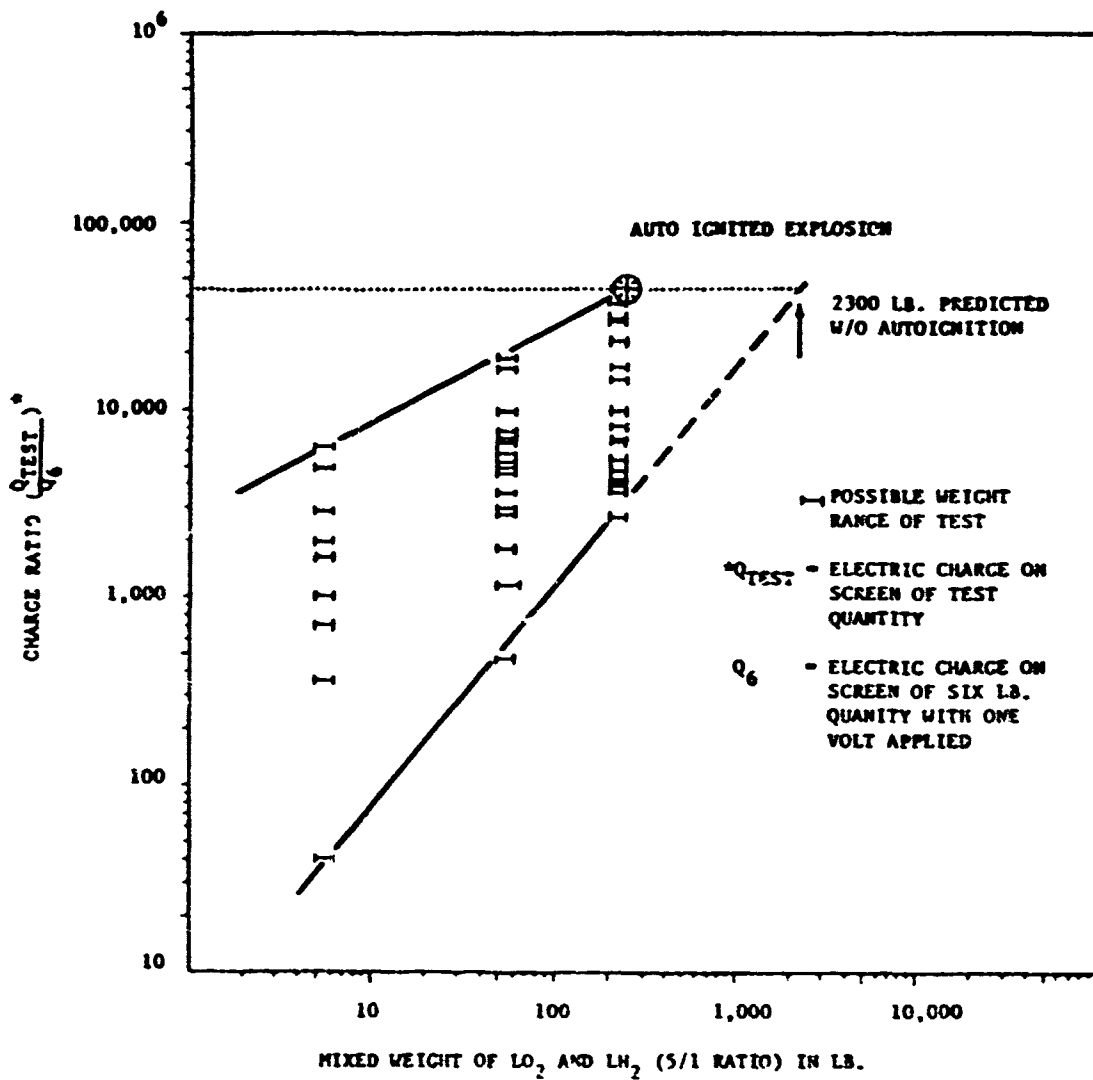
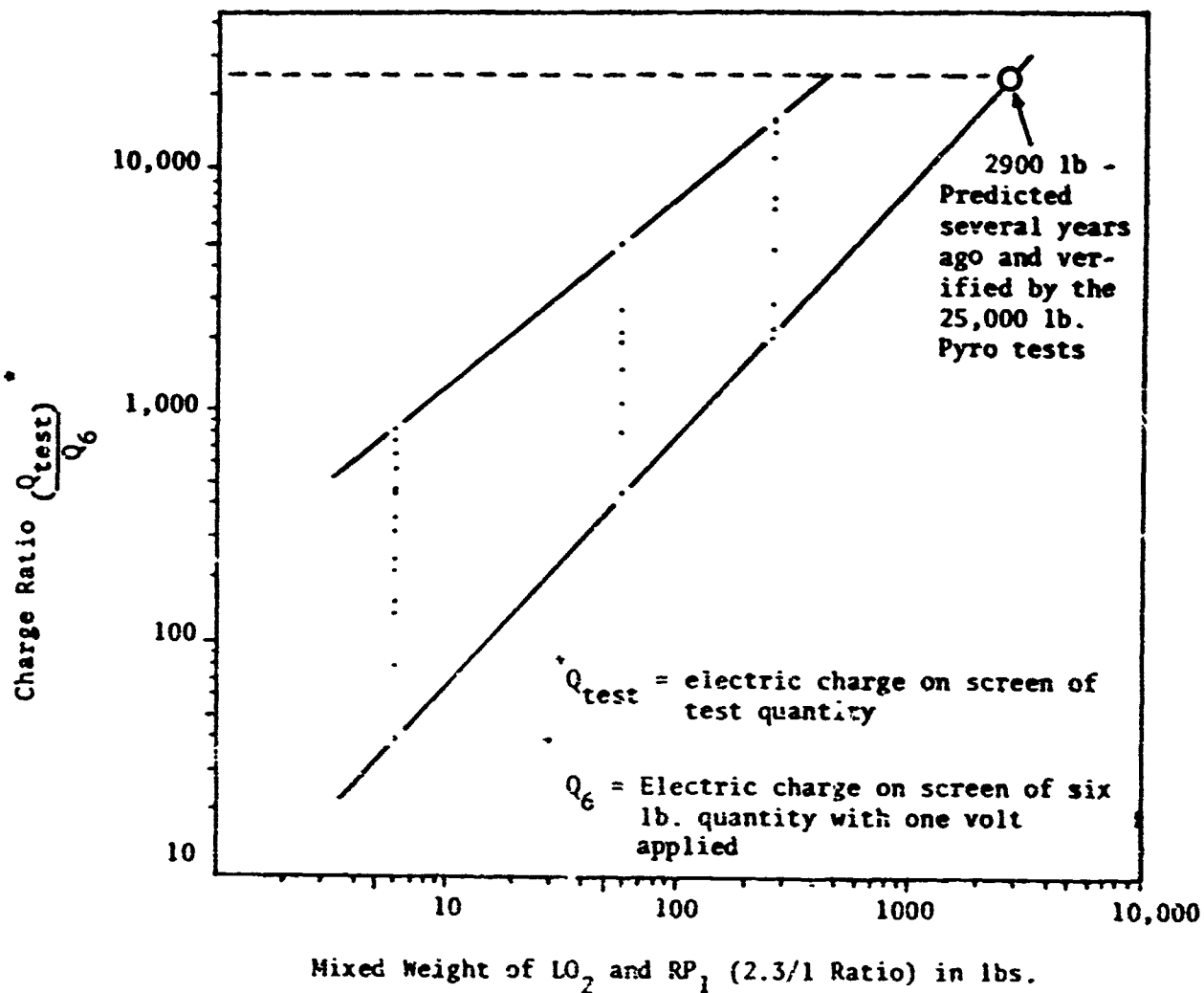Fig. 6 Charge Ratio as a Function of Propellent Weight (LO_2/LH_2 Mixtures)

Fig. 7   Charge Ratio as a Function of Propellant Weight
          (LO_2/RP_1 Mixtures)

Acknowledgements

It is with sincere appreciation that the author thanks the many faculty members in Engineering, Mathematics, Statistics, and Chemistry who have worked on this project; the many graduate students who have given assistance with the experimentation; and the many Engineering students who have helped with the computations, preparation of graphs, etc.

The help given by NASA personnel at the Kennedy Space Center and personnel of the Subcontractors made it possible to carry out the auto-ignition experiments at the Kennedy Space Center which verified the Electrostatic Charge Generation and Critical Mass Hypothesis.

Special thanks are due Mr. J.H. Deese who greatly contributed to the execution of this project through active participation in the auto-ignition experiments and through administrative action, and to Mr. W.H. Boggs who took over the duties of NASA's Technical Representative after Mr. Deese's retirement.

BIBLIOGRAPHY

1. Farber, E.A., et al. "Feasibility Study to Explore the Explosive Effects of Liquid Propellants to Define the Mathematical Behavior of Physical Processes Involved," Final Report, Phase I, Contract No. NAS10-1255, University of Florida, February, 1965.

2. Farber, E.A., "A Mathematical Model for Defining Explosive Yield and Mixing Probabilities of Liquid Propellants," Third Space Congress Proceedings, March 1966 (Preceding paper).

3. "Thermocouple Grid Analysis of Two 25,000-lb LOX/RP Liquid Propellant Explosion Experiments," E.A. Farber, Technical Paper No. 396, Florida Engineering and Industrial Experiment Station, Vol. XXI, No. 11, November, 1967.

4. "Explosive Yield Estimates for Liquid Propellant Rockets Based Upon a Mathematical Model," E.A. Farber, Technical Paper No. 415A, Florida Engineering and Industrial Experiment Station, Vol. XXII, No. 7, July, 1968.

5. "Interpretation of Explosive Yield Values Obtained from Liquid Rocket Propellant Explosions," E.A. Farber, Technical Paper No. 415B, Florida Engineering and Industrial Experiment Station, Vol. XXII, No. 7, July, 1968.

6. Arthur D. Little, Inc. "Summary Report on a Study of the Blast Effect of a Saturn Vehicle," February, 1962.

7. E.A. Farber and R.L. San Martin, "Studies and Analyses of the Mixing Phenomena of Liquid Propellants Leading to a Yield-Time Function Relationship," Proceedings of the New York Academy of Sciences Explosives Symposium, November, 1966.

8. Farber, E.A., et al., "Fireball Hypothesis Describing the Reaction Front and Shock Wave Behavior in Liquid Propellant Explosions," New York Academy of Sciences, Explosives Symposium Proceedings, 1967. Available as Technical Paper 387, Florida Engineering and Industrial Experiment Station.

9. Farber, E.A. and Deese, J.H., "A Systematic Approach for the Analytical Analysis and Prediction of the Yield from Liquid Propellant Explosions," Proceedings of the Third Space Congress, March, 1966.

10. Farber, E.A. and Richardson, M.R., "The Gamma Ray Densitometer and Concentration Meter," Proceedings of Annual Meeting of Instrument Society of America, April, 1957.

11. Farber, E.A., "200 A Thorium Oxide Slurry Test Loop Density and Concentration Data," Oak Ridge National Laboratory Report, January, 1957.

12. Farber, E.A., "Bubble and Slug Flow in Circulating Gas-Liquid and Gas (Vapor)-Liquid-Solid Mixtures," Oak Ridge National Laboratory Report, May, 1957.

13. Farber, E.A., "Bubble and Slug Flow in Circulating Gas-Liquid and Gas-Liquid-Solid Mixtures," Oak Ridge National Laboratory Report, February, 1958.

14. Farber, E.A., et al., "Fireball and Post-Fireball Composition and Atmospheric Chemistry of Fuel/Oxygen-Fluorine Propellants," NASA report, Contract NAS10-1255, July, 1967.

15. Farber, E.A., et al., "A Bibliography of Authoritative Sources Defining the Physical and Chemical Properties of Fluorine and Its Oxidizing Mixtures and Compounds," Part I, Contract NAS10-1255, University of Florida, April 1965.

16. Farber, E.A., et al., "A Bibliography of Authoritative Sources Defining the Physical and Chemical Properties of Fluorine and Its Oxidizing Mixtures and Compounds," Part II, Confidential, Contract NAS10-1255, University of Florida, April 1966.

17. Farber, E.A., et al., "Thermocouple Grid Method Applied to Studying Liquid Mixing," Contract NAS10-1255, University of Florida, March 1966.

13. Farber, E.A. and Deese, J.H., "A Systematic Approach for the Analytical Analysis and Prediction of the Yield from Liquid Propellant Explosions," Proceedings of the Third Space Congress, March 1966. (Paper No. II in this series).

19. Farber, E.A., et al., "A Systematic Approach for the Analytical Analysis and Prediction of the Yield from Liquid Propellant Explosions," Third Space Congress Proceedings, March 1966. Available as Technical Paper No. 347, Florida Engineering and Industrial Experiment Station.

20. Farber, E.A., et al., "Fireball Hypothesis Describing the Reaction Front and Shock Wave Behavior in Liquid Propellant Explosions," New York Academy of Sciences, Explosives Symposium Proceedings, 1967. Available as Technical Paper 387, Florida Engineering and Industrial Experiment Station.

21. Farber, E.A., et al., "Fireball and Post-Fireball Composition and Atmospheric Chemistry of Fuel/Oxygen-Flourine Propellants," NASA Report, Contract NAS10-1255, July 1967.

22. Farber, E.A., "A Mathematical Model for Defining Explosive Yield and Mixing Probabilities of Liquid Propellants," Technical Paper Series No. 346, Florida Engineering and Industrial Experiment Station, Vol. XX, No. 3, March 1966.

23. Farber, E.A., et al., "Prediction of Explosive Yield and Other Characteristics of Liquid Propellant Rocket Explosions," Final Report, Contract No. NAS10-1255, University of Florida, October 31, 1968.

24. Farber, E.A., et al., "A Systematic Approach for the Analytical Analysis and Prediction of the Yield from Liquid Propellant Explosions," Annals of the New York Academy of Sciences, Vol. 152, Art. 1, pp. 645-665.

25. Farber, E.A., et al., "Studies and Analyses of the Mixing Phenomena of Liquid Propellants Leading to a Yield-Time Function Relationship," Annals of the New York Academy of Sciences, Vol. 152, Art. 1, pp.654-684.

26. Paper (77) reprinted as Technical Paper No. 386, Florida Engineering and Industrial Experiment Station, Vol. XXI, No. 8, August 1967.

27. Farber, E.A., "Thermocouple Grid Analysis of Two 25,000 lb LOX/RP Liquid Propellant Explosions Experiments," Technical Paper No. 396, Florida Engineering and Industrial Experiment Station, Vol. XXI, No.11, November 1967.

28. Farber, E.A., "Explosive Yield Estimates for Liquid Propellant Rockets Based Upon the Mathematical Model," Technical Paper No. 415A, Florida Engineering and Industrial Experiment Station, Vol. XXII, No. 7, July 1968.

29. Farber, E.A., et al., "Fireball and Post-Fireball Composition and Atmospheric Chemistry of Fuel/Oxygen-Fluorine Propellants," NASA report, Contract NAS10-1255, July 1967.

30. Farber, E.A., Klement, F.W. and Bonzon, C.F., "Prediction of Explosive Yield and Other Characteristics of Liquid Propellant Rocket Explosions," University of Florida, Contract No. NAS10-1255, Final Report, October, 1968.

31. "Liquid Propellant Explosive Hazards," Project PYRO, Af RPL, Final Report, December 1968.

32. Farber, E.A. and Gilbert, J.S., "Fireball Hypothesis Describing the Reaction Front and Shock Wave Behavior in Liquid Propellant Explosions," Technical Paper No. 387, Florida Engineering and Industrial Experiment Station, Vol. XXI, No.8, August 1967.

33. San Martin, R.L.,"A Theoretical Investigation and Experimental Verification of the Mixing of Insoluble Liquids," Ph.D. Dissertation, University of Florida, March 1969.

34. Farber, E A.,"Prediction of Explosive Yield and Other Characteristics of Liquid Propellant Rocket Explosions," Technical Paper No. 448, Part VIII, Florida Engineering and Industrial Experiment Station, Vol. XXIII, No. 11, November 1969.

35. Bonzon, C.F., "Generation of Static Electricity Caused by the Mixing of Insoluble Fluids," Ph.D. Thesis, University of Florida, December 1970.

36. Farber, E.A., "Critical Mass (Hypothesis and Verification) of Liquid Rocket Propellants," Report No. IX, Contract No. NAS10-1255, University of Florida, September 14, 1971.

37. Deese, J.H., "Test Conductors Damage Assessment Report on Auto-Ignition LO_2/LH_2 Mixing Test Experimental Explosions of March 2, 1972, Vols. 1 and 2. Systems Engineering Division, Design Engineering Director, J.F.K. Space Center NASA, March 23, 1972.

38. Farber, E.A., et al., "Electrostatic Charge Generation and Auto-Ignition Results of Liquid Rocket Propellants Experiments," NASA Report, Contract NAS10-1255, October 1972.

39. Farber, E.A. and San Martin, R.L., "Part III. Studies and Analysis of the Mixing Phenomena of Liquid Propellants Leading to a Yield-Time Function Relationship." Available as Technical Paper 386, Florida Engineering and Industrial Experiment Station.

40. Farber, E.A. and Gilbert, J.S., "Part IV Fireball Hypothesis Describing the Reaction Front and Shock Wave Behavior in Liquid Propellant Explosive." Available as Technical Paper 387, Florida Engineering and Industrial Experiment Station.

41. Farber, E.A., "Part VIII. Prediction of Explosive Yield and Other Characteristics of Liquid Propellant Rocket Explosions." Available as Technical Paper 448, Florida Engineering and Industrial Experiment Station.

42. Proceedings Eleventh Explosive Safety Seminar, Armed Forces Explosive Safety Board, Washington, D.C. September 1969.

43. Generation of Static Electricity Caused by the Mixing of Insoluble Fluids," C.F. Bonzon, Ph.D. Dissertation, December 1969, University of Florida.

44. "Statistical Analysis of Project PYRO Liquid Propellant Explosion Data," P. Gunter, G.R. Anderson, Bell Comm, Inc., July 1969.

BLAST HAZARDS OF CO/N_2O MIXTURES

CAPT Charles R. Mastromonico
Forrest S. Forbes
Air Force Rocket Propulsion Laboratory
Edwards Air Force Base
Edwards, California

ACKNOWLEDGEMENTS

ABSTRACT

Blast Hazards of CO/N_2O Mixtures

Capt C. R. Mastromonico
Forrest S. Forbes

The propellants carbon monoxide (CO) and nitrous oxide (N_2O) are presently being investigated as candidates for laser applications. While there is significant data concerning the combustion and detonation properties of each of the individual propellants, little information exists about them in combination.

The purpose of this program is to make blast hazard determinations on CO and N_2O in their various physical states under several mixing conditions. This information will provide the basis for establishing structural and quantity distance safety criteria for an AF test facility. Consideration is also given to CO and air mixtures.

The propellants were combined in semi-confined and unconfined configurations designed to simulate the boundary conditions imposed on them by their surrounding environment in the event of line or component failure. Several mixing modes were investigated including liquid/liquid, gas/liquid, and gas/gas combinations. Several hundred pounds of CO and N_2O were combined as described above and ignited using blasting caps or squibs. The overpressure produced was then measured as a function of time and distance using field mounted transducers. This data was then used to calculate percent TNT equivilence.

The tests completed to date have indicated that semi-confined liquid/ liquid combinations of CO and N_2O represent the primary detonation hazard for these two propellants. The gas/liquid, and gas/gas mixtures exhibited rapid deflagration in all test configurations, however, no detonation wave was observed.

TABLE OF CONTENTS

FIGURES

TABLES

INTRODUCTION

BACKGROUND:

The Air Force Rocket Propulsion Laboratory was requested by the Weapons Laboratory to conduct a preliminary investigation into the blast and fire hazards associated with combinations of the propellants, carbon monoxide (CO) and nitrous oxide (N_2O). These propellants are presently being considered as candidates for a gas dynamic laser (GDL) system. In the course   planning a facility for testing these propellants, it has become apparent that hazard classification data required for facility design and siting is lacking for this specific propellant combination. It was the purpose of this program to obtain preliminary data concerning the explosive yield and damage mechanisms associated with mixtures of CO and N_2O.

SCOPE:

In designing a test facility, it is generally desirable to consider all of the hazards associated with a given propellant combination such as toxicity, fire, blast and fragmentation hazards. Once this information is known, a detailed failure mode analysis can be performed on the specific system of interest. Since the toxicity, flamability, and explosion limits of CO and N_2O (1),(4), (5), (9), and (10) individually are already fairly well known, this effort considered only the blast, thermal, and fragmentation hazards associated with the two propellants in combination. In addition, because only a small number of potential applications exist for this propellant combination, a limited test program was conducted to determine whether any explosion hazard is present for the type of propellant interactions (mixing modes) possible in the specific system of interest. The matrix of parameters investigated

was developed using the approach of similar studies performed on the blast hazards of liquid propellants (6) and detonable gases (7). The pertinant information obtained consisted of the TNT equivalence of these mixtures, the corresponding peak overpressures and impulse, and a qualitative assessment of the potential for thermal and fragmentation hazards.

APPROACH

GENERALIZED FAILURE CONCEPT:

As was mentioned earlier, the approach taken in this program was to
perform a limited number of tests designed to delineate potential explosive
effects associated with the types of propellant interaction possible in
the system in question. This implied that a generalized approach was
needed which concentrated on the basic modes of mixing that the two propel-
lants could credibly experience rather than one which would take into account
all of the possible failure modes that may exist in the system. To implement
this approach one must assume that the gross spacetime history of the propel-
lants determines the fraction, geometry, and motion of the propellants
undergoing each mixing mode. Each basic mixing mode could then be tested
for explosive effects as a function of initial propellant properties, geometry,
velocity distribution, and time. This can be seen more clearly by utilizing
a generalized concept for system failure as outlined in Table 1.

There are five general variables to consider when addressing a failure
in a specific system. Of these, the propellant type is perhaps the most
important for it determines the energy available for release in an explosion
and the initial state of the propellants at the time ignition occurs.
Carbon monoxide and nitrous oxide are the two propellants to be evaluated
in this investigation. The propellant tank configuration is also a major
factor for it sets some of the boundary conditions imposed upon the propel-
lants during the mixing process. For example, in a missile tank configuration
it is common for propellants to be stored one above the other and to share
a common bulkhead. A failure of this bulkhead would create a situation

1313

TABLE - 1

GENERALIZED CONCEPT OF SYSTEM FAILURE
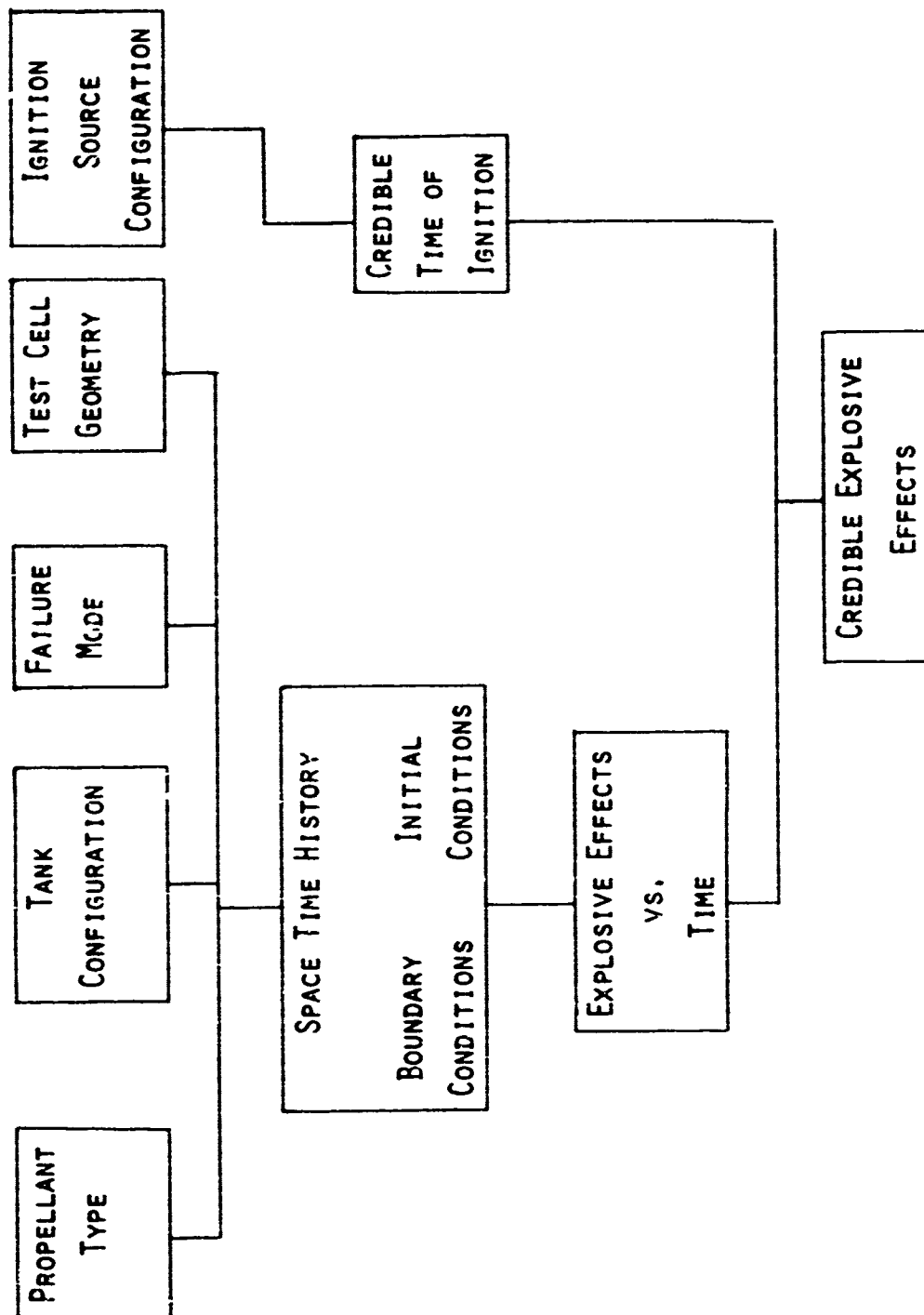
where the propellants were mixing in a completely confined configuration. The tanks in the test facility of concern, however, are separated by a significant distance (approximately fifteen feet) so that, should a tank failure occur, the propellants would only be able to come together in a semiconfined or unconfined condition. They are spherical tanks with an approximate volume of 27 cubic feet. One hundred and eighty pounds of cryogenic liquid CO is stored in one tank and five hundred pounds of N_2O are divided equally between two other tanks. The storage conditions for the N_2O have not been established as yet and may range from a high pressure gas to a cryogenic liquid. The lines and components leading to and from the propellant tanks must also be included in the tank configuration since they will influence the velocity distribution, the state, and quantity of the propellants that will mix. Line sizes no larger than 1.5 inches in diameter are included in the system design.

Since a detailed failure mode analysis was not found to be appropriate for this priliminary study, only credible general failure modes were considered. Previous experience with liquid rocket propellant feed systems has indicated that the three general failure modes are line, component, or tank failures. While tank failure is always a possibility it is usually much less probable than the remaining two modes. Hence, it is most likely that the rate and subsequent mixing of propellants released during a failure would be heavily dependent on line sizes and separation of release points.

Ignition sources are required for initiation of CO and N_2O mixtures since they are not hypergolic. It was assumed that chemical, thermal,

electrical, or shock sources of sufficient energy were available in the laser test system. Number six blasting caps were used to supply this energy in actual explosive testing.

The geometry of the test cell was also considered because the walls and floor of the structure can contribute various constraints on the propellants once they are released through a system failure. Liquid propellants will tend to pool and spread on the floor and collect in instrumentation throughs or drains, while gases or dispersions will expand into the air and fill the volume of the room. Each of these situations is influenced to a degree by the semiconfining surfaces of the test cell. The particular cell of interest is rectangular (65 ft x 45 ft x 26 ft) having a volume of approximately 68000 cubic feet.

SPECIFIC TEST PROGRAM DESIGN CONSIDERATIONS:

As can be seen in Table 1, the variables discussed above will fix the boundary and initial conditions of two propellants when they come together and mix, thus allowing one to determine their gross space-time history and establish credible times for ignition to occur. The properties of these propellants will also be fixed once the propellants types and initial conditions are fixed. The initial conditions of the propellants may be expressed in terms of their states, spatial distribution, and velocities at the time they first come into contact. From the range of storage conditions that the CO and N_2O will have in the operational system of interest, it can be shown that the release of both liquids or gases of either propellant is possible.

The shape and position of these propellants, when they come together, will depend on whether they are in a semiconfined or unconfined condition. In the semiconfined condition, liquid state propellants are released in narrow streams impinging on the floor and pooling. To maximize mixing in this situation it is necessary to have the maximum diameter release streams available with a minimum credible separation. The timing of release of each propellant and the ignition also have significant effects on the shape and position of the propellant mixture at the time of detonation. These effects must be determined experimentally to discover which conditions will result in the maximum yield. Finally, the presence of vertical confinement must also be considered in shaping the charge of mixed liquids available for detonation.

The unconfined condition is generally brought about when gas or liquid is released into the ambient air and reflected off minor confining surfaces such as pipes and valves forming relatively unconfined clouds of vapor and droplets. In this situation, simultaneous released of two propellants would provide the best mixing. The separation between release points is not so critical in this case as long as it is representative of that which will be found in the system being evaluated. The time for ignition that will produce maximum yield must be determined experimentally.

In the semiconfined condition, the velocity of the streams of liquid propellant released will determine the rate of growth and spreading of the pools of liquid formed. High velocities will cause the propellants to splash preventing them from accumulating on the ground and mixing. Since

CO and N_2O are cryogenics in the liquid state, the optimum velocity for mixing in the testing situation would be the lowest possible with a tolerable boiloff so that the quantity of propellant mixed could be estimated. The velocity distribution of the vapors and droplets released in the unconfined condition should also be a minimum so as not to form narrow streams of propellant and prevent early mixing.

CO and N_2O are cryogenics in the liquid state, the optimum velocity for mixing in the testing situation would be the lowest possible with a tolerable boiloff so that the quantity of propellant mixed could be estimated. The velocity distribution of the vapors and droplets released in the unconfined condition should also be a minimum so as not to form narrow streams of propellant and prevent early mixing.

EXPERIMENTAL

TEST CONFIGURATIONS:

As a result of the arguments above the test matrix shown in Table 2 was outlined. The tests to be performed were divided into two types of configurations corresponding to the semiconfined and unconfined boundary conditions discussed earlier. The open can test configuration depicted in Figure 1 was designed to simulate the pool or vertically confined situations. It consisted of a 3 ft diameter by 3 ft high aluminum can open at the top. The two cryogenic propellants entered the can through 1.5 inch lines near the bottom of the can. The feed lines came from an underground system which will be discussed later (see Figures 9, 1ú). Two No. 6 blasting caps were mounted to the side of the container with the face of each cap exposed to the propellant in the can. The can was mounted on top of a concrete or steel witness plate.

During a test, 60 gallons each of LN_2O and LCO were ejected into the can. Using 50 psi tank pressure this took approximately 25 seconds. Liquid N_2 and N_2O were used to calibrate flow rates and determine how much liquid would remain in the can after the flow had stopped. It was found that approximately 180 pounds of LCO and 270 pounds of LN_2O would consistently be left in the bottom of the can. The mixture which resulted was a 12 inch deep pool of LN_2O/LCO slush, since the boiling point of CO was lower than the freezing point of N_2O. If the propellants were released separately the flow time was doubled. Ignition was initiated immediately after all the propellants were down or 10 seconds after to allow for additional mixing condensation, or stratification that might occur.

TABLE - 2

TEST MATRIX

SEMICONFINED:

OPEN CAN TEST — Pool Confinement of LCO and LN_2O Stochiometric Mixtures (300 - 500 lbs of propellant)

— Simultaneous and Sequenced Release

— Immediate and Delayed Ignition

— Blasting Cap and Squib Ignition

TENT TEST — Ground Confinement of LCO and LN_2O Stochiometric Mixtures (approx 800 lbs of propellant)

— Simultaneous Release

— Ignition At All Down

— Blasting Cap and Squib Ignition

UNCONFINED:

BALLOON TEST — Unconfined Mixtures of CO and Air and CO and N_2O Ranging from Fuel To Ox Rich (50 lbs of propellant)

— Simultaneous Release

— Blasting Cap and Squib Ignition

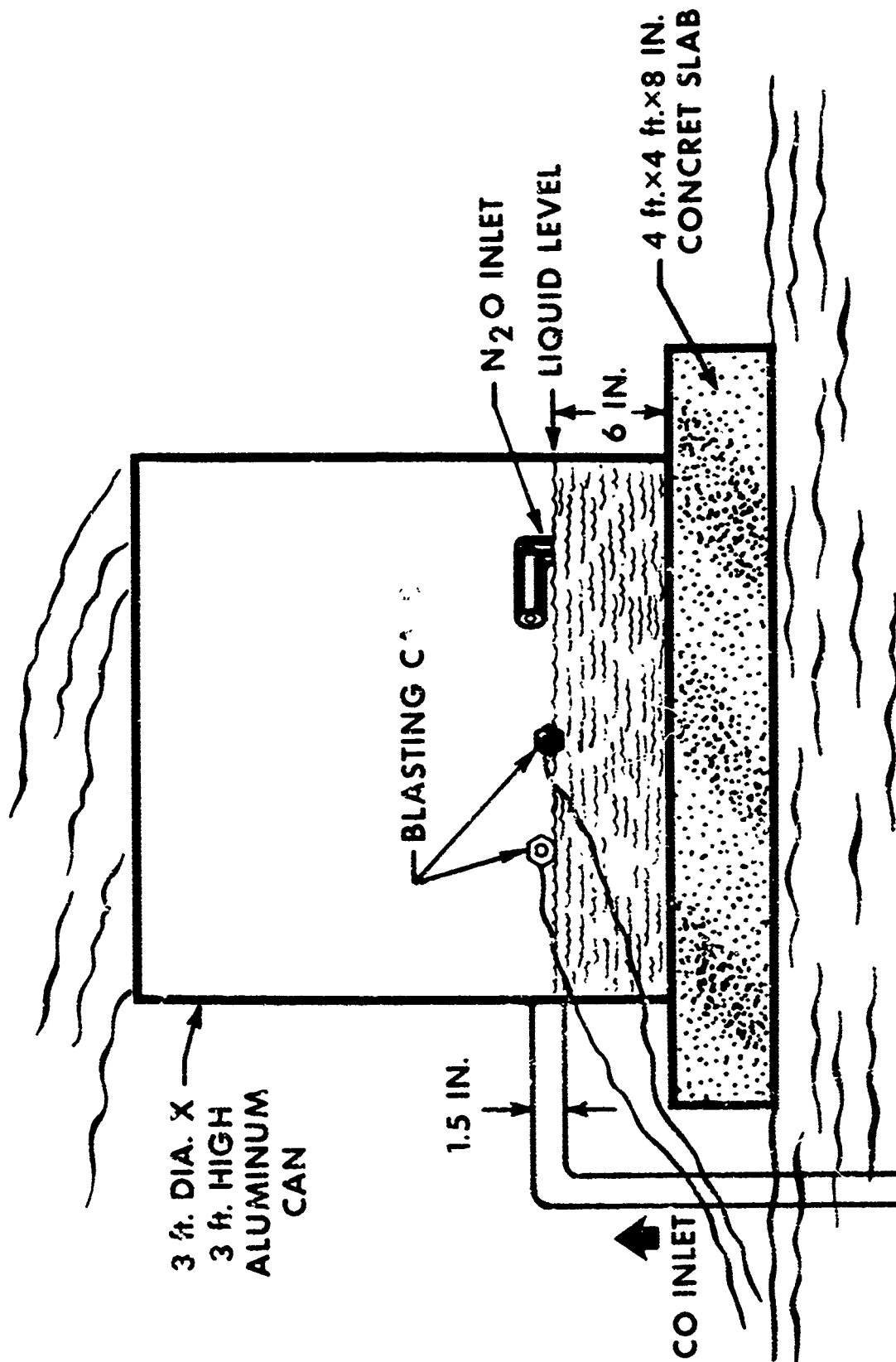# LCO/LN₂O SEMICONFINED TEST CONFIGURATION

FIGURE - 1

CO/N₂O TENT TEST CONFIGURATION

BLASTING CAP & SQUIB

METAL FRAME

N₂O INLET

PARACHUTE MATERIAL
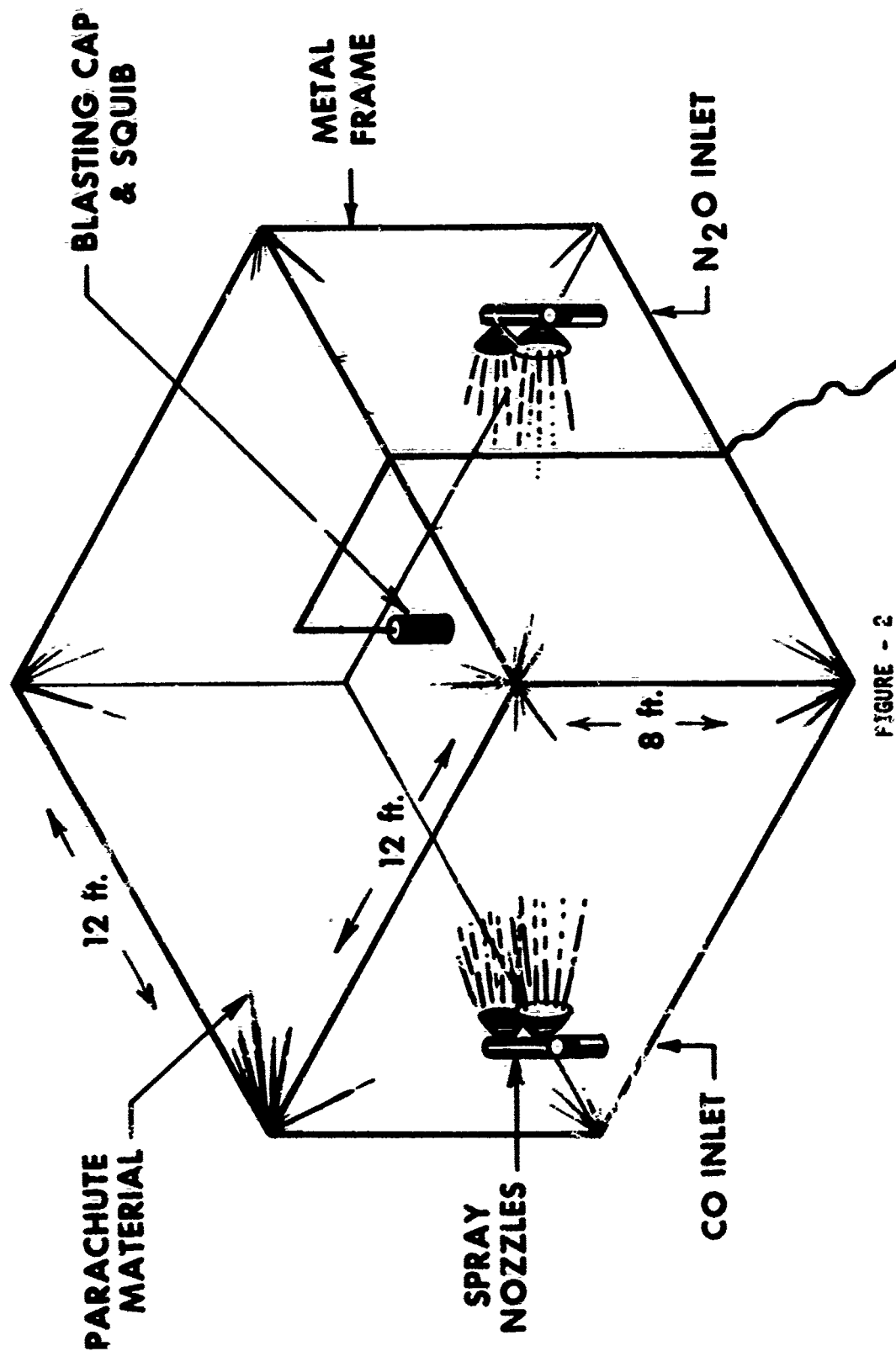
SPRAY NOZZLES

CO INLET

12 ft.

12 ft.

8 ft.

FIGURE - 2

1322

The tent test configuration is shown in Figures 2, 3, and 4. This configuration provides for two kinds of semiconfinement, ground confinement and reflection off of minor surfaces. Each propellant is released into the air through a bank of spray nozzles shown in Figure 4. This method of release is designed to simulate the reflection of liquid and gaseous streams off of minor surfaces such as lines and valves. The result is a despersion of liquid drops in a gas made up of CO, N_2O, and air. In addition, there will be some pooling of liquids on the ground. The tent enclosure consists of a metal frame covered with parachute material. I' was used to provide a means of keeping the propellants in the local tes area so that the approximate geometry and quantity of the propellants would be known at the time of ignition.

The propellants entered the tent through the two banks of nozzles shown in Figure 2. They were fed by the same underground feed system used for the can tests. Using 50 psi tank pressures it took 40 seconds to eject 60 gallons of each propellant into the tent. Detonation was initiated by a combination of a No. 6 blasting cap and a small squib suspended in the center of the tent. This arrangement was varied by putting the blasting cap on the ground in an effort to detonate any liquid that would pool there.

The balloon tests were designed to simulate the condition of having a unconfined mixture of the two propellants and air. Figure 5, 6, and 7, shows the details of this configuration and its appearance in the deflated and inflated state. These balloons were standard meteorological balloons which were designed for about a 16 ft diameter expansion. The propellants
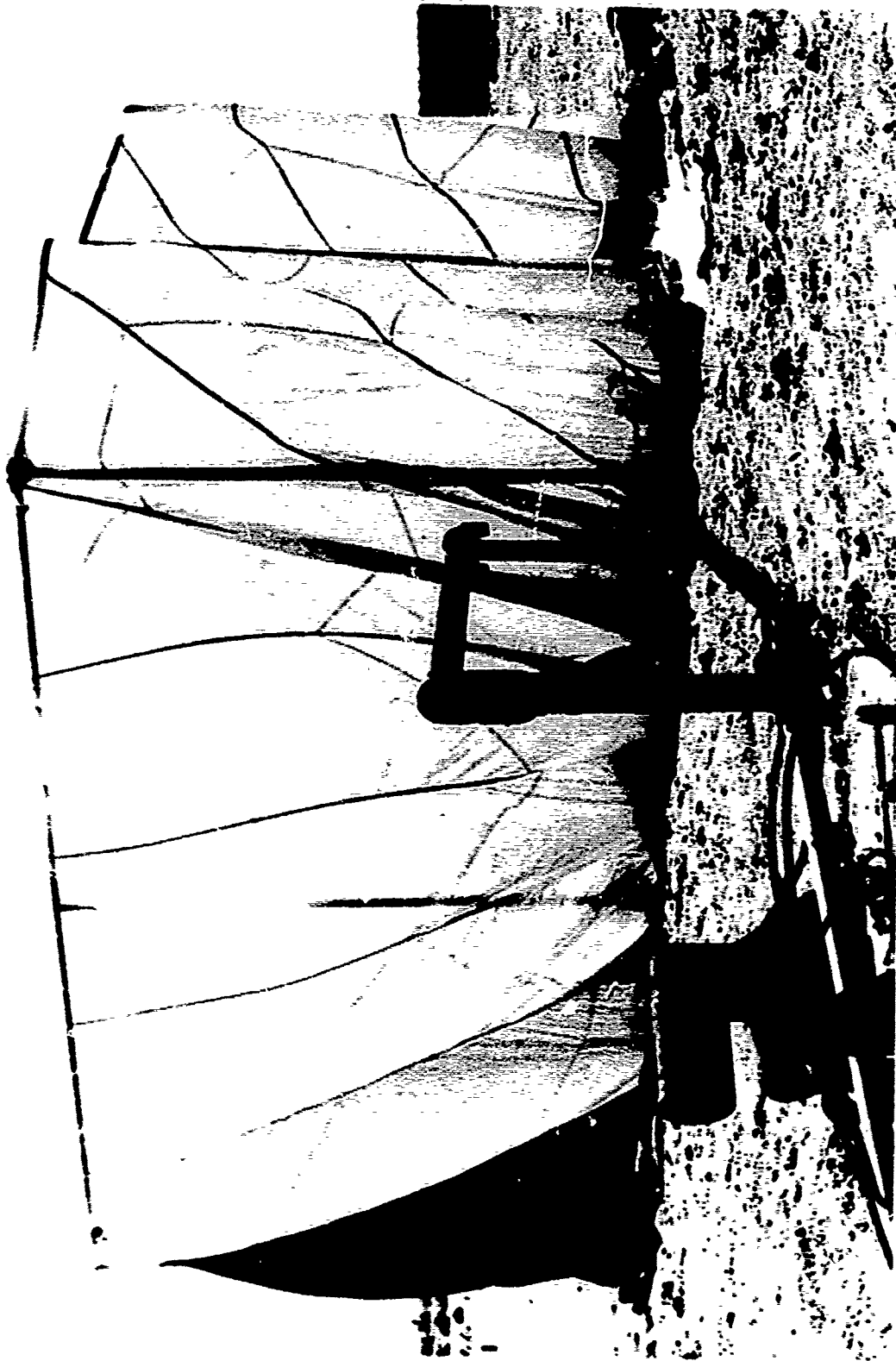
FIGURE - 3 : TENT TEST CONFIGURATION
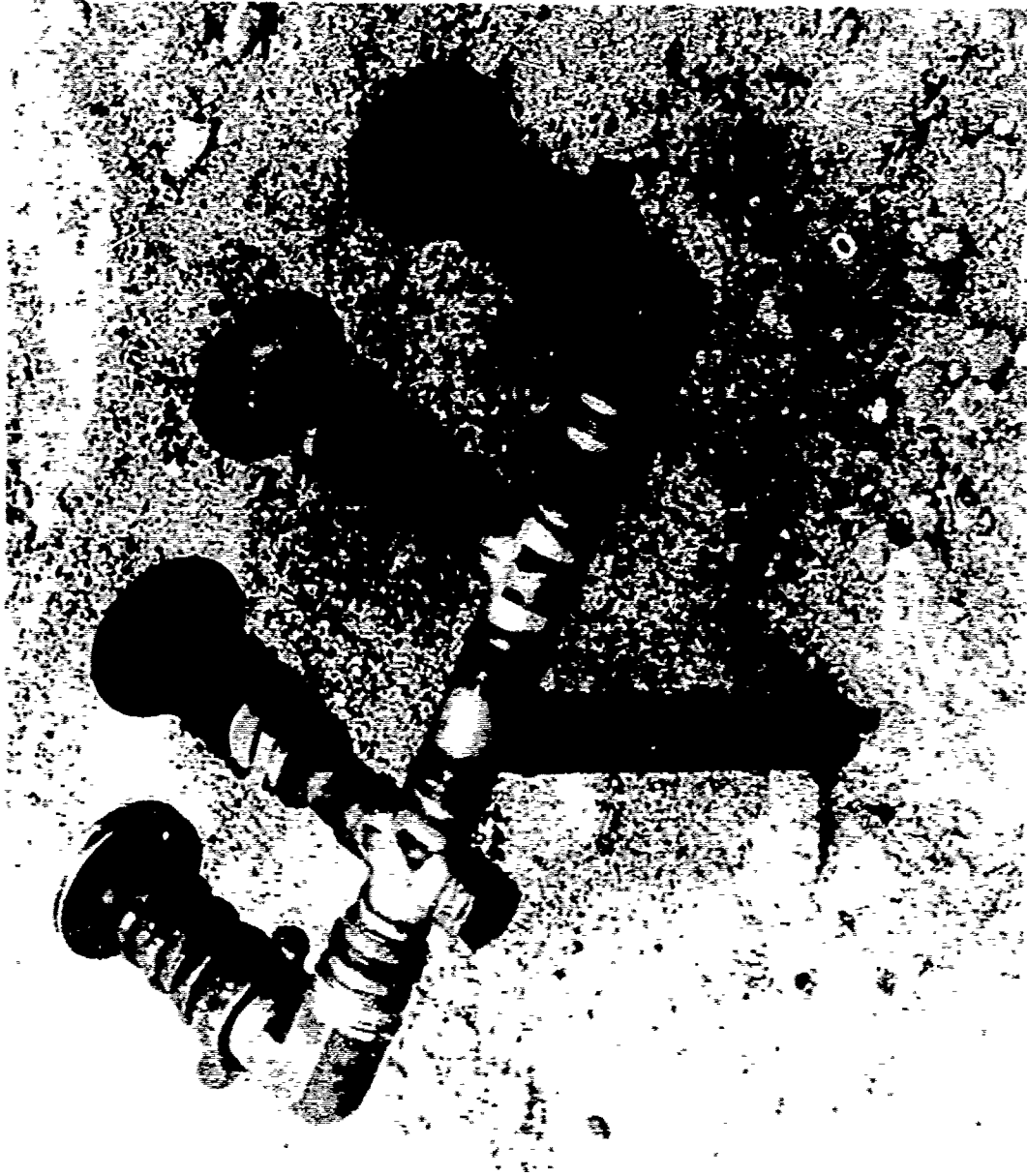
FIGURE - 4 SPRAY NOZZLES USED IN TENT TEST.

CO/N$_2$O BALLOON TEST CONFIGURATION

BLASTING CAP

ANCHOR

16 ft. DIA.
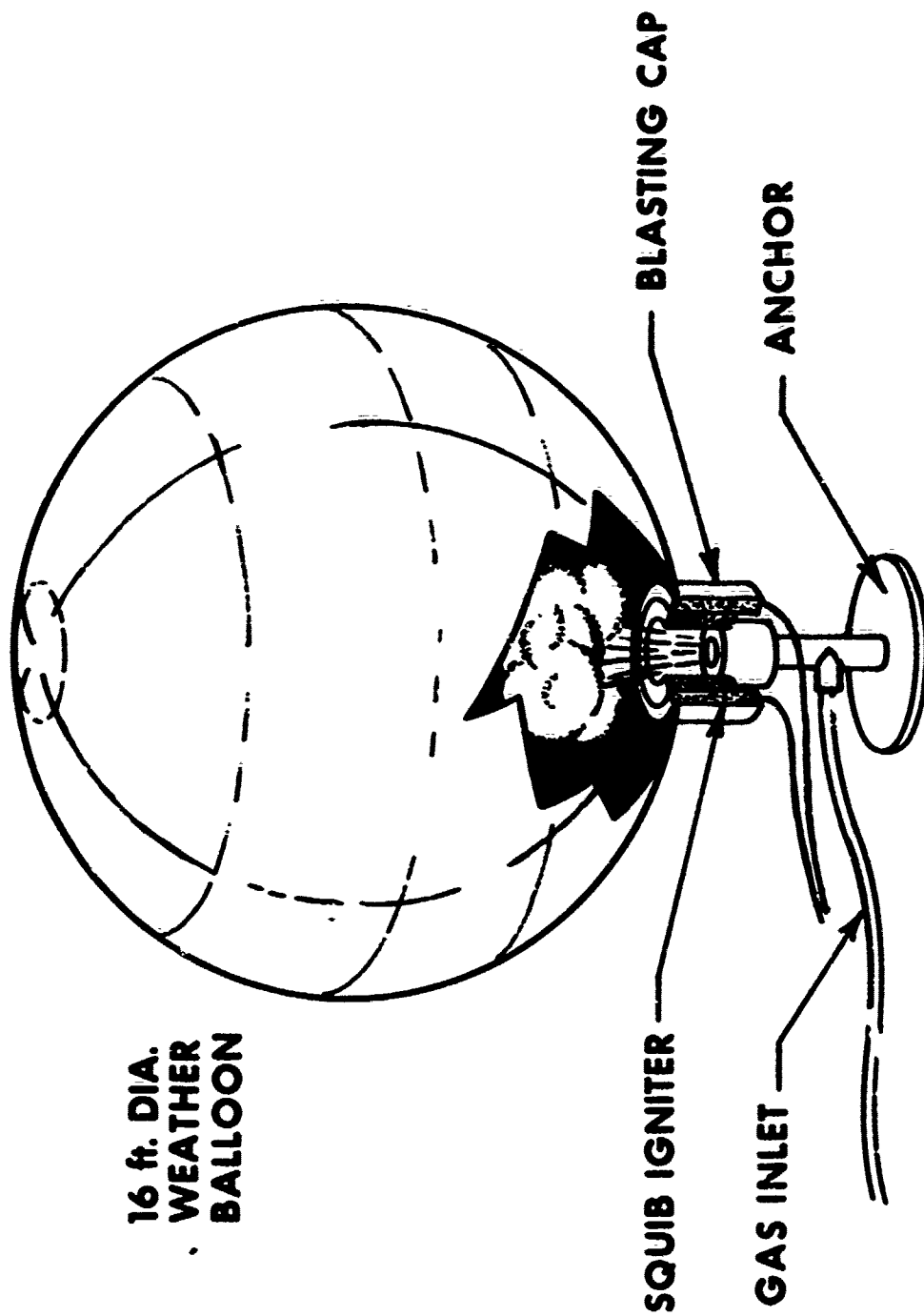WEATHER
BALLOON

SQUIB IGNITER

GAS INLET

FIGURE - 5

1326
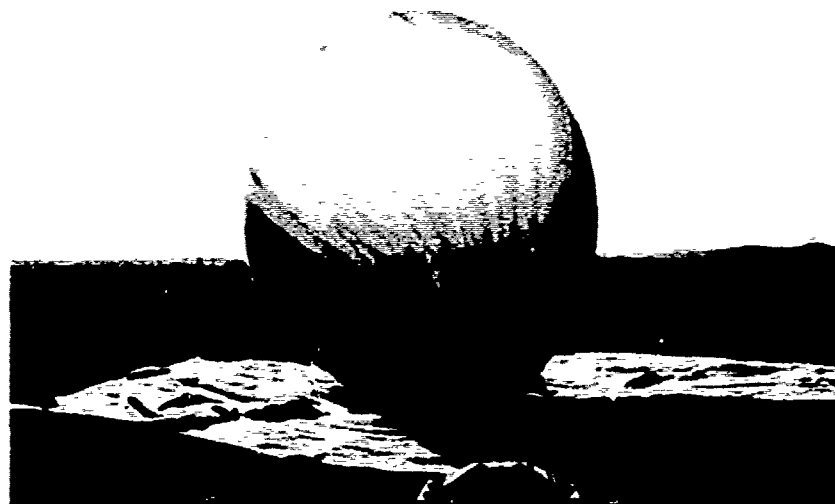
FIGURE - 6 TOP: MOUNTING THE BLASTING CAPS ON A BALLOON.

BOTTOM: BALLOON READY FOR DETONATION.

FIGURE - 7 DEFLATED BALLOON READY FOR FILLING.
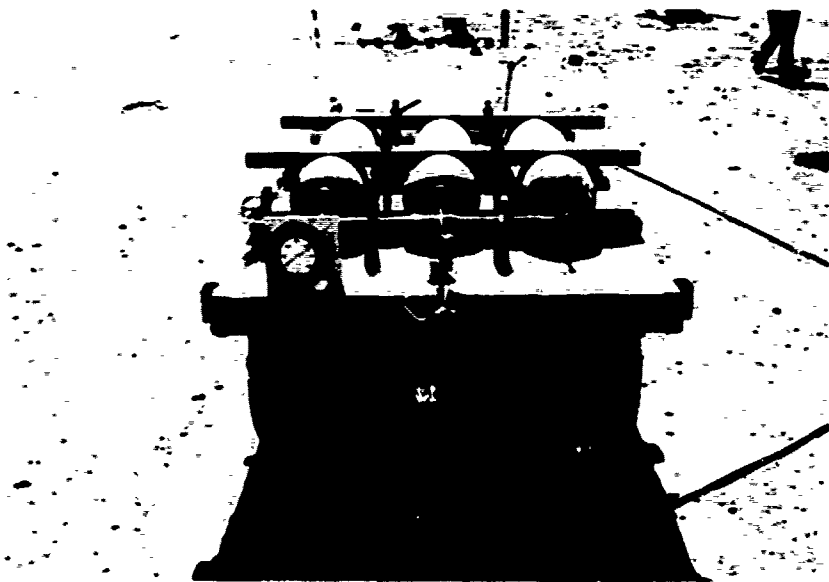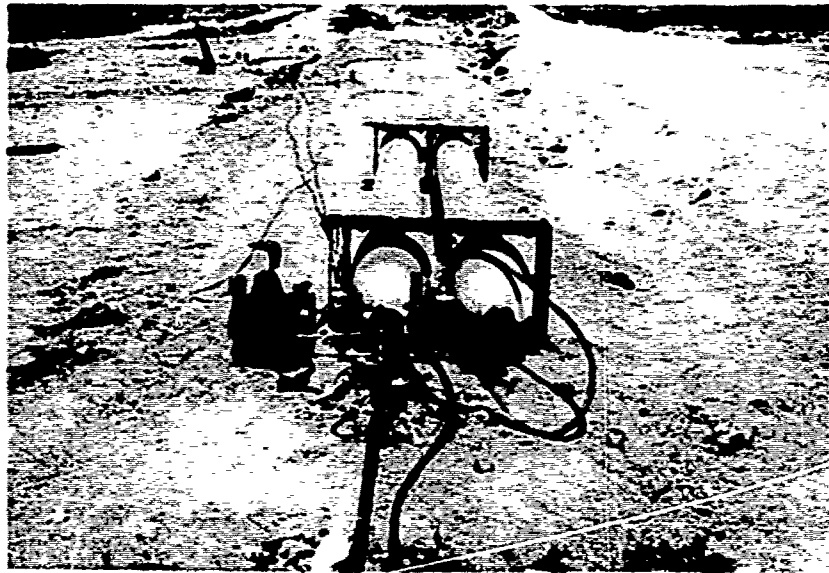
FIGURE - 8   TANKS USED TO FEED GASES TO DETONABLE BALLOONS.

were added in various combinations of CO, air, and N_2O. Fifty pounds total of propellant were used for each test. Each gas was added separately through a common feed line at the bottom of the balloon running from two separate banks of K-bottles as shown in Figure 8. Filling took 45 minutes to an hour and permitted ample time for mixing. The diameter of the resulting sphere ranged between 10 and 12 feet. A squib and a blasting cap were taped to the base of the balloon as shown in Figure 6. The base of the balloon was approximately four inches off the ground, but the balloon usually tipped and layed on its side due to the heavier than air gases used.

TEST FACILITY:

The configurations above were all tested at the center of the test pad shown in Figure 9. When the can tests were being performed, a witness plate was placed at ground zero for the cans to rest on (see Figure 10). The witness plate shown is made of steel with the dimensions 10' x 10' x 6". Its slightly cupped in the center as a result of previously performed hazards tests.

The tank trenches indicated in Figure 9 are the locations of the underground propellant feed system used for the can and tent tests. A portion of these trenches can be seen in Figure 10. This system was placed underground to protect it from damage and to avoid having obstructions above ground which could interfere with detonation waves formed during a test.

TRENCH LAYOUT-PROJECT HELP

VENT

(TYP.) TANK TRENCH

WITNESS PLATE

N

INSTRUMENT TRENCH

STA 0+40 (TYP)

STA 0+40 (TYP)

STA 0+70 (TYP)

STA 1+40(TYP)

ROAD

FIGURE - 9

1331
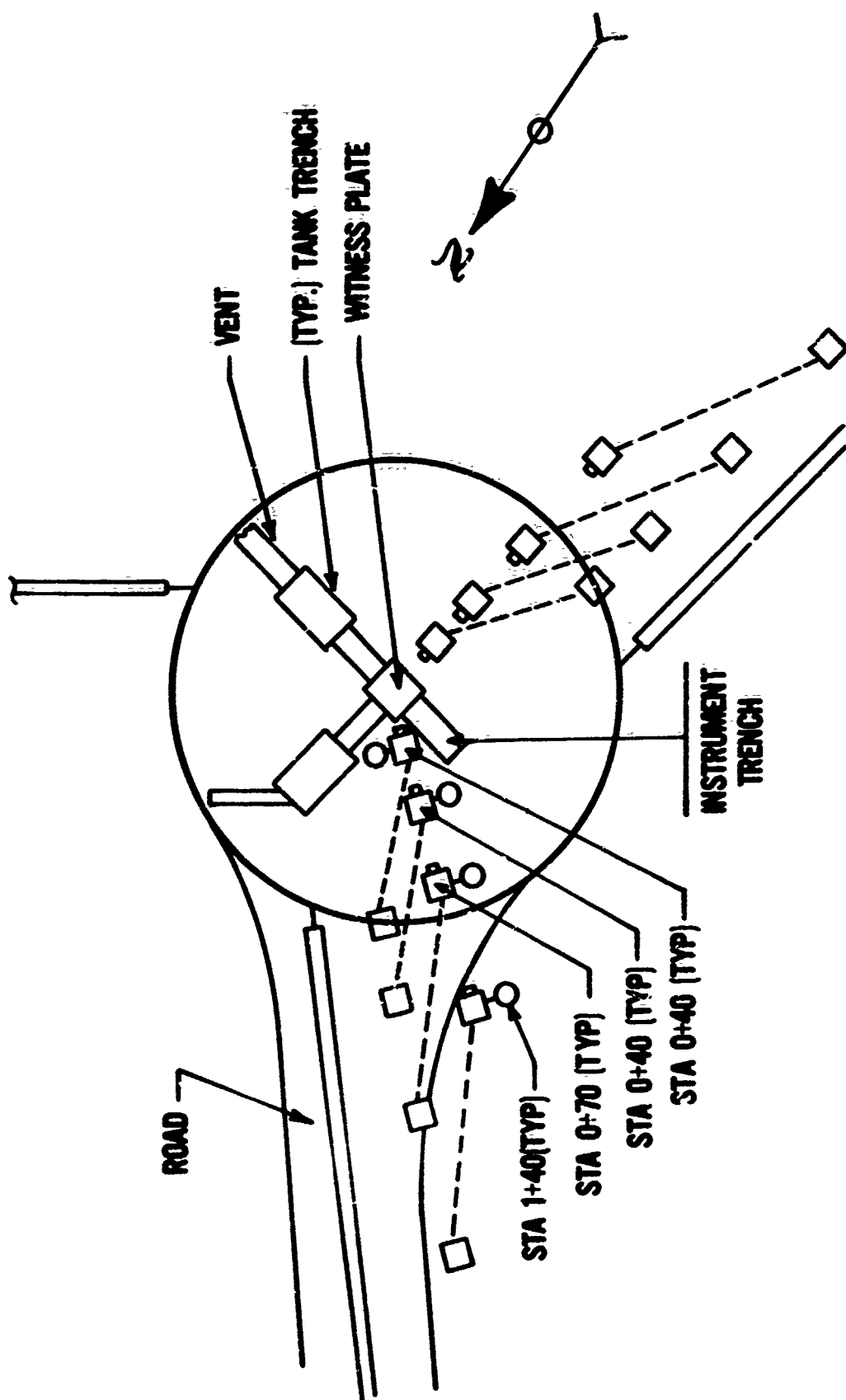
FIGURE – 10 STEEL WITNESS PLATE FOR CAN TEST, 10'X10'X6"

MECHANICAL SCHEMATIC—"PROJECT HELP"
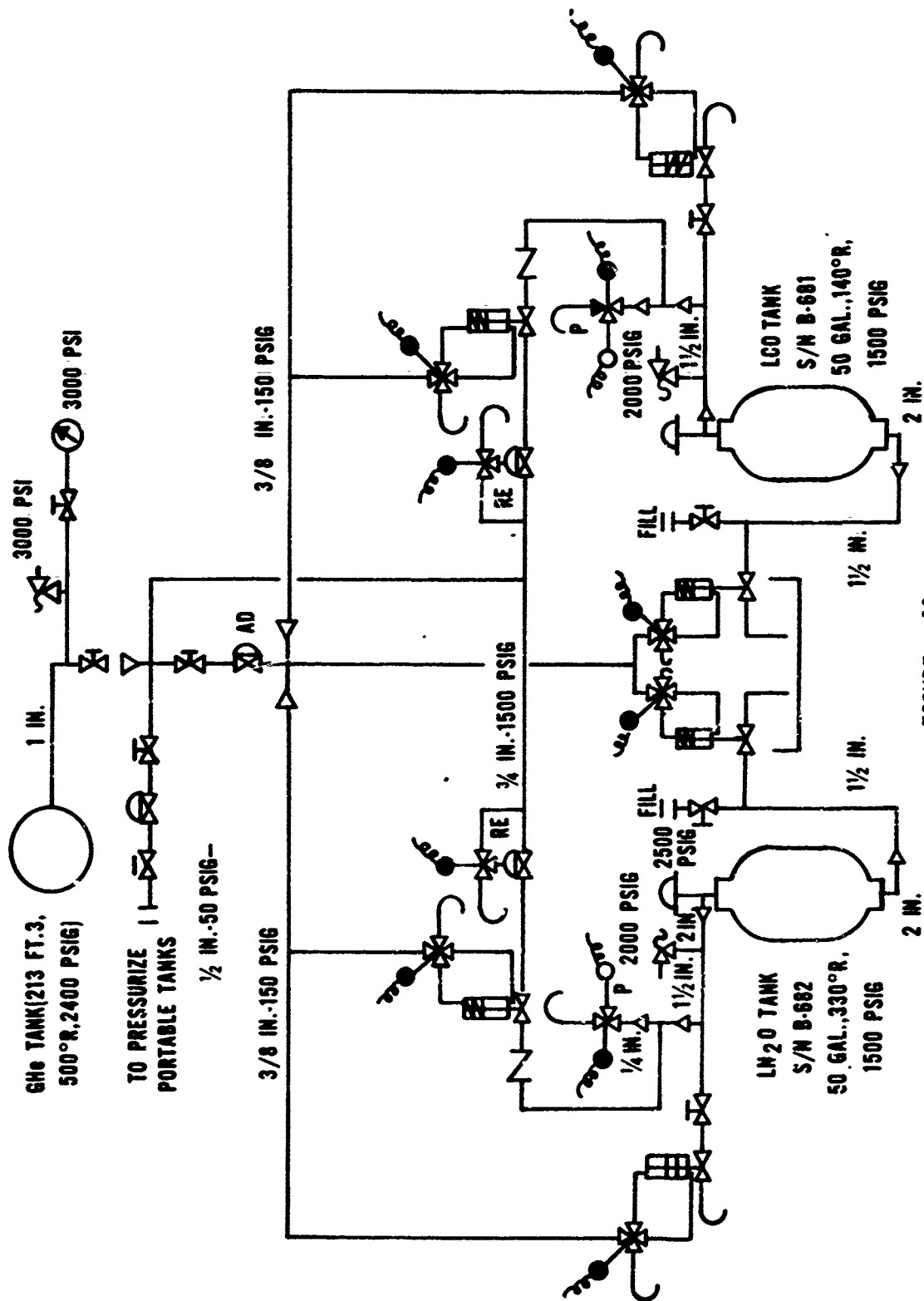
FIGURE - 11

The mechanical feed system buried underground is shown in Figure
11. It is very similar to a bipropellant rocket feed system with LCO
as the fuel and LN_2O as the oxidizer. Helium was used as the tank
pressurizing gas and to actuate the remote valving. The entire system
was operated from a block house sixteen hundred feet away.

INSTRUMENTATION:

Ten Kistler pressure transducers were placed on two legs radiating
from ground zero. Two thermal measurements of the fireball were also attempted.
These twelve data sources, along with voice and time base were fed into
a 14 channel tape recorder. Documentary photography was used to obtain
information on mixing parameters.

To provide adequate documentation of the explosive characteristics
of the propellant explosions, it was necessary to measure the pertinent
blast characteristics as a function of both distance and azimuth. Blast
gages were installed on two of the existing radial gage lines, passing
through ground zero and oriented 120° with respect to each other as shown
in Figure 11. It was decided to install side-on pressure gages at six
distances on Leg A; 7.5, 13, 25, 40, 70, and 140 ft, and at four distances
on Leg B; 25, 40, 70, and 140 ft. The estimated peak overpressures at
each of these gage locations for a 1%, 10%, and 100% of a 200-lb TNT
charge are presented in Table 3. It was anticipated, however, that the
close-in pressures for the propellant explosions would be somewhat lower
than these estimated values. Figures 12 and 13 illustrates the transducer
mounts used for close-in (7.5' and 13.0') and distance peak overpressure
measurements. The close-in mounts were almost flush with the ground so

TABLE - 3

ESTIMATED PEAK OVERPRESSURE FOR 1, 10, AND 100 PERCENT OF A 200-LB TNT CHARGE

DISTANCE (feet)	1% (psi)	10% (psi)	100% (psi)
7.5	28	100	700
13	8.4	40	260
23	3.5	9	65
38	1.7	5.2	22
67	0.8	1.7	7.5
117	0.4	0.8	3

1335

FIGURE - 12 CLOSE-IN TRANSDUCER MOUNTS BEING INSTALLED
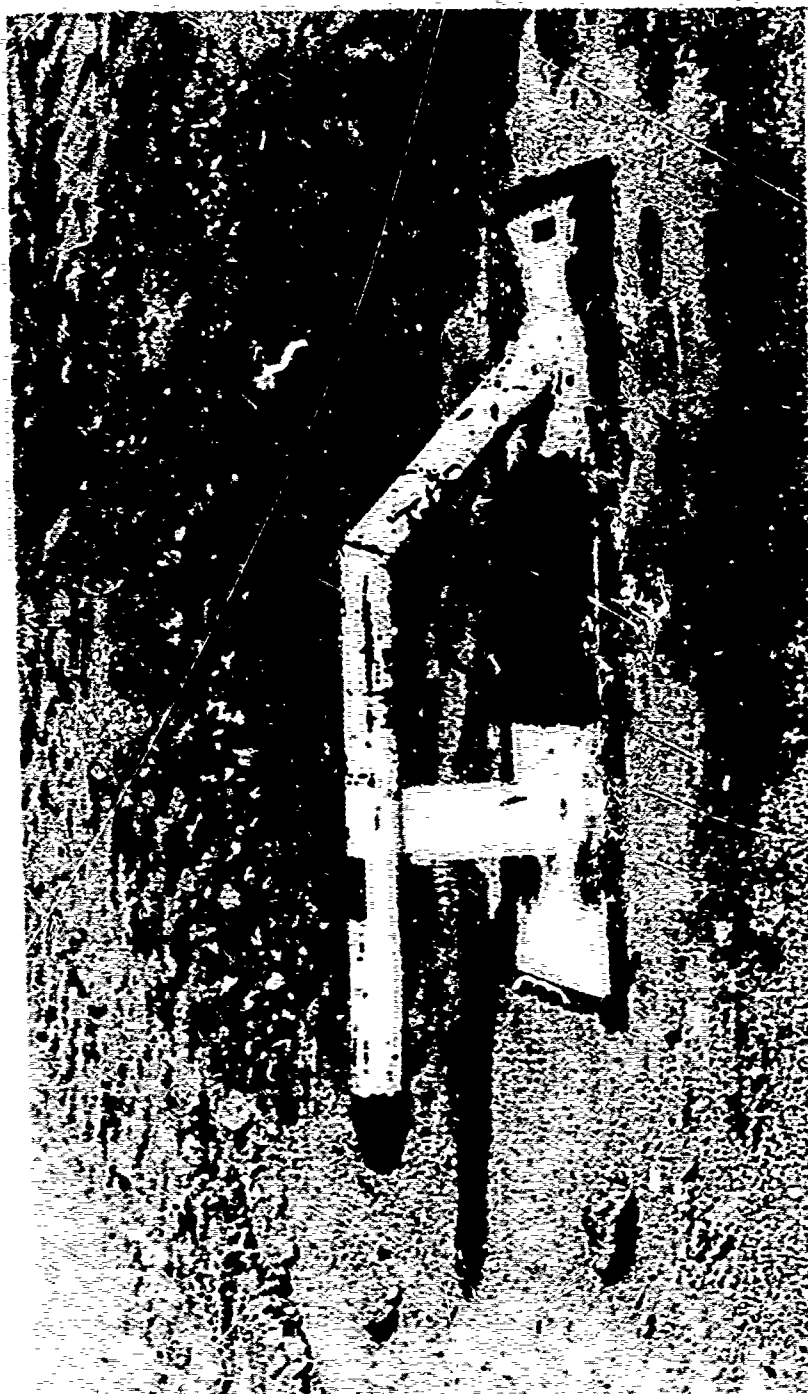
FIGURE -13 DISTANT TRANSDUCER MOUNT

that they would not interfere with the shock wave as it travelled away from ground zero. The bullet shape of the distant mounts provided an aerodynamic surface for a developing detonation wave to pass over before reaching the transducer placed several inches back from its nose. The purpose of this was to obtain an overpressure measurement of an undisturbed shock wave.

Deldrin inserts were used to isolate all gages which were installed with a slight recess to allow for application of silicone grease to protect the gages from thermal shock. It was also necessary that the cabling from the gage mounts to the amplifier boxes be encased in conduit to avoid damage to the wires and the pickup of noise signals.

The types of thermal devices used for these tests were: an intra-fireball thermocouple probe at the 13-ft distance on Leg A, and an external radiometer at the 67 or 117-ft distance on Leg A. The radiometer was mounted on the side of the raised pressure gage mount. The thermocouple probe was mounted in a length of thick-walled pipe, installed to one side of the 13.5 ft station.

DATA:

Pressure, as a function of time and distance, were measured. From this peak, overpressure and positive-place impulse were determined and reference curves plotted. A measure of the gas temperature within the fireball provided an indication of damage that might occur to nearby equipment Calibration of pressure transducers was provided by tests using pentolite and C-4 charges. Motion pictures documented each test

with both real-time and high-speed cameras. Single-point data obtained.
No effort was made to study the system parametically.

RESULTS

Six liquid can tests were performed using the quantities of propellants listed in Table 4. Tests #4 and 24 involved ejecting LCO into a can first and LN_2O second. Ignition was initiated two seconds after all the propellants were down. The quantities of propellants listed represent the amount remaining as liquid at the time of ignition.

Test #4 produced a detonation while Test #24 yielded only a deflagration. The peak overpressure and explosive yield data for Test #4 is shown in Table 5 and Figure 14. Data from both instrumentation legs are shown. The dashed lines are the reference curves for a TNT charge having 30 and 60% of the total propellant weight tested. It can be seen that the experimental points are bounded by these two curves approaching the 30 percent curve as they diverge from ground zero. The close-in data shows a significant difference between the two legs due to the non-spherical geometry of the test configuration. In addition it does indicate some anomalous behavior.

A pressure pulse produced by a charge of TNT (8) is initially very sharp and the peak overpressure curves produced are similar to those shown in Figure 14. Liquid propellant explosions normally produce a broad initial impulse. If the TNT equivalence of the propellant is known, a plot of peak overpressure versus distance should fall below the equivalent TNT curve near the point of the detonation and approach the TNT curve with

TABLE 4

SEMICONFINED CAN TEST RESULTS

TEST NO.	LCO (LB)	LN2O (LB)	YIELD (TNT Equiv)	REMARKS
4	180	270	30-60%	Put Hole in 6" Steel Plate
5	180	270	—	No Visible Reaction
6	180	270	10-20%	Destroyed 8" Reinforced Concrete Block
23, 24	180	270	—	Fireball
25	180	—	—	Fireball

TABLE - 5

PEAK OVERPRESSURE AND EXPLOSIVE YIELD DATA FOR TEST#4 LCO/LN₂O CAN TEST

DISTANCE (FEET)	2 O'CLOCK LEG		6 O'CLOCK LEG	
	PEAK OVERPRESSURE (psi)	EXPLOSIVE YIELD (%TNT)	PEAK OVERPRESSURE (psi)	EXPLOSIVE YIELD (%TNT)
25	83	69	64	52
40	-	-	18	37
70	6.1	34	5.8	31
140	1.9	28	-	-

TEST #4 SEMI-CONFINED LIQUID CAN TEST

Figure 14

13 -
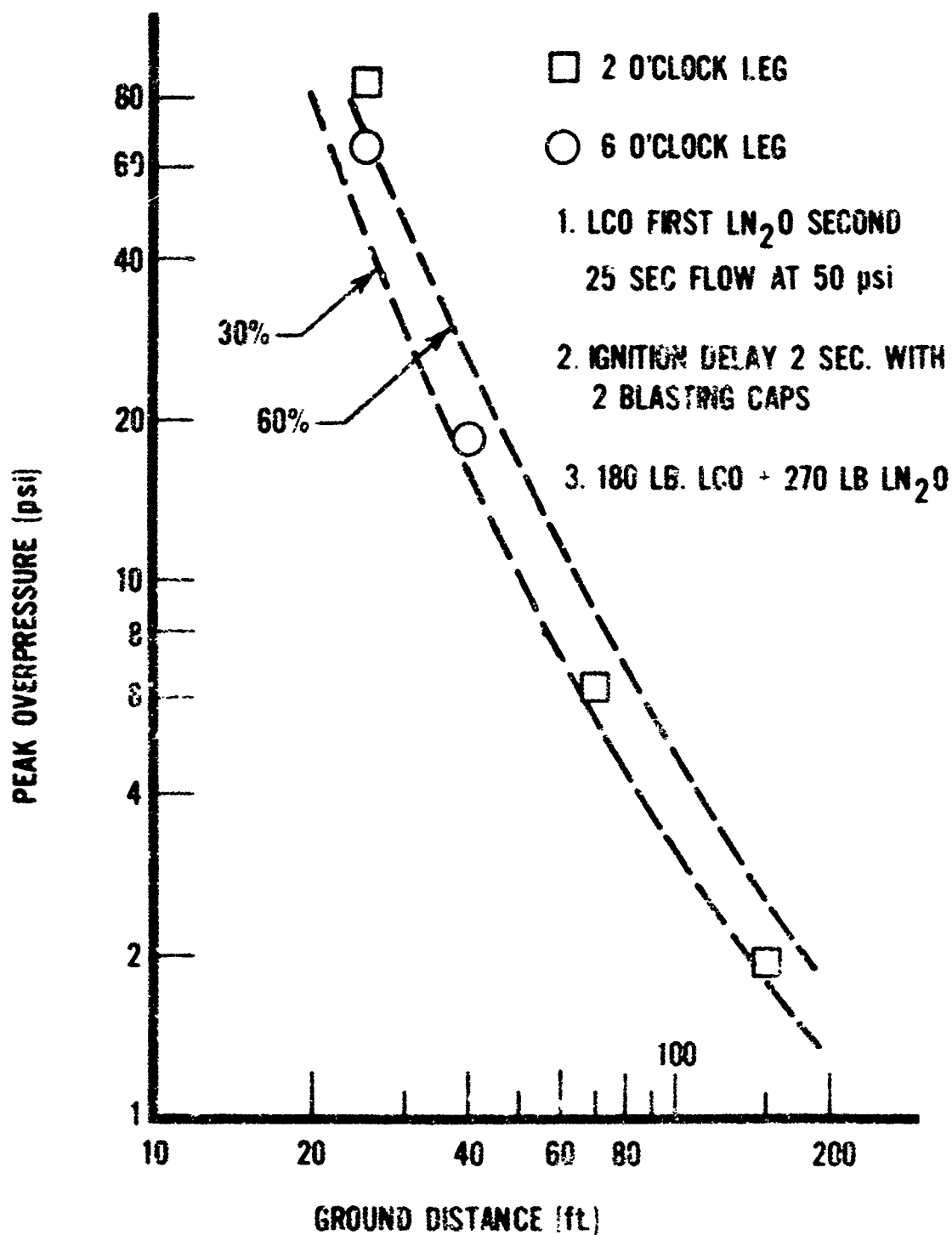
increasing distance since the effects of charge and impulse shape decrease with distance away from t. point of detonation. This is indicated by the convergence of the data for the two legs with distance.

Tests #5 and 6 were identical to those above except that the propellants were released simultaneously (see Table 6 and Figure 15). In Test #6 a detonation occurred, however, in Test #5 no reaction was observed. The peak overpressure data for Test #6 is presented in Figure 15. Here the yields ranged between 10% for the close-in data and 20% for the distance pressure gauges. The dropoff of the peak overpressure in the close-in data, as previously discussed, is observed in this case.

Test #25 was conducted to see whether enough liquid oxygen could be condensed from the air by LCO to form a detonable mixture without N_2O present. The result was a fireball but no detonation.

There are several possible explanations for the absence of detonations on a majority of the can tests. An analysis of similar type tests on LOX/H_2, LOX, RP1, and LCO/LOX (4), (6) indicates that the energy of initiation and mixture ratios are very critical in determining whether a mixture will detonate, deflagrate, or not react at all. Unlike flamability limits, detonation limits usually cover a much narrower range of mixture ratios. In the present case it appears that the energy provided by the blasting cap squib arrangement is marginal for initiating a detonation. However, once detonation is initiated it is of a significant order. The physical damage produced

TABLE - 6

PEAK OVERPRESSURE AND EXPLOSIVE YIELD DATA FOR TEST#6 LCO/LN$_2$O CAN TEST

DISTANCE (FEET)	2 O'CLOCK LEG		6 O'CLOCK LEG	
	PEAK OVERPRESSURE (psi)	EXPLOSIVE YIELD (%TNT)	PEAK OVERPRESSURE (psi)	EXPLOSIVE YIELD (%TNT)
13	-	-	56	6
25	30	18	-	-
40	10	14	8.4	11
70	3.6	13	3.5	13
140	1.5	16	-	-

1345

TEST #6 SEMI-CONFINED LIQUID CAN TEST
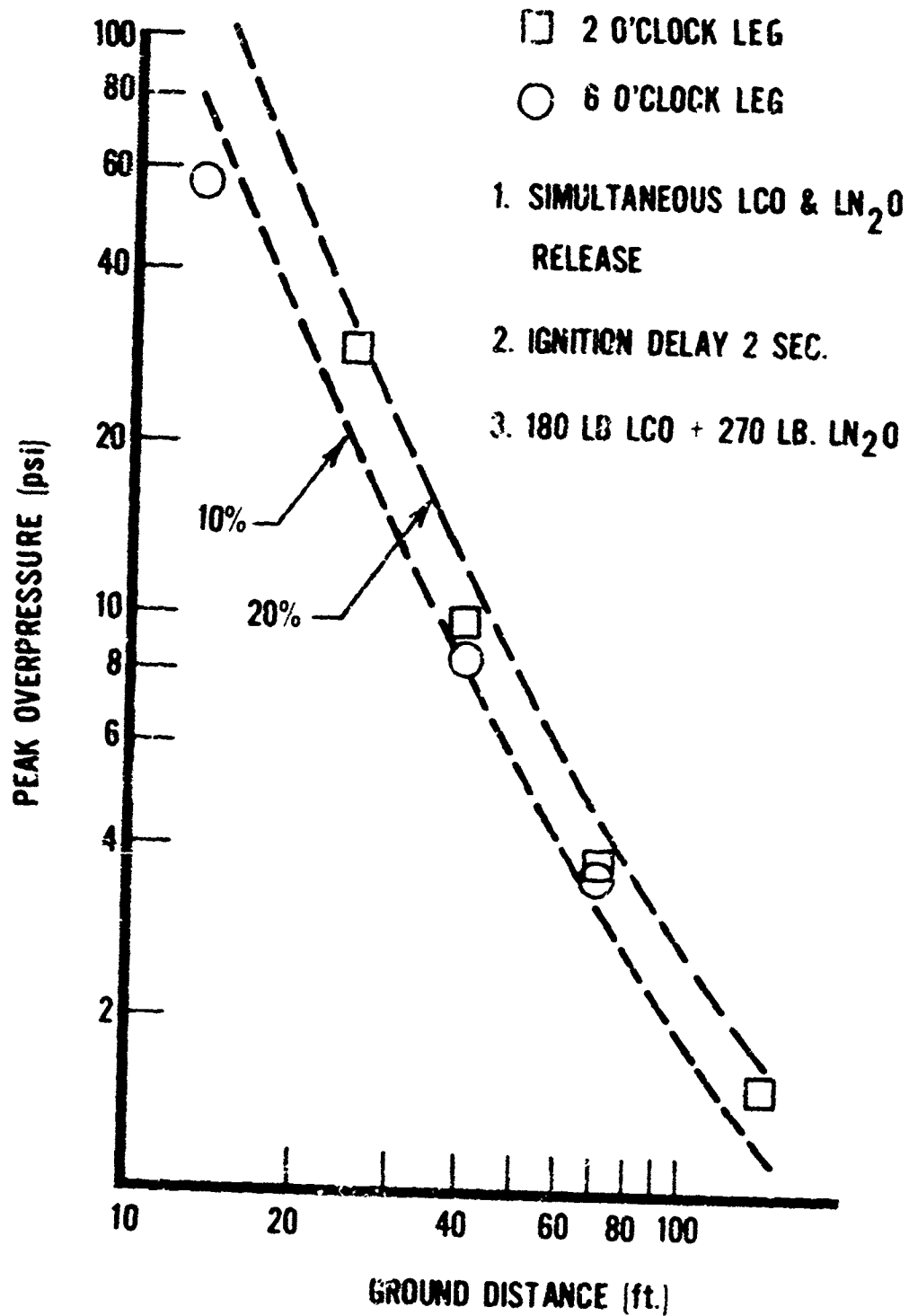
Figure-15

by such detonations is illustrated by the condition of the six inch steel witness plate in Figure 16. The aluminum can was completely destroyed. Two inch pieces of aluminum shrapnel were found as far as 250 feet from ground zero. The thermal devices were not successful in detecting the fireball temperature, however, bits of melted aluminum at ground zero gives some indication of the temperatures reached.

Four semiconfined tent tests were completed using the quantities of propellant indicated in Table 7. No detonations were obtained in the CO/N_2O or CO/air tests. In each test the gases ignited and the parachute tent was destroyed; however, no damage was sustained to the mechanical system or tent frame. The parachute seams and webbing remained indicating a relatively cool flame. The propagation of the flame front through the cloud of propellants in the tent was an order of magnetude slower than that observed in the can tests. In 10 thousanths of a second a major portion of the propellants were initiated in the can tests while in the tent tests there was about 10 thousanths of a second delay after ignition before a slowly expanding fireball was observed for approximately one tenth of a second. The lack of any detonation in the tent tests was not surprising since previous investigations into fuel air-explosions (2) have also encountered agreat deal of difficulty in propagating a detonation. The most important factor was the large amount of energy required. Benedict et al (3) used charges of Dupont El 506-A.5 explosive of more than 100 grams to detonate mixtures of air, propane, propylene and butane. For charges less than 400 grams the flamibility and detonation limits were strongly dependent on charge size and mixture ratio.

FIGURE - 16   WITNESS PLATE AFTER LCO/LN$_2$O CAN TEST#4

TABLE - 7

SEMICONFINED TENT TEST RESULTS

TEST NO.	CO (LB)	N_2O (LB)	REMARKS
15	110	-	Orange Fireball
16	327	343	White Fireball
17	334	514	White Fireball
18	334	514	White Fireball

No Detonations

1349

A second factor which can effect detonability is the shape and size of the volume of propellants to be detonated. Just as a critical diameter is required before a detonation will propagate through a solid grain it has been shown (3) that the dimensions of a detonable vapor mixture will influence whether a shock wave will be extinguished or propagated. The smaller the volume of gases, the more severe is the effective radius of curvature and, the more difficult it is to sustain a shock front. The final factor to consider is the mixture ratio. In all of the tests we have attempted to work around the stoichiometric ratio of CO to N_2O (2:1) since this would presumably be the easiest to ignite. Inside the tent, it is possible for local mixture ratios to deviate significantly from this ratio due to bouyancy effects from hot rising fans and the presence of two phases.

Five balloon tests were conducted using the gas mixtures presented in Table 5. The nitrogen and oxygen shown are the two components of air and are listed separately to indicate that nitrogen is merely a diluent and that CO reacts with the oxygen. Four CO/air tests were performed with mixture-ratios ranging from CO rich to O_2 rich. No detonation was obtained. A fireball was observed once having a flame propagation rate similar to the tent tests. The final test with CO and N_2O produced the same result. In these tests the initial mixture ratios were known much more precisely than in the can or tent tests and were well within the known flamability limits. Detonations were not obtained in these tests for many of the same reasons already discussed concerning the tent tests. These include

TABLE 8

CO/AIR AND CO/N₂O UNCONFINED BALLOON TEST RESULTS

TEST NO.	CO (LB)	N₂ (LB)	O₂ (LB)	CO: O₂	REMARKS
11	16.5	29.7	9.5	2:1	No Fireball No Detonation
12	12.0	27.6	8.3	1.65:1	Fireball No Detonation
13	19.0	35.5	10.1	2:1	No Fireball No Detonation
14	29.4	28.0	8.3	3.9:1	No Fireball No Detonation
21	CO/N₂O 31 LBS N₂O 19.5 LB CO				FIREBALL ONLY

Figure 17- Resulting Damage From a CO/N_2O Balloon Test

greater energy requirements, size and shape factors, and variations in local mixture ratios once ignition has been initiated.

Calibration tests using C-4 and pentolite charges were conducted periodically to insure the Kistler pressure transducers were calibrated. Figure 18 shows the typical results from a series of C-4 tests using 20 pound spheres placed on a 2.7 ft high box at ground zero.

TESTS #1,2,3 CALIBRATION

PEAK OVERPRESSURES (psi)

20 LB. C-4 SPHERES

H.O.B. -2.7 FT.

— REFERENCE CURVE-20 LB.
SPHERES AT H.O.B. =1.0

$\mathbf{I}$ DATA SPREAD

$ft/lb^{1/3}$
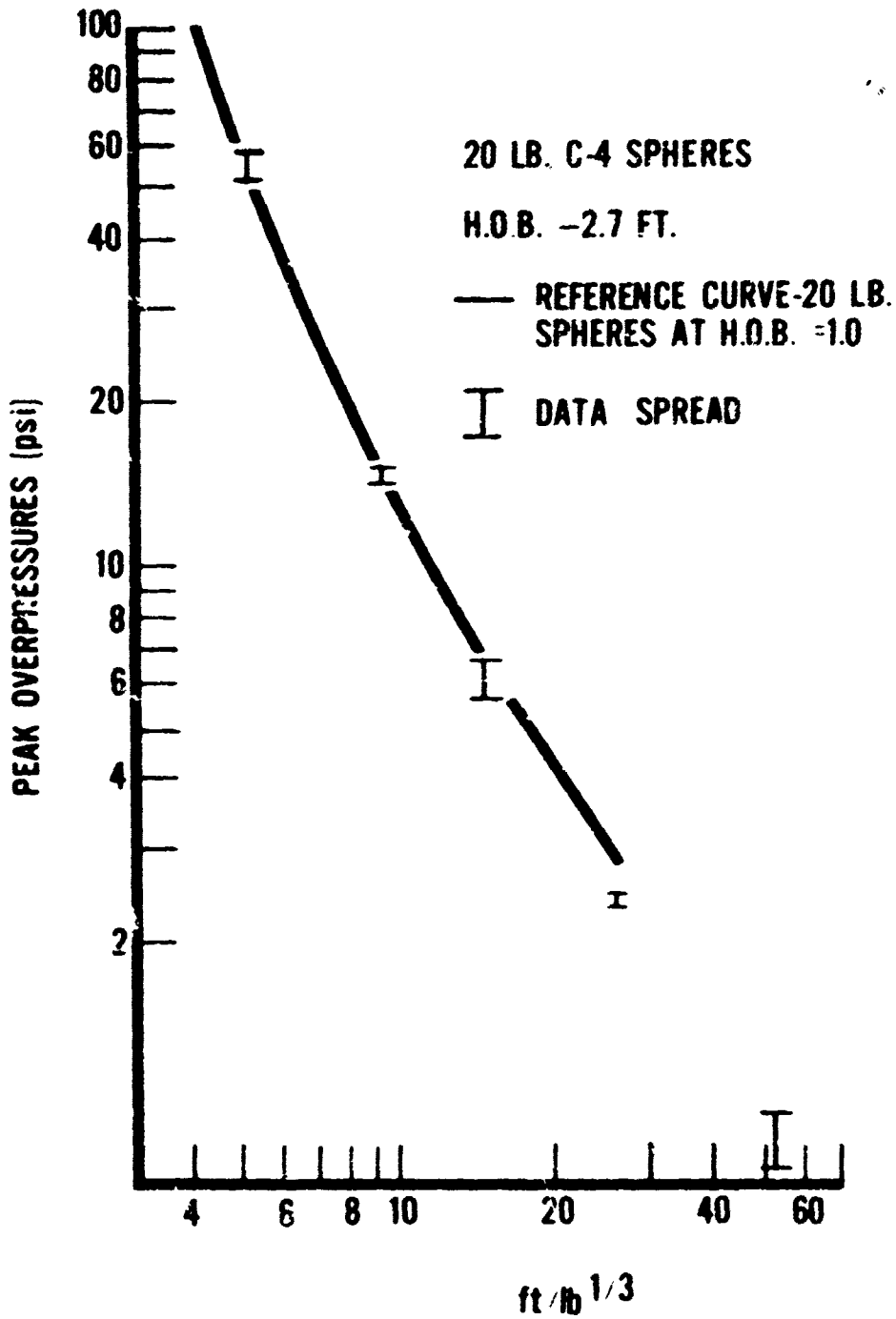
CONCLUSIONS AND RECOMMENDATIONS

A series of tests have been conducted to obtain a preliminary evaluation of the explosive hazards associated with CO/N_2O mixtures. This data is to be used for establishing facility siting criteria for a specific Air Force test facility. The test configurations and initiation energy selected represent the worst case situations which might occur in that system.

Semiconfined and unconfined mixtures of CO and N_2O were tested for explosive effects in the liquid and gaseous states. It was found that semiconfined cryogenic liquid mixtures of LCO and LN_2O, at stoichiometric mixture ratios, are detonable and will produce yields of over 60% of TNT. The detonability of these mixtures was dependent on the energy of the initiating source and the mixture ratio. The energy supplied by two No. 6 blasting caps and a squib appeared to be marginal for initiating a detonation. Once detonation was initiated the thermal and fragmentation hazards associated with the blast were significant.

Liquid - gas and gaseous mixtures of CO, air, and N_2O exhibited only a fire hazard. No detonations were obtained from fuel rich, oxidizer rich or stoichrometric mixtures. The lack of detonation was attributed to three factors: (1) the energy of initiation was not sufficient, (2) localized mixture ratios varied significantly from stoichrometric due to buoyancy effects and the existence of two phases, (3) the size and shape

of the test configurations were not sufficient to allow for the propagation of a detonation wave in CO/N_2O mixtures.

It is recommended that further studies be conducted on a bench scale level to determine detonation and flamability limits for CO/N_2O mixtures. This can then be followed, if application of the propellants is justified, by more estensive large scale testing particularly in the cryogenic liquid state.

BIBLIOGRAPHY

1. Bradley, J.N., Kistiakowsky, G.B., J. Chem Phys, 35, No. 1, Pg 256-263, July 1961.

2. Robinson, C.A., Aviation Week and Space Technology, Pg 42, February 19, 1973.

3. Strehlow, Roger A., "Unconfined Vapor Cloud Explosions - An Overview", Dept of Aeronautics and Astronautics Engineering Report., University of Illinois at Urbana - Champaign.

4. Kirshenbaum, A.D., "Fundamental Studies of New Explosive Reactions for Office of Ordinance Research", OOR Contract No. DA-36-034, ORD-1489, Project TB2-0001 (916), 1956.

5. Mitchell, R.C. et al, "Carbon Monoxide Fueled Gas Generation Reactant Stream Characterization", AFWL Contract No. F29601-71-C-0117, Rocketdyne Report No. 71RC7727, October 1971.

6. Willoighby, A.B., Wilton, C. et al, AFRPL TR-65-144, June 1965.

7. Balarzak, H.J., "Detonable Gas Explosion", General American Transportation Co. Report, Project 1.10, October 1965.

8. Kinney, G.F., "Explosive Shocks in Air", MacMillan Company, NY, 1962.

9. Lewis, B., Von Elbe, G., "Combustion Flames, and Explosions of Gas", Academic Press NY, 1961.

10. Krisjamson, J.O. et al, ARL Report 62-431, September 1962.

AIR-BLAST PRESSURE MEASUREMENT SYSTEMS AND TECHNIQUES

Louis Giglio-Tos, Ballistic Research Laboratories
T. E. Linnenbrink, General American Transportation Corp.

ABSTRACT

This paper details a procedure for specifying and implementing instrument-
ation for the acquisition of air-blast overpressure data. The air-blast
overpressure resulting from the detonation of a high explosive is modeled
as a forcing function in terms of overpressure versus time with charge
weight and ground range. System bandwidth requirements are determined
by system simulation driven by the actual air-blast model. The accuracy
of the peak overpressure presented after data aquisition is derived as
a function of the air-blast model and the frequency response of a first
order system. The derivation is included in its entirety as an appendix.
Curves and tables representing peak overpressure accuracy versus system
bandwidth are presented. A typical system is constructed using the system
response technique developed above to establish bandwidth requirements.
The system is implemented using techniques proven to be effective in the
field. Both static and dynamic calibration techniques are discussed.
Test site selection and transducer installation are presented as essentials
to obtaining the expected results. Finally data reduction and analysis
are discussed.

I. INTRODUCTION

The primary concern in a data acquisition system is maintaining
data accuracy over all operational and environmental conditions. The
purpose of this paper is to present a method of selecting an appropriate
data acquisition system.

Preceding page blank 1379

II. APPROACH

2.1 Forcing Function Definition

In order to assemble a system capable of recording the required information with high fidelity, the measurand must be defined. Figure 2.1 shows an idealized representation of an overpressure-time history from a detonation. Four (4) parameters which characterize the shock wave are shown. These parameters should be recorded as the shock wave traverses the instrument stations at selected locations. These parameters are:

(a) Time of Air-blast Shock Arrival (milliseconds, msec). This is the time interval between the electrical pulse used to detonate the charge and the shock front arrival at the point of measurement.

(b) Peak and/or Maximum Overpressure (pounds per square inch, psi). If the overpressure wave form has more than one peak, then the peak overpressure is the height of the first peak, while the maximum overpressure is the highest overpressure measured.

(c) Positive Phase Duration (msec). This is the time interval from shock arrival to where the overpressure has returned to ambient pressure.

(d) Positive Phase Impulse (psi-msec). Impulse is the integral with respect to time of overpressure from the time of shock arrival to the end of the positive phase.

The negative phase has a negative pressure, duration, and impulse. ese parameters may require consideration as part of the experiment design.
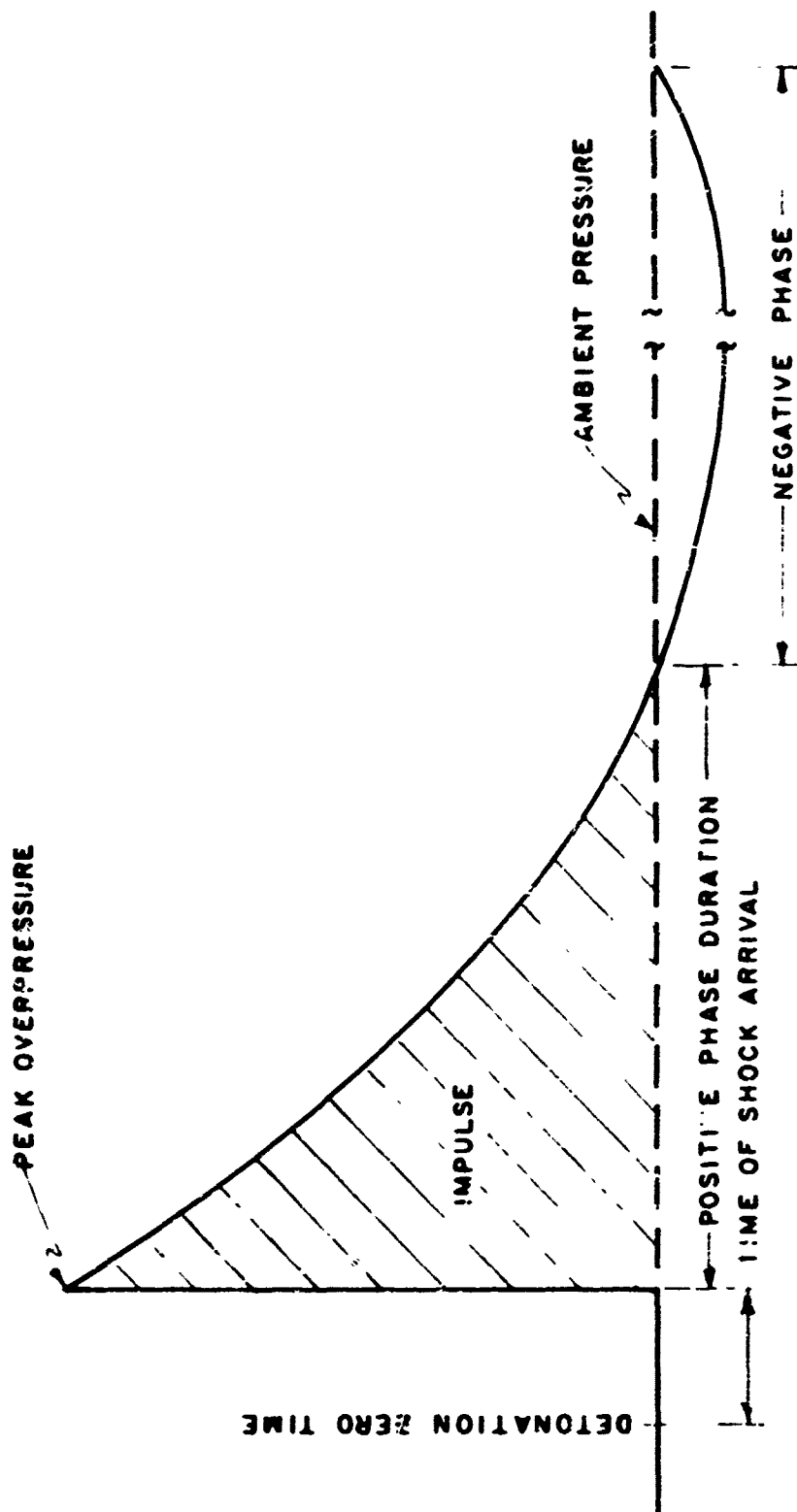
Figure 2.1 Ideal Overpressure vs. Time History

2.2 System Capability

The first consideration in the selection of a data acquisition system is that it be capable of faithfully measuring and recording the desired data. The primary consideration is the total system response to the leading edge (rise time) of the shock wave. Tracking of this leading edge with instrumentation can be difficult. Knowing that recording systems have response limitations, the problem then becomes one of determining a relationship between the actual and recorded parameters of interest. In selecting a data acquisition system, the frequency response must be considered the most important factor. By examining Figure 2.2, it is readily apparent that if the positive phase duration is short and the system frequency response is low, a large percentage of the peak over-pressure and impulse will be lost

There are other considerations which should not be overlooked in the interest of a successful test. These are: (a) equipment reliability, (b) system preparation. The requirement for equipment reliability is increased due to the nature of the testing. If we are dealing with a one-shot event that is very expensive and requires a long preparation period reliability and careful system preparation is a must. These will be discussed further in Section III.

2.3 Bandwidth Requirement by System Simulation

A computer program was written and checked using equations developed at the Ballistic Research Laboratories to describe the overpressure time-history from hemispherical TNT and nuclear explosions. The program is developed in Appendix A. The program determines the recording system bandwidth necessary to acquire data of predetermined accuracy as a
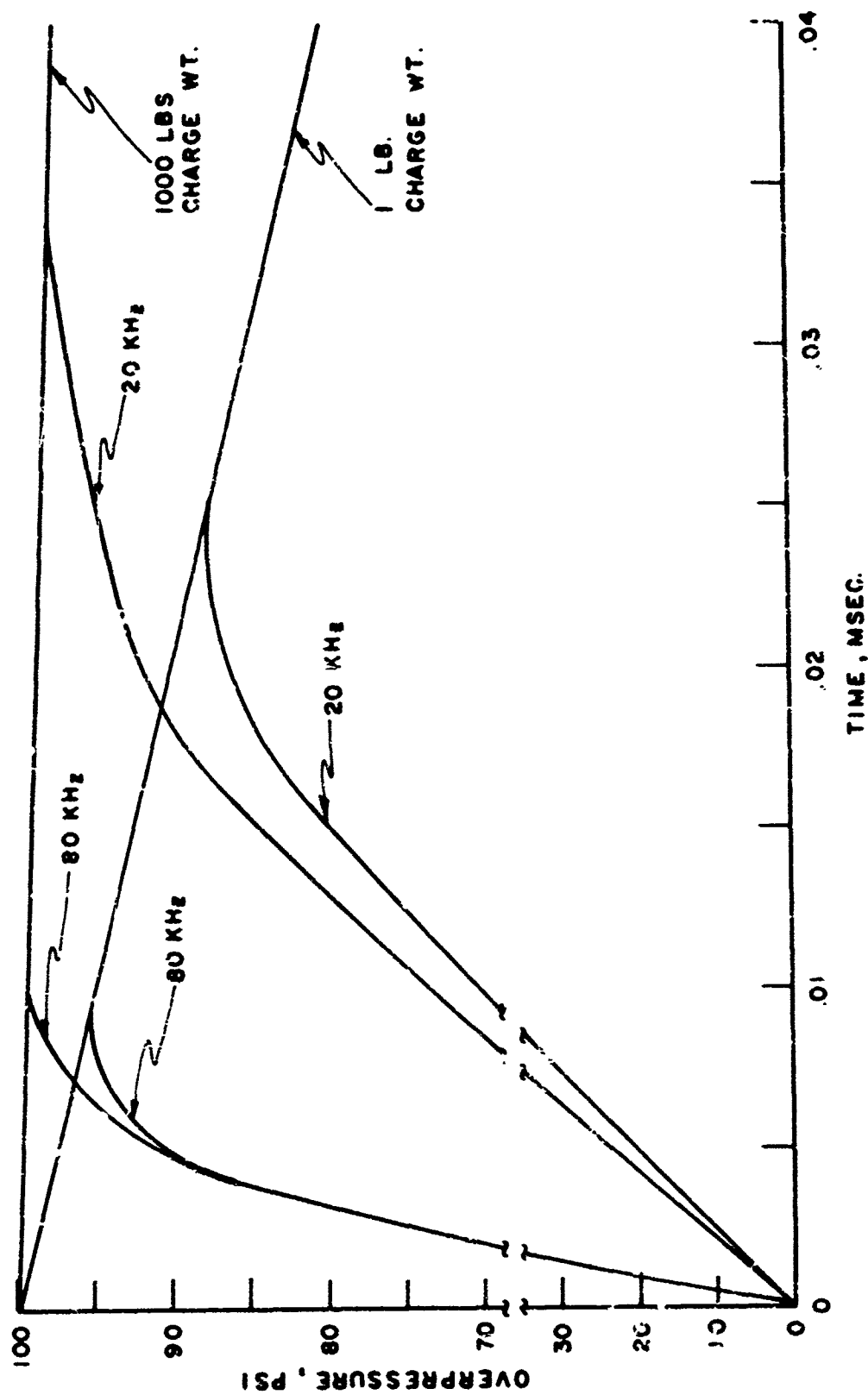
Figure 2.2 Ideal Overpressure vs. Time Compared to 20 and 80 KHz System Response vs. Time

function of charge weight and peak overpressure. The program has been
used to determine minimum system bandwidth required to yield selected
data accuracies ranging from 75% to 99% in the 1 psi to 1000 psi
incident overpressure range for a one pound hemispherical charge of TNT.

The results are tabulated in Table I and plotted in Figure 2.3.
These results directly relate error in peak overpressure, system band-
width, and peak overpressure for a 1 lb. charge. The graph and/or table
may be used with charge weights larger than 1 lb. An example is given
as follows:

There is a need to measure 10 psi overpressure produced by a 10,000
lbs. charge weight to a peak pressure accuracy of 99%. By using the
graph (Fig. 2.3) or Table 1 the required system bandwidth for a 1 lb.
charge to achieve 99% of peak for 10 psi is 112,000 Hertz. By employing
the following formula:

$$\text{bandwidth required } (BW_R) = \frac{\text{Bandwidth required for 1 lb. charge at stated incident overpressure and at the stated accuracy}}{\sqrt[3]{\text{Charge weight required}(CW_R)}}$$

$$BW_R = \frac{BW_R \; 1 \; lb.}{\sqrt[3]{CW_R}} = \frac{112,000}{\sqrt[3]{10000}} = \frac{112,000}{21.54} = 5200 \; \text{Hertz}$$

This indicates that a system with a minimum bandwidth of 5200 hertz
would be required to make the above stated measurement.

Table 2 and Figure 2.4 show how the required system frequency response
is reduced for incident overpressure measurements from 1 to 1000 psi with
charge weights of 1, 125, and 1,000 lbs. Secondly, it also shows that
bandwidth scales with the cube root of the charge weight.
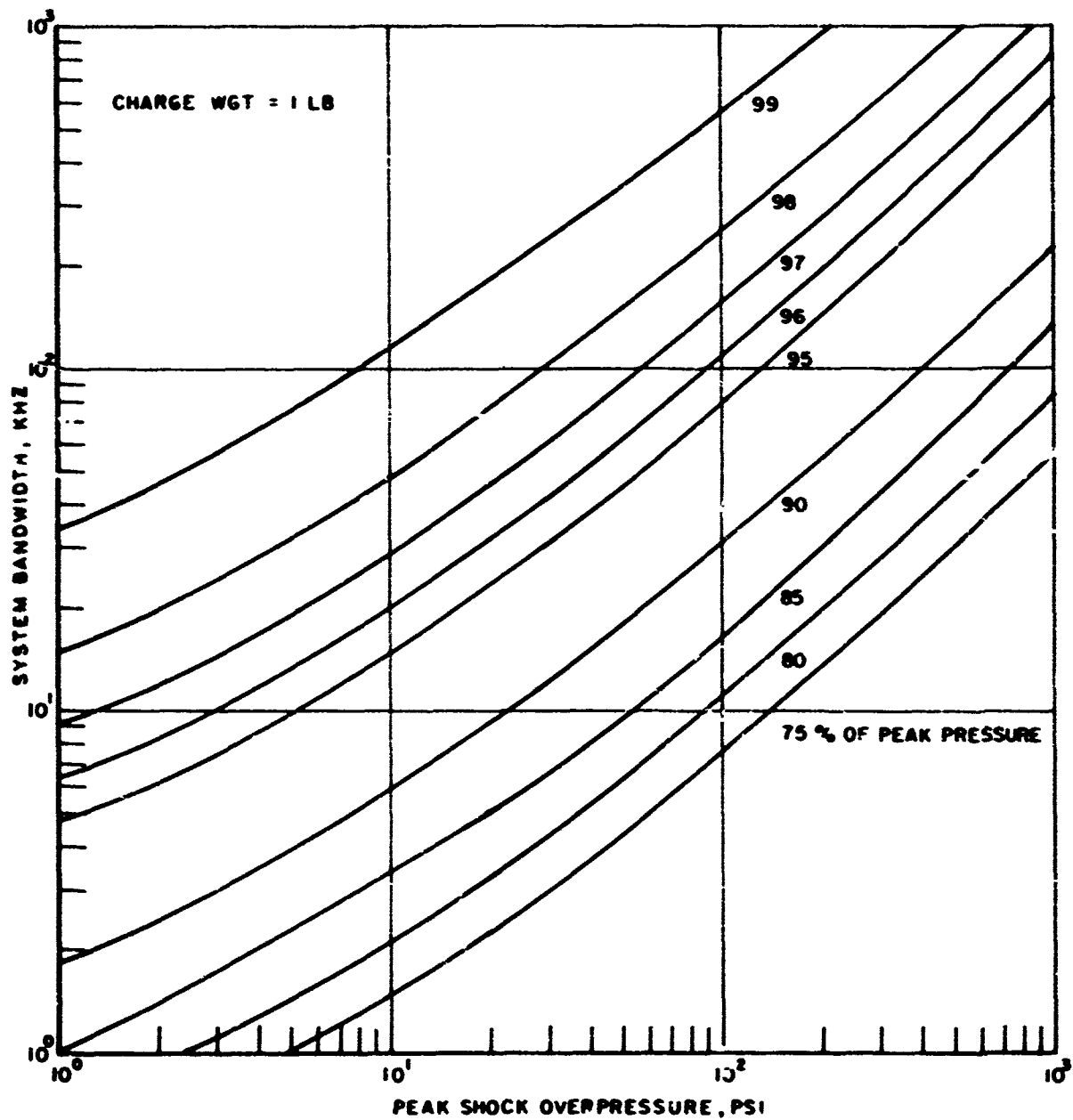
Figure 2.3 System Bandwidth vs. Various Peak Overpressure Accuracy

Charge Weight (lbs):1
Percent of Peak (0 to 1):.99

Peak Pressure (psig)	Ground Range (feet)	Time to Percent Peak (msec)	System Time Constant (msec)	Min System Bandwidth (hertz)
1	45.53	0.0301	0.0047	34288
2	25.61	0.0220	0.0034	45861
5	14.39	0.0137	0.0021	75221
10	9.80	0.0092	0.0014	112642
20	6.98	0.0059	0.0009	175429
50	4.62	0.0031	0.0005	354783
100	3.41	0.0018	0.0003	571367
200	2.50	0.0010	0.0002	1014454
500	1.60	0.0005	0.0001	2301700
1000	1.09	0.0002	0.0000	4477985

Charge Weight (lbs):1
Percent of Peak (0 to 1):.98

Peak Pressure (psig)	Ground Range (feet)	Time to Percent Peak (msec)	System Time Constant (msec)	Min System Bandwidth (hertz)
1	45.53	0.0605	0.0107	14889
2	26.61	0.0442	0.0078	20347
5	14.39	0.0276	0.0049	32659
10	9.80	0.0184	0.0033	48905
20	6.98	0.0118	0.0021	76176
50	4.62	0.0062	0.0011	145368
100	3.41	0.0036	0.0007	248103
200	2.50	0.0021	0.0004	440462
500	1.60	0.0009	0.0002	999414
1000	1.09	0.0005	0.0001	1944238

Charge Weight (lbs):1
Percent of Peak (0 to 1):.97

Peak Pressure (psig)	Ground Range (feet)	Time to Percent Peak (msec)	System Time Constant (msec)	Min System Bandwidth (hertz)
1	45.53	0.0911	0.0177	9018
2	26.61	0.0667	0.0129	12323
5	14.39	0.0416	0.0081	19780
10	9.80	0.0278	0.0054	29618
20	6.98	0.0178	0.0035	46135
50	4.62	0.0093	0.0018	88043
100	3.41	0.0055	0.0011	150262
200	2.50	0.0031	0.0006	266784
500	1.60	0.0014	0.0003	605267
1000	1.09	0.0007	0.0001	1177588

Table I. System Bandwidth Requirements for a 1 Pound Hemispherical Charge Weight

Charge Weight (lbs):1
Percent of Peak (0 to 1):.96

Peak Pressure (psig)	Ground Range (feet)	Time to Percent Peak (msec)	System Time Constant (msec)	Min System Bandwidth (hertz)
1	45.53	0.1221	0.0254	6268
2	26.61	0.0894	0.0186	8565
5	14.39	0.0557	0.0116	13749
10	9.80	0.0372	0.0077	20588
20	6.98	0.0239	0.0050	32067
50	4.62	0.0125	0.0026	61195
100	3.41	0.0073	0.0015	104446
200	2.50	0.0041	0.0009	185436
500	1.60	0.0018	0.0004	420726
1000	1.09	0.0009	0.0002	818534

Charge Weight (lbs):1
Percent of Peak (0 to 1):.95

Peak Pressure (psig)	Ground Range (feet)	Time to Percent Peak (msec)	System Time Constant (msec)	Min System Bandwidth (hertz)
1	45.53	0.1535	0.0339	4701
2	26.61	0.1123	0.0248	6424
5	14.39	0.0700	0.0154	10312
10	9.80	0.0467	0.0103	15441
20	6.98	0.0300	0.0066	24050
50	4.62	0.0157	0.0035	45896
100	3.41	0.0092	0.0020	78334
200	2.50	0.0052	0.0012	139072
500	1.60	0.0023	0.0005	315545
1000	1.09	0.0012	0.0003	613861

Charge Weight (lbs):1
Percent of Peak (0 to 1):.90

Peak Pressure (psig)	Ground Range (feet)	Time to Percent Peak (msec)	System Time Constant (msec)	Min System Bandwidth (hertz)
1	45.53	0.3152	0.0864	1843
2	26.61	0.2307	0.0632	2519
5	14.39	0.1437	0.0394	4043
10	9.80	0.0960	0.0263	6054
20	6.98	0.0616	0.0169	9430
50	4.62	0.0323	0.0089	17995
100	3.41	0.0189	0.0052	30714
200	2.50	0.0107	0.0029	54529
500	1.60	0.0047	0.0013	123718
1000	1.09	0.0024	0.0007	240692

Table I. Continued

Charge Weight (lbs):1
Percent of Peak (0 to 1):.85

Peak Pressure (psig)	Ground Range (feet)	Time to Percent Peak (msec)	System Time Constant (msec)	Min System Bandwidth (hertz)
1	45.53	0.4862	0.1561	1020
2	26.61	0.3558	0.1142	1394
5	14.39	0.2217	0.0711	2237
10	9.80	0.1480	0.0475	3350
20	6.98	0.0951	0.0305	5218
50	4.62	0.0498	0.0160	9958
100	3.41	0.0292	0.0094	16996
200	2.50	0.0164	0.0053	33174
500	1.60	0.0073	0.0023	68462
1000	1.09	0.0037	0.0012	133188

Charge Weight (lbs):1
Percent of Peak (0 to 1):.80

Peak Pressure (psig)	Ground Range (feet)	Time to Percent Peak (msec)	System Time Constant (msec)	Min System Bandwidth (hertz)
1	45.53	0.6676	0.2449	650
2	26.61	0.4886	0.1792	888
5	14.39	0.3044	0.1117	1425
10	9.80	0.2033	0.0746	2134
20	6.98	0.1305	0.0479	3325
50	4.62	0.0684	0.0251	6344
100	3.41	0.0401	0.0147	10829
200	2.50	0.0226	0.0083	19225
500	1.60	0.0100	0.0037	43618
1000	1.09	0.0051	0.0019	84857

Charge Weight (lbs):1
Percent of Peak (0 to 1):.75

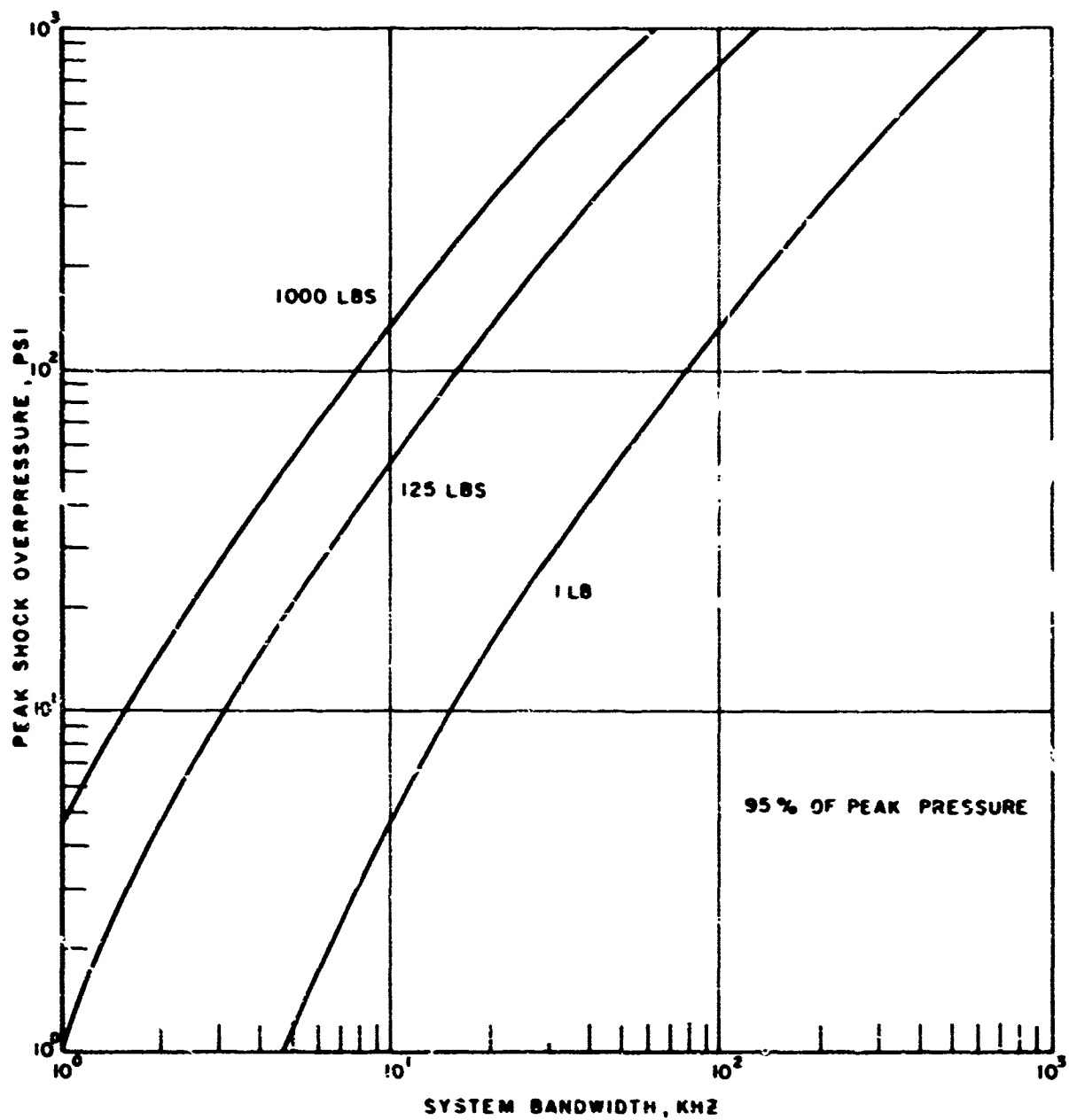| Peak Pressure (psig)	Ground Range (feet)	Time to Percent Peak (msec)	System Time Constant (msec)	Min System Bandwidth (hertz)
1	45.53	0.8607	0.3563	447
2	26.61	0.6299	0.2608	610
5	14.39	0.3924	0.1625	980
10	9.80	0.2621	0.1085	1467
20	6.98	0.1683	0.0697	2285
50	4.62	0.0882	0.0365	4361
100	3.41	0.0517	0.0214	7461
200	2.50	0.0291	0.0121	13214
500	1.60	0.0128	0.0053	29980
1000	1.09	0.0066	0.0027	58323

Table I. Continued

Figure 2.4 Influence of Charge Weight on System Bandwidth Requirement

Charge Weight (lbs):1
Percent of Peak (0 to 1):.95

Peak Pressure (psig)	Ground Range (feet)	Time to Percent Peak (msec)	System Time Constant (msec)	Min System Bandwidth (hertz)
1	45.53	0.1535	0.0339	4701
2	26.61	0.1123	0.0248	6424
5	14.39	0.0700	0.0154	10312
10	9.80	0.0467	0.0103	15441
20	6.98	0.0300	0.0066	24050
50	4.62	0.0157	0.0035	45896
100	3.41	0.0092	0.0020	78334
200	2.50	0.0052	0.0012	139072
500	1.61	0.0023	0.0005	315545
1000	1.09	0.0012	0.0003	613861

Charge Weight (lbs):125
Percent of Peak (o to 1):.95

Peak Pressure (psig)	Ground Range (feet)	Time to Percent Peak (msec)	System Time Constant (msec)	Min System Bandwidth (hertz)
1	227.63	0.7673	0.1693	940
2	133.03	0.5615	0.1239	1283
5	71.93	0.3498	0.0772	2063
10	48.99	0.2336	0.0515	3088
20	34.91	0.1500	0.0331	4810
50	23.11	0.0786	0.0173	9179
100	17.06	0.0461	0.0102	15662
200	12.50	0.0259	0.0057	27815
500	8.00	0.0114	0.0025	63108
1900	5.44	0.0059	0.0013	122773

Charge Weight (lbs):1000
Percent of Peak (0 to 1):.95

Peak Pressure (psig)	Ground Range (feet)	Time to Percent Peak (msec)	System Time Constant (msec)	Min System Bandwidth (hertz)
1	455.26	1.5346	0.3386	470
2	266.06	1.1230	0.2478	642
5	143.86	0.6996	0.1544	1031
10	97.99	0.4672	0.1031	1544
20	69.82	0.3000	0.0662	2405
50	46.23	0.1572	0.0347	4590
100	34.12	0.0921	0.0203	7834
200	25.00	0.0519	0.0115	13908
500	16.00	0.0229	0.0051	31554
1000	10.87	0.0118	0.0026	61387

Table II. System Bandwidth Requirement for Various Charge Weights

III. SYSTEMS AND TECHNIQUES

3.1 Acquisition Systems

The previous discussion of the function to be measured has established a number of requirements for the system. Figure 3.1 is a block diagram of the system that has been developed at the Ballistic Research Laboratories (BRL). The system consists of six (6) basic components: (1) the transducer, (2) the signal conditioning equipment, (3) data amplifiers, (4) FM or direct record amplifiers, (5) magnetic tape deck, and (6) a multiplexing unit.

Air blast transducers may be classed as mechanical or electronic. The BRL mechanical self-recording gages are limited in useage by their frequency response of 1000 Hertz. The electronic transducers may be divided into two types: (a) self-generating, (b) AC or DC driven. The piezoelectrics are of the self-generating type and are excellent for high frequency response above 100 KHz and up to 4,000 KHz. AC coupling is used on all piezoelectric transducers to avoid the effects of DC shift and base line temperature drift. A judicious choice of coupling circuit time constant must be made which balances the temperature drift cancellation against the necessity of recording accurately the positive phase duration. This time constant is often 20 times the positive phase duration. The AC or DC driven type have a lower frequency response (below 100 KHz) depending on pressure range. The unbonded strain gages and variable reluctance gages usually have frequency response below 10 KHz.

It must be remembered that the transducer is the weakest link in the data aquisition chain. This is because little protection may be added to the transducer without affecting its dynamic characteristics. The detonation produces deleterious effects such as heat and debris (this is a function of
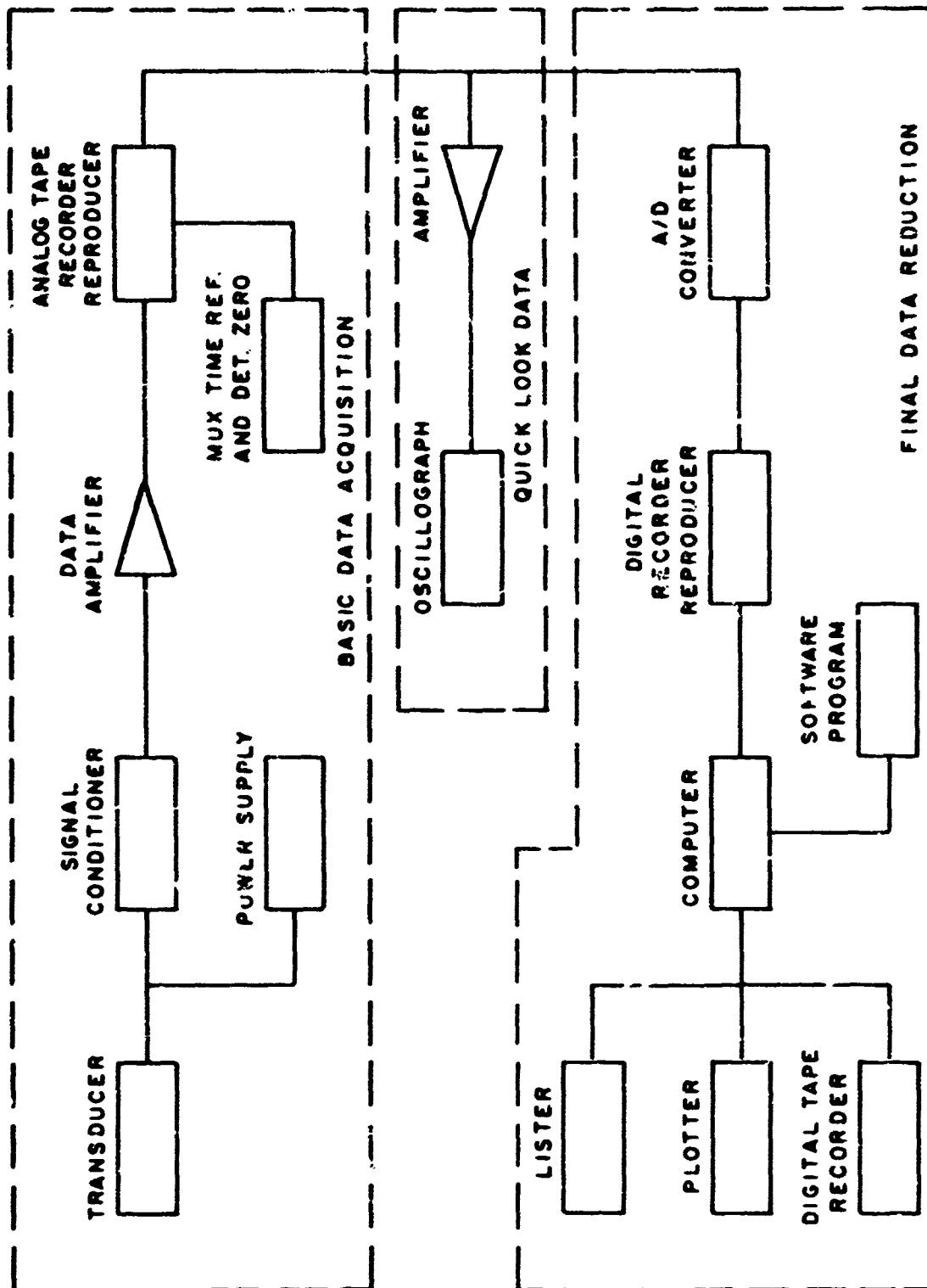
Figure 3.1 Data Acquisition/Reduction System

experimental set-up), which at times precedes the air blast wave which may also carry debris. Thus in trying to select the correct transducer for a given measurement application consideration must be given to balancing transducer characteristics against test conditions and type of information required.

Different kinds of signal conditioning are required for each of the transducer types. The strain gages transducers are operated with standard strain gage signal conditioning equipment. This equipment incorporates a constant voltage and/or constant current power supply and provisions for bridge balancing, shunt calibration, and most of the transducer functions. The equipment used in conjunction with the variable inductance or eddy current loss transducers consists of an oscillator drive and a demodulator with provisions for zero balance, phase shift adjust and electrical calibration.

The self-generating piezoelectric transducers usually drive a charge amplifier located near the recorder or an impedance converter (source follower) located near the transducer. Either device presents a high impedance load to the transducer. The charge amplifier is not required to have provision for the electrical calibration, where the source follower requires special circuity to provide the electrical calibration step.

The data amplifiers used are high gain, differential input, DC type amplifiers. These amplifiers are used to increase the transducer signal level to that required by the FM record amplifier.

The magnetic tape transport includes three basic components. The record (FM and/or direct) amplifiers or reproduce electronics. The FM mode has a DC-80KHz response and are wide band + 40% deviation, the direct record mode has a bandwidth from .4-700KHz at 120 ips. The electromagnetic head records data on, and recovers data from the magnetic tape. The tape transport moves the tape across the magnetic head smoothly and at a constant speed.

The multiplexing unit is used to record a reference timing signal as the data is being recorded. The timing reference is usually five (5) times to FM frequency response.

Other recording systems have been assembled and successfully used at BRL. A complete mechanical transducer of the self-recording type developed at BRL has a corrugated diaphragm which scratch records on a moving metal tape. This type of system by its inherent design is limited in usage to long duration (longer than 20msec) at low pressures because of their low frequency response of DC-1000 hertz or less. A record system used to measure low pressure and long duration consisted of a variable reluctance transducer and its signal conditioning unit having its output recorded on a pen recorder with DC-100 hertz response, or to a magnetic tape recorder with a DC-500 hertz response.

When the requirement exists to measure very high overpressures, or overpressures from small charge weights a high performance system may be assembled by incoporating a piezoelectric transducer with a tourmalive element, a source follower for signal conditioning, and feeding its output into a digital recorder, this type of system is capable of frequen response of DC-400 KHz.

1374

3.2 Calibration Procedure

Calibration of the selected data acquisition system should be accomplished in two phases. Phase 1 is the laboratory calibration and acceptance of the transducer and electronics. Phase II is the total system calibration in the field.

Phase I of the calibration procedure is accomplished when a transducer is received from the manufacturer or when it is to be re-used. The transducer is statically calibrated by applying the expected physical forcing function over its rated range to determine its sensitivity, non-linearity, hysterisis, and repeatability. Acceptable transducers are then exposed in a shock tube to determine its dynamic characteristics and to verify its ability to measure a shock-wave over-pressure based on the static calibration. See figure 3.2. If the transducer can reproduce a known shock wave profile then it should be tested to determine its resistance to other deleterious effects such as acceleration and themal levels expected during a test. Independent of the transducer calibration, the recording system has to be checked and corrected for any electrical and/or electronic deficiencies.

Phase II of the calibration procedure is the field static and dynamic calibration of the total system (see Figure 3.3). The transducer is installed int its field mount, and connected by signal cable to the recording system. The predicted forcing function is then applied statically (for d-c coupled transducers) and semi-dynamically (for a-c coupled transducers). The various amplifier and VCO gains are adjusted to the correct recording levels. At this point, an electrical calibration level (ECl) equal to the 100% forcing function is established. This electrical calibration step is also recorded on magnetic tape prior to each shot as a reference

Figure 3.2 Laboratory Calibration

120 %
100 %
80 %
60 %
40 %
20 %
0 %

STATIC CALIBRATION

100 %

0 %

QUASI-DYNAMIC CALIBRATION

SHOCK TUBE DYNAMIC CALIBRATION
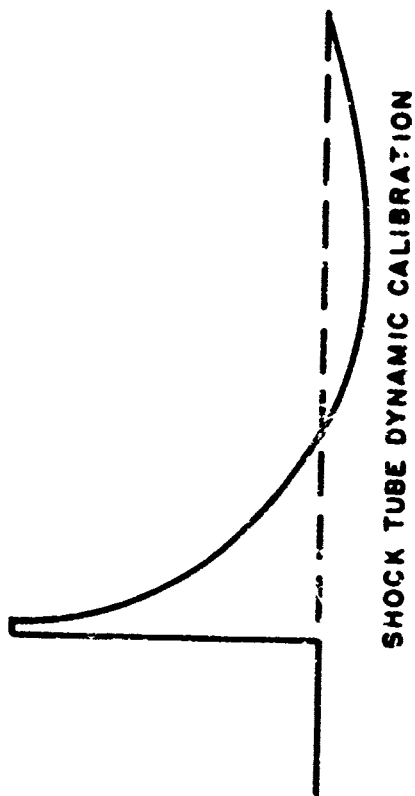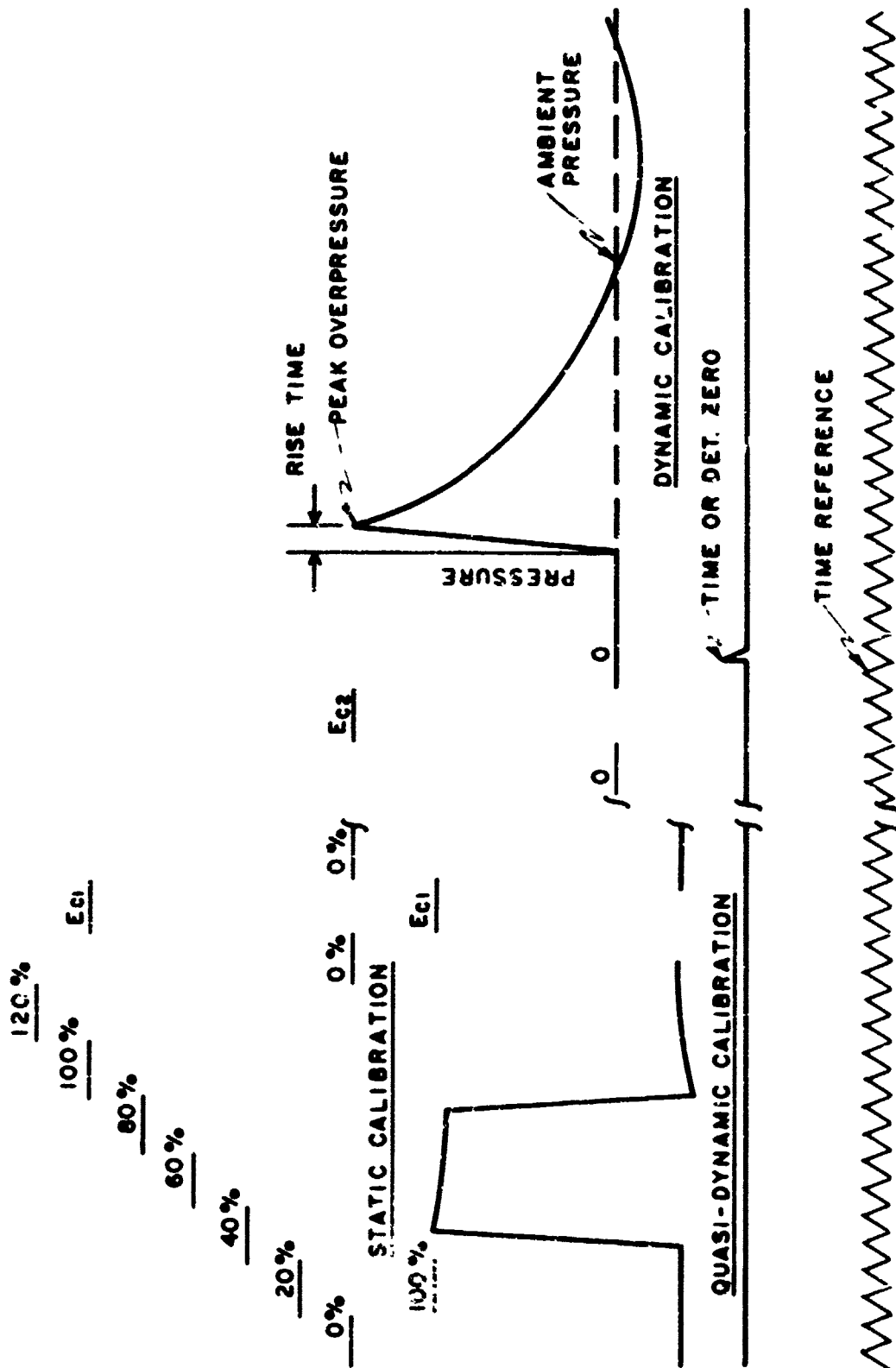
Figure 3.3 Field Calibration

which represents the 100% predicted forcing function. Within seconds
of actual data acquisition, the 100% level electrical calibration is
repeated (EC2). This serves to check the overall system gain change
between field static and quasi-static calibration and event time.
The field dynamic calibration is done to check for anomelies in the
recording system or field test set-up. To best accomplish this, one
should determine the base charge weight required to produce the same
blast overpressures as expected of the test item. By employing this
determined charge weight of a well known explosive (Pentolite preferred
because of its repeatability) of either spherical or hemispherical shape
the blast output is well known and recorded data should check well with
predictions. For large scale tests or where the charge yield is not
known, then the transducer stations should be calibrated individually
using 8 lb charge weights positioned at predetermined distances.

3.3 Site Selection and Installation of Transducers

Considerations in test site selection include the following:

a) Test area should be as flat as possible.

b) Test area should be as free as possible from gravel and
debris which could be picked up and hurled at transducers.

c) Test area should be free of obstruction from trees, hills
and buildings that might cause reflections or perturbations
of the shock wave.

d) The size of the required cleared area will depend on charge
weight and the overpressure level to be measured.

The field layout and transducer mounting require that certain guide
lines be followed. If gauges are mounted above the surface then the

support should be rigid so that it will not move when the blast wave traverses the measuring point. Secondly a baffle should be employed. the baffle may consist of 1/2-inch thick aluminum disc 18 inches in diameter, with the gauge mounted flush in the center of the disk. The baffle allows the blast wave to develop laminar flow past the inlet part of the gauge. One must remember to orient the face of the disk parallel to the shock wave propagation. Large errors in data may occur otherwise. A clear flat area about 2 feet in diameter should also be maintained when transducers are installed flush with the ground. The ground mounts should be large and heavy to minimize movement during the passage of the shock wave. Appropriate cable should be used to transmit the signal from gauge to recording system. Cable should be buried at least one foot below ground for protection against:

a) Rodents

b) Vehicles and pedestrian traffic

c) Fragmentation and other debris

3.4 Data Reduction & Analysis

Data reduction may be accomplished either manually or automatically. Generally, field data is read by hand and is used for quick analysis and reporting. Where equipment is available, in particular, back at home base, final data reduction is accomplished automatically with an analog to digital converter, computer, printer and plotter.

The calibration and data tapes are converted to digital form and stored on magnetic tape for computer usage. The overpressure time history is converter automatically with the digitizer triggered by

the detonation-zero time pulse. Time is then accumulated from this point for the purpose of determining the following parameters:

a) Time of shock arrival

b) Peak and/or maximum overpressure

c) Positive phase duration

c) Positive phase overpressure impulse

The digital information is then converted to engineering units using the computer. The data output is then available in three forms for further analysis:

a) Tabular listings

b) Overpressure time history plots

c) Digital magnetic tape

The magnetic tape output may be used for data input to any of the various smoothing or filtering routines that might be desired.

3.5 Typical Data

A well designed data acquisition system should yield data similar to the typical record shown in Figure 3.4. This particular record was acquired at Ballistic Research Laboratories (BRL). The air blast was generated by an 8.43 lb. sphere of Pentolite in free air at a height of 12 feet above ground. The piezoelectric transducer was mounted 6.5 feet from ground zero in the side-on, incident configuration. The data was recorded on an 80KHz FM magnetic tape recorder and later digitized to 11 bits+precision prior to computer processing. The record shown is a computer plot of the data as digitized.
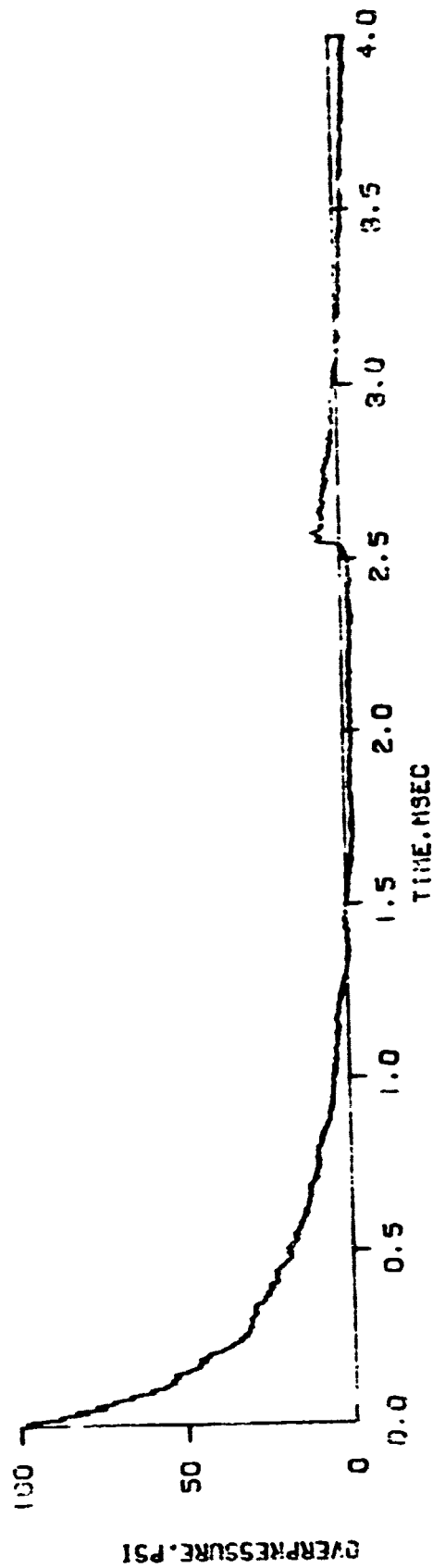
Pentolite-8.43 lbs.
Distance--6.5 feet
HOB--12 feet

Figure 3.4 Typical Record

The percentage of peak loss curves based on an idealized recording system, indicates that an 80KHz bandwidth system would yield data, for a 1 lb charge at the 100 psi overpressure with a less of 5%. Now since these curves scale as the cube root of the charge weight, $w^{1/3}$, we can then consider our recording system as having a bandwidth of 160KHz for the actual eight pound charge used for the record (Figure 3.4). Therefore, the error expected will be less than 3% due to the system response.

IV. SUMMARY

To acquire reliable data at minimum cost, it is necessary to first establish the purpose of the measurements, the parameters to be measured, and the minimum accuracy required. The data acquisition system must have predictable and demonstratable performance. The system must be highly dependable, easy to operate and repair. and as inexpensive as permitted by other requirements. When data must be acquired on the first and only attempt (e.g., large-scale events), the techniques and procedures described in this paper are especially vital to the success of the project.

APPENDIX A

DATA ACCURACY AS DETERMINED BY SYSTEM SIMULATION

The degree to which peak pressure and impulse data represent actual peak pressure and actual impulse is a function of the data acquisition/ reduction system used. The relationship of acquisition systems to error has been the subject of considerable study over the past years. As a result, standard procedures have evolved for determining acquisition system requirements in terms of sensitivity, response, bandwidth, etc.

With regard to air blast data, the most difficult problem lies in system response to the leading edge of the shock wave. Briefly, the pressure level rises so fast in time (1 - 10ns) that none of the standard instrumentation available today can reliably track it. Given that the acquisition system will not actually track the blast wave, the question then becomes one of the relationship between actual and indicated parameters of interest. Foremost of these parameters are peak pressure and positive overpressure impulse.

The approach taken to establishing a relationship between actual phenomena and apparent phenomena (i.e. data) involves mathematical models for both the actual phenomena and the acquisition system. While one blast wave model was used throughout, two distinct types of system model are discussed. The overpressure model was implemented and the resulting data included. While, it was not within the scope of this program to implement the positive overpressure impulse model, it is briefly discussed.

1384

1.1 Air Blast Over Pressure Model

The model used throughout this work is one developed by C. N. Kingery[1] of the BRL based on high explosive data from a wide range of yields. After extensive study of actual blast data, he determined that positive phase overpressure versus time could be accurately modeled in two segments as shown in Figure 1. The first segment is an exponential decay of pressure with time from the peak pressure, PM, to some arbitrary pressure PC which occurs at time TC. The second segment is a logarithmic decay from PC to zero pressure, occurring at time TD. Mr. Kingery's work relates all the secondary parameters (PC, TC and TD) to PM, the scaled peak overpressure. Another model developed by C. N. Kingery and B. F. Pannill[2] relating peak overpressure to scaled distance was also used. Both models were developed for high explosive, hemispherical charges on the earth's surface. Appendixces B and C contains the actual equations used.

1.2 Peak Pressure Modeling

The peak pressure model was developed first because the simplification possible led to a less complex, easier to implement model. Both the blast wave and the system were modeled in the simplest possible terms.

Since our range of interest is roughly 90% to 99% accuracy, it can be shown that the system peak (i.e. data peak) will be almost entirely a function of the first segment of the pressure model, the initial exponential decay from PM to the crossover pressure PC. Therefore, it is sufficient for this model to use just the first term,
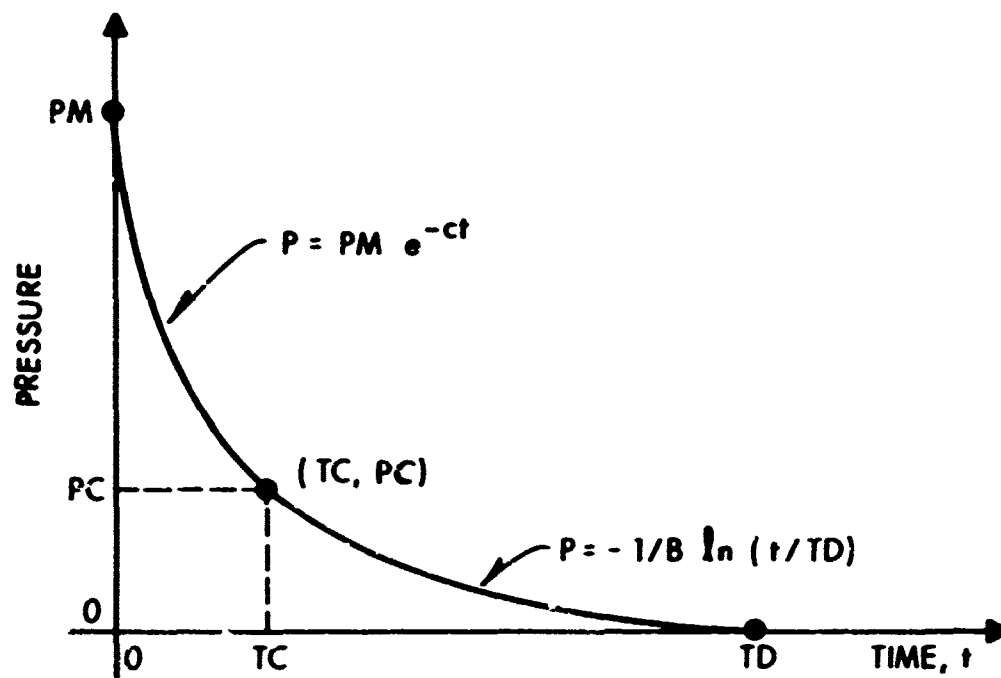
Figure 1 Air Blast Overpressure Model

1386

$$P(t) = PM e^{-ct}, \quad 0 \leq t < TC \tag{1}$$

The La Place transform of the model,

$$X(s) = PM \left(\frac{s}{s + c} \right) \tag{2}$$

is activated by a step of height PM at $t = 0$.

After considerable deliberation on what kind of system model to use, an idealized, Type 0 system was chosen. One may note that the system is free of complex poles which produce the overshoot and resonance sometimes seen in actual data. However on this first model, an overly complex model may lead to more confusion that insight. At sometime in the future when this model and its implication have become familiar, a more complex model may be appropriate. Both the frequency domain response,

$$C(s) = \frac{1/t_c}{s + 1/t_c} \, X(s) \tag{3}$$

and the time domain response,

$$c(t) = (1 - e^{-t/t_c}) \, x(t) \tag{4}$$

are shown in Figure 2, where t_c is the system time constant. For the sake of clarity, in the following expressions, b will replace $1/t_c$. Then the system time constant is $1/b$.

When the pressure model and acquisition system model are combined, the result is a total system model capable of producing data output in
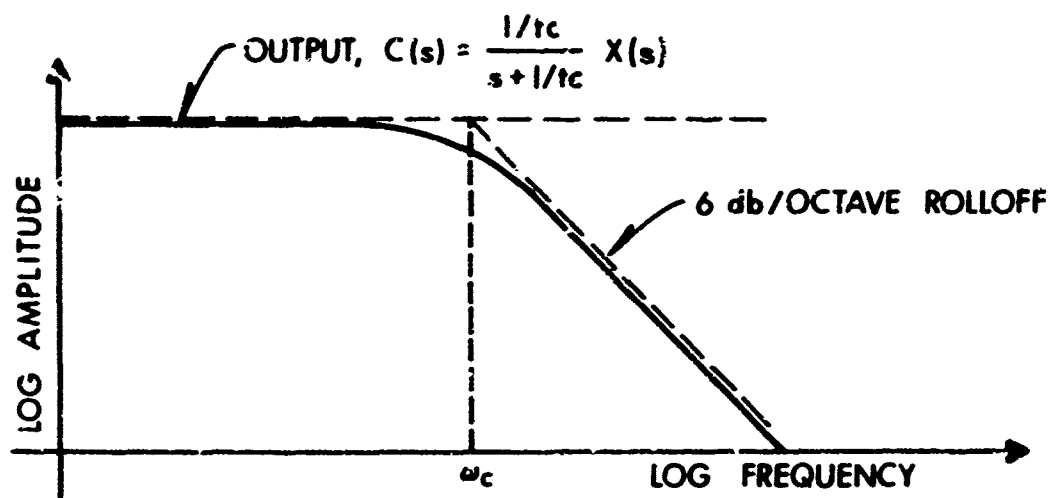
A) FREQUENCY DOMAIN
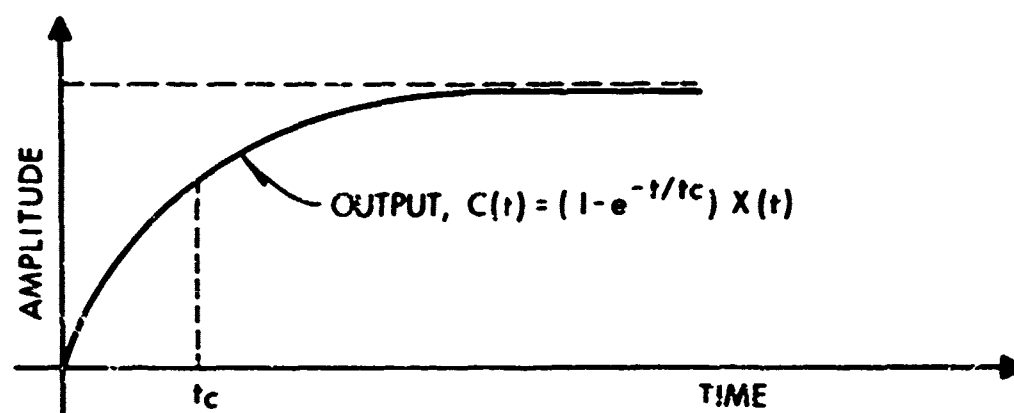
B) TIME DOMAIN RESPONSE TO UNIT STEP

Figure 2. Simple Acquisition System Model

response to a step of height PM. This system is shown in Figure 3. The system itself is described by

$$C(s) = (\frac{s}{s + c})\ (\frac{b}{s + b})\ R(s) \qquad (5)$$

when the appropriate input, $\frac{PM}{s}$, is substituted for R(s), the output, C(s) becomes,

$$C(s) = \frac{b}{(s + c)\ (s + b)}\ PM. \qquad (6)$$

Taking the inverse LaPlace yields the time domain solution,

$$c(t) = (\frac{b}{b - c})\ (e^{-ct} - e^{-bt})\ PM \qquad (7)$$

Now to determine the peak of the output, which is the indicated or data peak pressure, the first derivative of c(t) is taken, yielding

$$\frac{dc(t)}{dt} = (\frac{b}{b - c})\ (-ce^{-ct} + be^{-bt})\ PM \qquad (8)$$

This is then set to zero to determine the time at which the peak occurs, t_p, where,

$$t_p = \frac{1}{b - c}\ \ln(\frac{b}{c}) \qquad (9)$$

The maximum output, $c(t)_{max}$, will then occur at t_p. This output is to be some percentage of the maximum pressure, PM. Then,

$$C(t_p) = \%\ PM = (\frac{b}{b - c})(e^{-ct_p} - e^{-bt_p})\ PM \qquad (10)$$

or,

$$\% = (\frac{b}{b - c})\ (e^{-ct_p} - e^{-bt_p}) \qquad (11)$$

1389
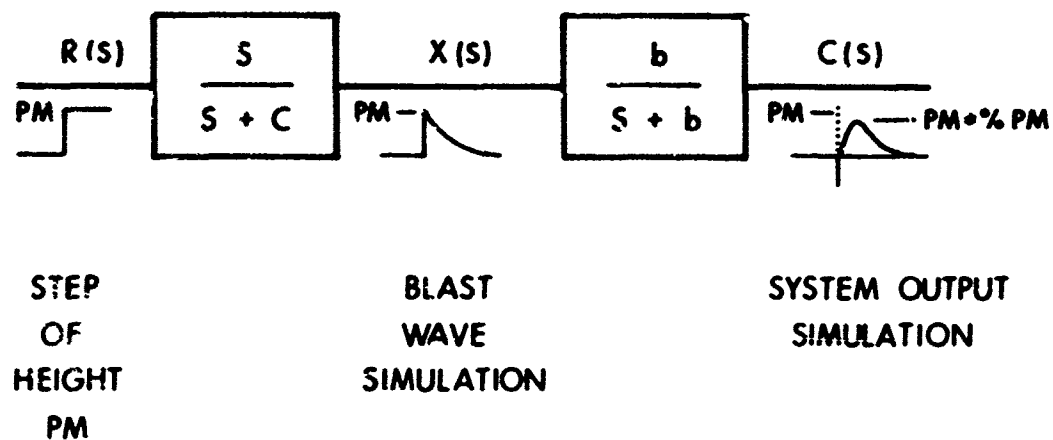
Figure 3. Laplace System Model With Time Domain Waveforms

1390

which may be reduced by substitution of (9) to

$$\text{\%} = (\frac{b}{c})^{(\frac{-c}{b-c})} \qquad (12)$$

Note that %, the ratio of indicated to actual pressure is a function
solely of c, the blast wave decay constant, and 1/b, the acquisition
system time constant.

A solution for 1/b as a function of c and % would be ideal, but
such a direct solution is not possible as equation (12) is transcendental.
However, aided with a computer an iterative procedure will yield results
to any desired accuracy.

All that remains is to implement the following algorithm:

    a) Find peak pressure PM given charge weight and distance

    b) Find blast wave decay constant c as function of PM and charge
       weight

    c) Find acquisition system time constant 1/b as a function of
       c and desired accuracy cf indicated peak pressure, %

A program based on this algorithm was written and debugged. Results
are presented in Tables 1 and 2. A plot of the one pound charge results
is shown in Figure 4. Another program was developed to plot shock wave
and acquisition system response as functions of time. Figure 5 is a
typical example of this plot as executed by the computer's teletypewriter.

Charge Weight (lbs):1
Percent of Peak (0 to 1):.9

Peak Pressure (psig)	Ground Range (feet)	Time to Percent Peak (msec)	System Time Constant (msec)	Min System Bandwidth (hertz)
1	45.5	0.315	0.086	1843
2	26.6	0.231	0.063	2519
5	14.4	0.144	0.039	4043
10	9.8	0.096	0.026	6054
20	7.0	0.062	0.017	9430
50	4.6	0.032	0.009	17995
100	3.4	0.019	0.005	30714

Charge Weight (lbs):1
Percent of Peak (0 to 1):.91

Peak Pressure (psig)	Ground Range (feet)	Time to Percent Peak (msec)	System Time Constant (msec)	Min System Bandwidth (hertz)
1	45.5	0.282	0.075	2136
2	26.6	0.207	0.055	2919
5	14.4	0.129	0.034	4686
10	9.8	0.086	0.023	7016
20	7.0	0.055	0.015	10528
50	4.6	0.029	0.008	20855
100	3.4	0.017	0.005	35595

Charge Weight (lbs):1
Percent of Peak (0 to 1):.92

Peak Pressure (psig)	Ground Range (feet)	Time to Percent Peak (msec)	System Time Constant (msec)	Min System Bandwidth (hertz)
1	45.5	0.250	0.063	2513
2	26.6	0.183	0.046	3434
5	14.4	0.114	0.029	5512
10	9.8	0.076	0.019	8253
20	7.0	0.049	0.012	12855
50	4.6	0.026	0.007	24532
100	3.4	0.015	0.004	41870

Table 1 System Requirements - 1# Charge

Charge Weight (lbs):1
Percent of Peak (0 to 1):.93

Peak Pressure (psig)	Ground Range (feet)	Time to Percent Peak (msec)	System Time Constant (msec)	Min System Bandwidth (hertz)
1	45.5	0.217	0.053	3012
2	26.6	0.159	0.039	4116
5	14.4	0.099	0.024	6607
10	9.8	0.066	0.016	9893
20	7.0	0.043	0.010	15409
50	4.6	0.022	0.006	29405
100	3.4	0.013	0.003	50139

Charge Weight (lbs):1
Percent of Peak (0 to 1):.94

Peak Pressure (psig)	Ground Range (feet)	Time to Percent Peak (msec)	System Time Constant (msec)	Min System Bandwidth (hertz)
1	45.5	0.185	0.043	3700
2	26.6	0.136	0.032	5057
5	14.4	0.084	0.020	8117
10	9.8	0.056	0.013	12154
20	7.0	0.036	0.009	18931
50	4.6	0.019	0.005	36126
100	3.4	0.011	0.003	61660

Charge Weight (lbs):1
Percent of Peak (0 to 1):.95

Peak Pressure (psig)	Ground Range (feet)	Time to Percent Peak (msec)	System Time Constant (msec)	Min System Bandwidth (hertz)
1	45.5	0.154	0.034	4701
2	26.6	0.112	0.025	5424
5	14.4	0.070	0.016	10312
10	9.8	0.047	0.010	15441
20	7.0	0.030	0.007	24050
50	4.6	0.016	0.004	45896
100	3.4	0.009	0.002	78334

Table 1. Continued

Charge Weight (lbs):1
Percent of Peak (0 to 1):.96

Peak Pressure (psig)	Ground Range (feet)	Time to Percent Peak (msec)	System Time Constant (msec)	Min System Bandwidth (hertz)
1	45.5	0.122	0.025	6268
2	26.6	0.089	0.019	8565
5	14.4	0.056	0.012	13749
10	9.8	0.037	0.008	20588
20	7.0	0.024	0.005	32067
50	4.6	0.013	0.003	61195
100	3.4	0.007	0.002	104446

Charge Weight (lbs):1
Percent of Peak (0 to 1):.97

Peak Pressure (psig)	Ground Range (feet)	Time to Percent Peak (msec)	System Time Constant (msec)	Min System Bandwidth (hertz)
1	45.5	0.091	0.018	9018
2	26.6	0.067	0.013	12323
5	14.4	0.042	0.008	29780
10	9.8	0.028	0.005	29618
20	7.0	0.018	0.004	46135
50	4.6	0.009	0.002	88043
100	3.4	0.006	0.001	150262

Charge Weight (lbs):1
Percent of Peak (0 to 1):.98

Peak Pressure (psig)	Ground Range (feet)	Time to Percent Peak (msec)	System Time Constant (msec)	Min System Bandwidth (hertz)
1	45.5	0.061	0.011	14889
2	26.6	0.044	0.008	20347
5	14.4	0.028	0.005	32559
10	9.8	0.019	0.003	48905
20	7.0	0.012	0.002	76176
50	4.6	0.006	0.001	145368
100	3.4	0.004	0.001	24 103

Table 1. Continued

Charge Weight (lbs):1
Percent Of Peak (0 to 1):.99

Peak Pressure (psig)	Ground Range (feet)	Time to Percent Peak (msec)	System Time Constant (msec)	Min System Bandwidth (hertz)
1	45.5	0.030	0.005	34288
2	26.6	0.022	0.003	46861
5	14.4	0.014	0.002	73221
10	9.8	0.009	0.001	112542
20	7.0	0.006	0.001	175429
50	4.6	0.003	0.001	334783
100	3.4	0.002	0.000	571367

Table 1. Continued
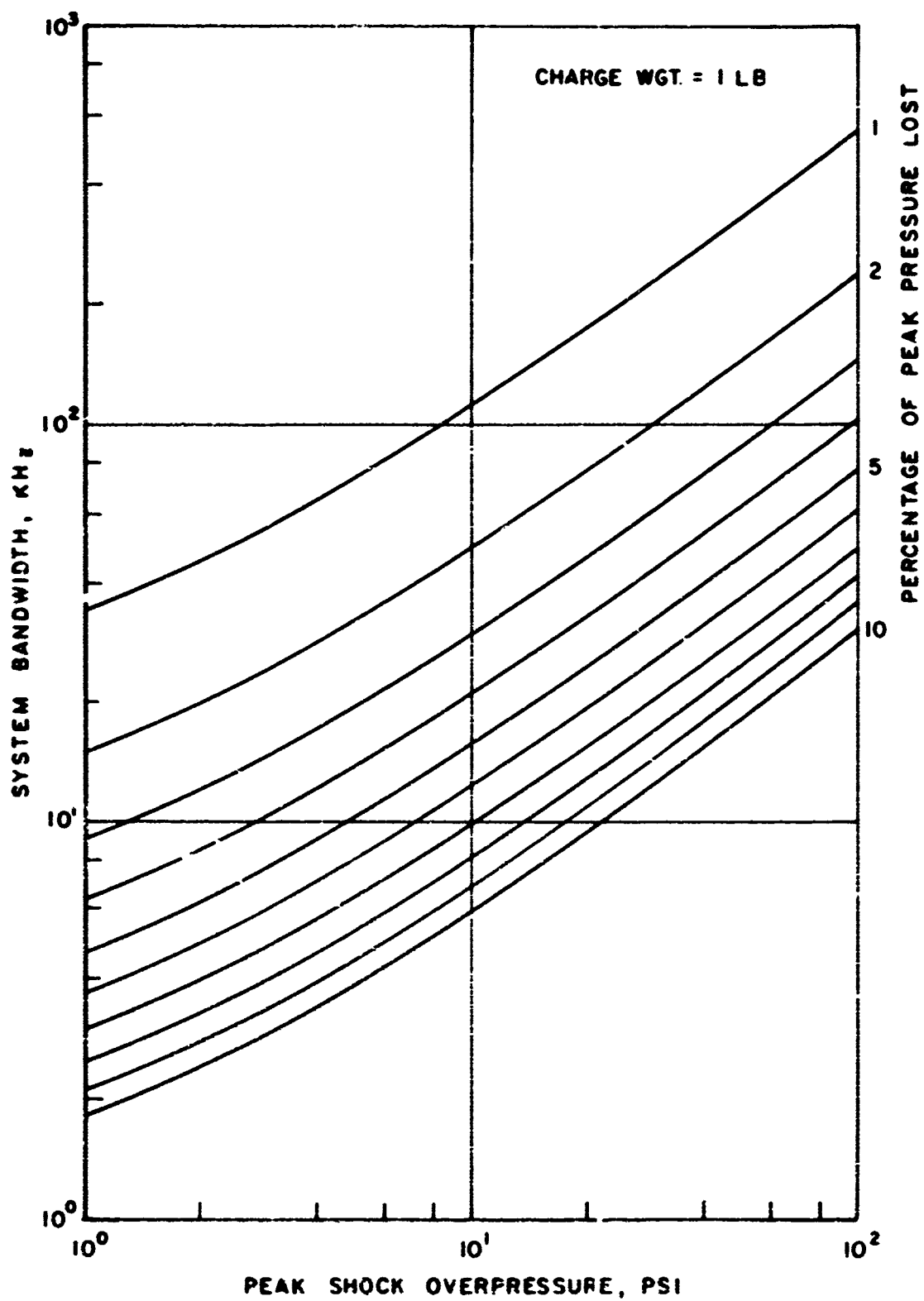
Figure 4.   System Bandwidth Required versus Peak Overpressure
at Various Accuracies for a 1ᵃ Charge

1395

CHARGE WT. = I LB.
90% PEAK OVERPRESSURE ACCURACY
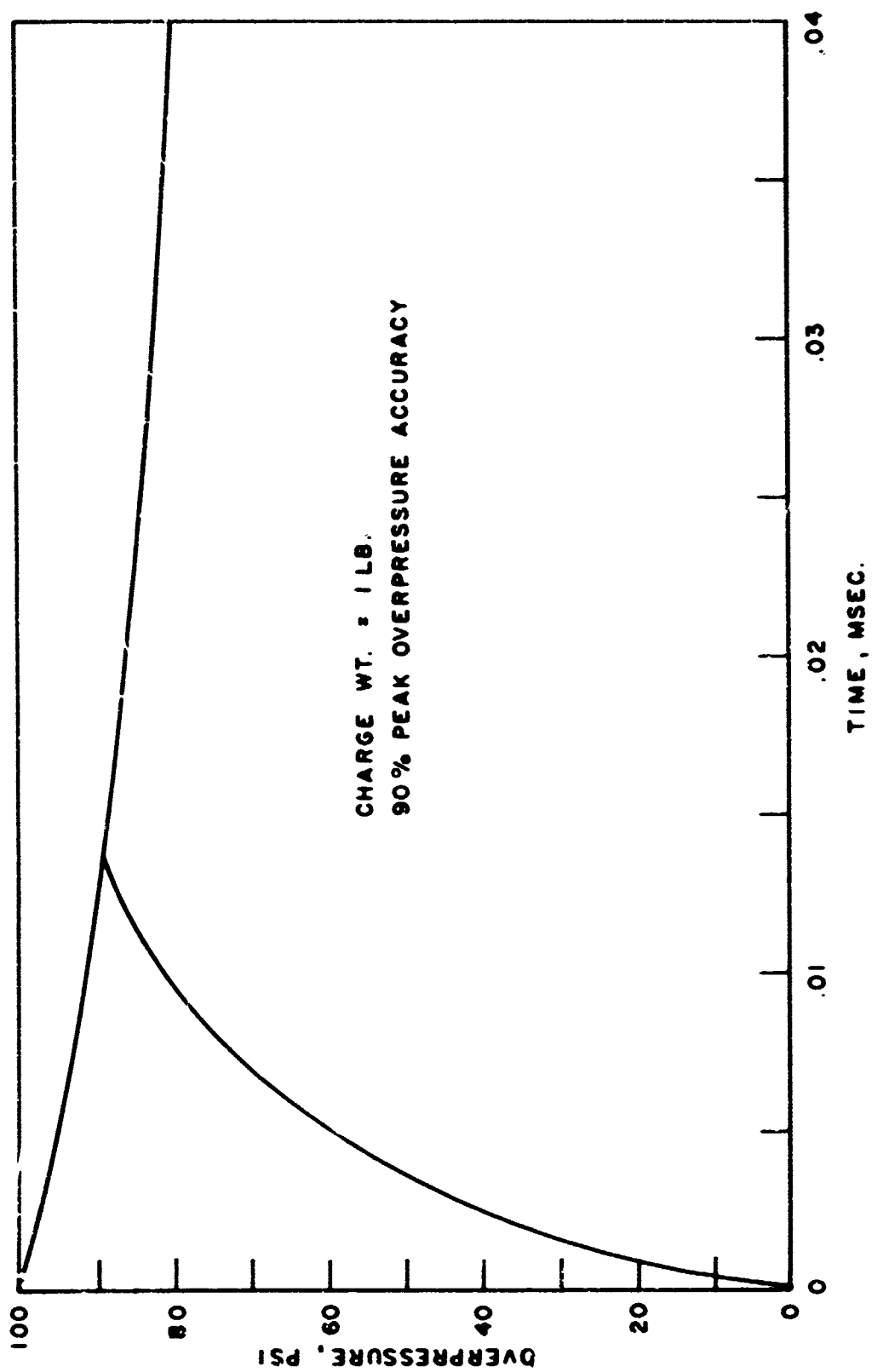
OVERPRESSURE, PSI

TIME, MSEC.

Figure 5. Digital Plot of Shock Wave and System Response

The acquisition system bandwidth (BW) and time constant (1/b) data is scalable with the inverse cube root of charge weight. First, note that the decay constant, c, a time related blast parameter scales inversly with the cube root of charge weight.

$$C_2 = C_1 \frac{\sqrt[3]{W_1}}{\sqrt[3]{W_2}} \tag{13}$$

Now, if both b and c are multipled by the same constant, observe from equation (12) that ‰ remains constant:

$$\left(\frac{kb}{kc}\right)^{\left(\frac{-kc}{kb-kc}\right)} = \frac{k}{k}\left(\frac{b}{c}\right)^{-\frac{k}{k}}\left(\frac{-c}{b-c}\right) = \left(\frac{b}{c}\right)^{\left(\frac{-c}{b-c}\right)} = \% \tag{14}$$

Then:

$$b_2 = b_1 \frac{\sqrt[3]{W_1}}{\sqrt[3]{W_2}} \tag{15}$$

Bandwidth is related to system time constant by

$$BW = \frac{1}{2\pi \ (1/b)} = \frac{b}{2\pi} \tag{16}$$

then bandwidth scales as follows

$$BW_2 = BW_1 \frac{\sqrt[3]{W_1}}{\sqrt[3]{W_2}} \tag{17}$$

If W_1 is a one pound charge, its cube root is one and equation (17) becomes:

$$BW_2 = \frac{BW_1}{\sqrt[3]{W_2}} \tag{18}$$

1398

Then the system bandwidth requirement for a particular peak pressure and charge weight can be derived from the one pound charge tables or curves as demonstrated in the following example:

EXAMPLE 1. It is necessary to measure the 10 psi overpressure produced by a 100 pound charge to an accuracy of 95%. From Table 1, for 1 pound charges, a bandwidth of 15441 HZ is required. Using equation (18),

$$BW_{100} = \frac{BW_1}{\sqrt[3]{100}} = \frac{15441}{4.6416} = 3327\ HZ \qquad (19)$$

Checking the 100 pound table (Table 2) indicated the same result.

EXAMPLE 2. There is a need to measure the 75 psi overpressure produced by a 1000 pound charge to an accuracy of 98%. From Figure 4, for a 1 pound charge, a bandwidth of 197,000 HZ is required. Using Equation (18),

$$BW_{1000} = \frac{BW_1}{\sqrt[3]{1000}} = \frac{197,000}{10} = 19,700\ HZ \qquad (20)$$

One would probably use a 20KH system for this measurement.

One should keep in mind that an elementary ideal acquisition system model was used. Real acquisitions often contain complex poles, leading to faster response at the expense of possible overshoot and resonance. Therefore, the results presented here should be regarded only as a guide.

APPENDIX B

The following equation from work by C. N. Kingery and B. F. Pannill[2] was used to relate scaled overpressure, PM, to scaled ground range, λ.

$$\ln PM = 7.0452041 - 1.6277561 \ln\lambda$$
$$- .27399088(\ln\lambda)^2 - 0.065973136(\ln\lambda)^3$$
$$+ 0.0065412563(\ln\lambda)^4 - 0.048236359(\ln\lambda)^5$$
$$- 0.020072553(\ln\lambda)^6 - 0.0030190449(\ln\lambda)^7$$
$$- 0.00015984026(\ln\lambda)^8$$

for $0.5 \leq \lambda \leq 440$

also: $PM = 226.61762\lambda^{-1.4065913}$

for $40 \leq \lambda \leq 1000$

APPENDIX C

The following equations are from work by C. N. Kingery[1]. Designations reference Figure 1 of Appendix A.

$$\ln\ PC = -0.68130202 + 0.8202848\ \ln\ PM$$

$$\ln\ TC = 5.0860601 - 0.32650031\ \ln\ PC - 0.089162767(\ln\ PC)^2$$

$$\ln\ TD = 6.0713887 - 0.2030581\ \ln\ PM - 0.017906738(\ln\ PM)^2$$
$$- 0.00001508165(\ln\ PM)^4 + 0.0000029357740(\ln\ PM)^9$$
$$- 0.00000046832248(\ln\ PM)^{10}$$

$$\ln\ c = -5.7010608 + 0.42205260(\ln\ PM) + 0.041003678(\ln\ PM)^2$$

$$\ln\ b = 0.43327169 - 0.89790991(\ln\ PM) + 0.0422564224(\ln\ PM)^2$$
$$+ 0.0000022628994(\ln\ PM)^8 - 0.000000071363505(\ln\ PM)^{10}$$

REFERENCES

1. C. N. Kingery, R. C. Kellner, *BRL Memorandum Report* No. 1638 March 1973

2. C. N. Kingery, B. F. Pannill, *BRL Memorandum Report* No. 1518 April 1964

DISTANT BLAST PREDICTIONS FOR EXPLOSIONS[*]

Jack W. Reed
Sandia Laboratories, Albuquerque, New Mexico

After one of the first Nevada nuclear tests in early 1951 broke windows in Las Vegas, 80 miles away, Sandia Laboratories began measurements and research to develop methods for avoiding recurrences. The techniques we derived are useful for blast prediction for various explosives where atmospheric refraction may cause nuisance or hazard outside a controlled danger area. Nuclear test data collections have been summarized to give a climatology of propagation amplitudes that may be expected under various meteorological conditions. These results are at variance with predictions in the Ballistic Research Laboratories Handbook, BRL-1240, of 1964, which is still used by some military agencies. That Handbook now appears to be obsolete, and based on limited data which were available and unclassified during the 1950's.

Atmospheric refraction, by wind and temperature effects, may duct and even focus blast waves to cause nuisance and possible minor damage at often unexpected distances from explosions. Blast ray paths may be returned to the ground, as shown by Figure 1, at ranges even beyond 100 miles, depending on upper air conditions. Strong propagation in the boundary layer may be carried downwind by strong winds, or in all directions during night-time surface temperature inversions. Jet-stream winds, at 25,000 to 40,000 ft altitudes can cause blast focusing at 30-50 mile downwind ranges. The warm layer in

the high stratosphere, or ozonosphere, near 150,000 ft, also allows ducting which carries relatively loud noise 100 to 150 miles downwind of seasonal monsoon winds at that altitude.

To predict amplitudes from these atmospheric ducted waves, we begin with a standard explosion overpressure versus distance curve, as shown in Figure 2. At low blast overpressures, below about 1/3 psi or 25 millibars, quasi-acoustic propagation in a homogeneous, calm atmosphere gives overpressures, or peak-to-peak amplitudes, that decrease about in proportion to the -1.2 power of distance. A variety of experimental data have been used to generate and confirm this rule for unrefracted, radially expanding explosive waves. This "standard" curve is shown for a 1-kt (4.2×10^{19} ergs) nuclear-explosive (NE), burst in free air away from reflecting surfaces, in 1000 mb ambient pressure.

Blast wave scaling laws, in Figure 3, show that distances to constant overpressures are proportional to the cube-root of yield as shown in Equations 1 and 2. In consequence, in the low pressure, $R^{-1.2}$ region, amplitudes are proportional to yield raised to the 0.4 power, as shown in Equation 3.

Most atmospheric nuclear tests were fired at or near a reflecting ground surface. Many generated fused Mach-stems, as shown in Figure 4, where incident and reflected waves are merged into one stronger shock wave. The strength of these Mach stem source waves depends primarily on yield-scaled height-of-burst (HOB). Figure 5 shows how apparent yield is enhanced by various scaled burst heights.

Far-field microbarograph records have been normalized to 1-kt NE free-air burst amplitudes, by adjusting for apparent yields, based on HOB, for 1953, 1955, 1957, and 1958 Nevada atmospheric nuclear tests in Figures 6, 7, 8, and

9. In spring and fall, storm winds and generally cooler surface temperatures occasionally caused blast ducting and larger-than-standard pressure amplitudes to propagate to considerable distances. Summer test data usually showed a rapid decrease of amplitude with increased distance because of the normally large gradient of sound velocity with altitude. As was shown earlier in Figure 1, a gradient in the surface layer causes the blast wave to turn away from ground, so that only relatively weak, scattered waves reach our ground level recorders. A rule-of-thumb for gradient propagation is that amplitudes decrease about in proportion to distance squared, beyond about 3km from 1-kt NE.

Nuclear data were usually gathered near or before dawn, when there was a strong surface temperature inversion in Yucca or Frenchman's Flats. This caused ducting and blast amplification on-site and until the wave passed the first range of hills surrounding the Flats. Beyond that distance, free air conditions of gradients or sound ducts determined the distant propagation.

At very high altitudes, near 50 km, relatively warm temperatures, near $0^{o}C$, and monsoon winds give downwind ducting into a noisy belt or ring near $2v^1$ km range. In winter, west winds at altitude carry blast waves eastward and in summer, east winds carry the blast west. The results are shown in Figures 10 and 11, with amplitudes again normalized for yield and HOB. St. George, Utah, east of Nevada Test Site, typically received "standard" amplitudes in winter, with considerable scatter, of course. Summer propagations, upwind, generally confirmed the R^{-2} rule for gradient propagation. To the west, Bishop, California, showed the monsoon pattern reversal, with strong, ducted waves in summer and weak, upwind waves in winter.

These climatological data were used to estimate off-site effects from several recent large HE tests in Colorado. Project MIDDLE GUST, by the USAF Weapons Laboratory, fired two 20-ton and three 100-ton HE yields near Ordway, in Southeastern Colorado. Proximity to various communities required that these tests be conducted with strong sound velocity-height gradients, to minimize nuisance damage and disturbance. Results from off-site microbarograph measurements of peak-to-peak amplitudes are shown in Figure 12, with an approximate threshold, at 4 mb for beginning window damage. By waiting for appropriate weather conditions, when necessary, it was possible to minimize such off-site damage and maintain good public relations with the neighborhood.

Project MIXED COMPANY, by the Defense Nuclear Agency, fired two 20-ton and one 500-ton HE tests near Grand Junction, in Western Colorado. Microbarograph measurements of the large yield event are shown in Figure 13. Window breaking amplitudes were held to about 20 km range where, under some weather conditions, they could have spread to 80 km. The weather-watch appears to have served its purpose in generally minimizing off-site propagations.

A similar prediction service was performed with a 150-ton HE test by Tooele Army Depot early this year, with successful results as shown by Figure 14. Although barely 4 mb would reach the distance of Ogden or Salt Lake City, the exposed population of near one million people caused need for special caution.

A primary source for empirical data on the nuisance damage from blast waves has been the accident at Medina Base, San Antonio, Texas, where 56-t HE exploded and broke over 3000 windows in the city, in 1963. Evaluation of the damage claims and the exposed pane population led to the relationships in

Figure 15. These have been used with fair success in evaluating other minor incidents in Nevada and Colorado tests. There is, however, no theoretical foundation for these power law relationships to pane area and incident overpressure. These damage probabilities also depend on the actual distribution of pane qualities and sizes -- area and thickness -- in San Antonio, Texas, in late 1963. A better theoretical basis would allow more confidence in extrapolation to other situations.

Figure 16 shows how the Medina result compares with Pittsburgh Plate Glass Co. Report 101, "Glass Product Recommendations - Structural". They assumed a normal distribution for failures with a 25% standard deviation that obviously fails at 4σ and does not account for real problems of actual exposure and installation. Their laboratory data may be re-interpreted with a better-fitting log-normal distribution, but it likewise fails to account for all of the variables in real installations.

A recent assembly of explosion test data, by Wilton and Gabrielsen, in DNA-2906F, is shown to give surprising agreement with the Medina equations, which obviously should fail at high breakage probability. A combination of a log-normal damage model which fits the two main explosion data sets is shown in Figure 17. Hopefully, the log-normal laboratory test data can be used, along with distributions of pane exposure and blast reflection factors, as well as distributions of incident overpressures which are randomized by atmospheric turbulence, to approximate the empirical log-normal connection from Medina data to the strong blast housing test results.

Details on blast prediction methods, as described in this paper, have been assembled for the American National Standards Institute (ANSI) in a draft, "Standard for Single Point Explosions in Air." This document is currently under committee review, and, hopefully, can be distributed during 1974.

1407

SELECTED REFERENCES

B. Perkins, Jr., and W. F. Jackson, "Handbook for Prediction of Air Blast
  Focusing," BRL-1240, Ballistic Research Laboratories, Aberdeen, Md,
  February 1964.

S. Glasstone, editor, The Effects of Nuclear Weapons, Rev. Ed., DOD/AEC,
  U. S. Government Printing Office, Washington, D.C., April 1962.

E. F. Cox, J. H. Plagge, and J. W. Reed, "Meteorology Directs Where Blast
  Will Strike," Bull. Am. Meteor. Soc., Vol. 35, No. 3, pp. 95-103, March
  1954.

J. W. Reed, "Explosion Wave Amplitude Statistics for a Caustic at Ranges of 30-
  to 45-Miles," SC-RR-67 860, Sandia Laboratories, February 1968.

J. W. Reed, "Climatology of Airblast Propagations for Nevada Test Site Nuclear
  Airbursts," SC-RR-69 572, Sandia Laboratories, December 1969.

J. W. Reed, "Airblast Overpressure Decay at Long Ranges," J. Geophys. Res.,
  Vol. 77, No. 9, March 20, 1972.

J. W. Reed, B. J. Paper, J. E. Minor, and R. C. DeHart, "Evaluation of Window
  Pane Damage Intensity in San Antonio Resulting from Medina Facility
  Explosion on 13 November 1963," Annals of the New York Academy of Sciences.
  Vol. 152, Art 1, October 28, 1968, pp. 565-584.

C. Wilton, and B. Gabrielsen, "House Damage Assessment," DNA-2906F, URS
  Research Co., San Mateo, CA, January 1973.

Pittsburgh Plate Glass Co., "Glass Product Recommendations - Structural,"
  Tech. Service Report No. 101, Pittsburgh, PA (1964).
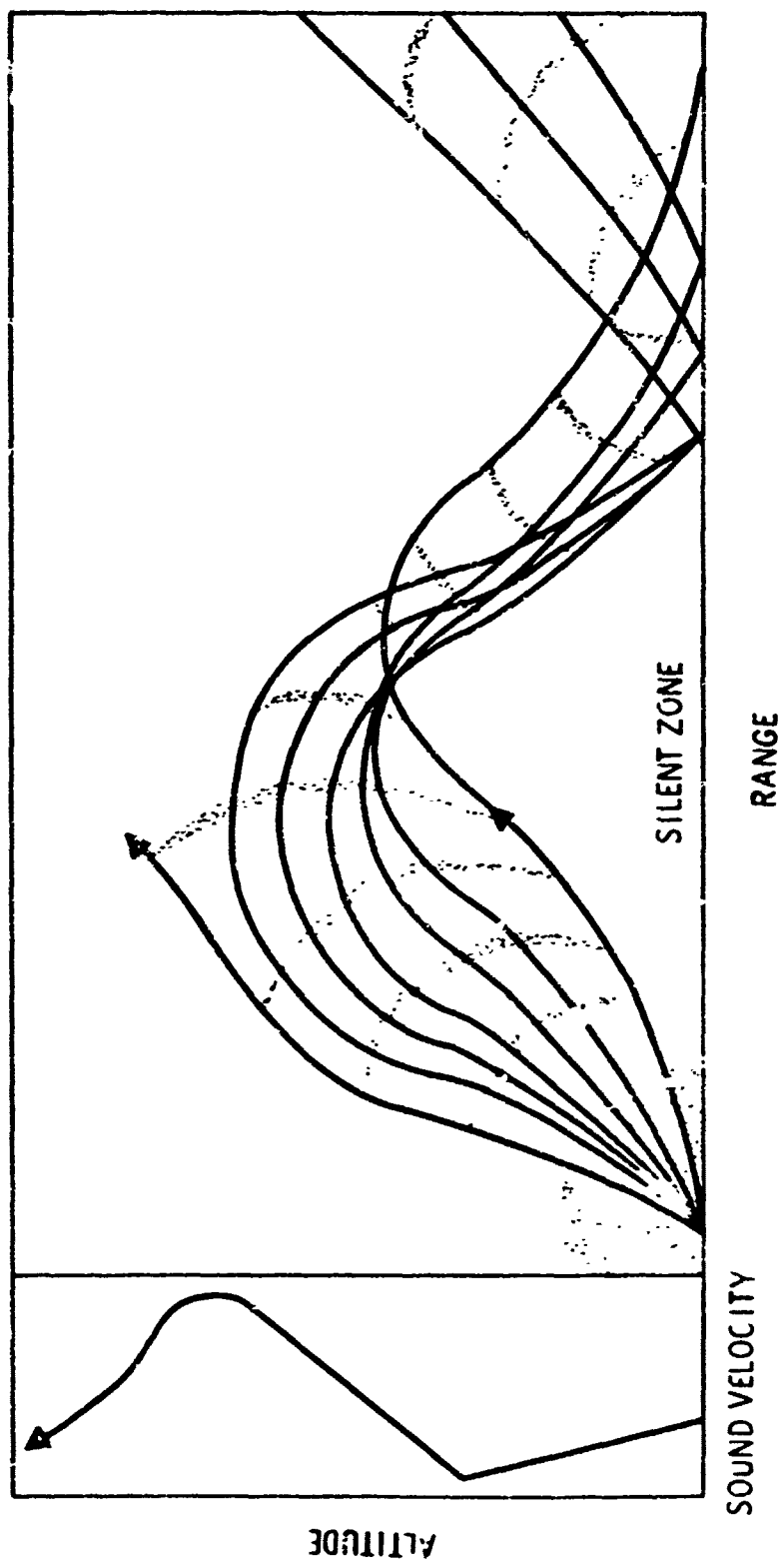
FIG. 1   TYPICAL EXPLOSION RAY PATHS

SOUND VELOCITY

ALTITUDE

SILENT ZONE
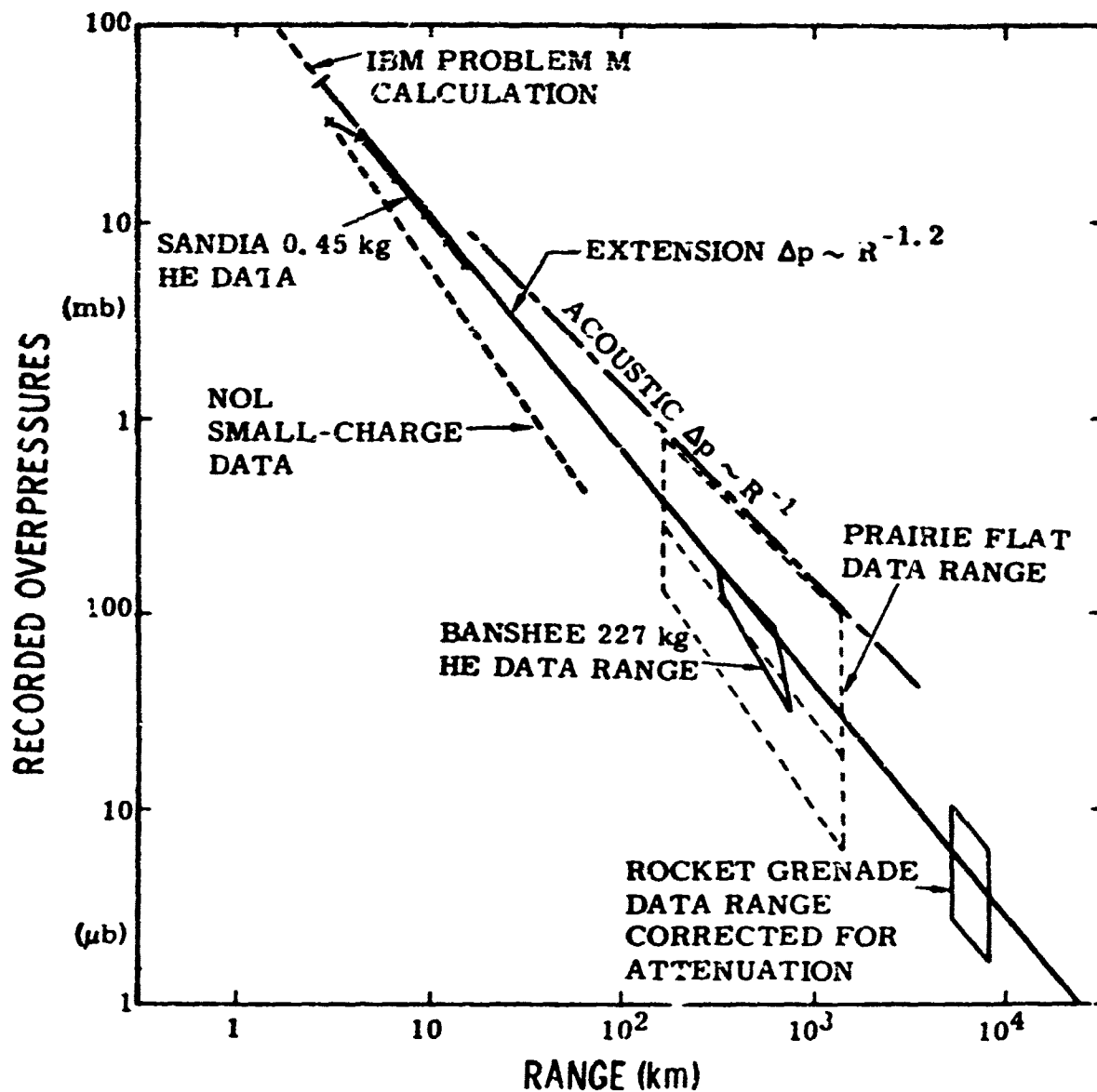
RANGE

FIG. 2   LONG-RANGE AIRBLAST DATA
SCALED TO 1-KT NUCLEAR
EXPLOSIVES

FIG. 3

p = pressure

Δp = overpressure

R = slant range

W = yield

SIMULTANEOUS SCALING EQUATIONS

$$\frac{\Delta p}{p} = \frac{\Delta p_0}{p_0} \tag{1}$$

$$\frac{R}{R_0} = \left(\frac{W}{W_0} \; \frac{p_0}{p} \right)^{1/3} \tag{2}$$

LOW OVERPRESSURE-DISTANCE EQUATION

$$\Delta p = k \, W^{0.4} R^{-1.2} p^{0.6} \tag{3}$$

k = constant
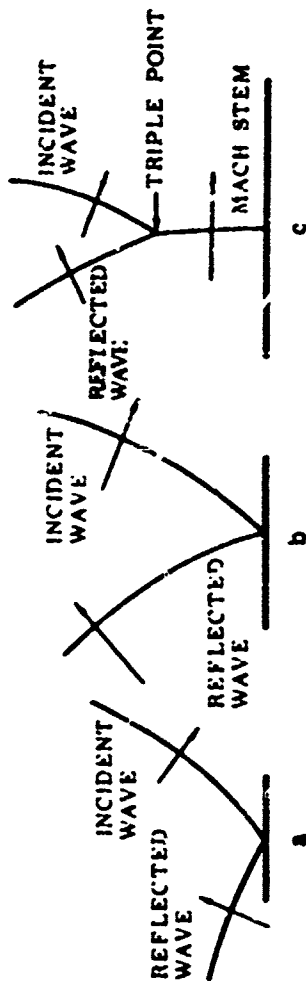
FUSION OF INCIDENT AND REFLECTED WAVES
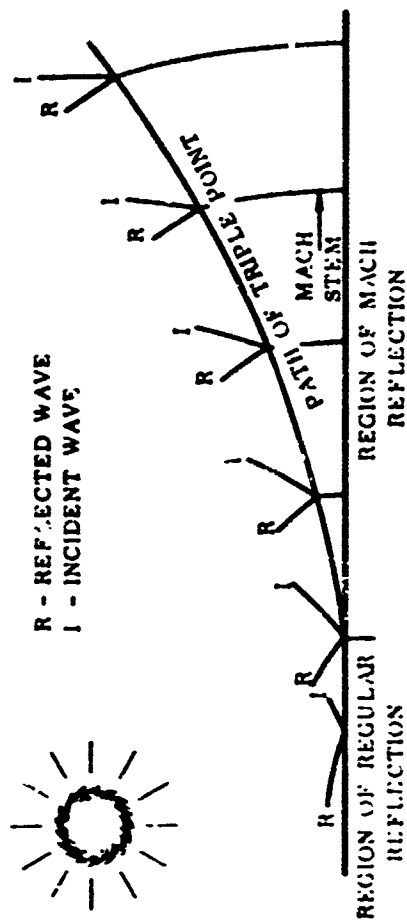
BLAST WAVE MOTION IN THE MACH REGION

FIG. 4   MACH STEM FORMATION FOR ABOVE-GROUND BURSTS
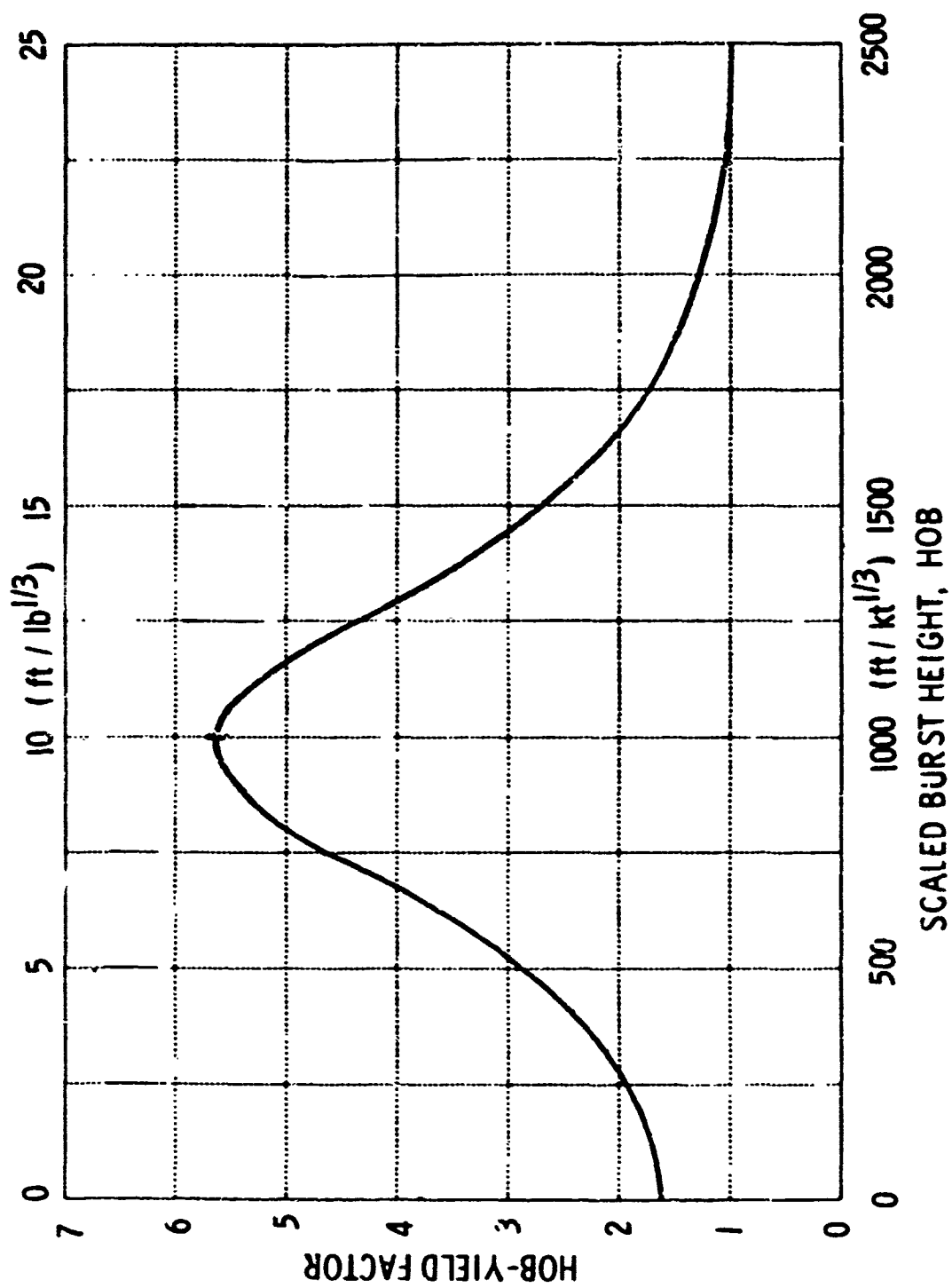
FIG. 5   AIRBLAST HEIGHT-OF-BURST EFECT ON APPARENT YIELD
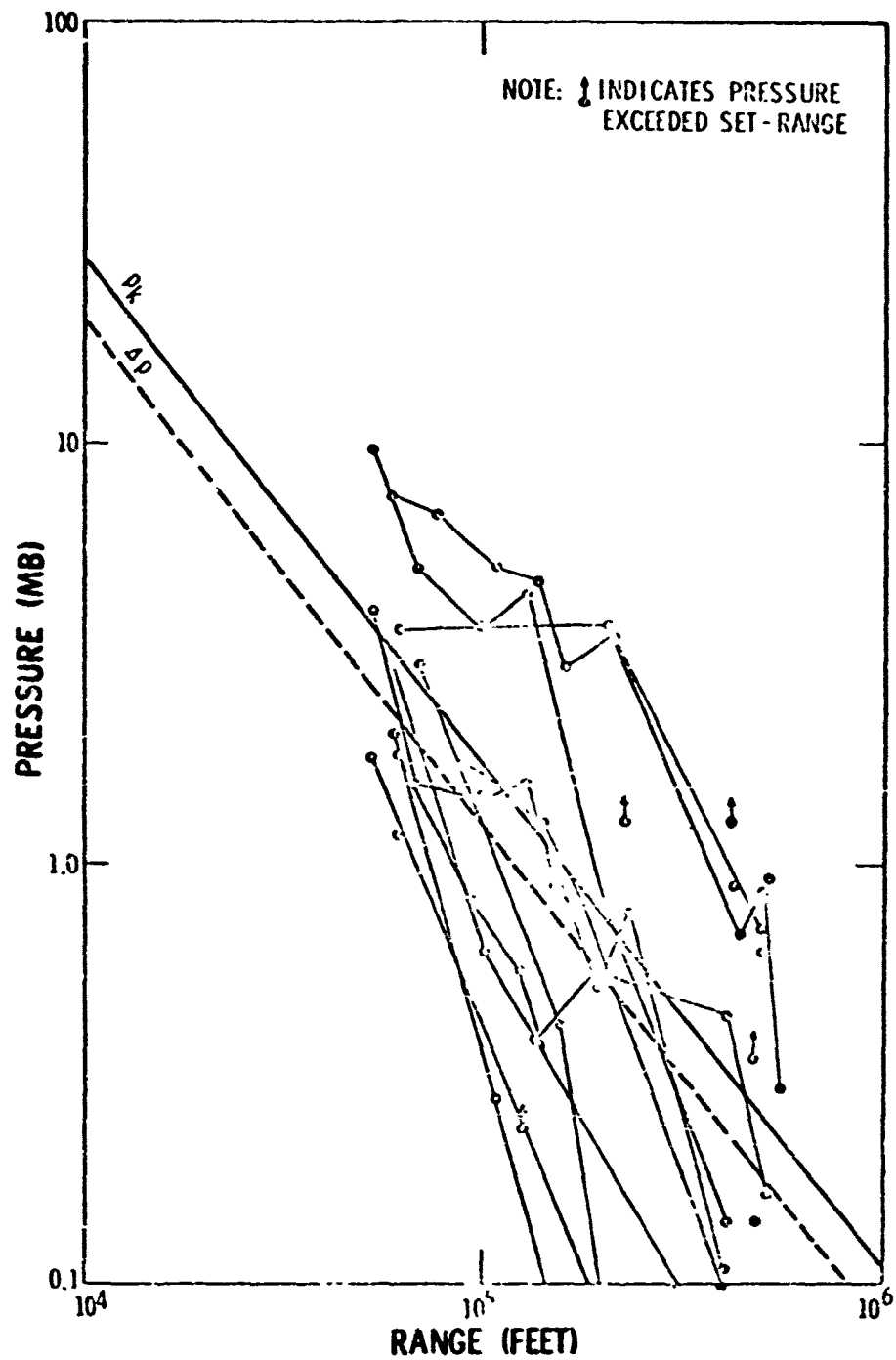
SUMMARY OF TROPOSPHERE PROPAGATIONS, uPSHOT-KNOTHOLE,
3/17 - 6/4, 1953 (SCALED TO 1-KT NE AIRBURST)

FIG. 6
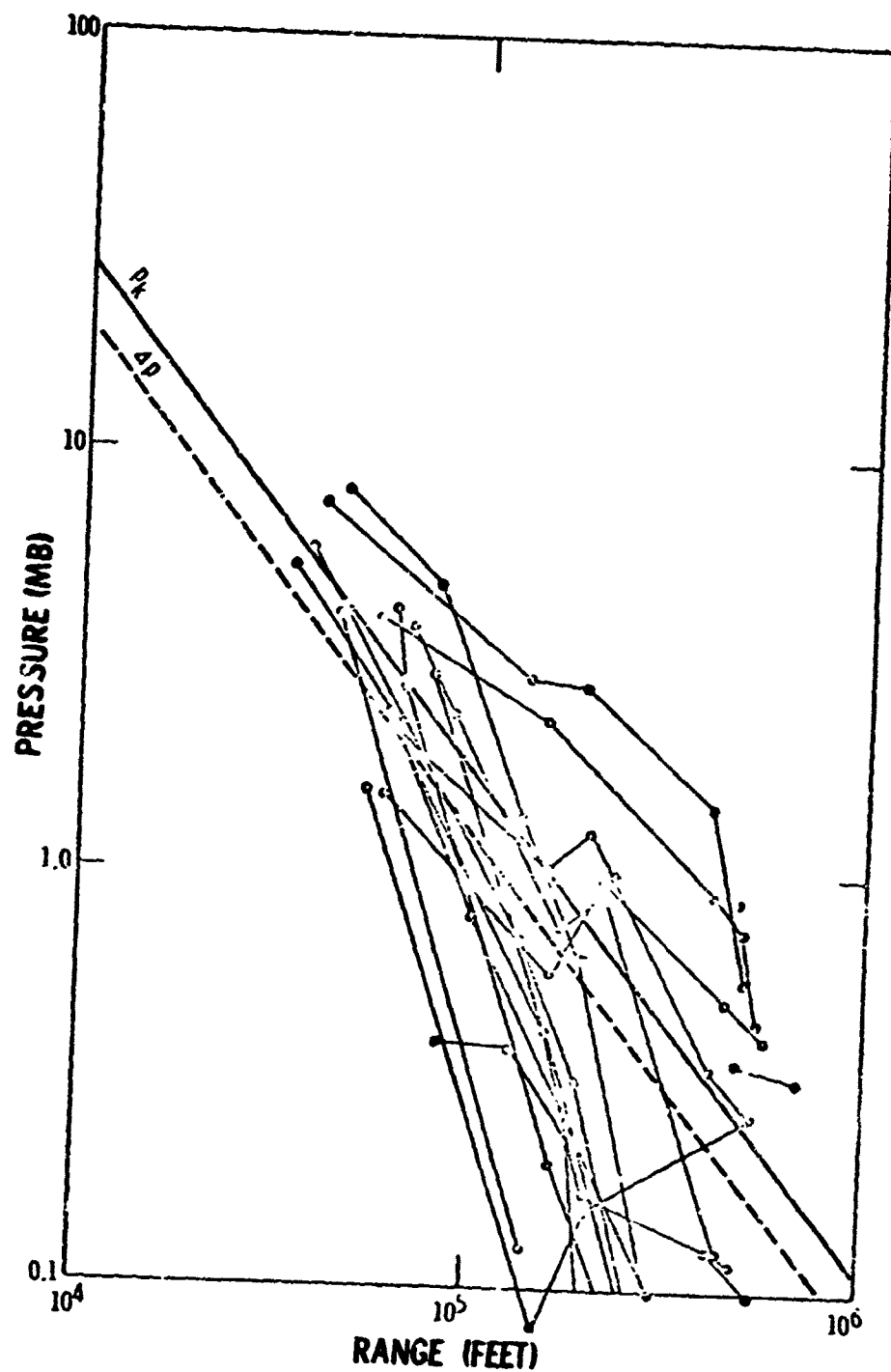
SUMMARY OF TROPOSPHERE PROPAGATIONS, TEAPOT, 2/18 – 5/15, 1955
(SCALED TO 1-KT NE AIRBURST)

FIG. 7
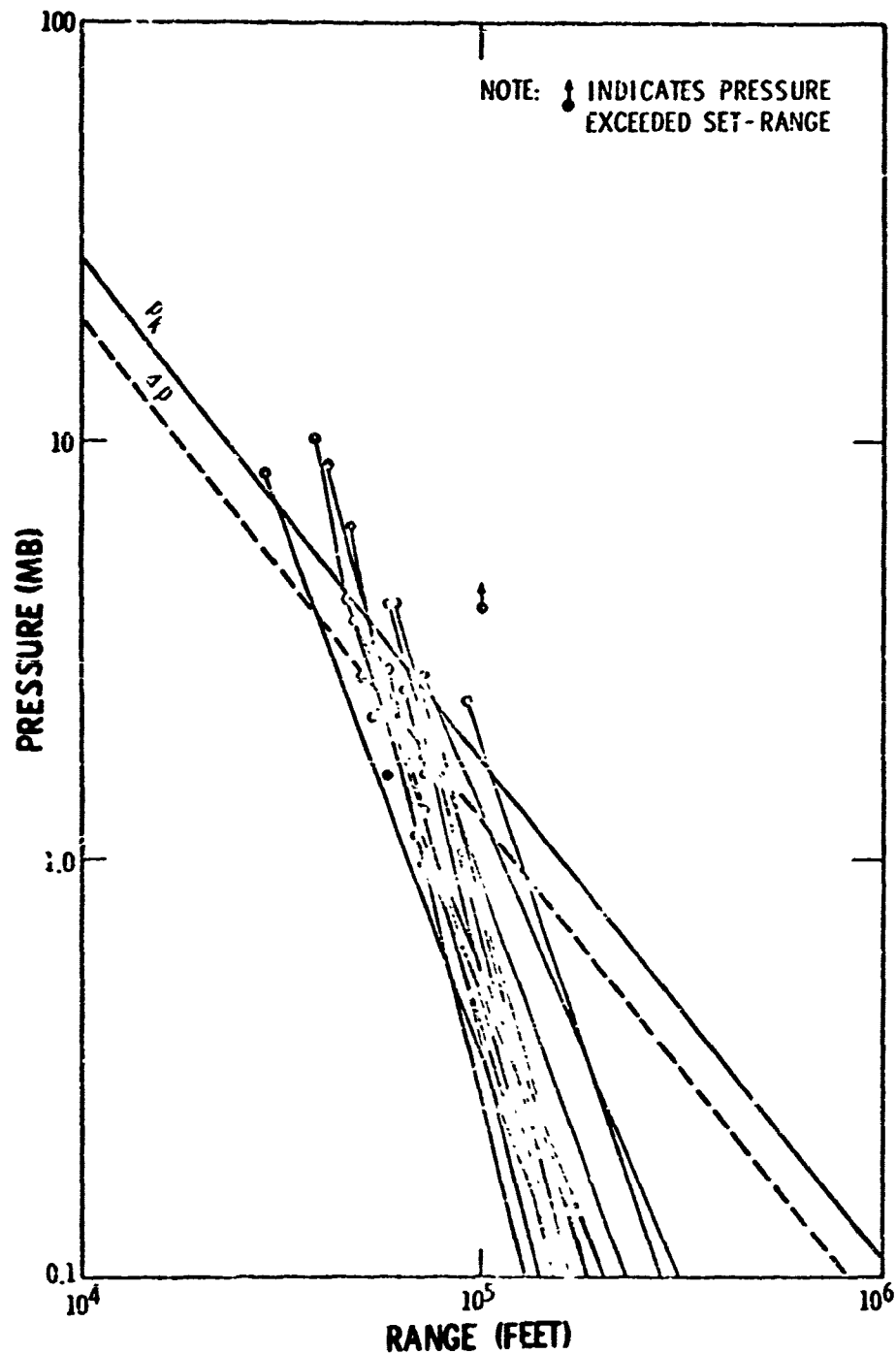
SUMMARY OF TROPOSPHERE PROPAGATIONS, PLUMBBOB, 5/28 - 10/7, 1957

(SCALED TO 1-KT NE AIRBURST)

FIG. 8
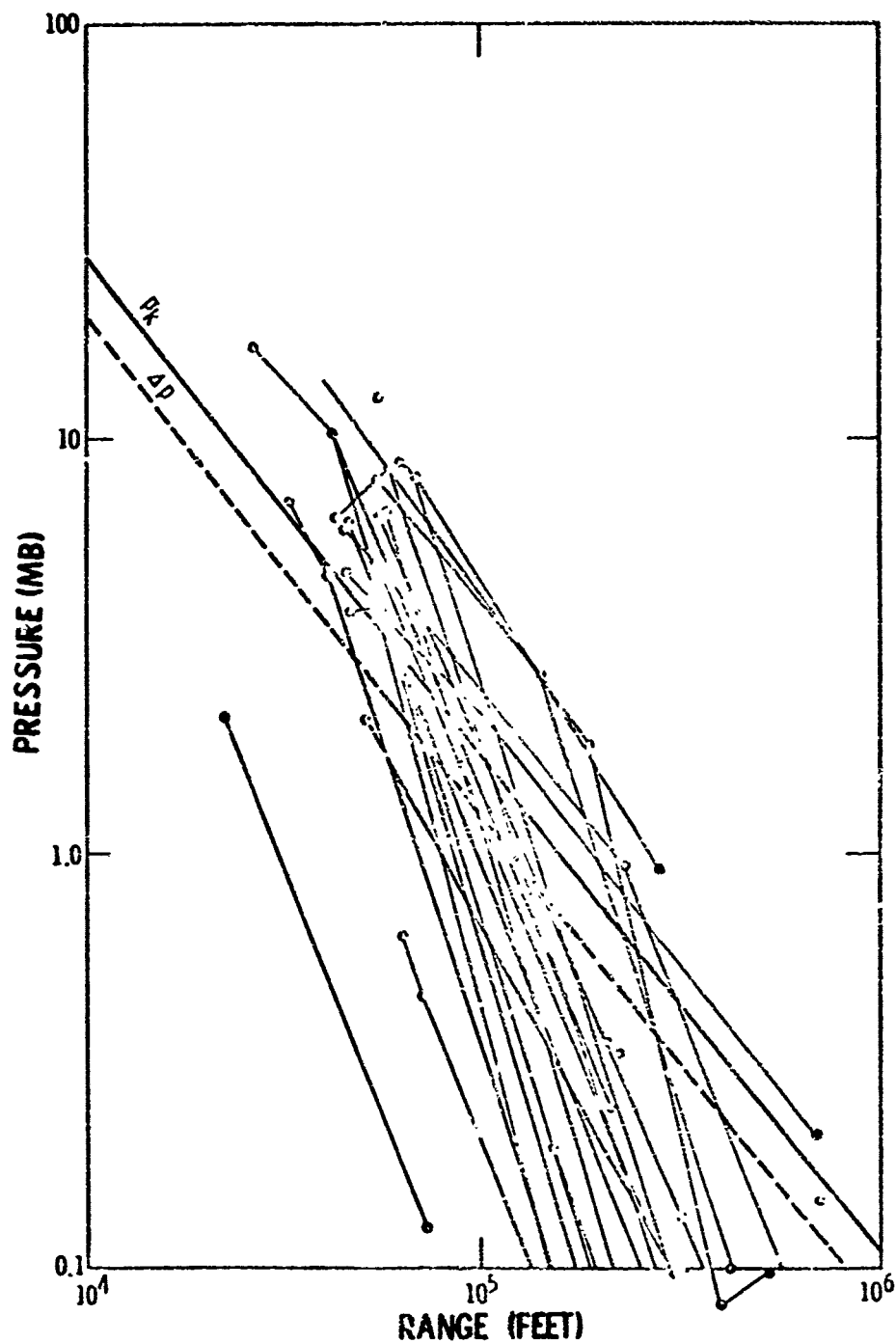
SUMMARY OF TROPOSPHERE PROPAGATIONS, HARDTACK II, 9/19 – 10/29, 1958
(SCALED TO 1-KT NE AIRBURST)

FIG. 9
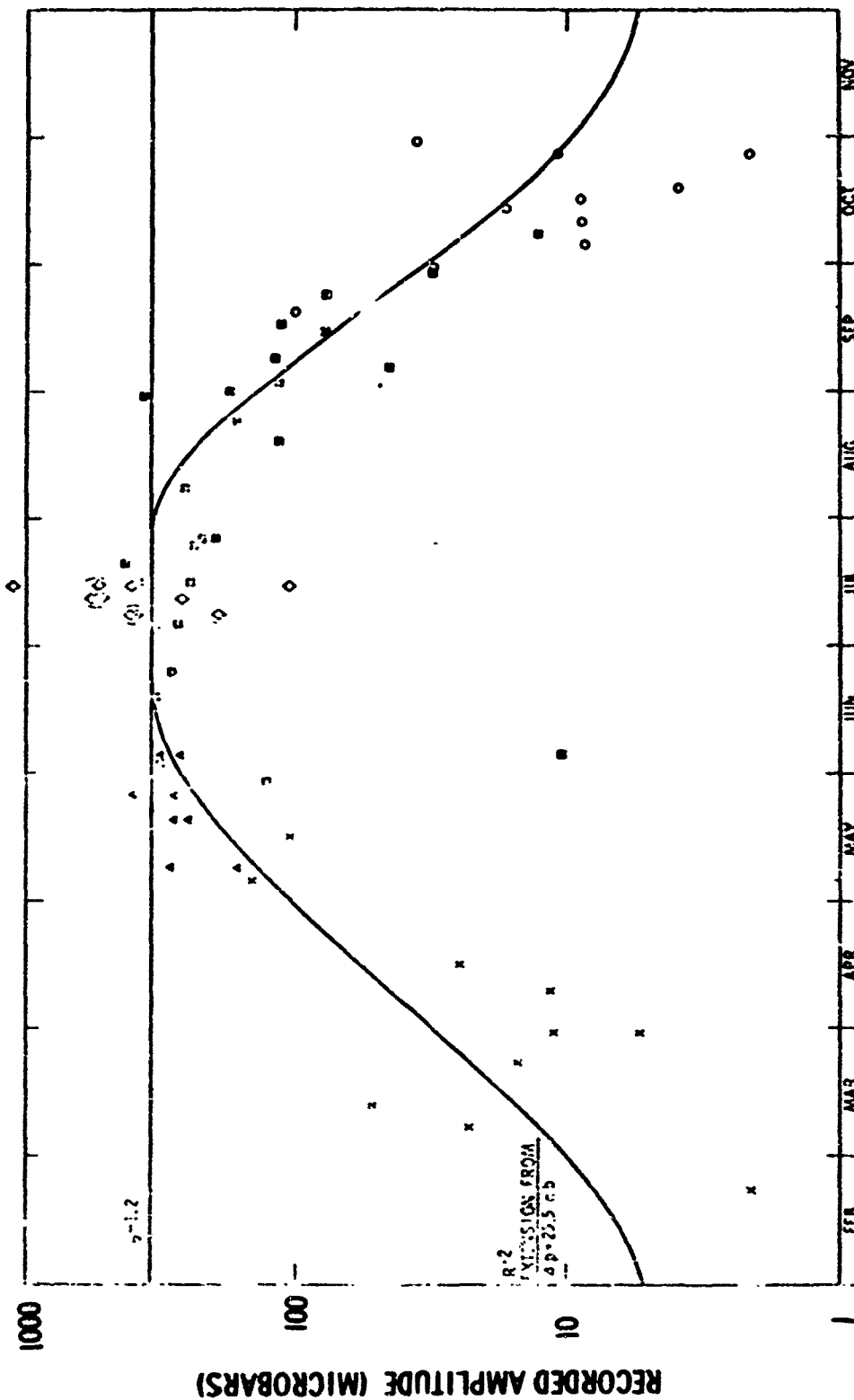
FIG. 10 OZONOSPHERE SIGNAL AMPLITUDES, BISHOP, CALIFORNIA, FROM
NEVADA NUCLEAR TESTS
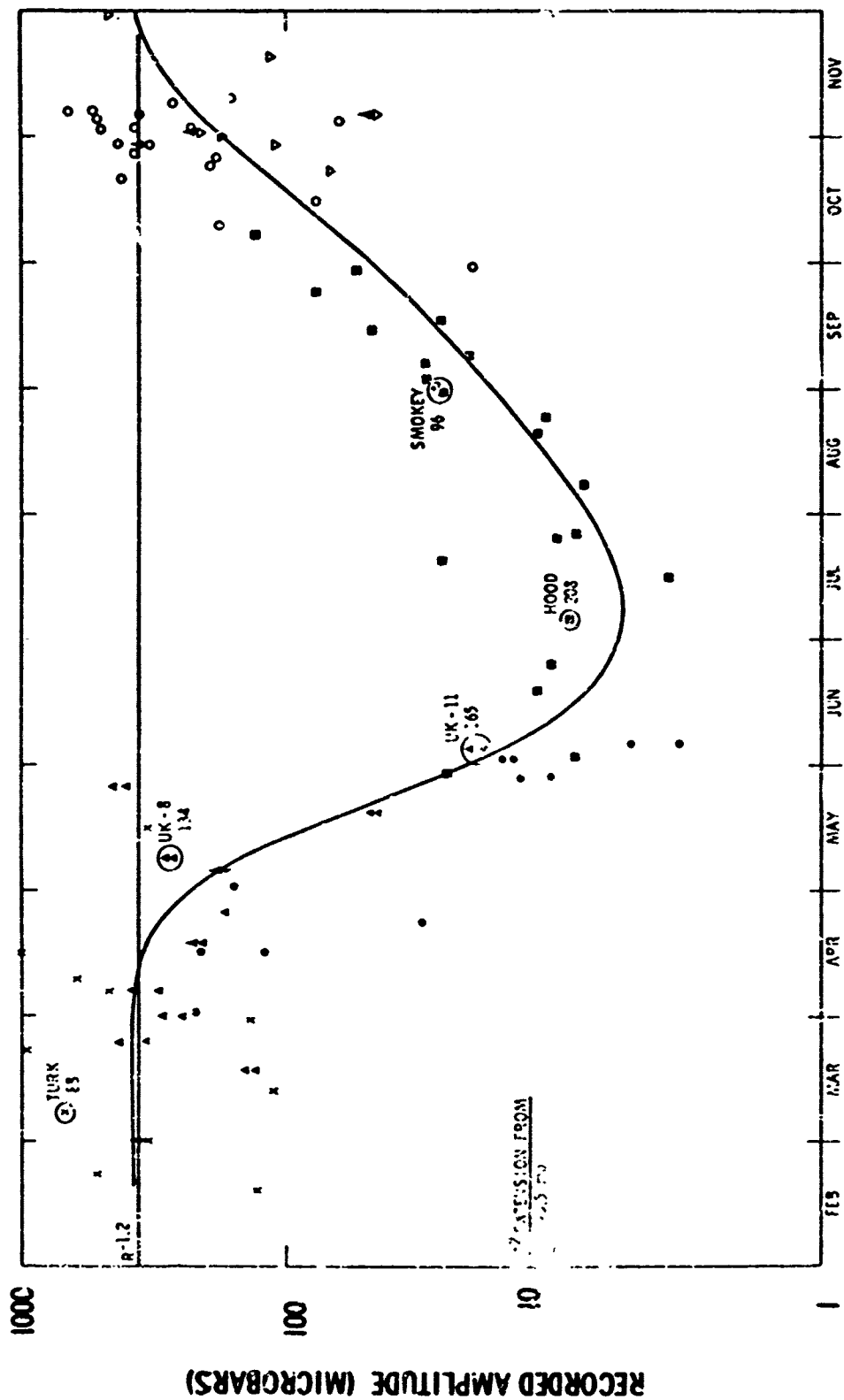
FIG. 11 OZONOSPHERE SIGNAL AMPLITUDES, ST. GEORGE, UTAH, FROM NEVADA NUCLEAR TESTS
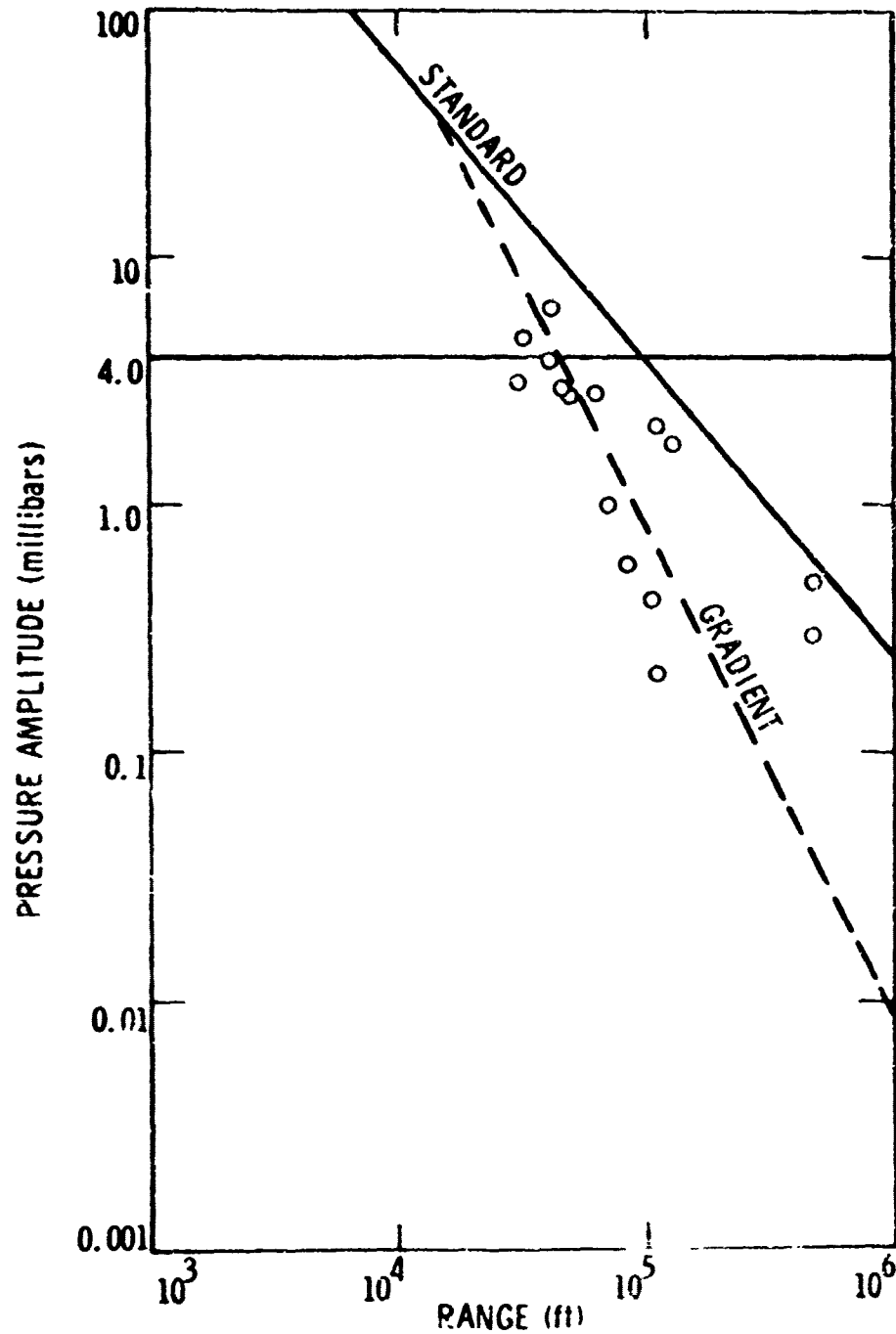
FIGURE 12   MIDDLE GUST SUMMARY OF PRESSURE AMPLITUDES,
SCALED TO 1-KT SEA LEVEL FREE-AIR BURST.
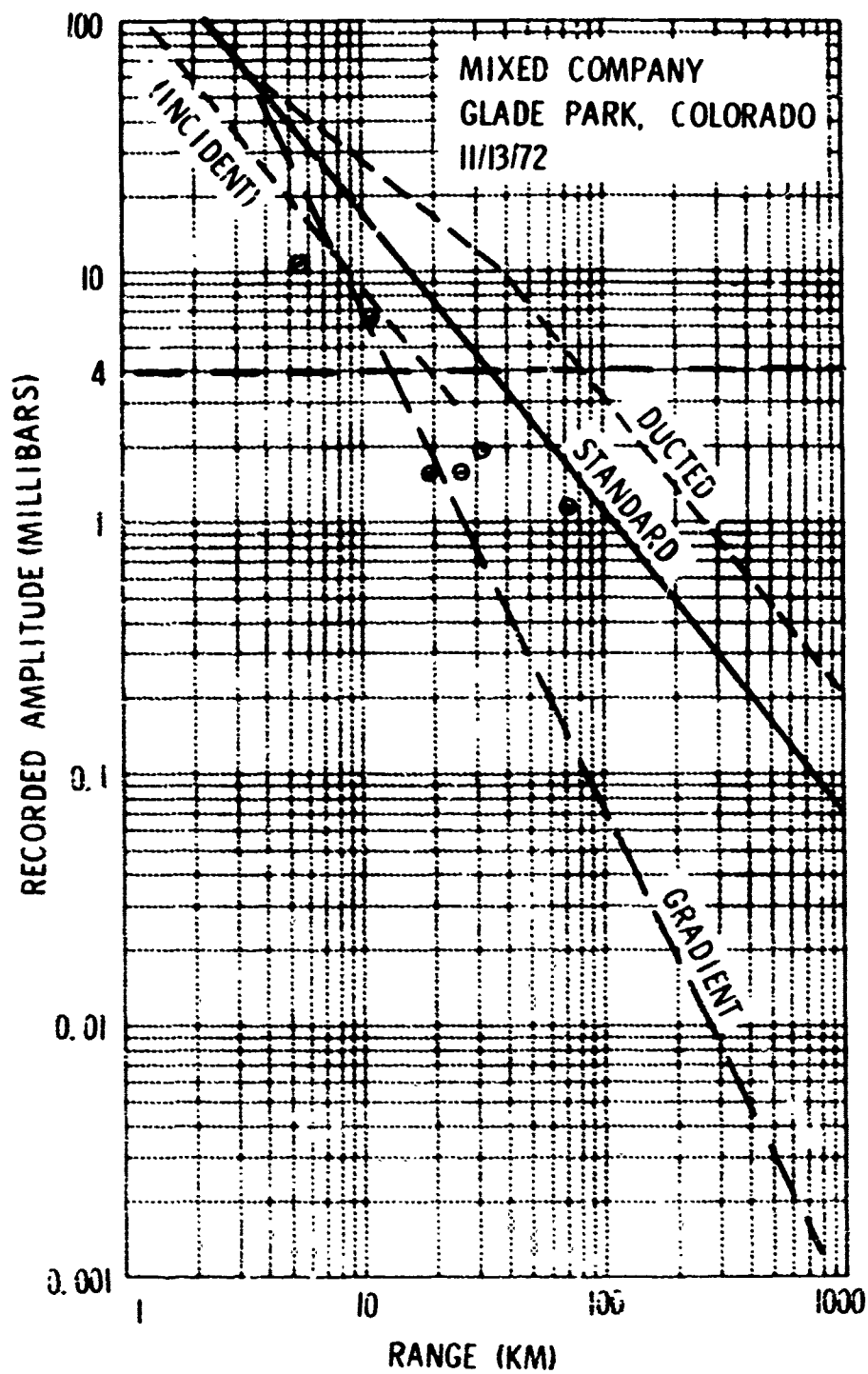
PEAK AMPLITUDES FROM 500-TON HE TEST

FIGURE 13
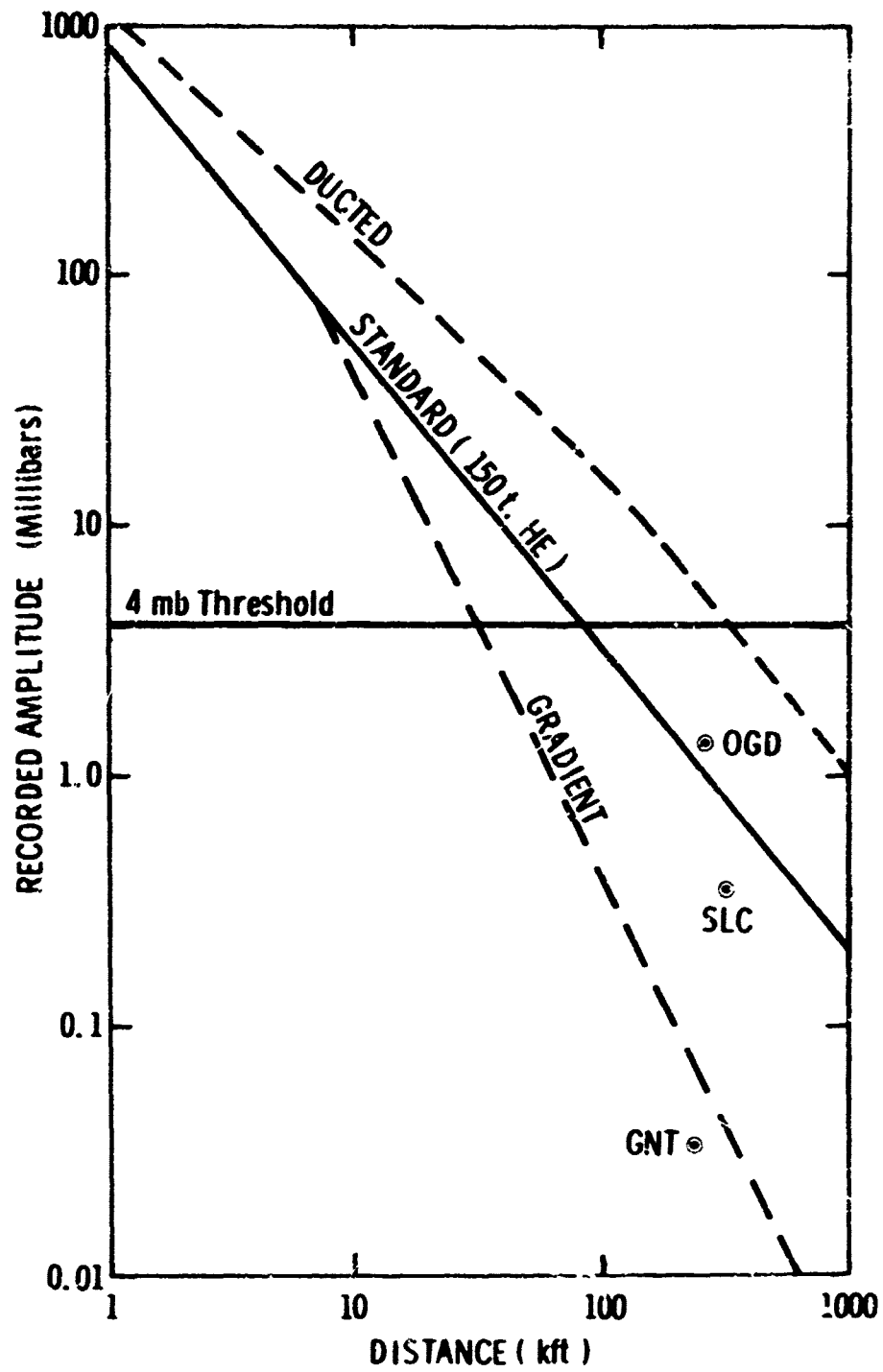
FIG. 14 TOOELE - HILL TEST
3 FEB. 1973
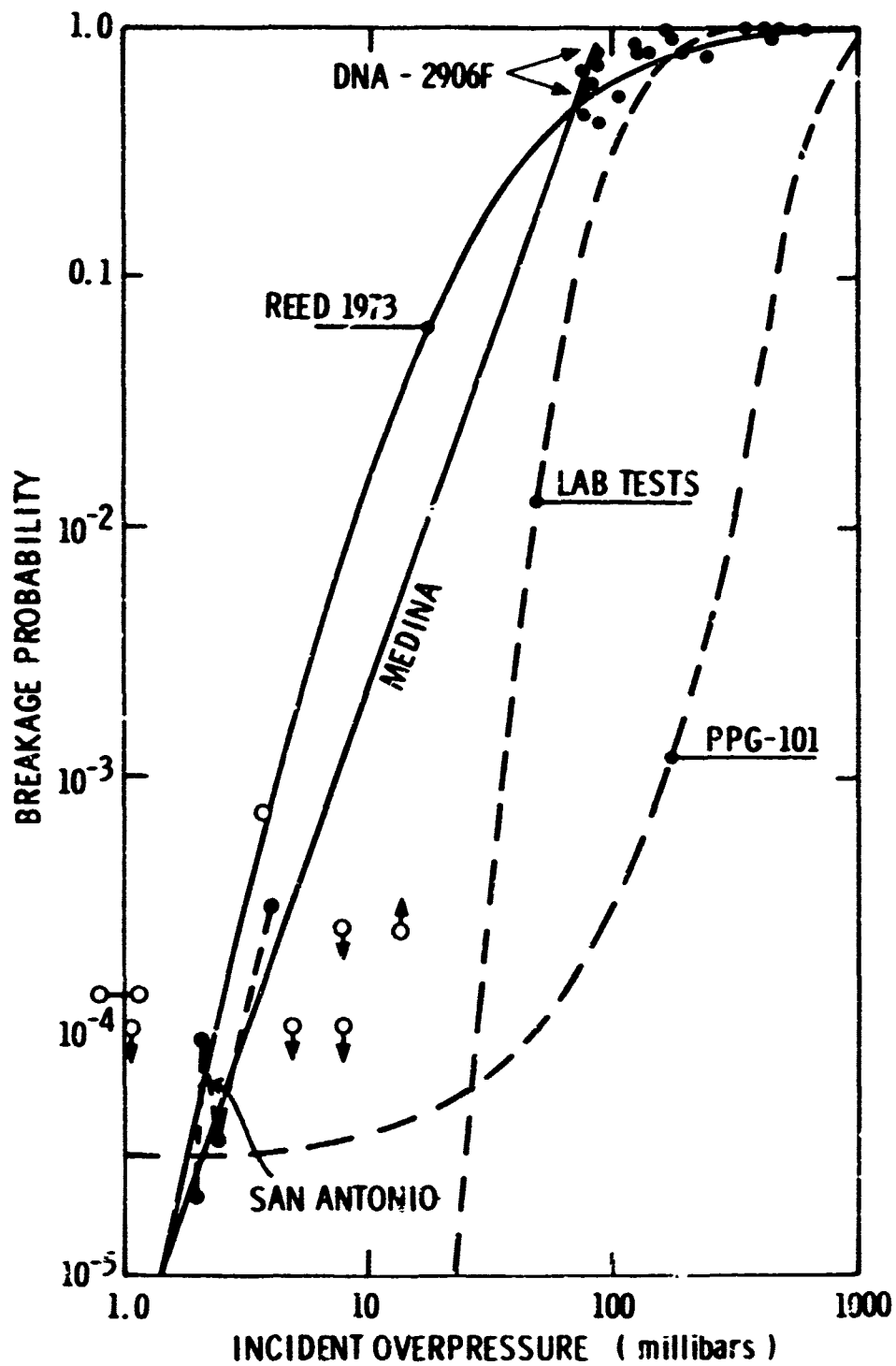
FIG. 16   WINDOW BREAKAGE FROM
AIRBLAST, THEORY & DATA

FIG. 15
WINDOW DAMAGES

DAMAGE PROBABILITY

$$P = 3.71 \times 10^{-6} \, (A \, ft^2)^{1.22} \, (\Delta p \, mb)^{2.78}$$

NUMBER OF BROKEN PANES

$$Q = 1.3 \times 10^{-4} \, N \, (\Delta p \, mb)^{2.78}$$

$$N = \text{Population (people)}$$

From: Medina Base Accident, November 1963,
San Antonio, Texas

FIG. 17

NEW WINDOW DAMAGE EQUATION

$$\Delta p \, (50) = 75 \times (2.5)^{\pm 1} \, mb$$

$\Delta p \, (50) : 50\% \, \text{Breakage Overpressure}$

$\text{Log Normal} \, \sigma = \text{Log}_e \, (2.5)$

An Investigation of the Sound Pressure Levels
Produced Around Bombproofs

by

Michael M. Swisdak, Jr.
Naval Ordnance Laboratory
Silver Spring, Maryland 20910

A major concern with any test involving high explosives is the effect of the test on the environment--both from the aspect of safety and from the aspect of noise "pollution". This study will describe some of the results of ? continuing program whose chief purpose is to investigate and reduce the noise and hazards produced by explosions in bombproofs located on the grounds of the Naval Ordnance Laboratory.

Currently, NOL operates 5 bombproofs. These are listed in Figure 1. Also shown in this figure are some of the salient features of each building. Building 324 is considered a "Typical" bombproof, so its construction will be examined in more detail. Figure 2 shows the configuration of this building. The actual test chamber is 10' x 15' x 8 1/2', with three viewports for camera observation. The walls of the test chamber are protected from fragments by 1-inch armor plate backed by 1 5/8-inch wood. A four-foot wide labyrinth leading out of the test chamber prevents fragments and blast from having a direct path to the outside. The heavy steel door in the labyrinth closes a 16.6 square foot vent area and encloses a total internal volume of 2,010 cubic feet. All walls, ceilings, and flooring in the test chamber are two-foot thick reinforced concrete (Ref. (1)).

Two distinct problems are involved in this study: (1) possible hearing damage to individuals located within a small radius (about 100-200 ft) of the bombproof and (2) long-range (several thousand feet) annoyance of the neighborhood surrounding the NOL grounds.

To help control the amount of noise produced by explosive tests, NOL has devised a "Noise Control System", which is outlined in Figure 3. Any firing of 1/2 pound or more of explosive in an unsealed bombproof must go through this system. Before a firing is approved, both the wind speed/direction and temperature are checked. For firing approval to be given the wind must be less than 5 mph from the N.E.-N.W. quadrant or less than 15 mph from the remaining directions. The lapse rate must be at least 2°F/100 ft. A temperature inversion, the opposite of a lapse, can result in the focusing and enhancement of the noise at locations outside NOL.

In spite of these precautions, complaints of excessive noise and vibration caused by our bombproof tests have been, and still are, being received from some of the neighboring private homes. NOL is completely surrounded by residential developments, consisting largely of single-family dwellings. Figure 4 is a map of NOL and its surroundings. The explosives test area is indicated as well as the general areas of complaint. At this point, it might well be advisable to put up some bench marks so that we can judge the results of our explosion tests. Threshold window damage can occur at 0.03 psi (Ref. (2)). The Bureau of Mines "recommended safe airblast pressure level for window breakage" is 0.5 psi (Ref. (3)). The Bureau of Mines also recommends as safe a level of 2 inches/second particle velocity. If the observed particle velocity exceeds this level in any of the three orthogonal components, there is a reasonable probability that damage will occur to residential structures. Under current government regulations (Ref. (4)) the maximum permissable level of any single impact noise is 140 dB (.03 psi) peak sound pressure level. If pressures are of this magnitude some form of hearing protection is necessary or loss of hearing can occur.

In 1966, NOL, in conjunction with the U.S. Bureau of Mines, made a series of measurements at a private residence which is located some 3000 feet from the bombproof, Building 314. The measurements consisted of airblast and three-component particle velocity. The airblast measurements were made outside the house, at the front and at the rear. They consisted of both pressure-time records and peak noise (recorded with a sound level meter equipped with an impact noise analyzer). The particle velocity gages were located in the center of the living room floor. Both the airblast and particle velocity data were recorded on a portable oscillograph. The noise source consisted of 4.5 pounds of pentolite detonated in Building 314. The results of these measurements are summarized in Figure 5. For comparison purposes, an additional test was included. This was the "heel drop" test. The "heel drop" test was conducted in the living room of the test residence. Oscillograph records were made of the response of the seismic gages to a man standing at the center of the room, rising on his toes and allowing his weight to drop on his heels. The peak amplitudes of the particle velocity gages on the heel drop are about 3 times as high as the amplitudes recorded on the explosion test. To bring the airblast results into the realm of the commonplace, another type of comparison test was also conducted. The sound level measured seven feet from the slamming of the front door on a Dodge sedan was the same level as that indicated in Figure 5 (Ref. (5)).

In 1969, a detailed study of the typical bombproof shown in Figure 1 was begun. Airblast measurements were included in this study with gages located 100 feet from the charge. The charge weights used were varied between 1 and 5 pounds, and the bombproof door was open, closed, and partially closed. Figure 6 summarizes the airblast results from this test. The overall findings of this study can be summarized as follows:

(1) For charge weights between 1 and 5 pounds, the effect of totally closing the chamber was to reduce the airblast pressures measured 100 feet from the charge by an average of 22.8 dB (Ref. (1)).

(2) The installation of heavy steel doors on bombproofs should eliminate all noise and vibration complaints from neighboring private home owners.

(3) Anyone within a 100-foot radius of this building at the time of an explosive firing should be required to have some form of hearing protection.

This present study has sought the answer to two other aspects of the noise problem: (1) what is the propagation law for the disturbance and (2) how do the sound pressure levels vary with charge weight at a fixed distance? Figure 7 is a synopsis of this present study. The charges were all pentolite cylinders and were initiated by means of an Engineer's Special Detonator.

Two types of airblast instrumentation were used in this study. The primary system consisted of B&K microphones and Celesco Corporation blast pressure transducers hard-wired into a magnetic tape recorder. The signals were played back on a Midwestern oscillograph. The frequency response of the system was 20 hz to 10 Khz. The secondary system consisted of General Radio Sound Level Meters equipped with Impact Noise Analyzers.

Measurements were made at four locations--three on NOL property, and the fourth at a private residence. The station at the private residence was equipped with a sound level meter/ impact noise analyzer.

Multiple-peaked records were obtained at each position on almost every shot. Figure 8 contains tracings from one shot and is typical of the type of records obtained on all the shots. In each case, the noise pulse begins as a well-defined series of shock waves and is degraded into what appears to be a damped sinusoid.

Figures 9-15 are plots of the pressure-distance data recorded for each bombproof. Straight lines have been fitted to the "far-field" data. The data taken at the private resistance are shown in these figures but have not been included in the straight line fit calculations. The author felt that these points should not be included in the fit because they would overly influence the results while themselves being strongly influenced by both the roughness of the terrain and the local meteorology. One assumption which has been made is that the pressure-distance decay slopes are independent of the charge weight for fixed door configurations in each bombproof. It is obvious from these plots that each bombproof appears to behave differently. Each has a characteristic pressure-distance decay slope and a pressure-charge weight scaling relationship. The decay slopes and weight-scaling exponents (scaled distance is obtained by dividing the distance by the charge weight raised to some appropriate exponent) are reported in Figure 16. With the exception of Bldg. 314, the decay is steeper than that caused by spherical spreading (R^{-1}). In Bldg. 314, for both the door open and door closed conditions, the decay was approximately that expected in the spreading of acoustic waves ($R^{-0.93}$ and $R^{-1.1}$).

The "noisiness" of the bombproofs can be characterized in at least two ways. The first is for a fixed charge weight, for example 2 lb, with the sound pressure level measured at a fixed distance (1000 feet in this example). The second method is to again use a fixed charge size (2 lb), and to measure the sound pressure level at the nearest non-government property line. The results of these calculations are presented in Figures 17 and 18. Thus, without a door, Bldg. 314 is the noisiest, while with a door, it is the next to the quietest. The door on Bldg. 324 produces a similar drop in the noise level.

In order to quantify the effect of doors on the sound pressure levels generated by bombproofs, let us define an attenuation or insertion loss, which is the difference in the sound pressure levels (in dB) between the door open operation and the door closed operation, for a given charge size, measured at the same distance. Because the decay rates are nearly the same for the door open and door closed operations in Bldg. 314, the attenuation will not vary appreciably with distance. For a 2-lb charge, the insertion loss is 33.4 dB, while for a 4-lb charge it is 40.3 dB. In Bldg. 324, the door open and door closed decay slopes do vary greatly, so that the attenuation for this building will vary with distance. This is shown in Figure 19, which is for both 2- and 4-lb charges in Bldg. 324.

1428

As a partial check on the data reported in this work, let us compare it with available previous results. For a 2-lb charge at 100 feet from Bldg. 324, Proctor (Ref. (1)) reports a pressure of 0.172 psi with the door open and 0.013 psi with the door closed. We measured 0.23 psi and 0.0119 psi under the same conditions. The maximum pressure reported by Sadwin and Swisdak (Ref. (6)) at a distance of 100 feet from Bldg. 331 was 0.36 psi for a 2-lb charge. We measured 0.56 psi under the same conditions. Reference (7) reports a peak of 132.5 dB (1.25×10^{-2} psi) at a position close to our third position for 2 lb fired in Bldg. 314 with the door open. At a nearby position we measured 134.5 dB (1.5×10^{-2} psi), and at a comparable distance (600 ft), Figure 9 indicates a pressure of 1.8×10^{-2} psi.

In summary, each bombproof behaves differently and should not be lumped together with any other bombproof. The observed far field sound pressure levels generally decay faster than acoustic waves subjected to spherical spreading only. The effect of a door on the noise produced by bombproofs seems to vary with the individual structure. As these tests have indicated there were no combinations of charge size and bomb-proof which even produced airblast pressures approaching those needed to cause threshold window damage (0.03 psi). However, the psychological results of these tests can be quite distressing. The sound level at 0.001 psi compares with the sound generated at 2 feet from a trumpet, auto horn, or automatic punch press. No amount of objective data can convince a person who is startled by a sudden sharp blast that the actual air blast pressures correspond to those of something as mundane as an auto horn. (Ref. (3)) Personal contact and public relations help alleviate the problem but convince few.

The only solution is to keep the airblast and vibration levels as low as possible (i.e., well below the safe levels) and to take as many measures as practical to further reduce the noise. These measures can include any or all of the following: (1) meteorological observations--don't conduct the tests under indicated conditions of ray focussing or enhancement, (2) close the test chamber, if possible, and (3) use the surrounding terrain to your advantage--trees and shrubs can help reduce the pressures in waves passing over them.

REFERENCES

1. Proctor, J. F., "Structural Analysis of NOL Explosion Test Facilities", NOLTR 69-84, 24 April 1969 (U)

2. Reed, J. W., et al, "Evaluation of Window Pane Damage Intensity in San Antonio Resulting from Medina ₋acility Explosion on November 13, 1963", Annals of the New York Academy of Sciences, Vol. 152, Article 1, 28 Oct 1968 (U)

3. Nicholls, H.R., Johnson, C. F., and Duvall, W. E., "Blasting Vibrations and Their Effects on Structures", U.S. Bureau of Mines Bulletin 656, 1971 (U)

4. "Primer of Plant-Noise Measurement and Hearing Testing", published by General Radio Company, 1971 (U)

5. Sadwin, L. D., "Memorandum to Code 241, Subj: "NOL Produced Explosion Noise at 10803 Bornedale Drive, Airblast and Seismic Measurements", dated 21 Dec 1966 (U)

6. Sadwin, L. D. and Swisdak, M. M., Memorandum, Subj: "Bombproof Tests at Bldg. 331 of 29 August 1970", dated 29 Aug 1970 (U)

7. Johnston, T. F., Code 221 memo to NOL Files, Subj: "Explosion Noise Tests of 14 Sep 1971", 20 Sep 1971 (U)

FIGURE 1. OPERATIONAL BOMBPROOFS AT NOL

BUILDING NUMBER	TYPE OF CLOSURE	BUILDING VOLUME (ft^3)
314	DOOR	1750
317	NONE	1100
324	DOOR	2010
325	NONE	1560
331	NONE - HAS A CHIMNEY-MUFFLER	1200

Figure 2   **CONFIGURATION OF TYPICAL BOMBPROOF**

VOLUME ENCLOSED WITH
DOOR CLOSED = 2010 FT³

VENT AREA WITH DOOR
OPEN = 16.6 FT²

STEEL DOOR

C.C.C. PRESSURE GAGE

CAMERA PORT

4' TYP

5'

4.5'

10'

EXPLOSIVE

A

2' TYP CONCRETE

A

ACCELEROMETERS

CAMERA PORT

PLAN

21'

EXPLOSIVE

8.5'

4'
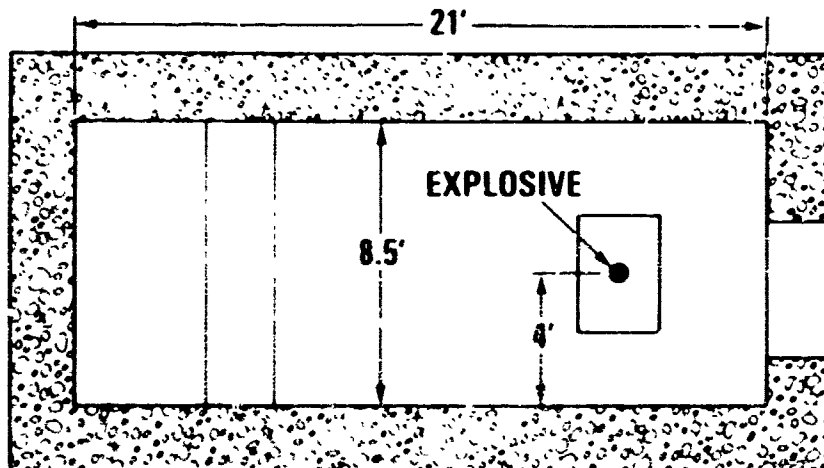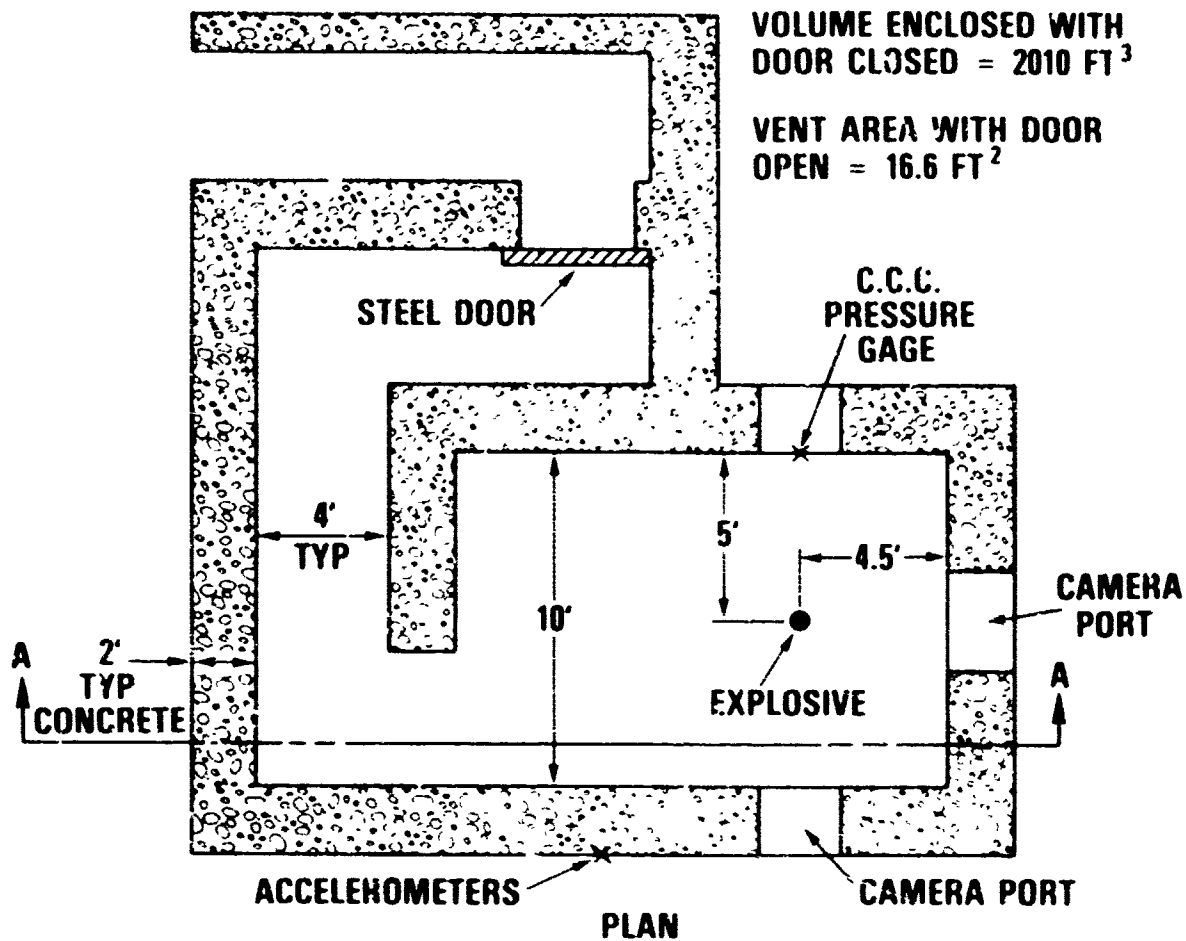
SECTION A-A

Figure 3

NOISE CONTROL SYSTEM
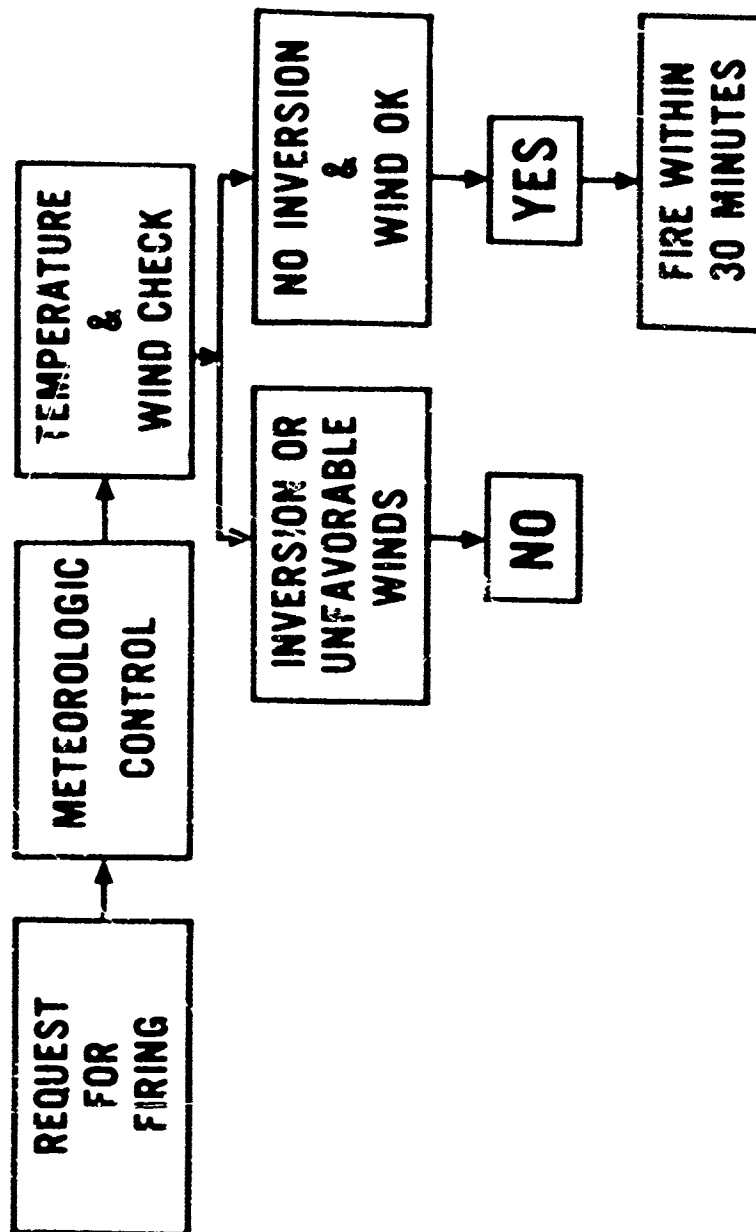
FIGURE 4. NOL AND ITS SURROUNDINGS
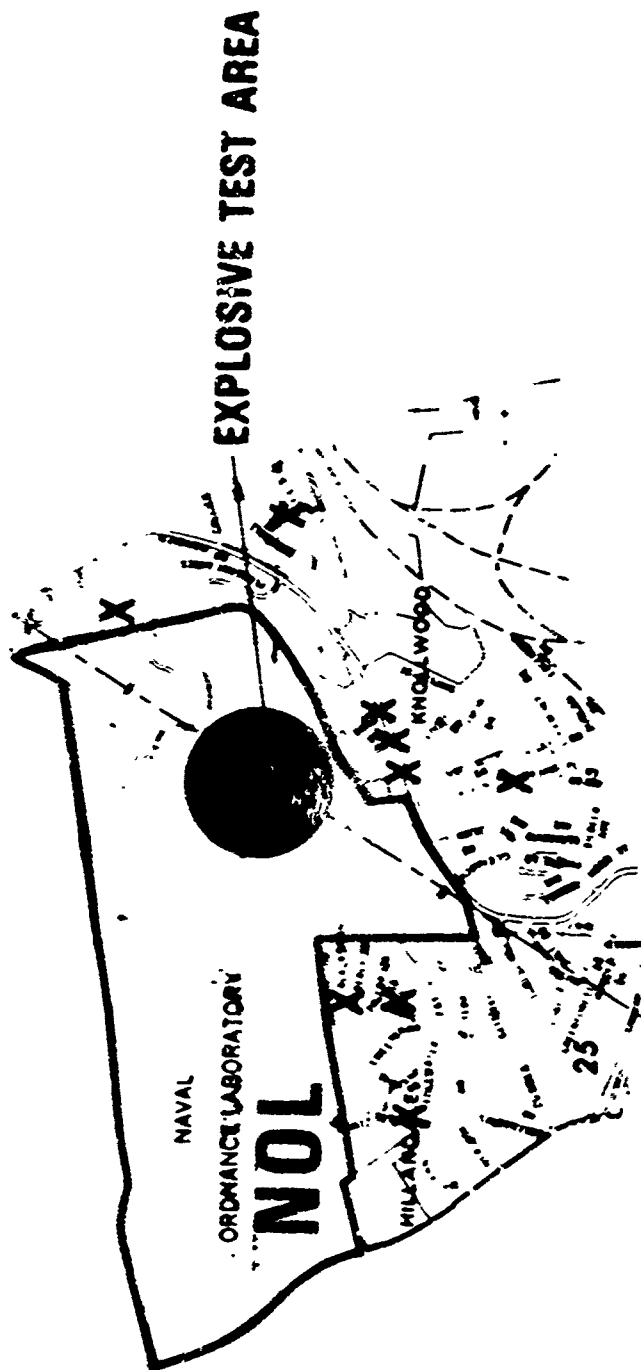
Figure 5

RESIDENCE TEST
(NOV. '66)

- 4½ LB EXPLOSIVE IN BOMB PROOF
- MEASUREMENTS AT 3000 FT DISTANCE

AT HOUSE

BLAST PRESSURE	0.0007 PSI (MAX)
FLOOR VIBRATION	0.046 IN/SEC (MAX)
(HEEL DROP FLOOR VIBRATION)	0.16 IN/SEC (MAX)

FIGURE 6. SOUND PRESSURE MEASUREMENTS OUTSIDE BUILDING 324

CHARGE WEIGHT (POUNDS)	DOOR	AVERAGE OVERPRESSURE AT 100 FEET (psi)
1	OPEN	8.43×10^{-2} (149.2)*
1	CLOSED	5.6×10^{-3} (125.7)
2	OPEN	1.72×10^{-1} (155.4)
2	CLOSED	1.27×10^{-2} (132.8)
5	OPEN	3.15×10^{-1} (160.7)
5	CLOSED	2.41×10^{-2} (138.3)

*NUMBERS IN ( ) ARE PRESSURES IN dB, RE: 2×10^{-5} N/M^2

FIGURE 7. SUMMARY OF TEST PROGRAM

BUILDING	DOOR	CHARGE WEIGHT AND SIZE			
		0.5 LB 2 x 2.68*	1.0 LB 2 x 5.36*	2.0 LB 4¼ x 2.37*	4.0 LB 4¼ x 4.74*
314	OPEN			X	X
314	CLOSED			X	X
317	NONE	X	X		
324	OPEN			X	X
324	CLOSED			X	X
325	NONE	X		X	
331	MUFFLER	X		X	

*DIAMETER X LENGTH (BOTH IN INCHES)

Figure 8

REPRESENTATIVE WAVE FORMS FROM FIRING
2 POUNDS OF EXPLOSIVE IN BLDG. 325

0.68
psi

93 FEET

$\longmapsto$ 10 msec

5.73×10^{-3}
psi

750 FEET

$\longmapsto$ 10 msec

3.72×10^{-3}
psi

1,400 FEET

$\longmapsto$ 10 msec

143
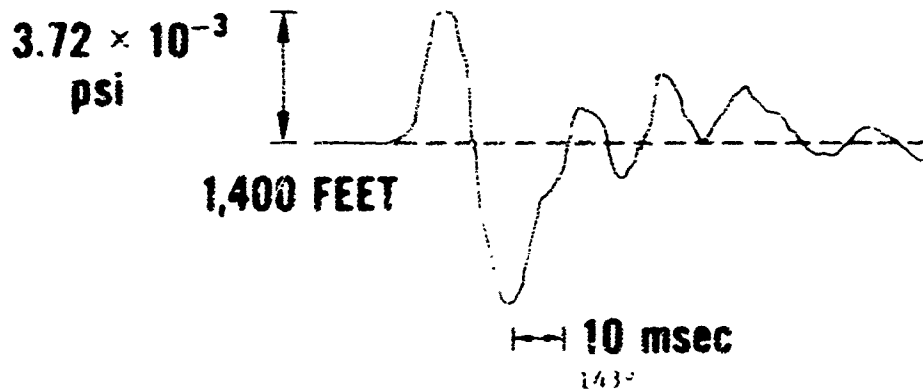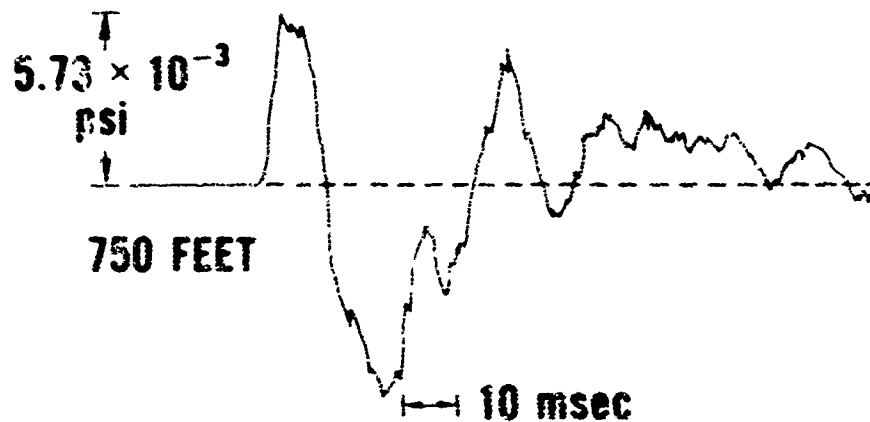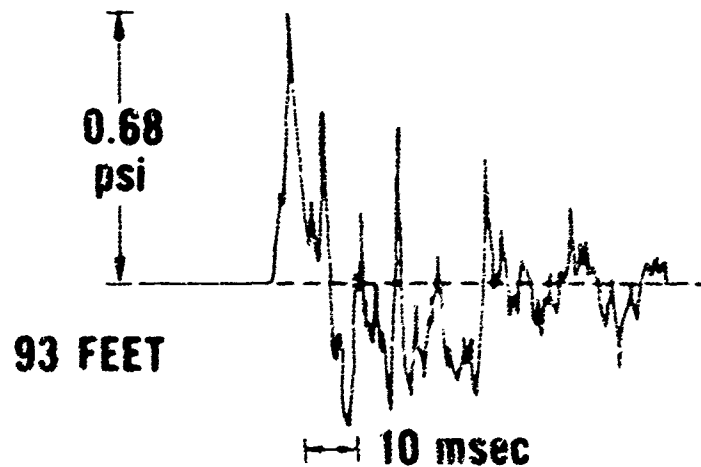
Figure 9

PRESSURE VS DISTANCE FOR BLDG. 314 WITH DOOR OPEN FOR TWO CHARGE WEIGHTS

14 14
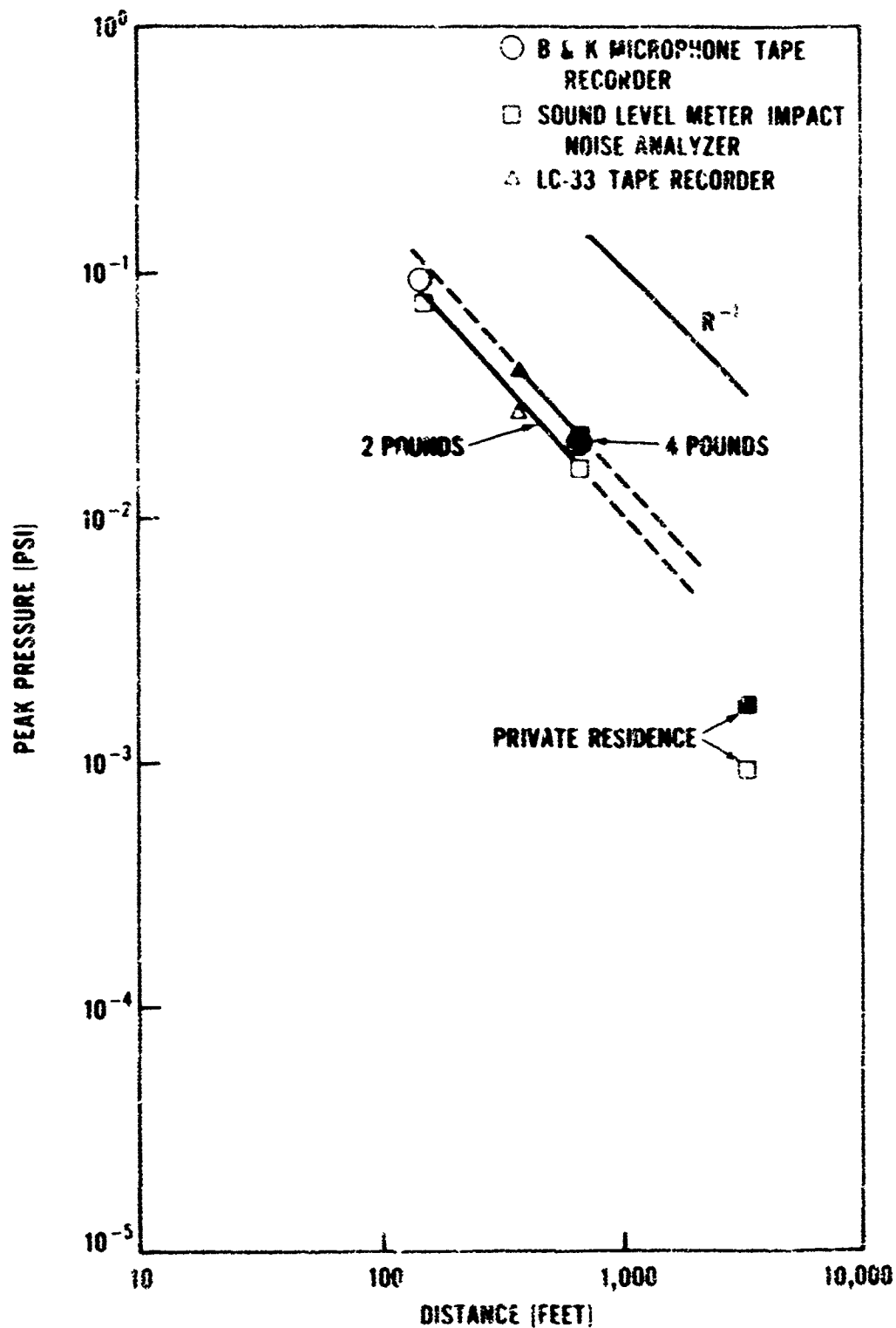
Figure 10

PRESSURE VS DISTANCE FOR BLDG . 314
WITH DOOR CLOSED FOR TWO CHARGE WEIGHTS
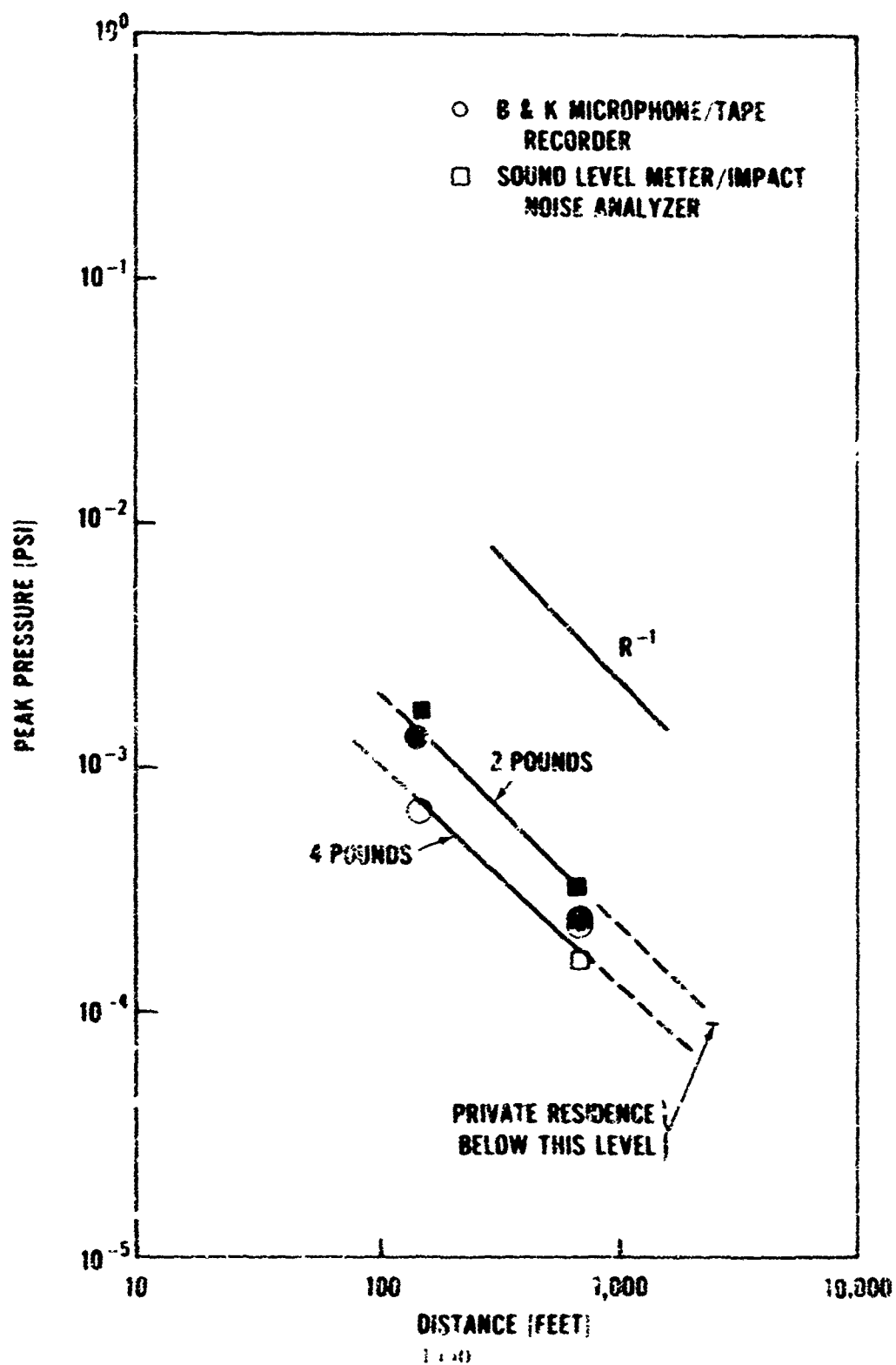
Figure 11

PRESSURE VS DISTANCE FOR BLDG. 317
FOR TWO CHARGE WEIGHTS

o B & K MICROPHONE/TAPE
  RECORDER
□ SOUND LEVEL METER/IMPACT
  NOISE ANALYZER
△ LC-33/TAPE RECORDER

1 POUND
½ POUND
R^{-1}

PRIVATE RESIDENCE
(BOTH CHARGE SIZES)

PEAK PRESSURE (PSI)
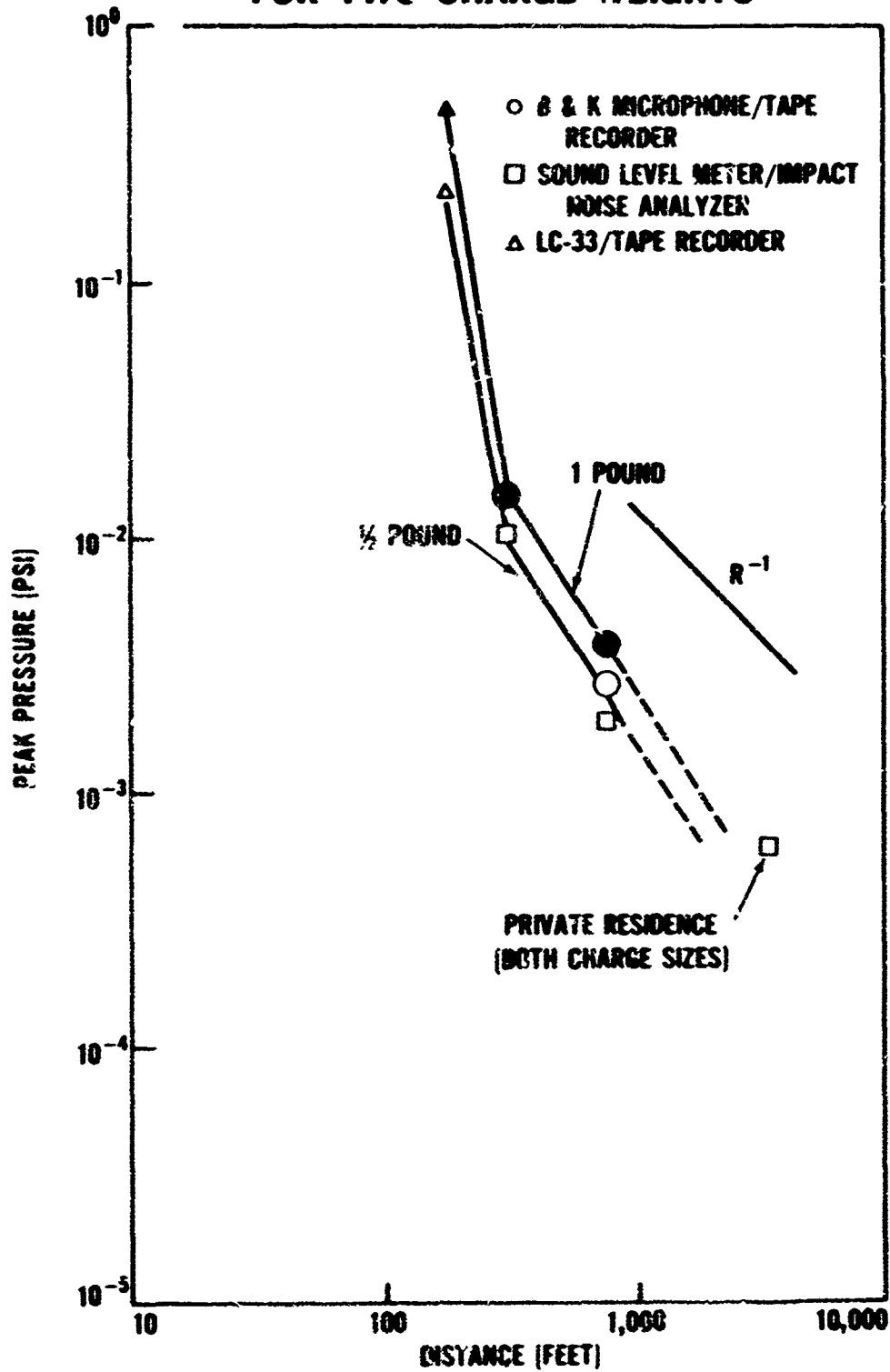
DISTANCE (FEET)

Figure 12

PRESSURE VS DISTANCE FOR BLDG. 324 WITH DOOR OPEN FOR TWO CHARGE WEIGHTS
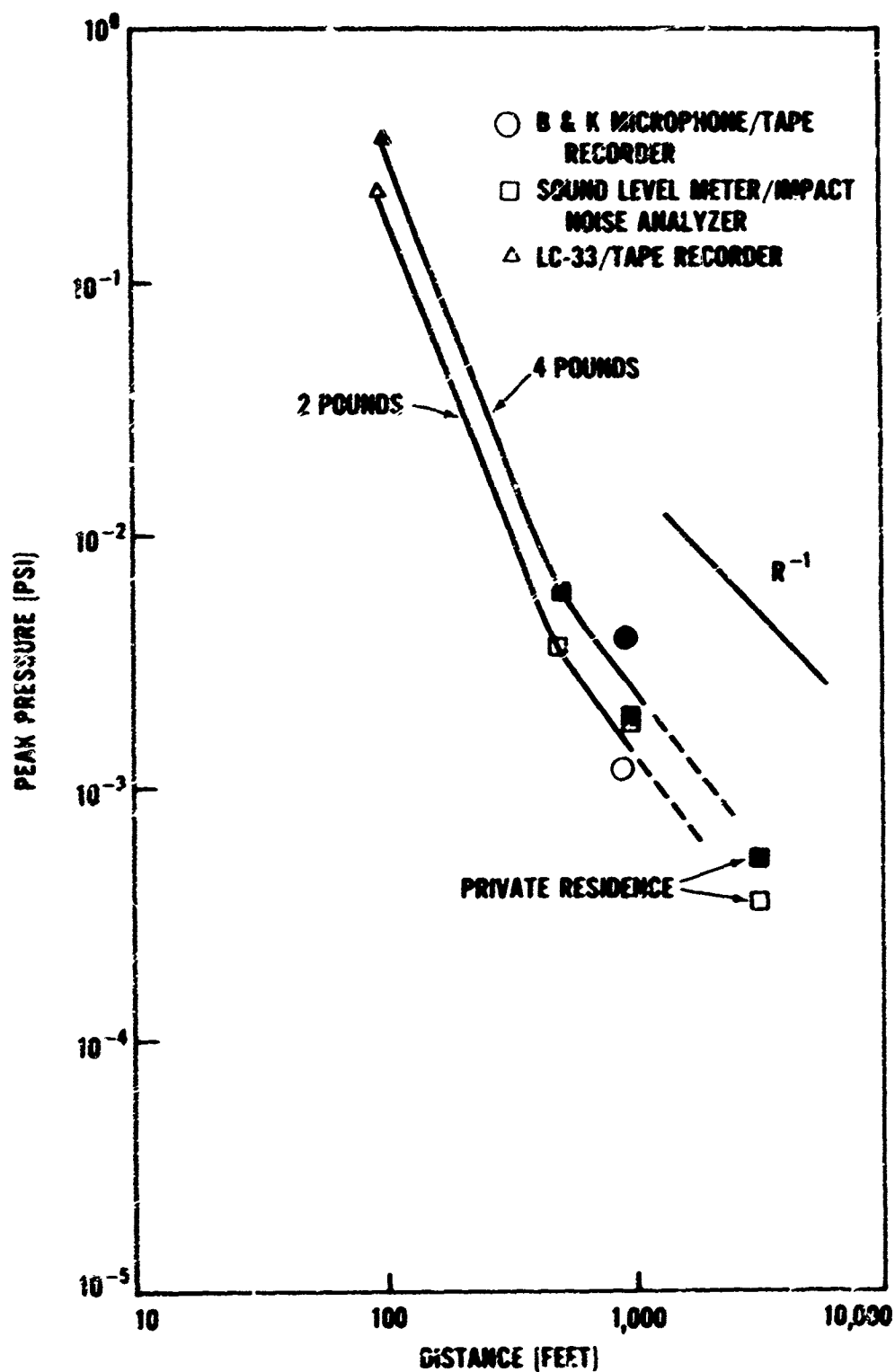
Figure 13

PRESSURE VS DISTANCE FOR BLDG. 324 WITH DOOR CLOSED FOR TWO CHARGE WEIGHTS

Figure 1

PRESSURE VS DISTANCE FOR BLDG. 325
FOR TWO CHARGE WEIGHTS

1444
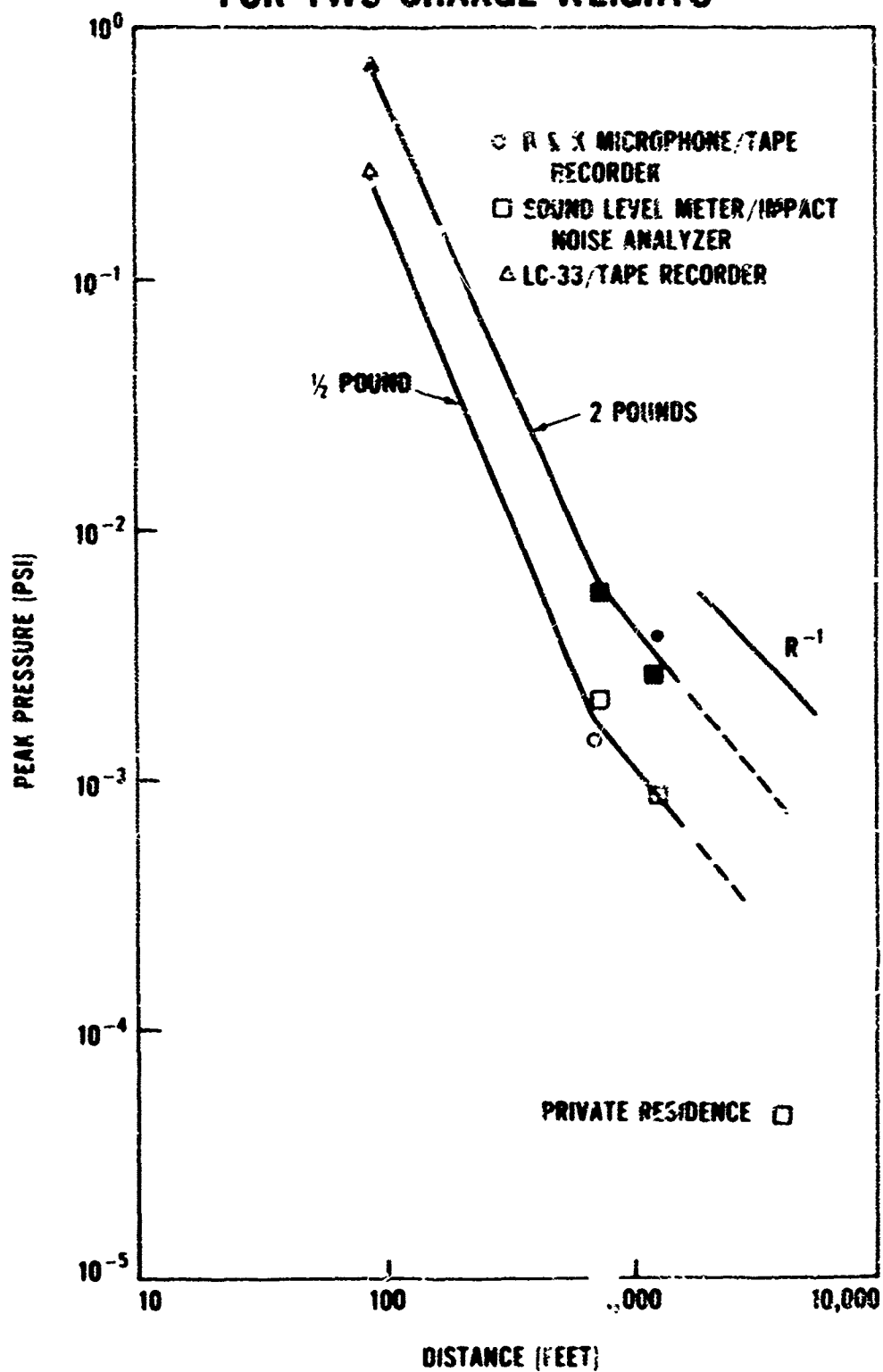
Figure 15

PRESSURE VS DISTANCE FOR BLDG. 331
FOR TWO CHARGE WEIGHTS

PEAK PRESSURE (PSI)

DISTANCE (FEET)

○ B & K MICROPHONE/TAPE RECORDER

□ SOUND LEVEL METER/IMPACT NOISE ANALYZER

△ LC-33/TAPE RECORDER

2 POUNDS

½ POUND

R^{-1}

PRIVATE RESIDENCE □
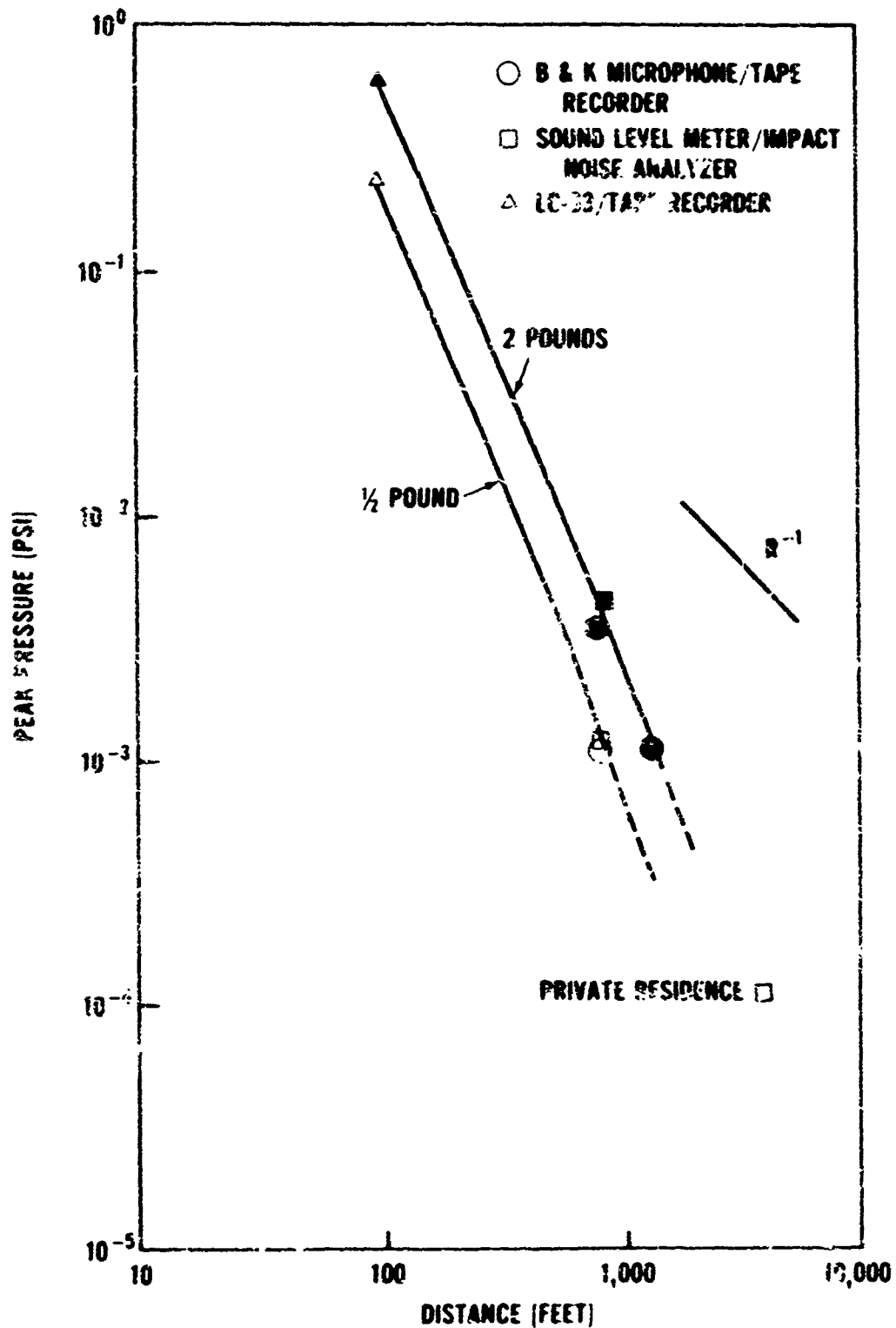
DECAY SLOPES AND WEIGHT SCALING EXPONENTS

BUILDING	DOOR	FAR FIELD PRESSURE VS DISTANCE [1] DECAY SLOPE (x)	FAR FIELD WEIGHT SCALING [2] EXPONENT (n)
314	OPEN	-1.1	0.64
314	CLOSED	-0.93	0.28
317	NONE	-1.54	0.67
324	OPEN	-1.3	0.76
324	CLOSED	-2.25	0.60
325	NONE	-1.22	0.69
331	MUFFLER	-2.74	0.38

(1) FOR $P^+_{max} \sim R^x$, WHERE P^+_{max} IS THE PEAK POSITIVE PRESSURE (psi) AND R IS DISTANCE IN FEET.

(2) FOR SCALING OF THE FORM $P^+_{max} \sim R/W^n$, WHERE P^+_{max} AND R ARE THE SAME AS ABOVE AND W IS THE CHARGE WEIGHT IN POUNDS.

Figure 17

NOISINESS RANKING FOR 2 POUND CHARGES AT 1,000 FEET

BUILDING	DOOR	PEAK PRESSURE (psi)	(dB)	NOISINESS RANKING (1 = LOUDEST)
314	OPEN	1.01×10^{-2}	130.9	1
314	CLOSED	2.22×10^{-4}	97.7	6
317	NONE	5.8×10^{-3}	126.1	2
324	OPEN	1.49×10^{-3}	114.3	5
324	CLOSED	4.72×10^{-5}	84.2	7
325	NONE	4.18×10^{-3}	123.2	3
331	MUFFLER	2.36×10^{-3}	118.3	4

Figure 18

NOISINESS RANKING FOR 2 POUND CHARGES AT NEAREST NON-GOVERNMENT PROPERTY

BUILDING	DOOR	DISTANCE (FT)	PEAK PRESSURE (psi)	(dB)	NOISINESS RANKING (1 = LOUDEST)
314	OPEN	810	1.29×10^{-2}	133.0	1
314	CLOSED		2.72×10^{-4}	99.5	6
317	NONE	990	5.8×10^{-3}	126.1	2
324	OPEN	1220	1.17×10^{-3}	112.2	4
324	CLOSED		3.12×10^{-5}	80.7	7
325	NONE	1390	2.78×10^{-3}	119.7	3
331	MUFFLER	1570	6.5×10^{-4}	107.1	5

Figure 19

ATTENUATION INTRODUCED BY DOOR VS DISTANCE FOR BLDG. 324
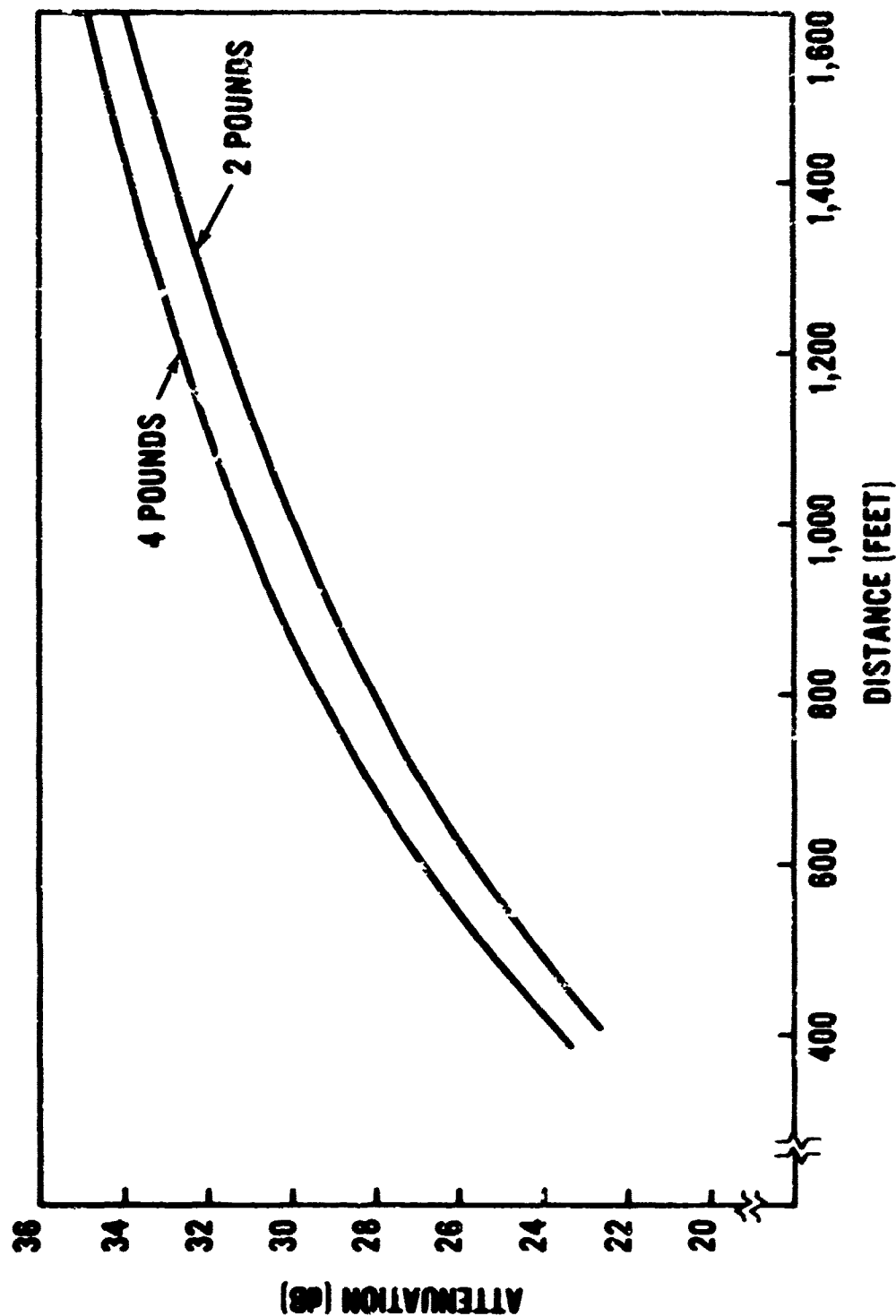
SAFE DISTANCES FROM UNDERWATER EXPLOSIONS

Donald R. Richmond
Lovelace Foundation for Medical Education & Research
Albuquerque, New Mexico 87108

Introduction

The purposes of this paper are (1) to summarize the results of tests run to determine how the biological effects of underwater blast fall off with range in the far field from small charges, and (2) to present a tentative underwater-blast safety criterion for unprotected swimmers based on the results of the animal experiments and information gained from volunteer swimmers.

The only safety criterion existing today for unprotected personnel in the water is--get out of the water during the explosion. Although there is some information on the response of personnel clothed in diving gear, summarized in reference 1, data for unprotected swimmers are notably meager. Since volunteer swimmers were at such great distances from underwater explosions and conditions were not well documented, the findings were of limited use (references 1 through 3).

The Naval Ordnance Laboratory—Lovelace Underwater Test Facility on Kirtland Air Force Base, New Mexico provided a facility to conduct systematic tests to determine the far-field underwater-blast effects in biological specimens. Tests could be run under carefully controlled conditions wherein the blast-wave parameters were measured precisely with the most up-to-date piezoelectric gages.

The Test Pond Facility

The test pond was 220 by 150 ft and was 30 ft deep over its 30-by 100-ft center portion, figures 1 and 2. The entire pond was lined with black polyvinyl plastic 20 mils thick. A 6-inch-deep layer of sand was located beneath the plastic in the 30-ft-deep portion of the bottom. The sides of the pond had a 2-to-1 slope. Two sets of rigging spanned the pond in a north-south direction. The main rigging, located 80 ft from the west end, consisted of a grid 14 by 24 ft which could be raised and lowered by an electric winch on the south bank. The east rigging was approximately 30 ft from the east end of the pond. Its center grid was 5 by 10 ft and was operated by a hand winch on the south bank. The test pond contained approximately 3.2 million gallons of tap water.

The ambient air pressure at the pond was 12.0 psia.

Test Procedures With Animals

Animals and pressure-time gages were usually slung from beneath the main rigging and the explosive charges hung from a cable that spanned the pond to the east of the rigging. When greater stand-off distances were required, the test specimens and gages were attached to the east rigging and the charges were toward the west end of the pond.

One hundred and one Columbia-Rambouillet female sheep, 37 Dalmatian dogs, and six rhesus monkeys were utilized on these tests.
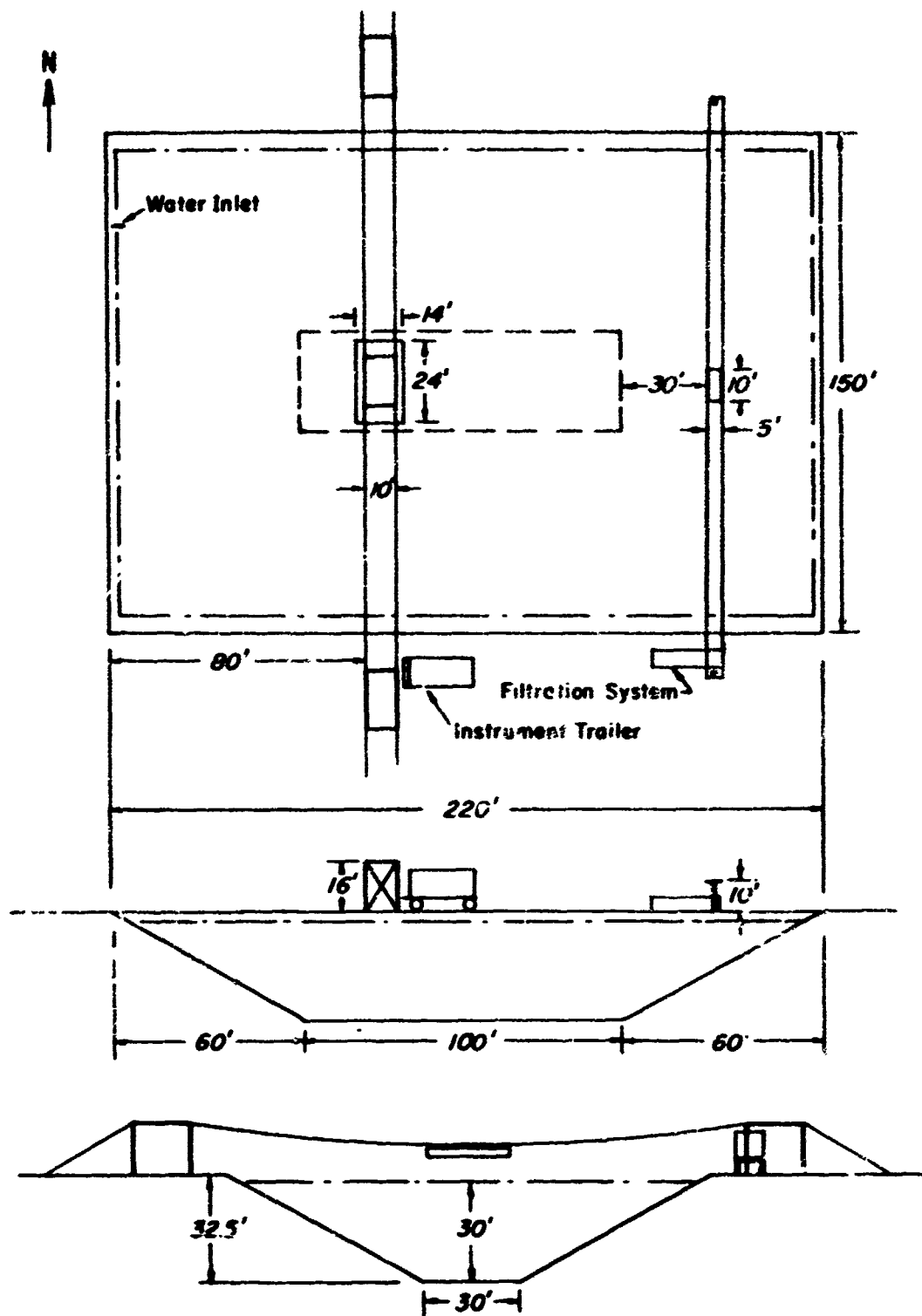
Figure 1. Diagram of Test Pond Facility.

Figure 2. Underwater Test Facility Viewed From the West.

Usually, three animals were tested on each shot at the same range. All the test subjects were mounted vertically in the water (long axis perpendicular to the surface). The depth of the sheep was measured from the water surface to their xiphisternum. Dogs and monkeys were submerged to about their glottis level, shoulders beneath the surface, but were designated as 1-ft depths. All animals were right-side-on to the charge. About one third of the sheep were exposed to underwater blasts at 2- and 10-ft depths.

The life-support system that supplied air to the sheep beneath the water surface consisted of a face mask (made from polyethylene bottles) having an air inlet hose in the side and a one-way outlet valve in the front of the mask. It covered the animal's nose and mouth and was held in place by four strings tied to the back of the head. The compressed air was delivered to the mask via plastic tubing connected to air bottles in series located above the main rigging. When animals were exposed at 10-ft depths, 2 psi was applied to the system once the mask was attached to the animal. The pressure then was increased to 6 psi and the rigging lowered to place the animals at the 10-ft depth. Following the detonation, the animals were returned to the surface within 1 min. All the test subjects were autopsied 2 hours following the blast. At postmortem, the entire length of the G.I. tract was examined carefully. It was slit open, its contents washed out, and the condition of the mucosal lining in the contused areas was recorded.

Eight tests were run with 24 dogs specifically for eardrum response data. Dogs were used because the size and geometry of the

eardrum and middle ear approximate man's more so than other animals. They were oriented vertically in the water with their ears exactly at a 1-ft depth. They were right-side-on to the charge with their right ear facing the charge. In order to maintain the exact position of the head, freshly sacrificed animals were used. After sacrifice, the pinna of the ear was clipped to approximate the size of the human's. To evaluate the extent of ear injury, the middle ear was dissected open form the brain side of the skull and then photographed.

Explosive Charges

The explosive charges used in these experiments were bare spheres of cast Pentolite and 1-lb blocks of pressed TNT. The Pentolite spheres had 5/16-inch-diameter detonator wells. The charges were fired with electric blasting caps, DuPont No. E-99. The charge weights were designated as 0.5 lb, 1 lb, 3 lb, and 8 lb. The actual measured weights of these charges, mean and range, were as follows: 0.5 lb, 0.487 (0.485 to 0.492) lb; 1 lb, 1.052 (1.047 to 1.058) lb; 3 lb, 2.618 (2.608 to 2.626) lb; and 8 lb, 8.373 (8.369 to 8.377) lb. All the charges were detonated at 10-ft burst depths.

Procedures for Measuring Underwater Blasts

There were four channels of pressure-time measuring instrumentation. The methods and equipment used for measuring and recording the underwater-blast wave basically are those described

in references 4 and 5. The pressure-time gages were a recent modification of the NOL gage Type B. Sensing elements of the gages consisted of four 1/4-inch-diameter tourmaline discs mounted in a Tygon® tube filled with silicone oil (Dow-Corning No. 200 dielectric oil). Signals from the gages were passed through a cathode-follower K amplifier unit and recorded on a dual-beam oscilloscope (Tektronix Model 555 with Type D preamplifier plug-in units). To ensure accurate time measurements, timing marks were placed on the oscilloscope with a time-marker generator.

On each trial, recording gages were placed at the same ranges and depths as the animals. Trigger gages were located just upstream from the recording gages so that their signals would initiate the sweep of the oscilloscope.

The system was calibrated by the voltage-step method. A voltage-step generator supplied a known voltage impulse to the system. The calibration voltage step and time markings were placed on separate oscillograph records immediately before each test.

Pressure recordings were enlarged photographically and semilogarithmic plots made for each one. Pressure values were obtained from the records by the following equation:

$$P = \frac{C_s E_c}{KA} \frac{\Delta P}{\Delta V} \qquad (1)$$

P = pressure, psi

C_s = standard capacitance, microfarads

E_c = calibration voltage, volts

ΔP = deflection on record due to pressure

ΔV = deflection on record due to calibration

KA = gage sensitivity, coulombs x 10^{-12}

The KA of the gages was determined at NOL.

A computer program was developed to extrapolate the pressure curve back to one-half the rise time on a particular record to obtain the peak pressure. This added area under the curve was included in the integration for the impulse. The theta and energy parameters likewise were furnished by the computer. In determining the peak pressure in the bottom reflection records, the curves were not extrapolated back to one-half the rise time.

Incident Shock Waves

Pressure-time records showing the pattern of the incident shock waves, at selected ranges, are illustrated in figure 3. These records show that there is little to be desired from the NOL underwater-pressure gages which have the tourmaline crystals inside a Tygon® tube filled with silicone oil. The mean values for peak pressure, impulse, and cutoff time measured at 1-ft depths on the 1-lb charge firings in relation to slant range are plotted in figure 4. The curves in figure 4 are those calculated from these empirically derived equations:

$$P_m = 18300 \left(W^{1/3}/R\right) 1.10 \tag{2}$$

$$\theta = 0.0603 \left(W^{1/3}/R\right)^{-0.168} W^{1/3} \tag{3}$$

$$t_c = \left(\sqrt{R^2 + 4 D_w D_g} - R\right)/C_o \tag{4}$$

Shot No.: 188   Slant Range: 13 ft

Gauge No.	Vertical Scale	Horiz. Scale
3257	565 psi/div	0.1 msec/div
3412	571 psi/div	0.1 msec/div

Shot No.: 199   Slant Range: 60 ft

Gauge No.	Vertical Scale	Horiz. Scale
3414	100 psi/div	0.02 msec/div
3264	100 psi/div	0.02 msec/div

Shot No.: 194   Slant Range: 20 ft

Gauge No.	Vertical Scale	Horiz. Scale
3414	329 psi/div	0.05 msec/div
3264	339 psi/div	0.05 msec/div
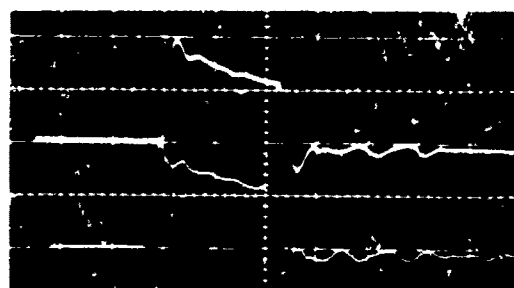
Shot No.: 205   Slant Range: 78 ft

Gauge No.	Vertical Scale	Horiz. Scale
3257	75 psi/div	0.02 msec/div
3412	73 psi/div	0.02 msec/div
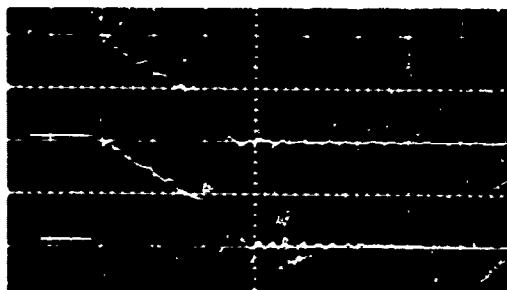
Shot No.: 204   Slant Range: 40 ft

Gauge No.	Vertical Scale	Horiz. Scale
3257	158 psi/div	0.05 msec/div
3412	158 psi/div	0.05 msec/div
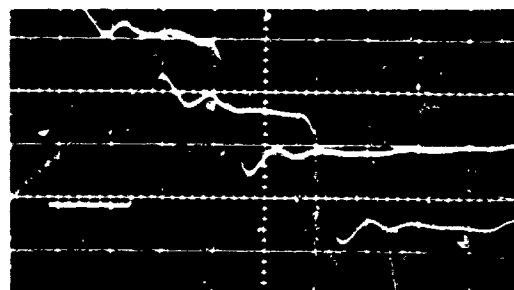
Shot No.: 193   Slant Range: 130 ft

Gauge No.	Vertical Scale	Horiz. Scale
3257	43 psi/div	0.01 msec/div
3412	43 psi/div	0.01 msec/div

Figure 3.   Oscillograms of Incident Shock Waves From 1-Lb
Charges at 10-Ft Depths Recorded by Gages at
1-Ft Depths.
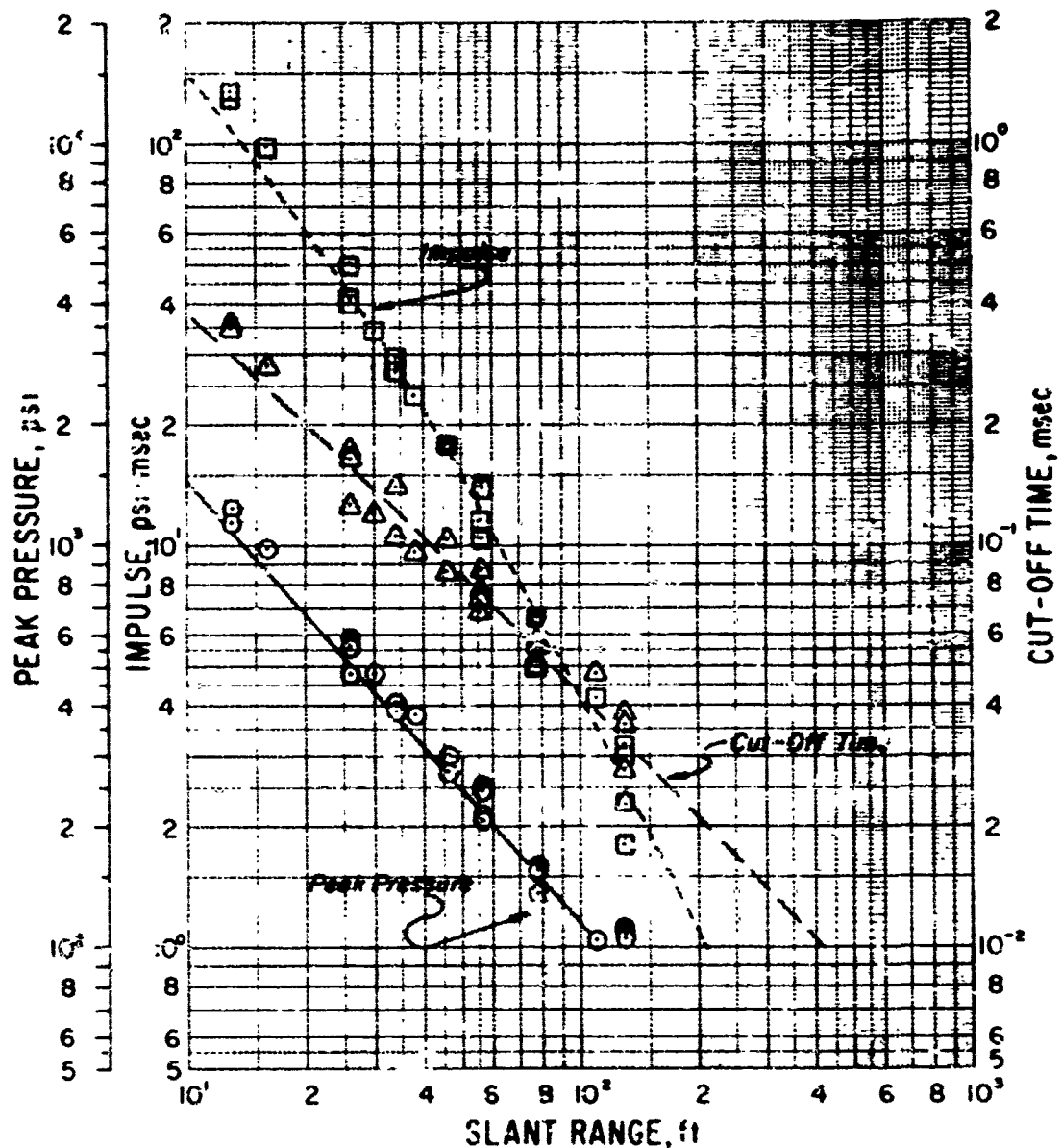
Figure 4. Pressure-Time Parameters in the Incident
Shock Wave at 1-Ft Depths as a Function of
Range From 1-Lb Charges Detonated at
10-Ft Depths. [The data points were
measured: the curves were computed.]

$$I = P_m \theta \left[\frac{9}{11}\left(1 - e^{-\frac{11t_c}{10\theta}}\right) + 1 - e^{-\frac{t_c}{10\theta}} \right]$$ (5)

where W = charge mass, lb; R = slant range, ft; t_c = time of arrival of the surface cutoff wave, msec; θ = time constant, msec; P_m = peak overpressure, psi; I = impulse to cutoff time, psi·msec; D_w = depth of charge, ft; D_g = depth of gage, ft; and C_o = speed of sound in water, 4.75 ft/msec.

As seen in figure 4, the measured data points for peak pressure, impulse, and cutoff time fell closely along the calculated curves. Moreover, there was little variation in the values measured by different gages on a given shot in regard to peak pressure, impulse, and cutoff times. Reference 6 gives pressure-time parameters measured on all the charge firings.

Negative Pressures

The peak negative pressures were read off the records from the preshock baseline to the maximum deflection the trace went below baseline. The magnitude of the negative pressures decreased with increasing slant range. They ranged from 110 to 150 psi at scaled ranges of 17 and 16 ft to 20 to 25 psi at scaled ranges of 140 ft. The negative pressures were of short duration—on the order of 10 μsec, which, in terms of the frequency response of gages, could account for some of the scatter in these measurements.

Bottom Reflections

A limited number of measurements were made of the waves that reflected from the bottom of the pond. The waveforms of these bottom reflections, recorded by gages at 1-ft depths on 1-lb charge firings, are illustrated in figure 5. As seen in the figure, the reflected waves recorded over the 13- to 45-ft ranges were altered markedly from the ideal form that could be expected. The peak pressures were not on the leading portion of the waves. At and beyond the 60-ft range, the reflected waves appeared more normal in their pattern. The peak pressures in the bottom reflected waves were well below the calculated ones within the 45-ft range. Beyond 45 ft they approached theoretical values. Measured impulses in the reflected waves were an order of magnitude below theoretical.

Bottom Reflection Effects

There are several reasons why bottom reflections encountered in the test pond were not significant in regard to adding to the underwater-blast dose that the animals received.

First, based on the response of animals to air blasts having various waveforms (reference 7), the aberrant waveform of the bottom reflection over the ranges out to approximately 45 ft would not be expected to produce damage. Even though these impulses appear rather high in some instances, 10 to 15 psi·msec, the associated peak pressures were low and the peak pressure did

Shot No.: 188   Scale:
Gauge No.: 3414   Vertical: 583 psi/div
Slant Range: 13 ft   Horiz.: 2.0 msec/div
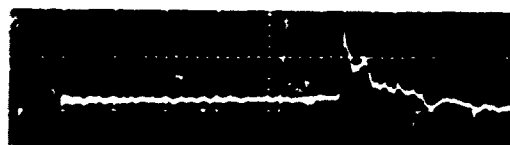
Shot No.: 205   Scale:
Gauge No.: 3264   Vertical: 124 psi div
Slant Range: 56 ft   Horiz.: 0.1 msec/div

Shot No.: 189   Scale:
Gauge No.: 3414   Vertical: 450 psi/div
Slant Range: 16 ft   Horiz.: 2.0 msec/div

Shot No.: 199   Scale:
Gauge No.: 3264   Vertical: 42 psi/div
Slant Range: 66 ft   Horiz.: 0.1 msec/div

Shot No.: 194   Scale:
Gauge No.: 3257   Vertical: 243 psi/div
Slant Range: 20 ft   Horiz.: 2.0 msec/div

Shot No.: 169   Scale:
Gauge No.: 3412   Vertical: 89 psi/div
Slant Range: 66 ft   Horiz.: 0.1 msec/div

Shot No.: 196   Scale:
Gauge No.: 3264   Vertical: 145 psi/div
Slant Range: 40 ft   Horiz.: 0.1 msec/div

Shot No.: 201   Scale:
Gauge No.: 3264   Vertical: 42 psi/div
Slant Range: 80 ft   Horiz.: 0.1 msec/div
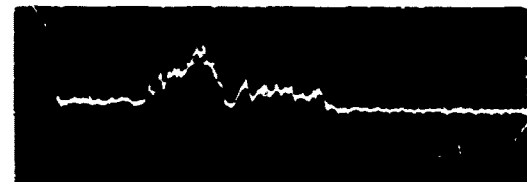
Shot No.: 200   Scale:
Gauge No.: 3264   Vertical: 169 psi/div
Slant Range: 45 ft   Horiz.: 0.1 msec/div
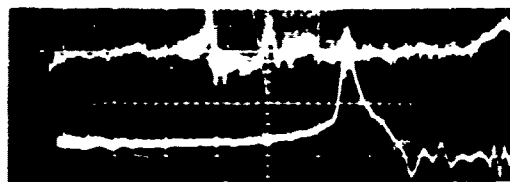
Shot No.: 193   Scale:
Gauge No.: 3264   Vertical: 43 psi/div
Slant Range: 130 ft   Horiz.: 0.05 msec/div

Figure 5.   Oscillograms of Bottom Reflected Waves Recorded by Gages at 1-Ft Depths When 1-Lb Charges Were Detonated at 10-Ft Depths.

not occur at the leading edge of the wave. Beyond 50 ft, the waves were more ideal-like but the peak pressures were low, and, more importantly, the pulses had short durations so that the impulses were small.

Second, if the bottom reflections were to add to the incident blast-wave dose, one could expect to find a rise in the incidence of injuries at ranges that correspond to those where the reflected pressure waves are greater. That is, from 40 to 60 ft, the pressure and impulse in the bottom reflections were the highest; yet the biological effects decreased over those ranges for targets at the 1-ft depths.

Third, some unpublished information exists in this laboratory that suggests that two pulses do not add to the damage effect unless they are delivered within a very short time--less than 2 msec. Furthermore, if these pulses are of low intensity, they are not additive even if delivered within the critical time. In order to have an additive effect from two pulses, they must be near lethal levels to begin with

The reason that the bottom reflections are altered markedly from their classical waveforms cannot be given at this time. This effect is probably associated with the reflected wave having to travel through the bubble pulse and surrounding disturbed water, cavitation of the water, nature of the bottom, its angle of incident to the bottom, etc. Whatever the reason, it is beneficial not to have a strong reflection from the bottom in this test pond.

Nature and Severity of Underwater-Blast Injuries

The only animals that appeared hurt from external signs were the three sheep tested at a 1-ft depth and at a slant range of 26 ft from a 1-lb charge. They appeared docile and remained lying down for a few minutes after the shot, but were on their feet at 5 min.

The immersion-blast injuries were, for the most part, confined to the lungs and G.I. tract. Some eardrums were ruptured in those animals tested beneath the surface at the shorter ranges. The dog eardrum data appear in the following section. The injuries were similar to those repeatedly described in the literature but of minor severity. There were no instances of either ruptured lungs or ruptured G.I. tracts.

At the shorter ranges, animals sustained slight amounts of lung hemorrhages and multiple contusions of the G.I. tract. The contusions were small in area and scattered throughout the small intestine, caecum, large intestine, and rectum. There was only one case of contusions in the stomach. Some of these contusions, even though small in area (1/2 inch or less), were of sufficient severity to ulcerate the mucosal layer of tissue that lines the lumen of these organs. These ulcerations would account for small blood clots found in the feces of many of the animals. In no instance did the blood clots in the feces amount to more than a few drops of blood. This commonly would cause the animals to defecate soon after their removal from the water. In general, the number and size of these contused areas

would decrease with distance from the charge. The contusions of the G. I. tract were term. .' as contusions (a moderate degree of injury) if ulcerations of the mucosal lining were associated with any of them and were termed as mild contusions (slight injury) if there were no ulcerations of the mucosal lining. Detailed listings of the lesions found in each animal appear in reference 6.

Ear Injury in Dogs

Table 1 gives the eardrum rupture data for dogs in terms of the percent of area destroyed and the corresponding range and pressure-time parameters. In general, the eardrums on the right side of the head (the heads were right-side-on) were more damaged than the left ones. The right ears from animals at the 20-ft range were more damaged than those at the 40-ft range in terms of the area of the tympanum destroyed and ossicular damage. In three cases, eardrum rupture was bilateral; the rest were unilateral.

A probit analysis was run relating right eardrum rupture as a function of the log impulse. The results predict that 50 percent of the right ears would be ruptured at an impulse of 22.6 psi· msec. The 85-percent confidence limits were 21.7 to 25.2 psi· msec. For both right and left ears there was a 36-percent incidence of eardrum rupture in dogs at the 40-ft range. The mean impulse measured on these four shots was 22.0 psi· msec; the mean peak pressure was 320 psi.

TABLE 1

EAR INJURY IN DOGS EXPOSED RIGHT-SIDE-ON WITH THEIR EARS AT 1-FT DEPTHS TO UNDERWATER BLASTS FROM 1-LB TNT CHARGES DETONATED AT 10-FT DEPTHS

Shot No.	Slant Range, ft	Peak Pressure, psi (Impulse, psi·msec) [Cut-Off Time, msec]	Dog No.	Eardrum Rupture, Percent Destroyed Right Ruptured	Right Intact	Left Ruptured	Left Intact	Totals
194	20	676[a] (68.2) [0.214]	204 217 215	90%[b] 80%[b] 100%[b]		60%	– –	4/6 (66.7%)
195	40	319 (23.5) [.113]	1 217' 218	60% 60%	N/A[c]	40%	– –	3/5
204	40	327 (22.7) [0.108]	200 116 210	90%[b] – –		5% 50%	N/A	3/5
208	40	328 (21.5) [0.103]	261 102 262	– – –		50%	– –	1/6
210	40	307 (20.4) [0.105]	263 117 163'	30% – –			– –	1/6
								8/22 (36.4%)
200	45	292 (19.2) [0.099]	120 253 200'		– – –		– – –	0/6
206	45	293 (19.0) [0.092]	220 100 208		– – –	20%	N/A	1/5
								1/11 (9.1%)
197	60	215 (12.4) [0.078]	205 163 202		– – –		– – –	0/6

[a] Pressure time was measured at 1-ft depths.
[b] Ossicles fractured or disrupted; otherwise intact.
[c] Not assessible.
– Indicates eardrum intact.

Underwater-Blast Injuries as a Function of Impulse

The incidence of lung hemorrhages and G. I. tract lesions, along with the associated impulse values for all the animals exposed to the underwater blast in a vertical position, appears in figure 6. The impulse values corresponding to each animal data point were those measured at the animals' designated depth, 1, 2, or 10 ft. As already mentioned, all these animals survived the underwater blast.

As seen in figure 6, slight lung hemorrhages and contusions of the G. I. tract occurred in animals subjected to impulse levels on the order of 20 psi·msec or more. The incidence of petechial lung hemorrhages and mild contusions of the G. I. tract dropped off sharply in animals that received less than 10 psi·msec. There were no lesions detectable in the 26 specimens given impulses of between 1.5 to 5 psi·msec.

Figure 7 summarizes the impulse levels over which the different degrees of immersion-blast injuries extended. Included in the figure is the corresponding slant range data adjusted to a 1-lb charge, depth of burst of 10 ft, and gage at a 1-ft depth. Moderate injuries in the form of slight lung hemorrhage and contusions of the G. I. tract extend to 42 ft, impulse of 20 psi·msec. Slight injuries, petechial lung hemorrhages, and G. I. tract lesions extend out to approximately 63 ft with a low probability out to 82 ft and 6 psi·msec. Eardrum rupture could occur out to 52 ft, head beneath the water surface. The corresponding impulse of 14 psi·msec was taken as the lower confidence limit associated with the 1-percent probability of dog eardrum rupture.

1467
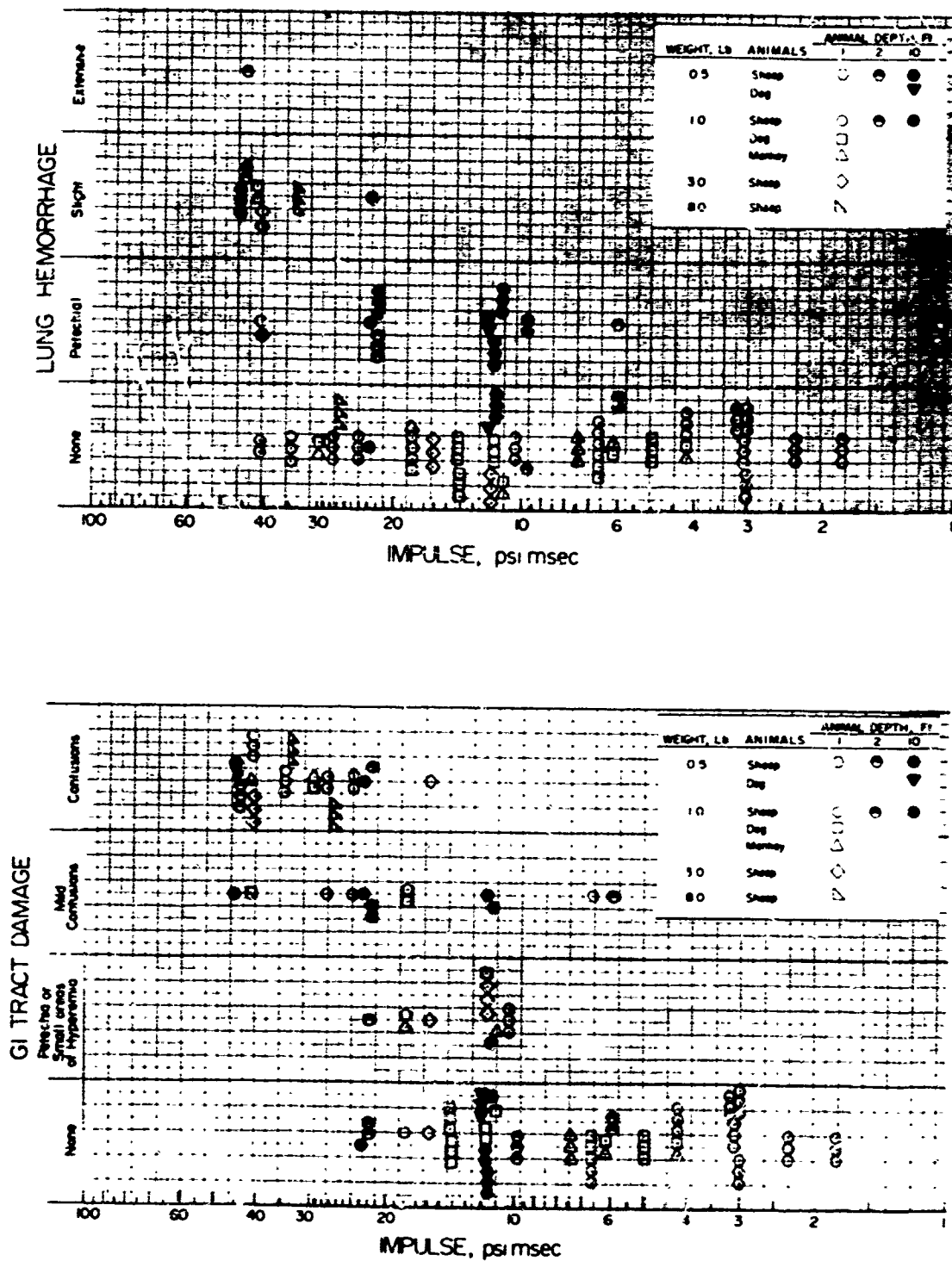
Figure 6. The Incidence of Lung Hemorrhage and G.I. Tract Injuries as a Function of Impulse.
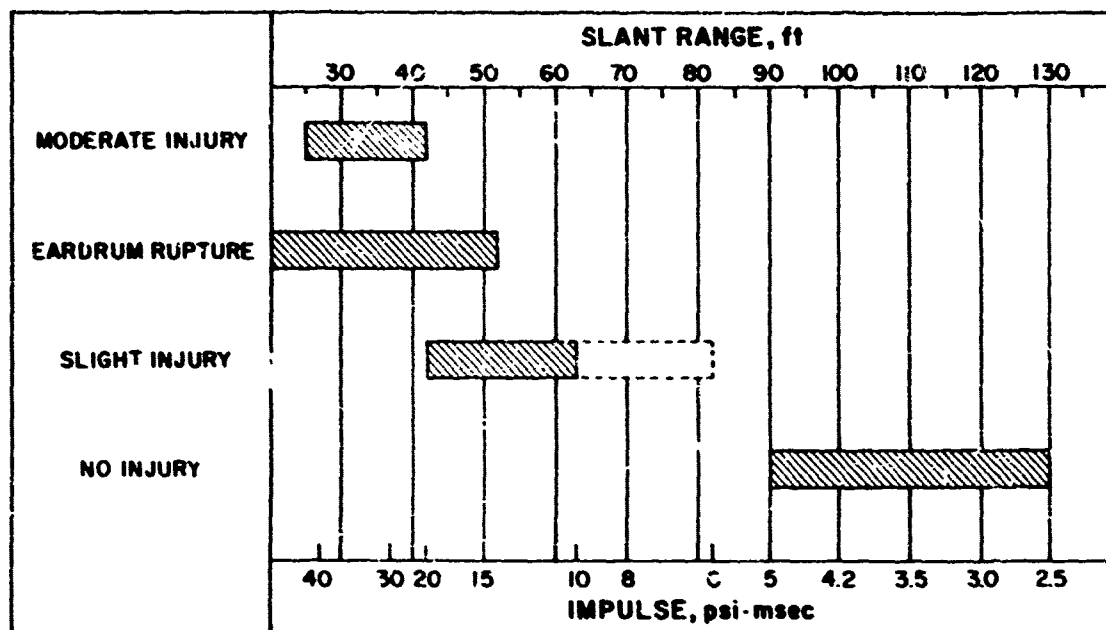
Figure 7.   Injuries in Relation to Range and Impulse.

There were no injuries beyond 90 ft where the impulse was 5 psi·msec or less.

That the impulse corresponds to the animal's underwater-blast dose better than does peak pressure or energy can be shown in the following sample of data. Three sheep at a 1-ft depth and at a slant range of 26 ft from a 1-lb charge sustained the same amount of G. I. tract damage as did three sheep at a 10-ft depth and at a slant range of 48 ft from a 1-lb charge.

The peak pressure was 478 psi at the 1-ft deep animals and the energy was 2.32 in·lb/in^2. The peak pressure at the 10-ft deep animals was 269 psi and the energy was 0.97 in·lb/in^2. The impulses were 42 psi·msec at the 1-ft deep animals and 45 psi·msec at the 10-ft deep ones. The impulses were nearly the same, yet the peak pressure and energy varied by a factor of about 2.

Swimmer Tests

Based on the results of the animal experiments it was predicted that a swimmer upright in the water, head above the surface, should not be injured by an impulse of 5 psi·msec or less. However, one could not predict from the animals' response whether or not underwater shocks of that intensity would be unpleasant to a swimmer. Consequently, the volunteer swimmer first evaluated the sensations produced by underwater shocks of low impulses while standing knee deep, then waist deep, and then neck deep in the southeast corner of the test pond, 153 ft from the charge. The subject felt nothing more than very mild ping or click sensations. These were not the least bit uncomfortable. Test conditions were a 1-lb charge, 10-ft deep, 60 ft

from the west bank of the pond with sheep beneath the east rigging 130 ft from the charge.

On the next shot (number 193), the swimmer was treading water at the 130-ft range adjacent to the sheep. The pressure-time pattern recorded in the incident wave from shot 193 appears in figure 3. The peak pressure measured was 108 psi with an impulse of 3.0 psi·msec and a cutoff time of 0.036 msec. The negative pressure was 28 psi. The shape of the bottom reflection that arrived 1.44 msec after the incident shock wave is illustrated in figure 5. The peak pressure in the reflected wave was 98 psi with an impulse of 2.5 psi·msec. Its duration was 0.130 msec. The swimmer only felt one slight transient pressure about his navel which was about 1.5 ft beneath the surface. Nothing was felt over other portions of the body. These results are summarized in table 2 along with those obtained on later tests when 1-lb charges were located to the east of the main rigging and the swimmer was standing neck deep in the southeast corner of the pond. The pressure-time parameters listed in table 2 were taken from the curves in figure 4. The sensations experienced at 120 ft (impulse, 3.0 psi·msec) were very mild, like those at 130 ft. At the 115-ft and 100-ft ranges (impulses, 3.3 and 4.2 psi·msec respectively) the swimmer experienced multiple moderate to intense stings over his upstream surface but no pressure sensation. The latter may have been masked by the cold water (65 °F).

Limitations to the Safety Criteria

At the present time the 2 psi·msec underwater-blast safety criteria should only be applied to the charge weight and charge depth

TABLE 2

DATA FOR SWIMMER UPRIGHT IN WATER
HEAD ABOVE THE SURFACE

Range, ft	Location	Peak Pressure, psi	Impulse, psi·msec	Cut-Off Time, msec	Remarks of Swimmer
153	Standing SE corner neck deep.	71	1.8	0.027	Slight ping only, no reflections.
130	Near center of east span neck deep.	90	2.5	0.032	Felt ping and slight abdominal pressure, no reflections.
120	Standing SE corner neck deep.	96	3.0	0.035	Ping or click sensation only; no pressure, no reflections.
115	Standing SE corner neck deep.	98	3.3	0.037	Moderate stings from incident and reflected waves; no pressure.
100	Standing SE corner neck deep.	115	4.2	0.042	Strong stings from incident and reflected waves; no pressure.

1-lb Pentolite charges detonated at 10-ft depths.

Parameters at 1-ft depths, taken from curves in Figure 4.

Subject in swim shorts facing the charge.

of burst conditions reported herein and limited to swimmers having their heads above the water surface. There are at least three areas of uncertainty that need checking out before one can confidently extend the criteria to underwater-blast conditions in general.

The first uncertainty is whether or not there may be a limit in the peak pressure that can be tolerated with the 2 psi·msec impulse. In the present study, peak pressures on the order of 80-90 psi were connected with that impulse. Charges fired at much shallower depths of burst would produce blast waves of 150-300 psi yet have impulses of 2 psi·msec. For example, 1-lb at a 2-ft depth of burst gives that impulse at 69 ft (gage at 1 ft) with a peak pressure of 185 psi. Experiments will be conducted in the near future to evaluate the effects of underwater shocks having high peak pressures and small impulses.

The second unknown is in connection with the effects of the underwater shock on the ears of a swimmer diving beneath the surface. There is an absence of information in the literature on eardrum rupture from underwater blast that could be compared with that from the present study. According to the results from the dogs, one would not expect eardrum rupture in swimmers with heads immersed at 2 to 3 psi·msec impulse levels. How obnoxious the sound intensity would be to a person at that impulse can not be stated at this time and will be the subject of future tests.

The third problem area is in regard to reflections of the underwater shock from the bottom, ships, and various underwater

obstacles adding to the underwater-blast dose. For reasons already stated in the section on bottom reflections, it is unlikely that reflections would be important. This, together with information to be obtained from records of the reflected shock waves taken adjacent to the volunteer swimmer, should establish the fact that reflections of underwater shocks of 2 psi·msec under any geometry of exposure would be safe.

In the following presentation the speaker will talk more about the physics of underwater blast. The speaker will also illustrate curves that can be used in determining the ranges for an impulse of 2 psi·msec as a function of charge weight and charge depth.

The experimental work discussed in this manuscript was conducted according to the principles enunciated in the "Guide for Laboratory Animal Facilities and Care," prepared by the National Academy of Sciences—National Research Council.

REFERENCES

1. Clemedson, C. J. "Table 53. Effects of Underwater Blast: Man and Other Animals." Environmental Biology (P. L. Altman and D. S. Dittmer, Editors), pp. 225-228 Federation of American Societies for Experimental Biology, 9650 Rockville Pike, Bethesda, Maryland. 1966.

2. Corey, E. L. "Medical Aspects of Blast." U. S. Naval Med. Bull. 46(5), pp. 623-652. 1946.

3. Wright, H. C. "Subjective Effects of Distant Underwater Explosions." Med. Res. Council (London), Roy. Naval Personnel Res. Committee, Report R. N. P. 47/3. April 1947.

4. Tussing, R. B. "A Four Channel Oscilloscope Recording System." U. S. Naval Ordnance Laboratory RPT. NOLTR 65-21. May 1965.

5. Slifko, J. P. and Farley, T. E. "Underwater Shockwave Parameters for TNT (U)." U. S. Naval Ordnance Laboratory NAVORD Report 6634. June 1959.

6. Richmond, D. R., Yelverton, J. T. and Fletcher, E. R. "Far-Field Underwater-Blast Injuries Produced by Small Charges." Technical Progress Report, DNA 3081T, Defense Nuclear Agency, Department of Defense, Washington, D. C. July 1973.

7. Richmond, D. R. et al. "The Relationship Between Selected Blast Wave Parameters and the Response of Mammals Exposed to Air Blast." Technical Progress Report, DASA 1860, Defense Nuclear Agency (formerly Defense Atomic Support Agency), Department of Defense, Washington, D. C. November 1966. Subsequently published in Ann. N. Y. Acad. Sci. 152, pp. 103-121. 1968.

MINIMUM ALLOWABLE STANDOFF RANGES FOR SWIMMERS OPERATING NEAR UNDERWATER EXPLOSIONS

Ermine A. Christian and C. J. Aronson

NAVAL ORDNANCE LABORATORY
White Oak, Silver Spring, Maryland 20910

ABSTRACT: The Lovelace Foundation has recently shown that minor injuries inflicted by underwater explosions can be correlated with the impulse of the pressure wave, and has proposed a 2 psi-msec impulse as a "safe" level for swimmers with head above the surface. Factors that are involved in translating the Lovelace test results into operational configurations are discussed. Using 2 psi-msec impulse criterion, minimum allowable standoff ranges are derived for swimmers operating in deep, open water. These new "safe impulse" ranges are compared with ranges for constant overpressure.

SLIDE 1

We have just heard a talk by Dr. Richmond entitled "Safe Ranges from Underwater Explosions". This paper treats exactly the same problem and in fact the same kinds of ranges, but as you can see, the title has now been changed to read "Minimum Allowable Standoff Ranges for Swimmers Operating Near Underwater Explosions". This backing down from the handy word "safe" to the longer title of "minimum allowable standoff" ranges is not merely our contribution to the obfuscation of governmentese. The psychological impact of these two titles is very different and indeed that fact has governed our selection of the less euphemistic words "minimum allowable" rather than "safe".

SLIDE 2

The question that we will be treating is that of "how do you extrapolate the small scale test results we have just heard about to real operational conditions?" Since the Navy rarely has occasion to use underwater ordnance in a swimming pool, even a rather large one, we must extrapolate the actual test conditions to quite different ones in order to make estimates for operational activities. The Navy prefers to have no one in water during detonations, and so arranges its planned operations.

Preceding page blank

There are, however, some circumstances under which the swimmer/diver is not in complete control of the situation and these are the circumstances we are addressing. In the far future, if one really can predict safety ranges with confidence, one might consider the possibility of revising operational procedures--improving them and allowing options.

SLIDE 3

Let us review briefly those conditions for which "safe ranges" could be taken directly from the experiments. First of all, we must have the swimmer at or near the surface, the explosive charge must weigh no more than 1/2 to 8 lbs and be at a depth of 10 ft, the water depth can be no more than 30 ft at the charge and 15 ft or less at the swimmer, and the type of shock wave must be only a simple exponential. These are the actual test conditions that obtained in the Lovelace pond, which is sketched at the top of the slide. The restriction on conditions to which we may extrapolate can be largely summarized in the last item shown here, namely, the type of shock wave. Let us look first at what that particular constraint means in terms of the conditions to which we can extrapolate.

SLIDE 4

Here is a sketch of the kinds of shock waves that were used in the tests and from which the impulse criterion for damage were derived. An explosion sends out a spherical shock wave which spreads equally in all directions from the charge. When this shock wave is bounced off the surface of the water, it is reflected back into the water as a wave of the same shape but one which has negative rather than positive pressure. That means that at some point "A" fairly near the water surface we will have two waves arriving: first, the so-called direct wave which comes out from the charge and then a little later the reflected wave from the surface. The sketches at the bottom of the slide show the kinds of shock wave that results. As we see at the lower right, the composite of both direct and reflected waves that arrive at point "A" will give us a truncated exponential wave. The area under such curves or the integral of the pressure time curve is the quantity we call impulse, and it is that area that we are looking at for determining allowable standoffs. This is what an exponential wave will look like from a free water shot. We do not find waves of this particular kind under all conditions.

SLIDE 5

For example, suppose we require only a maximum allowable impulse of 2 psi milliseconds. The next slide shows some

of the types of shock waves that we might find under different typical application conditions. First of all is the simple exponential wave such as we have just seen. This is the kind of shock wave you will find if swimmers are operating in fairly deep open water and you have a moderate charge size and depth. When you change any of these conditions, however, you may get rather different looking waveforms from that of the simple exponential. For example, the next sketch shows a distorted pulse such as you might find near a swimmer who is very far from a very large charge; or you might find such a distorted waveform if your charge is buried in the mud or is up against hard rock instead of being in free water. Next we see a double pulse wave. This is the kind of shock wave you might have if your swimmer is operating near a hard reflecting surface. In that case, the reflection comes back in as another compressional wave rather than having an inverted polarity as the surface reflected wave has. And finally, we see what you might find if you have re-peated pulses, such as you would have when several small explo-sions detonated nearby. Now in each of these four waveforms that we have seen on Slide 5, the area under the curve, that is the integral of pdt or the impulse, is still only equal to 2 psi milliseconds. But they are rather different waveforms, and we do not at this time have information that will allow us to say that the response of the biological target will be the same regardless of the waveform. Consequently, it is this constraint--a lack of knowledge on the effects of different waveforms--that restricts us for the present to using only the simple exponential wave which is the only kind of shock wave that has been used in any of the tests to date.

SLIDE 6

Here then are the conditions for which we can extrapolate the Lovelace data into operational form. We will treat only those operations that take place in open water that is deeper than about 50 ft. From various considerations of the available data, we also feel that we must limit the depth of our swimmer to no deeper than 10 ft, and for the explosive charge we should treat none that are larger than 50 lbs or deeper than 30 ft. These conditions shown here represent a fair extrapolation of the actual test variables that were shown earlier, and we believe are justifiable extrapolations. They do take us rather further than our man in the swimming pool with an 8-lb charge maximum weight, although they do not cover, by any means, the actual range of charge weights and configurations that the swimmers and divers in the operating Navy are apt to encounter. Within this range of variables, let us now look at how the impulse changes as we change the charge weights and depths and the swimmer depths.

SLIDE 7

Here we have an explosion being registered by someone
at point "A" and someone at point "B". Both of these positions
"A" and "B" are the same radial distance away from the explo-
sion so that they both see the same peak pressure in the front
of the exponential wave. The shallower of these two observers
sees less impulse, however, than the deeper one. This is true
because the surface-reflected wave arrives sooner at the
shallow position than it does at the deeper position. In other
words, the surface reflection chops off the compression wave
sooner at locations near the surface than it does at locations
at depth because the travel paths for the direct and reflected
waves are more nearly equal at shallower depth than at greater
depth. Consequently, although there is the same peak pressure
at these two locations, there is considerably more impulse at
location "B" than at the near-surface location "A". Since the
arrival time of the reflected wave is due to the geometry, that
is the depth of both the charge and the observer and also the
distance away from the charge, the effect of depth on impulse
is reciprocal. By that I mean we would have the same effect
if, instead of having two observers and one explosion, we have
one observer and two explosions.

SLIDE 8

So as shown here we get a smaller impulse for a shallow
charge just as we had on the previous slide a smaller impulse
for a shallow target.

SLIDE 9

In brief, with an impulse damage criterion, we can say
categorically: "shallower is safer". Let us look now at the
kinds of curves that have been generated; these can be generated
easily with a computer and the program such as we have at NOL
for estimating the contours along which we will have a particular
impulse level. In this case we are interested in a 2 psi-
millisecond impulse level.

SLIDE 10

As we have just been seeing, the impulse at a particular
spot depends upon both the charge depth and the swimmer depth.
If the depth of both of these are fixed, we can move them out
along horizontal dimension and calculate with our computer
program the location at which different explosive charge weights
will give us our desired impulse. The curves look like this.
Here charge weight is plotted along the abcissa and horizontal
range on the ordinate. In this example, both the charge and
the swimmer are at a depth of 5 ft, and the curve shown is the

contour of the positions at which the impulse is always
equal to 2 psi milliseconds. On this particular curve,
then, if we are underneath the curve, the impulse will be
greater than 2 psi milliseconds, and the upper portion of
the curve will be less. If our damage criterion is 2 psi
milliseconds, that would be translated to read: the swimmers
are definitely unsafe if they are below the curve, and they
are probably will not be harmed if they are above the curve.
The curve itself represents our minimum allowable standoff
measured horizontally to the charge. We have made a number
of such calculations and have curves of this kind for a
variety of charge weights, charge depths, and swimmer depths.
A convenient format, since we must hold some of the variables
constant to display them, is that shown in the next slide.
SLIDE 11
        Here we have a whole family of such curves for swimmers
at 5-ft depth. We have elected to hold a swimmer depth constant
and vary the charge depth as shown on each of the curves. If
it were more desirable for some reason, we could have held the
charge depth constant and shown the variation in our minimum
horizontal standoff for a variable swimmer depth. So again we
see that for our swimmer at a fixed depth at 5 ft, the minimum
horizontal standoff for 2 psi millisecond impulse (which is the
quantity shown on the left) increases very rapidly with increasing
charge weight for the first little bit and then becomes essen-
tially a flat curve. One would not expect that the required
standoff from a 50-lb charge, for example, would be so little
different from the standoff required for a 5 or 10-lb charge.
This is, however, the characteristic of curves based on an
impulse criteria because we must remember that the prime
controlling quantity in this case is the surface-reflected wave.
If your geometry stays constant and you increase the charge
weight, you do not increase the impulse nearly so rapidly as you
might expect since the surface reflection stays constant and
cuts the wave off at the same short time. We see here also
another demonstration of our comment that with an impulse
criterion shallower is safer. As the charge depth increases
from the shallow 2-ft depth on the lowest curve up to greater
and greater depths and finally 30 ft deep shown on the upper
curve, we find a marked increase in the range to which you must
go before your impulse is as low as 2 psi milliseconds. Now,
do we really believe these curves, would we be willing to say
to a swimmer at 5-ft depth that he can be a 100 yards away from
a 50-lb charge detonated at 2-ft depth and not be in any danger?
Before we make such a grave commitment,   let us look at any
other guidance that might be available concerning the safety of
swimmers operating in the vicinity of underwater explosions.

SLIDE 16

Here we have the allowable standoffs controlled by the
peak pressure of 50 psi for charge depths that are shallower
than about 10 ft, and we have a larger required standoff for
charges that are deeper than 10 ft. And here we have shown
the two previous curves for charge depths of 20 ft and 30 ft.

SLIDE 17

In summary, the present extrapolations of test results
must be limited to operations in deep open water with swimmers
somewhere between the surface and a 10-ft maximum depth and charges
that weigh no more than 50 lbs of TNT and a firing depth no
greater than about 30 ft. Secondly, we feel that we must
consider both the peak pressure and the impulse and the tentative
limits that we have used for demonstration purposes here are a
pressure of 50 psi maximum and an impulse of 2 psi-millisecond
maximum. Because of the nature of the impulse in the shock
wave from an explosion, the minimum allowable standoff increases
for deeper swimmers and deeper charges. Now obviously more work
is needed, and we must explore the relative significance of
impulse and peak pressure further before we can arrive at curves
that we are willing to offer as estimates of minimum allowable
standoffs. Perhaps in due time after adequate checking these
may become acceptable as guidance documents for use in the field
under those operating circumstances in which it is necessary to
have swimmers operating in the water at the time that explosives
charges detonate. We have made great strides towards this in
that we now have some quantitative basis for making such estimates
In the words of one of our backwoods cousins: we ain't
as far as we ought to be and we ain't as far as we're gonna be
but we are further than we were.

SLIDE 13

Here we can see how these standoff ranges can change if
we varied our allowable overpressure limits. Here we have
the same coordinates that we used earlier in the impulse plots,
that is horizontal range in yards vs the charge weight in lbs
of TNT. At the bottom is shown in the darkened region the
area where the peak pressure is 500 psi or greater. The peak
pressure you recall does not depend upon the depth of the
charge or the depth of the observation point; it is strictly
a radial quantity so here we do not have any geometric considera-
tions to take into account. The next line up that is shown here
is the contour at which there is a 100 psi pressure from charge
weights of these different sizes; and finally, at the top, is
the limit at which the pressure has fallen to 50 psi. The
question we are raising now is "Can we judge some allowable
limit of pressure as a possible alternative damage criterion?"

Lacking any real guidance on this point, aside from that
which has been observed in the Lovelace tests in conjunction
with particular impulses, it seems reasonable to think that
perhaps somewhere between, say, 100 and 50 psi might be an
allowable pressure level at which we would not expect to receive
damage.

SLIDE 14

On the next slide, let us see how the ranges described in
terms of pressure compare with those we saw earlier for an
impulse level of 2 psi milliseconds. Here we have superimposed
the two peak pressure curves for 100 psi and 50 psi on the 2
psi millisecond impulse curves that we saw earlier for our
swimmer at a 5 ft depth. The impulse curves are shown in red
and the pressure curves in blue. Some of the contours for
constant impulse fall at shorter ranges than the 50 psi peak
pressure curves. On the other hand if our charge depth is deeper
than about 10 ft, the impulse criterion gives us curves that are
at greater ranges than those of the peak pressure curves. At
our present state of understanding it seems that the better part
of valor to take the worst of both worlds and say we will require
that the peak pressure be no higher than some value at the same
time that we require that the impulse be no larger than some value.

SLIDE 15

For demonstration purposes let us assume that for safety
we must have a peak pressure less than or equal to 50 psi, the
outermost curve we have shown there, and an impulse that is our
same criterion of being less than or equal to 2 psi milliseconds.
With that pair of criteria the curves that we just saw would
look like this.

MINIMUM ALLOWABLE STANDOFF RANGES

FOR

SWIMMERS OPERATING NEAR

UNDERWATER EXPLOSIONS

BY

ERMINE A. CHRISTIAN AND C. J. ARONSON

NAVAL ORDNANCE LABORATORY
SILVER SPRING, MARYLAND

NOL

1485

HOW DO YOU TRANSLATE

SMALL-SCALE TEST RESULTS

TO

OPERATIONAL CONDITIONS?

NOL

1486

CONDITIONS FOR WHICH "SAFE" RANGES CAN BE TAKEN DIRECTLY FROM EXPERIMENTS
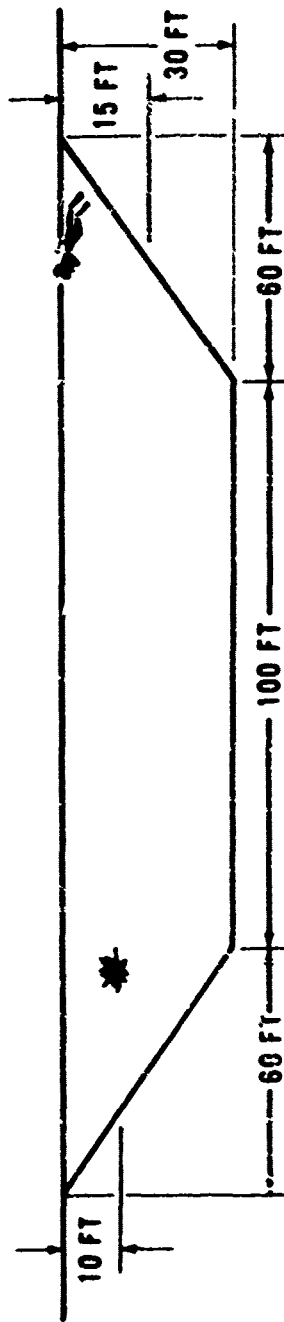
SWIMMER DEPTH: AT OR NEAR SURFACE

EXPLOSIVE CHARGE: WEIGHT - 1/2 TO 8 POUNDS
FIRING DEPTH - 10 FT

WATER DEPTH: 30 FT AT CHARGE
15 FT AT SWIMMER

TYPE OF SHOCKWAVE: SIMPLE EXPONENTIAL

NOL

DIRECT AND SURFACE-REFLECTED PRESSURE WAVES

IMPULSE = $\int p\,dt$

WAVE AT A

DIRECT

REFLECTED

(+)

AMBIENT PRESSURE

(−)

TIME

NOL

1488
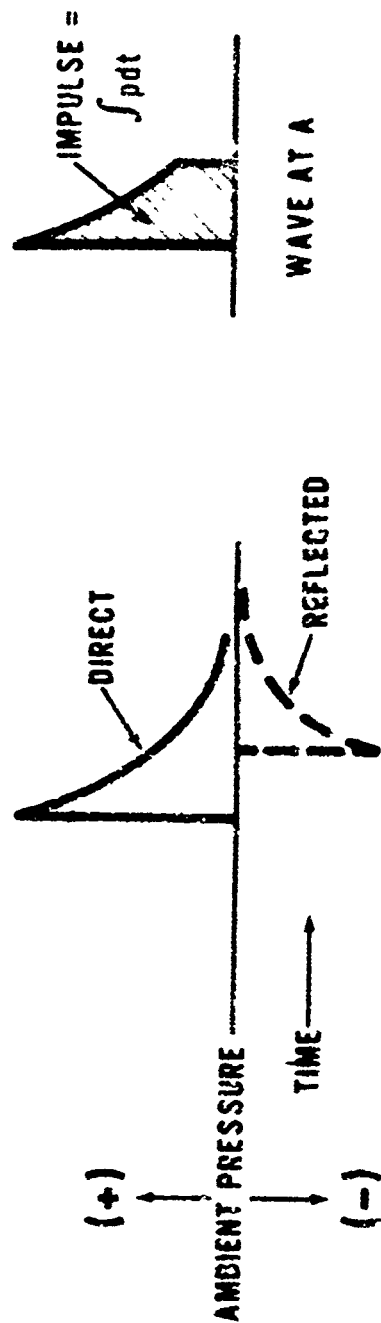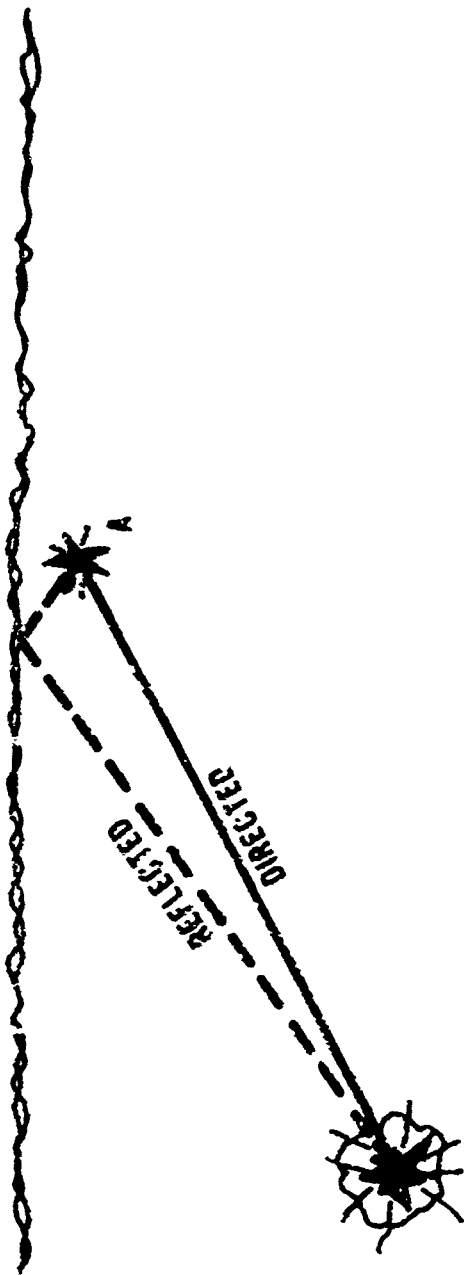
TYPICAL U/W SHOCKWAVES HAVING AN IMPULSE 2 PSI-MSEC

NOL

TYPE OF SHOCKWAVE

1) SIMPLE EXPONENTIAL	2) DISTORTED PULSE	3) DOUBLE PULSE	4) REPEATED PULSES

TYPICAL OPERATIONAL SITUATION

- SWIMMERS IN FAIRLY DEEP, OPEN WATER AND - MODERATE CHARGE SIZE AND DEPTH	- SWIMMER FAR FROM VERY LARGE CHARGE OR - CHARGE BURIED IN MUD, OR AGAINST LARGE ROCK	- SWIMMER NEAR HARD REFLECTING SURFACE	- SEVERAL SMALL EXPLOSIONS NEARBY

1489

LIMIT OF EXTRAPOLATION FROM ACTUAL EXPERIMENTAL
CONDITIONS JUDGED TO BE WARRANTED

NOL

AT PRESENT TIME CAN CONSIDER ONLY OPERATIONS IN OPEN WATER

DEEPER THAN ABOUT 50 FT
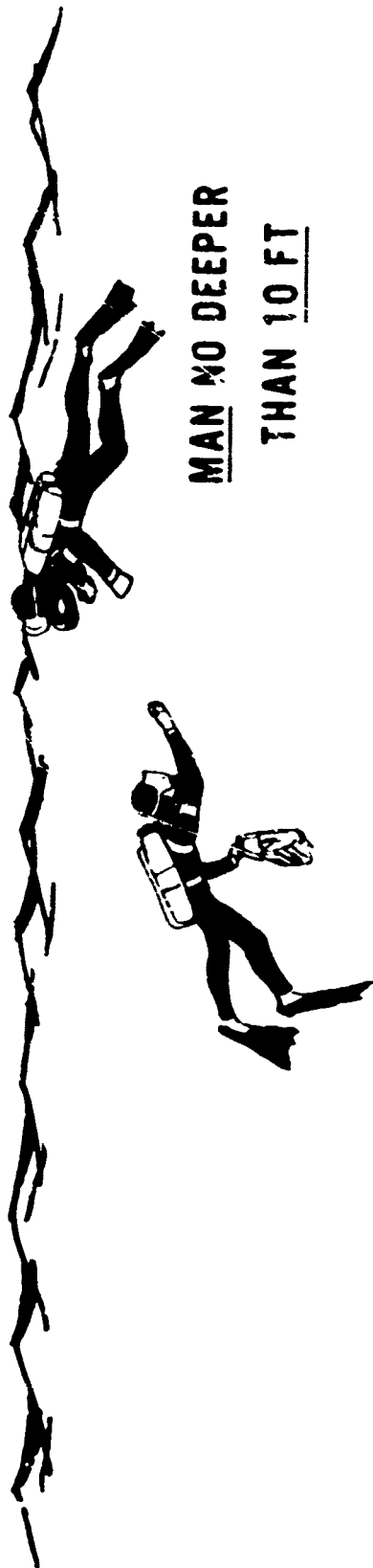
MAN NO DEEPER

THAN 10 FT

EXPLOSIVE CHARGE

NO LARGER THAN 50 LB

NO DEEPER THAN 30 FT

1490

IMPULSE VARIATION WITH SWIMMER DEPTH
(NO CHANGE IN PEAK PRESSURE)

CONSTANT PEAK PRESSURE
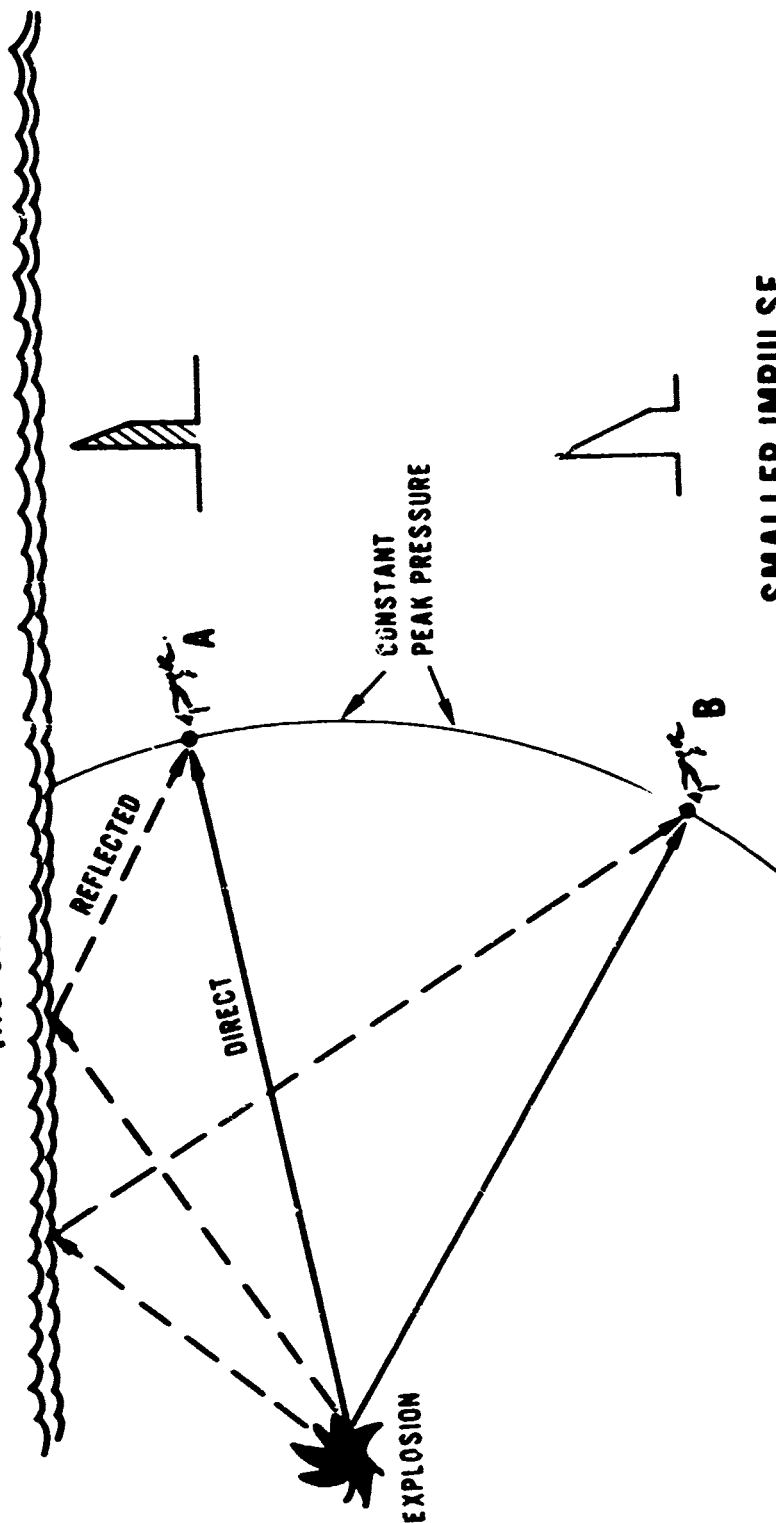
SMALLER IMPULSE FOR SHALLOW SWIMMER

REFLECTED

DIRECT

A

B

EXPLOSION

NOL

1491

IMPULSE VARIATION WITH CHARGE DEPTH

(NO CHANGE PEAK PRESSURE)

NOL

SHALLOW CHARGE

DEEP CHARGE
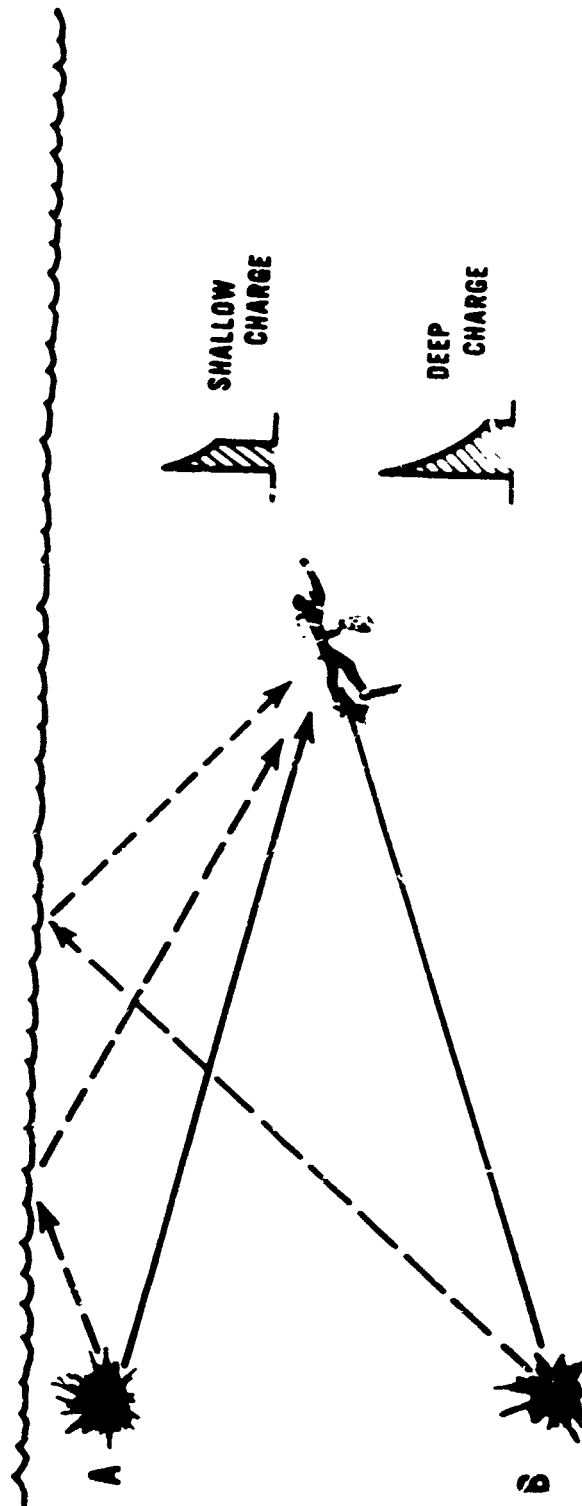
SMALLER IMPULSE FOR

SHALLOW CHARGE

A

B

WITH AN IMPULSE DAMAGE CRITERION

SHALLOWER
IS
"SAFER"

NOL

MINIMUM ALLOWABLE STANDOFF VS. CHARGE WEIGHT

IMPULSE <2 PSI-MSEC FOR CHARGE AND
SWIMMER AT 5 FT DEPTH

IMPULSE >2 PSI- MSEC FOR CHARGE
AND SWIMMER AT 5 FT DEPTH

HORIZONTAL RANGE (YDS)

160

140

120

100

80

60

40

20

0

0   10   20   30   40   50

CHARGE WT (LB OF TNT)

NOL

1494
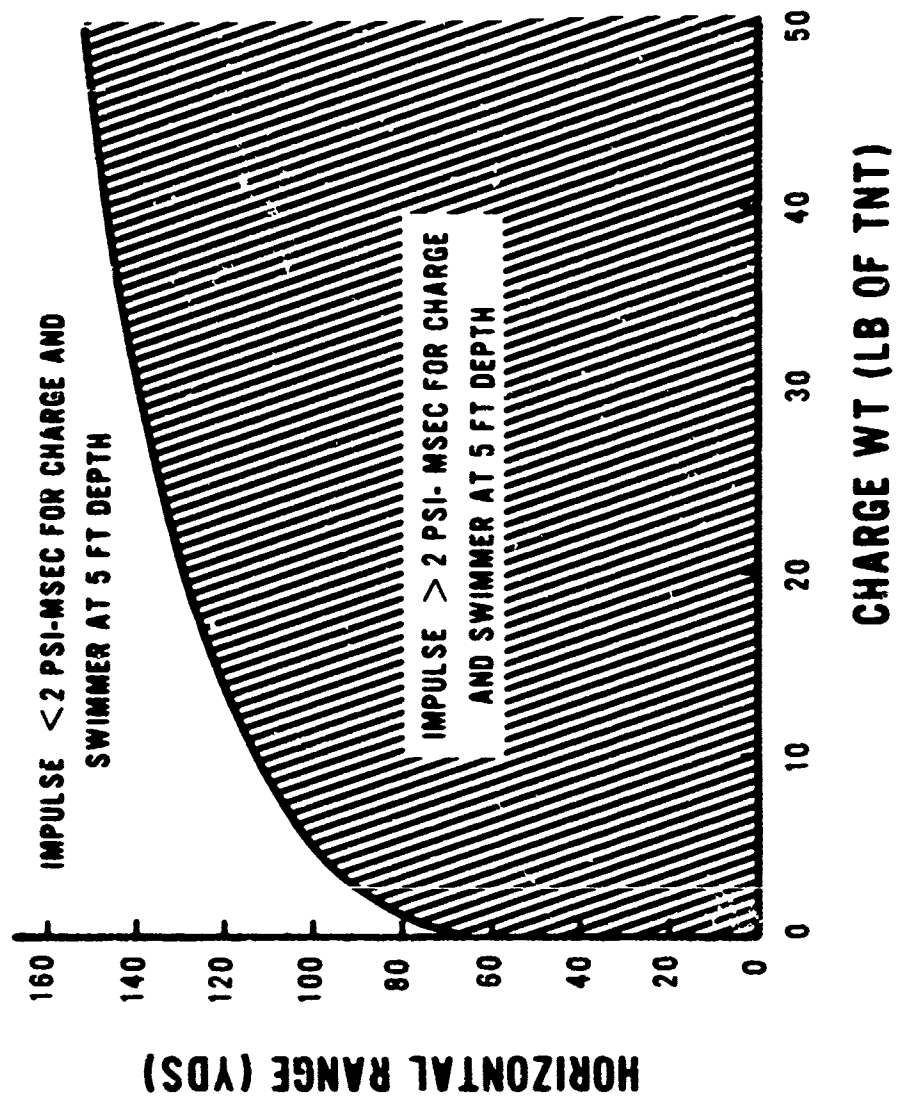
MINIMUM ALLOWABLE STANDOFF VS. CHARGE WEIGHT FOR SWIMMERS VARIOUS CHARGE DEPTHS

FOR SWIMMERS AT 5 FT DEPTH

CHARGE DEPTH

- 30 FT
- 20 FT
- 10 FT
- 5 FT
- 2 FT

CHARGE WT. (LB OF TNT)

MINIMUM HORIZONTAL STANDOFF(YD) FOR 2 PSI-MSEC IMPULSE

NOL

1495
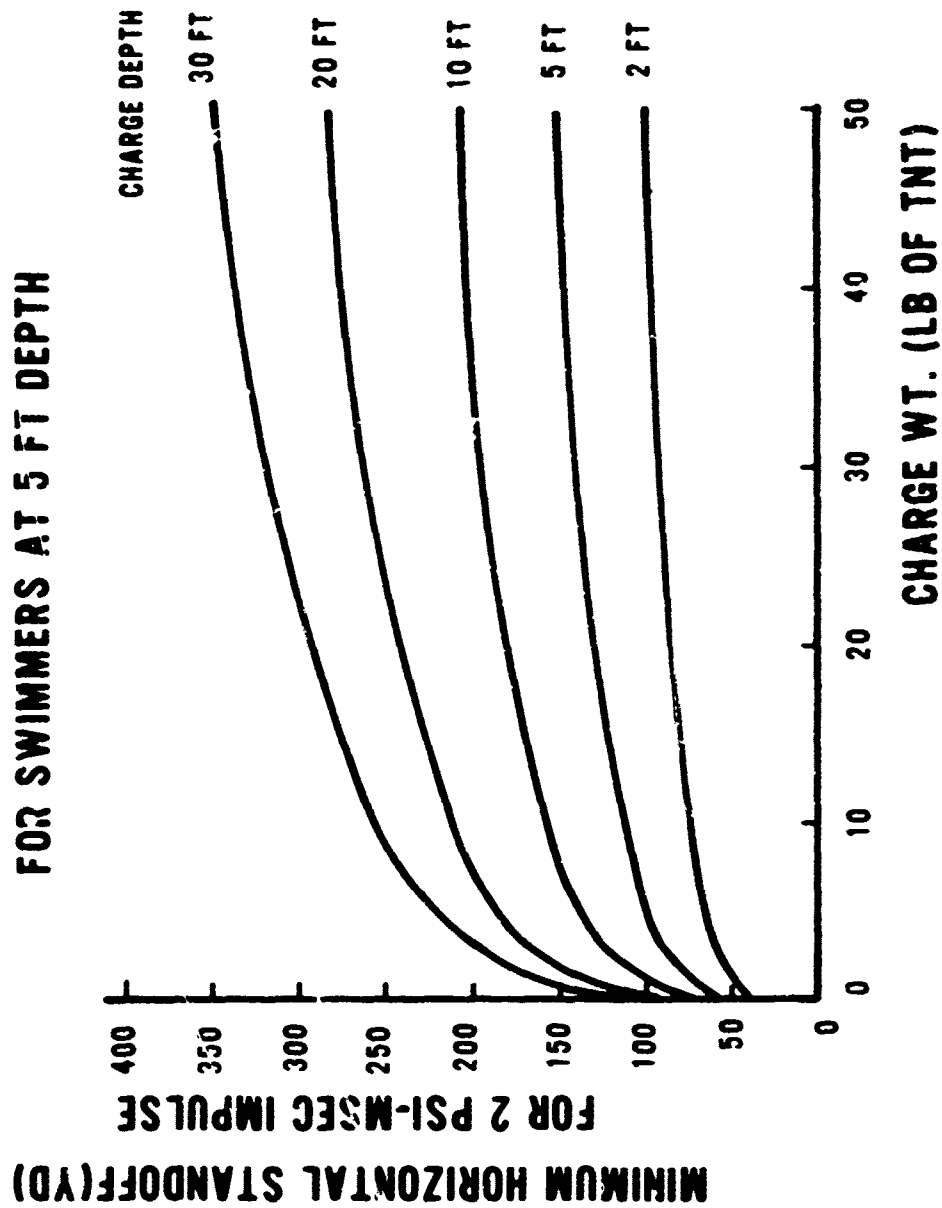
U.S. NAVY DIVING MANUAL

(NAVSHIPS 0994-001-9011)

1.3.14 UNDERWATER EXPLOSIONS

"PRESSURE OF 500 psi
         IS SUFFICIENT TO CAUSE INJURY....."

"DEGREE OF INJURY INFLUENCED BY DIVER'S DEPTH"

"SOMETIMES DEPTH OF WATER AND TYPE OF BOTTOM INFLUENCE DEGREE OF INJURY....."

"PROTECTIVE CLOTHING.... OFFERS SOME PROTECTION.... BUT IMPRACTICAL..."

"IF DIVER EXPECTS EXPLOSION AND HAS TIME... GET AS MUCH OF BODY OUT OF WATER AS POSSIBLE..."

"IF THERE IS TIME, THE DIVER SHOULD OBVIOUSLY GET AS FAR AWAY AS POSSIBLE FROM....THE EXPLOSION."

NOL.

1490

RANGE VS CHARGE WEIGHT FOR CERTAIN PEAK UNDERWATER PRESSURES

50 PSI PRESSURE

? ALLOWABLE LIMIT ?

100 PSI PRESSURE

500 PSI PRESSURE

CHARGE WT. (LB OF TNT)

HORIZONTAL RANGE (YD)
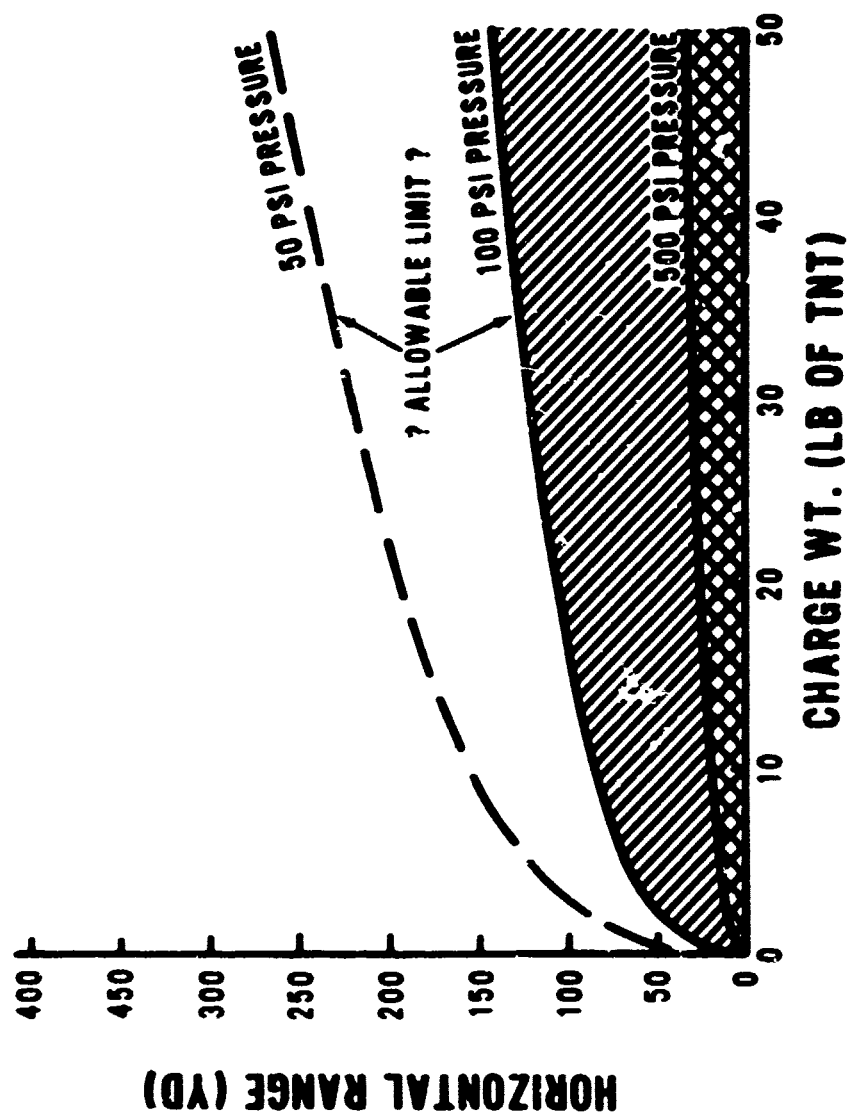
NOL

SHOCKWAVE CONTOURS FOR SWIMMER AT 5 FT DEPTH

PEAK PRESSURE

2 PSI-MSEC IMPULSE FOR VARIOUS CHARGE DEPTHS

30 FT
20 FT
50 PSI
10 FT
5 FT
100 PSI
2 FT

HORIZONTAL RANGE (YD)

CHARGE WT. (LB. OF TNT)
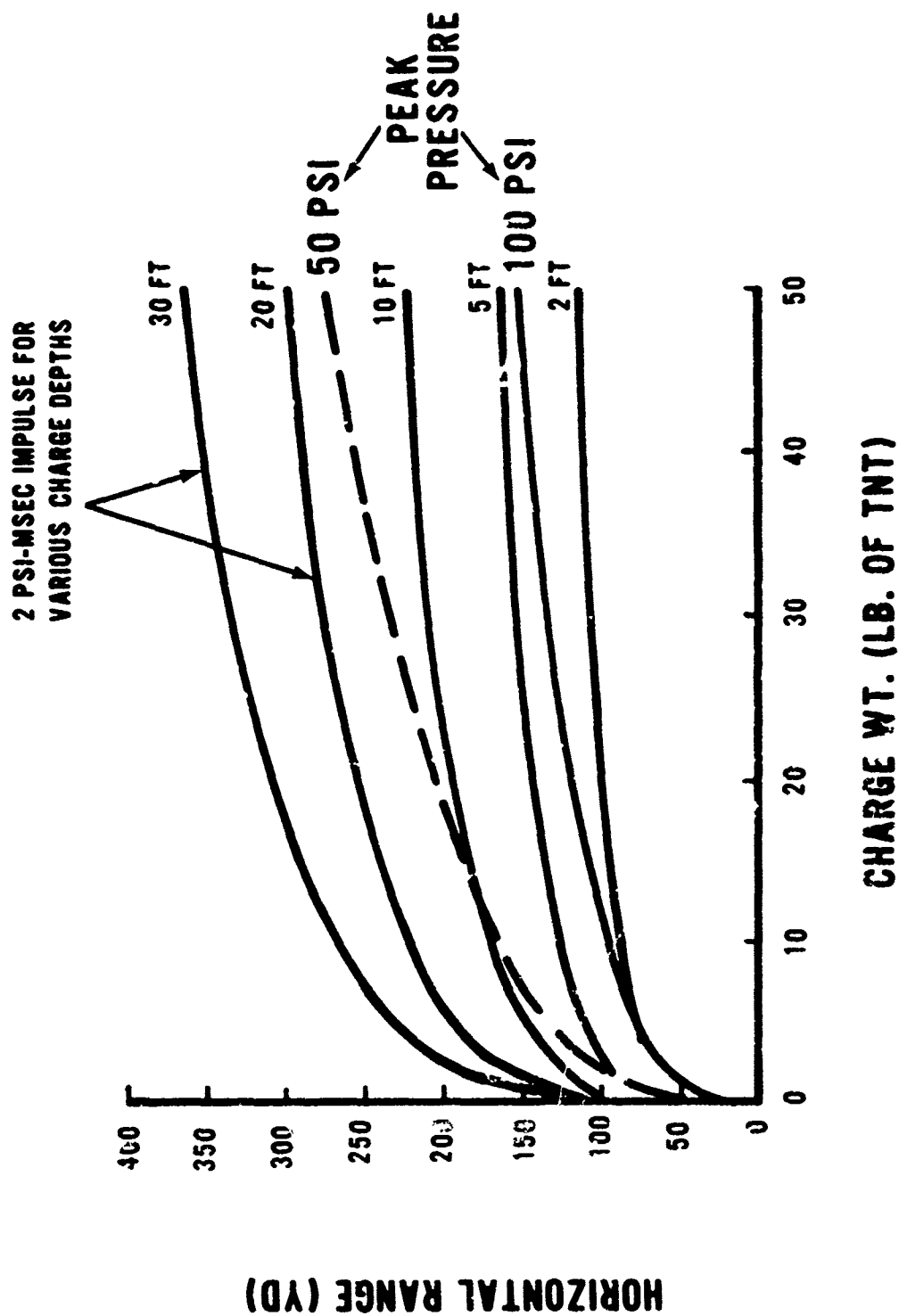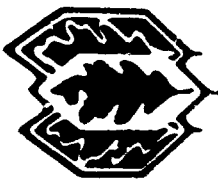
NOL

ASSUME FOR SAFETY:

PEAK PRESSURE ≤ 50 psi

AND

IMPULSE ≤ 2 psi-msec

NOL

1499

MINIMUM ALLOWABLE STANDOFFS VS CHARGE WEIGHT
FOR SWIMMERS AT 5 FT DEPTH

(COMBINED IMPULSE AND PEAK PRESSURE CRITERIA)

1500
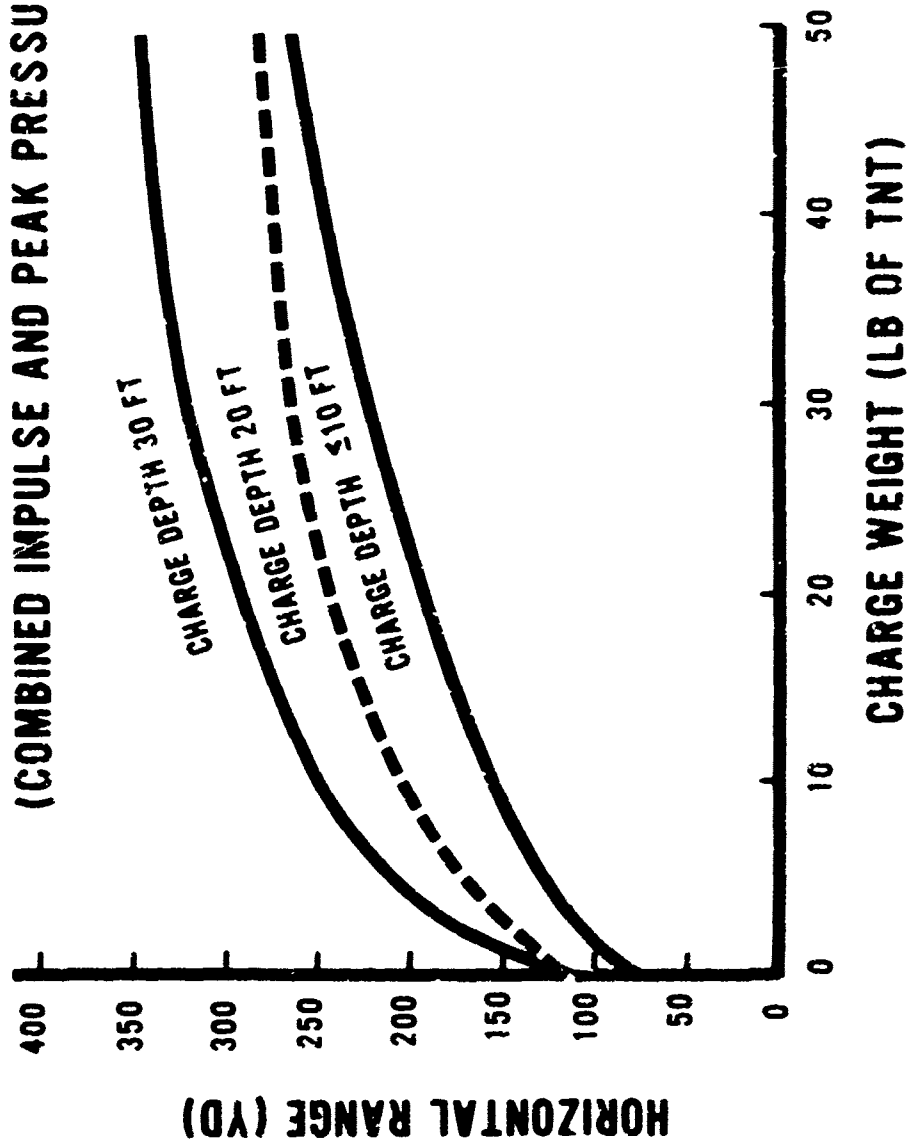
SUMMARY

1. PRESENT EXTRAPOLATIONS OF TEST RESULTS LIMITED TO:

   - OPERATIONS IN DEEP, OPEN WATER
   - SWIMMERS AT SURFACE-10 FT DEPTHS
   - CHARGES ≤50 LB (TNT) AT DEPTHS ≤30 FT

2. MUST CONSIDER BOTH PEAK PRESSURE AND IMPULSE:

   TENTATIVE { • PRESSURE - 50 PSI MAXIMUM
   LIMITS   { • IMPULSE - 2 PSI -MSEC MAXIMUM

3. AS SWIMMER GOES DEEPER OR AS CHARGES GO DEEPER THE MINIMUM ALLOWABLE STANDOFF INCREASES

NOL

1501

INITIATION MECHANISMS OF SOLID ROCKET PROPELLANT DETONATION

H.S. Napadensky, C.A. Kot, Y.A. Shikari, A.H. Wiedermann

IIT Research Institute
Chicago, Illinois

Preceding page blank

ABSTRACT

An experimental and analytical investigation was conducted to determine the mechanisms which may lead to the initiation of detonation in solid rocket propellants under accidentally applied low-amplitude stimuli. In particular, the effects of moderate speed impact are studied. A two-dimensional Lagrangian tensor computer code was developed to study in detail the hydrodynamic (or elastic-plastic hydrodynamic) and thermal behavior of explosive and propellant materials under unconfined or partially confined impact conditions. Results indicate that under partially confined impact, the local temperature rise in the material is substantially higher than in the unconfined impact case. This is due to the multiple shock reflections from the rigid boundaries. Based on several numerical experiments, it is concluded that the primary mechanism responsible for significant temperature rise is the adiabatic shock compression of the material. The energy due to distortion or friction contributes little to the total temperature increase. The effects of air pockets and inclusions of higher or lower density materials were investigated. It is found that, due to their high compressibility, soft inclusions, such as air or low density materials, undergo very substantial temperature increases during impact. The present calculations indicate that in order to reduce the hazards associated with the impact of propellant and explosive materials, care should be taken to eliminate inhomogeneities in the form of soft inclusions or gas pockets, as they represent high probability sites of initiation.

Impact experiments on solid propellants and on inert simulants were carried out in support of the analysis. Composite and double base propellants were used. These experiments covered the range of impact velocities between that where no reaction occurs and that where transition to detonation occurs. The observed features of the deformation of the propellant are in good agreement with the analytical predictions.

The work was sponsored by the Air Force Office of Scientific Research (AFOSR), Directorate of Aerospace Sciences, United States Air Force, under Contract F44520-71-C-0060.

734

1. INTRODUCTION

In evaluating the hazards to explosives and propellants, it is essential to obtain an understanding of the phenomena which may lead to the initiation of detonation. As far as this investigation is concerned, interest is limited to stimuli which are representative of typical accidental conditions, i.e., stimuli of moderate amplitude.

The existing detonation theories describe, reasonably well, the steady-state detonation of propellants and explosives by strong shock waves. However, detonation of propellants and explosives can occur under low amplitude shocks and by impact at speeds and pressures well below those predicted by classical hydrodynamic theory of detonation. Equally important as high order detonation is the class of chemical decompositions referred to as subdetonation reactions. Such reactions occur when the stimulus is not sufficient to cause high order detonation but is sufficient to cause disturbances with intensity levels from mild burning to low order detonation. Subdetonation reactions occur at relatively low pressures; hence, they are of interest in determining the potential hazards of propellants to common accidental stimuli such as impact or mechanical action.

The mechanical response of solid propellants in realistic accidential impact situations is characterized by large deformation. These deformations occur prior to initiation. To understand the mechanism leading to propellant ignition it is necessary to delineate the material flow and energy conversion processes during dynamic compression. One of the purposes of the investigation described in this paper is to provide an understanding of the processes leading up to initiation. Further, it is intended to investigate in some detail the process of ignition and to arrive at recommendations regarding the formulation and employment of solid propellants in order to minimize their hazard potential.

This investigation included both experimental and theoretical efforts. The experimental work involved flyer plate impact experiments for the determination of deformation modes, impact speeds required for initiation, and intensity of reaction. Instrumentation consisted primarily of high speed photographic coverage. The gross overall phenomena were observed and data on initiation

thresholds were collected in these experiments. However, it was not possible to gain insight by experimentation alone into the detailed mechanisms contributing to the initiation of the propellant material under impact conditions. Therefore theoretical and numerical modeling of the propellant impact problem was undertaken. In contrast to experimental work the numerical effort permits a detailed investigation of the phenomena taking place during impact. This in turn leads to a better understanding of the parameters which may play an important role in the initiation of propellants. Theoretical calculations can also enhance the interpretation of experimental results, while the latter may be used to check the computations.

The present version of the code is capable of handling multi-material problems with a choice of variable mesh size. This permits high resolution in a desired region while not increasing computer storage requirements substantially. It can also treat inhomogeneities in the material in the form of air pockets and higher or lower density inclusions.

2. SENSITIVITY EXPERIMENTS

Sensitivity of an explosive or ease of initiation may be defined as an inverse function of the energy expended in creating a disturbance that is just sufficient to cause initiation. Accidents involving solid propellant rocket motors have resulted in considerable damage to the surrounding environment. These effects are similar to that of a detonation of a high explosive. In the laboratory however, the propellants, subjected to a high pressure-short duration load from a detonating high explosive donor, cannot be ignited and they usually shatter. On the other hand, initiation of burning and detonation reactions occur at a much lower pressure by the long duration loads occurring as a result of low-speed impact.

Flyer plate impact experiments (Figure 1) on solid propellant materials and their inert mechanical simulants were carried out in order to determine deformation modes, impact speed required for initiation, intensity of the reaction, and to assist in the development of the theoretical model and substantiation of the predictions of the analysis. The Beckman & Whitley model 189 framing camera, operating at a framing rate of four microseconds between frames, was used to observe the deformation of the propellant during the early times, the first 100 μsec. Fastax cameras operating at 5000 fps were used for late time phenomena. Details of the experimental setup can be found in Reference 1. The experiments were conducted on two composite solid propellants, similar in composition except for binder, and one double base propellant. Their corresponding inert mechanical simulant was also tested at the same loading condition. The two composite propellants (PBAN and ANP) had aluminum as the fuel and ammonium perchlorate as the oxidizer. The binder materials were PBAN and polyurethane, respectively. The double base propellant consisted of aluminum as the fuel, HMX as oxidizer and EJC as binder. Experiments were carried out on EJC, PBAN and ANP to bracket the ignition threshold and intense reaction region. Each of the propellants were impacted at speeds ranging from 200 fps to 800 fps. The samples were cylindrical in shape, 5 in. in diameter by 5 in. high. The results of these tests are summarized in Table 1. Tests on an inert simulant, HDLK, carried out at the same impact speeds resulted in recovery of the compressed and fractured material.
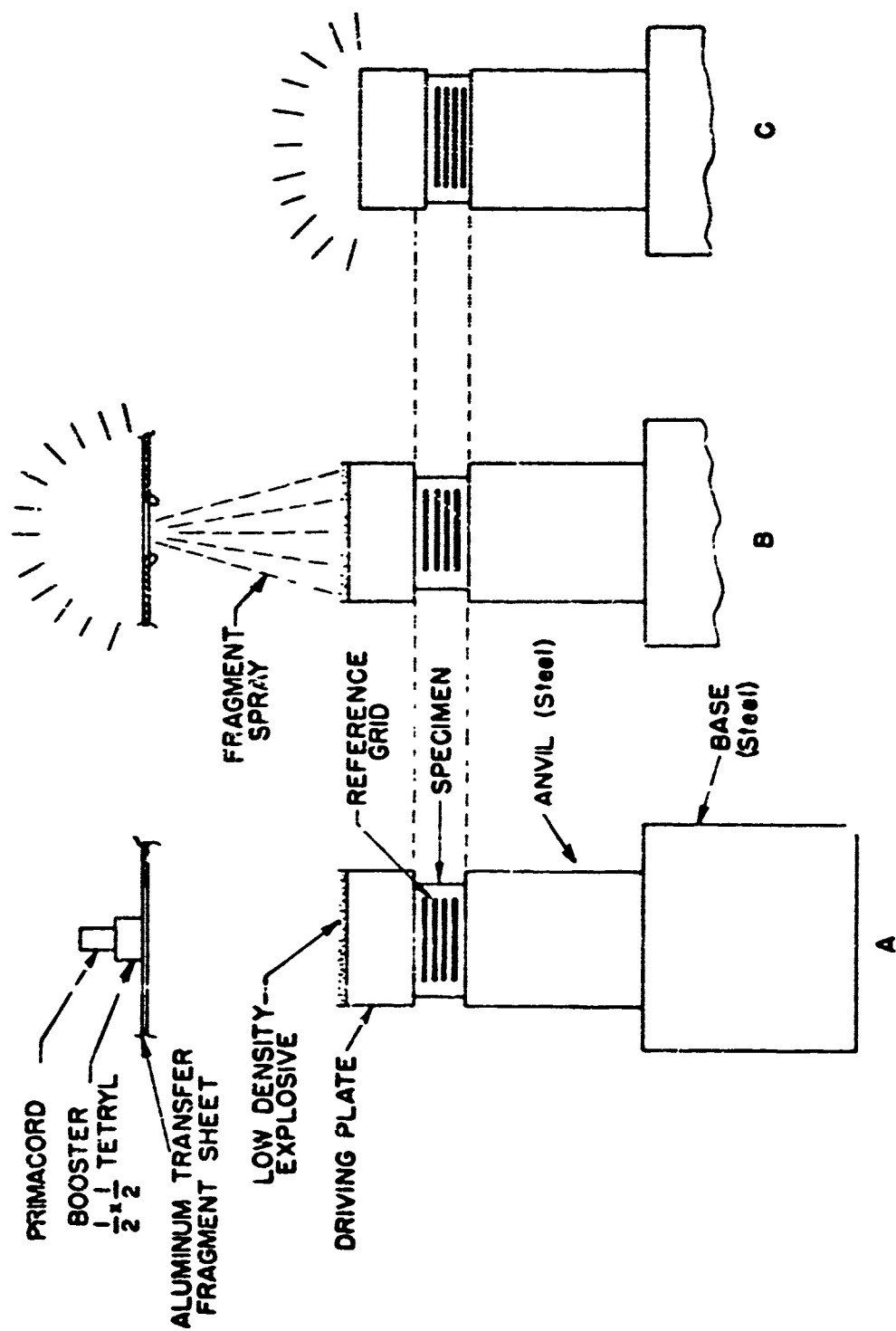
Figure 1 Test Arrangement

PRIMACORD

BOOSTER
$\frac{1}{2} \times \frac{1}{2}$ TETRYL

ALUMINUM TRANSFER
FRAGMENT SHEET

LOW DENSITY
EXPLOSIVE

DRIVING PLATE

FRAGMENT
SPRAY

REFERENCE
GRID

SPECIMEN

ANVIL (Steel)

BASE
(Steel)

A

B

C

Table 1

SUMMARY OF IMPACT EXPERIMENTS ON SOLID PROPELLANTS

IMPACT VELOCITY (fps)	PROPELLANT		
	EJC HMX/EJC/AL	PBAN AP/PBAN/AL	ANP AP/PU/AL
200	No Go	No Go	No Go
300	Scattered Burning	Partial Burn, Fragments	Partial Burn, Fragments
600	Burn In Place	Burn In Place	Partial Burn, Firebrands
800	Bowed Plate, Metal Flow	Burn In Place	Bowed Plate, Metal Flow

One of the important observations made is that composite and
double base propellants can exhibit intense reactions, resembling
low-velocity detonation, at impact speeds of ~800 fps. These mate-
rials were considered to be insensitive by other tests. The dimen-
sions of these materials were well below their critical diameter
for detonation, which was determined to be of the order of 60 in. for
PBAN (Ref. 2).

Other experiments were carried out to determine the ignition
threshold as a function of charge size for PBAN solid propellant.
Sample sizes ranged from 1 in. to 10 in. in length and 4 to 10 in. in
diameter. It was found that the PBAN propellant is exceedingly easy
to ignite by impact, requiring a plate impact speed of 150 to 300
fps, depending on charge size. However, the intensity of the reac-
tion at these impact speeds is a mild burning. Even at higher impact
speeds, reactions of the PBAN propellant were less intense than
those observed for the polyurethane propellant.

PBAN is found to be the more sensitive material but ANP is more
explosive where explosiveness denotes the intensity of reaction of
the material when ignited. Although the materials may be charac-
terized by these terms, the physical and/or chemical properties
governing sensitiveness and explosiveness of a material to a given
input stimulus are not yet clear.

It was also observed in Fastax film records that the ANP propel-
lants, in particular, produced firebrands. That is, upon impact
the material fragmented into a large number of burning pieces.
These pieces of lit propellant, firebrands, traveled hundreds of
feet. Thus there is not only the blast or overpressure hazard but
also the fire hazard associated with low speed impact. EJC on the
other hand did not produce firebrands. It is the intent of the
analytical work described in the next section to provide a detailed
understanding of the impact and material flow processes to determine
the way in which the mechanical energy is converted to thermal
energy, and to determine the effects of material properties on this
conversion process.

3. COMPUTATIONAL EFFORT

This work consists of the numerical modeling of the flow phenomena occurring in material billets subjected to impact. The primary tool employed in the modeling of propellant impact is a two-dimensional Langrangian code developed specifically for this purpose. Both plane two-dimensional and axisymmetric cases may be handled. Material behavior can be hydrodynamic or elastic-plastic where stress levels are not sufficient to permit a hydro-dynamic idealization of the material for low-velocity impacts.

The code is based on well established numerical techniques (Ref. 3) and detailed information regarding the same can be found in Reference 4. The code is capable of computing both unconfined impact and the impact of a flyer plate which simulates the most common experimental configuration. The materials considered were both propellants and explosives. The latter were included for comparison purposes and also because more information regarding their behavior, properties and equation of state data was available. A caloric form of the equation of state, relating pressure, density, and specific internal energy, is required to perform hydrodynamic or elastic-plastic computations. However, in order to study possible initiation mechanisms, an estimate of the temperature field must be made. This in turn requires a thermal equation of state which relates temperature to the other thermodynamic variables. While caloric equations of state may be derived from rather simple experimental data, more detailed information is required to describe the thermal behavior. These data are usually not available for complex propellant materials.

Since temperature is a good measure of the likelihood of initiation occurrence in the propellant, the capability of computing this variable was introduced into the computer program for at least one form of the equation of state (Ref. 4). Also the treatment of surface friction at the rigid surface was incorporated into the code. Other boundary conditions that may be simulated at this surface are free-slip or no-slip conditions. To aid in the interpretation of the computational results, a capability for graphical display

of the deformed propellant billet has been developed. Basically the generated plots represent the current location of the computational grid.

The program is capabile of handling simultaneous calculations in two liquid and/or solid materials, air and a detonating explosive. The equations of state for air and the detonating explosive are fixed but can readily be modified. For the nonreactive solids and/cr liquids the equations of state can be changed by simply replacing the appropriate equations of state subroutines with new ones. This approach, rather than a change in input values, was chosen because different materials may require not only different equation parameters but also different equation of state formulations.

The other significant feature of the code is the incorporation of varible size mass zoning. This adds to the computational flexibility in that regions requiring high definition may be zoned finely while coarser zoning can be used elsewhere. The obvious advantage of this zoning is that while high resolution can be obtained the computer storage requirements may not increase substantially. Another important flexibility provided into the code enables one to consider inhomogeneities in billet material in the form of gas pockets or higher and lower density inclusions.

4. PESULTS - SUMMARY AND DISCUSSION

Results obtained from the computational efforts of this program are described in brief herewith. In the case of an unconfined impact, the impact generates a shock wave moving upwards from the rigid interface. However, since the lateral surface of the cylinder is free, rarefaction waves move in to relieve the pressure. The flow field behind the original shock is simply one-dimensional. Once the rarefaction wave moves in, the flow field becomes two-dimensional. After sweeping through the entire billet the shock encounters the top free surface reflecting a strong rarefaction down into the material. This wave interacts with the rarefaction waves coming in from the lateral boundary, setting up a complex wave pattern in the billet. Further interactions of these waves with the rigid and free boundaries take place. In general these tend to relieve the pressure. Finally regions of strong tension may appear in the material, particularly along the centerline. Figure 2 illustrates the pressure field for the PBAN calculations at a certain time. Also shown are displacements and distortions which occur in the material due to the impact. As should be expected, the largest lateral displacement occurs along the rigid boundary.

The behavior of other materials in unconfined impact is qualitatively the same as described above. This is illustrated in Figure 3 which shows the displacements and temperatures for impact on an EJC billet. Similar results for TNT are contained in Reference 4. A comparison of the mechanical behavior of the three materials is shown in Figure 4. For all cases hydrodynamic behavior is assumed. Shown are the velocities and displacements at the corner of the billet. Again the similarity in behavior may be observed. Largest displacements and velocities are obtained for TNT.

In general, displacements and velocities in the hydrodynamic approximation are primarily the function of the density. This is clearly borne out by the results of Figure 4. To ascertain the influence of material strength on the mechanical behavior, impact calculations were performed for TNT assuming elastic-perfectly

Computation Cycle 230 , Time = 27.8 μ sec
Time Step = 0.008 μ sec. Last Cycle at
Which Original I-D State of 7.1 k Bar
Exists at x = 0 , z = 3.25 cm
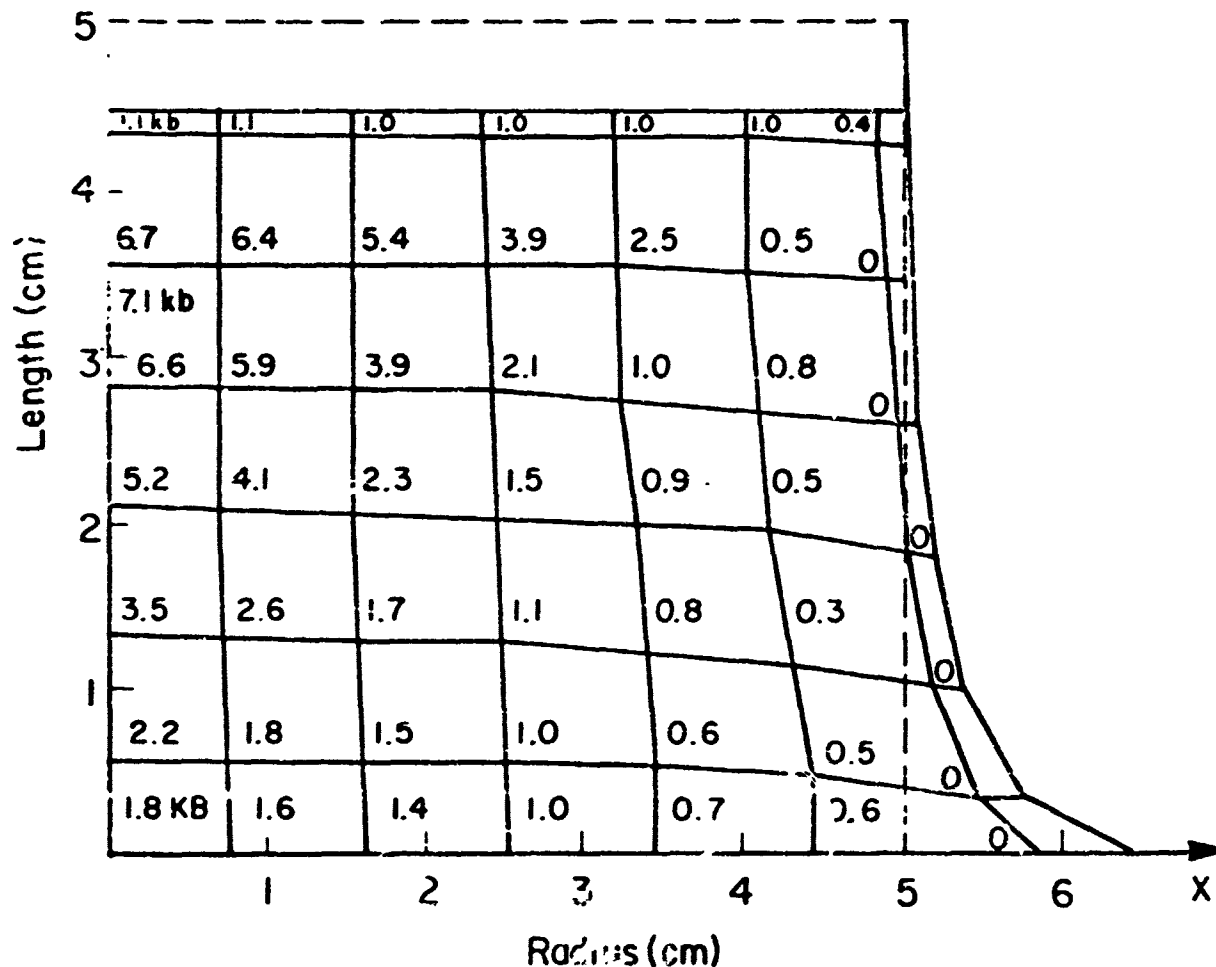
V_0 = Impact Speed = 2 cm/msec = 700 ft/sec

Radius = 5 cm   Length = 5 cm

✳ Numbers In Corners of Rectangles Are Values
Of Pressure In Kilobars

Figure 2   PRESSURE AND DISPLACEMENT FIELD IN UNCONFINED IMPACT -
PBAN (Hydrodynamic)

1514
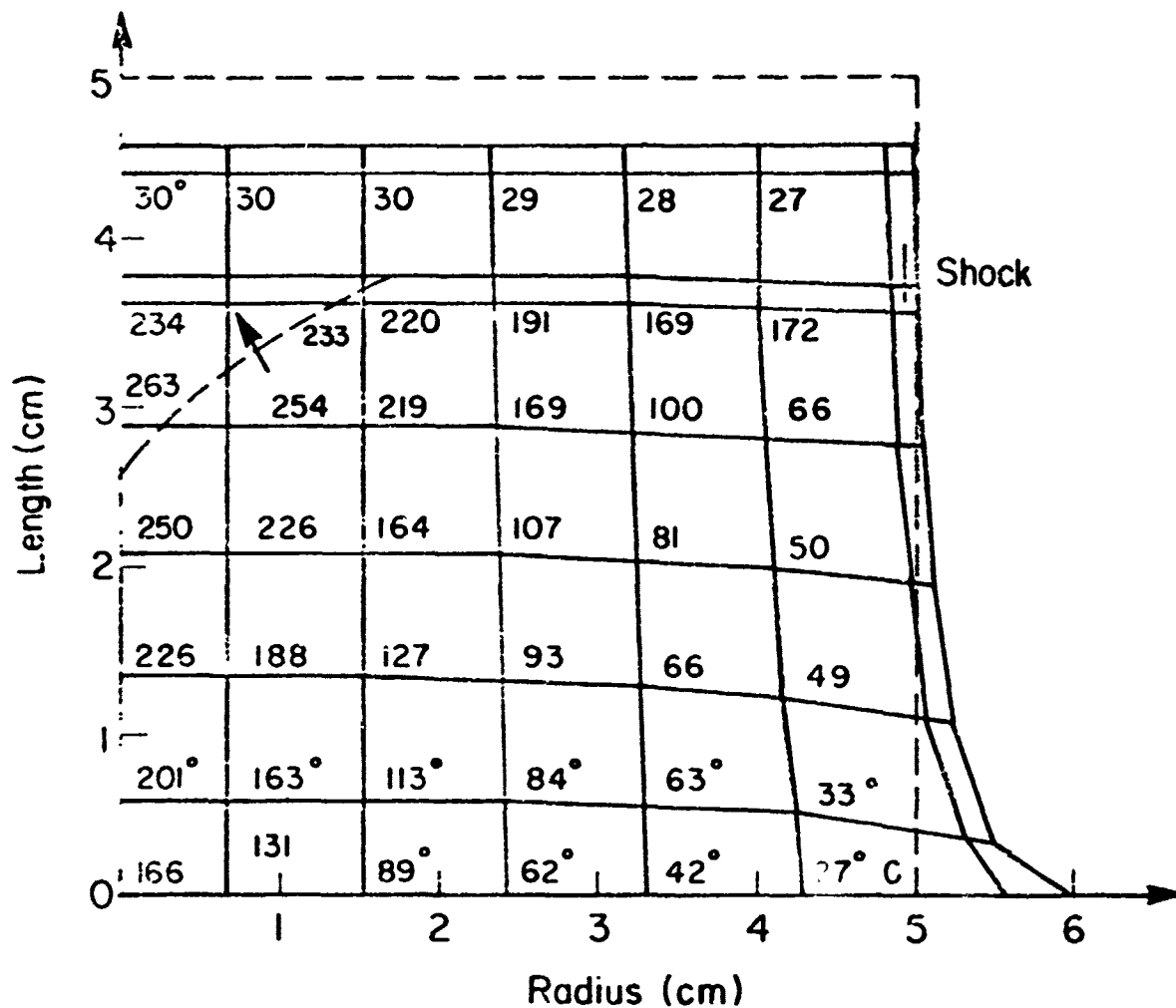
Impact Speed 21cm /msec Time =20.6 μsec
Shock At 3.75 cm Head Of Rarefaction at (0, 2.6 cm)
Initial Radius and Length 5 cm X 5 cm

✳ Numbers In Corners Represent Temperature
In °Centigrade

Figure 3   DISPLACEMENT AND TEMPERATURE FIELD IN UNCONFINED IMPACT -
EJC (Hydrodynamic)

1515
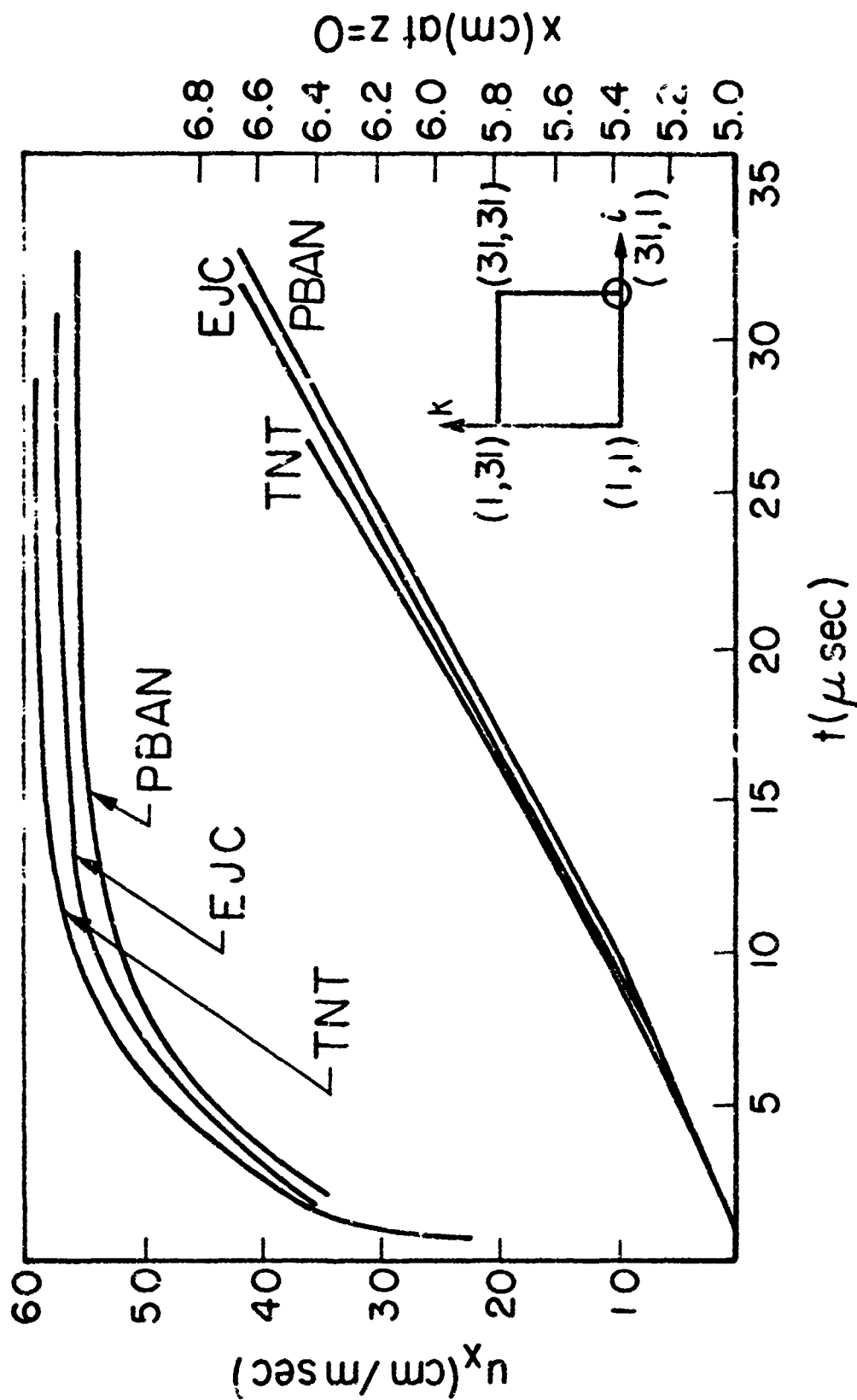
Figure 4 VELOCITY AND DISPLACEMENT VS. TIME AT CORNER OF BILLET i = 31, k = 1, EFFECT OF MATERIAL TYPE

plastic behavior. The effect of material strength is clearly demonstrated in Figure 5 which again shows the corner displacement and velocity. Both the velocity and the displacements are considerably reduced when material strength is taken into account.

Since the purpose of this study is to delineate possible initiation mechanisms for propellant and explosive materials, the most significant computational results are the temperature distributions. Typical of the calculated temperature fields is the one for EJC shown in Figure 3. The highest temperatures in unconfined impact occur generally behind the propagating shock wave. It has been observed that the maximum temperature never occurs at locations close to the free surfaces. The location of maximum temperature approximately follows the shock path upwards through the billet.

Figure 6 shows the effect of taking into account the strength of a material on the temperature field. As should be expected, higher temperatures prevail when a purely hydrodynamic behavior is assumed. The pressures in the hydrodynamic material are also higher. When material strength is included, part of the impact energy is dissipated in distorting the material, i.e., in mechanical work.

To determine the significance of surface friction in unconfined impact, computations were performed including the friction effect at the rigid surface. It was found that the effect of friction on the temperature increase was minimal. More significant was a slight reduction of the radial velocity and displacement along the rigid surface.

Since the computed temperatures in unconfined impact were found to be quite moderate, calculations were performed for partially confined impact. The same size billet was used but now resting on a rigid surface, and being impacted by a rigid flyer plate from above. The impacting plate was assumed to have the same initial velocity as the free impacting billet. Considerable higher temperatures were now computed. This is shown in Figure 7 which compares the maximum temperatures as a function of time for the plate impact case with the unconfined impact. Identical material
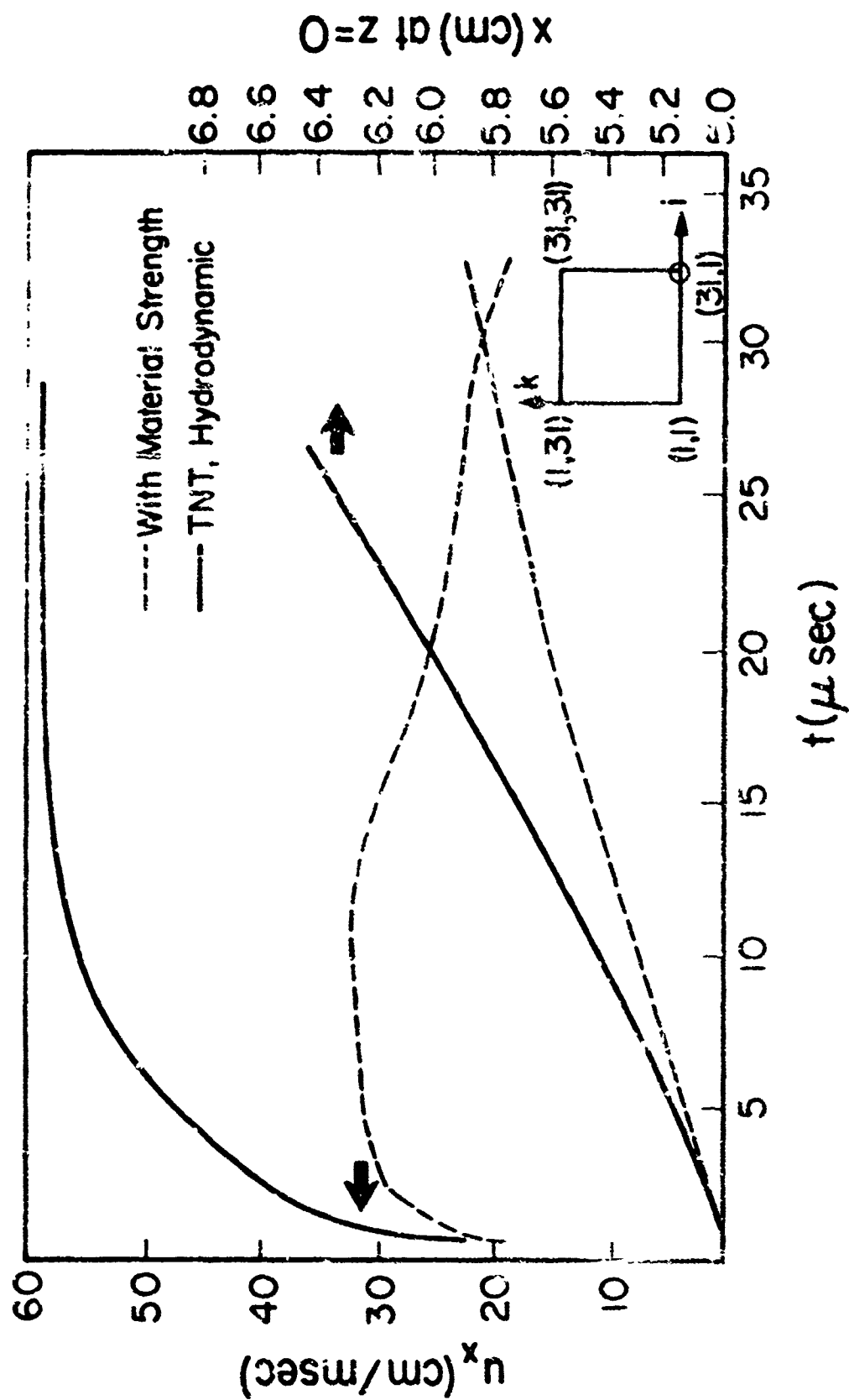
Figure 5   VELOCITY AND DISPLACEMENT VS. TIME AT CORNER OF BILLET, $i = 31$, $k = 1$, EFFECT OF MATERIAL STRENGTH
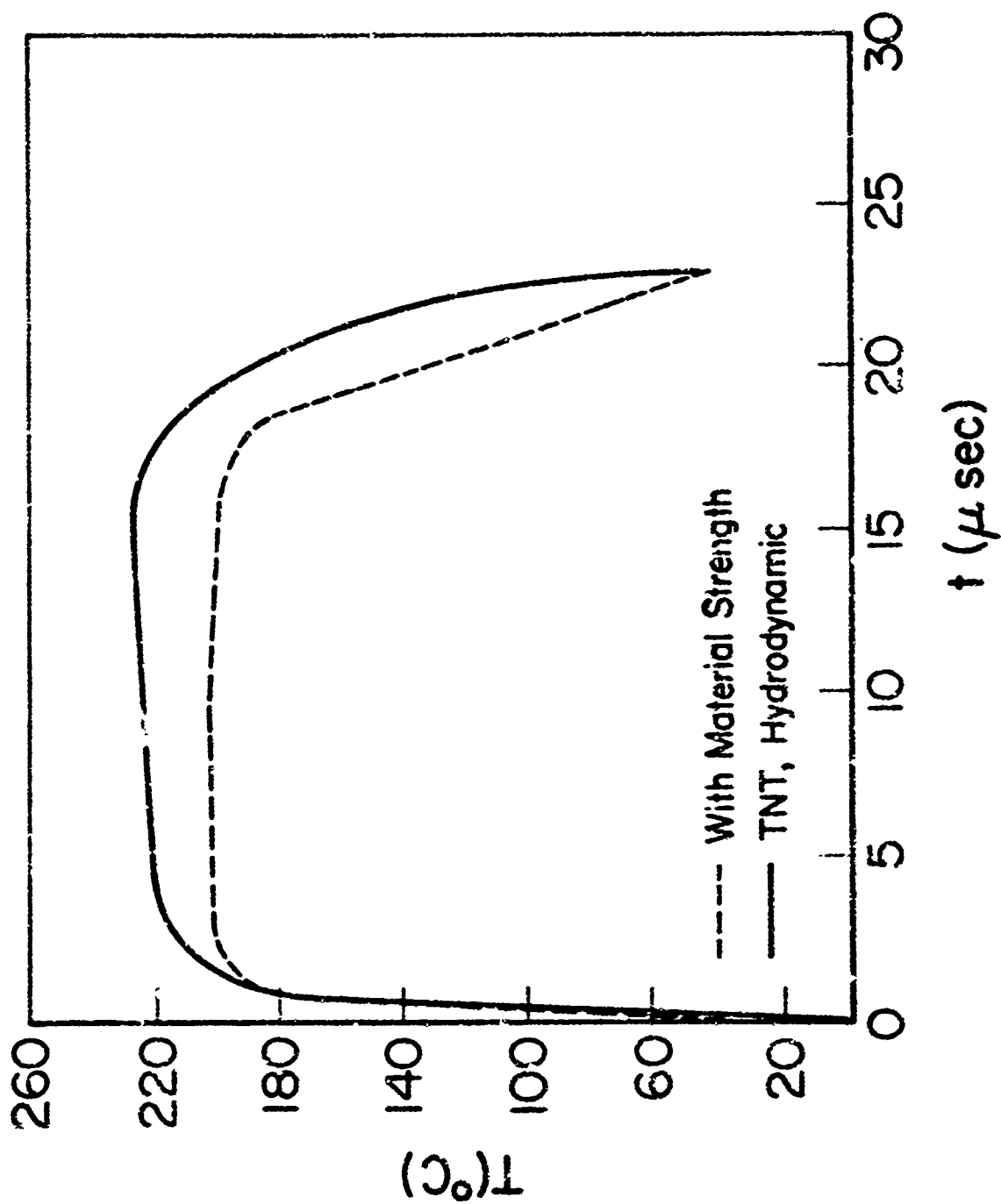
Figure 6   MAX. TEMPERATURE VS. TIME $V_0 = 21$ cm/msec
EFFECT OF MATERIAL STRENGTH
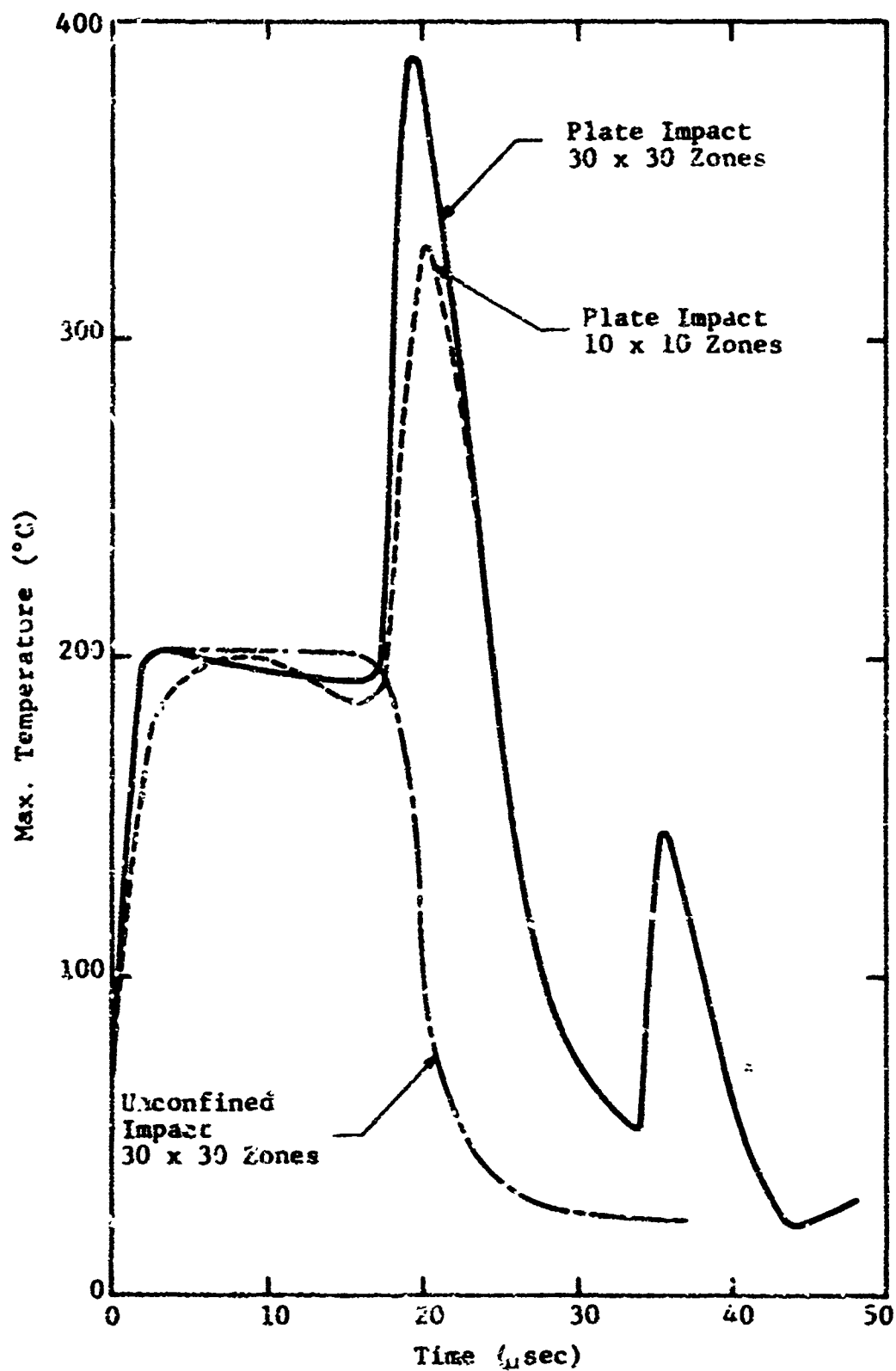
Figure 7   Max. Temperature vs Time for TNT
            Elastic-Plastic Material Behavior

picperties were assumed for both cases. The particular computation
is for TNT with material strength. Also shown in this figure are
results for plate impact obtained with a coarser computational grid
(10 zones in each direction rather than 30). The temperature
predicted is seen to be lower. This indicates that a coarse
computational grid is not capable of sufficiently resolving the
flow field to determine the maximum temperatures since these are
normally restricted to a small region. The maximum temperature occurs
on the interior of the billet close to the centerline. A rapid
initial temperature rise is followed by about 20 μsec of nearly
constant maximum temperature, as the shock caused by the plate
impact traverses the billet in the downward direction. Upon shock
reflection at the bottom rigid surface the temperature takes a
rapid jump to its maximum value of nearly 400°C. Due to the absence
of such a reflecting surface in unconfined impact, the temperature
does not experience a second rapid increase and the maximum temperature
obtained is much lower. After reaching this peak value the maximum
temperature decreases rapidly as the rarefaction waves originating
from the lateral free surface relieve the pressure in the material.
During the temperature increase the region through which the maximum
temperature prevails in the radial direction shrinks continuously
as the rarefaction waves progress toward the centerline of the
cylindrical billet.

From these results it seems that the primary mechanism
responsible for the temperature rise is the adaibatic shock compression
of the material. To further test this inference, additional compu-
tations were performed, again assuming a flyer plate impact but
for a narrower cylinder (2.5 cm radius and 5.0 cm height). The
maximum temperatures as a function of time for these calculations
are shown in Figure 8 as a dashed line. While the behavior s
qualitatively similar to that of the wider cylinder, the second
temperature peak due to shock reflection is actually lower than the
temperature behind the original shock. This is due to the fact
that the rarefaction waves coming from the lateral surface had
sufficient time in the narrow cylinder to penetrate to the center-
line and thus lower the pressure behind the incident shock before
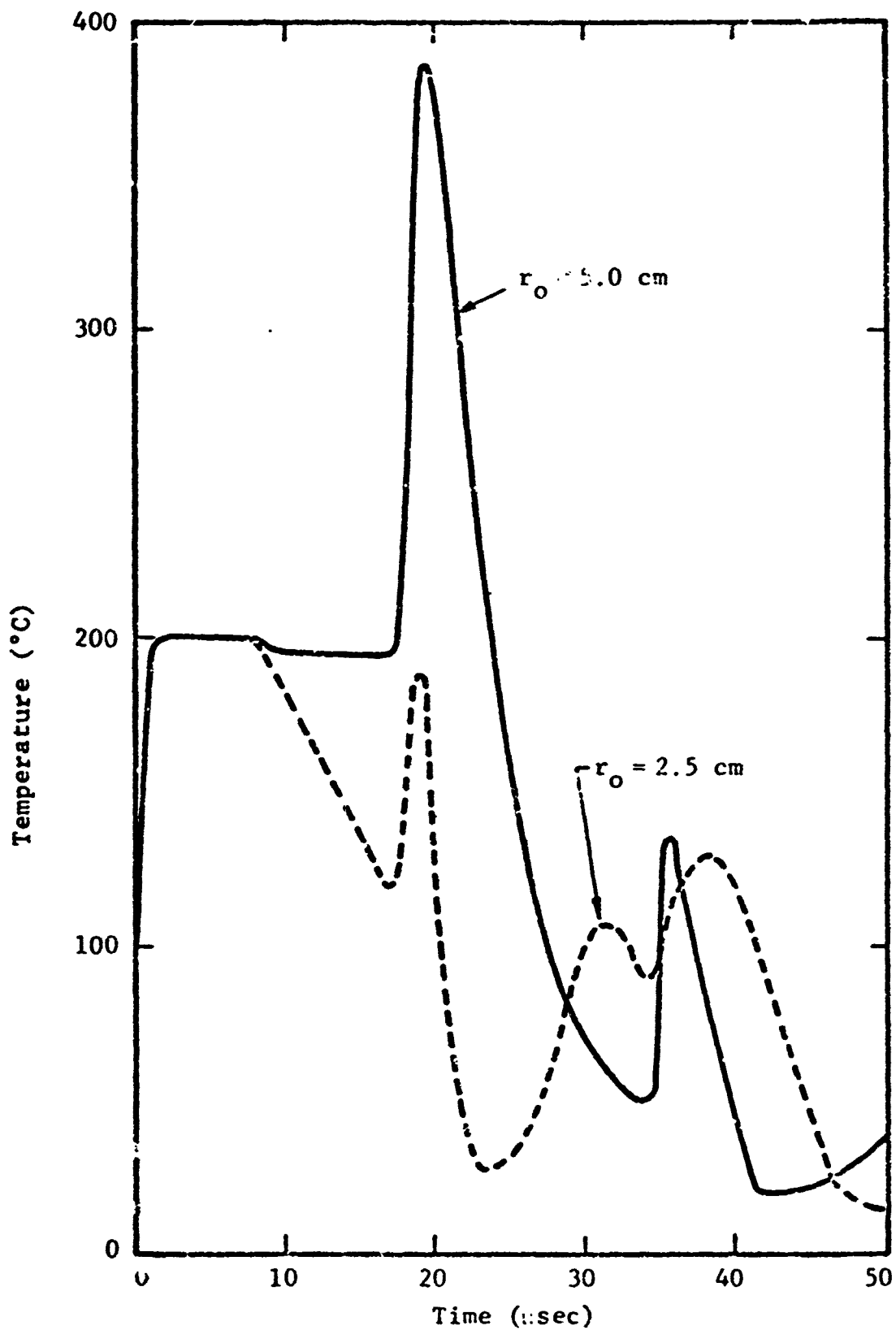
Figure 8   Maximum Temperature versus Time for TNT Elastic-
Plastic, Free-Slip Boundary

reflection took place. This confirms the earlier conclusion that high temperatures in the material are produced by adiabatic shock compression. The deformation of the narrower cylinder is as great or greater than that experienced by the large cylinder. This can be seen in Figure 9, which represents the mesh distortion of the cylinders at approximately equal times.

The computations modeling the flyer plate impact were carried out both for a free-slip and no-slip boundary condition at the bottom or anvil rigid surface. The resulting maximum temperatures were found to be virtually the same in both cases. This can be seen by comparing Figure 8 with Figure 10, where the latter presents the maximum temperature as a function of time for the no-slip case. The deformation has only insignificant influence on the temperature; adiabatic compression is the dominant effect.

The highest temperatures in the material are limited to a small spatial region (approximately a sphere of 0.08 cm radius) and occur only for very short durations (a few microseconds). However, other investigators have shown (Ref. 5) that at a temperature around 400°C initiation sources or hot-spots of these dimensions and durations are sufficient to cause initiation. Thus our calculations indicate that initiation may take place in a completely homogeneous material due to purely hydrodynamic mechanisms of energy concentration. This focusing of energy depends on the geometry and details of the applied load.

To investigate the significance of inclusions or material inhomogeneities the presence of a small gas bubble can be modeled numerically. Similarly the influence of further material confinement by bulkheads or casing can be numerically studied. While the presence of inclusions such as voids, bubbles or impurities may enhance the chance of initiation, they are not a necessary condition for initiation. During the course of this investigation concern was also focused on the effects produced by material inhomogeneities. This problem is of great importance because typical propellant grains may be expected to exhibit some inhomogeneities.
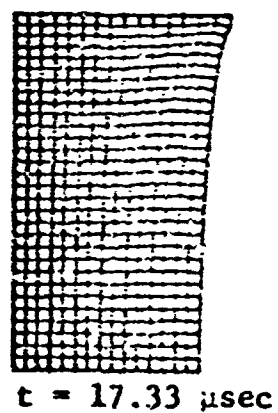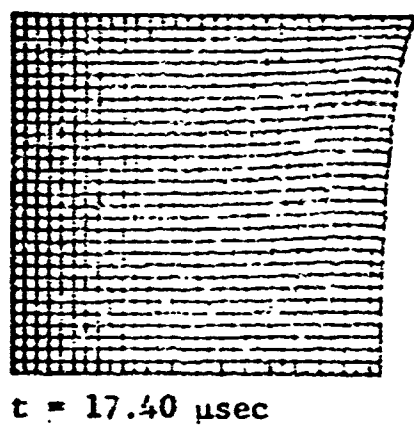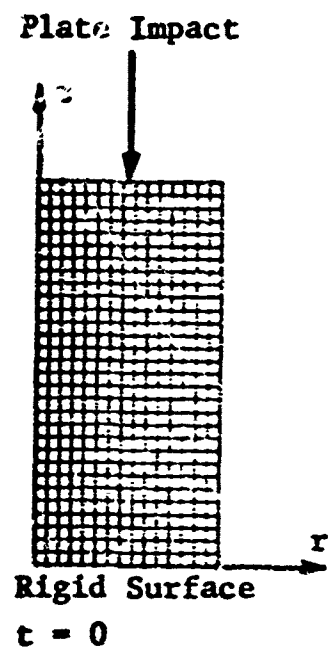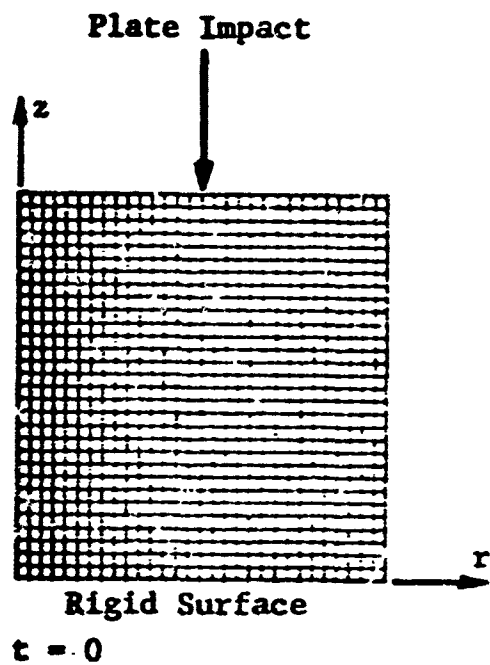
Figure 9a   Comparison of TNT Billet Deformations,
             Plate Impact Vo = 21 au/msec

t = 33.49 μsec

t = 33.05 μsec

t = 54.36 μsec
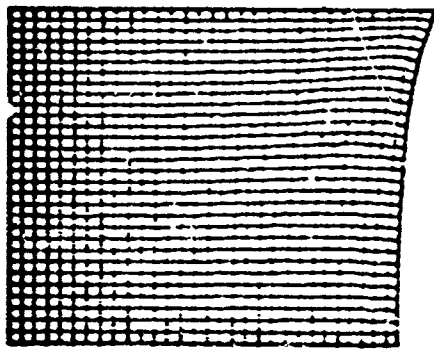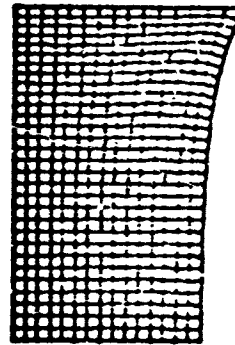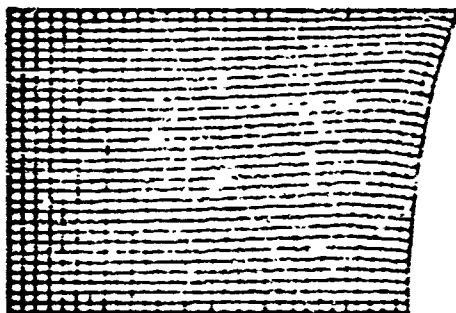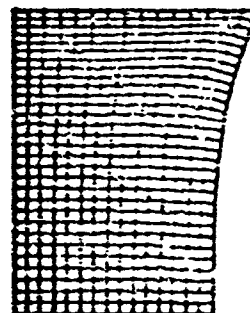
t = 52.90 μsec

Figure 9b   Comparison of TNT Billet Deformations (Cont.)
            Plate Impact Vo = 21 cm/msec
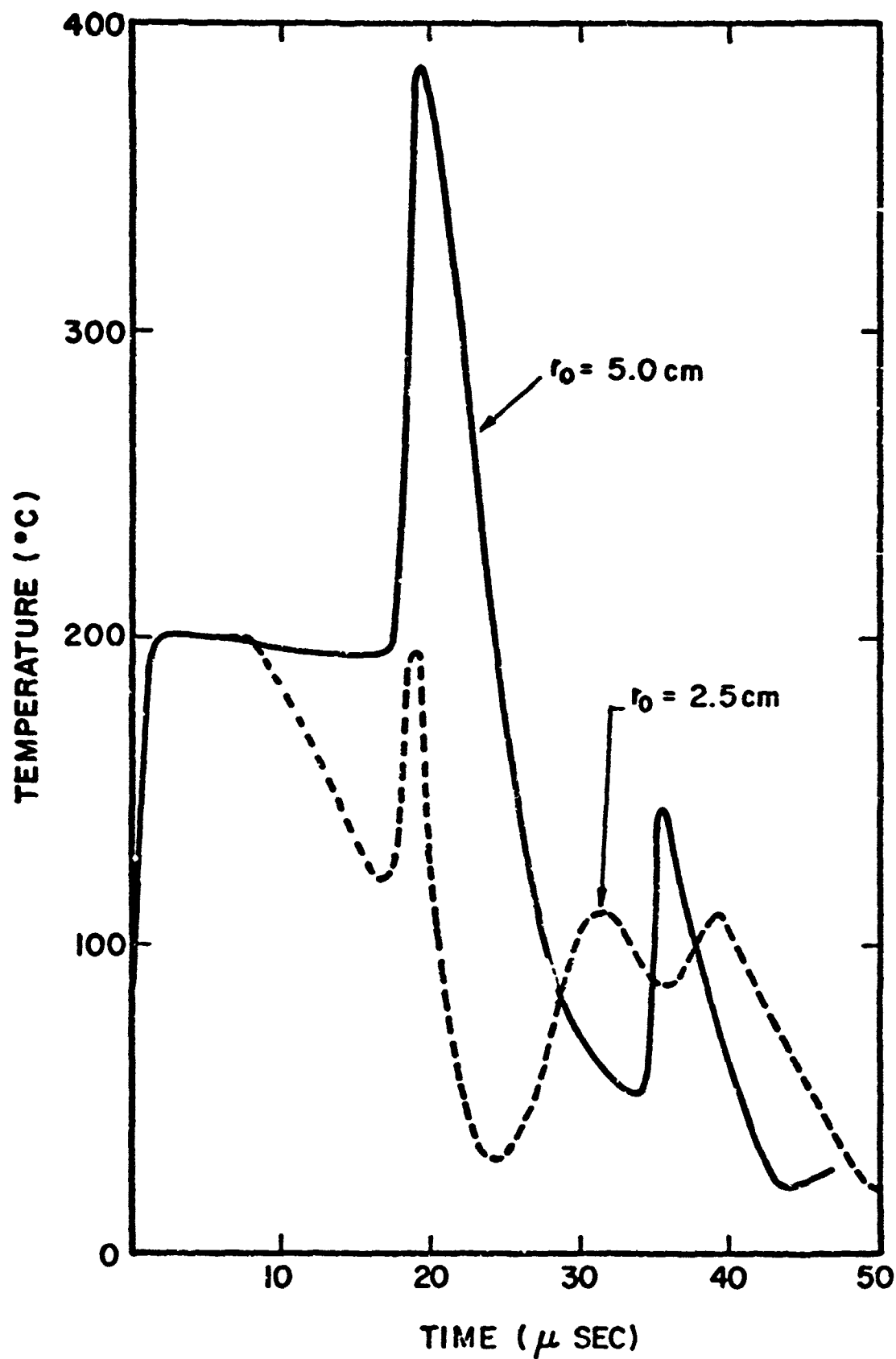
Figure 10   Max. Temperature VS. Time for TNT
Elastic-Plastic, No Slip Boundary

1526

Calculations were carried out for the flyer plate impact on a cylinderical billet of TNT with hydrodynamic material behavior. The inhomogeneity in the cylinder was limited to a single inclusion 0.5 cm in radius and 0.5 cm in height located approximately at mid-height. Three types of material inclusions were considered, viz. air, a material having half the density of the surrounding TNT, and a material having twice that density. In all calculations adiabatic behavior was assumed, neglecting heat transfer. The air was taken to be a perfect gas with a specific heat ratio of 1.4. The calculations were carried out past the time of shock reflection from the rigid bottom surface except for the case of an air inclusion, where the computations had to be terminated due to excessive zone distortion and actual air pocket collapse shortly after the shock passage.

The material distortion of the TNT billet and air inclusion is graphically illustrated in Figure 11 which shows a succession of computational grid distortions for this case. Some material distortions in the neighborhood of the inclusion occurred also in the case of the low density inclusion. For the high density inclusion distortions were insignificant.

A comparison of the maximum temperature for the low and high density inclusion is shown in Figure 12. The second temperature peak in all cases is due to reflection from the rigid bottom surface, and is of less interest here. One sees that the passage of the shock produces a very significant temperature rise for the case of a low density inclusion. This rise occurs in the inclusion proper. The effect of a high density inclusion is much less and the slight temperature rise indicated in Figure 12 occurs in the material immediately adjacent to the inhomogeneity. These results are not unexpected. The high density inclusion acts like a small reflecting surface while the low density inclusion undergoes substantial compression and thus a higher temperature rise. In this case the surrounding higher density (harder) material serves as a large reflecting surface for the low density (softer) inclusion, thus focusing the energy in this region.
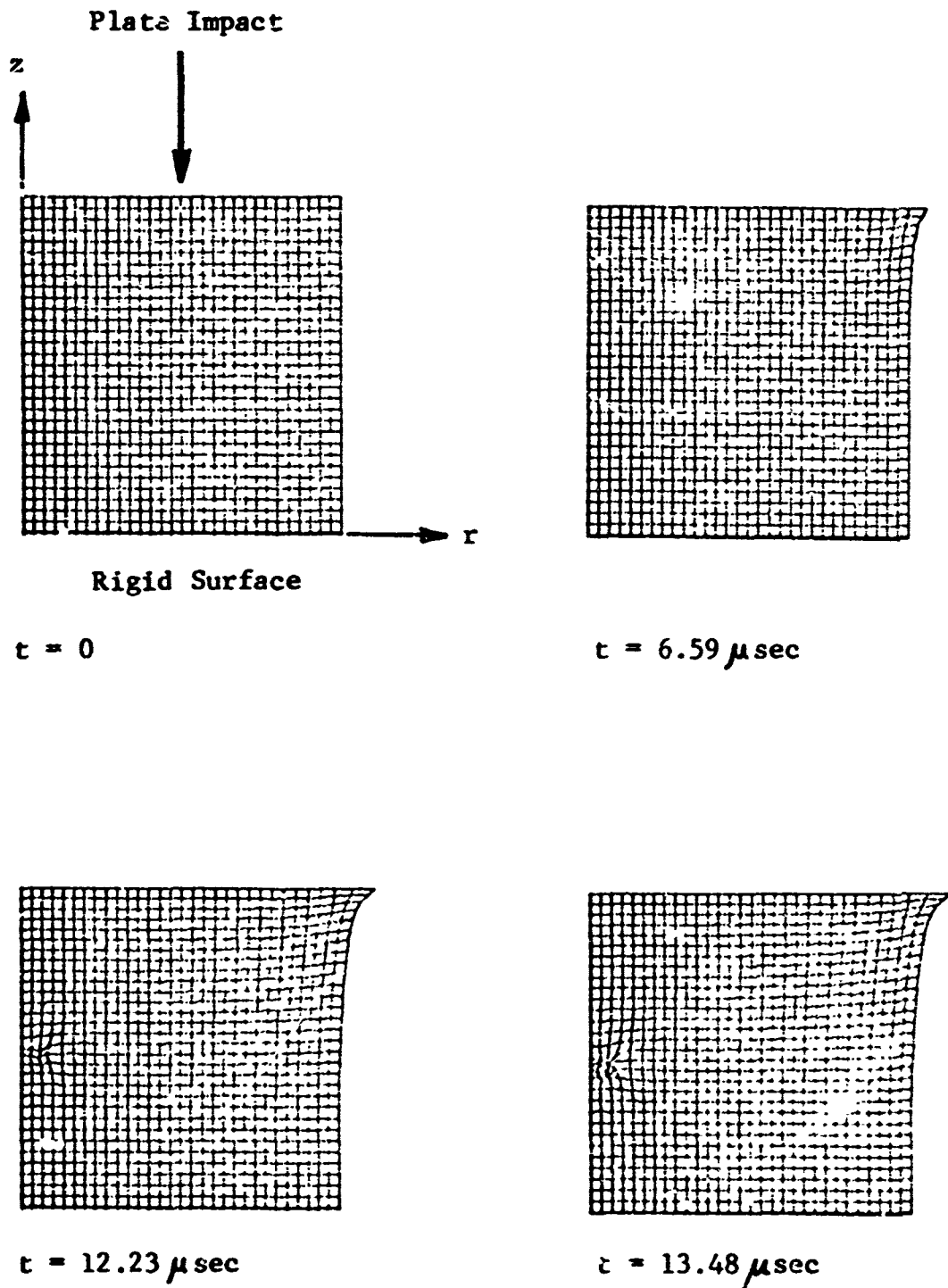
Figure 11   DEFORMATION OF TNT CYLINDER WITH AN
AIR INCLUSION - HYDRODYNAMIC COMPUTATION
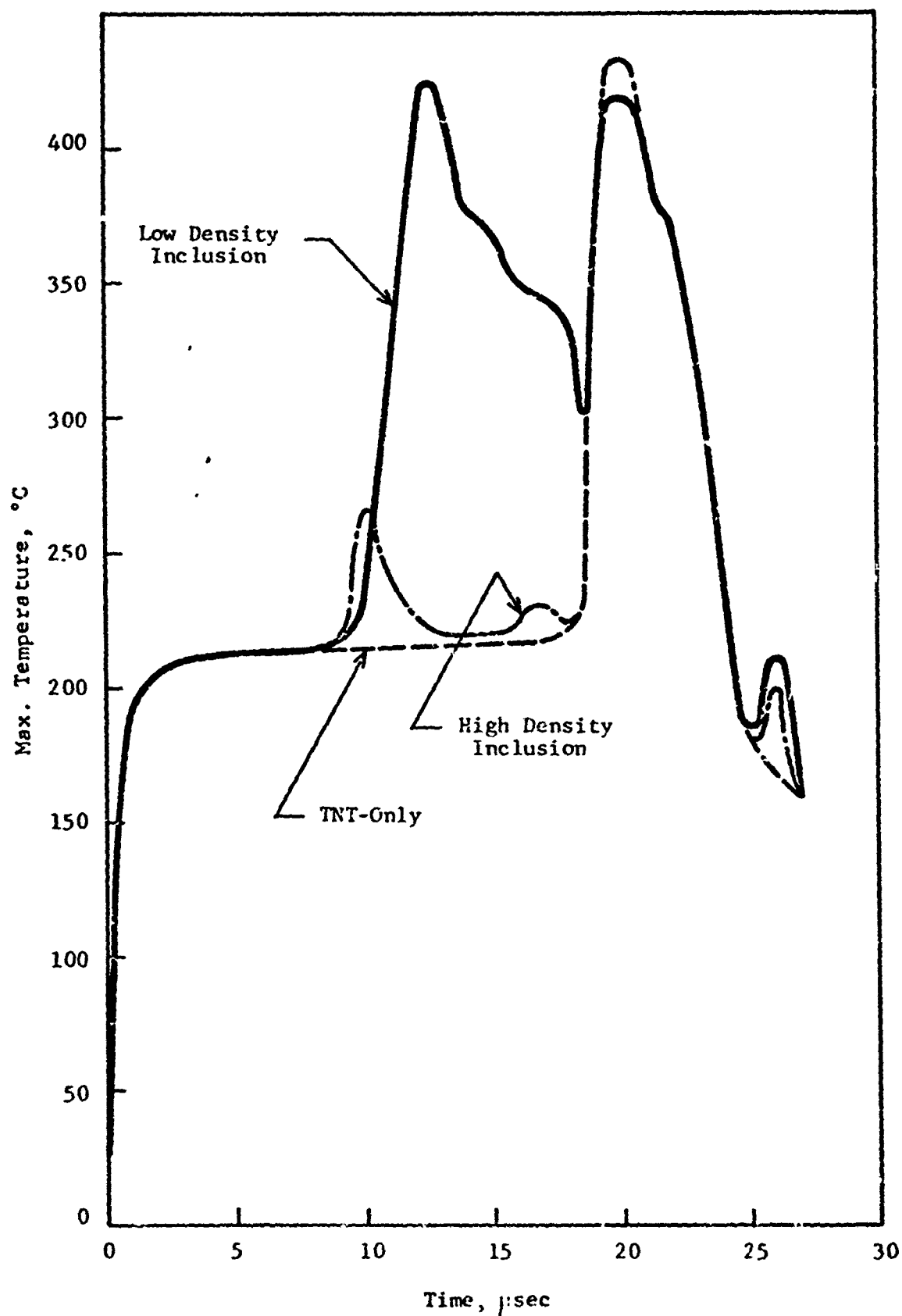
Figure 12 COMPARISON OF MAXIMUM TEMPERATURES
TNT HYDRODYNAMIC COMPUTATION

1520

The temperature and pressure effects caused by inhomogeneities
are further illustrated in Figures 13 through 16 which show profiles
of these variables in the vertical direction through the cylinder,
Figure 13 is for the homogeneous TNT. In all cases, the vertical
profile is along the centerline of the cylinder. Except for the
case of air, the profiles are taken at a time when the incident
shock wave has just passed the location of the inhomogeneity.
For the air inclusion the profiles correspond to the time of air
pocket collapse. The homogeneous material exhibits vertical profiles
typically associated with the passage of a step shock wave. For
the case of an air pocket (Fig. 14) the high temperature spike in
the air is shown.

It should also be noted that the pressure in the air is quite
low in comparison to that in the surrounding material. Therefore,
complete collapse of the air bubble should be expected. The temperature
and pressure profiles obtained with the low density inclusion are
presented in Figure 15. The highest pressure and temperature occur
in the inclusion proper. The profiles exhibit a rapid drop above
the inclusion caused by the pressure wave reflection from the softer
material. The profiles for the high density inclusion are depicted
in Figure 16. As indicated earlier, the highest pressure and tempera-
ture occur immediately adjacent to the inclusion due to the initial
pressure wave reflection from the harder insert. At this instant,
it should be noted that at later times the pressure both in the soft
and hard inclusion equalizes with that of the surrounding material,
however the temperatures remain at different values. As should be
expected the temperature in the soft inclusion is higher while that
in the hard inclusion is lower than the temperature of the surrounding
material.

The results thus far obtained, at least qualitatively, describe
the effect of material inhomogeneities in explosives or propellants
subjected to impacts of moderate amplitudes. The presence of a low
density (softer) inclusion produces a stronger temperature effect which
is comparable to that produced by a reflection from a rigid surface
(Fig. 10). Obviously the most pronounced effect is caused by the
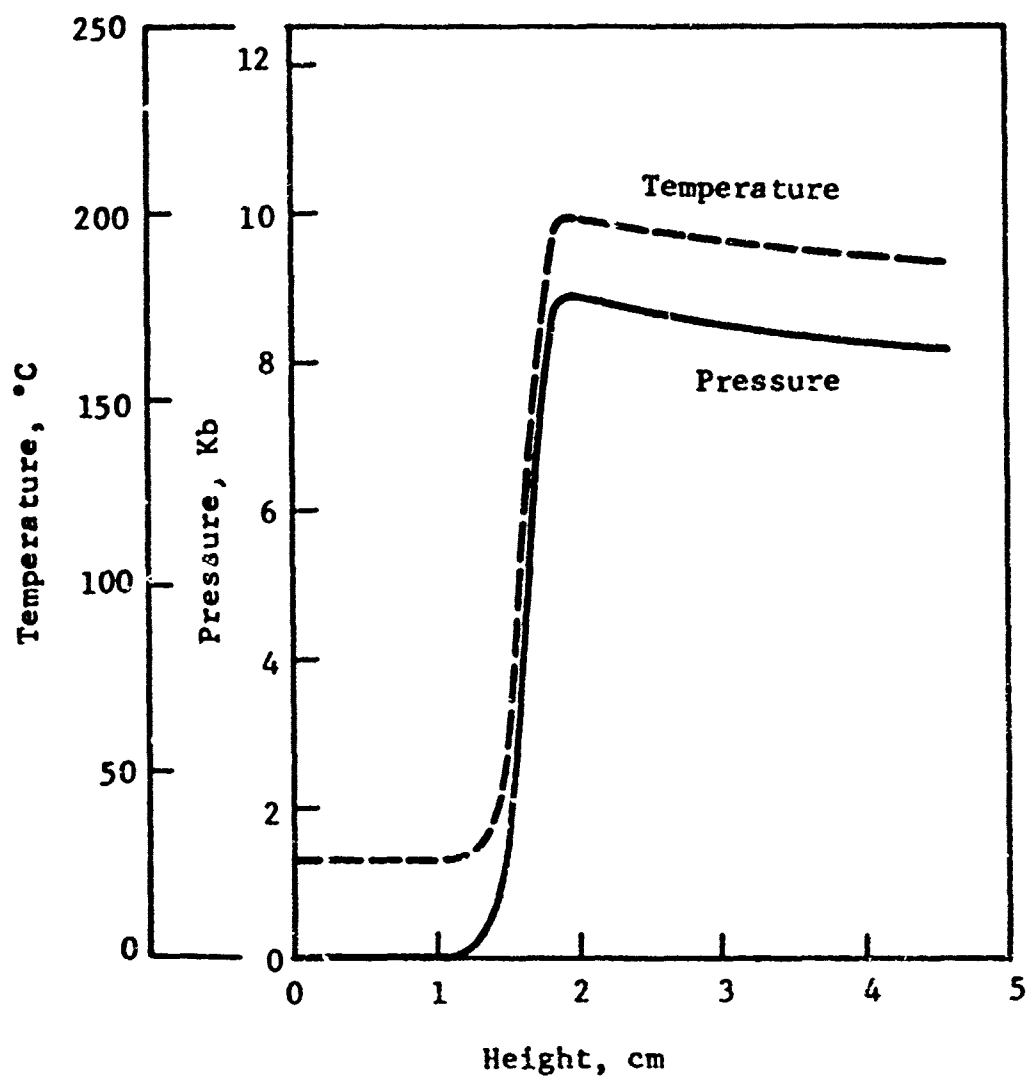
Figure 13   VERTICAL TEMPERATURE AND PRESSURE PROFILES
TNT-HYDRODYNAMIC COMPUTATION
(r = 0, t - 12.23 μsec)

1531
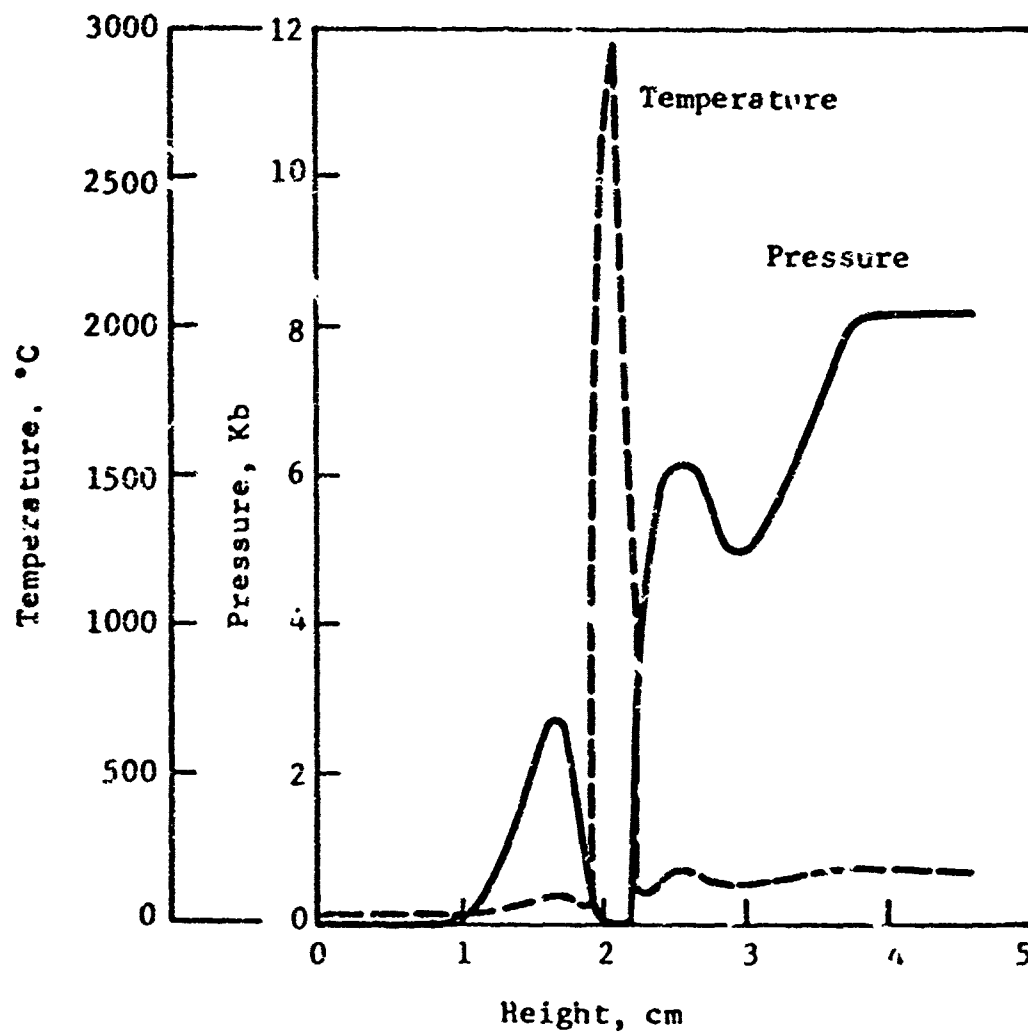
Figure 14   VERTICAL TEMPERATURE AND PRESSURE PROFILES
TNT-HYDROCYNAMIC WITH AIR INCLUSION
$(r = 0, t - 13.48 \mu sec)$

1532
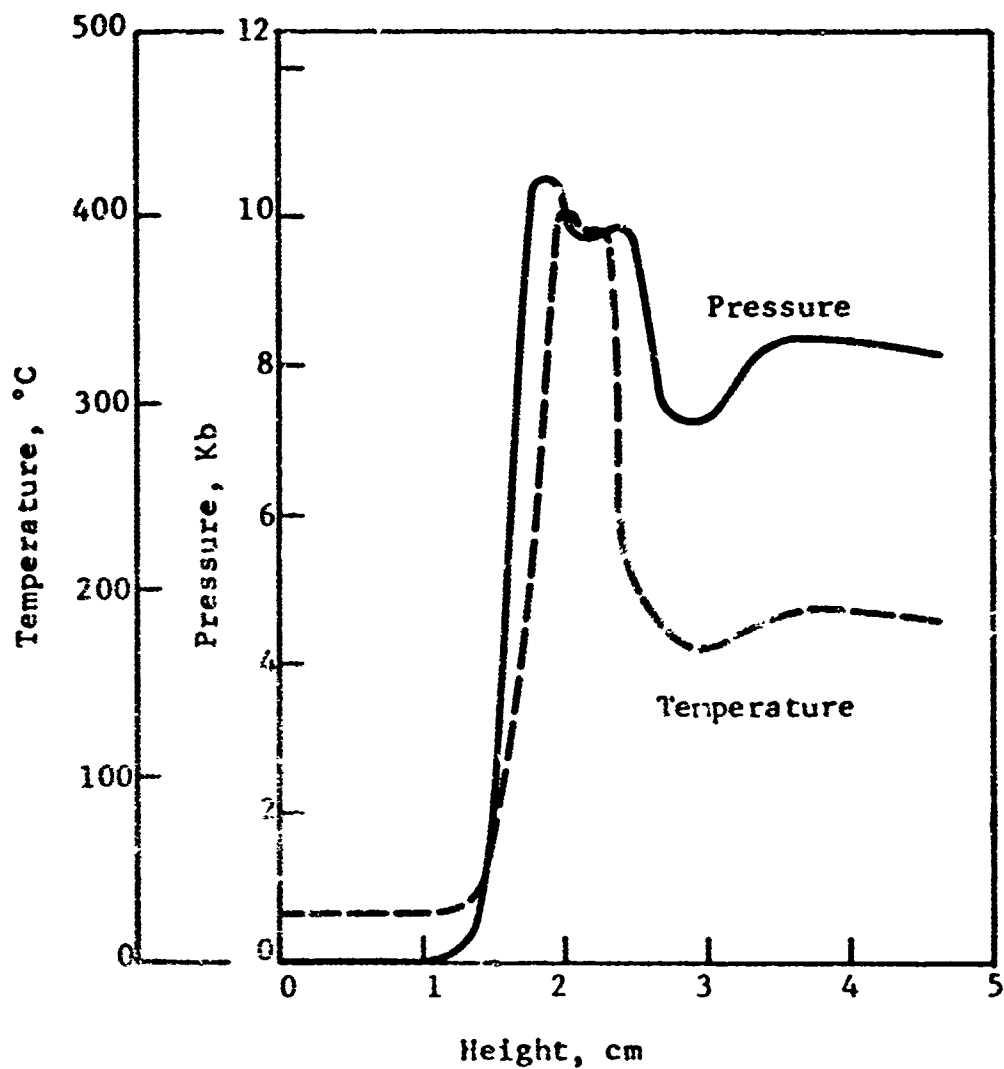
Figure 15 VERTICAL TEMPEFATURE AND PRESSURE PROFILES
TNT-HYDRODYNAMIC WITH LOW DENSITY INCLUSION
$(\rho_i = 0.5\ \rho_o,\ r = 0,\ t = 12.23\ \mu sec)$

1533
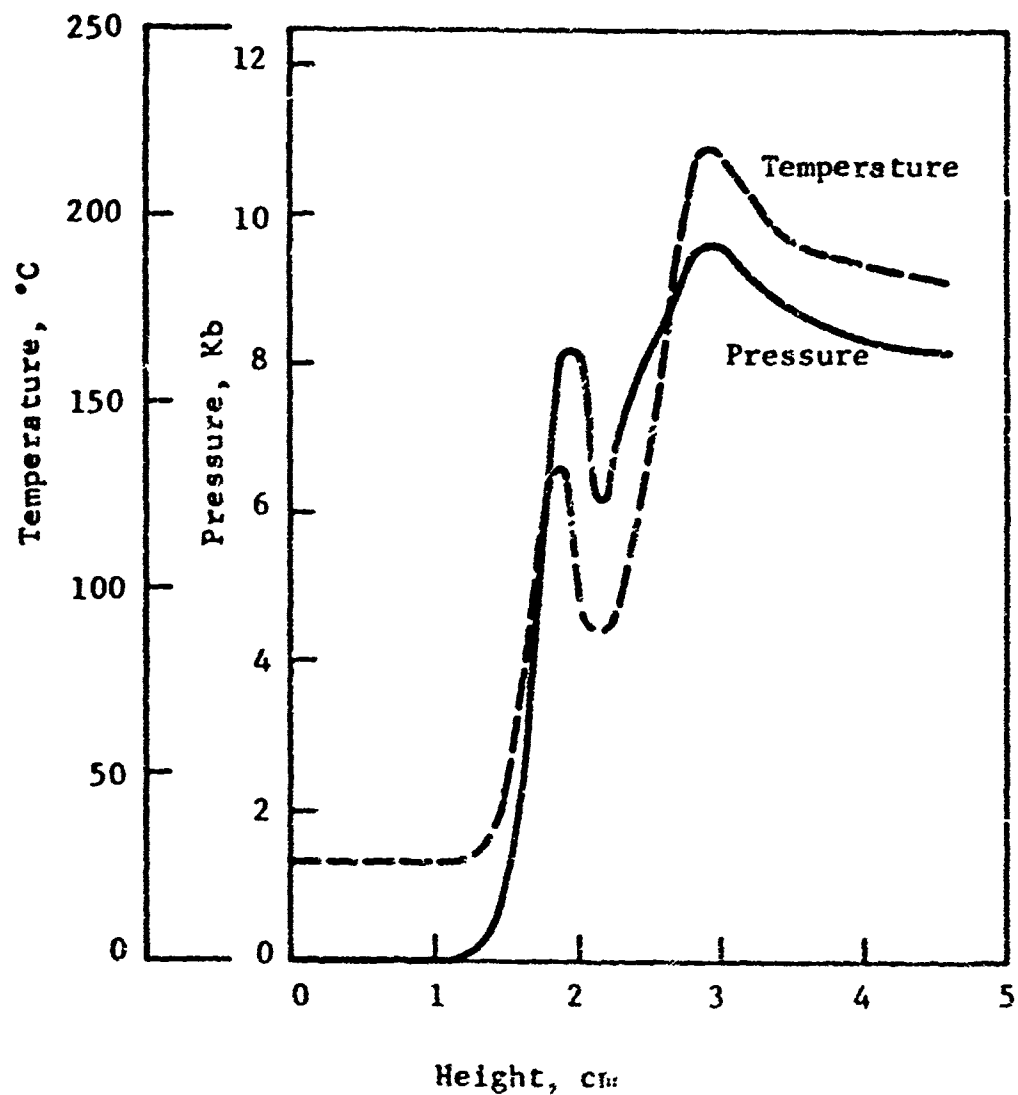
Figure 16   VERTICAL TEMPERATURE AND PRESSURE PROFILES
TNT-HYDRODYNAMIC WITH HIGH DENSITY INCLUSION
$(\rho_i = 2.0 \ \rho_o, \ r = 0, \ t = 12.23 \ \mu sec)$

1534

presence of an air bubble. A more realistic estimate of the effect
of a gas inclusion will require the treatment of heat transfer
and real gas behavior. However, even these preliminary computations
indicate that severe temperature rises may be expected in the
vicinity of the gas pocket and thus the likelihood of initiation
is enhanced by its presence. In general it can be stated that to
reduce the hazards associated with impact of explosive or propellant
materials care should be taken to eliminate material inhomogeneities
and in particular soft inclusions and gas pockets.

5. CONCLUSIONS

The results of this investigation have shown that explosive reactions can occur for composite and double base propellants under conditions of laterally unconfined low-speed impact by a rigid flyer plate. The mathematical model of the impact process shows that there is an almost twofold increase in temperature, under conditions of flyer plate impact, with the propellant resting on a rigid target, compared with the case of the propellant impinging directly on the rigid target. The maximum temperature achieved, $\sim 400°C$, is sufficiently high to cause chemical reaction.

In addition numerical test, using different computational mesh sizes showed higher temperatures are achieved using finer meshes, indicating that the development of high temperatures is a very local phenomenon. For low-speed impact the total applied energy is never sufficient to cause a rise in temperature of more than a few degrees throughout the bulk of the material. Hence it has been recognized that in order to effect an explosion the energy must be concentrated in a small region of the material. In our computations we see that this region is a sphere about 0.08 cm radius which achieves a temperature of ~ 400 °C. Bowden (Ref. 5) has calculated hot-spot radii for explosion of 10^{-3} to 10^{-5} cm with temperatures ranging from $400°$ to $600°C$ depending upon the explosive.

Further, it has been concluded that the primary mechanism responsible for significant temperature rise is the adiabatic shock compression of the material. The energy due to friction or distortion seems to be contributing little to the total temperature increase.

The results obtained for the material with inhomogeneities suggest that due to their high compressibility, soft inclusions, such as air or low density materials, undergo very substantial temperature increases during impact. Therefore, in order to reduce the hazards associated with the impact of propellant and explosive materials, care should be taken to eliminate inhomogeneities in the form of soft inclusions or gas pockets.

Finally, the observed features of the deformation of the propellants during experimentation are in good agreement with the analytical predictions.

REFERENCES

1. H.S. Napadensky, Sensitivity of Solid Propellants to Impact, AFRPL-TR-67-145, AD 316625, April 1967.

2. R.B. Elwell, et. al., Project SOPHY - Solid Propellant Hazards Program, AFRPL-TR-67-211, Vol. I, August 1967.

3. M.L. Wilkins, Calculation of Elastic Plastic Flow, Methods in Computational Physics 3, 211-263, Academic Press, Inc., New York, 1964.

4. H.S. Napadensky, Deformation of a Cylinder of Explosive Material in Unconfined Impact, Fifth Symposium (International) on Detonation, August 1970.

5. F.P. Bowden and A.D. Yaffe, Initiation and Growth of Explosion in Liquids and Solids, Cambridge, 1952.

CLOSING REMARKS

Captain P. F. Klein, USN
Chairman
Department of Defense Explosives Safety Board

The Fifteenth Seminar has been completed successfully, and I hope profitably. I hope you will all feel that it has been sufficiently rewarding and that you will be encouraged to attend the Sixteenth next year.

The agenda was interesting to me and I have received many favorable comments which I pass along to those deserving persons who earned them for us.

I would like to extend my thanks to the moderators and session speakers that I have not yet had a chance to thank personally and to my Secretariat for the arrangements which provided such an excellent setting and meeting place.

In closing, let me extend to all of you my thanks for your past support of the Board, my hope that this support will continue in the future, and my best wishes for a safe journey home.

The Seminar is now closed.

LIST OF ATTENDEES
15th ANNUAL EXPLOSIVES SAFETY SEMINAR
SAN FRANCISCO, CA.
18-20 SEPTEMBER 1973

ABERNETHY, D. F.   ODCSPER, DA, Washington, D. C.
ADDOR, H. S.   OOAMA, Hill AFB, Utah
ALLEN, R.   Teledyne McCormick Selph, Hollister, Cal.
ALLISON, J. C., LTC, USAF   HQ USAF, IG, Washington, D. C.
AISOP, B. E.   Embassy of Australia, Washington, D. C.
AMIG, Patricia M.   Naval Plant Rep Ofc, Sunnyvale, Cal.
AMLIE, June T.   Naval Ship R&D Center, Bethesda, Md.
AMSTER, A. B.   NAVORDSYSCOM, Washington, D. C.
ANDERSON, A. H.   United Technology Ctr, Sunnyvale, Cal.
ANDERSON, D. C.   TRW Systems, Inc., Redondo Beach, Cal.
ANDERSON, R. W.   Agbabian Associates, El Segundo, Cal.
ANDERSON, S.E., COL, USA   Sierra Army Depot, Herlong, Cal.
ARDIS, R. J.   NAPEC, Crane, Ind.
ARCHER, J.W., MSG, USA   Presidio of San Francisco
ARNOLD, W. K.   Holston Defense Corp., Kingsport, Tenn.
ARONSON, C. J.   NOL, Silver Spring, Md.
ATKINS, J. R.   Kennedy Space Center, Fla.
ATKISSON, J. B.   Jet Propulsion Lab., Pasadena, Cal.
AUGUSTINE, S. A.   Harry Diamond Labs., Washington, D. C.

BACHTELL, N. D.   DDESB, Washington, D. C.
BAGG, J. C.   Sandia Labs., Albuquerque, N. M.
BAILETS, R. J.   AFFTC/SEK, Edwards AFB, Cal.
BAILEY, M. R.   USAMC Field Safety Agency, Charlestown, Ind.
BAITY, W. M.   BRL, Aberdeen Proving Ground, Md.
BAKER, C. F.   Lawrence Livermore Labs, UC, Livermore, Cal.
BAKER, H. O.   CofEngrs, USA, Huntsville, Ala.
BALDWIN, W. J.   DSA, Alexandria, Virginia
BALL, J. G.   NASA, Pasadena, Cal.
BALL, L. W.   NASA, Marshall Space Flight Ctr., Ala.
BANNISTER, R. J.   U. S. Army Europe
BARAN, C.   HQ 21 AF, McGuire AFB, N. J.
BARRETT, B. J.   Delco Electronics Div, GMC, Goleta, Cal.
BARRETT, F. S.   AMC Ammunition Center, Savanna, Ill.
BARRON, M. A.   Jet Propulsion Lab., Pasadena, Cal.
BATCHELDER, M. C.   OOAMA, Hill AFB, Utah
BEARDEN, J. L., LTC, USAF   HQ AFISC/SESS, Norton AFB, Cal.
BECHER, A. F.   Edgewood Arsenal, Aberdeen PG, Md.
BELL, J. A.   British Embassy, Washington, D. C.
BELLES, F. E.   NASA, Cleveland, Ohio
BELMONT, A. J., COL, USA   USA Nuc & Chem Surety Grp, Ft Belvoir, Va.

BENGTSON, G. L.	Navajo Freight Lines, Oakland, Cal.
BENN, D. M.	Vandenberg AFB, Cal.
BENT, R. L.	Sperry Rand Corp., Louisiana AAP, La.
BERRY, J. C.	AMC Ammunition Ctr., Savanna, Ill.
BINGHAM, B. L.	Naval Plant Branch Rep, Hercules Inc, Magna Ut
BISHOP, R. H.	Wright-Patterson AFB, Ohio
BLOOM, G. E., MAJ, USAF	DCASR-Los Angeles, Cal.
BLOWER, H. E.	AF.CO Steel Corp., Lafayette, Cal.
BODDORFF, D.	Hercules Inc., Wilmington, Del.
BOGGS, W. H.	NASA, Kennedy Space Center, Fla.
BOGUNOVICH, R. A.	DCASR-San Francisco, Cal.
BOHLMAN, M. T., LT, USCG	U. S. Coast Guard, Washington, D. C.
BOURDON, C. F.	Naval Electronics Lab Ctr, San Diego, Cal.
BOYD, G. F.	Tri-State Motor Transit Co., Joplin, Mo.
BOYLE, V. M.	BRL, Aberdeen Proving Ground, Md.
BRAKE, R. L. CDR, USN	Naval Missile Center, Point Mugu, Cal.
BRAMEIER, H. A.	Aberdeen Proving Ground, Md.
BRASWELL, A. T.	Red River AD, Texarkana, Texas
BRATTON, T. R.	ARTEC Associates Inc., Hayward, Cal.
BREEN, C. F.	NASA, Langley Research Ctr., Virginia
BRETTEL, E. G.	Day & Zimmerman, Inc, Kansas AAP, Kansas
BRIARD, K. P., CAPT	Canadian Forces, Nat'l Defence HQ, Ottawa,C.
BROCK, N. H.	Air Products & Chemicals, Inc, Allentown, Pa.
BROOKS, I. G.	AF Special Wpns Ctr., Albuquerque, N. M.
BROWN, G.L.,LCDR, USN	DNA, Washington, D. C.
BROWN, J. W.	California Highway Patrol, Sacramento, Cal.
BROWN, W. D., Jr.	Iowa AAP, Burlington, Iowa
BRYANT, J.B.,COL, USA	HQ USA Armament Cmd, Rock Island Ars, Ill.
BUCHANAN, H. C	BRL, Aberdeen Proving Ground, Md.
BURCH, C. A.	USADC, Albuquerque, N. M.
BURT, D.	MTMTS, Oakland, Cal.
BUSH, P.R.,CAPT, USN	Staff, CINCUSPACFLT & COMSERVFPACFLT
BUTAS, J. A.	USA Safeguard Systems Cmd, Huntsville, Ala.
BYRD, V. E.	NOL, Silver Spring, Md.
CADY, C. M.	Badger AAP, Baraboo, Wisc.
CAIN, W. M.	MTMTS, Oakland, Cal.
CALLAHAN, H. L.	Black & Veatch, Kansas City, Mo.
CAMPBELL, C. J.	Rock Island Arsenal, Ill.
CARLTON, C. E.	United Technology Ctr, Sunnyvale, Cal.
CARPER, W. Ed.	NAVORDSYSCOM School, Bloomington, Ind.
CARY, E. C.	NWS Concord, Cal.
CASSADY, D. C.	CofEngr, Huntsville, Ala
CASWELL, C. R.	BuAlcohol,Tobacco,Firearms, San Francisco, Cal.
CAVIN, D. L.	NAD Hawthorne, Nevada
CERONE, J. R.	A. T. Kearney, Inc., Chicago, Ill.
CHAMBLISS, J.E.,CAPT, USN	NAD McAlester, Okla.
CHAMPION, M. W.	duPont Company, Wilmington, Del.

CHILDRESS, W. L.   Thiokol Chemical Corp. Brigham City, U.
CHRISTNER, R. K.   HQ, OCAMA, Del City, Okla.
CHURCHILL, W. I.   CofEngr, Mo River Div, Omaha, Neb
CLARK. W. G.   Naval Undersea Center, Pasadena, Cal.
CLARY, J. W.   Umatilla AD, Hermiston, Ore
COBERLY, J.A. MGYSGT, USMC   Camp Pendleton, Cal.
COFFIN, J. P.   Thiokol Chemical Corp., Bristol, Pa.
COLE, J. E.   BRL, Aberdeen Proving Ground, Md.
COLLINSWORTH, K. L.   HQ USAF, AFISC/SEOE, Norton AFB, Cal.
COMBS, M.F., CDR, USN   NCL Missile Test Facility, White Sands, N. M.
COMINS, T. E.   OOAMA, Hill AFB, Utah
CONLEY, J. H.   Aberdeen Proving Ground, Md.
CONNELL, G. N.   DCASR-San Francisco, Cal.
CONNELLY, J. W.   OFC, Ch Naval Operations, Washington, D.C.
COOK, M. A.   IRECO Chemicals, Salt Lake City, Utah
COOK. W. J.   Lockheed Propulsion Co., Redland, Cal.
COPENHAGEN, D.   Western Pacific RR, San Francisco, Cal.
CORBIN, C.C.   NAD Crane, Indiana
CORNEY, J.K., CAPT, USAF   AF Armament Lab., Eglin AFB, Fla.
COTTER, M. F.   Celesco Industries, Saugus, Cal.
COUCH, G.   United Technology Ctr., Sunnyvale, Cal.
COULSON, J. R.   duPont, Wilmington, Del.
COUPTRIGHT, C.   Los Alamos Scientific Lab., Los Alamos, N.M.
COWAN, G. H.   HQ USA MUCOM, Dover, N. J.
COWELL, A.D.   Custom Materials, Inc., Chelmsford, Mass.
CRAIG, B. G.   Los Alamos Scientific Lab., Los Alamos, N.M.
CROOK, A. M.   Indiana AAP, Charlestown, Ind.
CROSLEY, W. A.   Detector Electronics Corp., Minneapolis, Minn.
CROSS, J. F.   Hercules Inc., Magna, Utah
CRUPI, J. S.   Ofc, Asst SecNav (I&L), Washington, D. C.
CUMMINS, G. R.   MTMTS, Oakland, Cal.
CUNNIFF, R. E.   Uniroyal Inc., Joliet AAP, Ill

DAVIDSON, T. W.   Redstone Arsenal, Ala
DAVIS, C. T.   US AEC, Oakland, Cal.
DAVIS, J. O.   Sandia Labs., Albuquerque, N. M.
DAVIS, W. C.   NOSSOPAC, San Diego, Cal.
DAY, J. D.   CofEngr, Vicksburg, Miss.
DEANS, H. L.   DDESB, Washington, D. C.
DeJONG, R.V., CAPT, USA   Presidio of San Francisco, Cal.
DEMBERG, E.   Picatinny Arsenal, Dover, N.J.
DEWEY, L.   Southern Pacific Trans Co., San Francisco, Cal.
DEXTER, R. F.   BuAlcohol,Tobacco & Firearms, Washington, D.C.
DIAS, W. C.   SAMTEC (ROGF), Vandenberg, AFB, Cal.
DICKERSON, C. L.   NAVORDSYSSUPPOLANT, Norfolk Nav Shpyd, Va.
DIETEMANN, A. B.   NOL, Silver Spring, Md.
DIGGS, B.W., LCDR, USN   Naval EOD Facility, Indian Head, Md.
DITTMER, R. E.   Southern Pacific Trans Co., San Francisco, Cal.

DOBBS, N.	Ammann & Whitney, New York, New York
DONALDSON, L. O.	HQ 22AF/SEV, Travis AFB, Cal.
DONNADIEU, Roger	Societe Nat Des Poudres & Explosifs, Paris
DOW, G. S.	DCAS, Pittsburgh, Pa.
DOWD, T. H.	Tri-State Motor Transit Co., Joplin, Mo.
DOWDY, R. W.	Agbabian Associates, El Segundo, Cal.
DOWLING, T. P.	Trojan-U.S.Powder Div Commercial Solvents Corp., Allentown, Pa.
DOYLE, J. E.	J. E. Doyle Associates, Concord, Cal.
DRAKE, J. L.	Waterways Experiment Station, Vicksburg, Miss.
DRAKE, J. T.	DDESB, Washington, D. C.
DRAKE, R. W.	Los Alamos Scientific Lab., Los Alamos, N.M.
DREYER, O. F.	Lockheed Missiles & Space Co., Sunnyvale, Cal.
DRISCOLL, T. W.	DCASR-Atlanta, Georgia
DUBIE, L. W.	Teledyne McCormick Selph, Hollister, Cal.
DUFF, R. E.	Systems Science & Software, San Diego, Cal.
DUNN, D. J.	USA BRL, Aberdeen Proving Ground, Md.
DUNN, M. L.	DDESB, Washington, D. C.
DUNWOODY, C. C.	62 MAW (MAC) SEV, McCrord AFB, Wash.
EDDY, W. J.	NAVFACENGCOM, Alexandria, Va.
EDWARDS, C. R.	Hercules, Inc., Radford AAP, Va.
EHLERS, B.	HQ 59th ORD GRP, Pirmasens, Germany
EHRINGER, A. G.	AMC Ammunition Center, Savanna, Ill.
ELEUTERIO, H. S.	duPont., Wilmington, Del.
ELSASSER, F. M.	60 MAWG/SEV, Travis AFB, Fairfield, Cal.
ERICKSON, C. L.	Sierra AD, Herlong, Cal.
EVANS, K.	NWS Concord, Cal.
EWING, H. M.	Sacramento AD, Sacramento, Cal.
FAIRCHILD, J. M.	Aerojet-General Corp., Sacramento, Cal.
FART, G. D.	AMC HQ, Alexandria, Va.
FARBER, E. A.	University of Florida, Gainesville, Fla.
FEIL, J.A., LTC, USAF	DCASR-Boston, Mass
FENGER, F. H.	Tudor Engineering Co., San Francisco, Cal.
FERNANDES, A.	NAVORDSYSCOM, Washington, D. C.
FICHTER, A.A.	FMC Corporation, Santa Clara, Cal.
FIDELL, F. J.	Frankford Arsenal, Philadelphia, Pa.
FINE, W. T.	NOL, Silver Spring, Md.
FINGER, M.	Lawrence Livermore Lab., Livermore, Cal.
FINKEL, M. G.	USA Matl Sys Analysis Agcy, Aberdeen PG, Md
FISHER, R. E.	duPont, Pompton Lakes, N.J.
FLEMING, L. U.	Dugway Proving Ground, Utah
FLETCHER, E. R.	Lovelace Foundation, Albuquerque, N. M.
FORBIS, K. V.	Anniston AD, Ala
FORSYTHE, F. J.	Joliet AAP, Ill.
FOWLER, W. T.	Radford AAP, Va.
FRANKOVICH, S.	Explosives Transports, Okle City, Okla.

FREEDMAN, E.	USA BRL, Aberdeen Proving Ground, Md.
FUGELSO, L. E.	General American Research Div, Niles, Ill
GAITHER, D.	NAD Crane, Indiana
GALLES, F. P.	NTS, Keyport, Wash.
GERA, J.	Rockwell International, Downey, Cal.
GERHARDS, J. E.	NWS Concord, Cal.
GIBPLE, J. W.	NAVAIRSYSCOM, Washington, D. C.
GIGLIO-TOS, L.	BRL, Aberdeen Proving Ground, Md.
CILL, J. O.	NAPEC Crane, Indiana
GILMAN, R.D., CAPT, USAF	Armament Dev Test Ctr, Eglin AFB, Fla.
GILMORE, A. E.	NAD Crane, Indiana
GOFF, C. R.	Day & Zimmerman, Inc., Texarkana, Texas
GOLEBIEWSKI, J. J.	HQ 9th Infantry & Ft. Lewis, Wash.
GOOCH, T. R.	Thiokol Chemical Corp., Huntsville, Ala.
GOTT, R. W.	Hercules Inc., Magna, Utah
GOUGLER, G. M.	AFPRO (Thiokol Chemical Corp) Brigham City, Ut
GRAHAM, K. J.	Naval Postgraduate School, Monterey, Cal.
GRAVATT, G. D.	Dept of Labor. OSHA, Indianapolis, Ind.
GREEN, J. P.	NOSSOPAC, San Diego, Cal.
GREEN. L. G.	Lawrence Livermore Lab., Livermore, Cal.
GRIFFIN, K. T.	Arnold Research Org, Arnold EDC, Tenn
GROSS, C. E.	NAVFACENGCOM, San Bruno, Cal.
GROVE, H.	Doudell Trucking Co., San Jose, Cal.
GRYTING, H. J.	NWC China Lake, Cal.
GUARIENTI, R. P.	Lawrence Livermore Lab., Livermore, Cal.
CURRY, S., CAPT, USN	NAD Oahu
HALL, G. W.	Pan American World Airways, Patrick AFB, Fla.
HALPIN, J.	NWC China Lake, Cal.
HAMILTON, H.	ICI America Inc., Volunteer AAP, Tenn.
HAMMOND, J. W.	NASA, Kennedy Space Center, Fla.
HANNA, R. J.	Boeing Aerospace Co., Seattle, Wash.
HANNAH, M. M.	63MAWG/SEV (MAC), Norton AFB, Cal.
HARRIS, N. A., LCDR, USN	Pacific Missile Range, Point Mugu, Cal.
HARRIS, R. M.	Red River AD, Texarkana, Texas
HART, R. E.	Bu of Explosives, Assn of Am RR, San Fran, Cal.
HARTON, I. E.	Department of Transportation, Washington, D.C.
HASSLER, J. W.	Holex, Inc., Hollister, Cal.
HAWS, L. D.	Monsanto Research Corp., Miamisburg, Ohio
HEACOCK, F.	Presidio of San Francisco, Cal.
HECKLEY, P. J.	Naval Biomedical Research Lab., Oakland, Cal.
HEESEMAN, A.	Wyle Laboratories, Norco, Cal.
HEFFAN, H.	NWS Concord, Cal.
hELLE, C. J.	Remington Arms Inc., Sao Pualo, Brazil
HEMM, W. H., COL. USAF	HQ AAC/SE, Elmendorf AFB, Alaska
HEMPHILL, WM.	Martin Marietta Aerospace, Vandenberg AFB, Cal.
HENRY, R. E.	Lawrence Livermore Lab., Livermore, Cal.

HERMAN, R. C.   DDESB, Washington, D. C.
HERMAN, P. J.   Naval Plant Rep, Sunnyvale, Cal.
HERSCHKORN, J. A.   HQ AFCMD/SE, Kirtland AFB, Albuquerque, N. M.
HERSOM, G. F.   Southern Pacific Transp Co., San Francisco, Cal
HESS, V. J.   Priority Air Dispatch, Washington, D. C.
HICKEY, E. C.   TRW Systems, Redondo Beach, Cal.
HILL, R. H.   AMC Ammunition Center, Savanna, Ill.
HILL, W. V.   Black & Veatch, Kansas City, Mo.
HILLARD, L. F.   HQ US Army Pacific
HILLMAN, R. S.   Martin Marietta Aerospace, Denver, Colo.
HILLS, D. J.   Presidio of San Francisco, Cal.
HIRSCH, D.   Norris Industries, Inc., Vernon, Cal.
HOFFMANN, J. M.   Southern Pacific Trans Co., Los Angeles, Cal.
HOFFMAN, P. D.   Hercules Inc., Cumberland, Md.
HOLDEN, J. E.   Tudor Eng. Co., San Francisco, Cal
HOSKING, C. H.   Picatinny Arsenal, Dover, N. J.
HOUSER, J. J.   Consolidated Freightways, Hayward, Cal.
HOWARD, J.N., CAPT, USN   Ofc, Ch of Naval Operations, Washington, D.C.
HOWE, P. M.   BRL, Aberdeen Proving Ground, Md.
HOWELL, E. D.   Air Force Systems Cmd, Andrews AFB, Md.
HUANG, P. C.   NOL, Silver Spring, Md.
HUEHN, W., CAPT   WEHRBEREICHSKOMMANDO V (HQ MIL Dist), W. Ger.
HUFFMAN, J. P., COL, USAF   AF Insp & Safety Ctr., Norton AFB, Cal.
HUGHES, G. F.   NWS Yorktown, Virginia
HURT, R. K.   Rocky Mountain Arsenal, Denver, Colo.
HUTCHINS, S.   DCASR-Los Angeles, Cal.

IRWIN, B. F.   HQ Alaskan Air Cmd., Elmendorf AFB, Alaska
ISAACS, N.   MRC Corporation, Baltimore, Md.

JAMISON, J. E.   Mason & Hanger-Silas Mason Co., Burlington, Io.
JANG, J. F.   DCAS San Francisco, Cal.
JENKINS, D M.   NWL Dahlgren, Va.
JOHNSON, C. N.   Tri-State Motor Transit Co., Joplin, Mo.
JOHNSON, L. P. E.   Polaris Missile Facy Pacific, Silverdale Wash
JOHNSON, R. E.   Olin Corporation, Badger AAF, Baraboo, Wisc.
JOHNSON, R. H., MAJ, USA   Presidio of San Francisco, Cal.
JOHNSON, R. W.   Baggett Transp Co., San Francisco, Cal.
JONES, C. P.   NAVORDSYSCOM, HQ, Washington, D. C.
JONES, C. S.   NWS Concord, Cal.
JONES, F. M.   Aerojet Solid Prop Co., Sacramento, Cal.
JONES, L. L.   NAVORDSYSCOM, NAPEC Crane, Ind.
JOPHLIN, D. F.   Hercules Inc., Wilmington, Del.
JUNKIN, W. P.   Edgewood Arsenal, Aberdeen Proving Ground, Md.

Kaplan, K.   URS Research Co., San Mateo, Cal.
KASDORF, F. W.   NWL Dahlgren, Va.
KEENAN, W. A.   Naval Civil Eng Lab, Port Hueneme, Cal.

KEISER, S.P., MAJ, USAF   DCASR-St. Louis, Mo.
KEITH, A. W.   Southern Pacific Transp Co.,San Francisco, Cal.
KELLY, J. E.   Naval Weapons Handling Lab.,NAD Earle,N.J.
KELLER, G. R.   Keller & Gannon, San Francisco, Cal.
KELLEY, P. G., COL, USA   DDESB, Washington, D. C.
KELLY, J.P.H.   AEC, Washington, D. C.
KEIDRICH, H. E.   AEC, Las Vegas, Nev.
KIMBALL, F.   Southern Pacific Transp Co., San Francisco Cal.
KINDIG, J.M., LCDR, USN   Naval Missile Center, Point Mugu, Cal.
KING, L. R.   United Technology Ctr, Sunnyvale, Cal.
KING, R. L.   Southern Pacific Transp Co., San Francisco, Cal
KINGERY, C. N.   BRL, Aberdeen Proving Ground, Md.
KINNEY, G. F.   NWC China Lake, Cal.
KINNEY, R. B.   ADC, Colorado Springs, Colo.
KINNISON, R. L.   DCASD Phoenix, Ariz.
KIRSCHKE, E. J., CAPT, USN   NAD Hawthorne, Nev.
KLEHS, H.J.W.   Southern Pacific Transp Co., San Francisco Cal
KLEIN, P.F., CAPT, USN   Chairman, DDESB, Washington, D. C.
KNIGHT, J.   Embassy of Australia, Washington, D. C.
KNOTT, E. F.   NOL Test Unit, Patrick AFB, Fla.
KOMOS, J. N.   DSA, Alexandria, Virginia
KORMAN, H. F.   TRW Systems, Redondo Beach Cal.
KOSKETAR, P., CAPT, USA   Sierra AD, Herlong, Cal.
KUNZI, E. J.   NAD Hawthorne, Nevada
KRUSE, J. C.   Dept of Justice, Washington, D. C.
KRUSE, K., COL, USAF   HQ SAC, Offutt AFB, Neb.

LAMOTHE, R. M.   USA Mat & Mech Res Ctr, Watertown, Mass
LANDERS, R. C.   Aerojet Ord Mfg Co., Pomona, Cal
LANDRUM, R. G., CDR, USN   NWS Concord, Cal.
LANG, R. A.   DCASR-Chicago, Ill.
LARIMER, E. M.   Federal Cartridge Corp., Twin Cities AAP, Minn.
LARSEN, T. E.   Detector Electronics Corp., Minn., Minn.
LATHAM, J. F.   NAD EARLE, N. J.
LAURENCE, E. A.   Lockheed Missiles & Space Co., Sunnyvale, Cal.
LEAVITT, C. L.   Reynolds Ind., Los Angeles, Cal.
LECHNER, G. J.   Teledyne McCormick Selph, Hollister, Cal.
LEEHY, L. R.   CofEngr, Omaha, Neb.
LEMKE, J. C.   AMC, Alexandria, Va.
KEVEY, D. V.   Gearhart Owen Ind., Inc., Fort Worth, Texas
LESLIE, E. B.   Anniston AD, Anniston, Alabama
LEWIS, H.   duPont, Wilmington, Del.
LIGHTBODY, A.   NOL, Silver Spring, Maryland
LINDLER, H. L.   USAMCESA, Charlestown, Ind.
LINNENBRINK, T. E.   General American Trans. Co., Niles, Ill.
LLOYD, J. D.   AMC, Alexandria, Va.
LOGAN, J. F.   Western Electric Co., Greensboro, N. C.
LOWADIER, F. D.   Monsanto Research Corp., Miamisburg, Ohio

LOVELACE, G.M., MAJ, USA	USAMMCS, Redstone Arsenal, Ala.
LOVELL, P. K.	Sandia Labs., Livermore, Cal.
LOVING, F. A.	duPont, Martinsburg, W. Va.
LUNGREN, J. G.	Philco Ford Corp., Newport Beach, Cal.
McCAY, W. C.	Longhorn AAP, Marshall Texas
McDONALD, J. B.	Brunswick Corp., Sugar Grove, Va.
McDOWALL, M. E.	National Defence Hq., Ottawa, Canada
McKIBBEN, R. B.	NAVFACENGCOM, San Bruno, Cal.
MacDONALD, H. J.	Reynolds Industries, Inc., San Ramon, Cal.
MACK, Jr., J. O.	Hercules, Inc., Sunflower AAP, Lawrence, Dan.
MAHER, F. J.	Keller & Gannon, San Francisco, Cal.
MAJOWICZ, J. M.	HQ, DA, Washington, D. C.
MALM, D. O.	Booz Allen Applied Research, Bethesda, Md.
MAPLES, J. D.	Station Supply & Stock Control Div, Redstone Arsenal, Ala.
MARCHITELLI, T. T.	NAVORDSYSCOM, Washington, D. C.
MARSISCHKY, G. W.	NAD Crane, Indiana
MARTINELLI, J. A.	Aerospace Corp., El Segundo, Cal.
MASSIE, S. A.	MTMTS, Oakland Army Base, Oakland, Cal.
MASTROMONICO, C., CAPT, USAF	AF Rocket Propulsion Lab., Edwards AFB, Cal.
MAUCK, C.	Sandia Lab., Livermore, Cal.
MAYBERRY, L. J.	Navy Ships Parts Control Ctr, Mechanicsburg,Pa
MAYER, F. H., MAJ, USA	DCASR-New York, N.Y.
MEAD, J. M.	Uniroyal Inc., Joliet, Ill.
MENDOLIA, A. I.	Asst Secretary of Defense (I&L)
METCALF, H. L.	OASD(I&L), Washington, D. C.
MIGUEL, J.	USN Underwater Sys Ctr., Newport, R. I.
MILIBAND, H.	DCASD, Springfield, N.J.
MILLER, J. L.	Honeywell, Inc, Govt & Aeronautical Prod. Minneapolis, Minn.
MITCHELL, W. D.	Research & Eng. Redstone Arsenal, Ala.
MOBLEY, A. C.	Newport AAP, Indiana
MOODY, H. E.	DCASR-Los Angeles, Cal.
MOORE, C. D.	Martin Marietta Aerospace, Vandenberg AFB,Cal
MOORE, W. J.	NAVFACENGCMD, San Bruno, Cal.
MORRIS, C. W.	NWL Dahlgren, Virginia
MOUNT, C. T.	Lexington Blue Grass AD, Lexington, Ky.
MULLINS, R. K.	Lawrence Livermore Lab., Livermore, Cal.
MUNSON, E. H.	NWS Concord, Cal.
MURCHISON, B. F.	March AFB, Cal
MURPHY, J. L., JR.	Thiokol Chemical Corp., Huntsville Ala.
MUSTAHICH, J. M.	Southern Pacific Transp Co., San Francisco Cal
MYERS, R. L.	AMC Fld Safety Agcy, Charlestown, Ind.
NATALI, G.	NWS Concord, Cal.
NEWCOMB, F. N.	USA Human Eng. Lab. Aberdeen, Md.
NICKERSON, H. D.	NAVFACENGCOM, Alexandria, Virginia

POPLE, D. S., LCDR, USN   NWS Concord, Cal.
NYSTROM, W. K.   NWS Concord, Cal.

O'DEA, J. P.   Cornhusker AAP, Grand Island, Neb.
OLSEN, F. N.   Boeing Aerospace Co., Seattle, Wash.
OPEL, M. C.   ICI America Inc., Indiana AAP, Charlestown Ind.
OSBORN, D. M.   NAD Earle, Colts Neck, N. J.
OSHEROFF, B. J., Capt   US Dept Health Ed. & Welfare, Washington, D.C.
OZBURN, J. E.   Leonard Bros. Trucking Co., Pensacola, Fla.

PAKULAK, J. M.   NWC China Lake, Cal.
PARKER, F. J., Jr.   Red River AD, Texarkana, Texas
PARKER, P. L.   AF Armament Lab., Eglin AFB, Fla.
PARKS, D. K.   Falcon R&D, Denver, Colo.
PARRISH, D. D., Jr.   Holex, Inc., Hollister, Cal.
PASZEK, J. J.   USA BRL, Aberdeen Proving Ground, Md.
PELL, H. D.,   Custom Materials, Inc., Chelmsford, Mass
PENA, A. O.   NOMTF, White Sands Missile Range, N.M
PERKINS, R. G.   DDESB, Washington, D. C.
PETERSEN, A. H.   Detector Electronics, Corp., Minn. Minn.
PETERSON, R. J.   AEC, Las Vegas, Nev.
PETES, J.   NCL White Oak, Silver Spring, Md.
PFEIFER, H. E.   Lawrence Livermore Lab., Livermore, Cal.
PHILLIPS, H.   Mason & Hanger-Silas Mason Co., Amarillo, Tex.
PIERCE, Richard B. LTC, USA   HQ DNA, Washington, D. C.
PINE, D. W., LT, USN   Oceanographer of the Navy, Alexandria, Va.
PLANK, D. A.   NWS Concord, California
PLATE, S. W.   Tri-State Motor Transit Co., Joplin, Mo.
PLEDGER, D. E.   NAVFACENGCOM, Alexandria, Va.
POLLEY, C. J.   USA Mat & Mech Research Ctr, Watertown, Mass.
PONDER, E E.   Lanson Industries, Inc., Cullman, Ala.
POWER, J. M.   National Defence Hq., Ottawa, Canada
PRATT, V.   Dugway Proving Ground, Ut.
PRESTERA, JR., M.R.   Prestera Trucking Co., Inc., Huntington, W.Va.
PRIOR, L. C.   Jet Propulsion Lab., Pasadena, Cal.
PRITCHARD, G. C.   NWC China Lake, Cal.
PROVINES, J. C.   American Farm Lines, Oklahoma City, Okla
PROWS, Rodney G.   DCASR, Dallas, Texas
PUCHALSKI, V.   Frankford Arsenal. Philadelphia, Pa.

RAIFORD, J. P.   HQ SAC, Offutt AFB, Neb.
RANDALL, H. J.   DCAS, Burlingame, Cal.
RANES, W. A.   NWS Concord, Cal.
REED, J. W.   Sandia Lab., Albuquerque, N. M.
REEVES, H.   BRL, Aberdeen Proving Ground, Md.
REGAN, L. F.   USAMC. Alexandria, Va.
REID, R. J.   FMC Corp., Santa Clara, Cal.
REXON, C. J.   DCASD Anaheim, Cal.

REZETKA, W. L.   Pacific Missile Range, Point Mugu, Cal.
RHODES, D. B.   Lone Star AAP, Texarkana, Texas
RHODES, J. L.   Munitions Sys., Hill AFB, Utah
RICHARDSON, K. M.   Ft. MacArthur, San Pedro, Cal.
RICHMOND, D. R.   Lovelace Foundation, Albuquerque, N.M.
RILEY, W. E.   Space & Missile Test Ctr., Vandenberg AFB, Cal.
RINGENBERG, M. G.   USA Armaments Cmd, Aberdeen PG., Md.
RINGHAM, A., JR.   A.T.Kearney, Inc., San Francisco, Cal.
RITTMAN, H. T., JR.   duPont Company, Wilmington, Del.
ROACH, J. R.   NAPEC, Crane, Ind.
ROBERTS, C.   DCASR-Los Angeles, Cal.
ROBINSON, P. E.   Military Airlift Wing (MAC), McGuire AFB,NJ
ROBINSON, R. M.   Presidio of San Francisco, Cal.
RODIO, P. A.   USAMC, Alexandria, Va.
ROMINE, E. A.   Sandia Lab., Livermore, Cal.
ROSENVINGE, R. C.   Union Carbide Corp., Oak Ridge, Tenn.
ROST, D. L.   Sandia Lab., Albuquerque, N. M.
RUTH, J.   Management Science Assoc., Palo Alto, Cal.
ROTHERY, C. M.   DCASR-St. Louis, Missouri
ROURE, J. J.   Svc Technique Des Poudres Et Explosifs, Paris
ROUSE, J. H., COL, USA   US Army Claims Svc, Ft. Meade, Md.
ROWLAND, S. W.   Gulf Energy & Environmental Sys, Del Mar, Cal.
ROYLANCE, H. M.   NAVORDSYSCOM, Washington, D. C.
RUMBLE, M. W., CAPT,USN   NAVAIRSYSCOM, Washington, D. C.
RUSSELL, B. A.   Dow Chemical Co., Midland, MI
RUSSELL, P. V.   US Forest Service, San Francisco, Cal.

SANCHEZ, F. B.   US NWL Dahlgren, Va.
SANDERS, B. L.   Tri-State Motor, Joplin, Missouri
SAPORITO, M.   Seneca AD, Romulus, NY
SAVITT, J.   Lockheed Missiles & Space Co., Santa Cruz, Cal.
SAWYER, R. B.   DDESB, Washington, D. C.
SCHAICH, E. CAPT   German Ministry of Defence, Bonn, Germany
SCHIFFMAN, T. H.   General American Research Div., Niles, Ill.
SCHUETT, K. A.   United Technology Ctr., Sunnyvale, Cal.
SCHULFER, E. R.   Hill AFB, Utah
SCHUMACHER, H. R.   NWS Concord, Cal.
SCHUMACHER, R. N.   BRL, Aberdeen Proving Ground, Md.
SCOTT, R. A., JR., DR.   DDESB, Washington, D. C.
SCOTT, R. L.   NWS Concord, Cal.
SEAVERS, R. H.   Army Missile Cmd., Redstone Arsenal, Ala.
SEAY, G. E., DR.   Systems Science & Software, San Diego, Cal.
SHALABI, G. K.   Olin Corporation, Badger AAP, Wisc.
SHARPS, A. R., LT, USN   HQ 5th Naval Dist., Norfolk, Va.
SHAY, R. M.   AEC, Albuquerque, N.M.
SHERIDAN, G. E.   Reynolds Ind., Inc., Los Angeles, Cal.
SHEFFIELD, O. E.   Picatinny Arsenal, Dover, NJ.
SHIPMAN, C. E.   Western Pacific Railroad, San Francisco, Cal.

SHOPHER, K. R.	AF Log Cmd., Wright-Patterson AFB, Ohio
SHORT, P. E.	Martin-Marietta, Milan AAP, Tn.
SHULTZ, L.	Lockheed Missiles & Space Co., Sunnyvale, Cal.
SILVA, L. F., MAJ	DNA, Washington, D. C.
SIMPSON, J. L.	Martin-Marietta Aerospace, Denver, Colorado
SIMS, W. H.	NAVORDSYSCOM Support Ofc (Atlantic), Portsmouth, Va.
SISSON, G. D., JR, COL, USAF	Edgewood ARsenal, Aberdeen Proving Ground, Md.
SKAAR, K. S.	NWC China Lake, Cal.
SKAGG, D.	Explosive Transports Inc., Okla City, Okla.
SKAGG, G.	Explosive Transports Inc., Okla City, Okla.
SKAGGS, L. F.	Explosive Transports Inc., Okla City, Okla.
SKINNER, C. S.	Design & Development, Inc., Cleveland, Ohio
SLIGHT, G. F.	NAD Crane, Indiana
SLYKER, R. W.	Naval Missile Center, Point Mugu, Cal.
SMITH, D.	Hercules Inc., Magna, Utah
SMITH, E. L.	March AFB, Cal.
SMITH, J. R.	Aerospace Corp., Los Angeles, Cal.
SMITH, P. J.	NAD Crane, Indiana
SMITH, R. J.	NSA, Ft. Meade, Md.
SMITH, W. D.	NWL Dahlgren, Va.
SNELLER, G.	Kelley AFB, San Antonio, Texas
SPERBER, H. H.	HQ Space & Missiles Sys, El Segundo, Cal.
STECKER, E. J.	Holex, Inc., Hollister, Cal.
STEVENS, C. J.	NAVFACENGCMD, Alexandria, Va.;
STEVENSON, T. D.	Lockheed Missiles & Space Co., Sunnyvale, Cal.
ST. HILAIRE, A. R.	Sandia Corp., Livermore, Cal.
STOFFERS, F. W.	Jet Propulsion Lab., Pasadena, Cal.
STOOPS, R. R., LCDR, USN	NAVAIRSYSCOM, Washington, D. C.
STOREY, R. B.	OOAMA, Hill AFB, Utah
STOTHERS, M. Q.	WESTNAVFACENGCOM, San Bruno, Cal.
STARR, L. D.	NAPEC, NAVORD, Washington, D. C.
STUCKEY, G. B.	USA Armament Cmd, Rock Island, Ill.
SULLIVAN, E. P., JR.	Atlantic Research Corp, Gainesville, Va.
SULIIVAN, T. J.	NOS Indian Head, Maryland
SUTHERLAND, J. L.	USA MEMCMS, Redstone Arsenal, Ala.
SUMIDA, T. A.	Lockheed Missile & Space Co., Sunnyvale, Cal.
SWEARINGEN, P. LTC, USA	Joint Chiefs of Staff, Washington, D. C.
SWISDAK, M. M., Jr.	NOL White Oak, Silver Spring, Md.
TAKAHASHI, T. H.	Sandia Laboratory, Livermore, Cal.
TALLEY, R. R.	WESTNAVFACENGCOM, San Bruno, Cal.
TANCRETO, J. E.	Naval Civil Eng. Lab., Port Hueneme, Cal.
TEOPFER, R. E., CAPT, USN	1st Marine Div., Camp Pendleton, Cal.
TEICHMANN, E. C.	60th ORD GP., Germany
TEREO, M.	NAD Earle, Colts Neck, N. J.
THATCHER, D. N.	Teledyne McCormick Selph, Hollister, Cal.
THOMAS, C. A.	Hughes Aircraft Co., Tucson, Arizona

THOMAS, W. C.	Naval Undersea Ctr., San Diego, Cal.
THUMM, H.	Chateau Yaldara Propriety, Lyndoch, Australia
TORRES, J., CAPT, USAF	Pacific Air Forces
TOWNSEND, J. E.	NWL Dahlgren, Va.
TRAFTON, J. C.	General Electric Co., Burlington, Vt.
TRAVERS, P. B.	Custom Materials, Inc., Chelmsford, Mass.
TREDREA, D. R.	USA Armament Cmd., Rock Island, Ill
TULL, J. D.	Lockheed Missile & Space Co., Santa Cruz, Cal.
TURNER, D.	Ofc, DCSLOG, Washington, D. C.
TWOHY, G. W.	Mission Airlines, California City, Cal.
VAN ERP, D.	Keller & Gannon, San Francisco, Cal.
VAN WINKLE, J. C.	NAD Crane, Indiana
VINING, J. O.	Battelle Northwest Lab., Richland, Wash.
VINSON, J. L.	Remington Arms Co., Lake City AAP, Mo.
WALL, M. F.	Thiokol Chemical Corp., Longhorn Div., Marshall, Texas
WALLACE, R. D., JR., COL, USA	AMC, Alexandria, Va.
WARE, W. W.	Rockwell International Corp., Downey, Cal.
WARNER, R. C.	TRW Systems Group, Redondo Beach, Cal.
WATSON, J. B.	NAVFACENGCOM, San Bruno, Cal.
WATSON, R. R.	Ministry of Defence, London, England
WATSON, R. W.	US Bureau of Mines, Pittsburgh, Pa.
WEALS, F. H.	NWC China Lake, California
WEISS, H.	Rocketdyne, Canoga Park, Cal.
WENZEL, A. J.	Southwest Research Institute, San Antonio, Tx.
WHITBREAD, E. C.	Home Office, London, England
WHITE, R. W.	NWS Concord, Cal.
WHITE, W.	Frankford Arsenal, Philadelphia, Pa.
WEIDERMAN, A. H.	IIT Research Institute, Chicago, Ill.
WIGGER, G. F.	OCE, Washington, D. C.
WIGHT, R. L.	OCE, Washington, D. C.
WILLIAMS, R.	Harry Diamond Lab., Washington, D. C.
WILLIAMS, F.	Bechtel Power Corp., San Francisco, Cal.
WILLIAMSON, T. C.	AFPRO Boeing Co., Seattle, Washington
WILLIS, F. M.	E.I.duPont de Nemours &Co., Martinsburg, W. Va.
WILLIS, V. G., SR.	NAD Crane, Indiana
WILLOUGHBY, W. F.	USA Mat'l Sys Analysis Agcy, Aberdeen PG, Md.
WILKINSON, W.	Stanford Research Institute, Menlo Park, Cal.
WILSON, D. E.	NOS Indian Head, Md.
WILSON, P. D.	Pacific Missile Range, Point Mugu, Cal.
WILTON, C.	URS Research Corp, San Mateo, Cal.
WINER, H.	ARADCOM, ENT AFB, Colorado Springs, Colo.
WON, W.	Naval Supply Center, Oakland, Cal.
WOODMAN, F.	Presidio of San Francisco, Cal.
WOWAK, W. E.	DNA, Kirtland AFB, N. M.
WRIGHT, H. W.	Twin Cities AAP, Minnesota

YOUNG, R. E.   Picatinny Arsenal, Dover, N.J.

ZAKER, T. A., Dr.   DDESB, Washington, D. C.
ZAUGG, M. M.   Tooele AD, Utah
ZELLER, A. F., Dr.   AF Insp & Safety Ctr., Norton AFB, Cal.
ZIMMERMAN, C. A.   Lockheed Missile & Space Co., Sunnyvale, Cal.